# Toxic Species and Particulate Emissions from Synthetic Polymer Fires

Miss Hasimawaty Binti Mat Kiah

Submitted in accordance with the requirements for the degree of Doctor of Philosophy

The University of Leeds

School of Chemical and Process Engineering

March, 2020

The candidate confirms that the work submitted is her own, except where work which has formed part of jointly-authored publications has been included. The contribution of the candidate and the other authors to this work has been explicitly indicated below. The candidate confirms that appropriate credit has been given within the thesis where reference has been made to the work of others.

1) **Mat Kiah M.H.**, Mustafa B.G., Andrews G.E., Phylaktou H.N., Li H (2019). **PVC Sheathed Electrical Cable Fire Smoke Toxicity**, Proceedings of the Ninth International Seminar on Fire and Explosion Hazards, St. Petersburg, Russia (April, 2019).

*(Included in Chapter 4)*

All the experimental work, analysis of results and writing up of the publication were carried out by Miss Hasimawaty Binti Mat Kiah. Bintu Grema Mustafa participated in carrying out the experimental procedures as two students are required when undertaking experiments and I participated in her work relating to the toxic hazards of commercial wood products. Dr Herodotos Phylaktou, Professor Gordon Andrews and Dr Hu Li (particle number specialist) supervised the research work and proof-read the publication.

***On-going and other joint publications are listed in Appendix A.***

## Acknowledgements

I would like to thank my supervisors, *Dr Herodotos Phylaktou, Professor Gordon Andrews and Dr Hu Li* for their continuous support, great supervision, kind advices, valuable ideas and positive discussions through this research work.

I also would like to thank the staff and friends under the same department who helped me direct and indirectly during my study. My special thanks for whom always there to assist me when needed go to: my research mate, *Bintu Grema Mustafa* and the SCAPE laboratory technicians, *Ed Woodhouse, David Instrell, Dr Adrian Cunliffe, Karine Alves Thorne, Gurdev Bhogal, Stuart Micklethwaite, Ryan Smith and Lucy Leonard.* I also want to extend my thanks to *Professor David Purser* for his idea sharing and advices when I was at my initial stage of my PhD study.

Also not forgetting, special thanks to *Kevin O'Neill*, *Neil Duddy* and *Gavin Andrews* for their generosity on supplying some of research test materials. *Kevin O'Neill* had supplied Siemens' Wind Turbine and other LSZH cables, *Neil Duddy* had supplied bunding materials which mostly were Polyethylene type of materials and *Gavin Andrews* from Leeds Solar company had supplied high voltage Solar Energy cables.

Great thanks to the *Malaysian Government (Ministry of Higher Education, Malaysia)* and *Universiti Teknologi Malaysia* for sponsoring my PhD study.

My extraordinary thanks to *my husband also known as my soulmate* ***Izham,*** my lovely daughter ***Damia*** and my sweet son ***Daffa****.* My deepest thanks, love and gratitude for *my parents* and *all family members* in Malaysia. This work would not have been completed without their borderless love and endless support throughout the PhD journey.

## Abstract

Overall fire statistics and residential and industrial fires in which there have been large number of fatalities demonstrate that the cause of most deaths can be attributed to effects of toxic smoke produced in these fires. Despite this fact there are no national or international legal requirements to determine the toxic emissions from materials used in construction, electrical cabling or the wide range of polymer based products used in house construction and industry. Many polymers used commercially are fire retarded and the materials used for this can add to the toxicity. The only indirect control comes through some test requirements for product classification based on the volume of smoke production. However, this is not an adequate approach to the problem. Fire smoke contents can cause death directly or can impair escape so that people die indirectly from the effects of toxic gases, and in the first we need to identify and quantify these emissions for different materials and under different fire conditions. Currently, as a consequence of this lack of legal requirements, there is a dearth of data on toxic emissions from real industrial products under fire conditions.

This research was focused on toxic gas emissions under fire conditions from practical industrial polymeric materials: insulating foams, electrical cables, Polyethylene and Polystyrene goods together with some other polymeric materials: rubber, GRP, PVC pipes and clear Acrylic. All were either used by industry who gave samples for testing or were on sale in construction product retailers. Some of the goods were fire retarded and had HCl, HBr or HF in the product gases or had high ash content. These generally produced higher toxic emissions than non-fire retarded products.

Most of the work was carried out using the Leeds University modified Cone Calorimeter with raw gas sampling from a chimney above the cone outlet. A heated sample line, heated filter and heated sample pump with heated FTIR was the method of analysis used. All products were found to have significant toxic gas emissions, but the most important toxic gas depended on the material tested and was rarely CO. A data set of toxic emissions and toxic gas yields was produced which is greater than most data sources in the literature for synthetic polymer materials.

Part of this work was the modification of the Purser Furnace by adding raw hot gas sampling and eliminating the backflow of dilution air into the reaction tube. This took a long time to design and construct and was only available at the end of the research work where it was used with PE samples at lean and rich equivalence ratios.

A significant part of the work was the first use of this equipment for particle size analysis using the DMS 500 instrument. Ultra fine particles (<50nm) were present in all the fires and were a significant health hazard.

# Table of Contents

# List of Tables

# List of Figures

## Nomenclature and Symbols

| | |
|---|---|
| CO | Carbon monoxide |
| $CO_2$ | Carbon dioxide |
| HCN | Hydrogen cyanide |
| HBr | Hydrogen bromide |
| HCl | Hydrogen chloride |
| HF | Hydrogen fluoride |
| $N_2$ | Nitrogen |
| $O_2$ | Oxygen |
| $SO_2$ | Sulphur dioxide |
| Φ | Equivalence ratio |
| % | Percent |
| $^oC$ | Unit temperature – degree Celsius |
| kW | Unit energy – kilowatt |
| $m^2$ | Unit area – meters square |
| g/g | Yield unit – gram/gram |
| ppm | Part per million |
| s | Unit time – seconds |
| $dm^3$ | Unit volume – cubic decimetre |
| m3 | Unit volume – cubic metre |
| min | Unit time – minutes |
| mm | Unit length – millimetre |
| nm | Unit length – nanometre |
| g | Unit mass – gram |
| L | Unit volume – litre |
| vol. | Volume |
| wt. | Weight |
| ŋ | Combustion efficiency |

# Chapter 1
# Introduction

Fire toxicity is one of the main causes of death and injury in fires in buildings. Statistics in the UK [1] show that toxic smoke inhalation accounts for about 60% of the total deaths in fires. However, currently there are no regulations that require the toxic emissions from the burning of building to be determined and taken into account. This project tests the fire toxicity of various polymeric materials used in the construction and contents of buildings. Other than gas toxicity, small particle size also a significant fire hazard. This hazard had been studied and measured from a small range of size (5nm).

## 1.1 Fire Statistics

As reported by the recent World Fire Statistics 2018 [2] and reproduced in Table 1.1, in consideration of 53 countries, India gave the highest number in fire deaths from year 2012 to 2016 with the fire death average number per year of 20,668. Russia gave the highest number of fire deaths for year 2016 which was about 50 percent (8,749 deaths) of the total world fire deaths (17,310 deaths), followed by USA with 3,390 deaths and Ukraine with 1,872 deaths. Meanwhile the total fire deaths in Great Britain in 2016 was 367 deaths and in Malaysia was 142 deaths with average number per year 344 and 122 deaths. Figure 1.1 (a) shows the total number of world fires categorised by type of environment in which the fires took place – the biggest fraction, 35.5 percent involved structure fires, 22.1 percent involved grass and forest fires, 13.5 percent involved vehicle fires, highlighting the importance of structural fires. Structural fires are the most hazardous to human life as it is where the highest concentration of people.

In the last few decades, the development in the fire safety research has led to the growth of fire toxicological studies. Before that, the well-known fire hazards were limited to thermal hazards only [3]. Fire statistics now show that the main cause of fire deaths is by smoke inhalation, not by heat burns.

In Great Britain the cause of death in fires has been attributed mainly the effects of smoke typically 40% due to “smoke” and another 20% due to the combination of “smoke and heat” with only 20% attributed to “heat” alone (the balance being “unspecified” or “other”). The 2013/14 statistics [8] are typical of these with three

main categories being 41, 20 and 20 % respectively. The most recent (2018/19) breakdown [9], is shown in Fig. 1.1 (b).

**Table 1.1** Trends in fire deaths in the countries of the World in 2012-2016 [2].

| № | Country | Population, thous. inh. | Number of fire deaths | | | | | Average number per | | |
|---|---|---|---|---|---|---|---|---|---|---|
| | | | 2012 | 2013 | 2014 | 2015 | 2016 | year | 100,000 inh. | 100 fires |
| № | Страна | Население, тыс. чел. | Число погибших | | | | | Среднее число | | |
| | | | 2012 | 2013 | 2014 | 2015 | 2016 | в год | на 100 тыс.чел. | на 100 пожаров |
| | Staat | Einwohner in 1.000 | Anzahl der Brandtoten | | | | | Mittelwert | | |
| | | | 2012 | 2013 | 2014 | 2015 | 2016 | je Jahr | je 100.000 Einw. | je 100 Brände |
| 1 | India | 1 267 500 | 23 281 | 22 177 | 19 513 | 17 700 | - | 20 668 | 1.6 | - |
| 2 | USA | 323 128 | 2 855 | 3 420 | 3 275 | 3 280 | 3390 | 3 244 | 1.0 | 0.2 |
| 3 | Bangladesh | 154 331 | 210 | 161 | 70 | 68 | - | 127 | 0.1 | 0.7 |
| 4 | Russia | 146 270 | 11 652 | 10 601 | 10 138 | 9 405 | 8749 | 10 109 | 6.9 | 6.7 |
| 5 | Japan | 128 130 | 1 721 | 1 625 | 1 678 | 1 563 | - | 1 647 | 1.3 | 3.8 |
| 6 | Vietnam | 93 000 | 78 | 45 | 90 | 62 | 98 | 75 | 0.1 | 3.0 |
| 7 | Germany | 82 218 | 384 | 439 | 372 | 367 | - | 391 | 0.5 | 0.2 |
| 8 | Thailand | 70 498 | 20 | 110 | - | - | - | 65 | 0.1 | - |
| 9 | France | 66 628 | 362 | 321 | 280 | 335 | 289 | 317 | 0.5 | 0.1 |
| 10 | Great Britain | 63 786 | 380 | 350 | 322 | 325 | | 344 | 0.5 | 0.2 |
| 11 | Italy | 61 000 | 258 | 196 | 141 | 222 | 295 | 222 | 0.4 | 0.1 |
| 12 | Myanmar | 51 486 | 184 | 83 | 60 | - | - | 109 | 0.2 | 7.2 |
| 13 | Spain | 47 079 | 170 | 132 | 162 | 143 | 175 | 156 | 0.3 | 0.1 |
| 14 | Ukraine | 42 673 | 2 751 | 2 494 | 2 246 | 1 948 | 1872 | 2 262 | 5.3 | 3.2 |
| 15 | Poland | 38 454 | 564 | 515 | 493 | 512 | - | 521 | 1.4 | 0.3 |
| 16 | Canada | 35 544 | 149 | 141 | 150 | - | - | 147 | 0.4 | 0.4 |
| 17 | Malaysia | 31 800 | 98 | 72 | 139 | 158 | 142 | 122 | 0.4 | 0.3 |
| 18 | Nepal | 30 430 | 77 | 59 | 67 | - | - | 68 | 0.2 | 6.8 |
| 19 | Taiwan | 23 069 | 142 | 92 | 124 | 117 | 169 | 129 | 0.6 | 8.0 |
| 20 | Romania | 20 121 | 222 | - | - | 646 | 258 | 375 | 1.9 | 1.2 |
| 21 | Kazachstan | 17 500 | 518 | 455 | 401 | 386 | 371 | 426 | 2.4 | 2.9 |
| 22 | Netherlands | 16 979 | - | - | 75 | 81 | 42 | 66 | 0.4 | 0.1 |
| 23 | Greece | 10 788 | 49 | 33 | - | - | - | 41 | 0.4 | 0.1 |
| 24 | Belgium | 10 700 | 70 | 48 | - | - | - | 59 | 0.6 | 0.3 |
| 25 | Czech Republic | 10 579 | 125 | 111 | 114 | 115 | 124 | 118 | 1.1 | 0.6 |
| 26 | Sweden | 9 851 | 103 | 96 | - | 110 | - | 103 | 1.0 | 0.4 |
| 27 | Hungary | 9 830 | 140 | 112 | 94 | 108 | 114 | 114 | 1.2 | 0.5 |
| 28 | Jordan | 9 700 | 42 | 35 | 35 | 52 | 28 | 38 | 0.4 | 0.1 |
| 29 | Belarus | 9 505 | 927 | 783 | 737 | 578 | 538 | 713 | 7.5 | 5.7 |
| 30 | Austria | 8 544 | 30 | 20 | - | - | - | 25 | 0.3 | 0.1 |
| 31 | Israel | 8 300 | - | - | - | - | 19 | 19 | 0.2 | 0.2 |
| 32 | Serbia | 7 187 | - | 62 | 73 | - | - | 68 | 0.9 | 0.1 |
| 33 | Bulgaria | 7 154 | 53 | 106 | 103 | 109 | - | 93 | 1.3 | 0.3 |
| 34 | Singapore | 5 800 | 1 | 4 | - | - | 1 | 2 | 0.0 | 0.0 |
| 35 | Denmark | 5 710 | 65 | 70 | 84 | 68 | 52 | 68 | 1.2 | 0.5 |
| 36 | Kyrgyzstan | 5 522 | 90 | 80 | 80 | 48 | 80 | 76 | 1.4 | 1.9 |
| 37 | Finland | 5 463 | 77 | 58 | 86 | 74 | 82 | 75 | 1.4 | 0.6 |
| 38 | Slovakia | 5 412 | 44 | - | - | - | - | 44 | 0.8 | 0.3 |
| 39 | Norway | 5 109 | 40 | 62 | 54 | - | - | 52 | 1.0 | 0.7 |
| 40 | New Zealand | 4 596 | - | - | - | 13 | 19 | 16 | 0.3 | 0.2 |
| 41 | Croatia | 4 290 | 36 | - | 21 | 24 | 22 | 26 | 0.6 | 0.3 |
| 42 | Moldova | 3 553 | 150 | 120 | 118 | 107 | - | 124 | 3.5 | 2.5 |
| 43 | Kuwait | 3 415 | 21 | 17 | 19 | 38 | 50 | 29 | 0.8 | 1.5 |
| 44 | Mongolia | 3 120 | 75 | 53 | 61 | 59 | 60 | 62 | 2.0 | 1.6 |
| 45 | Armenia | 3 017 | - | - | - | - | 32 | 32 | 1.1 | 0.6 |
| 46 | Lithuania | 2 889 | 150 | 160 | 125 | 125 | 101 | 132 | 4.6 | 1.1 |
| 47 | Slovenia | 2 064 | 8 | 0 | 0 | 3 | - | 3 | 0.1 | 0.0 |
| 48 | Qatar | 1 975 | 22 | 4 | 18 | 18 | 1 | 13 | 0.6 | 1.0 |
| 49 | Latvia | 1 969 | 99 | 104 | 94 | 88 | 95 | 96 | 4.9 | 0.9 |
| 50 | Estonia | 1 315 | 54 | 47 | 54 | 50 | 39 | 49 | 3.7 | 0.9 |
| 51 | Cyprus | 858 | 2 | 5 | - | - | - | 4 | 0.4 | 0.0 |
| 52 | Brunei | 430 | 1 | 0 | 7 | 4 | 3 | 3 | 0.7 | 7.4 |
| 53 | Liechtenstein | 37 | 0 | 0 | 0 | 0 | - | 0 | 0.0 | 0.0 |
| **Total/Итого/Gesamt** | | **2 980 306** | **48 550** | **45 678** | **41 773** | **39 109** | **17 310** | **43 883** | **1.5** | **1.3** |

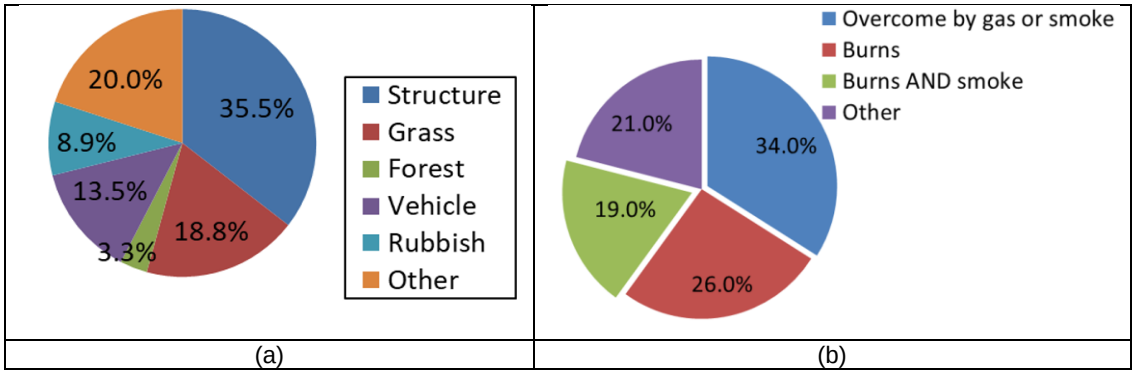


**Figure 1.1** Fire distribution by (a) types in worldwide (2016) [2] and (b) causes of fire deaths in Great Britain for 2018/19 [4].

The causes of fire-related deaths are fairly stable across recent years, except for 2017/18 where the 'other' category was higher (27% compared with a usual range of between 10–20%) due to the Grenfell Tower fire - a large proportion of the fatalities are recorded as 'unspecified' while the public inquiry is still ongoing [9].

Smoke produced in fires normally contains toxic gases, vapour and various sizes of particulates. While the fire deaths are mainly attributed to the effects of smoke in terms of visibility and toxicity and most of previous fire toxicity studies are found to be focused more on the determination of toxic potency of fire effluents based on gas-phase products compared to particle-phase products. the effect of particulates has only recently started receiving attention. There are currently only a limited number of studies [5-7] which focus on the determination of particulate size from fires. As awareness on the health and environmental impact from particles generated in fires has increased, it is vital to conduct research in order to investigate the particulates emissions from the combustion of different materials and their effects on human health other than to be only focused on the toxic gases emission from the fire. This work will present data on both gaseous and particulate yields.

The latest Fire Rescue and Incident Statistics in England for year ending September 2019 [1] as in Figure 1.2, it showed a decrease of 31 percent of fire deaths which gave 248 fire deaths compared with year 2017 which gave 362 fire deaths including 72 from the Grenfell Tower fire. From the data, most of fire deaths involve fires in dwellings and other buildings compared to other locations such as road vehicles and other outdoor. This statistic has raised a critical concern to researchers when knowing that between these fire locations, even number of fires occurred are much lower for building fires than for chimney, road

vehicle and other outdoor fires but it has contributed to a high number of the total fire deaths. This consideration has become one of the reasons why the present work focussing on investigating the toxic gases and particulate emissions from building material fires. Table 1.2 shows a statistic of fire incident number by type comparing the year ending September 2019 with the year ending September 2018, five years previously in 2013/14 and ten years previously (where available) in 2008/09 in Great Britain. Fire related fatalities in dwellings had shown an increase of 9% in 2019 compared to 2018.

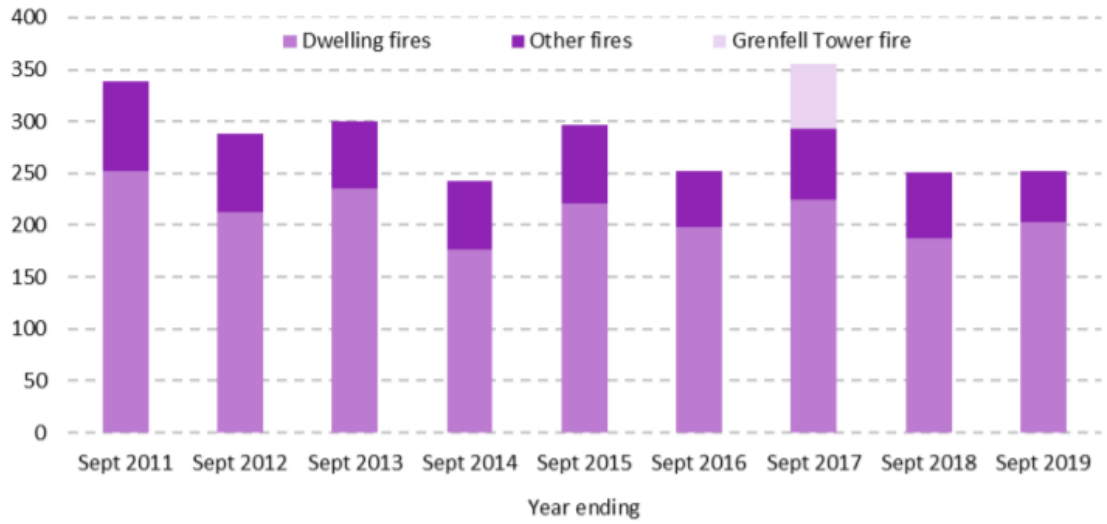


**Figure 1.2** Total fire-related fatalities, England; year ending September 2011 to year ending September 2019 [1]

**Table 1.2** Fire incident types in Great Britain from 2008 to September 2019 [1].

| Incident type | Year ending September 2019 compared with | | |
|---|---|---|---|
| | Year ending September 2018 | 2013/14 | 2008/09 |
| 554,269 **all incidents** | 584,408 -5% | 526,812 +5% | 717,805 -23% |
| | | | |
| 163,039 **fires** | 182,013 -10% | 171,349 -5% | 249,237 -35% |
| 69,534 **primary fires** | 74,730 -7% | 73,230 -5% | 104,348 -33% |
| 28,655 **dwelling fires** | 30,740 -7% | 31,910 -10% | 38,584 -26% |
| 25,755 **accidental dwelling fires** | 27,569 -7% | 28,613 -10% | 32,428 -21% |
| 90,236 **secondary fires** | 103,360 -13% | 92,132 -2% | 136,744 -34% |
| | | | |
| 228,309 **fire false alarms** | 231,856 -2% | 224,119 +2% | 312,914 -27% |
| 162,921 **non-fire incidents** | 170,539 -4% | 131,344 +24% | 155,654 +5% |
| 18,619 **medical incidents** | 25,630 -27% | 13,649 +36% | ..[1] |
| | | | |
| 252 **fire-related fatalities** | 251 = | 278 -9% | 323 -22% |
| 203 **fire-related fatalities in dwellings** | 187 +9% | 217 -6% | 255 -20% |
| 6,980 **non-fatal casualties** | 7,107 -2% | 7,819 -11% | 9,227 -24% |
| 3,083 **non-fatal casualties requiring hospital treatment** | 3,131 -2% | 3,453 -11% | 5,030 -39% |
| 5,164 **non-fatal casualties in dwellings** | 5,284 -2% | 6,118 -16% | 7,455 -31% |

## 1.2 Notable Relevant Fires

Below is a brief summary of some well known fires in which the toxicity of the fire products was the main contributor to the mass fatalities of these fires. A list of other fires relevant to this project, involving cladding materials is also given in Table 1.3.

### 1.2.1 Grenfell Tower

Grenfell Tower fire happened on June 14, 2017 and took away 72 lives including one victim who died in the hospital seven months after the incident and around 70 injured [8]. As generally reported, the fire on this 24-storey residential tower block was started by a malfunctioning fridge-freezer on the fourth floor which then spread rapidly up the building's exterior, bringing fire and smoke to all the residential floors. This fire incident is one example of cladding materials based fire cases. Zinc cladding was initially considered as cladding materials for the building construction of the Grenfell Tower in 2015 but due to cost saving purpose, cladding materials like Reynobond PE and aluminium with plastic filling were finally used. There are many buildings constructed with using flammable cladding materials and many more will be in future if no further objection by rules as safety guidance. In Dubai UAE, more 70% skyscrapers were constructed with flammable cladding materials which was mainly PE. In example, Burj Kalifa Hotel fire started with an explosion and this building were constructed with 100% PE as panel cores of the cladding part. There were many fire cases around the world that involved cladding materials and some examples were listed in Table 1.3.

Whilst currently the cause of death of the 72 people in the building is currently “unspecified” (as discussed above) one of the objectives of the Public Inquiry is the determination of the cause of death. The phase 1 report from the fire Toxicology expert witness Prof. Purser [9] reported that blood toxicology from a limited number of victims (15) showed high concentrations of carboxyl haemoglobin consistent with CO poisoning. He also states that these measurements and and 999 call transcripts indicate that people who died in their flats were overcome by asphyxiant gases (CO and HCN) and died before their bodies were burned. He also identified the building cladding, PVC windows and contents of the apartments as contributors to the fatal toxic emissions.

### 1.2.2 The Rose Park Nursing Home

In 2004, a fire at a residential care home, the Rosepark Care Home, located in Lanarkshire, Scotland resulted in 14 deaths of elderly residents and another four residents injured [10, 11]. Fire safety procedures at this care home were found to be inadequate and deficient. As reported, the staff waited nine minutes before they contacted the fire service [11]. From the accident investigation and reconstruction tests with detailed toxic species concentration measurements [12] concluded that the elderly population of 18 residents were exposed to the same

mix of fire effluents but at different levels of severity depending upon their location. Ten persons in open rooms were exposed to high concentrations, resulting in death at the fire scene within ~8–9 min of the start of the fire. Persons in more protected locations were found alive after much longer exposure times although they some of these subsequently died due to their exposure.

### 1.2.3 Piper Alpha

A very high number of deaths (at least 165 died) caused by the Piper Alpha initial explosion and subsequent fires at North Sea oil platform, near Aberdeen in July 1988 [13]. This incident involved pool and liquid and gas jet fires in multi-level buildings. The cause of the incident was a leak of condensate due to failures of the permit to work system which resulted in a small explosion and subsequent hydrocarbon fires which eventually destroyed the whole platform [14]. Of the diseased, a large number (109) died from smoke inhalation most of them while sheltering in the designated accommodation modules.

### 1.2.4 Kings Cross Fire 1988

31 died in this fire accident at the Kings Cross Railway Station which was started by smokers' matches falling through the gap at the edge of the escalator [15]. The dirt and grease accumulated over months was the fuel ignited by the falling match below the escalator. A flashover through the ticket hall resulting from the pyrolysis of multilayers of paint is thought to have contributed to the dense toxic smoke that was associated with the fire the public inquiry that followed concluded that the toxic smoke contributed to the deaths and recommended the removal of materials known to produce toxic fumes.

**Table 1.3** List of fire incidents involved cladding materials.

| No. | Incident | Location | Date of Event | Number of Deaths | Number of Injuries | Cause of Fires | Information |
|---|---|---|---|---|---|---|---|
| 1 | EPF Building | Jalan Gasing, PJ, Selangor Malaysia, 6 storey building | 13.02.2018 (14:15) | - | - | On the 1st floor due to renovation works at the back of the building | PE cladding |
| 2 | Grenfell Tower | North Kensington, London England, 24 storey flat | 14.06.2017 (00:54) | 72 (2 died in the hospital) | >70 | Fridge-freezer faulty on 4th floor | Cladding materials used in the building were PE filler, PIR foam insulation, PU seal for joints and PVC windows |
| 3 | The Marina Torch Tower | Dubai UAE, 79 storey building | 04.08.2017 (01:00) | - | - | Not known (Suspected caused by a thrown cigarette butt and it landed on a plant at a balcony) | During restorative works |
| 4 | The Marina Torch Tower | Dubai UAE, 79 storey building | 21.02.2015 (02:00) | - | 7 (due to smoke inhalation) | Fire started on the 50th floor | |
| 5 | Burj Khalifa Hotel | Dubai UAE, 63 storey building | 31.12.2015 (New Year's Eve) | | | An explosion in the 39th floor | Fire started with an explosion. Flammable cladding materials (100% PE as panel cores) |
| 6 | Tamweel Residential Tower | Jumeirah Dubai UAE, 34 storey building | 18.11.2012 | - | - | A cigarette butt thrown into a bin | |
| 7 | Sharjah Residential Tower (Tiger 3 Building in Al Taawun) | Sharjah Dubai UAE, 40 storey building | 04.03.2018 (07:03) | - | 7 | Flames allegedly started from a kitchen in an apartment on the 8th floor of the building. | |
| 8 | Al Buteenah Apartment | Al Buteenah, Sharjah Dubai UAE | 12.02.2018 (01:12) | 5 (due to suffocation) | | From investigation, fire might have started from the air-conditioning unit on the 1st floor. | |
| 9 | Al Manama Supermarket | Sharjah Dubai UAE | 14.04.2017 | 2 (died of suffocation) | 5 | | |
| 10 | Nasser Tower | King Faisal Street, Sharjah Dubai UAE, 32 storey building | 01.10.2015 | - | - | | |
| 11 | Hafeet Tower 2 (10 Apartments) | Al Tawun, Sharjah Dubai UAE | 22.04.2013 | | | Fire broke out on the 20th floor. | |
| 12 | 10 Apartments | Al Qasimiya, Sharjah Dubai UAE, 10 storey building | 12.03.2013 | - | - | A blaze gut 10 apartments on the 1st floor. | |

| | | | | | | | |
|---|---|---|---|---|---|---|---|
| 13 | Al Tayer Tower | Al Nahda Park, Sharjah Dubai UAE, 40 storey building | 28.04.2012 | | | | |
| 14 | Al Baker Tower 4 | Al Tawun Mall, Sharjah Dubai UAE | 25.01.2012 | | | The fire was caused by a lit cigarette that was thrown off the balcony from an upper floor and landed on the balcony on the 1st floor. | |
| 15 | A High-rise Residential Tower | Al Nahda, Sharjah Dubai UAE | 08.11.2011 | | 6 | | |
| 16 | Al Wahda Street Apartment | Sharjah Dubai UAE | 08.03.2011 | | | Fire caused by an electric short circuit. | |
| 17 | Bu Tinah Fire | Bu Tinah, Sharjah Dubai UAE, 14 storey building | 06.07.2010 | | | | |
| 18 | Al Buhaira Corniche Apartment | Sharjah Dubai UAE | 04.01.2009 | - | | Fire started from a kitchen and gutted the apartment on the 13th floor. | |
| 19 | Abdullah Khouri Building | Jamal Abdul Nasser Street, Sharjah Dubai UAE | 28.10.2008 | 2 | | Fire on the 4th floor. | |
| 20 | Al Ta'awun Residential Building | Sharjah Dubai UAE | 26.05.2008 | - | | The fire started on the 1st storey and extended to apartments up to the 7th floor. | |
| 21 | Al Tahira Tower | Al Nahda, Sharjah Dubai UAE | 21.07.2007 | 1 | 3 | Fire breaks out in an apartment at the 8th floor. | |
| 22 | Majaz 2 Residential Tower | Sharjah Dubai UAE | 09.04.2007 | | | Fire tore through four floors. | |
| 23 | Al Yasmeen Apartment | Sharjah Dubai UAE | 25.01.2007 | | | | |
| 24 | Dana Tower | Buhairah Corniche, Sharjah Dubai UAE, 47 storey building | 09.01.2007 | | | | |
| 25 | Baku Residence Building | Baku Azerbaijan, 16-level residence building | 19.05.2015 | 15 (toxic smoke inhalation) | 63 | | Flammable Styrofoam facing had been installed on exterior of buildings. Flammable materials used in facade renovation. |
| 26 | Sanghai Fire | Shanghai China, 28 storey high-rise building | 15.11.2010 (14:15) | 58 | >70 | Fire started with construction materials and spread throughout the building. | |
| 27 | The Beijing Television Cultural Center Fire | Beijing China | 09.02.2009 (20:27) | 1 (a fire-fighter) | 7 | A nearby unauthorised fireworks (Chinese New Year Celebration) display caused the fire. | The building was built far less steel than conventional skyscrapers. |

## 1.3 Particulates

Beyond the gaseous toxic emissions fires also emit large amounts of respirable particulates of various sizes which may harm the occupants and fire-fighters in different ways giving either a short term effect or a long term effect. Compared to ultra-fine particles, large particles usually will give a short term or immediate effect to the people who are exposed to them during the fire by causing irritancy to their eyes and skins which will reduce their capability to escape. As a long term effect, generation of nanoparticles (especially particle size below than 50 nm) from the combustion process may cause cancer disease to the people who has exposed to them when being absorbed through the blood line [16, 17].

The main aspects of particle toxicity relate to where they deposit in the respiratory tract, which depends on particle size, and their toxicity, which depends partly on their chemical composition and partly on their physical characteristics. In general large inhalable particles ~100-15 microns diameter, deposit in the upper respiratory tract and airways, If the carry toxic chemicals they cause acute airway inflammation, or following long term exposure (eg smoke from air pollution or tobbaco) chronic obstructive lung disease and lung cancer. Smaller particles ~0.5-5 microns diameter penetrate into the alveolar region of the lung and can cause acute lung inflammation and oedema a few hours after exposure during a fire, which can be fatal. Ultrafine and nano-particles may cause acute lung inflammation or emphysema but also cross into the blood stream where they can cause several effects depending on their chemistry and physical characteristics. These effects include polymer fume fever, cardiovascular disease (including heart attacks), and carcinogenicity.

Smaller particles can penetrate into the blood system easier than larger particles. These nanoparticles may act as transporters of absorbed and adsorbed toxic compounds (VOC or aerosols) into the lungs the blood stream and vital organs. Polycyclic aromatic hydrocarbons (PAH) such as Benzene and Naphthalene are the example of toxic compounds that may cause the cancer decease to the humans when they breathe in these particles during the fire. In 2014, there was a fire death case which was due to cancer decease where three fire fighters died on the same day after 13 years giving service as responders in the fire incident of the World Trade Centre, USA because of their direct exposure to the toxic species and particulates [17]. It is very important to do further investigations on the particle size and particle distribution from fires in order to be able to control

and prevent this kind of hazard from harming the people who are directly exposed.

Measurement of particulate yields and characterisation of particle size distribution is an important objective of this project.

## 1.4 Legislation

Most of fire deaths are generally involved in building fires. Building fire cases have involved various kinds of building structures such domestic or private home fires, high rise living accommodation fires, commercial and industrial building fires, public place building fires and also care centre fires.

There are various types of combustible materials used in building construction. Wood is the most common building material which is widely used compared to other materials like polymers. Due to an increase in demand for synthetic materials, cost savings with an advanced industrial production process, these synthetic materials have become a favourable option by the contractors and the end users. Even furniture, tools and small appliances are widely made by the synthetic materials.

Combustible building construction materials mostly used is wood, only 20 percent usage involved other materials which are mainly polymers. Polymer fires may produce gases which are more toxic than the wood fires depending to the type of polymer burnt, in example Polyisocyanurate (PIR) based materials will produce Hydrogen cyanide (HCN) which is toxic even at low concentration level. PVC based materials will produce irritant gases that can cause irritancy effects when burned which may impair the people who exposed to it from escape during the fire event. As for today, there is no regulation yet found to stop of using PVC or other harmful polymers in buildings.

The British standards for toxicity provide a guidance for the escape/safety of occupants where there is stated that there must be enough time to reach a place of safety without any harm [18-20]. From the existing standards, regarding the toxicity, only smoke obscuration is mentioned and the illustration of smoke alarms [18]. Smoke spread from the origin, hot gas layer and smoke optical density are the main parameters related to the application of fire safety engineering [19]. Although there are tenability limits defined in terms of exposure to toxic and irritants fire gases there is legal requirement to control the use of such materials based on their toxic yields in fire. The only control that may

translate to an indirect control of toxicity is the visibility requirement for safe escape and by controls of reaction-to-fire properties of products [20].

## 1.5 General Research Aims

In overall, the present work mainly aims to highlight and investigate the toxicity dangers of various electrical cables and polymers sold commercially for buildings using two different test methods, an existing modified Cone Calorimeter and a new developed Purser Furnace System with attachment to several external analysers such as Fourier Transform Infrared Spectroscopy (FTIR), Oxygen Analyser, Particle Sizer (DMS500) and Smoke Meter. The FTIR and Oxygen analyser were used to measure the toxic gases. For measurement of the particulate sizes, a particle size equipment called the Cambustion DMS500 was used. Smoke meter was also used to measure soot mass collected on the placed filter papers. Series of fire tests were conducted under different realistic fire conditions from well to under-ventilated fires. More than 40 polymers were burned and tested including the electrical cables. General research objectives are as follow:

a) Develop a methodology for the analysis of toxic gases and particulates in the Cone Calorimeter and the steady state tube furnace.

b) Design, construct and commissioning the new developed Purser Furnace System.

c) Provide data of combustion and fire toxicity properties such as heat release rate, equivalence ratio, mass loss rate, toxic gas concentration, total toxicity, major gas contribution, gas and particulate yields and particle size and number distributions from polymer fires.

d) Compare the results from both Cone Calorimeter and Purser Furnace methods.

# Chapter 2
# Literature Review

## 2.1 Toxic Gases and Particulate Emissions from Fires

The most common toxic component in most fire gases are Carbon monoxide (CO) yields. CO is normally produced from an incomplete combustion of the fuel, by low temperatures, flame quenching, or under-ventilation [21]. Exposure to asphyxiant gases such as CO and Hydrogen cyanide (HCN) primarily will cause incapacitation or loss of consciousness, then death. Irritant gases may cause immediate incapacitation mainly by effects on the eyes and upper respiratory tract, and longer term damage deeper in the lung. Toxic gases can be divided to two main groups, Asphyxiants and Irritants and the List of toxic gases is shown in the following Table 2.1. Henceforth the effects of toxic gases to human health is included in Table 2.2.

**Table 2.1** Asphyxiant and irritant gases [22, 23].

| **Asphyxiants** | **Irritants** | | |
|---|---|---|---|
| | **Carcinogens** | **Acidic gases** | **Other organic irritants** |
| Carbon dioxide $CO_2$ | Formaldehyde $CH_2O$ | Formic acid $CH_2O_2$ | Acrolein $C_3H_4O$ |
| Carbon monoxide CO | Benzene $C_6H_6$ | Nitrogen dioxide $NO_2$ | Ammonia $NH_3$ |
| Hydrogen cyanide HCN | | Acetic acid $C_2H_4O_2$ | Acetaldehyde |
| Ambient $O_2$ reduction | | Sulphur dioxide $SO_2$ | Crotonaldehyde |
| | | Hydrogen chloride HCl | Styrene |
| | | Hydrogen fluoride HF | Methyl styrene |
| | | Hydrogen bromide HBr | Phenol |
| | | | Fine particulates |

Nitrogen containing fuels typically would produce nitrogen based species like HCN, NO, $NO_2$, $NH_3$ etc when burned. However, in the present work, some fire tests that burning none nitrogen containing fuels had also produced these nitrogen based species as the main products. Referring to the work by Marro et al [24] as shown in the Figure 2.1, this condition could happen due to a chemical reaction between the fuels with the Nitrogen ($N_2$) from the air.

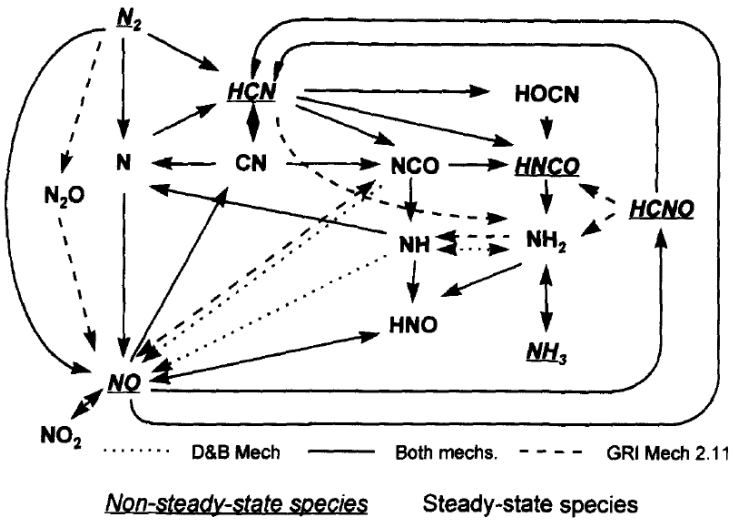


**Figure 2.1** Reaction path to formation Nitrogen based species from the reaction with the Nitrogen from the air in fires [24].

**Table 2.2** Toxic gases and their effects to human health.

| Toxic gases | Molecular Formula | Boiling point (°C) | Melting point (°C) | Molar mass (g/mol) | Density ($kg/m^3$) | Descriptions | Exposure effects to the humans |
|---|---|---|---|---|---|---|---|
| Carbon dioxide | $CO_2$ | -78.5 | -56.6 | 44.01 | 1.98 | A colorless and odorless gas vital to life on Earth | High concentrations can displace oxygen in air and cause suffocation. May cause frostbite. |
| Nitrogen | $N_2$ | -195.8 | -210.0 | | 1.25 | The lightest pnictogen and at room temperature, it is a transparent, odorless diatomic gas | Nitrogen is safe to breathe only when mixed with the appropriate amount of oxygen. Fashioning of nitro amines, which are known as one of the most common causes of cancer (nitrates and nitrites). |
| Propane | $C_3H_8$ | -42.0 | -188.0 | 44.10 | 2.01 | A gas, at standard temperature and pressure, but compressible to a transportable liquid | High concentrations can displace oxygen in air and cause suffocation; headache, nausea, dizziness, drowsiness and confusion. May cause frostbite. |
| Carbon monoxide | CO | -191.5 | -205.0 | 28.01 | 1.14 | A colorless, odorless and tasteless gas that is slightly less dense than air. It is toxic to hemoglobic animals when concentrations above 35 ppm | Breathing CO can cause headache, dizziness, vomiting, and nausea. If CO levels are high enough, you may become unconscious or die. Exposure to moderate and high levels of CO over long periods of time has also been linked with increased risk of heart disease. |
| Hydrogen cyanide | HCN | 25.6 | -13.4 | 27.03 | 687.00 | A colorless, extremely poisonous liquid that boils slightly above room temperature, at 25.6 °C | Headache, drowsiness, vertigo, weak and rapid pulse, deep and rapid breathing, a bright-red color in the face, nausea and vomiting. Follow with convulsions, dilated pupils, clammy skin, a weaker and more rapid pulse and slower, shallower breathing. |
| Cyanogen chloride | CNCl | 13.0 | | 61.46 | 1190.00 | An inorganic compound, linear, triatomic pseudohalogen, easily condensed colorless gas | Particularly affecting those organ systems most sensitive to low oxygen levels: the central nervous system (brain), the cardiovascular system (heart and blood vessels), and the pulmonary system (lungs). It has strong irritant and choking effects, can be rapidly fatal. |
| Hydrogen sulfide | $H_2S$ | -60.0 | -82.0 | 34.08 | 1.36 | A colorless gas with the characteristic foul odor of rotten eggs; it is heavier than air, very poisonous, corrosive, flammable, and explosive | Prolonged exposure may cause nausea, tearing of the eyes, headaches. Airway problems (bronchial constriction) in some asthma patients. Possible fatigue, loss of appetite, irritability, poor memory, dizziness and death. |
| Ammonia | $NH_3$ | -33.3 | -77.7 | 17.03 | 0.73 | A colourless gas with a characteristic pungent smell | High concentrations exposure may cause immediate burning of the nose, throat and respiratory tract. This can cause bronchiolar and alveolar edema, and airway destruction resulting in respiratory distress or failure. Inhalation of lower concentrations can cause coughing, and nose and throat irritation. |

| | | | | | | | |
|---|---|---|---|---|---|---|---|
| Bromine (vapor, Br2) | Br, $Br_2$ | 58.8 | -7.2 | | 3102.80 | A halogen, fuming red-brown liquid at room temperature, corrosive and toxic | Malfunctioning of the nervous system, stomach and gastrointestinal, disturbances in genetic materials, cause damage to organs such as liver, kidneys, lungs and milt, can even cause cancer. |
| Chlorine | Cl | -34.0 | -101.5 | | 3.20 | The second lightest halogen | The effects primarily due to its corrosive properties. May cause eye and skin irritation. |
| Formaldehyde | $CH_2O$ | -19.0 | -92.0 | 30.03 | 815.00 | The simplest aldehyde, also known as methanal | Exposure via inhalation are eye, nose, and throat irritation and effects on the nasal cavity. Effects of exposure to high levels of formaldehyde in humans are coughing, wheezing, chest pains, and bronchitis. |
| Hydrogen chloride | HCl | -85.1 | -114.2 | 36.46 | 1.49 | At room temperature, it is a colorless gas, which forms white fumes of hydrochloric acid upon contact with atmospheric humidity | Depending on the concentration, hydrogen chloride can produce from mild irritation to severe burns of the eyes and skin. Long-term exposure to low levels can cause respiratory problems, eye and skin irritation, and discoloration of the teeth. |
| Hydrogen fluoride | HF | 19.5 | -83.6 | 20.01 | 1.15 | A colorless gas or liquid | Can cause severe injury via skin and eye contact, inhalation, or ingestion. It also may cause severe burns to the eyes, which may lead to permanent damage and blindness. |
| Nitric oxide | NO | -152.0 | -164.0 | 30.01 | 1.34 | A mixture or a binary compound of oxygen and nitrogen, a sharp sweet smell, colorless to brown at room temperature | |
| Nitrogen dioxide | $NO_2$ | 21.0 | −11.2 | 46.01 | 2620.00 | A mixture or a binary compound of oxygen and nitrogen, colorless to brown liquid at room temperature, with a strong, harsh odor | Long-term exposure to nitrogen oxides in smog can trigger serious respiratory problems, including damage to lung tissue and reduction in lung function. Exposure to low levels of nitrogen oxides in smog can irritate the eyes, nose, throat, and lungs. It can cause coughing, shortness of breath, fatigue, and nausea. Acute exposure to higher concentrations can cause lung oedema and death. |
| Nitrous oxide | $N_2O$ | -88.5 | -90.9 | 44.01 | 1.98 | A mixture or a binary compound of oxygen and nitrogen | |
| Nitrogen pentoxide | $NO_5$ | | | | | A mixture or a binary compound of oxygen and nitrogen | |
| Dinitrogen pentoxide | $N_2O_5$ | 47.0 | 41.0 | 108.01 | 1640.00 | A mixture or a binary compound of oxygen and nitrogen | |
| Ozone | $O_3$ | -112.0 | -192.2 | 48.00 | 2.14 | A pale blue gas with a distinctively pungent smell | Chronic effects of ozone on human health are incidence of asthma, a decreased lung function growth, lung cancer and total mortality. |
| Phosgene | $COCl_2$ | 8.3 | -118.0 | 98.92 | 4.25 | A colorless gas gained infamy as a chemical weapon | Extremely toxic by acute (short-term) inhalation exposure. Severe respiratory effects, including pulmonary edema, pulmonary emphysema, and death. Severe ocular irritation and dermal burns may result following eye or skin exposure. |
| Phosphine | $PH_3$ | -87.7 | -132.8 | 34.00 | 1.38 | A colorless, flammable, toxic gas and odorless | |

| | | | | | | | |
|---|---|---|---|---|---|---|---|
| Diphosphane | P2H4 | 65.2 | -99.0 | 65.98 | | A colorless liquid with unpleasant odor like garlic or rotting fish | Severe lung irritation, difficulty breathing or shortness of breath (dyspnea) and accumulation of fluid in the lungs (pulmonary edema), and death. |
| Sulfur dioxide | $SO_2$ | -10.0 | -72.0 | 64.07 | 2.63 | At standard atmosphere, it is a toxic gas with a pungent, irritating smel | It can irritate the respiratory system. Exposure to high concentrations for short periods of time can constrict the bronchi and increase mucous flow, making breathing difficult. It can also aggravate existing heart and lung diseases. |
| Sulfuric acid | $H_2SO_4$ | 337.0 | 10.0 | 98.079 | 1840.00 | A highly corrosive strong mineral acid, pungent-ethereal, colorless to slightly yellow viscous liquid | It cause direct local effects on the skin, eyes, and respiratory and gastrointestinal tracts when there is direct exposure to sufficient concentrations. It also can cause severe skin burns, it can burn the eyes, burn holes in the stomach if swallowed, irritate the nose and throat, and cause difficulties breathing if inhaled. |
| Sulfur trioxide | $SO_3$ | 44.9 | 16.9 | 80.07 | 1.92 | A significant pollutant, being the primary agent in acid rain | |
| Acrolein | $C_3H_4O$ | 53.0 | -88.0 | 56.06 | 839.00 | The simplest unsaturated aldehyde, colourless liquid with a piercing, disagreeable, acrid smell, burnt fat smell (caused by the burned glycerol to form acrolein) | May cause eye, nasal and respiratory tract irritations in low level exposure |
| Benzene | $C_6H_6$ | 80.1 | 5.5 | 78.11 | 876 | Composed of 6 carbon atoms joined in a ring with 1 hydrogen atom attached to each | Can cause cancer and aplastic anaemia (a risk factor for acute nonlymphocytic leukemia). |
| Acetaldehyde | $C_2H_4O$ | 20.2 | -123.5 | 44.05256 | 788 | An organic chemical compound | Can cause significant damage to the liver where the bulk of alcohol metabolism occurs. |
| Acetic acid | $C_2H_4O_2$ | 118 | | 60.05 | 1050 | A colourless liquid organic compound, called glacial acetic acid when undiluted | Could produce some irritation of eyes, nose, and throat. |
| Styrene | $C_8H_8$ | 145 | -30 | 104.15 | 909 | Also known as ethenylbenzene, vinylbenzene, and phenylethen | Irritation of the skin, eyes, and the upper respiratory tract. Acute exposure may also result in gastrointestinal effects. Chronic exposure affects the central nervous system showing symptoms such as depression, headache, fatigue, weakness, and may cause minor effects on kidney function. |
| Phenol | $C_6H_6O$ | 181.7 | 40.5 | 94.11124 | 1070 | Known as carbolic acid, is an aromatic organic compound | Phenol poisoning can occur by skin absorption, vapor inhalation, or ingestion. May also cause muscle weakness, convulsions, and coma. |
| Toluene | $C_7H_8$ | 110.6 | -95 | 92.14 | 867 | A colorless, water-insoluble liquid with the smell associated with paint thinners | Chronic inhalation exposure may cause irritation of the upper respiratory tract and eyes, sore throat, dizziness, and headache. |
| Formic acid | $CH_2O_2$ | 100.8 | 8.4 | 46.02538 | 1.22 | An important intermediate in chemical synthesis and occurs naturally, most notably in some ants | Can cause chronic respiratory, skin, kidney, liver and eye disease. |
| Acrylonitrile | $C_3H_3N$ | 77 | -84 | 53.06 | 810 | A colorless volatile liquid, consists of a vinyl group linked to a nitrile | Liver damage may possibly occur in high concentrations exposure. |

### 2.1.1 Asphyxiant Gases

Asphyxiant gases which are also known as narcotic or choking gases prevent oxygen uptake by cells which then may lead to loss of consciousness and ultimately death to the people who are exposed to them [25]. In fire gases, Carbon dioxide ($CO_2$) is almost always present at high concentration levels, meanwhile its concentrations in fresh air vary from 300 ppm to 600 ppm depending on location. As one of the asphyxiant gases, $CO_2$ can stimulate the respiration rate, tidal volume and may cause acidosis (increase the blood acidity) when being inhaled by humans. Hence, it will increase their inhalation of oxygen and toxic gases produced by the fire.

Asphyxiants may cause a central nervous system depression by decreasing the supply of oxygen to body tissue where their increasing dose may cause the effects become more severe. In locations remote from the fire source of fire, toxicants such as CO and HCN can be presented in lethal quantities by considering that the oxygen depletion will not be harmful and by assuming that the survival has been prevented from hazards which are caused by the heat and other gases [25, 26].

### 2.1.2 Irritant Gases

Irritant gases can be divided to two different groups which are organic gases and inorganic gases. The organic gases usually contain carbonaceous molecules meanwhile the inorganic gases do not contain any carbon molecules. In the Table 2.1, Formaldehyde is one example of the organic irritant. Other organic irritants are Acrolein, Benzene, Acetaldehyde, Acetic acid, Styrene, Phenol, Toluene, Formic acid, Acrylonitrile, etc.

Each type of toxic gases produced from the combustion process has given different exposure effects to the humans [27-32]. The effects of toxic gases depend on what type of gases the occupants expose to, how much gas they breathe and for how long. In example, Hydrogen chloride (HCl) gas will be intolerable to humans at concentrations above 100 ppm, but will be lethal to rats only at concentrations around 5000 ppm [33] for 30 minutes of exposure. For certain gases, exposure to a high concentration can quickly lead to death.

Exposure to irritant smoke may influence the escape behaviour and walking speed of humans depending to the concentration they are exposed to. At high concentrations, exposure to these irritants may cause incapacitation and may impair their escape capability with the painful, sensory effects on the eyes and

respiratory tract. While at low concentrations, exposure may slow down their evacuation behaviour and can reduce their walking speed [34].

### 2.1.3 Particulates from Smoke

Particles or particulates are one of the components contained in the smoke. They can be unburned, partially burned and completely burned substances which their sizes are too small. Smoke particulates in solid and liquid form (aerosol) may cause smoke obscuration and impede escape. It also poses a major threat to human respiratory system. The smallest (nano particulates) can penetrate through the lung into the blood stream. Larger particles deposit in the respiratory tract at different locations depending on particle size. During inhalation process, air comes in from the nose and the mouth entering the throat and the pharynx (the entrance to the airways, divides into two tubes called the oesophagus and the trachea, which leads down towards the lungs). Contaminated air passes into the trachea (which itself divides into two large tubes, each called a bronchus), then enters a lung before passing through the blood vessels (capillaries). Other than the inhaled oxygen, tiny components such as chemical vapours, gases and mists which are toxic and harmful may reach the alveoli in the lungs and can also pass into the blood and be distributed around the body [16].

Solid dust-like particles or particulate matter less than 2.5 millionths of a metre across ($PM_{2.5}$, 2500 nm) which are produced from the combustion process can cause cancer to the people who are being exposed to them. Cancer-related fire deaths were mostly digestive, oral, respiratory, and urinary cancers [16]. Different size of particulates may affect human health in different ways and levels. Smaller particulates are more harmful than bigger particulates in terms of penetration ability which are easier for them to be absorbed into the blood system through breathing or respiration process. Most researchers stated that particle size below than 1 µm (1000 nm) can cause cancer to the humans [5]. However some of them agreed that the real danger due to cancer might happen when people exposed to the size of particulates smaller than 0.1 µm (100 nm). Whether particulates cause cancer at a particular site depends on two main aspects, the extent to which they reach that site and their toxicity (carcinogenicity). So, particle size is very important because it determines the site of deposition in the respiratory tract. Particles deposit by impaction, sedimentation and diffusion. Larger particles deposit mainly by impaction and sedimentation. So, for example one important site for cigarette smoke (~1 micron) particles is the tracheal bifurcation, where the main bronchi to the two lungs branch. Impaction of tobacco

smoke at this point, combined with the chemical carcinogens in the smoke result in lung cancers often forming at this point.

Ultrafine or nano particles entering the blood stream may be carried to any body organ and cause cancer there if they carry carcinogenic chemicals like PAHs.

Despite the importance of smoke particulates, limited investigation has been conducted with respect to the particle size and distribution, as well as its composition. Therefore, smoke particle analysis is one of the main objectives in this research project.

## 2.2 Causes of Fire Deaths

Following the statistical reviews of fire casualties for several decades in the United Kingdom (UK) and United States of America (USA), the major cause of death for fire victims is the fire toxicity [3]. When fire victims are exposed to fire effluent, the first hazard encountered is commonly smoke, containing toxic gases and particulates [35, 36]. This hazard can cause instant visual obscuration and severe eyes and respiratory tract irritation which may be followed by incapacitation due to continuous exposure. In the early stages of fire, these effects are serious and could be taken into consideration in determining the possibility, speed and efficiency of escape.

It is also important to investigate and to determine the particulate size and its emission from fires in order to understand its effects to the humans in terms of health especially people who are exposed to it directly. There was a case which was related to these effects where three New York firefighters who worked at Ground Zero died of cancer on the same day less than two weeks after the 13$^{th}$ anniversary of the September 11, 2001 terrorist attacks. The first firefighter had colon cancer, the second one had leukaemia and the third one had oesophageal cancer [17]. They had served as first responders at the World Trade Centre in the immediate aftermath of 9/11. Other than the three men, the Fire Department of New York (FDNY) lost 343 firefighters on 9/11 and 89 more since then due to illnesses directly related to contaminated air at Ground Zero.

### 2.2.1 Smoke Inhalation

Most fire deaths are not caused by burns, but by inhalation of smoke and toxic gases [21, 37, 38]. The number of injuries from smoke and toxic fumes have

increased drastically from decades ago with an annual rate about 1000 to more than 6000 [21]. Often smoke incapacities so quickly that people are overcome and cannot reach an otherwise accessible exit. Smoke consists of particles, vapours and toxic gases that can each be lethal in its own way and may impair humans from escape safely during the fire.

Table 2.3 shows the limit concentration values by different toxic assessments provided by different authorities which are LC50, COSHH and AEGLs. LC50 method (BSI, 2016) [39], also expressed as the lethal concentration for 50% of the population to die. For impairment of escape, there is the European standard known as Control of Substances Hazardous to Health (COSHH) for short time exposure of 15 minutes (HSE, 2018) [40]. An equivalent standard is the American Acute Exposure Guideline Limits (AEGL-2) that causes impairment after 10 minutes of exposure (EPA Online, 2018) [41]. In order to quantify the toxicity of each gas measured, toxicity has been expressed in terms of a set of indices calculated by dividing the measured concentration by the toxic limit concentration for each toxicity endpoint (LC50, COSHH and AEGL-2). The index for each gas thereby represents a factor relating the measured concentration to each limit concentration. Where the measured combustion product atmosphere contains a mixture of toxic gases, a simple fractional additive model has been used to express the total toxicity of the mixture as described in Section 3.6.5, Chapter 3.

**Table 2.3** Limit concentration for major toxic species [39-41].

| Toxic Species | Chemical Formula | Limit Concentration Values | | | |
|---|---|---|---|---|---|
| | | $COSHH_{15min}$ | $LC50_{30min}$ | $AEGL\text{-}2_{10min}$ | $AEGL\text{-}3_{30min}$ |
| | | HSE 2018 (EH40/2005) | BSI 2016 | EPA Online (AEGL) | |
| Acetaldehyde | $C_2H_4O$ | 50 | - | 340 | 1100 |
| Acrolein | $C_3H_4O$ | 0.3 | 150 | 0.44 | 2.5 |
| Ammonia | $NH_3$ | 35 | 750 | 220 | 1600 |
| Benzene | $C_6H_6$ | 3 | - | 2000 | 5600 |
| Carbon monoxide | CO | 100 | 5700 | 420 | 600 |
| Formaldehyde | $CH_2O$ | 2 | 750 | 14 | 70 |
| Hydrogen bromide | HBr | 3 | 3800 | 250 | 250 |
| Hydrogen chloride | HCl | 5 | 3800 | 100 | 210 |
| Hydrogen cyanide | HCN | 45 | 165 | 17 | 21 |
| Hydrogen fluoride | HF | 3 | 2900 | 95 | 62 |
| Hydrogen sulfide | $H_2S$ | 10 | - | 41 | 59 |
| Nitrogen dioxide | $NO_2$ | 1 | 170 | 20 | 25 |
| Sulfur dioxide | $SO_2$ | 1 | 1400 | 0.75 | 30 |
| Toluene | $C_7H_8$ | 100 | - | 1400 | 5200 |

As explained earlier, most fire deaths arise from toxic gas inhalation, particularly Carbon monoxide (CO) and Hydrogen cyanide (HCN). Toxic smoke can cause rapid contamination of building spaces which is the main hazard to the building occupants. It also can cause irritancy to them when they are exposed to it and leads to visual obscuration which affects their escape behaviour, slowing travel speeds and impedes escape efficiency [42].

### 2.2.2 Burns (Heat Shock)

The potential effects of radiation exposure is a primary importance in any risk assessment because it presents a major hazard especially when accidental hydrocarbon fires occurred in the open or in large industrial facilities [43]. The most important criteria in assessing the effects of thermal radiation exposure is the thermal dose that is capable of causing particular levels of burn injury, the death risk from different levels of burn injury and how quickly people are assumed to escape from the affected area.

Thermal burns (from fire or flame) can cause an injury at different burn degree depending to how severe and how likely our body or skin has been directly

exposed. The effects of burns may cause fluid loss, electrolyte imbalance and hypovolaemic shock (a condition where the heart is unable to pump enough blood to the body, which may cause many organs to stop working). Heat is also a hazard to the respiratory system, as superheated gases may burn the respiratory tract. When the air is hot enough (~300$^{o}$C), even just one breath can kill [44].

### 2.2.3 Reduction of Oxygen Levels

In addition to producing heat and smoke, fire can incapacitate or kill by reducing oxygen levels, either by consuming the oxygen, or by displacing it with other gases. During the combustion process, oxygen has depleted or reduced when reacting with the fuel to produce the combustion products. When the occupants have exposed to the closed surface area which is containing less oxygen, they will experience a hard breathing condition, hence they will be incapacitated and the chance for them to escape from the affected place is lower. In the air, when oxygen concentration is below tenable levels (~6%), this depletion condition can be lethal to the humans [26].

## 2.3 Fire Stages

Fires can be divided into a number of stages which can be replicated by certain bench-scale fire apparatus such as the Purser furnace (BS 7990 and ISO TS 19700) based on fuel-to-oxygen ratios (equivalence ratio) [33]. Combustion fires produced in a compartment or tube furnace have four different stages and types such as smouldering or non-flaming, well-ventilated flaming (small and early), fully developed or post flashover (large and vitiated) and fully developed (well-ventilated). Figure 2.2 shows an illustration of the different development stages of a compartment fire.

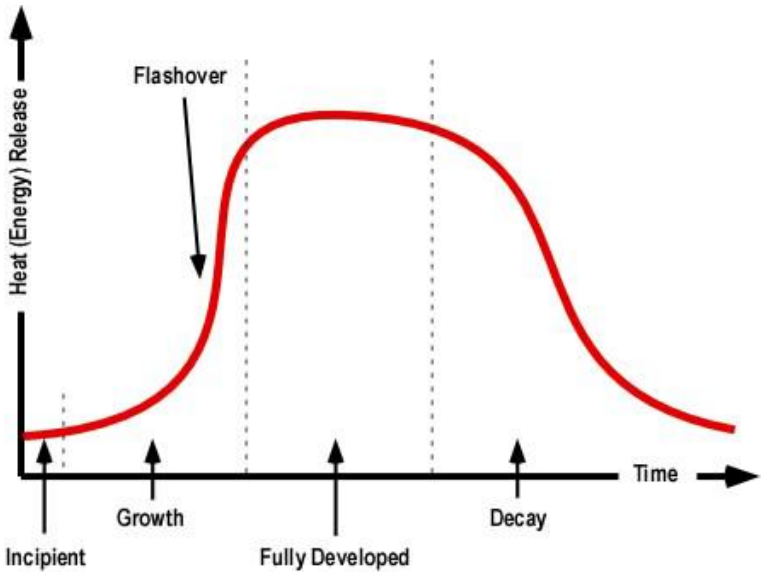


**Figure 2.2** Different development stages of a compartment fire [45].

### 2.3.1 Smouldering Fires (Incipient)

At this early stage, the fire may take a very long time to grow and may extinguish itself without reaching a fully developed state. This stage (non-flaming fire) normally occurred when the amount of fuel used was controlled. This first stage begins when heat, oxygen and a fuel source combine and have a chemical reaction resulting in fire. This is also known as “ignition” and usually represented by a very small fire which often goes out on its own, before the following stages are reached. Recognising a fire in this stage provides the best chance at suppression or escape.

### 2.3.2 Developing Fires (Well-ventilated Flame)

Well-ventilated flaming provides efficient combustion and produces mainly $CO_2$ and water with low yields of all toxic carbon and nitrogen compounds (other than $NO_x$) except for materials that contain halogen compounds [46]. Oxygen amount is in excess and more than sufficient for combustion process of materials in this stage with the phi value (equivalence ratio) is less than 1. A well ventilated flame may grow to a fully developed fire after experiencing the flashover, a rapid transition between the growth period and the fully developed fire stage. Flashover is also known as the transition point from a fuel-controlled fire to a ventilation-controlled fire.

### 2.3.3 Ventilation Controlled Pre-Flashover Fire

The ventilation controlled pre-flashover fire is a fire condition which the most common cause of death in building fires. In an enclosed fire compartment with restricted ventilation (i.e. most occupied buildings), the early well-ventilated stage is followed by a ventilation-controlled stage where the fire becomes under-ventilated due to the restricted ventilation and the equivalence ratio becomes >1. If the level of ventilation is sufficient or increases (for example following window failure or doors being opened) then the fire may grow and proceed to flashover.

### 2.3.4 Fully Developed Fires (Post-Flashover Phase)

When the growth stage has reached its maximum and all combustible materials have been ignited, the fire is considered fully developed. Value of combustion properties such as mass loss rate (MLR), heat release rate (HRR), flame temperature and oxygen depletion are at the highest at this stage.

### 2.3.5 Decay Phase

At this decay stage, the heat release has decreased because the fuel is fully being consumed which then lowering down the surrounding temperature. The fire has turned from a ventilation-controlled fire to a fuel-controlled fire when reaching this phase. This phase is usually the longest stage of a fire, giving a significant decrease in oxygen or fuel, putting an end to the fire. The existence of these non-flaming combustibles can potentially start a new fire if not fully extinguished.

## 2.4 Factors Influence the Emission of Toxic Gases from Fires

Emission factors for toxic gases and particulates depend the initial set on conditions such as primary and secondary air flow (determining ventilation conditions), operating temperatures or irradiance levels, fuel-air ratios and type of test materials (content different composition of components). The toxicity of fire effluents, like flammability is a function of both the material and the fire environment [47]. It is important to relate the toxicity results with the end-use fire situation. Furthermore, different methods used for assessing the fire effluents may also produce inconsistent data because they provide different fire scenarios [48]. Different fire conditions can have a significant effect on the effluent

produced. Smoke and toxic gases generation is markedly dependent upon temperature and oxygen concentration.

### 2.4.1 Equivalence Ratios of Fuel and Air Mixture

The equivalence ratio can be controlled by fixing the fuel (sample mass) and primary air feed rates. It can be calculated by dividing the actual fuel-to-air ratio with the stoichiometric fuel-to-air ratio [6, 25, 33, 36, 37, 49-56]. Equation 1 shows a typical formula which expresses the equivalence ratio.

$$\phi = \frac{\text{actual fuel/air ratio}}{\text{stoichiometric fuel/air ratio}} \qquad (1)$$

For $\phi < 1$, it represents the fuel lean flames, $\phi = 1$ represents the stoichiometric flames and $\phi > 1$ represents the fuel rich flames. The production of CO yield (g/g) increases with the increase of $\phi$ value (from lean to rich condition) which is also proportionate to the oxygen consumption. Oxygen concentrations decrease as $\phi$ increases [56]. CO yield increases with equivalence ratio. The average of typical CO yields obtained are 0.01 g/g at the lean condition, 0.05 at the stoichiometric condition and 0.2 g/g at the rich condition [54, 55]. The yield of other products such as $NO_x$, HCN, organic products and particulates are also expected to increase with equivalence ratio due to more amount of unburnt fuel left at the end of combustion.

Air-fuel ratio (AFR) can be determined through several ways such as a metered method (direct measurements of intake air and the injected fuel by using the measurement devices), a reaction based method and an exhaust emissions based techniques [57-61]. In the present study, the exhaust emissions based air-fuel ratio calculation is used in order to determine the amount of unburnt hydrocarbons from the conducted combustion tests.

The exhaust emissions based techniques had been improved and proposed for accurate determination of AFR which involved exhaust gas emissions analysis [57, 61]. Through this method, atoms balance for carbon (C), hydrogen (H) and oxygen (O) in the internal combustion engines can also be determined. In addition to the application of this method, parameters that may have a direct effect on the AFR calculations, such as the accuracy of the emission analysers, the assumed water-gas shift reaction constant, the humidity and the temperature of the atmospheric air and the inclusion of oxides of nitrogen in the AFR model should be taken into the consideration [57].

### 2.4.2 Variable Ventilation Conditions

Combustion conditions influence the generation of toxic product yields [36]. Fire stages and types can be individually created and replicated through the application of the steady state tube furnace (ISO TS 9700) either in terms of equivalence ratio or $CO_2$/CO ratio in order to measure various product yields.

In actual applications, the room doors normally would be closed and this considers that no ventilation flows in and flows out from the room. In case of a fire accident happened, the concentration of combustion products generated would be much higher and would appear much earlier, even when less amount of combusted material was involved. Any developed fire within an enclosure due to restriction of the ventilation, a higher mass loss rate (MLR) will lead to under-ventilated burning, and contribute higher yields of various toxic products [54].

In order to replicate different ventilation conditions (different fire stages), a fixed rate of sample is driven through the tube furnace (Purser Furnace) or is placed in the compartment of the Cone Calorimeter at a fixed flow of primary air.

### 2.4.3 Type of Test Materials

Every type of material that applied in the buildings will produce a variety of toxic gases when combusted, depends to its content. The toxic hazard produced from fire has increased due to the widespread use of polymers nowadays especially the flame retarded polymers which may produce a violent fire environment [49]. Common type of materials which have been used widely in building construction and its properties such as furniture and accessories are polymers (Polyethylene (LDPE), Polystyrene, Polypropylene, Polyvinyl chloride (PVC)), wool, cotton and wood.

Fluoropolymers especially Polytetrafluoroethylene (PTFE) had been used extensively in the building and cable industries due to their desirable character of having good resistance to fire. Their application became limited because of the concerns over their toxic thermal decomposition products which gave a toxic potency about 1000 times greater and contributed to $LC_{50}$ approximately ten times higher compared to wood and most other materials [62]. In addition, the wide usage of the polymeric materials based cables such as PVC and Polyolefin in building applications cannot be simply ignored because their combustion may result in an effluent with significant yields of toxic gases [54] which contributes to fire hazard. For example, an incapacitating irritant like Hydrogen chloride (HCl) gas that evolved from burning PVC and other Chlorine containing plastics may

reduce the chance and performance of escape by the humans due to its incapacitation effect to them [33].

The synthetic materials commonplace in today's homes produces especially dangerous substances. As a fire grows inside a building, it will often consume most of the available oxygen, slowing the burning process. This causes an incomplete combustion which is resulted in production of toxic gases.

From the research by Stec [26] who presented the results in terms of toxic product yields and predicted fire ratio for seven materials (LDPE, Nylon 6.6, Polystyrene, PVC, medium density fibreboard gas toxicity as a function of equivalence with and without flame retardant and glass reinforced polyester), the results showed that different test materials produced different toxicological significant species. As the result from the study, HCl and HCN were produced as the most toxic species for combustion of PVC and Nylon 6.6 types of material. Meanwhile, in other materials such as LDPE and Polystyrene, CO was the major toxicant observed.

Nitrogen based materials may produce hydrogen cyanide (HCN) during the combustion in fires which is very harmful and toxic to the people. Table 2.4 shows the elemental compositions of the materials and products as tested by the previous researchers [63].

**Table 2.4** Composition of test materials containing nitrogen [63].

| No | Material | Stoichiometric $O_2$ Demand | Elemental composition (%) | | | | | | | |
|---|---|---|---|---|---|---|---|---|---|---|
| | | g/g | C | H | O | N | Cl | Br | P | S |
| 1 | CMHR polyurethane foam - FR | 1.87 | 56.45 | 7.67 | 24.10 | 8.22 | 2.53 | - | - | - |
| 2 | Polyisocyanurate (PIR) rigid foam | 1.87 | 63.50 | 4.98 | 21.80 | 6.15 | 3.56 | - | - | - |
| 3 | Polyamide 6 (PA6) granules | 2.33 | 63.68 | 9.79 | 14.14 | 12.40 | - | - | - | - |
| 4 | MDF board | 1.35 | 47.90 | 6.13 | 41.66 | 3.69 | 0.62 | <0.50 | <0.01 | - |
| 5 | MDF - FR board | 1.25 | 45.10 | 5.77 | 39.22 | 6.73 | - | 2.66 | 0.63 | - |
| 6 | Acrylic / wool / polyester 38 / 38 / 24 boucle mixed fibre fabric | 2.02 | 63.10 | 6.40 | 16.70 | 12.89 | <0.30 | <0.50 | - | 0.94 |
| 7 | Acrylic / wool / polyester 38 / 38 / 24 boucle fabric - FR back-coated | 1.91 | 59.00 | 6.30 | 16.10 | 10.83 | 0.95 | 6.09 | - | 0.76 |
| 8 | Acrylic / cotton / polyester 52 / 31 / 17 velour mixed fibrefabric | 2.00 | 64.40 | 6.39 | 18.45 | 11.55 | <0.30 | <0.50 | - | - |
| 9 | Polyacrylonitrile (>85%) Jersey fabric | 2.33 | 65.62 | 5.71 | - | 23.24 | - | - | - | - |
| 10 | Plywood | 1.24 | 49.50 | 6.10 | 43.98 | 0.32 | - | - | - | - |

## 2.5 Review of Fire Toxicity Test Methods

To the author's knowledge, there are many fire toxicity studies which use different assessment methods such as closed cabinet tests, flow through tests and mathematical modelling, testing various types of material under different fire conditions [5, 6, 21, 25, 33-37, 42, 46-48, 50-56, 62-81]. However, only a few [5, 6] have focused on the determination of particulate size from the fire smokes and lack of particle size data is found as reference to other people. Most of previous studies focus on the measurement of toxic gases produced from the fire and their toxicity effects to the human behaviours during the fire based on the incapacitation effects of exposure and lethal concentration (see Table 2.5). Some put an interest on investigating and determining the combustion properties such as heat release rate and mass loss rate of various burning materials in order to control the fire hazards.

For present work, the fire toxicity studies were conducted using two different methods such as the Purser furnace and the Cone Calorimeter. Both methods are expected to give comparable results for a better fire toxicity analysis under various ventilation conditions. Modifications were done when required to this equipment and research implementation method in order to achieve the research objectives especially in measuring the particles size of the fire smoke and additional equipment or analysers were also used when necessary. It is important to highlight again that there are only sparse studies which focus on the determination of the particulate size from fires. In addition to this, the present study will contribute valuable results which will provide useful data for other researches. List of references related to the previous fire toxicity studies has been summarised in Table 2.5.

### 2.5.1 Using the Purser Furnace System

The Purser Furnace has been developed to widen the range of fire types amenable to laboratory-scale investigation. This furnace is used to study a wide variety of fire conditions (as detailed in ISO 9122) including unstable, vitiated combustion conditions. It can create steady-state combustion conditions and these conditions can be set to control the experiment with reasonable accuracy [56]. For fire toxicity studies, in order to investigate the fire behaviour, this equipment is useful and suitable due its ability to provide a constant combustion conditions during the test. It has been used extensively by the researchers [33,

36, 37, 49-52, 69, 76, 82] and is also newly designed and developed for the usage of the present study.

### 2.5.2 Using the Cone Calorimeter Method

This method is one of the tools of choice for determining the fire properties of products and materials. The Cone Calorimeter has been developed for the studies of fire hazards and as one of effective measurement techniques for the measurement of heat, smoke and toxic gas emissions from fires. It is also the first commercially available calorimeter to incorporate mass loss rate measurement [78]. The basic design and features of this equipment has been described in previous publications [83-85]. The standard operating procedures of this Cone Calorimeter method has been published by the International Organization for Standardization (ISO) as DIS 5660 [86] and also has been adopted by the American Society for Standards and Materials (ASTM). The toxic potency from fire smokes [78, 79, 87] and the heat release rate based on oxygen consumption from burning combustibles in fires has been investigated extensively using this method [81, 83, 88].

**Table 2.5** List of references related to the previous fire toxicity studies.

| Journal Title | Authors | Year | Descriptions | Test Method | Test Materials | Conclusions |
|---|---|---|---|---|---|---|
| Detailed determination of smoke gas contents using a small-scale controlled equivalence ratio tube furnace method [64]. | Blomqvist P., Hertzberg T., Tuovinen H., Arrhenius K. & Rosell L. | 2007 | Determination of yields of fire generated products at defined combustion conditions. The analysis also includes the measurement of the size, distribution and composition of fire generated particles for some selected materials. | Tube furnace (BS 7990:2003). | Solid wood, flexible polyurethane (PUR), fire-retarded rigid PUR, a polyvinyl chloride (PVC) carpet, a high-performance data cable with fluorine-containing polymer matrix, a PVC-based cable sheathing material and fire-retarded polyethylene cable insulation material. | This new furnace method is able to replicate the defined combustion conditions. For both fire stages (well ventilated and vitiated conditions), the quantification of toxic inorganic gases produced and the determination of typical yields from burning of various materials were successful regarding repeatability and stability. |
| Experimental parameters affecting the performance of the Purser furnace: a laboratory-scale experiment for a range of controlled real fire conditions [56]. | Carman J.M., Purser D.A., Hull T.R., Price D. & Milnes G.J. | 2000 | Assessment of the experimental paramaters that affect the performance of the Purser furnace where the yields of toxic combustion products from the burning materials are determined under different stages and types of fire, eg fully ventilated, vitiated. | Salford's Purser furnace (DIN 53436). | Low-density polyethylene (LDPE), poly methyl methacrylate (PMMA), polystyrene (PS), polypropylene (PP) & EVA. | The Purser furnace does create steady-state combustion conditions and it can be used to study various fire conditions. Recommendations to be followed are the sample feed-rate should be at least 1 $gmin^{-1}$ and the dilution air should be at least equal to the primary air flow rate. |
| Study on the real-time size distribution of smoke particles for each fire stage by using a steady state tube furnace method [6]. | Goo J. | 2015 | Measurement of size distributions of smoke particles by using an electric low-pressure impactor ($ELPI^{+}$) and their morphologies were analyzed using transmission electron microscopy (TEM). | A steady state tube furnace method ISO/TS 19700. | Wood and polypropylene (PP). | The number concentration distribution and shape of smoke particles differ considerably between fire stages and combustible materials. It is concluded that the different particle characteristics in terms of shape and smoke yield for wood and PP can be attributed to their different physical properties. |

| | | | | | | |
|---|---|---|---|---|---|---|
| Irritancy of the smoke (non-flaming mode) from materials used for coating wire and cable products, both in the presence and absence of halogens in their chemical composition [65]. | Hirschler M.M. & Purser D.A. | 1993 | Coating materials (PVC & XLPE) are assessed for their smoke irritancy under non-flaming conditions by using the respiratory depression method ($RD_{50}$). | Tube furnace (DIN 53 436 combustion tube). | Coating/insulation materials: PVC and XLPE. Animals (mouse) are exposed to the smokes for 10 min. | Result shows little difference between the irritancy of both PVC (containing halogens) and XLPE (no halogens) smokes even it is expected initially that PVC smoke would be much more irritating than XLPE smoke. This irritancy may be caused by long-lived free radicals in the XLPE smoke because PVC smoke does not contain them. |
| Continued:- | | | | | | |
| **Journal Title** | **Authors** | **Year** | **Descriptions** | **Test Method** | **Test Materials** | **Conclusions** |
| Combustion toxicity of fire retarded EVA [53]. | Hull T.R., Quinn R.E., Areri I.G. & Purser D.A. | 2002 | Combustion toxicity is investigated under steady state flaming combustion at equivalence ratios varying from 0.5 to 1.5 by driving the polymer materials through the furnace at 750ºC. 30% of EVA and 70% fire retarded composites, containing fire retarded fillers. | A Purser furnace. | Ethylene-vinyl acetate copolymer (EVA) with and without fire retardant fillers. | The yields of CO per g of polymer from the EVA-fire retardant composite samples show similar yields of CO under ventilated conditions to the pure EVA. Under the most toxic fuel rich conditions, the EVA-fire retardant gives higher CO yields than the base polymer. |
| Acidity, Toxicity And European Cable Classification [66]. | Hull T.R., Lebek K. & Robinson J.E. | 2006 | Fire effluent toxicity assessments of 10 cables are conducted using bench scale apparatus and correlated with acid gas data. 5 cables tested in the current study are also compared with previous published large scale toxicity data. | Purser furnace (EN 50267-2-3). | European cables (ten different cables). | Even CO is a significant contributor to fire effluent toxicity, the presence of acid gases is the major differentiator between the different types of cables tested. Low measured conductivity represents low toxicity and gives low FED. FED increases from smouldering to well-ventilated and to developed fire. |
| Polymers and Fire [89]. | Hull T.R. & Stec A.A. | 2009 | Comparison between the natural polymers and the synthetic polymers is discussed. Advancement of manufacturing technology causes a rapid shift of the polymer usage (from natural to synthetic). | - | - | Fire stages: smouldering (no flaming/induction period), ignition (when polymer surface is 200ºC hotter), well-ventilated (rise in temperature), low/controlled ventilation (800-1000ºC) and decay (fuel is fully consumed). |

| | | | | | | |
|---|---|---|---|---|---|---|
| Development of Standards for Assessment of Fire Effluent Toxicity and their Application to Cable Installations [54]. | Hull T.R., Stec A.A. & Robinson J. | 2008 | The assessment of fire effluent toxicity from the combustion based cables. Fire hazard is provided as Hazard = Toxicity x Yield x Mass loss rate. | The steady state tube furnace (Purser furnace). | Polyolefin (PO@LSZH type), EVA-ATH, NHMH, NHXMH, Cat 5e, etc. | If the ventilation becomes restricted, as it does in any developed fire within an enclosure, then a higher mass loss rate will lead to under-ventilated burning, and higher yields of many toxic products. |
| Comparison of toxic product yields of burning cables in bench and large-scale experiments [55]. | Hull T.R., Lebek K., Pezzani M. & Messa S. | 2008 | Determination of toxic product yields from five commercial cables and to establish a relationship by comparing the results between bench-scale (SSTF & a static tube furnace NF X 70-100 method) and large-scale (physical fire model prEN50399-2-2 test) toxic product yields for the burning cables. | A steady state tube furnace (SSTF) method (IEC 60695-7-50, Purser furnace). | PVC, LSZH (low-smoke zero-halogen), fire retarded (ethylene-vinyl acetate copolymer plus aluminium hydroxide, ATH) cables. | Cables have been formulated for low flammability and therefore do not burn consitently. The tube furnace burns the cable completely, whereas the large-scale test produces a combination effluent of flame spread and toxic product yields which both are fire scenario dependant. |
| Continued:- | | | | | | |
| **Journal Title** | **Authors** | **Year** | **Descriptions** | **Test Method** | **Test Materials** | **Conclusions** |
| Hydrogen chloride in fires [33]. | Hull T.R., Stec A.A. & Paul K.T. | 2008 | Fire effluent toxicity is compared between ISO 13571:2007 and ISO 13344 based on rat lethality by considering both asphyxiant and irritant gases which influence the safe escape performance. | Purser furnace ISO TS 19700 and Acid Gas test EN 50297-2-3:1998. | Unplasticised PVC, plasticized PVC cable and LDPE. | HCl concentrations above 100 ppm are intolerable, but only at HCl concentrations around 5000 ppm are lethal to rats. The result also shows that HCl gives the large contribution to the fire hazard. |
| Bench-scale assessment of combustion toxicity—A critical analysis of current protocols [48]. | Hull T.R. & Paul K.T. | 2007 | Review papers related to current fire effluent toxicity tests which use different test methods. | Closed cabinet tests and flow through tests (simple tube furnace, SSTF & other flow-through methods). | - | Different methods give apparently inconsistent data because they represent different fire scenarios. There is an improvement on the traditional methods towards fire risk assessments and engineering solutions. Essential elements such as reliable data of heat release, fire effluent toxicity and smoke generation are useful for such assessment. |
| Factors affecting the combustion toxicity of polymeric materials [47]. | Hull T.R., Stec A.A., Lebek K. & Price D. | 2007 | Different test methods are used in order to determine the factors affecting the fire toxicity of the burning polymers under various fire scenarios. | Simple tube furnace (NF X 70-100) & SSTF (Purser). | Polymeric materials (LDPE, PS, nylon 6.6 (PA 6.6) & PVC). | In many cases, CO which is assumed to be the most significant toxic gas becomes less importance than HCl and HCN, when present. |

| | | | | | | |
|---|---|---|---|---|---|---|
| Prediction of CO evolution from small-scale polymer fires [67]. | Hull T.R., Carman J.M. & Purser D.A. | 2000 | The CO concentrations from the decomposition of polymers are determined at equivalence ratios varying from 0.5 to 1.5. | Purser furnace. | Polymers: PE, PP, PS, polymethyl methacrylate (PMMA), vinyl acetate-ethylene copolymers (EVA). | CO yield of fire gases increase with the increase in fuel/air ratio (equivalence ratio). CO evolution depends only equivalence ratio but independent of the polymer. |
| Carbon monoxide generation in fires: effect of temperature on halogenated and aromatic fuels [21]. | Kaczorek K., Stec. A.A. & Hull T.R. | 2011 | Investigate the effect of ventilation condition and furnace temperature on the CO yield from burning mixtures of polymers containing halogens and aromatic rings. | A steady state tube furnace (ISO 19700). | PVC, PE, polyamide 6 (containing a brominated FR and antimony synergist) & PS. | Under well-ventilated burning, the high CO yields reduced at furnace temperatures above 850$^{o}$C, giving a diminution of fire toxicity. For the same fire stage, CO yields are higher at a furnace temperature of 650$^{o}$C. |
| Intoxication by cyanide in fires: a study in monkeys using polyacrylonitrile [69]. | Purser D.A., Patricia G. & Keith R.B. | 1984 | The effects of sublethal or low level exposures of HCN are determined. HCN may cause rapid incapacitation at low blood levels of cyanide in fires while death due to CO poisoning or other factors may follow later. | A dynamic steady state tube furnace is used to form the desired test atmosphere concentrations. | Monkeys are exposed to the pyrolysis products of polyacrylonitrile (PAN) or to HCN atmospheres. | The monkeys experienced loss of consciousness after 1-5 minutes and followed by a rapid recovery after exposure. The general results are applicable to other nitrogen-containing polymers which yield HCN and other nitriles during decomposition. |
| Continued:- | | | | | | |
| **Journal Title** | **Authors** | **Year** | **Descriptions** | **Test Method** | **Test Materials** | **Conclusions** |
| Modelling Toxic and Physical Hazard in Fire [68]. | Purser D.A. | 1989 | A mathematical model is presented for estimating toxic and physical hazard in fire in terms of time to incapacitation or death by taking the concentration/time profiles of the combustion products, smoke optical density, temperature and radiant heat flux. Fractional Effective Dose (FED) method is used to determine time to incapacitation. | Through a mathematical model with a reference to data profiles. | Primates and rodents. Exposure to many materials. | A victim would be able to escape from a fire without serious injury within 3 minutes after ignition if he or she is awake and aware of the fire, is not otherwise incapacitated, and does not stay after 2 minutes. |
| A bioassay model for testing the incapacitating effects of exposure to combustion product atmospheres using cynomolgus monkeys [70]. | Purser D.A. | 1984 | Incapacitating effects of exposure (30 minute periods) are tested at different atmosphere conditions, at different HCN and CO concentrations (80-150 ppm for HCN and 1000-8000 ppm for CO). | Various test atmospheres are established using a 70 litre rectangular chamber. | Monkeys are exposed to thermal decomposition products from polymeric materials. | HCN may produce a rapid "knock down" or incapacitation and causing the victim to remain in the fire and die from CO or other factors. The effects are minimal at HCN concentrations below 60 ppm. $O_2$ levels below 10% and $CO_2$ levels between 5-10% may also lead to incapacitation. |

| | | | | | | |
|---|---|---|---|---|---|---|
| The application of exposure concentration and dose to evaluation of the effects of irritants as components of fire hazard [34]. | Purser D.A. | 2007 | Determination of irritant potency for individual irritants and combustion products mixtures. The mouse $RD_{50}$ test is used with human data as reference for common irritants. | ISOTS19700 tube furnace method combined with the mouse $RD_{50}$ (Respiratory Rate Depression). | PVC cable jacket material (provides irritants: HCl). | Exposure to irritant smoke affects escape capability and influences walking/movement speed of humans. At high concentrations, the painful, sensory irritant effects on the eyes and respiratory tract can cause incapacitation. While at low concentrations, they affect evacuation behaviour and reduce the walking speed. |
| Influence of fire retardants on toxic and environmental hazards from fires [46]. | Purser D. | 2009 | Study provides the data of toxic yields (CO and HCN) versus equivalent ratios for wood and various fire retardant polymers and comparison with compartment fire data by Beyler and Gotuk. | BS7990 tube furnace | Wood and polymers (different types of fire retardant materials). | Fire retardant materials which contain halogens can reduce combustion efficiency and increase the CO yield even in well-ventillated fires although their application on product may provide a further performance benefit by slowing down the rate of flame spread or fire growth compared to that of an untreated product. Acid gases give high yields under all combustion conditions. |
| Continued:- | | | | | | |
| **Journal Title** | **Authors** | **Year** | **Descriptions** | **Test Method** | **Test Materials** | **Conclusions** |
| Bench scale generation of smoke particulates and hydrocarbons from burning polymers [51]. | Stec A.A. & Rhodes J. | 2011 | Determination of particle size distribution of combustion products (hydrocarbon and soot) from burning polymers under well ventilated, small under-ventilated and large under-ventilated fire conditions, comparing results between three test methods: NBS smoke chamber (cone heater), fire propagation apparatus & Purser furnace. | Tube furnace (ISO TS 19700) & smoke density chamber (ISO 5659-2). A cascade impactor is used to determine the particle size. | Polymers such as polyethylene, polystyrene, polyamide and polyvinyl chloride (PVC). | Well-ventilated flaming typically has high CO2/CO ratios and high combustion efficiency. Meanwhile, in under-ventilated flaming, higher yields of incomplete combustion products such as CO, soot and unburned hydrocarbons are observed. The result showed that predominance of 1-5 μm particulates for most of the test polymers under the test conditions, except PVC. |

| | | | | | | |
|---|---|---|---|---|---|---|
| Quantification of fire gases by FTIR: Experimental characterisation of calibration systems [90]. | Stec A.A., Fardell P., Blomqvist P., Valencia L.B., Saragoza L. & Guillaume E. | 2011 | FTIR calibration tests are performed for different concentrations of the gases. Volatile species in fire effluents have been obtained and identified at about 180$^{o}$C. | Gas phase FTIR spectroscopy. | Calibration gases used are CO, $CO_2$, HCl, HBr, HCN, NO, $NO_2$, $SO_2$ & $CH_4$. | Particular attention is required to minimize error of result especially to ensure constant temperature, pressure and gas flow are obtained in the sample lines and gas cell. |
| Analysis of toxic effluents released from PVC carpet under different fire conditions [76]. | Stec A.A., Readman J., Blomqvist P., Gylestam D., Karlsson D., Wojtalewicz D. & Dlugogorski B.Z. | 2013 | Measurement and quantification of acute and chronic toxicants including PAH and PCDD/F in different fire scenarios (oxidative pyrolysis, well-ventilated and under-ventilated fires). | The steady state tube furnace. | PVC carpet is selected as the fuel. | Significant quantities of respirable submicron particles are measured. The findings do have implications for the health and safety of fire and rescue personnel, fire investigators and other individuals exposed to the residue from unwanted fires. |
| Smoke and hydrocarbon yields from fire retarded polymer nanocomposites [52]. | Stec A.A. & Rhodes J. | 2011 | Comparison of toxic products yields for the separate materials and fire retarded and nanocomposite modifications of these materials under flaming conditions.FR used for PP is ammonium polyphosphate and for PA6 is a mixture of organic aluminium phosphinate and melamine polyphosphate (OP1311) and nanoclay (NC). | A steady state tube furnace (BS 9700, ISO TS 19700). | Polypropylene (PP) and polyamide 6 (PA6) with and without fire retardants (FR). | In under-ventilated fire conditions, the highest CO yields are occurred for both pure polymers when FR and NC are combined together. |
| Continued:- | | | | | | |
| **Journal Title** | **Authors** | **Year** | **Descriptions** | **Test Method** | **Test Materials** | **Conclusions** |
| Assessment of the fire toxicity of building insulation materials [37]. | Stec A.A. & Hull T.R. | 2011 | Usage of lightweight building insulation materials as replacement to the traditional building materials can contribute less fire load in terms of fire safety concern and energy saving (efficiency). | Purser furnace (a steady state tube furnace, ISO TS 19700). | Lightweight building insulation materials (increasing fire toxicity order: stone wool, glass wool, polystyrene foam, phenolic foam, polyurethane foam and polyisocyanurate). | Stone wool (least toxic) and glass wool fail to ignite and give consistently low yields of toxic products. Polyisocyanurate (most toxic) and polyurethane foam give significant contribution about doubling of the overall toxicity due to formation of hydrogen cyanide (from well-ventilated to under-ventilated fire condition). |

| | | | | | | |
|---|---|---|---|---|---|---|
| Comparison of toxic product yields from bench-scale to ISO room [36]. | Stec A.A., Hull T.R., Purser J.A. & Purser D.A. | 2009 | Large/full scale (ISO room) and small/bench scale (tube furnace ISO TS 19700) are used to measure toxic product yields from the burning materials. Product yield data (measured for $CO_2$, CO, HCN, $NO_x$, total hydrocarbons and smoke particulates) from both scales are expressed as fuctions of equivalence ratio and $CO_2$/CO ratio. | A steady state tube furnace (ISO TS 19700) & ISO 9705 room corner. | Building product materials (polypropylene (PP), polyethylene (PE), polyamide 6.6 (PA 6.6), polystyrene (PS), medium-density fireboard (MDF-FR) (A and B)). | The closest direct agreement between the large scale and small scale data are shown by pool fires involving PP and nylon (polyamide) 6.6 product yield. Smoke yields vary as influenced by the presence of different areas of flaming and non-flaming decomposition. |
| Characterisation of the steady state tube furnace (ISO TS 19700) for fire toxicity assessment [49]. | Stec A.A., Hull T.R. & Lebek K. | 2008 | Temperature profiles of the furnace, sample and effluent dilution chamber are determined to characterise the conditions in the apparatus. | The steady state tube furnace (Purser furnace, ISO TS 19700). | Polypropylene | The smoke distribution demonstrates the efficiency of mixing in the effluent dilution chamber. Heat flux application at various points through the furnace gives a vary fire condition to the sample from pre-flaming to full developed fires. |
| The effect of temperature and ventilation condition on the toxic product yields from burning polymers [33]. | Stec A.A., Hull T.R., Lebek K, Purser J.A. & Purser D.A. | 2008 | The Purser furnace is used in order to create different fire stages (from smouldering combustion to early well-ventillated flaming through to fully developed under-ventillated flaming) for identification and quantification of toxic combustion gases through the application of FTIR as a measuring device. | Purser furnace (BS 9700 & ISO TS 19700). | Polymers such as low density polyethylene, polystyrene (PS), nylon 6.6 and polyvinyl chloride (PVC). | For all tested polymers except PVC, product yields for incomplete combustion (CO and hydrocarbons) give a dramatic increase with increase in equivalence ratio. The PVC shows a consistently high level of products of incomplete combustion due to formation of HCL and oxygen depletion. |
| Continued:- | | | | | | |
| **Journal Title** | **Authors** | **Year** | **Descriptions** | **Test Method** | **Test Materials** | **Conclusions** |
| A comparison of toxic product yields obtained from five laboratories using the steady state tube furnace (ISO TS 19700) [50]. | Stec A.A., Hull T.R., Purser J.A., Blomqvist P. & Lebek K. | 2008 | Polymers are tested in 5 laboratories using the tube furnace for assessing the toxic product yields as a fuction of equivalence ratio ($\phi$). | A steady state tube furnace (BS 9700, ISO TS 19700). | Tested polymers are LDPE, PP, PVC, nylon and PS. | A high degree of reproducibility of toxic product yield is observed across the range of ventillation conditions. The CO yield shows consistent behaviour which is independent of a particular laboratory. |

| | | | | | | |
|---|---|---|---|---|---|---|
| Fire toxicity and its assessment [25, 26]. | Stec A.A. & Hull T.R. | 2010 | Describe types and effects of toxic effluents from fires and different methods in assessing fire toxicity (using animal exposure studies, laboratory scale and large scale tests). Discussion involves the influence of different materials and fire conditions on the generation of toxic products. | Various test apparatus: open tests, closed chamber tests & flow-through tests (bench scale fire tests) are compared. | LDPE, PS, PVC and nylon 6.6. | There are a large number of different methods for bench scale assessment of combustion toxicity. It is more appropriate to use the incapacitation methodology (ISO 13571) than the rat lethality methodology (ISO 13344) since incapacitation in a fire will result in a fire death in the same way as lethality (unless the incapacitated victim is rescued). |
| Numerical investigation of tube furnace toxicity measurement method (ISO 19700) [77]. | Mahalingam A., Jia F., Wang Z., Patel M.K. & Galea E.R. | 2012 | Simulation works of flow and combustion conditions inside the tube (Purser) furnace using CFD fire modelling technique and validation process by measurements/tests. | Tube (Purser) furnace (Standards: ISO TS 19700, BS 7990:2003, IEC 60695-7-50). | NYM (PVC type) and NHMH cables. | At 750$^{o}$C furnace temperature, air flow 15 L/min contributes to higher temperature inside the mixing chamber compared to air flow 4 L/min for test with the empty boat. Secondary air flow is used to generate a uniform mixture within the dilution chamber. |
| Effective measurement techniques for heat, smoke, and toxic fire gases [78]. | Babrauskaus V. | 1991 | Discuss about the differences between data obtained in large-scale and in bench-scale tests. Focus on the measurement techniques for measuring HRR (related to the amount of oxygen being consumed from the air stream). | Cone Calorimeter, NIST Furniture Calorimeter (ASTM E 1354). | Furniture. | Involve the measurement of heat, smoke and toxic fire gases. Data analysis techniques have been developed which express the material fire properties. |
| Toxic potency measurement for fire hazard analysis [79, 91]. | Babrauskaus V., Levin B.C., Gann R.G., Paabo M., Harris R.H., Peacock R.D. & Yusa S. | 1992 | Determination of smoke toxicity data for hazard analysis using a bench scale apparatus which provides the real fire conditions. | A descendant of the cup of furnace and the Weyerhaeuser radiant apparatus (represent the combustion condition in real fires). | Materials, products, composites and assemblies. | FED value ~1.1 at the $LC_{50}$. For $LC_{50}$ values greater than 8 g/m$^3$, post-flashover smokes are indistinguishable from each other. $LC_{50}$ of CO is ~ 5 g/m$^3$ (one-fifth of the smoke which is based only on $CO_2$ and CO). Total $LC_{50}$ value for post flashover smoke ~25 g/m$^3$. |
| Continued:- | | | | | | |
| **Journal Title** | **Authors** | **Year** | **Descriptions** | **Test Method** | **Test Materials** | **Conclusions** |
| Toxic hazard from fires: a simple assessment method [87]. | Babrauskaus V. | 1993 | Development of the simplest level toxic hazard analysis by taking into account both toxic potency and burning rate variables. | Test data on a number of products obtained from NBS combustion toxicity test and from the Cone Calorimeter. | Various inter-laboratory evaluation (ILE) materials; wood, wool & polymers. | Toxic fire hazard can be increased by increasing the pyrolisis of material (high mass loss rate), increasing flame spread rate or flame coverage area and decreasing room ventilation flow. |

| | | | | | | |
|---|---|---|---|---|---|---|
| A cone calorimeter for controlled-atmosphere studies [92]. | Babrauskaus V., Twilley W.H., Janssens M. & Yusa S. | 1992 | Involve the design of a new version Cone Calorimeter for investigating certain types of fires (under different controlled atmospheres/ventilation flows). | Modified Cone Calorimeter (ASTM E 1354, ISO DIS 5660). | - | Minimum combustion air flow is 12 L/s in order to make sure there is no combustion products would fail to be collected by the exhaust hood. The normal flow is 24 L/s and maximun flow limit is 32 L/min. |
| The phi meter: A simple, fuel-independent instrument for monitoring combustion equivalence ratio [93]. | Babrauskaus V., Parker W.J., Mulholland G. & Twilley W.H. | 1994 | Development of an equipment for monitoring the equivalence ratio in combustion systems based on an oxygen consumption measuring method. | Phi meter (include pyrolysing catalytic combustor, catalyst, two inlets for sample and oxygen). | Fuels; PVC, PU, PTFE, polysulfonates. | Phi meter will apply to fuels containing C,H & O. By assume that components such as $CO_2$, $H_2O$ (products of complete combustion) and others will be scrubbed out except $O_2$ and $N_2$. |
| Fire safety improvements in the combustion toxicity area: is there a role for $LC_{50}$ tests? [94]. | Babrauskaus V. | 2000 | Determine the dominant factor which contributes to combustion toxicity either $LC_{50}$ or mass loss rate value in both real/full scale and bench scale tests. | DIN 53436 tube furnace & ISO 5660 Cone Calorimeter. | A wide range of building materials. Rock wool, rubber foam, phenolic foam & other polymer foams (e.g. PE, PU, PS). | $LC_{50}$ is a minor constituent (far from being the dominant factor in fire toxicity picture and fire fatalities) for products in real & bench scale test. But mass loss rate vary tremendously. Fire toxicity hazard can be controlled by reducing the burning rate (low mass loss rate) rather than attempting to make the effluent less toxic. |
| Heat release rate: the single most important variable in fire hazard [95]. | Babrauskaus V. & Peacock R.D. | 1992 | Explain the important of heat release rate as the most significant variable in characterising the flammability of products and their consequent fire hazard. | Bunsen burner (full scale test) & Calorimeter ISO DIS 5660 (bench scale test which canrelate to the real scale test). | Non-fire retardants and fire retardants. | Heat release rate is closely related to the mass loss rate. The HRR is the best predictor of fire hazard even though fire deaths are primarily caused by toxic gases. |
| Experience plan for controlled-atmosphere cone calorimeter by Doehlert method [96]. | Guillaume E., Marquis D.M. & Chivas C. | 2013 | The application of Doehlert method in optimization of the number of tests. | Controlled-atmosphere cone calorimeter (CACC). | Specimen size (100 mm x 100 mm). | Polynomial approximations is applied to establish fire behaviour constitutive in order to optimize the experimental measurement. Time for measurement is reduced. |
| Continued:- | | | | | | |
| **Journal Title** | **Authors** | **Year** | **Descriptions** | **Test Method** | **Test Materials** | **Conclusions** |

| | | | | | | |
|---|---|---|---|---|---|---|
| Effect of gas cell pressure in FTIR analysis of fire effluents [97]. | Guillaume E., Saragoza L., Wakatsuki K & Blomqvist P. | 2015 | Analysis of fire effluents using FTIR increases due to this technique is very selective and precise if it is calibrated properly. | FTIR (ISO 19702). | - | Gas cell pressure has to be maintained to deviate not more than 10 Torr from the calibration pressure during the experiment. Results are sensitive to instrumental parameters such as the effects of pressure on the contents in the measurement cell. |
| Calibration of flow rate in cone calorimeter tests [98]. | Guillaume E., Marquis D. & Saragoza L. | 2014 | Present a calibration method for volumetric flow rate without using orifice place and determine C-factor (mass flow) without methane burner and calorimetry. | Cone Calorimeter | - | Dilution method used to calibrate volumetric flow rate is efficient enough to meet the acceptance limit of standard flow rates around 0.024 $m^3/s$. |
| Regulatory issues and flame retardant usage in upholstered furniture in Europe [99]. | Guillaume E., Chivas C. & Sainrat A. | 2008 | Evaluationof the risks and the benefits of introducing flame retardants into upholstered furniture within the life-cycle risk assessment. | Data sheets are referred. | Upholstered furniture (with flame retardants). | Risks (exposure risk during manufacture of the products, under normal living conditions, during recycling/incineration, during fires) due to the present of flame retardants in upholstered furniture are determined. |
| Particles and isocyanates from fires [5]. | Hertzberg T., Blomqvist P., Dalene M. & Skarping G. | 2003 | Presentation of the capacity for generation of particles and isocyanates as a result of combustion for many types of building materials. For comparison purpose, data from SBI method (EN13823), Room-Corner (ISO 9705) and other full/larger scale methods were collected. | Cone Calorimeter (ISO 5660). Low pressure impactor is used to measure particle size distribution. | 24 different building materials or products. | Results show a significant variance in the yield of particles generated for different test materials but the mass shape and number size distributions are very similar. Building materials (fire retardants) that did not burn well contributed to higher amount of particles compared to materials that burn well (wood materials, tend to oxidise all available combustibles). |
| Observations of urban airborne particle number concentrations during rush-hour conditions: analysis of the number based size distributions and modal parameters [7]. | Lingard J.J.N., Agus E.L., Young D.T., Andrews G.E. & Tomlin A.S. | 2006 | Measurement of the number concentration and the size distribution of combustion derived nanoparticles from diesel and spark-ignition (SI) engine emissions for urban airborne roadside particles by using Electrical Low-pressure Impactor and TSI Scanning Mobility Particle Spectrometer. | ELPI measures particles within the range of 30 nm to 10 µm and SMPS measures particles within the range of 6 to 225 nm. | - | Four component modes were identified: Two nucleation modes 1) More minor, sub-11 nm particles, 2) Much larger, particle size range from 10-20 nm, 3) Particles with size ranges of 28-65 nm & 4) 100-160 nm. |

## 2.6 Specific Research Objectives

The specific objectives of this research are divided to four (4) sections as follow:

a) Pre and Post Analysis
   i. Sample preparation before analysis
   ii. Perform pre and post analysis (proximate and ultimate analysis) for test sample materials.
   iii. Determine the group type of each test materials.

b) Cone Calorimeter
   i. Develop a methodology for the analysis of toxic gases and particulates for the Cone Calorimeter method.
   ii. Perform fire tests under different test conditions with varying air flow rates and heat fluxes.
   iii. Measure toxic gases, particle sizes and soot mass from various synthetic material (electrical cable and polymer) fires.
   iv. Determine combustion properties, gas toxicities, total toxicities, particle size distributions, gas and particulate yields.

c) Purser Furnace System
   i. Understand criticisms about the previous built Purser Furnace and come out with improvements in designing a new furnace.
   ii. Procure all parts for constructing the new furnace system.
   iii. Design, construct and install a new furnace system (the Purser Furnace), followed by commissioning work of the rig.
   iv. Produce and develop a methodology for the analysis of toxic gases and particulates for the Cone Calorimeter method.
   v. Perform some fire tests during and prior the commissioning of this new rig.
   vi. Measure toxic gases, particle sizes and soot mass from the selected polymeric material fire.
   vii. Determine combustion properties, gas toxicities, total toxicities, particle size distributions, gas and particulate yields.

d) Comparison
   i. Compare results with the same group of test materials from both test methods.
   ii. Compare test data with the published experimental data and literature.

# Chapter 3
# Research Methodology

## 3.1 Cone Calorimeter

The standard cone calorimeter (open-air Cone Calorimeter) [92] was modified [100] to enable the toxic gas yields from materials under fire conditions to be determined as a function of the fire equivalence ratio. The cone calorimeter was used with free ventilation for all materials and using the controlled atmosphere version for a few polymers. The most important modification of the Cone Calorimeter was the placement of chimney above the electrical heater cone from which a gas sample of the raw products of combustion could be obtained for analysis. This eliminated oxidation of the combustion products by the surrounding air during the cone calorimeter dilution process. In order to avoid backflow of the external air into the chimney, a grid plate restrictor with 90% flow blockage was placed at the exit to the chimney.

The cone calorimeter was also modified to add the controlled atmosphere enclosure with chimney for raw gas sampling, as detailed by Irshad et al. [100]. This enclosure was ventilated with a metered air supply and this enabled compartment fire conditions to be simulated and the fire ventilation varied. Rich combustion conditions were created where toxic emissions were very high. Figure 3.1 shows the configuration of the Cone Calorimeter for free ventilation tests without the controlled atmosphere box and Figure 3.2 shows the configuration for the controlled ventilation tests. For both free and controlled ventilation tests, on top of the cone heater there is a chimney having X sample probe, exhaust pipe and orifice plate mounted on top accordingly as shown in Figure 3.1.

The Cone Calorimeter was used to determine the fire heat release rate, total heat released, effective heat of combustion, mass loss rate, ignitability and the evolution of smoke particulates and various gas species. The heat radiation was calibrated as a function of the cone temperature prior to each test. The calibrated heat fluxes are shown in Table 3.1.

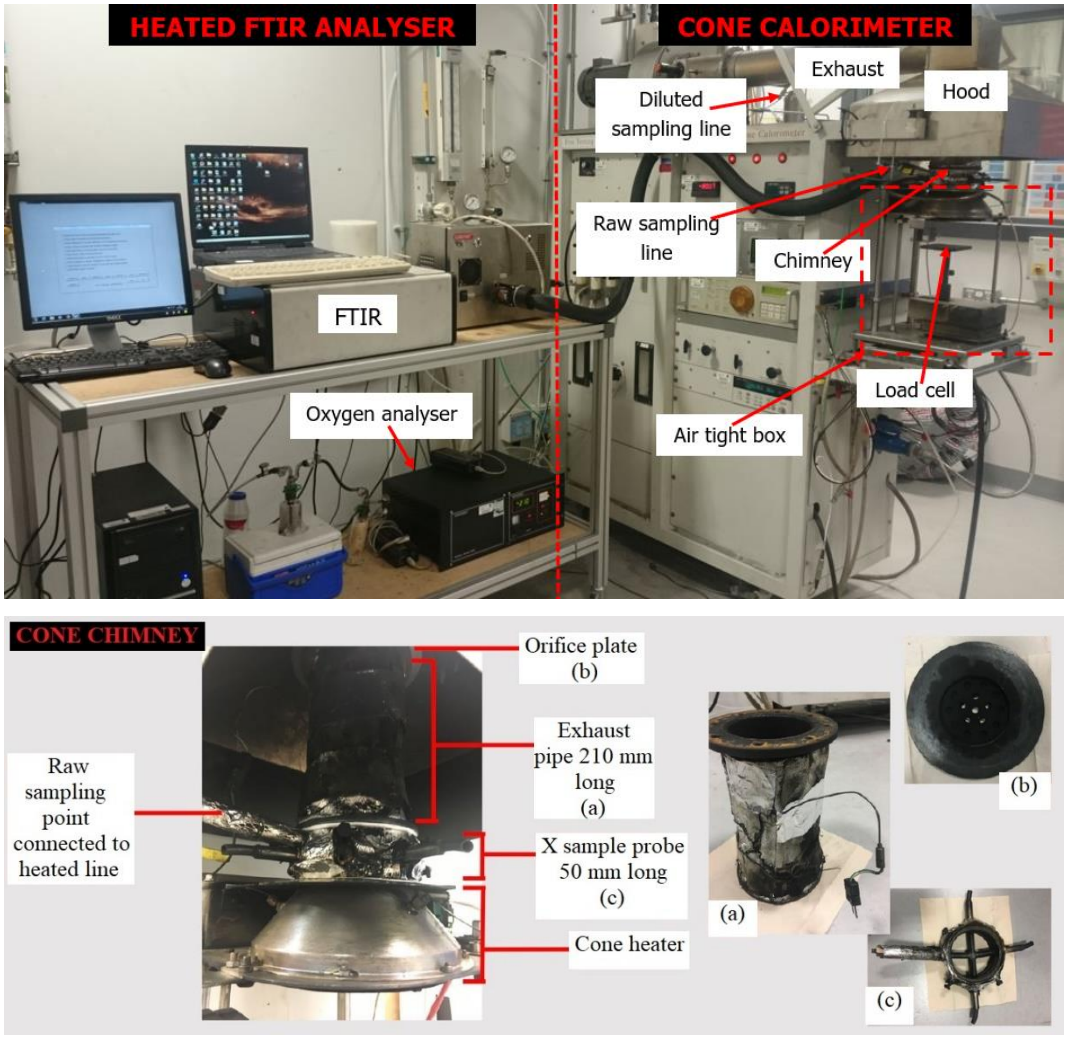


**Figure 3.1** Configuration of the Cone Calorimeter with a chimney.

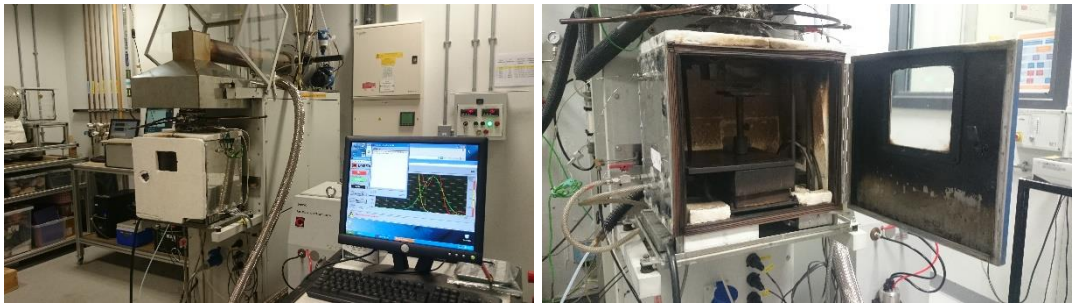

**Figure 3.2** Configuration of the Cone Calorimeter for restricted ventilation test (with the air tight box).

**Table 3.1** Calibrated irradiation level at certain Cone temperature.

| Irradiation Level ($kW/m^2$) | Cone Temperature ($^oC$) |
|---|---|
| 10 | 377 |
| 15 | 460 |
| 20 | 520 |
| 21 | 537 |
| 25 | 568 |
| 30 | 610-613 |
| 35 | 645 |
| 40 | 695 |
| 50 | 760 |
| 70 | 862 |

Properties of combustion products were determined from two different effluent streams which were the raw gases stream and the diluted gas stream. Raw gases were sampled from the cone calorimeter chimney using a multi-hole gas sample probe and were transported through electrically heated sample lines to the heated FTIR. The exit gases from the FTIR were hot and were passed to a water condenser for water removal and then to a paramagnetic oxygen analyser. This enabled the toxic products to be related to oxygen conditions in the fire.

### 3.1.1 Test Procedure for the Cone Calorimeter Method

The test started with calibration of the heater and the preparation of the specified test specimens. The heater was first turned on and equilibrated to the correct temperature and radiant heat flux. The controlled atmosphere compartment had an variable area flow meter to determine the ventilation air flow rate. The Cone Calorimeter exhaust fan flow is set up to achieve a positive value of chamber pressure approximately 5 Pa. The mass flowrate (MFR) of the total gas flow in the Cone Calorimeter diluted products duct was set to the standard 24 L/s (29 g/s) for the Cone Calorimeter. The air flow range for controlled atmosphere ventilation was 6 – 28 LPM which is a dilution ratio range in the cone calorimeter flow of 51 – 240. As this post dilution of the toxic gas products can result in oxidation of these products, particularly reduction of CO, the cone calorimeter is not suitable for toxic gas measurements, which is why the raw gas analysis from a chimney mounted above the electrical cone heater was used for gas samples. However, for particulate measurement the

cone calorimeter dilution is ideal as the sample has to be cooled ‘by dilution’ in automotive particulate regulations and hence the same procedure should be used for particulate measurement from fires. The cooling is to ensure that any hydrocarbons present are condensed or absorbed onto the particles, as will occur in the atmosphere. The particles on the filter paper can be analysed using TGA for the volatile and carbon fractions. For particle number cooling by dilution ensures there are no losses in the cooler and also produces an aerosol of hydrocarbons if there are high Hydrocarbons levels in the toxic gases, which will be shown to be a key feature of polymer fires. Particle number is thus not just solid particles of carbon or ash, but liquid particles of condensed Hydrocarbons.

The Cone Calorimeter has a shutter between the conical electrical radiant heater and the 100 mm square test material, The heater is switched on with the shutter closed and when it is up to the temperature required for the desired radiant heat, the shutter is manually opened and the test starts. The heater radiation with the shutter in the closed position causes the sample holder which contains the test specimen to heat up. Thus, delays before opening the shutter, once the heater is at the desired temperature, should be avoided.

The test specimen is placed in the sample holder on the load cell platform and the controlled atmosphere enclosure box door is shut. Before proceeding with the test, the inlet and exhaust oxygen meters should be checked properly to indicate the desired oxygen value. To start the test, the shutter is opened and the specimen is exposed to the cone heater. The test specimen is observed through the glass window in the controlled atmosphere enclosure door and the time to achieve flaming ignition is determined and this is the ignition delay. In most of the present work there was no pilot present and the auto-ignition delay time was determined for each polymer tested. An alternative test can be carried out using a pilot spark ignition during the heating period [92], but this was not used in the present work.

## 3.2 Purser Furnace

### 3.2.1 Principles of Operation

The Purser Furnace method (ISO 19700 [101]) is designed to enable the toxic gas yields to be determined as a function of equivalence ratio and so aims to simulated compartment fire burning conditions. The Purser Furnace [56] is

capable of reproducing the oxygen depleted conditions of a developed fire. In the present work, this apparatus was used for assessment of fire effluents including gas toxicity, smoke density, particulate mass and size. A feature of this method is the continual feed of fresh material into the furnace. Thus at steady state burning there is pyrolysis of the fire material at the base of the sample as it enters the furnace. This releases volatiles that give flaming combustion (which in the present work was observed through an end window), after the volatiles are burnt the leading edge of the sample undergoes char oxidation or pyrolysis depending on the air flow conditions. Thus all phases of a fire are included in the test and this is what happens in real fires where pyrolysis, flaming combustion and char oxidation are all occurring in the fire. However, the toxic products in each phase of the fire are difficult to separate. When the test starts raw material enters the heated zone and initially only pyrolysis occurs, then the sample ignites and flaming combustion is observed. Later on the initial front part of the sample starts to char. Thus the three zones can be separated if the FTIR results are recorded as a function of time.

The sample is heated in an air flow in a furnace at a constant temperature that is usually 600$^{o}$C, but could be used to determine toxic gas yields as a function of temperature. The sample is placed on a long Quartz ‘boat’ that can be moved at a set rate into the furnace, which has a set air flow. The rate of advance of the sample boat is equivalent to the fuel mass flow burning rate and this with the air flow enable the A/F mass ratio and fire equivalence ratio to be pre-set. The evolved toxic gases are discharged into an enclosure where dilution air is added prior to the mixed sample being analysed. The total flow rate is kept at 50 LPM and if say 10 LPM is passed into the furnace tube then 40 LPM is the dilution air and the dilution ratio is 4/1. This is much lower than on the cone calorimeter dilution ratio, but is still sufficient to give post furnace tube oxidation of the toxic gases.

The dilution flow changes the dew point of the gases and enables cold gas sampling to be used without risk of water condensation in the sample lines. If raw gas sampling is used, as in the present work, then fully heated gas sample lines, pumps and filters are required which most fire toxicity laboratories do not have. This is why most current fire toxicity experiments us sample dilution prior to toxic gas measurement. Unfortunately all these dilution techniques change the toxic gases being analysed and hot raw gas sampling should be used to avoid this, as in the present work.

### 3.2.2 Problems of the Purser Furnace Method

The Purser Furnace method has several problem areas that the present design equipment was intended to eliminate. The first has been mentioned above and that is the use of diluted samples with the potential for oxidation of the products of combustion. This was overcome in the present work by using raw gas samples directly from the heated Quartz tube upstream of the discharge into the diluted air flow.

An additional problem of the discharge into the air dilution volume is that the static pressure there will be higher than that in the tube, due to the velocity difference between the tube flow and the discharge. Also the method of gas flowing from the diluted volume to the discharge point with a relatively small discharge increases the backpressure. This causes air to backflow into the sample reaction Quartz tube, where it can promote oxidation of the toxic gases. In the development of the raw gas sample method for the Cone Calorimeter the same problem had been encountered [100] with air backflowing into the chimney and the sample. This was most clearly shown when the cone calorimeter was operated on Nitrogen and the gas samples of the volatiles was found to contain significant levels of Oxygen. The solution was to place a 75% blockage grid plate at the exit to the chimney. The same solution was used on the Purser Furnace with an orifice plate with 90% blockage being fitted to the exit of the Quartz tube. This made the static pressure in the test section higher than in the discharge volume so backflow of air was prevented. This issue was known about and that a flow restrictor is required by the current standard for lower primary air flow rates. The basic design is that the primary air flow is positive with respect to the mixing chamber, which is positive with respect to the exhaust duct. With the standard sized primary tube some evidence for a small back flow into the end of the tube was found for low primary air flow rates (1-2 litres/min). When this was tested (with and without flow restriction) at higher primary flow rates no evidence of secondary oxidation was found [102]. The other possible reason for mixing at the end of the tube at low flows is more to do with stratification within the tube than back pressure from the mixing.

In the original Purser design the mixing between the dilution air and the toxic gases from the Quartz tube was poor and so a sample taken from the discharge volume was not necessarily well mixed. In the new design the bypass air was injected into the discharge volume remote from the Quartz tube exit and impinged on the top of the discharge box, so that the air spread

out and was then entrained by the Quartz tube jet discharge. This discharge was located in the upper half of the discharge volume.

The outlet from the discharge volume to the extract discharge suction was placed near the bottom of the volume and used a very large diameter pipe (75 mm). Also this pipe was turned through two 90 degree bends before multi-hole gas sample probes were fitted across the pipe. There were three of these to enable simultaneous FTIR, particle mass and particle size measurements to be made simultaneously. This mean gas sample would be much more representative of the true mean than in the original equipment design where the mixing of the two streams was not shown to be adequate.

The inlet to the Quartz tube was a difficult design area as a seal against Quartz glass had to be achieved as well as a seal against the rotating pusher rod for the internal Quartz boat. Both seals were made with ‘O’ rings and the whole test facility was well engineered.

The auto ignition delay of the sample was not determined in the standard test, but in the modified equipment a small Quartz window was placed in the cold end of the Quartz tube and an angled mirror enabled the occurrence of flaming combustion to be determined, as well as the end of flaming combustion. These two times are marked on all the results. The volatile gases during the ignition delay were determined as well as those during flaming combustion. However, for char combustion the hydrocarbons were far too high, way beyond the range calibrated for and these results will not be discussed as they are unreliable. Many of the polymer samples studied had fire retardants added that should have acted to produce a long ignition delay. The ability to measure the ignition delay enabled the effectiveness of fire retardants to be determined.

### 3.2.3 Description of the Modified Purser Furnace Method

The Purser Furnace is shown in Figure 3.3 and was designed and constructed as part of this PhD research project. However, it took a long time to build the facility so that only limited toxic gas measurements were made for a commercial Polyethylene sample at two nominal equivalence ratios. However, these tests were carried out using the heated FTIR with simultaneous particle mass and particle number measurements, which is a first for this equipment.

The construction followed the ISO 19700 [101] standard and the method is similar to the fire emission DIN 53436 [103] method. The design has four main

sections which are a Quartz sample boat drive mechanism, a clear glass or Quartz tube, a tube furnace and an effluent mixture chamber. Other parts include a sample boat, several pipes for the primary and secondary air and exhaust gas outlet duct. The raw gas sample tube was positioned on the centreline of the Quartz tube and fed through the wall of the discharge volume. It was located 50 mm from the discharge end of the Quartz tube, which was considered to be the end of the furnace heating section. After the discharge volume the sample was connected to the FTIR using 180$^{o}$C heated sample lines, heated filter and heated pump. A Type K mineral insulated thermocouple was also placed on the centreline of the Quartz tube to measure the actual tube gas temperature separately from the furnace temperature. The overall length of this Purser Furnace was about 3 m.

A small Quartz window (15 mm diameter) was placed in the cold end of the external Quartz tube on the centreline for the Quartz tube. A mirror was then used so that the onset of flaming combustion could be determined. This enabled the ignition delay at 600$^{o}$C to be determined and by operating at different temperatures the delay as a function of temperature could be determined.

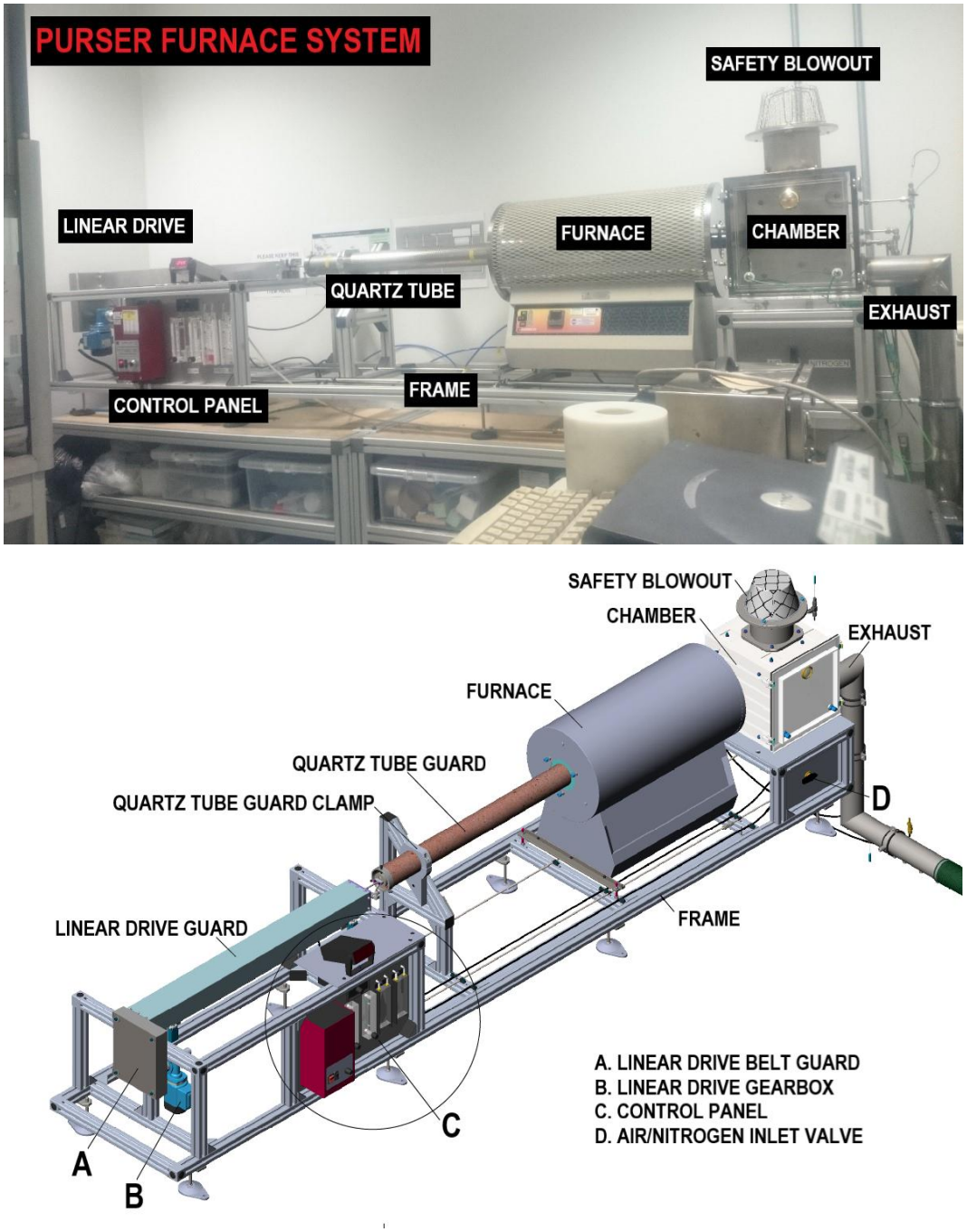


**Figure 3.3** The actual and schematic configuration of the Purser Furnace System.

### 3.2.4 Test Procedure for the Purser Furnace Method

For these experiments, a test specimen mass of 25-50 mg/mm was used and air-flows were varied between 2 to 13 L/min in order to cover the range of combustion conditions with the required equivalence ratios. The specimen is spread evenly along the furnace boat in granular or pellet form for each

conducted test. Typical rate of movement of the sample boat for most test materials which was advanced by the drive mechanism, was 40 mm/min. This drive advance rate can be up to 60 mm/min for some fast-burning or low-density materials [104]. During the test, experiments are observed to make sure they are conducted under constant steady flaming conditions at a furnace temperature of 650$^{o}$C. The furnace temperature would vary from 650$^{o}$C to 850$^{o}$C, sometimes lower or higher than that range depending on the type of material used in the study, in order to obtain steady flaming condition. The combustion products then were diluted to a standard total flow of 50 L/min and sampled from the mixing chamber. This gives a bypass air dilution ratio range of 3-24.

Experiments were set up initially close to stoichiometric, with one rich mixture and one lean mixture overall studied, but normally the nominal equivalence ratio would be varied over a wider range, between 0.5 and 2.5. The Standard Test Procedure for running the present modified Purser furnace is in Appendix C.

## 3.3 Analysers Used in Experimental Works

It was desired to measure gas concentration, particle size distribution and soot mass in the tests. In addition the material elemental composition was required to be determined, in order to calculate the stoichiometric A/F by mass. The Gasmet FTIR was fully used to measure gas concentration, the Cambustion DMS500 was used to measure particle size distribution and Smoke Meter was used to measure soot mass. In total, more than 100 fire tests were done in the present work (see Appendix D). Also the fixed Carbon, volatile content and ash were required to be known and TGA equipment was used for this.

### 3.3.1 Fourier Transform Infrared Heated Gas Analyser (FTIR)

A heated Gasmet FTIR analyser complete with Servomex Oxygen analyser were used in the study for measurement of toxic gases from the conducted fire tests. Up to 60 species could be measured by the FTIR analyser and this analyser was calibrated by the manufacturer to measure these species in certain measurement range of gas concentration as included in the following Table 3.2. In the present work, emissions of toxic gases from various polymer fires were determined and the results of species concentration for most of polymer fires were collected. However, some analysed data was giving too

high values, well beyond the calibration range. This occurred in the char smouldering combustion phase on the Purser furnace tests, when measuring concentration of gases for some species such as Benzene, THC, HBr and $NO_x$ from Polyethylene fires. In this case only the flaming combustion phase was reported. Gas measurement data by the FTIR analyser was recorded by the Calcmet software. The FTIR configuration is shown in Figure 3.4.

Table 3.2 shows that CO was calibrated up to 20% and thus the CO for very rich mixtures was valid. However, most other species were calibrated to 500 ppm and some to 1000 ppm. This is the range of interest for raw gas sampling in most fires. Another problem with diluted gas samples is that the toxic gas concentrated is diluted and FTIR analysis of very low concentrations is not very reliable.

**Table 3.2** Calibration and wavelength range for each species measured by the FTIR [105-107].

| Species | Calibration Range | | Wavelength Range ($cm^{-1}$) | Species | Calibration Range | | Wavelength Range ($cm^{-1}$) |
|---|---|---|---|---|---|---|---|
| Water vapour H2O | 50 | % | 4000-3400, 2000-1250 | Iso-pentane $C_5H_{12}$ | *200 | ppm | 3050-2800 |
| Carbon dioxide $CO_2$ | 30 | % | 3800-3500, 2450-2200, 800-600 | Hexane $C_6H_{14}$ | 500 | ppm | 3050-2800 |
| Carbon monoxide CO | 20000 | ppm | 2250-2000 | Heptane $C_7H_{16}$ | 500 | ppm | 3050-2800 |
| Nitrous oxide $N_2O$ | 500 | ppm | 2300-2150, 1350-1200 | Octane $C_8H_{18}$ | *200 | ppm | 3050-2800 |
| Nitric oxide NO | 2000 | ppm | 2000-1750 | Iso-octane $C_8H_{18}$ | *500 | ppm | 3050-2800 |
| Nitrogen dioxide $NO_2$ | 1000 | ppm | 1700-1500 | Cetane $C_{16}H_{34}$ | *200 | ppm | |
| Sulphur dioxide $SO_2$ | 1000 | ppm | 1450-1300 | Acetylene $C_2H_2$ | 500 | ppm | 800-650 |
| Carbonyl sulfide COS | 200 | ppm | 2150-1950 | Ethylene $C_2H_4$ | 500 | ppm | 1100-800 |
| Ammonia $NH_3$ | 500 | ppm | 1200-800 | Propene $C_3H_6$ | 500 | ppm | |
| Hydrogen cyanide HCN | 500 | ppm | 3450-3200, 1550-1300, 800-600 | 1,3-Butadiene $C_4H_6$ | 500 | ppm | |
| Hydrogen chloride HCl | 500 | ppm | 3100-2550 | Benzene $C_6H_6$ | 500 | ppm | 3200-2900, 750-600 |
| Hydrogen fluoride HF | 200 | ppm | 4000-3600 | Toluene $C_7H_8$ | 500 | ppm | 3150-2800, 800-650 |
| Hydrogen bromide HBr | 500 | ppm | 2750-2300 | m-Xylene $C_8H_{10}$ | 500 | ppm | 3150-2800, 1650-1350, 800-650 |
| Methane $CH_4$ | 1000 | ppm | 3200-2800, 1400-1200 | o-Xylene $C_8H_{10}$ | 500 | ppm | 3150-2800, 800-650 |
| Ethane $C_2H_6$ | 500 | ppm | 3100-2800 | p-Xylene $C_8H_{10}$ | 500 | ppm | 3150-2800, 1600-1350, 850-750 |
| Propane $C_3H_8$ | 500 | ppm | 3050-2800 | 1,2,3-Trimethylbenzene $C_9H_{12}$ | 500 | ppm | 3150-2800, 1650-1350, 850-700 |
| Butane $C_4H_{10}$ | 500 | ppm | 3150-2800 | 1,2,4-Trimethylbenzene $C_9H_{12}$ | 500 | ppm | 3150-2800, 1650-1350, 950-850 |
| 1,3,5-Trimethylbenzene $C_9H_{12}$ | 500 | ppm | 3150-2800, 1650-1350, 900-800 | Sulfur hexafluoride $SF_6$ | 50 | ppm | 1000-850 |
| Ethylbenzene $C_8H_{10}$ | *200 | ppm | | i-Butane $C_4H_{10}$ | *100 | ppm | |
| Indene $C_9H_8$ | *500 | ppm | | 1-Butene $C_4H_8$ | *500 | ppm | |
| Methanol $CH_4O$ | 500 | ppm | 3100-2700, 1100-900 | Trans-2-Butene $C_4H_8$ | *100 | ppm | |
| Ethanol $C_2H_6O$ | 500 | ppm | 3100-2750, 1150-950 | Cis-2-Butene $C_4H_8$ | *150 | ppm | |
| Propanol $C_3H_8O$ | 500 | ppm | 3050-2800, 1150-850 | i-Butene $C_4H_8$ | *150 | ppm | |
| Butanol $C_4H_{10}O$ | *200 | ppm | | Pentene $C_5H_{10}$ | *250 | ppm | |
| MTBE $C_5H_{12}O$ | 500 | ppm | 3050-2800, 1350-1000 | Hexene $C_6H_{12}$ | *500 | ppm | |
| Dimethyl Ether $C_2H_6O$ | *200 | ppm | | Heptene $C_7H_{14}$ | *500 | ppm | |

| Species | Calibration Range | | Wavelength Range ($cm^{-1}$) | Species | Calibration Range | | Wavelength Range ($cm^{-1}$) |
|---|---|---|---|---|---|---|---|
| Formaldehyde $CH_2O$ | 500 | ppm | 3100-2600, 1800-1600 | Octene $C_8H_{16}$ | *500 | ppm | |
| Acetaldehyde $C_2H_4O$ | 200 | ppm | 3000-2600, 1900-1700, 1550-1300 | Nonene $C_9H_{18}$ | *500 | ppm | |
| Formic acid $CH_2O_2$ | 200 | ppm | 1850-1700, 1200-1000 | Cyclopropane $C_3H_6$ | *500 | ppm | |
| Acetic acid $C_2H_4O_2$ | 500 | ppm | 1850-1700, 1350-1100 | Cyclohexane $C_6H_{12}$ | *500 | ppm | |
| Acrolein $C_3H_4O$ | 500 | ppm | 1800-1650 | alpha-Pinene $C_{10}H_{16}$ | *500 | ppm | |
| Naphthalene $C_{10}H_8$ | 500 | ppm | 3150-2900, 850-700 | $NO_x$ ($NO + NO_2$) | 3000 | ppm | |
| 1-Ethylnaphthalene $C_{12}H_{12}$ | 500 | ppm | 3150-2850, 850-700 | THC | 1000 | ppm | |
| Pentane $C_5H_{12}$ | 500 | ppm | 3050-2800 | TMB $C_{16}H_{20}N_2$ | 1500 | ppm | |
| | | | | * = Generic libraries used | | | |

Multi-species FTIR analysis was used for monitoring fire toxic gas emissions by the Leeds University toxic gas research group, one of the first fire toxicity groups to use heated FTIR [108-117]. Several other researchers have used FTIR in their studies for analysing combustion products and smoke gases in fires [108-111, 118, 119]. The present GASMET FTIR has MCERT certification for undertaking legislated quality flue gas toxic gas measurements. Detailed guidance has been published for the use of FTIR in measuring fire effluents [120]. The present fire toxicity research complied with the reference manuals and sampling methods for the measurement of toxic fire effluents [97, 121, 122]. However, the work of the Leeds group is one of the few groups using fire raw gas analysis with fully heated gas sampling systems and heated FTIR.

Gas phase FTIR has the potential to measure almost all volatiles, both organic and inorganic gases (where fire gases such as water and most organic species are heated to 180$^{o}$C) on a continuous basis during fire [90]. It is a powerful analytical tool, but requires a significant time investment to achieve reliable quantitative analysis. This kind of spectroscopy technique is used to obtain an infrared spectrum of absorption or emission of gases (raw gases) produced from the combustion process. It simultaneously collects high spectral resolution data over a wide spectral range. It is used to determine time based gas concentration data for a wider range of species (can measure wide variety of gases, up to 60 gases in the present work).

The FTIR detects gaseous compounds based on their absorbance of infrared radiation. Each molecular structure has a unique combination of atoms and will produce a unique infrared spectrum with different wavelengths or wavenumbers. The infrared spectrum is recorded by the FTIR computer (Calcmet software). Figure 3.5 shows an example of a recorded spectrum by the FTIR analyser. The Gasmet FTIR takes a new analysis at 10 Hz, but it is used in the present work time averaged over 2 s so that transient fires can be studied.

The largest concentration of gaseous species measured by FTIR in the present study were carbon monoxide (CO), carbon dioxide ($CO_2$) and water vapour ($H_2O$). Other gases at low concentrations have to have a calibration wavelength that is not coincident with the three large absorption peaks. This is done in many cases by using more than one wavelength in the analysis in the Calcmet software, as shown in the above Table 3.2.

The Paramagnetic Oxygen analyser, shown in Figure 3.4, is used for measuring the Oxygen composition from the fire effluents. Through this analyser, water has been removed from the sample stream by condensation and absorption of the remaining vapour in silica gel.

**Figure 3.4** FTIR and Oxygen analyser.

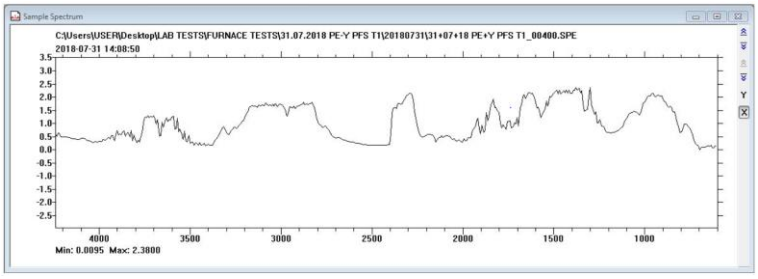


**Figure 3.5** Example of spectrum recorded by the FTIR analyser.

### 3.3.2 Differential Mobility Spectrometer (DMS500)

The Cambustion DMS500 measures the particle size spectral density of aerosol streams from engines and other sources [123]. The advantages of using this size analyser are its fast time response (200 ms $T_{10\text{-}90\%}$ @ 10 Hz), widest size range (from 5 nm to 1 µm or 2.5 µm), widest concentration range (nine orders) and best response sensitivity. The DMS500 used in the present

study is able to measure up to 1000 nm (1 um) diameter particle size with giving two readings in a second (2 Hz). Figure 3.6 shows the overall configuration of the Differential Mobility Spectrometer (DMS500). This equipment measures the particulate size based on electrical mobility. The aerosols produced from the combustion process in the main rig will be charged by an electrical charger when they enter the DMS system. The charged aerosols will then be introduced into the classifier column which contains many stages (the DMS500 used in the study contains 22 stages of classifiers) of size separators. In each stage of size separation has an electrometer that providing a continuous particle size reading to the DMS computer.

DMS 500 operating instructions:

a) Switch on the computer where DMS 500 software is installed.
b) Open the software via CD-R, Cambustion, My V4.11, Start DMS.
c) Select File Dialog: Biomondal_m7_m2cqw21.dmd.
d) Turn on the compressed air (2bar) and the DMS unit (Green bottom on the equipment).
e) Turn the DMS equipment to ON from STAND BY, and wait 30 mins for warming up the DMS equipment.
f) Autozero All after the warming up, and decide where the experiment data should be logged to.
g) Start and stop logging data.
h) After the experiment, turn the equipment from ON to STAND BY, and click EXIT from the FILE MENU.
i) Close the software and shut down the DMS equipment.
j) Turn off the compressed air.

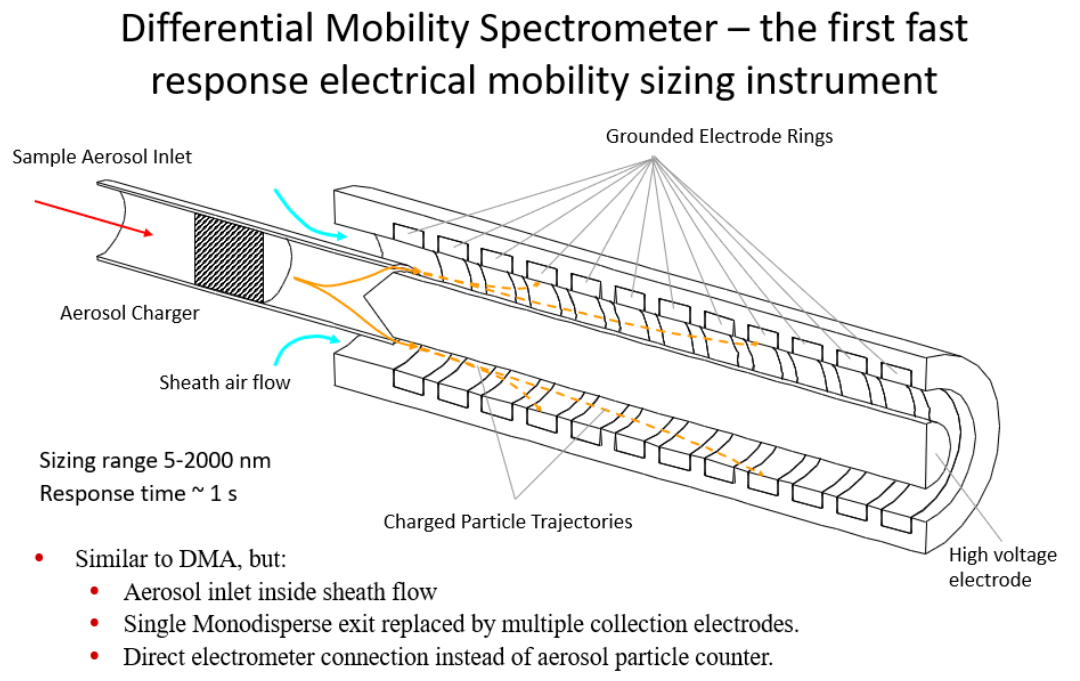


**Figure 3.6** Particle sizer, the DMS500 [124, 125].

The Dekati ELPI particle size analyser has been used by other fire researchers [5, 6, 126-128], this does not have as good a size resolution as the DMS500, particularly for the nano-particles with the greatest toxic health effects. The particles in the sample are measured in the ELPI using aerodynamic size separation on impactors. This consists of several impactor stages (ranges from 10 to 16 stages) arranged vertically. Larger particles are collected on the upper stages and smaller particles are collected on the lower stages.

The DMS500 is used in this research to measure the number of particle over a range of wavelengths to produce the particle size distribution of the diluted products from the fire, using the standard gas sampler on the cone calorimeter diluted products duct . It also can be used to measure solid particles by removing the volatiles using the Dekati thermodenuder. A typical particle size distribution is shown in Figure 3.7.

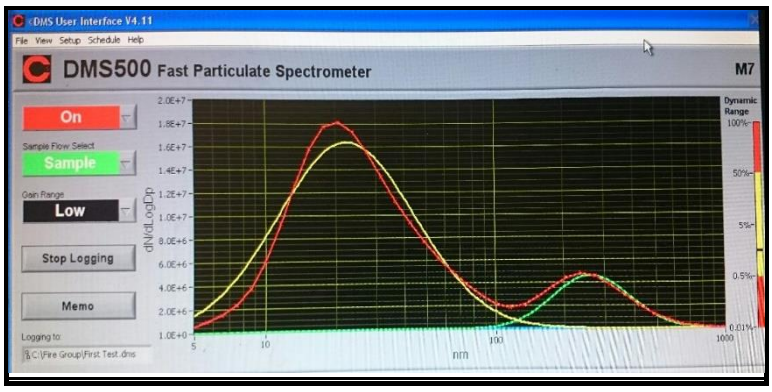


**Figure 3.7** An online graph as shown by the DMS500 computer.

### 3.3.3 Smoke Meter

Figure 3.8 shows the smoke meter equipment for soot mass measurement during the fire tests in the Cone Calorimeter. Particulate total mass emissions was determined by sampling onto a filter paper using raw gas samples from the fire or from the diluted stream. For raw sampling a heated sample system is used to prevent water condensing on the filter. Heating the filter to 50$^{o}$C was used in the present work to collect both solid and liquid particles, from Hydrocarbon condensation. The SAE Smoke Meter sampling system was used in the present work, this was originally developed for Engine Smoke Measuring Equipment. The filter paper is weighed before and after the test and the sample is flowed at 10 LPM through the filter and the sample time recorded so that the measurements in mg/m$^3$ can be determined, which can be converted into a particle yield. A filter paper particle sample can also be used for PAH (Polycyclic Aromatic Hydrocarbons) analysis, but there was not time to do this in the present work. Particulates which are collected from the filter paper (see Figure 3.9) can be analysed by scanning or transmission electron microscope (SEM/TEM) to study the morphology or physical structure of the particulate matters.

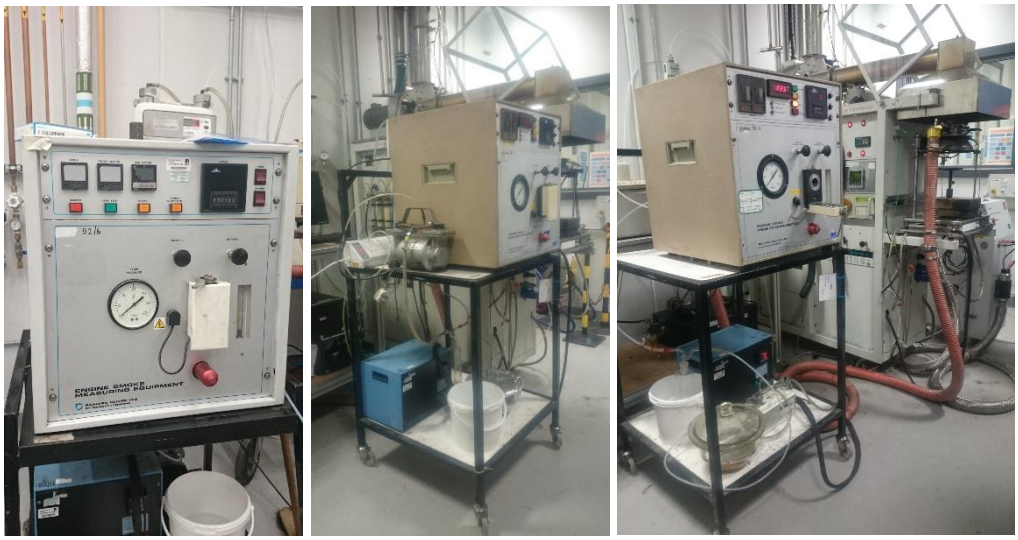

**Figure 3.8** Smoke meter equipment.

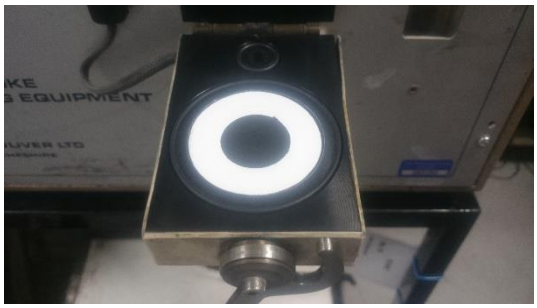

**Figure 3.9** Filter paper in the electrically heat holder after collection of particles. The black circle indicates mainly soot particles. If the volatiles are high the circular spot is brown.

### 3.3.4 Thermodenuder

A Thermodenuder is a highly effective tool to remove Hydrocarbon volatile matter and to produce a soot plus ash sample. If this is combined with the total particle mass measurement then the soot plus ash and the volatile mass fraction of the particles can be determined. The Dekati thermal denuder was available in the present work and was added to the particle sample system on the Cone Calorimeter. Unfortunately there was not time to commission the equipment with the Smoke Meter filter sampler.

The operating principle of the Thermodenuder involves the following steps:

a) The acceptable flow rate of exhaust sample which contains volatile compounds is about 10 to 20 L/min. These volatile compounds are first vaporised in an aerosol heater, which the sample are heated to over 250$^{o}$C with the maximum operating temperature of 300$^{o}$C.
b) After heating, the vaporised compounds are absorbed in active charcoal which has been designed to the form of mats for ease of use or is in the form of easily replaceable filter cartridges when entering the denuder section.
c) The sample is then also cooled in the denuder section using either air or water as cooling media.

The Dekati Thermodenuder was initially designed by the manufacturer for use with the Electrical Low Pressure Impactor (ELPI) and the Dekati Mass Monitor (DMM) but it could also be used with any measurement device with a suitable sample flow rate. This Thermodenuder was used in the present work with the Particle Size Equipment (the DMS500) in diluted sample or exhaust sample measurements for particle size determination. This thermodenuder will allow the DMS500 to measure soot amount produced from the combustion tests. Figure 3.10 shows the configuration of the Dekati Thermodenuder which was installed and reconstructed with the complete fittings and cooling line system. It was planned to use this Thermodenuder with the DMS500 in the Cone Calorimeter tests for comparison of experimental data with and without using the analyser. But due to time constraint, there was no opportunity to perform those tests in the current work. The plan of using this Thermodenuder has been added into the list of future works to be done. The configuration of the newly installed Thermodenuder complete with full fittings is shown in Figure 3.10.

**Figure 3.10** Volatile remover, the Dekati Thermodenuder.

## 3.4 Test Materials

More than 40 materials including electrical cables and polymers were analysed and tested for fire toxicities. All the selected materials are commonly used as building construction and electrical wiring materials. Test materials were grouped based on their type.

Electrical cables were divided into groups:

- PVC cables
- Non-PVC cables:
  Specialist cables: Solar Energy dc cables (supplied by Leeds Solar), Wind Power electrical cables (supplied by Siemens), Low Smoke Zero Halogen (LSZH) cables and other electrical cables.

Polymers were separated to several groups:

- Polyurethane foam
- Polyisocyanurate foam
- Polyethylene
- Polystyrene
- Other polymers:
  a. Glass reinforced plastic (GRP)
  b. Acrylic sheet
  c. PVC pipe
  d. Rubber Butyl

Some of test materials were provided by industrial users and some were bought directly from building material suppliers. Each selected polymer was used in certain application with specific functions. Table 3.3, 3.4 and 3.5 show the list of test materials and their application in buildings.

**Table 3.3** List of PVC electrical cables and their application in building.

| No. | Material | Code | Color | Details of Test Material | Standard | Applications |
|---|---|---|---|---|---|---|
| **PVC Electrical Cables** | | | | | | |
| 1 | PVC Prysmian A | PVC P A | Grey | PRYSMIAN (A) BASEC ELECTRIC CABLE 300/500V BS6004 6242Y 2X60+2.5 H MADE IN UK 2013 | BS6004 6242Y | Standard power cables - Fixed installation in dry or damp premises on wall, boards or trays, in channels or embedded in plaster |
| 2 | Doncaster 2 | DC2 | Grey | BASEC DONCASTER CABLES ENGLAND ELECTRIC CABLE 300/500V BS6004 H6242Y 2X6+2.5 | BS6004 H6242Y | Light industrial and domestic wiring such as meter tails |
| 3 | Twin & Earth Cable 1 | TEC1-G / EC-GB1 | Grey | Twin & Earth Cable 6242YH BS 6004:2012 (SK BASEC ELECTRIC CABLE 300/500 V BS 6004:2012 6242Y 2X10+4 SQMM 2016 H CE P), Max. rating at 240 volts = 52 amps | 6242YH BS 6004:2012 | Suitable for light duty cookers and showers over 7kW |
| 4 | Twin & Earth Cable 3 | TEC3-G / EC-GB2 | Grey | Twin & Earth Cable 6242YH BS 6004:2012 (SK BASEC ELECTRIC CABLE 300/500 V BS 6004:2012 6242Y 2X6+2.5 SQMM 2017 H CE Eca P), Max. rating at 240 volts = 38 amps | 6242YH BS 6004:2012 | Suitable for light duty cookers and showers up to 7kW |
| 5 | Twin & Earth Cable 4 | TEC4-G / EC-GB3 | Grey | Twin & Earth Cable 6242YH BS 6004:2012 (SEVAL KABLO BASEC ELECTRIC CABLE 300/500 V BS 6004:2012 6242Y 2X2.5+1.5 mm2 2016 H CE), Max. rating at 240 volts = 23 amps | 6242YH BS 6004:2012 | Suitable for ring mains and socket outlets |
| 6 | Twin & Earth Cable 5 | TEC5-G / SK1-GB | Grey | 394048 BNS25W25 Twin & Earth Cable 2.5mm2 6242Y Grey 25M BS 6004:2012 (SK BASEC ELECTRIC CABLE 300/500 V BS 6004:2012 6242Y 2X2.5+1.5 SQMM 2017 H CE Eca P) | 6242Y BS 6004:2012 EN 50575:2014 + A1:2016 FLAT&EARTH | Supply of electricity in buildings and other civil engineering works with the objective of limiting the generation and spread of fire and smoke |
| 7 | Twin & Earth Cable 6 | TEC6-G / SK2-GS | Grey | 394046 BNS1W25 Twin & Earth Cable 1.0mm2 6242Y Grey 25M BS 6004:2012 (SK BASEC ELECTRIC CABLE 300/500 V BS 6004:2012 6242Y 2X1+1 mm2 2017 H CE Eca P) | 6242Y BS 6004:2012 EN 50575:2014 + A1:2016 FLAT&EARTH | Suitable for fixed installation in industrial, commercial and domestic premises, installation in wells, on boards, in conduit, trunking or embedded in plaster |

**Table 3.4** List of non-PVC electrical cables and their application in building.

| No. | Material | Code | Color | Details of Test Material | Standard | Applications |
|---|---|---|---|---|---|---|
| **LSZH Electrical Cables** | | | | | | |
| 8 | Prysmian B | P B | Red | PRYSMIAN (B) 2013 HLPCB 0771 FP200GOLD LSOH BS7629-1 BS6387 CWZ EN50200 PH30 PH60 BS8434-1 30MIN 2X15 300/500V BASEC | BS7629-1 BS6387 CWZ EN50200 PH30 PH60 BS8434-1 30MIN | Fire resistance for fire detection and alarm systems, emergency lighting, other essential service circuits |
| 9 | Armoured Marine | AMI G | Grey | ELECTRIC CABLE BS 7917 TYPE SW4 FO 1,5MM/1PR (i) 150/250 V ONTEL IEC 60332-3A & IEC 60331 - 7553 - 0547 m | BS 7917 | Fire resistance - Instrumentation, Power & Control Cable ships and offshore units |
| 10 | Armoured Marine | AMI B | Black | ELECTRIC CABLE BS 6883 TYPE SW4 2,5MM/2C 600/1000 V ONTEL IEC 60332-3A UKODA WB203 - 99527 - 1 | BS 6883 | Instrumentation, Power & Control Cable on ships and mobile offshore units |
| 11 | Standard 6701B | 6701B-W | White | 026 BASEC <HAR> H07Z-K 6701B 2.5SQMM 450/750V CE | BASEC 6701B BS 7211 | Standard normal applications |
| 12 | Twin & Earth Cable 2 | TEC2-W | White | Low Smoke Zero Halogen Twin & Earth Cable 6242B BS 7211:2012 (SK BASEC ELECTRIC CABLE 300/500 V BS 7211:2012 6242B 2X2.5+1.5 mm2 2017 H CE P, Max. rating at 240 volts = 23 amps | 6242B BS 7211:2012 | Suitable for ring mains and socket outlets |
| **Other Electrical Cables** | | | | | | |
| 13 | High Voltage 1 | HV1-4C | Black | BASEC ELECTRICAL CABLE 600/1000 V BS 5467 2015 ATOM KABLO 4X4 mm2 1464m | BS 5467 | Standard power cables |
| 14 | High Voltage 2 | HV2-3C | Black | ebion kablo BASEC ELECTRICAL CABLE 600/1000 V BS 5467 3X6 SQMM 2015 CE 2653m | BS 5467 | Standard power cables |
| 15 | Doncaster 1 | DC1 | Grey | BASEC DONCASTER CABLES ENGLAND BASEC 300/500V 6242Y 2.5 | BASEC 6242Y | Light industrial and domestic wiring such as meter tails |
| 16 | FLEX 1 | FL1-BG | Brown | 3 Core Round Flex 2183Y BS EN 50525-2-11 (HO3VV-F 3G0.5MM2 <VDE> HIGH PROJECT TIME), Max. rating at 240 volts = 3 amps 720 watts | BS EN 50525-2-11 | Suitable for decorative lighting, e.g. brass lamps |
| 17 | FLEX 2 | FL2-W | White | 3 Core Round Flex 3183Y BS EN 50525-2-11 (HO5VV-F 3G1.5MM2 <VDE> HIGH PROJECT TIME), Max. rating at 240 volts = 16 amps 3840 watts | BS EN 50525-2-11 | Suitable for washing machines, dishwashers, extension leads etc |
| 18 | FLEX 3 | FL3-W | White | 3 Core Round Flex 3183Y BS EN 50525-2-11 (HO5VV-F 3G0.75MM2 <VDE> HIGH PROJECT TIME), Max. rating at 240 volts = 6 amps 1440 watts | BS EN 50525-2-11 | Suitable for televisions, videos, HiFi, computers etc |

**Table 3.5** List of polymers and their application in building.

| No. | Material | Code | Color | Details of Test Material | Standard | Applications |
|---|---|---|---|---|---|---|
| **Polymers** | | | | | | |
| 19 | PIR Foam | PIR-F GT | Yellow | Celotex CW4050 RS500 (50mmt), 25mmt | | Grenfell Tower - Test sample (Frame and wall insulation) |
| 20 | PU from Spray Can | PU-FSC | Yellow | 25mmt | | Sealant for joints (e.g. frame) |
| 21 | Polyurethane Sheet | PU-FM | Brown | 20mmt Polyurethane Floor Mat | | Floor mat |
| 22 | PU Foam B | PU-FB | Black | 24 mmt Black Foam for packing material | | As packing material |
| 23 | PS Packaging Material | PS-TV | White | 23mmt PS type of TV packaging material | | Packaging material for TV |
| 24 | Polystyrene Sheet | PS-CB | White | 3mm Polysyrene bonded with Cardboard - 18% reducting heat (PS faces up) | | Wall insulation |
| 25 | Polystyrene Sheet | PS-CB2 | White | 3mm Polysyrene bonded with Cardboard - 18% reducting heat (Cardboard faces up) | | Wall insulation |
| 26 | Polystyrene Sheet | PS2 | White | 2mm Polystyrene Sheet - 13% heat reduction | | Wall insulation |
| 27 | Clear Polystyrene Sheet | CPS2 | Clear | 2mm Clear Polystyrene - ariel | | Clear door/window |
| 28 | Clear Polystyrene Sheet | CPS4 | Clear | 4mm Clear Polystyrene (melting with the heat of sawing) | | Clear door/window |
| 29 | Polystyrene Coving | PS Cove | White | Arthouse: Quality Polystyrene Coving | | Roof, ceiling |
| 30 | PS Skirting Board | SB-W H | White | Hard skirting board | | Roof |
| 31 | PS Packaging Material | PM-G | Green | Instrument packaging material | | Packaging material for flowmeter @ instrument |
| 32 | PE Blue | PE-BE | Blue | 9mmt | | Liquid storage |
| 33 | PE Black | PE-BK | Black | 9mmt | | Liquid storage |
| 34 | PE Yellow | PE-Y | Yellow | 9mmt | | Liquid storage |
| 35 | PE Storage Box | SB-P | Purple | Storage Box | | For storage purpose |
| 36 | PE Pipe | PEP15 | White | 15mm OD PE Tube | | Piping (water pipe) |
| 37 | Glass Reinforced Plastic | GRP | Blue | 9mmt | | Liquid storage |
| 38 | PMMA-B | PMMAB | Black | 18mmt | | Perspex |
| 39 | Acrylic (Liteglaze) Sheet | CA-B | Clear | 2mm Clear Acrylic (Liteglaze) | | Clear door/window |
| 40 | PVC Square Tube | ST | White | 20mm Square Tube | | Cable trunking |
| 41 | Polypropylene Rope | PPR10 | Yellow | Syneco 10mm Polypropylene Rope, 10 metres, 260kg maximum safe working load | | For lifting purpose |
| 42 | Cable Trunk | CT | Grey | Control Panel Trunking (Betaduct Halogen-Free) NH510E BS EN ISO 4589-2:1999 BS 6853 | NH510E BS EN ISO 4589-2:1999 BS 6853 | Public buildings such as shopping centres, hospitals, airport terminals, etc |
| 43 | Rubber Butyl Sheet | RBS | Black | | | Ferrybridge - Test sample |
| 44 | Rubber Butyl Crumbs 1 | RBG | Black | 3mm thk Butyl ground with P24 grit disc / 11000 rpm | | Ferrybridge - Test sample |
| 45 | Rubber Butyl Crumbs 2 | RBG-B | Black | Ground 3mm butyl from bonded steel sheet using Bostik 2 part adhesive + primer hand -grinder P24 grit | | Ferrybridge - Test sample |
| 46 | Lamp1-C | L1C | Clear | Flood light | | Ferrybridge - For lighting |
| 47 | Lamp2-Y | L2Y | Yellow | Flood light | | Ferrybridge - For lighting |

### 3.4.1 Sample Preparation Before Test for the Cone Calorimeter

Each sample was cut to fit the space of 100 mm width and 100 mm length in the sample holder as shown in Figure 3.11 and Figure 3.12.

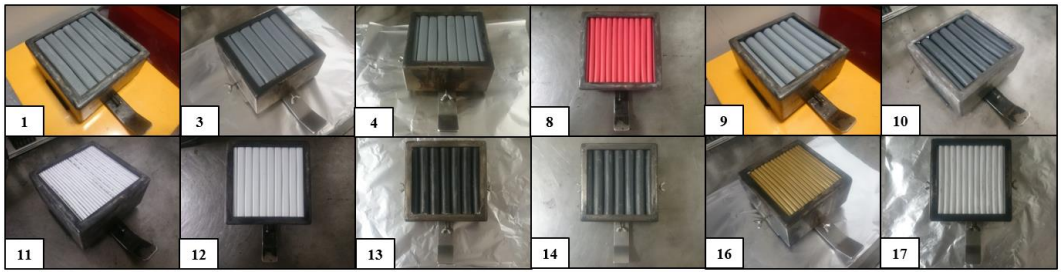


**Figure 3.11** Electrical cable samples in sample holder.

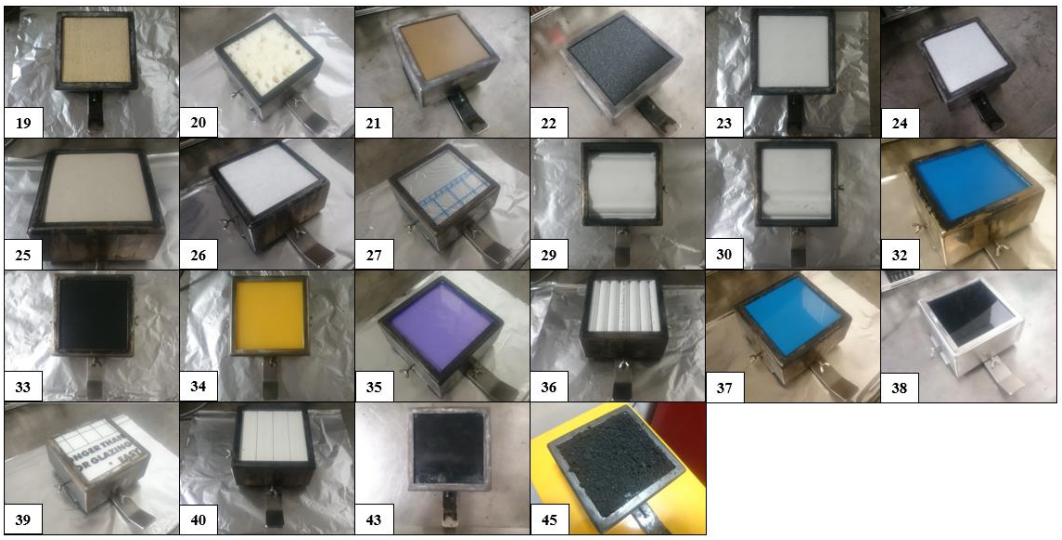


**Figure 3.12** Polymer samples in sample holder.

### 3.4.2 Sample Preparation for Pre and Post Analysis

All solid samples for elemental and TGA analysis were ground into a uniform composition powder using a Cryomil. Figure 3.13 shows a picture of the Cryomill and the tools used to grind the samples. For larger size of samples, they were crushed first to smaller size using the crushing machine shown in Figure 3.1, before being ground.

**Figure 3.13** Cryomill used to grind samples.


**Figure 3.14** Crushing machine and ball mill PM100.

## 3.5 Pre and Post Analysis Equipment

Various pre and post analysis were done before and after the fire tests to determine the chemical composition and properties of sample materials and the char remaining at the end of the tests. Proximate (by TGA) and ultimate (by elemental analysis) data were determined for all the samples as summarised in Table 3.11.

Raw polymer samples were initially ground and prepared in powder form before the TGA and elemental analysis took place, as shown in Figure 3.15. In the present work, about 50 polymers including electrical cables were analysed and had been grouped in several groups (PVC, PU, PIR, PE, PS, others) for comparison of results. Material groups and empirical formula for each group are shown in Table 3.6.

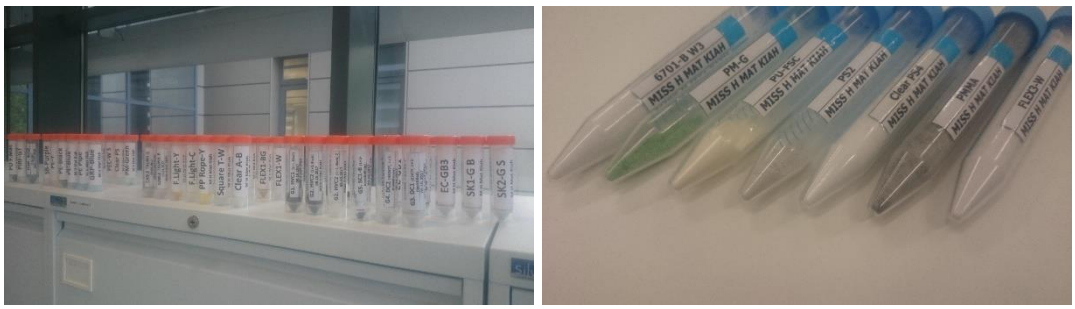

**Figure 3.15** Ground polymer samples in powder form.

**Table 3.6** Chemical formula for various groups of polymers.

| **Material Group** | **Short Name** | **Empirical Formula** | **$CH_yO_zN_w$** | **Stoichiometric $A/F_{mass}$** |
|---|---|---|---|---|
| Polyvinyl Chloride | PVC | $(C_2H_3Cl)_n$ | $CH_{1.5}Cl_{0.5}$ | 5.5 |
| Polyisocyanurate | PIR | $C_3H_3N_3O_3$ | CHNO | 2.4 |
| Polyurethane | PU | $C_{27}H_{36}N_2O_{10}$ | $CH_{1.33}O_{0.37}N_{0.074}$ | 5.2 |
| Polystyrene | PS | $(C_8H_8)_n$ | CH | 13.3 |
| Polyethylene | PE | $(C_2H_4)_n$ | $CH_2$ | 14.8 |
| Poly(methyl methacrylate) | PMMA | $(C_5O_2H_8)_n$ | $CH_{1.6}O_{0.4}$ | 8.3 |
| Polyacrylic | PAA | $(C_3H_4O_2)_n$ | $CH_{1.33}O_{0.67}$ | 5.7 |
| Polyacrylate | PAC | $(C_3H_3NaO_2)_n$ | $CHO_{0.67}Na_{0.33}$ | 4.0 |
| Polypropylene | PP | $(C_3H_6)_n$ | $CH_2$ | 14.8 |

### 3.5.1 CHNS-O Analyser

The elemental analysis was carried out using a CHNS-O analyser which provides weight percentage of Carbon, Hydrogen, Nitrogen, Sulphur and Oxygen. This analyser does not analyse for Oxygen, but assumes that the missing mass is Oxygen. For PVC compounds it is assumed that the missing mass is Chlorine. 40+ polymer samples including various types of electrical cables had elemental analysis undertaken. Samples were crushed or grinded before weighted and prepared properly in a silver capsule (see Figure 3.16), then they were mixed with oxidiser and burnt in a reactor at 1000$^{o}$C. The

combustion products were then carried by a constant flow of Helium gas to a packed column, and quantified with a thermal conductivity detector (TCD) at 290$^{o}$C which gave an output signal proportional to the concentration of the individual elements of the sample, with C, H, N and S content determined. For PVC type materials the rest of sample weight was assumed as Chlorine (Cl), meanwhile for other samples the rest of weight was assumed as Oxygen (O). Composition of elements obtained from this analysis were used to determine the chemical formula for each test material. The results for all the materials are in Table 3.11.


**Figure 3.16** Thermo EA2000.

### 3.5.2 Thermo-Gravimetric Analyser (TGA)

Thermo-Gravimetric Analysis (TGA) determines the weight loss as a function of temperature in a flow of Nitrogen. It was used to measure the moisture ($H_2O$), volatile Hydrocarbons, fixed Carbon and dry ash. The sample size tested was between 2 and 50 mg (at least the most minimum of 1 mg of

sample needed if only small amount of sample is available) [129]. Figure 3.17 shows the configuration of the TGA-50 Shimadzu with a TA60WS processor that was used in the study for the proximate analysis of the materials.

**Figure 3.17** Shimadzu TGA-50.

Analysis was run by the TGA following the steps which was set initially in the TGA software. The details of test procedure are as follow:

a) Initially, the sample was heated up from the ambient temperature to 110$^{o}$C at the heating rate of 10$^{o}$C/min under nitrogen atmosphere which flows at 50 mL/min. The sample was held up at 100$^{o}$C for 10 minutes to remove completely the moisture content from it. The mass of the moisture in the sample was then determined by measuring the weight loss of the sample.

b) After that, the sample temperature (110$^{o}$C) was increased to 910$^{o}$C at the heating rate of 25$^{o}$C/min and was held up again for 10 minutes in order to measure the weight of the volatile loss.

c) Determination of fixed carbon of the sample was then done by introducing the air at a temperature of 920$^{o}$C, which allowed the $O_2$ to react with the fixed carbon in the char. Therefore, the fixed carbon content of the material was obtained by measuring the mass loss. In addition, the dry ash which was left was also measured as the mass difference.

### 3.5.3 Bomb Calorimeter

The Bomb Calorimeter is shown in Figure 3.18 and was used to determine the calorific value of the test materials. From the analysis, normally high Hydrocarbon (HC) content of materials produced high calorific (CV) values. For fire retardant or fire resistance materials, the CV values were lower. Following are the procedures used for the Bomb Calorimeter analysis.

1) Sample preparation and weighing process

a) Sample was weighted with 5-figure mass balance between 0.25 to 0.33 g. Sample mass <0.3 g is recommended for slow burning materials or less HC contained materials.
b) The weighted sample then pressed using the Presser (see Figure 3.18) to transform powder into the pellet or pill form. Safety glass should be worn when using the Presser. Valve was closed when pumping the pressure. Pumping pressure should not exceed 4 bar to standardise the formed pellet. Samples formed by the Presser is shown in Figure 3.19.

2) Analysis steps with the Bomb Calorimeter (BC)

a) Flow valve from the main cylinder was turned on to let $O_2$ flow to the Bomb Calorimeter line system.
b) For sample placement in the pressure vessel (PV), U-shape wire for ignition was formed and hanged with its curved end closest to the sample in the crucible bowl but not touching the sample.
c) PV wall then wetted with ~10 mL deionised water. The surrounding o ring of the PV closure was also wetted. The closure was lifted by holding the PV valve and was placed on top of the PV to close and seal it tightly. Then, valve was closed by twist it softly.
d) Then, PV valve was connected to allow the flow of the $O_2$ into the PV. To start the $O_2$ filling, $O_2$ fill button was pressed on the BC screen. The process normally took about 60 s for $O_2$ to completely filled the PV. The sound of pressure relief was the sign of $O_2$ filling completion.
e) The BC water bucket was filled with exact before was placed into the BC correctly on the position with ensuring it did not touch the BC wall.
f) Special lifter or holding tool was used to hold and lift the PV into the bucket inside the BC. Leakage check by observing any bubble formation was done to ensure no leakage on the PV.

g) After that, the thermocouple was placed into the holes on the PV without touch the water in the bucket. BC door then was closed slowly and carefully. Thermocouple wires was repositioned to ensure it did not too close or touch the stirrer inside the BC.
h) Prior to start test, the details of the test should be entered. Spike mass was set to 0 and sample weight was also entered.
i) Pressure inside the PV is ~40bars. So to release the pressure after the test the PV should be placed inside the fume cupboard. This process was done slowly and carefully to release it little by little by opening the PV valve.

3) Tidy up after the test

a) Mass balance was off and water was emptied from the BC bucket.
b) All used crucibles from the sample residue was cleaned with wet paper towel.
c) All apparatus was kept in the appropriate storage place or drawer. PV closure was placed into the plastic container which was filled with deionised water and its top was covered with the glass saucer.


**Figure 3.18** Bomb Calorimeter – Parr 6200.

**Figure 3.19** Samples formed by the presser.

### 3.5.4 Scanning Electron Microscopy (SEM)

SEM produced a magnified image of a sample through a scanning process by the electron beam. Hitachi SU8230 FESEM is shown in Figure 3.20. Other than SEM Hitachi, the SEM Carl Zeiss was also available at the University of Leeds for the same image analysis. Through SEM analysis, size, shape, texture and composition of the sample were determined. Figure 3.21 shows the spectrums and image from SEM analysis. From Figure 3.21, the Spectrum 35 and Electron Image 10 were produced by the SEM Carl Zeiss for PVC Prysmian A raw sample. The Electron Image 19 was produced by the SEM Hitachi for PE-Y raw sample. Figure 3.21 shows that the elements in the sample can be determined, which was used for the determination of presence of elements in fire retardants.

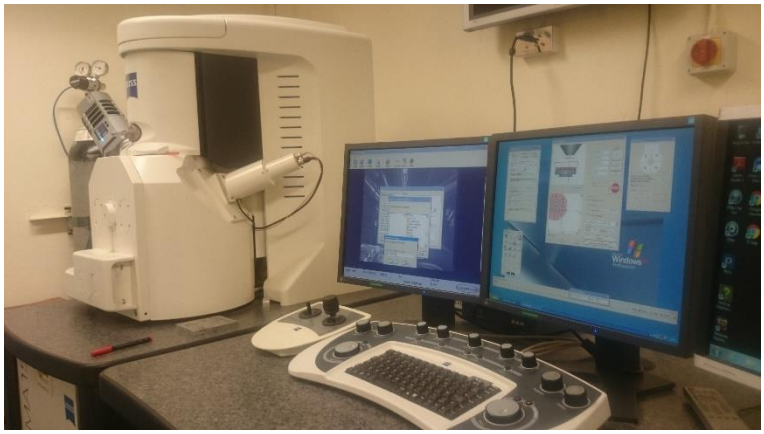

**Figure 3.20** Photo of SEM Hitachi SU8230 FESEM.

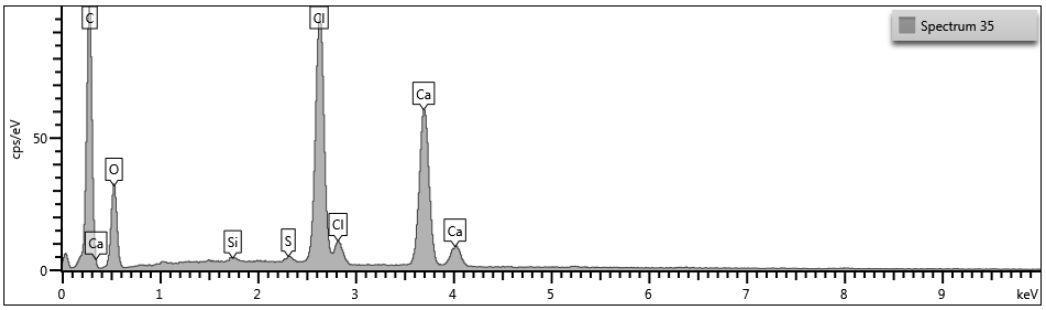

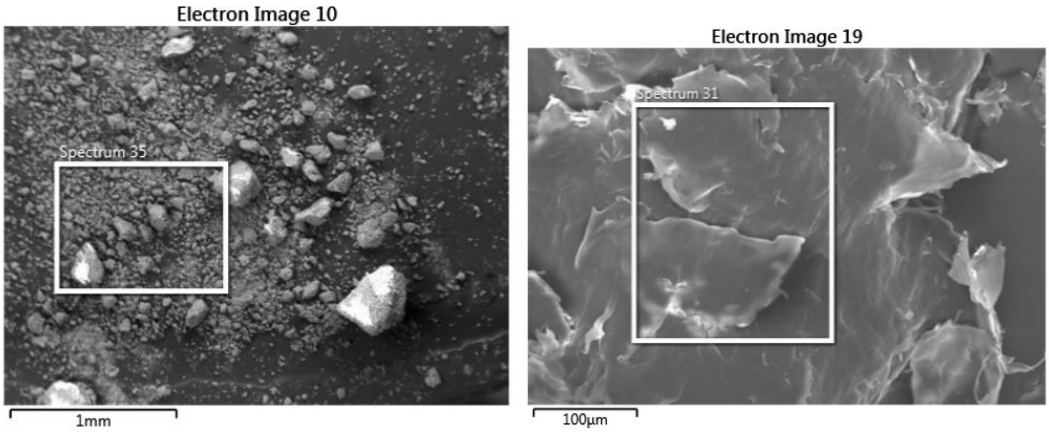


| SEM Carl Zeiss | | | SEM Hitachi | | |
|---|---|---|---|---|---|
| PVC Prysmian A Cable (Raw) | | | PE-Y (Raw) | | |
| Element | Wt% | Wt% Sigma | Element | Wt% | Wt% Sigma |
| O | 47.07 | 0.34 | C | 100 | 0 |
| Si | 0.35 | 0.04 | | | |
| S | 0.5 | 0.05 | | | |
| Cl | 25.81 | 0.2 | | | |
| Ca | 26.27 | 0.21 | | | |
| Total: | 100 | | Total: | 100 | |

**Figure 3.21** Spectrums and image from SEM analysis.

### 3.5.5 Gas Chromatography (GC-MS)

Future work is planned using pyrolysis Gas Chromatography with Mass Spectrometry species detection. The filter paper particulate samples are put into the pyrolysis unit and rapidly heated, which devolatilises the particles. The pyro probe unit is places at the head of the capillary column so devolatilised components are condensed there and can be separated by Gas Chromatography to measure the composition of the volatile fraction of particulate material. This includes the cancer formatting PAH component.

## 3.6 Calculations and Data Interpretations

Analysis of experimental data from the Cone Calorimeter and Purser Furnace tests including pre and post analysis data involves many calculations in order to present the results in mass yield terms. In this section the calculations and formulas used are presented which include the determination of the chemical formula of the test materials from the elemental analysis, the use of this for the calculation of the air to fuel ratio by mass and then the fire equivalence ratio. The heat release is calculated by oxygen consumption for both the Cone Calorimeter raw gas sample and for the mean diluted gas composition. The difference is the heat release in the dilution process. The conversion of the toxic gases from volume concentration measurement to mass and then to

yield is detailed. The toxicity concentrations are converted into relative concentrations normalised to the toxic limit for that gas and then summated to get the total toxicity. Normalising each species normalised toxicity to the total normalised toxicity gives the contribution of each species to the total toxicity. The conversion of number volume concentration data to mass concentration and yields is detailed, together with the conversion of particle number to mass and then the summation to give a measure of the total particulate mass yield. This can then be compared with mass yields converted from smoke obscuration measurements.

### 3.6.1 Determination of Sample Chemical Formula

In 3.5.1 the CHNS-O analyser described that was used to determine the elemental analysis of each test sample in weight percentage (wt.%) for Carbon, Hydrogen, Nitrogen and Sulphur with an assumption that the balance percent was either Oxygen for non PVC samples or Chlorine for PVC samples (CHNS-O or CHNS-Cl). The results are shown in Table 3.11 for all the materials tested. The mole ratio of each atom or element in the substance were determined by dividing the weight percentage of each element to its molecular weight as shown in Equation 2. This mole ratio of the atoms becomes the subscripts in the chemical formula of the substance that correspond to that element.

$$n = \frac{m}{M} \qquad (2)$$

where,

n is the molar ratio for each element (C, H, N, S and O or Cl), m is the weight percentage of each element (wt.%) and M is the molecular weight of each element (g/mol).

Chemical formula determination for *PVC Prysmian A electrical cable* sample;

Weight percentage of each element, C = 35.83 %, H = 3.84%, N = 0.00% and S = 0.00%. For PVC type of materials, the balance percentage is assumed as Cl which 60.53%.

Molecular weight of each element, C = 12 g/mol, H = 1 g/mol, N = 14 g/mol, S = 32 g/mol and Cl = 35.45 g/mol.

Molar ratio for each element, C = 1, H = 1.29, N = 0, S = 0 and Cl = 0.57.

The chemical formula for *PVC Prysmian A electrical cable* sample, $CH_{1.29}Cl_{0.57}$. The element composition and chemical formula for all test samples are summarised in Table 3.11.

### 3.6.2 Air to Fuel Ratio (AFR) and Equivalence Ratio, Φ (ER)

The stoichiometric AFR by mass for a combustion process was determined by Carbon balance. Pure Hydrocarbons can be treated as $CH_y$ where y is the H/C molar ratio.

$CH_y + a\ O_2 \rightarrow b\ CO_2 + c\ H_2O$

This is in volume units (*molar units or mols).*

Carbon balance gives 1 = b, Hydrogen balance gives y = 2c, Oxygen balance gives a = b + c/2 = 1 + y/4 and Oxygen/Fuel by volume = 1 + y/4.

$$Fuel\ concentration\ by\ volume = \frac{Fuel}{(Fuel + Oxygen)} \qquad (3)$$

Divide through by Fuel,

Fuel concentration = 1/ [1+(1 + y/4)] = 33.3% for y=4.

To convert from volume to mass ratios,

$$(Oxygen/Fuel)_{Mass} = \frac{[(Oxygen/Fuel)_{Volume}][(2)(16)]}{[12+y]} = \frac{\left[(1+\frac{y}{4})(32)\right]}{[12+y]} \qquad (4)$$

For y = 4 this gives 4 kg/kg, for y = 2 this gives 3.43 kg/kg and for y = 1 this gives 3.08 kg/kg.

We are usually more interested in combustion in air and all we have to do to convert the above into Air/Fuel ratios is to utilise the fact that there is 20.9% oxygen in air by volume and 23.2% by mass. Also 4.31 kg of air is required to give 1 kg of Oxygen to the fire.

The proof of the mass concentration of Oxygen in air is below (Equation 5).

$$\text{Average molecular weight, M of air}$$

$$= \left[0.791\ \frac{\text{mol } N_2}{\text{mol air}}\ \text{x}\ 28\ \frac{\text{g } N_2}{\text{mol } N_2}\right] + \left[0.209\ \frac{\text{mol } O_2}{\text{mol air}}\ \text{x}\ 32\ \frac{\text{g } O_2}{\text{mol } O_2}\right]$$

$$= 22.148 \frac{\text{g } N_2}{\text{mol air}} + 6.688 \frac{\text{g } O_2}{\text{mol air}}$$

$$= 28.836 \frac{\text{g}}{\text{mol air}}$$

Oxygen mass by mass in air

$$= \frac{6.688 \text{ g } O_2}{28.836 \text{ g air}}$$

$$= 0.232 \frac{\text{g}}{\text{g}} @ \frac{\text{kg}}{\text{kg}} \quad (5)$$

Air/Fuel ratios for a general Hydrocarbon $CH_y$.

$$(Air/Fuel)_{Volume} = [(Oxygen/Fuel)_{Volume}] \left[\frac{1}{0.209}\right] = \frac{\left(1 + \frac{y}{4}\right)}{0.209} \quad (6)$$

For y = 4 this gives 9.57 as previously shown for Methane, the fuel concentration [Fuel/(Fuel + Air)] as 9.46%.

For higher Hydrocarbons the volume ratio for the fictitious $CH_y$ fuel has to take into account the real Carbon number, n. The fuel is really $n(CH_y)$, where n is the Carbon number.

e.g. For Propane ($C_3H_8$) with H/C = 2.67 the above equation gives the air/fuel by volume for $CH_{2.67}$ as 7.98, but this should be multiplied by 3 to give a ratio of 23.94. This then gives a fuel concentration in air + fuel of 4.01%.

Air/Fuel ratios by mass for a general Hydrocarbon $CH_y$.

$$(Air/Fuel)_{Mass} = [(Oxygen/Fuel)_{Mass}] \left[\frac{1}{0.232}\right] = \frac{\left[\left(1 + \frac{y}{4}\right)(32)\right]}{[12 + y]} \Big/ 0.232$$

$$= 137.93 \frac{\left(1 + \frac{y}{4}\right)}{(12 + y)} \quad (7)$$

For y = 4 this gives 17.24 as previously shown for Methane, for y = 2 this gives 14.78 (Polyethylene) and for y = 1 this gives 13.26.

Thus for all Hydrocarbons the stoichiometric A/F by mass varies only between about 13 and 17, whatever the Hydrocarbon. An average value of 15 is often used for any Hydrocarbon combustion.

Hydrocarbon polymers are a common fire load and are a major topic in this research.

$$Stoichiometric\ (Air/Fuel)_{Mass} = 137.93\frac{\left(1+\frac{y}{4}\right)}{(12+y)} \quad (8)$$

**Table 3.7** Stoichiometric A/F by mass for various Hydrocarbons.

| Polymer | Formula | y = H/C | Stoichiometric A/F (by mass) |
|---|---|---|---|
| Poly α-methyl styrene | $C_9H_{10}$ | 1.1 | 13.4 |
| Polyisoprene | $C_5H_8$ | 1.6 | 14.2 |
| Polyisobutylene | $C_4H_8$ | 2 | 14.8 |
| Polystyrene | $(C_8H_8)_n$ | 1 | 13.3 |
| Polypropylene | $(C_3H_6)_n$ | 2 | 14.8 |
| Polyethylene | $(CH_2)_n$ | 2 | 14.8 |
| Polymethylene | $(CH_3)_n$ | 3 | 16.1 |
| Polydivinyl benzene | $C_{10}H_{10}$ | 1 | 13.3 |
| Polybenzyl | $C_7H_7$ | 1 | 13.3 |

General formula for a HCO combustion = $C_\alpha H_\beta O_\gamma$.

This would normally be expressed in terms of H/C and O/C ratios using y = H/C and z = O/C as $CH_yO_z$.

$CH_yO_z + a\ O_2 \rightarrow b\ CO_2 + c\ H_2O$

This is in volume units (molar balance). Carbon balance gives 1 = b, Hydrogen balance gives y = 2c and Oxygen balance gives z + 2a = 2b + c = 2 +y/2. Thus, a = [(2 + y/2) – z] / 2.

$$(Oxygen/Fuel)_{Volume} = \frac{\left[\left(2+\frac{y}{42}\right)-z\right]}{2} \quad (9)$$

$$(Oxygen/Fuel)_{Mass} = \{[(2+y/2)-z]/2\}\left[\frac{(2)(6)}{(12+y+16z)}\right] \quad (10)$$

$$(Air/Fuel)_{Mass} = \{[(2+y/2)-z]/2\}\left[\frac{(2)(6)}{(12+y+16z)}\right]\left(\frac{1}{0.232}\right)$$

$$= \frac{\left[\left(2+\frac{y}{2}\right)-z\right](68.97)}{(12+y+16\,z)} = \frac{\left[\left(1+\frac{y}{4}\right)-\frac{z}{2}\right](137.94)}{12+y+16z} \quad (11)$$

Many polymers have a HCO composition and these are common fire loads.

Polymethylmethacrylate (PMMA) n($C_5H_8O_2$) > $CH_{1.60}O_{0.40}$, $(Air/Fuel)_{Mass}$ = 8.28. Polymethyl acrylate (PMA) n($C_4H_6O_2$) > $CH_{1.5}O_{0.5}$, $(Air/Fuel)_{Mass}$ = 7.27. Polyethylene oxide n($C_2H_4O$) > $CH_2O_{0.5}$, $(Air/Fuel)_{Mass}$=7.84.

It may be shown using similar methods as for CHO that a general formula for CHON materials is,

$$(Air/Fuel)_{Mass} = \left\{ \frac{\left[\left(1+\frac{y}{4}\right)-\frac{z}{2}-\frac{w}{4}\right](137.94)}{12+y+16z+14w} \right\} \qquad (12)$$

where, w = N/C.

A common CHON fire load is Polyurethane foam and this is studied in the present work. The elemental formula is $CH_{1.74}O_{0.323}N_{0.07}$ (Gottuk and Roby, 1995) [130].

The stoichiometric A/F may be shown from the above formula to be an A/F of 8.71 (this compares with 8.78 in the SFPE Handbook). Table 3.11 shows the elemental analysis of two PU foam samples in the present work and the stoichiometric A/F was 8.45 and 8.99, which are slightly different from that for pure PU foam and this indicates that these foams are not entirely pure PU.

Similarly Chlorine is a common fire load particularly in PVC in electrical wiring, this means CHONCl 5 element fire loads are possible.

The formula for the stoichiometric A/F is now:

$$(Air/Fuel)_{Mass} = \left\{ \frac{\left[\left(1+\frac{y}{4}\right)-\frac{z}{2}-\frac{w}{4}-\frac{k}{4}\right](137.94)}{12+y+16z+14w+35.45k} \right\} \qquad (13)$$

where k=Cl/C.

e.g. PVC $CH_{1.5}Cl_{0.5}$, k = 0.5, y = 1, z and w = 0.

Stoichiometric A/F by mass for PVC = 155.18/30.725 = 5.05.

This is quite different than the ~15/1 stoichiometric A/F for say a Polypropylene electrical cable insulation. The present PVC materials in Table 3.11 have a stoichiometric A/F of 2.74 – 5.12, and the difference from 5.05 for

pure PVC indicates that these PVC electrical cables are, apart from the one at stoichiometric 5.12, not pure PVC and have other materials added. These materials generally give rise to an ash fraction as shown in Table 3.11. A formal proof of the stoichiometry for PVC is given below.

From the burning of PVC materials, the main products of complete combustion are carbon dioxide ($CO_2$), Hydrogen chloride (HCl) and water ($H_2O$). Example the balanced chemical reaction for *PVC Prysmian A electrical cable* fire as follows;

$CH_{1.29}Cl_{0.57} + 1.18O_2 \rightarrow CO_2 + 0.57HCl + 0.36H_2O$ (complete combustion)

From the chemical reaction, 1.18 molar $O_2$ is consumed to burn 1 molar fuel. So, the $O_2$ to fuel ratio is 1.18 (volume/volume, v/v) and converted to (mass/mass, m/m) by multiplying each element with molecular weight, M (refer Equation 2);

Total $O_2$ mass = 1.18 x (16 g/mol x 2 mol) = 37.76 g

Total fuel ($CH_{1.29}Cl_{0.57}$) mass = 1 x [(12 g/mol x 1 mol) + (1 g/mol x 1.29 mol) + (35.5 g/mol x 0.57 mol)] = 33.53 g

$O_2$ to fuel ratio, 1.13 (g/g) or (m/m).

Stoichiometric AFR is obtained by dividing $O_2$ to fuel ratio (1.13 g/g) with $O_2$ to air ratio (0.232 g/g) which equal to 4.86 for the *PVC Prysmian A electrical cable fire*. All calculated stoichiometric AFR for polymers are in Table 3.11.

The actual AFR and equivalence ratio (ER) in the present work is determined from the gas composition using Chan's equation [57] by the Carbon balance method with referring to CO, $CO_2$ and THC concentration (vol.% in wet basis) produced from the FTIR measurement. Chan's equation uses CO and $CO_2$ measurements on a dry basis, as it was derived for automotive use where dry NDIR measurements are used. The concentration value in ppm was converted to vol.% by multiplying it with $10^{-4}$ and the value in vol.% is then multiplied with $10^{-2}$ to get in mole fraction, while the wet basis concentration of gases measured by the FTIR are also corrected to the dry basis using following Equation 14.

$$X_{\mathrm{i}}\ \mathrm{wet} = (1 - X_{H_2O}\ \mathrm{wet})\ (X_{\mathrm{i}}\ \mathrm{dry})$$

$$(X_{\mathrm{i}}\ \mathrm{dry}) = \frac{X_{\mathrm{i}}\ \mathrm{wet}}{(1 - X_{H_2O}\ \mathrm{wet})} \quad (14)$$

where,

$X_{\mathrm{i}}$ dry is the dry mole fraction of species i, $X_{\mathrm{i}}$ wet, is the wet mole fraction of species i and $X_{H_2O}$ wet is the wet mole fraction of water vapour measured by the FTIR.

Detailed of Chan's equation is shown in Equation (15). Oxygen changes during a fire representing the Oxygen consumption by the burning material and it is measured by the paramagnetic Oxygen analyser (in volume percentage, vol.% and dry basis) that receives the gases from the FTIR analyser outlet after drying. The dry mole fraction $O_2$ would be used in the Chan's equation to calculate the actual AFR and ER values. Another way to determine the actual AFR and ER is based on the fuel and air flow mass measurements on the test rig. This is difficult on a transient basis, whereas the fast response FTIR gives time resolution of the A/F of the fire.

Given an example of chemical formula determined from the elemental analysis by the CHNS-O analyser is $C_\alpha H_\beta O_\gamma N_\delta S_\varepsilon$ with α is number of mole for element C, while β, γ, δ and ε are for element H, O, N and S as calculated using Equation 2.

$$AFR_{Chan} = \left[\frac{138.324}{12.011\alpha + 1.008\beta + 15.999\gamma + 14.007\delta}\right] \mathrm{x}$$
$$\left[\frac{\alpha A_1 - \gamma + \left(\frac{\beta \mathrm{K}(CO_2)}{2A_2}\right) - \left(\frac{\alpha A_3 A_4}{2A_2}\right)}{2.0038 + A_5 - \left(\frac{A_5 \mathrm{K}(CO_2)}{A_2}\right) + \left(\frac{0.0019 A_3\ A_4}{2A_2}\right) - 0.0019\ A_1}\right]$$

where,

$$A_1 = \frac{[CO] + 2[CO_2] + 2[O_2] + [NO] + 2[NO_2]}{[CO] + [CO_2] + [HC]}$$

$$A_2 = K[CO_2] + [CO]$$

$$A_3 = \frac{K[CO_2]}{[CO]\{[CO] + [CO_2] + [HC]\}}$$

$$A_4 = x[HC][CO]$$

$$A_5 = 4.7755 \frac{P_v}{P_A - P_v} \quad (15)$$

$x$ is H to C ratio for the fuel type, [ ] is volumetric concentration of specified species (CO, $CO_2$, $O_2$ and HC) in %, $P_A$ is atmospheric pressure (atm) and $P_v$

is pressure of water vapour (atm). $A_5$ is determined by considering the following calculations with $P_A$ = 1 atm (1.01325 x $10^5$ Pa).

$P_v = \frac{R}{P_w}$ which R is 0.6 (Relative humidity) and $P_w$ is calculated by using the Antoine equation [131],

and,

$$log_{10}P_w = A - \frac{B}{C+T} = 8.07131 - \frac{1730.63}{233.426 + 20} = 1.242 \quad (16)$$

Antoine Constants for water;

**Table 3.8** Antoine Constants for water.

| $T_{low}$ (°C) | $T_{high}$ (°C) | A | B | C |
|---|---|---|---|---|
| 1 | 99 | 8.07131 | 1730.63 | 233.426 |
| 100 | 374 | 8.14019 | 1810.94 | 244.485 |

*T is taken as 20°C (water temperature) and $P_w$ is in mmHg

$$P_w = P_s = 10^{\left(A - \frac{B}{C+T}\right)} = 17.473\ mmHg = \frac{17.473}{(760)(10^5)} = 2299\ Pa$$

From the actual $AFR_{Chan}$ that determined using Equation 15, the actual equivalence ratio, Φ (ER) then can be also determined by dividing the stoichiometric AFR value with the actual AFR value as in Equation 17. The general formula for ER determination was also included in Chapter 2 (Equation 1). In the present work, the set or metered ER for restricted ventilation tests and the ER by Chan method are both referred.

$$\text{Equivalence Ratio, } \phi = \left[\frac{(\text{FAR})_{\text{Actual}}}{(\text{FAR})_{\text{Stoichiometric}}}\right] = \left[\frac{\left(\text{m}_{\text{Fuel}}/\text{m}_{\text{O}_2}\right)_{\text{Actual}}}{\left(\text{m}_{\text{Fuel}}/\text{m}_{\text{O}_2}\right)_{\text{Stoichiometric}}}\right] = \left[\frac{\left(\text{n}_{\text{Fuel}}/\text{n}_{\text{O}_2}\right)_{\text{Actual}}}{\left(\text{n}_{\text{Fuel}}/\text{n}_{\text{O}_2}\right)_{\text{Stoichiometric}}}\right] = \left[\frac{(\text{AFR})_{\text{Stoichiometric}}}{(\text{AFR})_{\text{Actual}}}\right] = \left[\frac{\left(\text{m}_{\text{O}_2}/\text{m}_{\text{Fuel}}\right)_{\text{Stoichiometric}}}{\left(\text{m}_{\text{O}_2}/\text{m}_{\text{Fuel}}\right)_{\text{Actual}}}\right]$$

$$= \left[\frac{\left(n_{O_2}/n_{Fuel}\right)_{Stoichiometric}}{\left(n_{O_2}/n_{Fuel}\right)_{Actual}}\right] \quad (17)$$

For the test with the Purser Furnace, the ER is set to a certain constant value by adjusting the dial number of the driver which corresponding to the fuel feed rate (mm/min) before the start of each test. This would allow the conduction of toxicity test at different fire conditions. The dial number that needs to be set to represent the certain equivalence ratio was calculated and summarised in Table 3.9. In order to investigate the lean fires for smaller range equivalence ratios (Φ<0.8), it is suggested to use the small scale of driving dial with a higher accuracy and recalibration of speed rate with the total travel time should be done for setting up it precisely to represent the correct equivalence ratio. The travel time will be longer than 87.85 minutes for Φ less than 0.8.

**Table 3.9** Dial number points of the driver at certain Φ.

| Equivalence Ratio, Φ | Travel Time for 685 mm Distance (min) | Speed Rate (mm/min) | Dial No. |
|---|---|---|---|
| 0.5 | | 4.93 | 0.32 |
| 0.6 | | 5.92 | 0.38 |
| 0.7 | | 6.91 | 0.45 |
| 0.8 | 87.85 | 7.89 | 0.51 |
| 1.0 | 78.96 | 9.87 | 0.66 |
| 1.2 | 70.11 | 11.84 | 0.80 |
| 1.5 | 56.82 | 14.80 | 1.03 |
| 1.8 | 43.53 | 17.76 | 1.25 |
| 2.0 | 34.71 | 19.74 | 1.40 |
| 2.5 | 29.12 | 24.67 | 1.67 |
| 3.0 | 23.55 | 29.60 | 1.94 |

Some calculations involved in setting up the ER with the right adjustment of the dial number. In the Purser Furnace, during commissioning of this rig, tests were done with burning the Polyethylene samples. In example, the ER (Φ) to be set before the test is 2.0 for PE-Y fire. The actual AFR is obtained by dividing the stoichiometric AFR with the set ER. The stoichiometric AFR for PE-Y sample is 14.92 and the estimated actual AFR is about 7.43. Other parameters involved in the calculation as follow;

A constant initial air flowrate to be supplied is 10 L/min (0.2 g/s), this will give fuel mass flowrate or speed rate of 0.03 g/s.

Measured mass of fuel sample (PE-Y) is 49.3 g and the fuel is cut to a length of 600 mm. By dividing the fuel mass with the fuel length, the mass per unit length is determined which is equal to 0.0822 g/mm for this PE-Y sample. The speed rate in mm/min (19.74 mm/min) is obtained by dividing the mass per unit length of 0.0822 g/mm with the speed rate in g/s (0.3 g/s) and then the value is multiplied with 60 s. The calculated speed rates and the calibrated total travel time for the sample boat is shown in Table 3.9.

### 3.6.3 Normalised Mass Loss (NML) and Mass Loss Rate (MLR)

Normalised mass loss (wt.%) is determined by Equation 18 and the graphs are presented in the chapter of results and discussion,

$$\text{Normalised Mass Loss, NML (wt.\%)} = \left[\left(\frac{m_0 - m_i}{m_0}\right)(100)\right] \quad (18)$$

where,

$m_0$ is the measured sample mass at certain time before (at time = 0 s = initial mass of sample) and $m_i$ is the measured sample mass at certain time after (at time = i s) with the value difference is the total mass within that period. The mass loss rate (MLR, in g/s) is then obtained by dividing the mass loss value with the total time in s as the formula shown in Equation 19. The sum of MLR and initial air flowrate (IAF) is the total mass flowrate (MFR).

$$\text{Mass Loss Rate (MLR)} = \left[\frac{m_0 - m_i}{t_i - t_0}\right] \quad (19)$$

$$\text{Mass Flow Rate (MFR)} = \text{Mass Loss Rate (MLR)} + \text{Initial Air Flow (IAF)} \quad (20)$$

The original unit of the set IAF is L/min (i.e. 9.4, 18 and 28 L/min) and it is converted to g/s and kW/m$^2$ with considering 3.05 MJ/kg$_{air}$ when required while presenting the results. The air flowrates in different unit are summarised in Table 3.10. Beside using the Chan method, the actual AFR can also be determined by dividing this constant air flow (IAF) with the mass loss rate (MLR). Fuel mass loss rate (MLR) has a similar graph pattern with the equivalence ratio (Φ) variation as the set air flow is constant.

**Table 3.10** Air flowrates (IAF) in different units.

| | Unit | | |
|---|---|---|---|
| | L/min | g/s | kW/m$^2$ |
| IAF | 9.4 | 0.192 | 59 |
| | 18 | 0.368 | 112 |
| | 28 | 0.572 | 174 |

### 3.6.4 Heat Release Rate (HRR)

There are two methods used to calculate the heat release rate (HRR) which is based on Oxygen ($O_2$) consumption and mass loss rate (MLR). $O_2$ consumption or changes in dry basis during the test was recorded by the $O_2$ analyser connected to the FTIR analyser sample outlet. This gave the raw HRR and the $O_2$ consumption HRR measured on the diluted sample in the normal way gave the total HRR including the HRR after the discharge of the raw gases from the chimney. The mass flowrate (MFR) of the diluted gases in the cone calorimeter was set to 24 L/s (29 g/s). The heat of combustion released per kg of $O_2$ consumed is a constant with the value of 13.1 MJ/kg oxygen [132] which is the same as 3.05 MJ/kg air. The HRR based on $O_2$ consumption can be determined by Equation 21 [81, 133].

$$q = E\left(m_a {Y^a}_{O_2} - m_e {Y^e}_{O_2}\right) \quad (21)$$

where,

q is heat release rate (HRR) in kW, E is heat release per mass unit of $O_2$ consumed (13.1 MJ/kg or 13.1 kJ/g), $m_a$ is mass flow rate of the inlet air in g/s, $m_e$ is mass flow rate of the exhaust gases, ${Y^a}_{O_2}$ is mass fraction of the combustion air and ${Y^e}_{O_2}$ is mass fraction of the exhaust gases.

For the HRR based on MLR, it is determined by multiplying the heat of combustion (Calorific Value, CV in MJ/kg) of the fuel obtained from the Bomb Calorimeter analysis with the MLR (kg/s) value.

### 3.6.5 Gas Concentration, Total Toxicity and Major Gas Contribution

The gas concentration is measured by the FTIR analyser in ppm or vol.%. There are three toxic assessment methods used in the present study which are $LC50_{30min}$, $COSHH_{15min}$ and $AEGL\text{-}2_{10min}$ as described in Section 2.2.1, Chapter 2. The following Equation 22 to 24 are used to determine the total

toxicity indices for all three methods with referring the provided limit concentration values [39-41] as summarised in Table 2.3, Chapter 2.

$$Total\ LC50_{30min}\ index, N = \frac{[CO]}{LC50_{CO}} + \frac{[HCN]}{LC50_{HCN}} + \frac{[HCl]}{LC50_{HCl}} + \frac{[HF]}{LC50_{HF}} + \frac{[Formaldehyde]}{LC50_{Formaldehyde}} + \sum \frac{[Species\ i]}{LC50_{Species\ i}} \quad (22)$$

where,

$LC50_{Species\ i}$ is the lethal limit concentration of toxic species provided in [39] and $[Species\ i]$ is the measured concentration of toxic species by the FTIR analyser.

$$Total\ COSHH_{15min}\ index, N = \frac{[CO]}{COSHH_{CO}} + \frac{[HCN]}{COSHH_{HCN}} + \frac{[HCl]}{COSHH_{HCl}} + \frac{[HF]}{COSHH_{HF}} + \frac{[Formaldehyde]}{COSHH_{Formaldehyde}} + \sum \frac{[Species\ i]}{COSHH_{Species\ i}} \quad (23)$$

$COSHH_{Species\ i}$ is the limit concentration of toxic species that cause impairment to escape provided in [40] and $[Species\ i]$ is the measured concentration of toxic species by the FTIR analyser.

$$Total\ AEGL-2_{10min}\ index, N = \frac{[CO]}{AEGL-2_{CO}} + \frac{[HCN]}{AEGL-2_{HCN}} + \frac{[HCl]}{AEGL-2_{HCl}} + \frac{[HF]}{AEGL-2_{HF}} + \frac{[Formaldehyde]}{AEGL-2_{Formaldehyde}} + \sum \frac{[Species\ i]}{AEGL-2_{Species\ i}} \quad (24)$$

$AEGL-2_{Species\ i}$ is the limit concentration of toxic species that cause impairment to escape provided in [41] and $[Species\ i]$ is the measured concentration of toxic species by the FTIR analyser. AEGL-2 assessment for 10 minutes of exposure is equivalent to COSHH assessment for 15 minutes of exposure.

### 3.6.6 Emission Index for Pollutants or Toxic Gas Yields for Fire Toxicity

Pollutants or toxic gases are measured in ppm or % and must be converted to mass. It can be shown that for hydrocarbon/air combustion with y = 2 the mean atomic mass (or MW) of the combustion products is to better than 1% the same as that for air at 29 (actually 28.84 for 20.9% $O_2$ and 79.1% $N_2$). This is because the products of combustion of $CO_2$ (MW 44) and $H_2O$ (MW 18) are 37% higher and 44% lower respectively than oxygen and they are produced in roughly equal volumes. When the 79% $N_2$ is included the MW of the products are within 1% of those of air.

For Φ = 1, the exhaust composition (wet) is $CO_2$ = 14%, $H_2O$ = 12% and $N_2$ = 74%.

MW = (0.14 x 44) +(0.12 x 18) +(0.74 x 28) = 29.04.

Air is 28.84 error is 1% and lower for lean mixtures.

This allows a great simplification in conversion of pollutant volume to mass. This approximation has been used for all the fire material compositions.

Measured pollutant concentration p = pollutant / exhaust gas %.

To convert to mass x the MW ratio,

Mass Pollutant / Mass exhaust gas = p x $MW_p$ / 29 = $m_p$ / $m_e$

$$\frac{m_p}{m_e} = \frac{m_p}{(m_a + m_f)} \tag{25}$$

Now,

$$\left(\frac{m_p}{m_e}\right)\left(\frac{m_e}{m_f}\right) = \left(\frac{m_p}{m_f}\right) = Emission\ Index, EI \tag{26}$$

EI = p x $MW_p$ / 28.84 x $m_e$ / $m_f$

Now,

$$\left(\frac{m_e}{m_f}\right) = \left(\frac{m_a + m_f}{m_f}\right) = \left(1 + \frac{A}{F}\right) \tag{27}$$

Hence EI = $MW_p$ / 28.84 x p x (1 + A/F).

For CO the MW is 12 + 16 = 28, for $CH_4$ the MW is 12 + 4 = 16 (unburnt HC is measured as $CH_4$ equivalent) and for $NO_2$ the MW is 14 + 32 = 46.

The EI are thus:

$EI_{CO} = 0.971\ p_{co}\ (1 + A/F)$, $EI_{CH4} = 0.555\ p_{CH4}\ (1 + A/F)$, $EI_{NOx} = 1.595\ p_{NOx}\ (1 + A/F)$ and $EI_{CO2} = 1.526\ p_{CO2}\ (1 + A/F)$ in $kg/kg_{fuel}$.

In the above p is the volumetric fraction, 1% = 0.01 and 1 ppm = 0.000001.

The kg/kg EI is in fire toxicity referred to as the toxic gas yield.

For pollutants it is more normal to express the EI in units of g/kg. If the normal units in which concentration are measured are used then the EI equations become: $EI_{CO} = 9.71\ p_{CO}\ (1 + A/F)\ g/kg_{fuel}$ with $p_{CO}$ in %, $EI_{CH4} = 0.000554\ p_{CH4}\ (1 + A/F)\ g/kg_{fuel}$ with $p_{CH4}$ in ppm and $EI_{NOx} = 0.001595\ p_{NOx}\ (1 + A/F)\ g/kg_{fuel}$ with $p_{NOx}$ in ppm.

Note that in all these equations p must be expressed as the wet volumetric fraction (which the heated FTIR measures) and hence either must be measured wet (i.e. a hot sample) or converted from a dry gas measurement by calculating the volume fraction of $H_2O$ that has been removed in the sample drier. This is often assumed to be all of the $H_2O$ produced and hence can be calculated if y (H/C) is known.

The determination of the toxic gas yield ($g_{toxic}/g_{fuel)}$ is shown in Equation 28 and the MW of the gas sample is taken as the same as that of air, as explained above.

$$\text{Gas Yield, } Y_{Species\ i} = \left[\left(\frac{MW_{Species\ i}}{MW_{Gas\ Sample}}\right)\right][Measured\ concentration\ fraction][1 + (AFR)_{Actual}]\ \text{g/g} \quad (28)$$

where,

$\left(\frac{MW_{Species\ i}}{MW_{Gas\ Sample}}\right)$ is the molecular weight ratio of toxic species to the sample gas, $\left(\%_{Species\ i}\right)$ represents the measured volume concentration of toxic species and $(AFR)_{Actual}$ is the actual AFR value determined from the Chan method.

Combustion Inefficiency

The combustion inefficiency is the summation of the energy content of the CO, unburnt fuel ($CH_4$ equivalent) and unburnt Carbon in ash (solid fire loads) that

is emitted (as Equation 29). The energy content is the EI x the CV ratio for CO/fuel or $CH_4$/fuel (usually taken as 1).

$$1 - \eta_c = (EI_{CO})\left(\frac{CV_{CO}}{CV_{Fuel}}\right) + \left(EI_{CH_4}\right) + (EI_{Soot})\left(\frac{CV_{Carbon}}{CV_{Fuel}}\right) \quad (29)$$

EI must be in kg/kg to use the above Equation. In the present work the soot emissions were ignored in the combustion efficiency.

For an inefficiency of 1% it may be shown that for an A/F of 15/1 that 1130 ppm of $CH_4$ is required, which is not often seen in gas burners. However, for CO ~ 0.12% is required and much higher values than this occurs in fires >>1%, as will be shown in the present results. The unburnt Hydrocarbons (UHC) are often not considered [108] in determining the combustion efficiency in fires, but it is the dominant term in the present work on polymer fires.

### 3.6.7 Particle Number and Mass Distributions, Particulate Yields and Cumulative Mass

Particle number concentrations (p/cm$^3$) are measured by the particle size equipment, the Cambustion DMS500. These number concentrations can be converted to the mass concentrations by using the following Equation 30.

Dilution correction in the Cone Calorimeter is also considered in this number to mass conversion with multiplying the dilution factor which determined using Equation 31 with the number concentrations. The dilution correction in the Cambustion DMS500 is not required because the device is already set up internally to 10 to 1 of dilution for the measurement process of particle size during the test. Exhaust flow of the cone is 24 L/s (1440 L/min or 29 g/s).

$$Particulate\ Mass, P_m = (V)(D)(P_n)(D_F) \quad (30)$$

where,

$P_m$ is the particulate mass in g/m$^3$, $V$ is the sphere volume of particle $[(\frac{\pi}{6})(r^3)]$ with r is the measured size of the particle, $D$ is the assumed density of solid Carbon (1000 kg/m$^3$), $P_n$ is the measured particle number in p/cm$^3$ by the Cambustion DMS500 and $D_F$ is the dilution factor [134].

$$Dilution\ Factor, D_F = \frac{MFR_{g/s}}{(MLR + MFR_{inlet\ air})_{g/s}} \quad (31)$$

where,

$MFR$ is the set mass flowrate of the exhaust gas for the Cone Calorimeter test (29 g/s), $MLR$ is the average mass loss rate of the fuel and $MFR_{inlet\ air}$ is the set initial air flowrate in g/s. For determination of the $MFR_{inlet\ air}$, the FTIR flow (3 L/min or 0.0611 g/s) is also taken in consideration by subtracting the set $MFR_{inlet\ air}$ value with it to get the corrected $MFR_{inlet\ air}$.

For the Purser furnace test, the dilution ratio is 4 to 1 with the initial air flowrate of 10 L/min and the diluted air flowrate of 40 L/min.

Smoke obscuration, k (1/m) data recorded by the ConeCalc software of the Cone Calorimeter is also presented on the same graph with the particle mass concentration profile for some of the polymer fires. Cumulative mass of particulate is also determined by total up all the particulate mass concentration produced from the combustion of fuel.

For the calculation of the particulate yield (number and mass basis), Equation 32 and 33 are used.

$$\text{Particulate Yield}, Y_{P_n} = \left[\frac{P_n}{1.18}\right][1 + (AFR)_{Actual}]\ \text{p/kg (number basis)} \quad (32)$$

$$\text{Particulate Yield}, Y_{P_m} = \left[\frac{P_m}{1.18}\right][1 + (AFR)_{Actual}]\ \text{g/kg (mass basis)} \quad (33)$$

where,

$P_n$ is the particle number (p/cm$^3$) and $P_m$ is particle mass in g/m$^3$.

Meanwhile, 1.18 is the density of air in kg/m$^3$ (at P = 1 atm, T = 15$^o$C) of the sample gas flow meter and $(AFR)_{Actual}$ is the actual air to fuel ratio of the sample.

### 3.6.8 Soot Mass from Filter Papers

In the Purser furnace tests, soot on the filter paper are collected from the Smoke Meter equipment for Polyethylene (PE-Y) fires under fuel lean and fuel rich equivalence ratios. The soot mass is then measured manually using the mass balance with 4 decimal points to get the total soot mass in mg. Soot yield is calculated using Equation 34.

$$Y_{P_{Soot}} = \frac{M_{Soot}}{M_{Fuel}} \quad (34)$$

where,

$Y_{P_{Soot}}$ is the soot yield, $M_{Soot}$ is the total soot mass collected and $M_{Fuel}$ is the initial mass of fuel.

### 3.6.9 Summarised Data for Proximate and Ultimate Analysis

The following Table 3.11 shows the summarised data for proximate and ultimate analysis of test materials. The stoichiometric A/F by Carbon balance that determined was a theoretical value based on the composition of the actual tested polymer. Basically, the proximate analysis shows the results of the TGA analysis for each product. Columns 3 and 4 show the measured proportions of (in dry basis) combustible matter released as volatiles and oxidisable fixed Carbon. Column 5 shows the measured moisture content. The following columns 7-10 shows the measured % of combustible matter in the form C, H, N and S. As stated, the balance in the form of O or Cl in columns 11 and 12 is an estimate based on the assumed nature of the test material. For PVC cables the balance is assumed to be Cl and for non-halogen materials the balance is assumed to be Oxygen. As discussed, although this is considered in general to be the case it is recognized that there were some deviations, especially for the cables. Column 13 shows the measured gross calorific value (GCV) by the Bomb Calorimeter.

**Table 3.11** Proximate and ultimate analysis results for test materials.

| No. | Material | Proximate analysis (wt.%)(daf) | | | | Ultimate analysis (wt.%)(daf) | | | | | | | Other information | |
|---|---|---|---|---|---|---|---|---|---|---|---|---|---|---|
| | | Volatile matter | Fixed carbon | Moisture (as received) | Ash (as received) | C | H | N | S | O | Cl | GCV (MJ/kg) | Stoichiometric A/F by Carbon balance | Chemical formula |
| **PVC Electrical Cables** | | | | | | | | | | | | | | |
| 1 | PVC Prysmian A | 96.36 | 3.64 | 0.40 | 28.91 | 35.63 | 3.84 | 0.00 | 0.00 | 0.00 | 60.53 | 17.95 | 4.86 | $C_1H_{1.29}Cl_{0.57}$ |
| 2 | PVC Doncaster (H6242Y)-DC2 | 94.67 | 5.33 | 0.40 | 26.99 | 37.11 | 4.21 | 0.00 | 0.00 | 0.00 | 58.69 | 15.36 | 5.12 | $C_1H_{1.36}Cl_{0.54}$ |
| 3 | PVC EC-GB 1 | 96.50 | 3.51 | 0.11 | 37.73 | 29.90 | 3.02 | 0.00 | 0.00 | 0.00 | 67.07 | 10.57 | 3.82 | $C_1H_{1.21}Cl_{0.76}$ |
| 4 | PVC EC-GB 2 | 98.03 | 1.97 | 0.21 | 38.47 | 31.62 | 3.30 | 0.00 | 0.00 | 0.00 | 65.08 | 12.04 | 3.94 | $C_1H_{1.25}Cl_{0.74}$ |
| 5 | PVC EC-GB 3 | 95.69 | 4.32 | 0.15 | 39.01 | 30.15 | 3.00 | 0.00 | 0.00 | 0.00 | 66.85 | 10.84 | 3.82 | $C_1H_{1.20}Cl_{0.76}$ |
| 6 | PVC SK1-GB | 96.39 | 3.61 | 0.05 | 36.91 | 31.45 | 3.28 | 0.00 | 0.00 | 0.00 | 65.27 | 11.99 | 3.94 | $C_1H_{1.25}Cl_{0.74}$ |
| 7 | PVC SK2-GS | 98.15 | 1.85 | 0.34 | 40.87 | 28.98 | 2.88 | 0.00 | 0.00 | 0.00 | 68.15 | 10.02 | 3.77 | $C_1H_{1.19}Cl_{0.77}$ |
| **LSZH Electrical Cables** | | | | | | | | | | | | | | |
| 8 | Prysmian B | 97.01 | 2.99 | 0.36 | 39.21 | 29.43 | 6.29 | 0.00 | 0.00 | 64.28 | 0.00 | 16.30 | 2.78 | $C_1H_{2.57}O_{1.64}$ |
| 9 | Armoured Marine-I (BS 7917) AMI-G | 99.75 | 0.25 | 0.14 | 44.13 | 26.16 | 5.95 | 0.00 | 0.00 | 67.89 | 0.00 | 12.53 | 2.13 | $C_1H_{2.73}O_{1.95}$ |
| 10 | Armoured Marine-P (BS 6883) AMI-B | 99.89 | 0.11 | 0.32 | 43.67 | 26.89 | 6.06 | 0.00 | 0.00 | 67.06 | 0.00 | 12.81 | 2.29 | $C_1H_{2.70}O_{1.87}$ |
| 11 | 6701B-W 2.5 | 99.98 | 0.02 | 0.35 | 39.81 | 20.75 | 4.41 | 0.00 | 0.00 | 74.84 | 0.00 | 17.97 | 0.69 | $C_1H_{2.55}O_{2.7}$ |
| 12 | TEC2-W Electrical Cable | 99.82 | 0.17 | 1.07 | 40.62 | 30.02 | 5.72 | 0.00 | 0.00 | 64.25 | 0.00 | 14.89 | 2.64 | $C_1H_{2.29}O_{1.61}$ |

| No. | Material | Proximate analysis (wt.%)(daf) | | | | Ultimate analysis (wt.%)(daf) | | | | | | | Other information | |
|---|---|---|---|---|---|---|---|---|---|---|---|---|---|---|
| | | Volatile matter | Fixed carbon | Moisture (as received) | Ash (as received) | C | H | N | S | O | Cl | GCV (MJ/kg) | Stoichiometric A/F by Carbon balance | Chemical formula |
| **Other Electrical Cables** | | | | | | | | | | | | | | |
| 13 | High-V Power 1-4C | 94.97 | 5.02 | 0.07 | 30.82 | 33.46 | 3.62 | 0.00 | 0.00 | 62.92 | 0.00 | 13.37 | 2.39 | $C_1H_{1.30}O_{1.41}$ |
| 14 | High-V Power 2-3C | 89.68 | 10.32 | 0.45 | 25.71 | 36.27 | 3.91 | 0.00 | 0.00 | 59.82 | 0.00 | 16.02 | 2.93 | $C_1H_{1.29}O_{1.24}$ |
| 15 | Doncaster (6242Y)-DC1 | 95.71 | 4.29 | 0.04 | 27.80 | 35.18 | 3.84 | 0.00 | 0.00 | 0.00 | 60.99 | 14.74 | 2.74 | $C_1H_{1.31}O_{1.30}$ |
| 16 | Flex 1 BG Cable | 89.90 | 10.10 | 0.71 | 2.00 | 49.24 | 6.42 | 0.00 | 0.00 | 0.00 | 44.34 | 26.65 | 7.46 | $C_1H_{1.57}O_{0.68}$ |
| 17 | Flex 2 W Cable | 98.46 | 1.55 | 0.29 | 31.02 | 38.26 | 4.50 | 0.00 | 0.00 | 57.24 | 0.00 | 16.81 | 3.49 | $C_1H_{1.41}O_{1.12}$ |
| 18 | Flex 3 White Cable | 93.91 | 6.09 | 0.08 | 25.40 | 37.86 | 4.44 | 0.21 | 0.00 | 57.50 | 0.00 | 16.64 | 3.41 | $C_1H_{1.41}O_{1.14}N_{0.00}$ |
| **Polymers** | | | | | | | | | | | | | | |
| 19 | GT PIR Foam | 96.04 | 3.96 | 0.94 | 29.61 | 60.81 | 4.99 | 6.09 | 0.00 | 28.11 | 0.00 | 26.36 | 7.44 | $C_1H_{0.98}O_{0.35}N_{0.09}$ |
| 20 | PU Foam SC | 94.43 | 5.57 | 1.09 | 8.14 | 62.03 | 6.77 | 6.11 | 0.00 | 25.10 | 0.00 | 25.45 | 8.45 | $C_1H_{1.31}O_{0.30}N_{0.08}$ |
| 21 | PU Floor Mat | 94.83 | 5.17 | 0.85 | 0.00 | 62.92 | 8.24 | 4.00 | 0.00 | 24.84 | 0.00 | 30.78 | 8.99 | $C_1H_{1.57}O_{0.30}N_{0.05}$ |
| 22 | Foam-B | 99.56 | 0.44 | 0.37 | 0.00 | 65.30 | 7.74 | 7.02 | 0.00 | 19.94 | 0.00 | 29.65 | 9.32 | $C_1H_{1.42}O_{0.23}N_{0.09}$ |
| 23 | PS-TV | 99.97 | 0.03 | 0.02 | 0.69 | 90.70 | 7.89 | 0.14 | 0.00 | 1.27 | 0.00 | 41.76 | 13.12 | $C_1H_{1.04}O_{0.01}N_{0.00}$ |
| 24 | PS Cardboard | 94.79 | 5.21 | 7.96 | 0.00 | 46.23 | 5.61 | 0.12 | 0.00 | 48.04 | 0.00 | 18.68 | 5.19 | $C_1H_{1.46}O_{0.78}N_{0.00}$ |
| 25 | PS-CB 2 | 94.79 | 5.21 | 7.96 | 0.00 | 46.23 | 5.61 | 0.12 | 0.00 | 48.04 | 0.00 | 18.68 | 5.19 | $C_1H_{1.46}O_{0.78}N_{0.00}$ |
| 26 | PS2 | 99.94 | 0.07 | 0.30 | 1.56 | 89.55 | 7.79 | 0.19 | 0.00 | 2.47 | 0.00 | 41.77 | 12.91 | $C_1H_{1.04}O_{0.02}N_{0.00}$ |
| 27 | PS Clear | 99.97 | 0.03 | 0.46 | 0.08 | 82.25 | 7.08 | 0.15 | 0.00 | 10.52 | 0.00 | 42.26 | 11.39 | $C_1H_{1.03}O_{0.10}N_{0.00}$ |
| 28 | PS4 Clear (without plastic cover) | 99.87 | 0.13 | 0.22 | 0.81 | 91.76 | 8.06 | 0.18 | 0.00 | 0.00 | 0.00 | 42.13 | 13.35 | $C_1H_{1.05}O_{0.00}N_{0.00}$ |
| 29 | PS Cove S | 99.82 | 0.17 | 0.48 | 1.71 | 89.97 | 7.88 | 0.14 | 0.00 | 2.01 | 0.00 | 41.8 | 12.93 | $C_1H_{1.05}O_{0.02}N_{0.00}$ |
| 30 | PS Skating Board H | 99.78 | 0.23 | 0.12 | 2.16 | 91.56 | 8.44 | 0.00 | 0.00 | 0.00 | 0.00 | 41.33 | 13.44 | $C_1H_{1.11}O_{0.00}$ |
| 31 | Packaging Material Green | 99.62 | 0.37 | 0.23 | 1.26 | 85.86 | 7.53 | 0.18 | 0.00 | 6.44 | 0.00 | 41.35 | 12.14 | $C_1H_{1.05}O_{0.06}N_{0.00}$ |

| No. | Material | Proximate analysis (wt.%)(daf) | | | | Ultimate analysis (wt.%)(daf) | | | | | | | Other information | |
|---|---|---|---|---|---|---|---|---|---|---|---|---|---|---|
| | | Volatile matter | Fixed carbon | Moisture (as received) | Ash (as received) | C | H | N | S | O | Cl | GCV (MJ/kg) | Stoichiometric A/F by Carbon balance | Chemical formula |
| **Polymers** | | | | | | | | | | | | | | |
| 32 | PE SB Sheet Blue | 99.76 | 0.24 | 0.30 | 1.13 | 84.16 | 15.68 | 0.16 | 0.00 | 0.00 | 0.00 | 47.06 | 15.11 | $C_1H_{2.24}O_{0.00}N_{0.00}$ |
| 33 | PE SB Sheet Black | 99.84 | 0.16 | 0.28 | 0.42 | 83.44 | 16.42 | 0.14 | 0.00 | 0.00 | 0.00 | 47.34 | 15.28 | $C_1H_{2.36}O_{0.00}N_{0.00}$ |
| 34 | PE SB Sheet Yellow | 99.92 | 0.08 | 0.31 | 0.72 | 84.90 | 14.91 | 0.19 | 0.00 | 0.00 | 0.00 | 47.36 | 14.92 | $C_1H_{2.10}O_{0.00}N_{0.00}$ |
| 35 | PE Storage Box Purple | 99.78 | 0.22 | 0.05 | 0.00 | 76.81 | 9.68 | 0.65 | 0.00 | 12.85 | 0.00 | 47.14 | 11.51 | $C_1H_{1.51}O_{0.13}N_{0.01}$ |
| 36 | PE Pipe | 99.94 | 0.06 | 0.26 | 2.72 | 68.00 | 7.52 | 0.00 | 0.00 | 24.48 | 0.00 | 44.42 | 9.36 | $C_1H_{1.33}O_{0.27}$ |
| 37 | PAA GRP SB Sheet Blue | 99.95 | 0.05 | 1.45 | 26.28 | 54.19 | 4.59 | 0.14 | 0.00 | 41.09 | 0.00 | 23.07 | 6.03 | $C_1H_{1.01}O_{0.57}N_{0.00}$ |
| 38 | PMMA | 100.00 | 0.00 | 0.44 | 1.52 | 59.34 | 8.51 | 0.20 | 0.00 | 31.95 | 0.00 | 26.81 | 8.43 | $C_1H_{1.72}O_{0.40}N_{0.00}$ |
| 39 | Clear Acrylic B | 99.74 | 0.26 | 0.20 | 1.33 | 62.21 | 7.67 | 0.00 | 0.00 | 30.12 | 0.00 | 27.57 | 8.53 | $C_1H_{1.48}O_{0.36}$ |
| 40 | PVC Square Tube White | 83.71 | 16.29 | 0.10 | 10.28 | 36.62 | 4.46 | 0.27 | 0.00 | 0.00 | 58.65 | 19.9 | 4.48 | $C_1H_{1.46}Cl_{0.66}N_{0.00}$ |
| 41 | PP Rope Yellow | 98.50 | 1.50 | 1.32 | 1.03 | 78.47 | 8.09 | 0.00 | 0.00 | 13.44 | 0.00 | 46.57 | 11.21 | $C_1H_{1.24}O_{0.13}$ |
| 42 | Cable Trunk S | 80.43 | 19.57 | 0.41 | 8.19 | 73.53 | 6.25 | 0.00 | 0.00 | 20.23 | 0.00 | 34.74 | 9.69 | $C_1H_{1.02}O_{0.21}$ |
| | Cable Trunk B | 80.62 | 19.38 | 0.76 | 7.71 | 74.45 | 6.31 | 0.00 | 0.00 | 19.23 | 0.00 | 33.88 | 9.97 | $C_1H_{1.02}O_{0.19}$ |
| 43 | FB Rubber Butyl Sheet | 67.85 | 32.15 | 0.06 | 23.52 | 64.12 | 6.04 | 0.17 | 2.24 | 28.14 | 0.00 | 31.13 | 8.34 | $C_1H_{1.13}O_{0.32}N_{0.00}S_{0.01}$ |
| 44 | FB Rubber Butyl Crumbs | 67.85 | 32.15 | 0.06 | 23.52 | 64.12 | 6.04 | 0.17 | 2.24 | 28.14 | 0.00 | 31.13 | 8.34 | $C_1H_{1.13}O_{0.32}N_{0.00}S_{0.01}$ |
| 45 | FB Rubber Butyl Crumbs B | 64.43 | 35.57 | 0.06 | 27.03 | 64.60 | 5.57 | 0.15 | 2.07 | 26.61 | 0.00 | 29.74 | 8.20 | $C_1H_{1.03}O_{0.32}N_{0.00}S_{0.01}$ |
| 46 | Flood Light C | 82.50 | 17.49 | 0.13 | 0.46 | 75.66 | 5.58 | 0.00 | 0.00 | 18.76 | 0.00 | 31.50 | 9.75 | $C_1H_{0.88}O_{0.19}$ |
| 47 | Flood Light Y | 84.08 | 15.92 | 0.08 | 2.11 | 72.71 | 5.57 | 0.14 | 0.00 | 21.57 | 0.00 | 31.1 | 9.40 | $C_1H_{0.92}O_{0.22}N_{0.00}$ |

*Key of terms: daf – dry ash free basis, GCV – gross calorific value

# Chapter 4
# Electrical Cable Fires in the Cone Calorimeter

## 4.1 Introduction

All the electrical cables tested on the Cone Calorimeter were tested mainly at 35 kW/m$^2$ radiant heat flux, but PVC Prysmian A was tested at 25 and 50 kW/m$^2$ as well. They had the results processed in two sets of results termed combustion properties and fire toxic gas emissions. Some of the cables were also tested for particulate emissions.

For combustion properties the following were analysed and graphs plotted as a function of time.

a) Normalised mass loss
b) Mass loss rate (MLR)
c) Oxygen in the raw gas exit chimney
d) Equivalence ratio
e) Heat Release Rate (HRR) based on the MLR
f) Heat Release Rate (HRR) based on the oxygen consumption
g) Primary HRR in the raw gas sample from the chimney
h) Secondary HRR for post oxidation of the gases from the chimney (difference in the Total HRR and Primary HRR.

The toxic gas emissions presentation of the results had the most significant toxic gases in ppm concentration and mass yield. The cumulative mass was also presented and the overall mean mass yield. The relative toxicity and the normalised toxicity was presented to show the most important toxic gases. The yield results for CO and THC were converted into a primary combustion efficiency. Yields of the most important toxic gases and combustion efficiency were also plotted as a function of the primary equivalence ratio.

## 4.2 General Combustion Properties of PVC and Other Types of Electrical Cable Fires

The 18 electrical cables studied in this work are shown in Table 4.1 and their chemical analysis is given in Table 3.11. Only 12 of the 18 cables were tested

for fire toxicity tests in the Cone Calorimeter tests, due to lack of time to test then all. These 12 electrical cables are divided to groups: PVC electrical cables; Solar Energy cables (supplied by Leeds Solar); Wind Turbine cables (supplied by Siemens Wind Turbine); Low Smoke Zero Halogen (LSZH) cables and other electrical cables. In Table 4.1, the thickness, mass and internal core mass (Copper or other type of metal) of each selected cables are given.

**Table 4.1** Thickness, sample mass and Copper mass for electrical cable samples.

| Cable Name | Thickness (mm) | Mass Range (100 $mm^2$ Sample) (g) | Copper Mass (g) |
|---|---|---|---|
| **PVC Electrical Cables** | | | |
| PVC Prysmian A | 6 | 150-155 | 86.8 |
| PVC Doncaster (H6242Y)-DC2 | | | |
| PVC EC-GB 1 | 10 | 215-220 | |
| PVC EC-GB 2 | 7 | 180-185 | |
| PVC EC-GB 3 | | | |
| PVC SK1-GB | | | |
| PVC SK2-GS | | | |
| **LSZH Electrical Cables** | | | |
| Prysmian B | 7 | 110-115 | 50.7 |
| 6701B-W 2.5 | 4 | 80-85 | 59.4 |
| TEC2-W Electrical Cable | 6 | 110-115 | |
| Armoured Marine-I (BS 7917) AMI-G | 15 | 205-210 | 62.3 |
| Armoured Marine-P (BS 6883) AMI-B | 15 | 220-225 | 74.2 |
| **Other Electrical Cables** | | | |
| High-V Power 1-4C | 15 | 315-320 | 201.6 |
| High-V Power 2-3C | 16 | 350-355 | 219.8 |
| Doncaster (6242Y)-DC1 | | | |
| Flex 1 BG Cable | 8.5 | 145-150 | |
| Flex 2 W Cable | 6 | 75-80 | |
| Flex 3 White Cable | | | |

PVC Prysmian A, PVC EC-GB 1 and PVC EC-GB 2 were in the PVC electrical cable group. High voltage power cables, HV1-4C and HV2-3C cables were in the Solar Energy group of cables. Siemens' Wind Turbine cables were AMI-G and AMI-B and were included in the LSZH electrical cable group together with Prysmian B, 6701B-W and TEC2-W electrical cables.

The group allocated to the cables was decided following the printed information on each cable and the available cable's specification details. For

other electrical cables such as FLEX1-BG and FLEX2-W cables, no further details were identified either these electrical cables were PVC, LSZH or non-PVC type of cables. However, it will be shown below that FLEX1-BG had very high HCl yields and hence must be a PVC cable, whereas FLEX2-W has very low HCl emissions and hence is likely to be a non-PVC cable. FLEX2-W is high in ash (Table 3.11) and this is likely to be a fire retardant such as Sodium bicarbonate, Calcium carbonate or Aluminium trihydrate that decomposes endothermically on heating and releases $CO_2$. These two cables will be directly compared and thus will show a direct comparison of a PVC and Non-PVC, high ash and low ash cables for the same application and from the same manufacturer.

Table 4.2 lists fire tests for PVC Prysmian A electrical cable. For this PVC Prysmian A cable fires, ten fire tests were carried out under various test conditions with varying radiant heat flux and initial air flowrate. Data for combustion properties, gas concentrations and particle size distributions were obtained for these electrical cable fires and were presented in this Chapter 4. A higher radiant heat was found to reach a flaming state in a shorter time than at lower radiant heat. Increasing the air flowrate reduced the time for an ignition for forced ventilation with the controlled atmosphere box around the sample.

**Table 4.2** Test details for PVC Prysmian A electrical cable fires.

| Test | Radiant heat ($kW/m^2$) | Air flow (L/min) | Air flow (g/s) | Ignition (s) | Flame out (s) |
|---|---|---|---|---|---|
| 1 | 25 | 9.4 | 0.192 | 52 | 1192 |
| 2 | 25 | 18 | 0.368 | 51 | 1066 |
| 3 | 25 | 28 | 0.572 | No | No |
| 4 | 35 | 9.4 | 0.192 | 21 | 1048 |
| 5 | 35 | 18 | 0.368 | 18 | 957 |
| 6 | 35 | 28 | 0.572 | 28 | 826 |
| 7 | 35 | FV | FV | 23 | 983 |
| 8 | 50 | 9.4 | 0.192 | 11 | 372 |
| 9 | 50 | 18 | 0.368 | 9 | 669 |
| 10 | 50 | 28 | 0.572 | 9 | 792 |

Other than PVC Prysmian A electrical cable, other PVC electrical cables such as PVC EC-GB 1 and PVC EC-GB 2 cables were also tested for fire toxicity determination at 35 $kW/m^2$ of irradiation level and free ventilation. Details of PVC EC-GB 1 and PVC EC-GB 2 electrical cable fires like ignition time and flame out time were included in Table 4.3. From the details, it can be

concluded that PVC EC-GB 1 electrical cable ignited faster but took more longer to reach the flame out condition compared to PVC EC-GB 2 electrical cable.

**Table 4.3** Test details for other PVC electrical cable fires at 35 kW/m$^2$ of irradiation level under free ventilation condition.

| Test | Cable Name | Ignition (s) | Flame out (s) |
|---|---|---|---|
| 1 | PVC EC-GB 1 | 23 | 1525 |
| 2 | PVC EC-GB 2 | 26 | 1162 |

Test details of Solar Energy cable fires, LSZH cable fires including Wind Turbine cable fires and also other electrical cable fires were shown in Table 4.4. In comparison between HV1-4C and HV2-3C power cables from Solar Energy company, for the test conducted at 35 kW/m$^2$ with free ventilation condition, the HV1-4C cable took much shorter time (37 s) to ignite than the HV2-3C cable (1084 s). Once ignited, both cable fires took more than half an hour for the flame to extinguish. For Wind Turbine cables from Siemens, AMI-G cable was tested at two different conditions which at 35 kW/m$^2$ with free ventilation and at 50 kW/m$^2$ with restricted ventilation (9.4 L/min of air flowrate). Meanwhile, AMI-B cable was only tested at one condition (35 kW/m$^2$ with free ventilation) for a comparison with the AMI-G cable fire. At 35 kW/m$^2$ and free ventilation test conditions, ignition time for both cable fires was not different much but the time gap for the flame out time was too much between those cable fires. The AMI-B cable fire was extinguished at 643 s and the AMI-G cable fire was extinguished at 2928 s, about 38 min different.

From the Table 4.4, test details for other LSZH electrical cable (Prysmian B, 6701B-W and TEC-W) fires were also included for reference. Each Prysmian B, 6701B-W and TEC-W cable fire gave an ignition at 112 s, 124 s and 217 s for test conditions at 35 kW/m$^2$ with free ventilation. Prysmian B cable fire took the shortest time (366 s) to reach the flame out state, followed by 6701B-W at 758 s and TEC2-W at 1032 s. For the electrical cable fires (PVC Prysmian A, AMI-G, Prysmian B and 6701B-W) that conducted at 50 kW/m$^2$ and 9.4 L/min air flowrate, comparison of results could also be made in future publications. Other electrical cable fires like FLEX1-BG and FLEX2-W, the FLEX1-BG cable fire gave an ignition at 35 s and a flame out at 727 s, meanwhile, the FLEX2-W cable fire ignited at 41 s and extinguished at 1229 s. In overall, from the details illustrated in Table 4.2, Table 4.3 and Table 4.4, from all conducted

electrical cable fires under various heat fluxes and ventilation conditions, the shortest time delay before having an ignition was 9 s for PVC Prysmian A electrical cable fire (at 50 kW/m$^2$ of heat flux with 18 and 28 L/min of air flowrates) and the longest time delay was about 1084 s (18 minutes) for Solar Energy cable HV2-3C fire (at 35 kW/m$^2$ of heat flux with free ventilation) from the time the sample was started being exposed to the source of heat.

**Table 4.4** Test details for non PVC electrical cable fires.

| Test | Cable Name | Radiant heat (kW/m$^2$) | Ventilation | Air flow (L/min) | Air flow (g/s) | Ignition (s) | Flame out (s) |
|---|---|---|---|---|---|---|---|
| Solar Energy Cables | | | | | | | |
| 1 | HV Power 1-4C | 35 | FV | | | 37 | 3327 |
| 2 | HV Power 2-3C | 35 | FV | | | 1084 | 3468 |
| LSZH Electrical Cables | | | | | | | |
| A. Wind Turbine Cables from Siemens | | | | | | | |
| 3 | AMI-G | 35 | FV | | | 322 | 2928 |
| 4 | AMI-G | 50 | RV | 9.4 | 59 | 43 | 1231 |
| 5 | AMI-B | 35 | FV | | | 315 | 643 |
| B. Other LSZH Electrical Cables | | | | | | | |
| 6 | Prysmian B | 35 | FV | | | 112 | 366 |
| 7 | Prysmian B | 50 | RV | 9.4 | 59 | 43 | 811 |
| 8 | 6701B-W 2.5 | 35 | FV | | | 124 | 758 |
| 9 | 6701B-W 2.5 | 50 | RV | 9.4 | 59 | 44 | 595 |
| 10 | TEC2-W | 35 | FV | | | 217 | 1032 |
| Other Electrical Cables | | | | | | | |
| 11 | Flex 1 BG | 35 | FV | | | 35 | 727 |
| 12 | Flex 2 W | 35 | FV | | | 41 | 1229 |

### 4.2.1 PVC Electrical Cable Fires

#### 4.2.1.1 PVC Prysmian A Electrical Cable Fires

Figure 4.1 shows combustion properties as a function of time for PVC Prysmian A electrical cable fires at 25 kW/m$^2$ for various air flow rates. At a heat flux of 25 kW/m$^2$ the maximum normalised mass loss for PVC Prysmian A cable fire was less than 50% for all three air flowrates. The mass loss rate increased with air flow, but at the highest air flow there was negligible heat release but significant, although lower, mass loss. An explanation of this is that the high air flow was cooling the sample and this reduced the material below its ignition temperature. The oxygen results for the highest air flow were very high and there was little combustion or heat release and no observably

flaming combustion. The mass loss with little heat release indicates that the PVC is being vaporised or pyrolysed but not burnt. It will be shown later that the emissions results are quite different at this 25 kW/m$^2$ heat flux with a high air flow, which produces volatiles that do not burn. Significant HCl toxic gas levels will be shown to be pyrolysed in this test, even though there is little heat release to heat the cable. It will be shown that Acrolein and other toxic gases are higher than for the flaming combustion air flows. Thus cables that do not burn but are heated by radiation can give off high levels of toxic gases, which are well acknowledged in the toxic gas literature. It will be shown in this thesis that this can occur for other polymers.

The PVC Prysmian A cable fire at a lower air flow rate showed richer burning. For the first 600 s of the burning period the mass loss rate (MLR) was highest at 60 g/sm$^2$ and lowest at 57.2 g/sm$^2$ with a MLR of 40 g/sm$^2$. Figure 4.1 (d) shows that the higher the air flowrate the leaner was the combustion and the equivalence ratios for most of these cable fires were less than 1.0 except for air flowrate of 19.2 g/sm$^2$, where equivalence ratios up to 1.1 were reached after 300 s.

Heat release rates (HRR) from the burning of PVC Prysmian A cable samples were low at less than 200 kW/m$^2$ for all three ventilation rates with primary HRR values that were less than 150 kW/m$^2$ and secondary HRR were not more than 30 kW/m$^2$ if compared to HRR from a polymer fire such as Polyethylene (> 500 kW/m$^2$).

The difference in the primary and total HRR is the secondary HRR and this shows that significant post chimney burning was occurring. This is why the standard Cone Calorimeter should not be used for fire toxicity as it will give low values due to the post cone oxidation as the primary combustion plume entrains ambient air. This is why raw hot gas sampling was used in the present work, for the first time on the Cone Calorimeter (other than for previous work at Leeds University for wood fires [100, 106] and other materials [112, 113, 135].

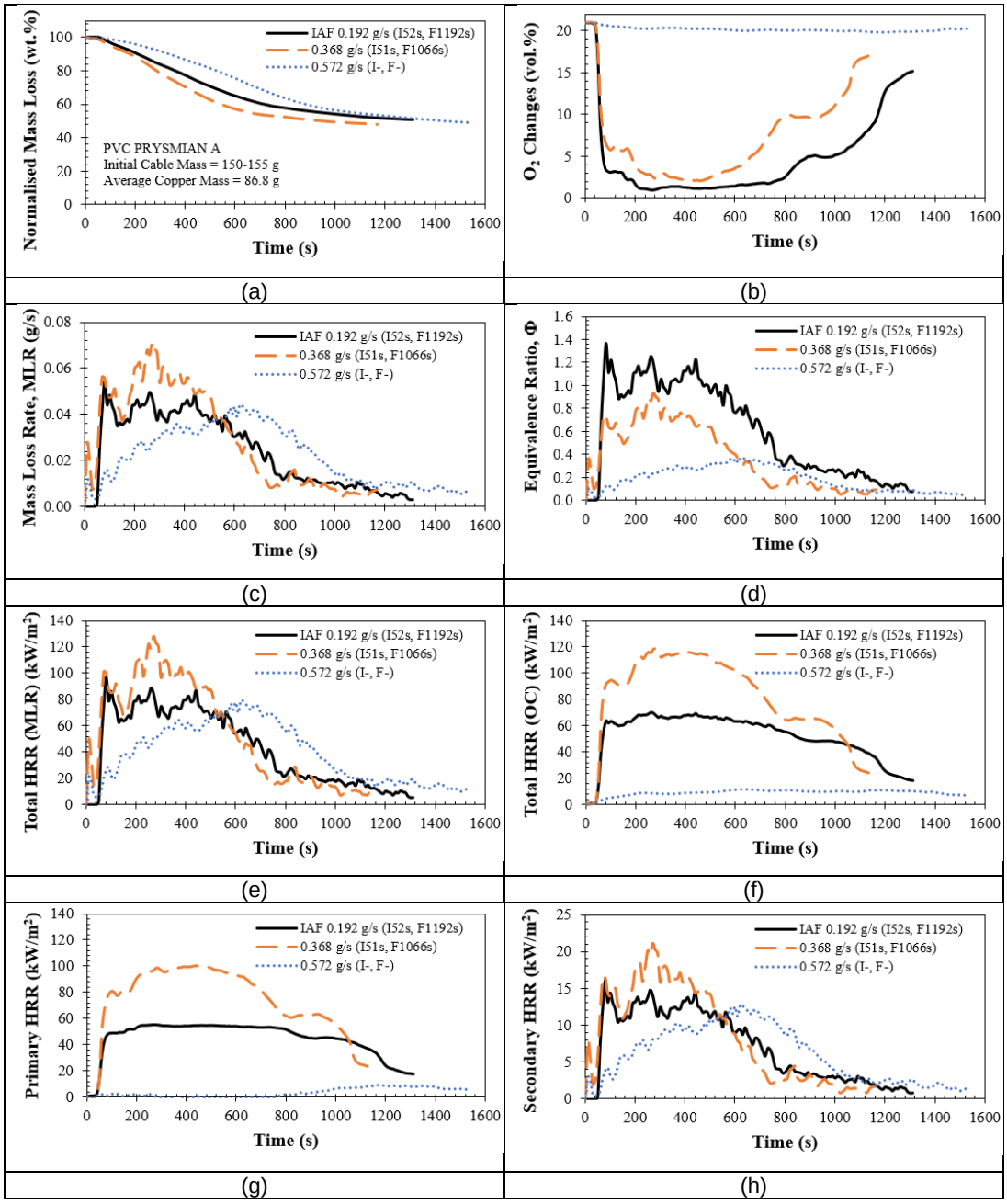


**Figure 4.1** Combustion properties against time for PVC Prysmian A electrical cable fires at 25 kW/m$^2$ with various air flow rates.

The combustion properties for PVC Prysmian A electrical cable fires at a heat flux of 35 kW/m$^2$ and for four air ventilation rates are shown in Figure 4.2. The highest normalised mass loss for these PVC cable fires was not more than 50%, even with an increase in heat flux. This is possibly due to fire resistance behaviour of this PVC cable which had controlled the fire growth during its burning and given a low burning rate. Under high ventilation rate of 0.572 g/s, the PVC Prysmian A cable fire had only consumed up to 11% by volume of

$O_2$. The mass loss rate for these cable fires were below than 0.08 g/s for all ventilation rates. PVC cable fires with the low air flowrate of 0.192 g/s showed rich burning with equivalence ratios more than 1.2 and the cable fires at higher air flowrates had shown a lean burning condition with equivalence ratios less than 0.9. At this 35 kW/m$^2$ of heat flux and varied air flowrates, the highest HRR values were less than 140 kW/m$^2$ for these PVC cable fires. These HRR values were slightly higher compared to the highest HRR values showed by PVC Prysmian A cable fires at a lower heat flux of 25 kW/m$^2$. The primary HRR values showed less than 120 kW/m$^2$ and secondary HRR values showed less than 25 kW/m$^2$.

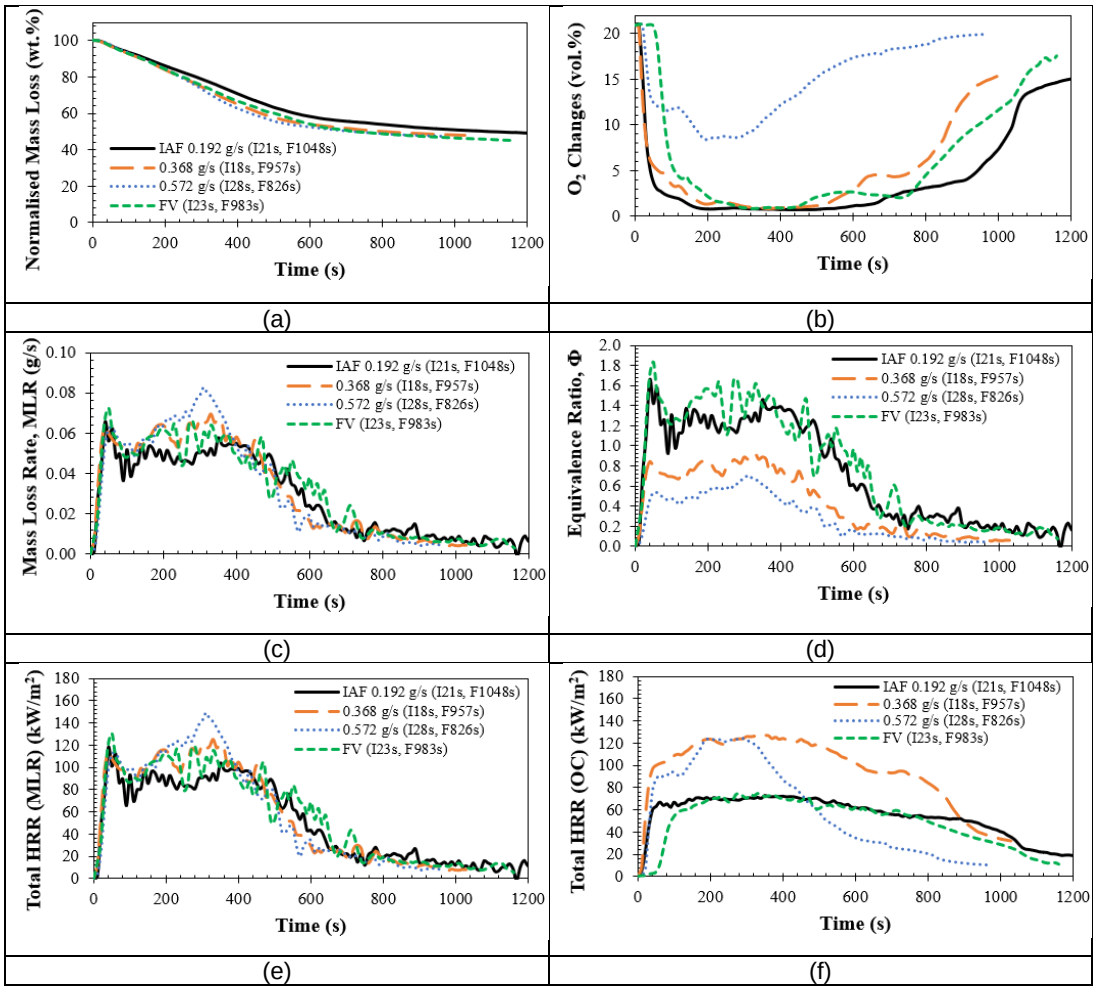

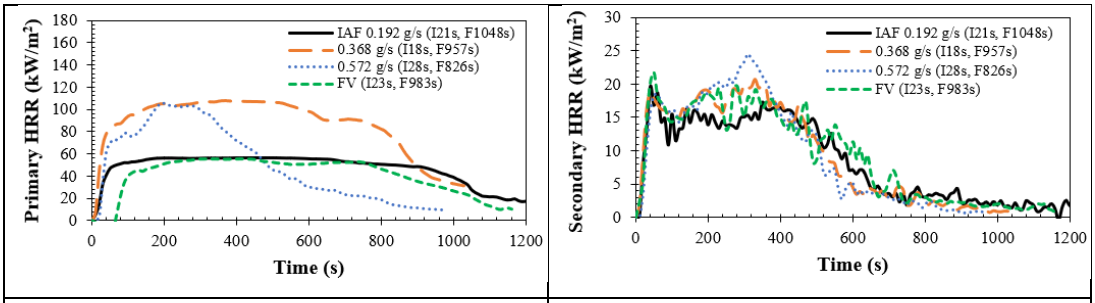


(g) (h)

**Figure 4.2** Combustion properties against time for PVC Prysmian A electrical cable fires at 35 kW/m$^2$ with various air flow rates.

The free ventilation results were unexpected and behaved in a similar way to the lowest ventilation with the controlled atmosphere box. This is possible due to the small air entrainment force of the Cone Calorimeter with natural draught governed by the distance from the base of the cone to the exit from the chimney ~0.4cm, which would only give a small induced draught. In contrast the diluted cone has a fan that draws in air and the cone products. The low entrained air for the freely ventilated cone gives rise to rich burning mixtures in the discharge pipe. The main reason that the two highest ventilation conditions have significantly different results is that both are burning lean compared with the rich mixtures in the chimney for the free and lowest ventilation conditions. This affects all the yield results discussed later.

Figure 4.3 showed combustion properties as a function of time for PVC Prysmian A electrical cable fires at 50 kW/m$^2$ irradiation level and various ventilation rates. Total burning period of about 800 s was the shortest for PVC cable fires at this heat flux compared to lower heat fluxes which giving a longer burning period. As expected, the highest mass loss given by these PVC Prysmian A cable fires was not more than 50% by weight for various fire conditions and this was discussed in the previous section. At 50 kW/m$^2$ the $O_2$ reduction due to consumption by the cable burning was high for all three ventilation rates. This indicated significant burning and a high mass loss rate of more than 0.08 g/s. Figure 4.3 (d) shows that the equivalence ratio was near stoichiometric and above 1.0, showed that most of these PVC Prysmian A cable fires had rich burning. The heat release rates for 50 kW/m$^2$ radiant heat were the highest at up to 180 kW/m$^2$ with the higher ventilation rate giving higher HRR. Primary and secondary HRR, each gave the HRR values of <150 kW/m$^2$ and <30 kW/m$^2$. In general, in comparison of the PVC Prysmian A

cable fires at different heat fluxes and ventilation rates, the higher the value of heat flux would give the higher burning rate and HRR value.

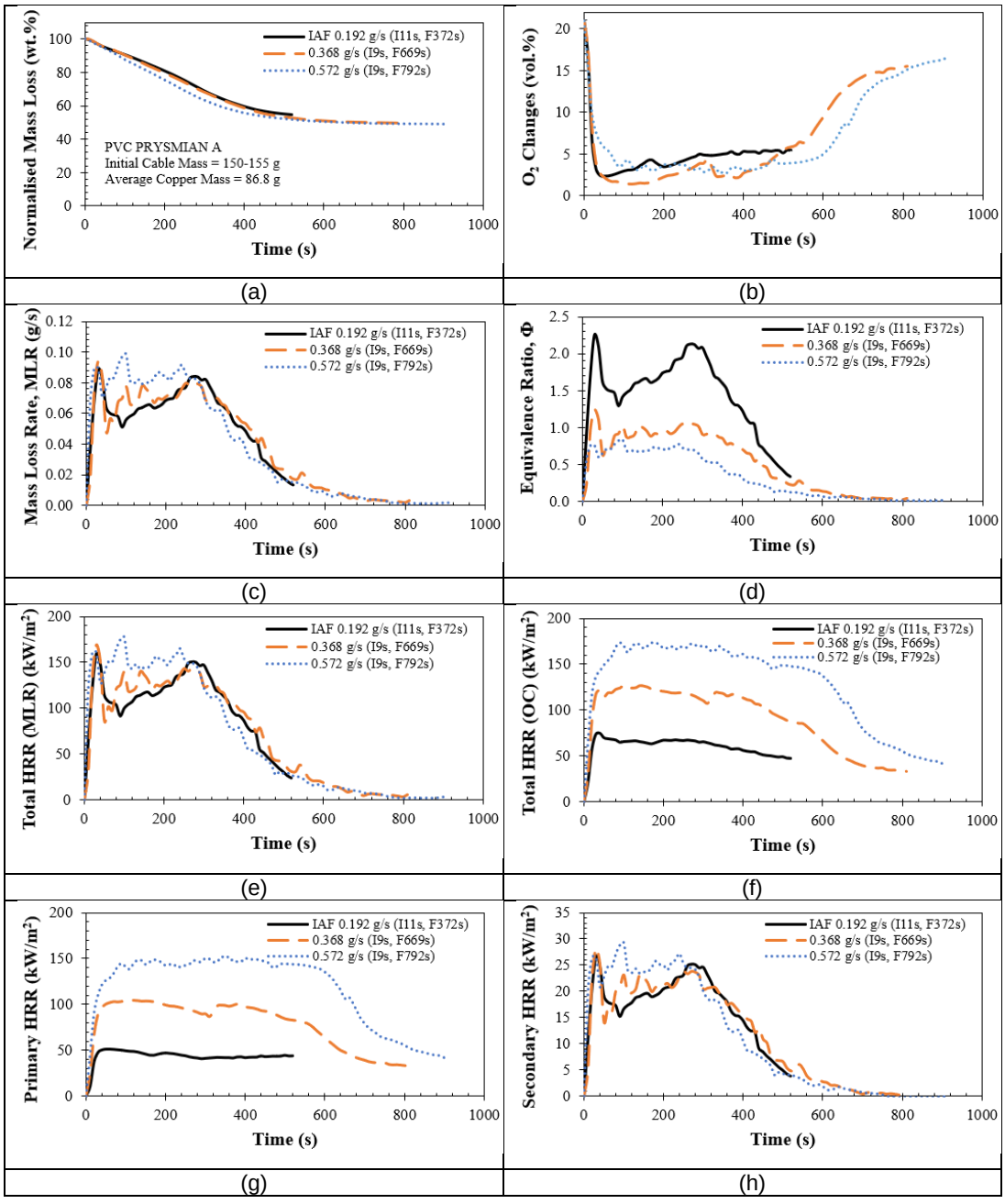


**Figure 4.3** Combustion properties against time for PVC Prysmian A electrical cable fires at 50 kW/m$^2$ with various air flow rates.

### 4.2.1.2 Other PVC Electrical Cable Fires

General combustion properties as a function of time for other PVC cable fires (PVC EC-GB 1 and PVC EC-GB 2 fires) were investigated at 35 kW/m$^2$ radiant

heat and the combustion results are shown in Figure 4.4. PVC EC-GB 1 fire took much more longer (1525 s) to reach the flame out condition compared to PVC EC-GB 2 fire (1162 s). PVC EC-GB 2 fire gave a slightly higher normalised mass loss of 12% than PVC EC-GB 1 fire (8%). Both cable fires showed the low consumption of $O_2$ which less than 2% by volume. As in Figure 4.4 (c), the highest mass loss rate (MLR) given by these electrical cable fires were about 0.07 g/s with very lean fire equivalence ratios (<0.12). Essentially these were very slow burning fires, but did have an observable flame.

Both PVC EC-GB 1 and PVC EC-GB 2 cable fires had a HRR <80 kW/m$^2$, lower than for PVC Prysmian A cable fires. EC-GB cable had a higher resistance to fire development than the Prysmian A cable, hence also giving a lower burning rate and HRR. This indicates the presence of an additional fire retardant in the EC-GB cables. The ash content in Table 3.11 was significantly higher in these cables and this indicates that a higher fire retardant compound was present, that decomposes to extract heat from the fire.

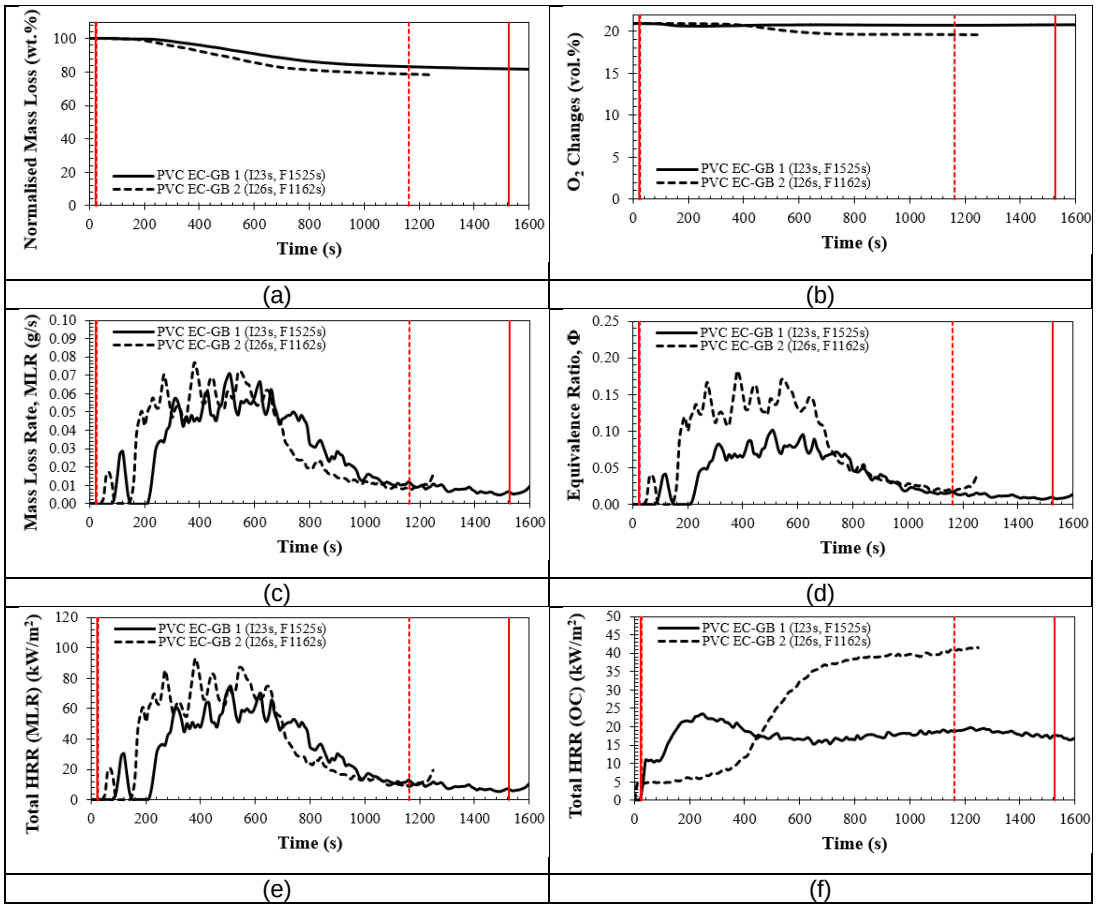

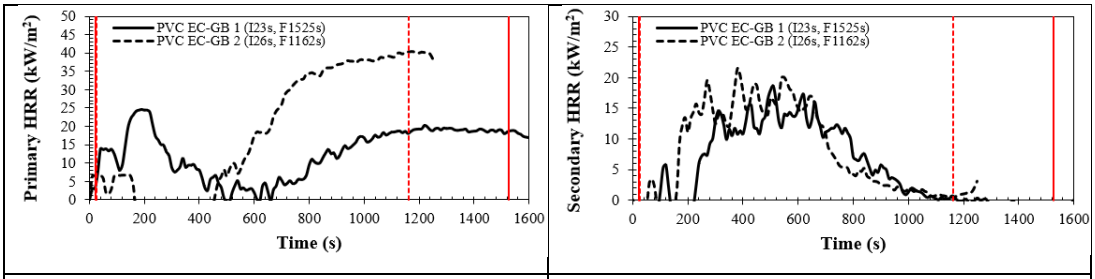


(g) (h)

**Figure 4.4** Combustion properties against time for other PVC electrical cable fires at 35 kW/m$^2$ with various air flow rates.

### 4.2.2 Non PVC Electrical Cable Fires

Solar Energy cables (HV1-4C and HV2-3C cables), Wind Turbine cables from Siemens (AMI-G and AMI-B cables), Low Smoke Zero Halogen (LSZH) cables (Prysmian B, 6701B-W and TEC2-W cables) and other non PVC cables such as FLEX1-BG and FLEX2-W electrical cables were grouped under the non PVC cable group. These cables were divided into five sub groups for comparison purpose. Chemical compounds of each cable including other details obtained from proximate and ultimate analysis were included in Table 3.11 in Chapter 3 for reference.

#### 4.2.2.1 Solar Energy Cable Fires

Solar Energy cables HV1-4C and HV2-3C were burned with a heat flux of 35 kW/m$^2$ under free ventilation and the results of combustion properties as a function of time for both cable fires are presented in Figure 4.5. The autoignition time for the two cables were substantially different with HV2-3C having an 1100 s delay and HV1-4C a 100 s delay. It is shown later in Figure 4.13 that both cables had high HCl emissions at 4000-8000 ppm, with HV2-3C emitting high HCl during the ignition delay due to devolatilisation. This indicates that both cables have PVC in their content there must be another fire retardant in HV2-3C that is not in HV1-4C. Table 3.11 shows that the ash is lower in HV2-3C so that fire retardant is unlikely to be one that forms an ash. For both cables the ash is relatively high at 25.7% for HV2-3C and 30.82% for HV1-4C.

Normalised mass loss values for both cable fires were less than 40% with the HV1-4C cable fire giving a higher mass loss of 40% than for the HV2-3C cable fire (30% mass loss). The MLR for both fires were < 0.045 g/s which the MLR

peak for HV1-4C cable fire was at 800 s and HV2-4C cable fire was at 1100 s. From Figure 4.5 (d), both cable fires showed equivalence ratios less than 0.7 which was a lean fire condition. Heat release rates for these cable fires were less than 80 kW/m$^2$ with the maximum primary HRR not more than 50 kW/m$^2$ and secondary HRR less than 13 kW/m$^2$. There is thus no obvious explanation of why HV2-3C has such a long ignition delay and this needs further investigation, which should include more details on the ash composition. Fig. 4.5 (d) shows that the equivalence ratio for HV2-3C is leaner than HV1-4C and it could be that the leaner mixture is too lean to burn, which would be valid if the gases were Hydrocarbons. The mixture goes richer and ignition occurs.

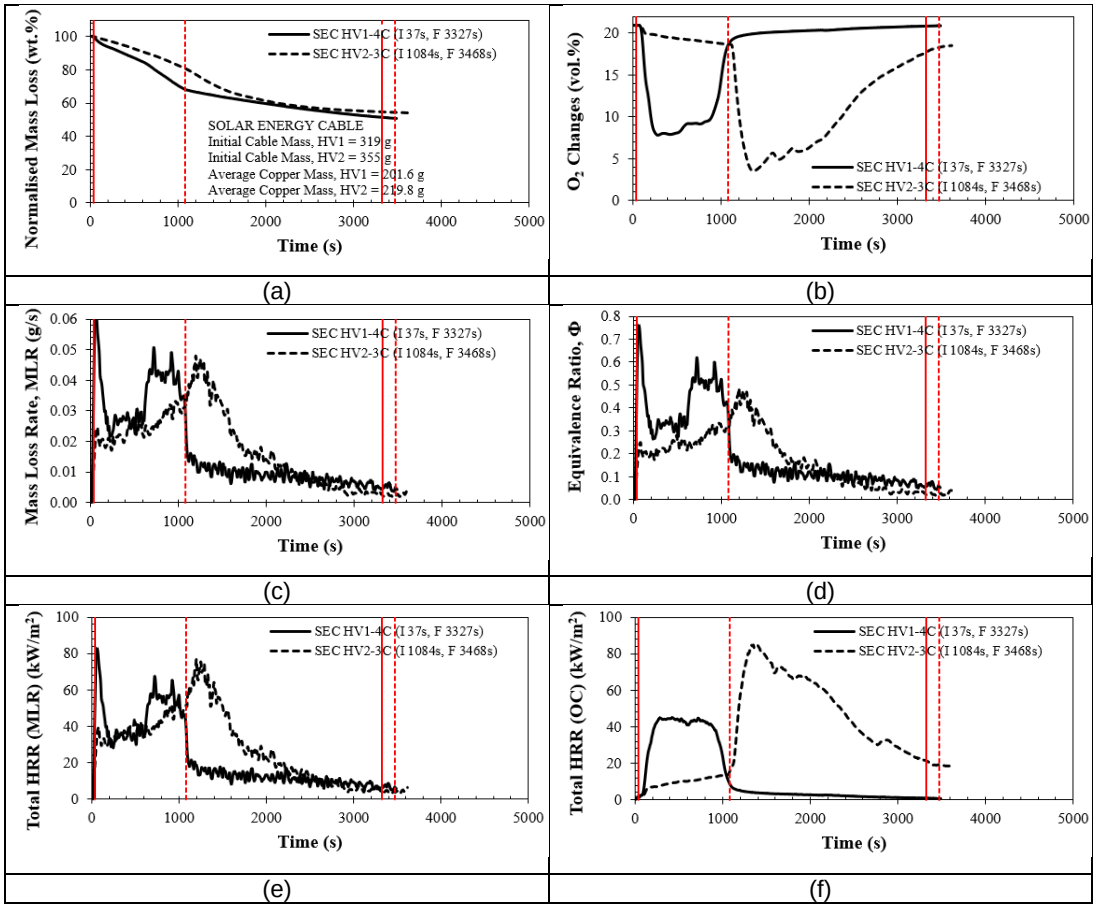

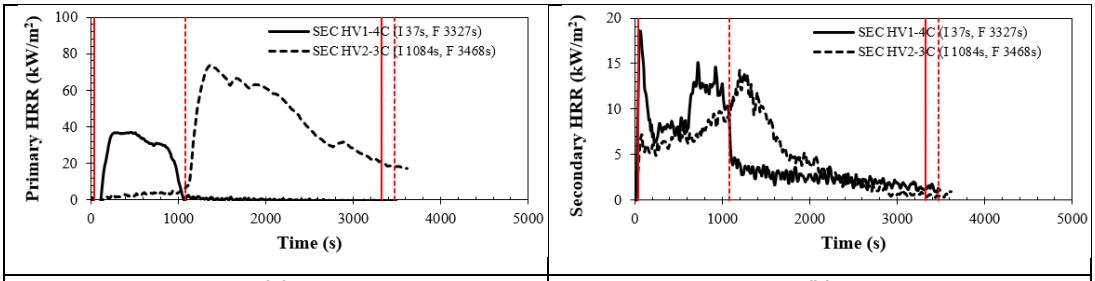


(g) (h)

**Figure 4.5** Combustion properties against time for Solar Energy cable fires at 35 kW/m$^2$ with free ventilation.

### 4.2.2.2 Siemens' Wind Turbine Cable Fires

Two different cables (AMI-G and AMI-B cables) from Siemens were tested in the Cone Calorimeter at 35 kW/m$^2$ irradiation level with free ventilation. Results of combustion properties as a function of time are shown in Figure 4.6. The ignition delay was the same for both cables, but the flaming combustion was much greater for AMI-G. This indicates that AMI-B had a flame retardant that was released in the flaming combustion phase. It is shown later that there was no significant HCl, so the retardant could not be PVC or any other Chlorine compound. It is not clear why these two cables had such significantly different performance. Table 3.11 shows that they had a similar GCV and similar ash content and similar stoichiometric A/F. It is shown later in the emissions section that during the early combustion phase both cables behaved in a similar way with the same peak emissions. The main fire retardant appeared to be Sulphur based as high $SO_2$ emissions were found for both cables. The emissions results do not show a reason for AM1-G to burn for substantially longer than AM1-B. The equivalence ratio shows a much leaner peak for AM1-B and it could be that the gas phase reactions that give flaming combustion were simply too lean to sustain combustion.

The AMI-B grey cable burned faster than AMI-G black cable with 10% of normalised mass loss while AMI-G cable fire gave 20% of normalised mass loss. It took about 643 s to reach the flame out condition for AMI-B compared to the AMI-G cable fire which burned much more longer before extinguished at 2928 s. AMI-B cable fire gave a maximum $O_2$ consumption of 11% while AMI-G showed two peaks of $O_2$ consumption with the first peak gave $O_2$ reduction level of 11% at 400 s and the second peak gave about 18% of $O_2$ reduction at 1600 s. The highest mass loss rate (MLR) for AMI-G cable fire was ~0.05 g/s which higher than the highest MLR by AMI-B cable fire (~0.04

g/s). Both cable fires experienced lean burning with equivalence ratios below than 0.4. The highest total heat release rate (HRR) for these cable fires was <100 kW/m$^2$ with a maximum primary HRR was less than 95 kW/m$^2$ and secondary HRR not more than 14 kW/m$^2$.

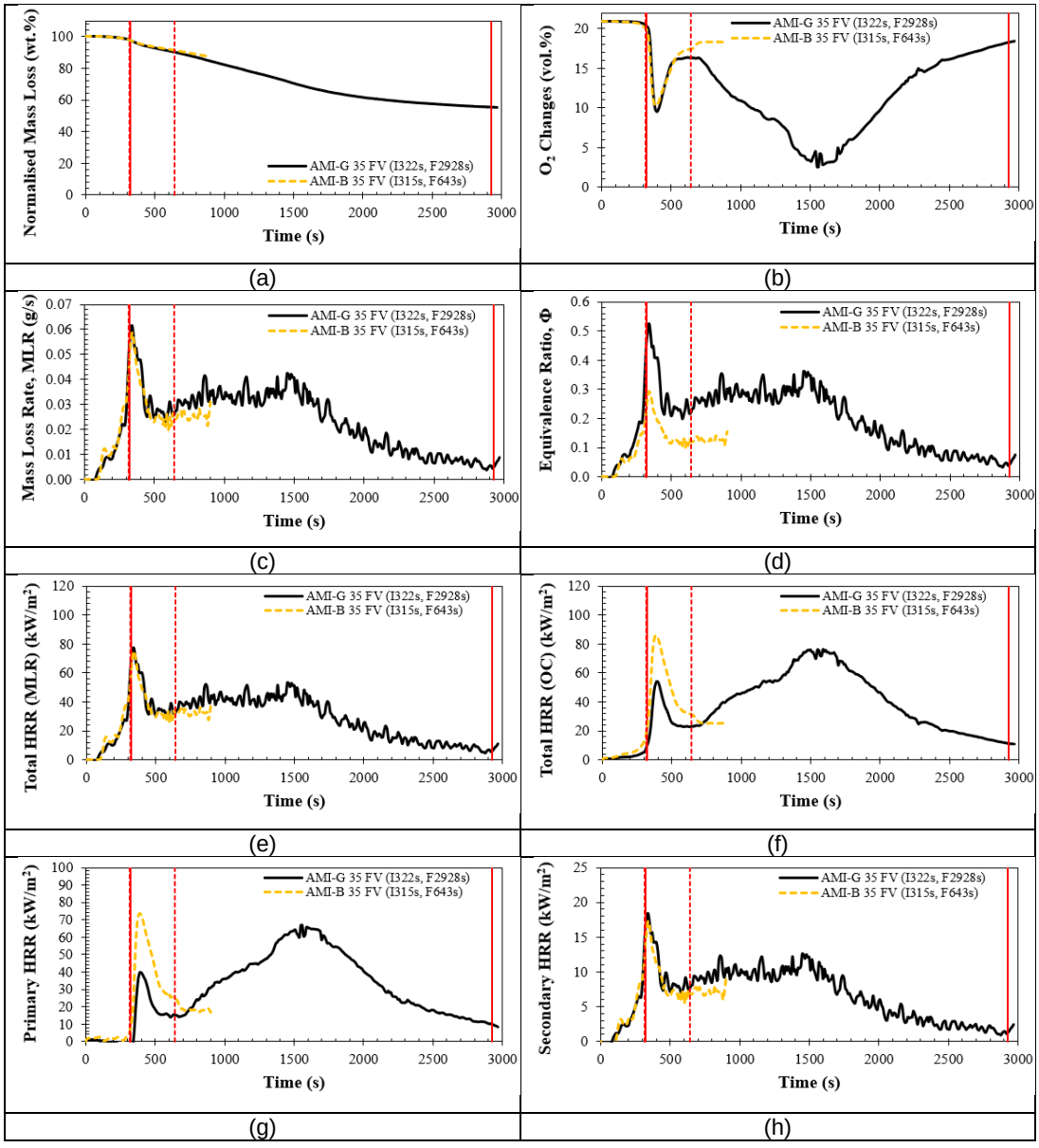


**Figure 4.6** Combustion properties against time for Siemens' Wind Turbine cable fires at 35 kW/m$^2$ with free ventilation.

### 4.2.2.3 LSZH Electrical Cable Fires

In addition to the Siemens' Wind Turbine cables (AMI-G and AMI-B cables), Prysmian B, 6701B-W and TEC2-W cables were also LSZH (Low Smoke Zero

Halogens) cables. In the Cone Calorimeter tests, these three LSZH cables (Prysmian B, 6701B-W and TEC2-W cables) were burned individually at irradiation level of 35 kW/m$^2$ with free ventilation. For fire conditions of irradiation level of 50 kW/m$^2$ and restricted ventilation (9.4 L/min or 0.192 g/s), only Prysmian B and 6701B-W cables were tested.

Figure 4.7 shows the combustion properties as a function of time for LSZH electrical cable fires at different heat fluxes and ventilation rates. For tests at heat flux of 35 kW/m$^2$ and free ventilation, Prysmian B cable burned quicker than 6701B-W and TEC2-W cable samples with the ignition at 112 s and the flame out at 366 s. TEC2-W cable fire had the longest burning period with auto ignition after 217 s and a flame out at 1032 s. TEC2-W cable fire gave higher values of mass loss, MLR and HRR compared to the other two cable fires under the same fire conditions. The fire equivalence ratios for the TEC2-W cable fire was rich at up to 1.2, while Prysmian B and 6701B-W cable fires had given fire equivalence ratios less than 0.4.

At 50 kW/m$^2$ with restricted ventilation Prysmian B and 6701B-W cable fires had a higher MLR, ER and HRR than the cable fires at 35 kW/m$^2$ radiation with free ventilation.

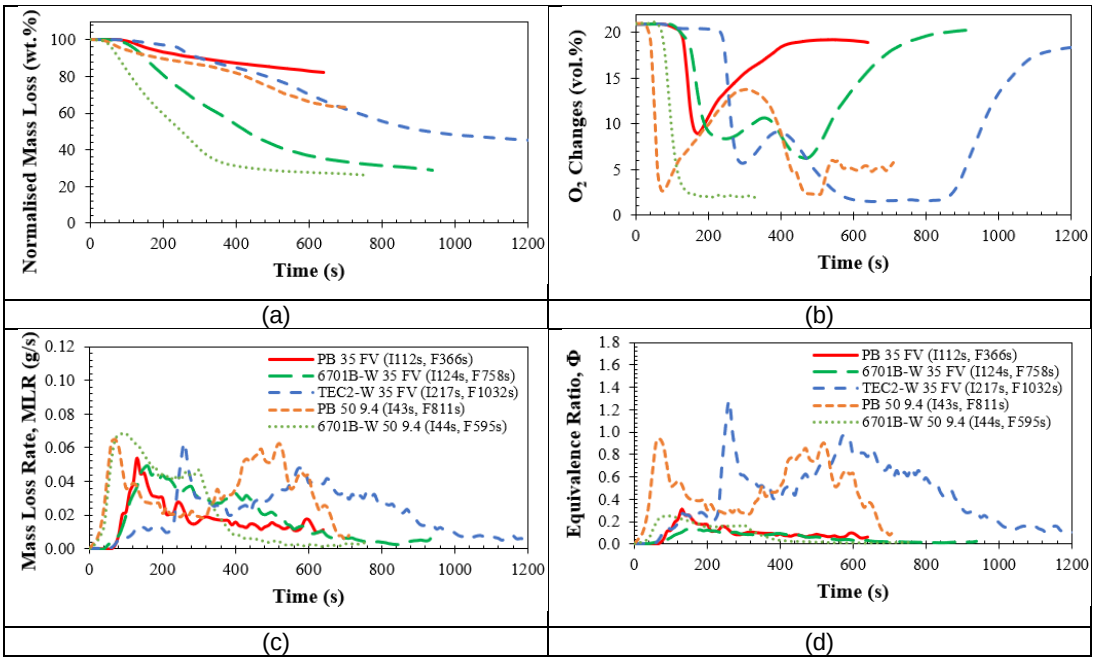

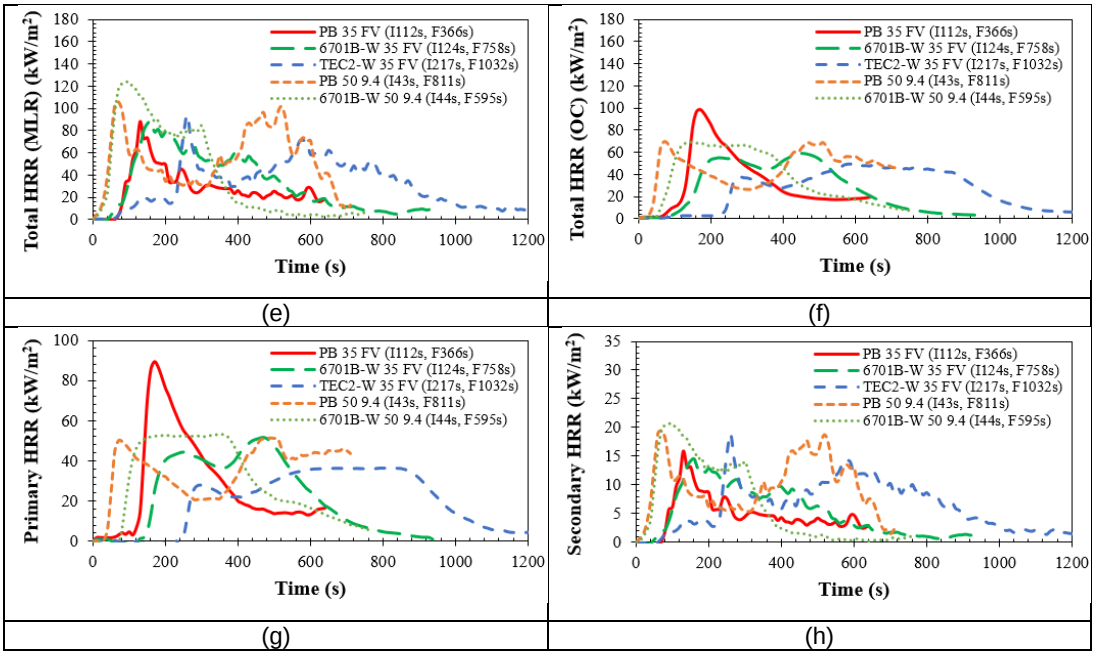


**Figure 4.7** Combustion properties against time for LSZH electrical cable fires at different heat fluxes and ventilation rates.

### 4.2.2.4 Other Non-PVC Electrical Cable Fires

The FLEX1-BG (high PVC content as HCl are high, as will be shown in the toxic gas section), with 35 kW/m$^2$ radiant heating, had a shorter burning period and a higher burning rate than the FLEX2-W electrical cable fire as shown in Figure 4.8 for free ventilation. The total mass loss for FLEX2-W burning was 30% which was lower than the 50% of mass loss for FLEX1-BG fire. FLEX1-BG fire consumed about 20% Oxygen by volume, whereas the FLEX2-W fire consumed about 3% Oxygen. The MLR for FLEX1-BG fire gave a maximum peak at 0.09 g/s and FLEX2-W fire had the highest MLR peak at 0.07 g/s. Both of these electrical cable fires showed lean burning combustion. FLEX1-BG fire had the highest equivalence ratio of 0.8 and FLEX2-W fire had very lean equivalence ratios of 0.15, during steady state burning. This contributed to a higher heat release rate (HRR) for FLEX1-BG fire in comparison with FLEX2-W fire as shown in Figure 4.8 (e) and (f). GCV value for FLEX1-BG was 26.65 MJ/kg and for FLEX2-W was 16.81 MJ/kg as shown in Table 3.11. A high GCV value of material would give a high total HRR value from its burning and this HRR based MLR was typically higher than the HRR based on Oxygen consumption (OC) as shown in Figure 4.8 (e) and (f). The primary HRR for the FLEX1-BG fire was double (160 kW/m$^2$) that of the FLEX2-W fire (80 kW/m$^2$) after 200 s of burning time.

This higher reactivity of FLEX1-BG was unexpected as it is shown in the toxicity section that the HCl was very high and this was likely to be due to a high PVC content of the cable polymer sheath. PVC is normally quite unreactive and the Chlorine released would normally act as a fire retardant. A significant difference in the two cables is shown in Table 3.11 to be the high ash content of FLEX2-W of 31% compared with 2% in FLEX1-BG. This is also why the GCV was much lower for FLEX2-W. One method of fire retardation is to add compounds such as Sodium bicarbonate to the polymer composition, which decomposes endothermically when heated and releases $CO_2$. The net effect is to retard the flame propagation and the compound appears as a high ash fraction in the polymer composition. It is possible that this type of fire retardant was incorporated into FLEX2-W, which was more effective that the natural low reactivity of the PCV cable composition of FLEX1-BG. The very lean equivalence ratio of the fire for FLEX2-W would also make it very difficult to propagate a flame due to flammability considerations.

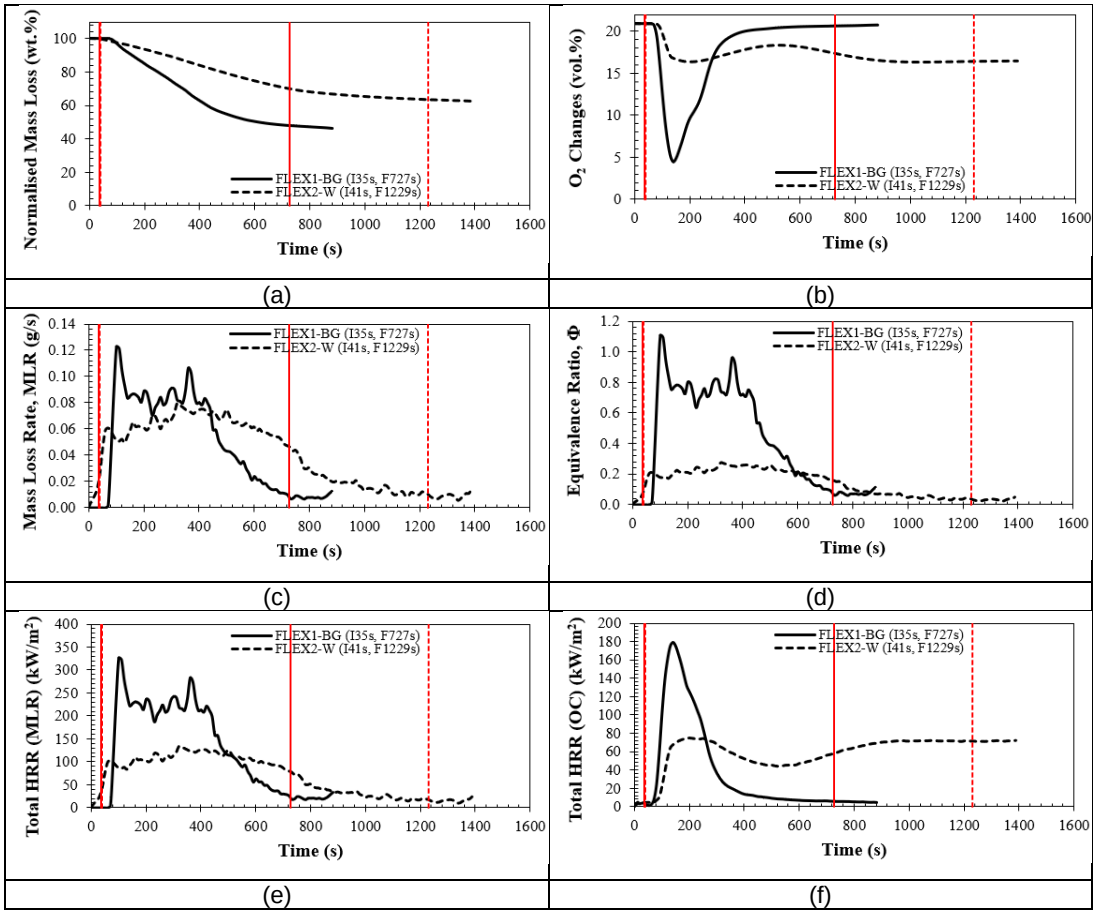

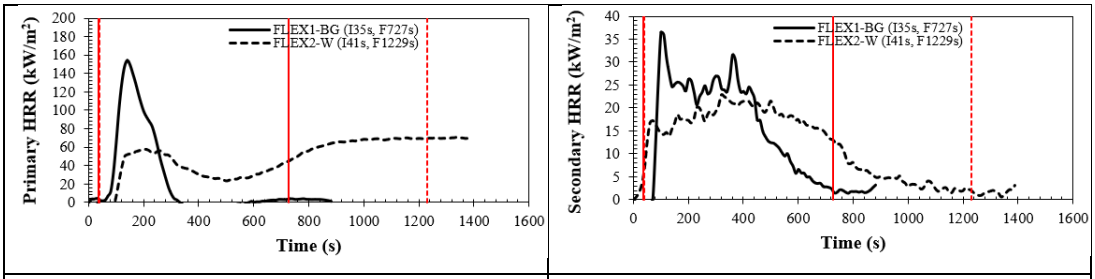


(g) (h)

**Figure 4.8** Combustion properties against time for other tested electrical cable fires at 35 kW/m$^2$ with free ventilation.

## 4.3 Toxicity from Various Types of Electrical Cable Fires

### 4.3.1 Gas Concentrations for PVC Prysmian A Cable Fires

Gas concentrations as a function of time for PVC Prysmian A electrical cable fires at 25 kW/m$^2$ and various ventilation rates are shown in Figure 4.9. The concentration of most of toxic gases was the highest for PVC Prysmian A cable fire under a ventilation rate of 19.2 g/sm$^2$ compared to higher air flowrates. At higher air flowrates leaner equivalence ratios were found as shown in Figure 4.1 (d). This would reduce the burning rate of burned materials and would release lower gaseous emission. However, concentrations of some species like Formaldehyde, Acrolein, $NH_3$, Acetaldehyde and Toluene were the highest for PVC Prysmian A cable fire for a ventilation rate of 57.2 g/sm$^2$. Well ventilated fires at low fire temperatures can produce partially oxidised Hydrocarbons such as the Aldehydes found in this work . The highest gaseous emissions were shown for PVC Prysmian A cable fire at an air flowrate of 19.2 g/sm$^2$ and occurred at 400 s, while the highest gaseous emissions from the PVC Prysmian A cable fire with an air flowrate of 57.2 g/sm$^2$ was after 700 s. HCl concentrations were high for these PVC cable fires, with concentrations up to 16000 ppm. $NH_3$ emission was observed at 500 s for PVC cable burning with non-flaming fire under an air flowrate of 57.2 g/sm$^2$. For PVC Prysmian A cable fires at this irradiation level, the highest THC concentration was about 100000 ppm or 0.1%.

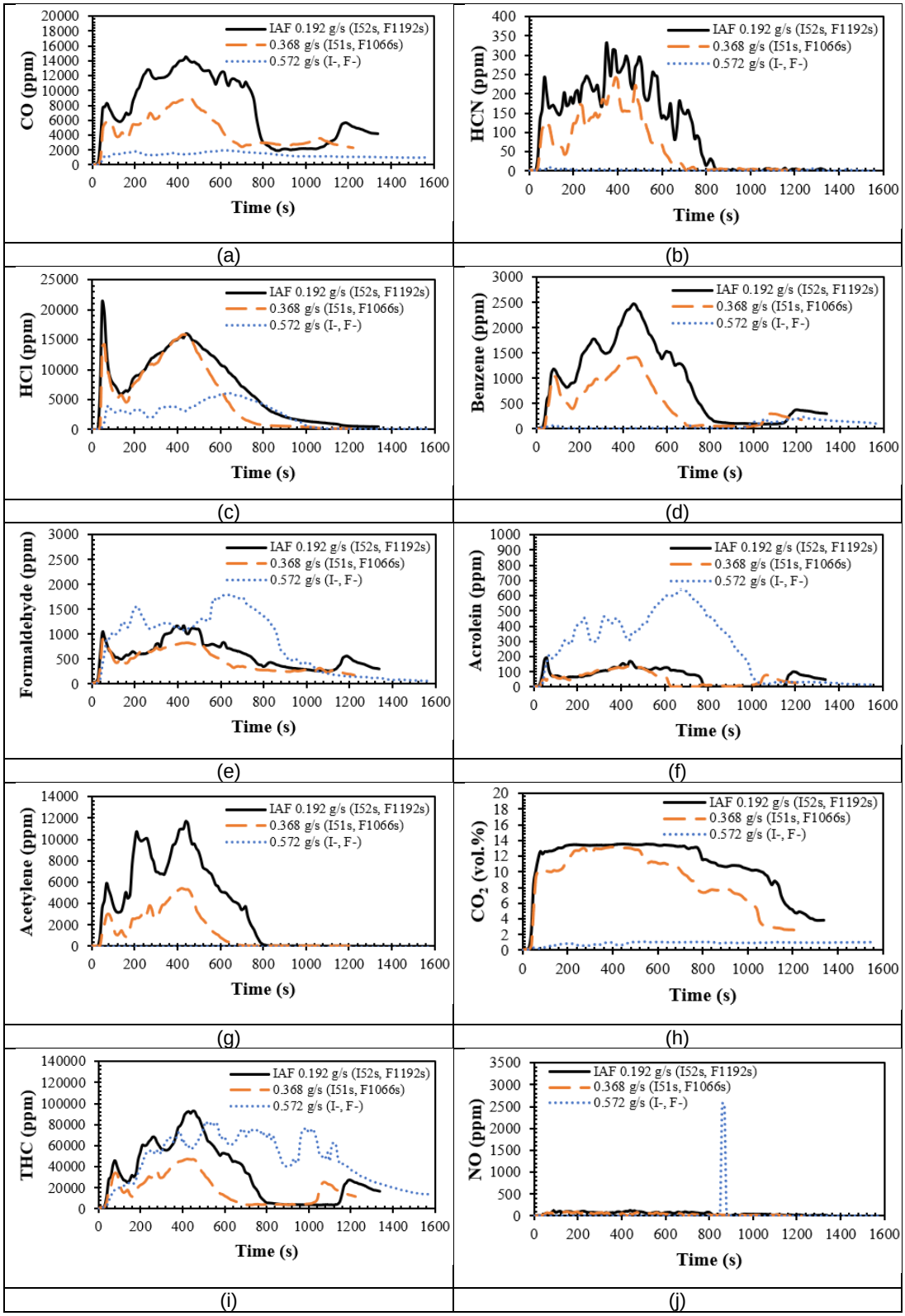
CO (ppm)
HCN (ppm)
HCl (ppm)
Benzene (ppm)
Formaldehyde (ppm)
Acrolein (ppm)
Acetylene (ppm)
CO2 (vol.%)
THC (ppm)
NO (ppm)
Time (s)
IAF 0.192 g/s (I52s, F1192s)
0.368 g/s (I51s, F1066s)
0.572 g/s (I-, F-)
(a)
(b)
(c)
(d)
(e)
(f)
(g)
(h)
(i)
(j)

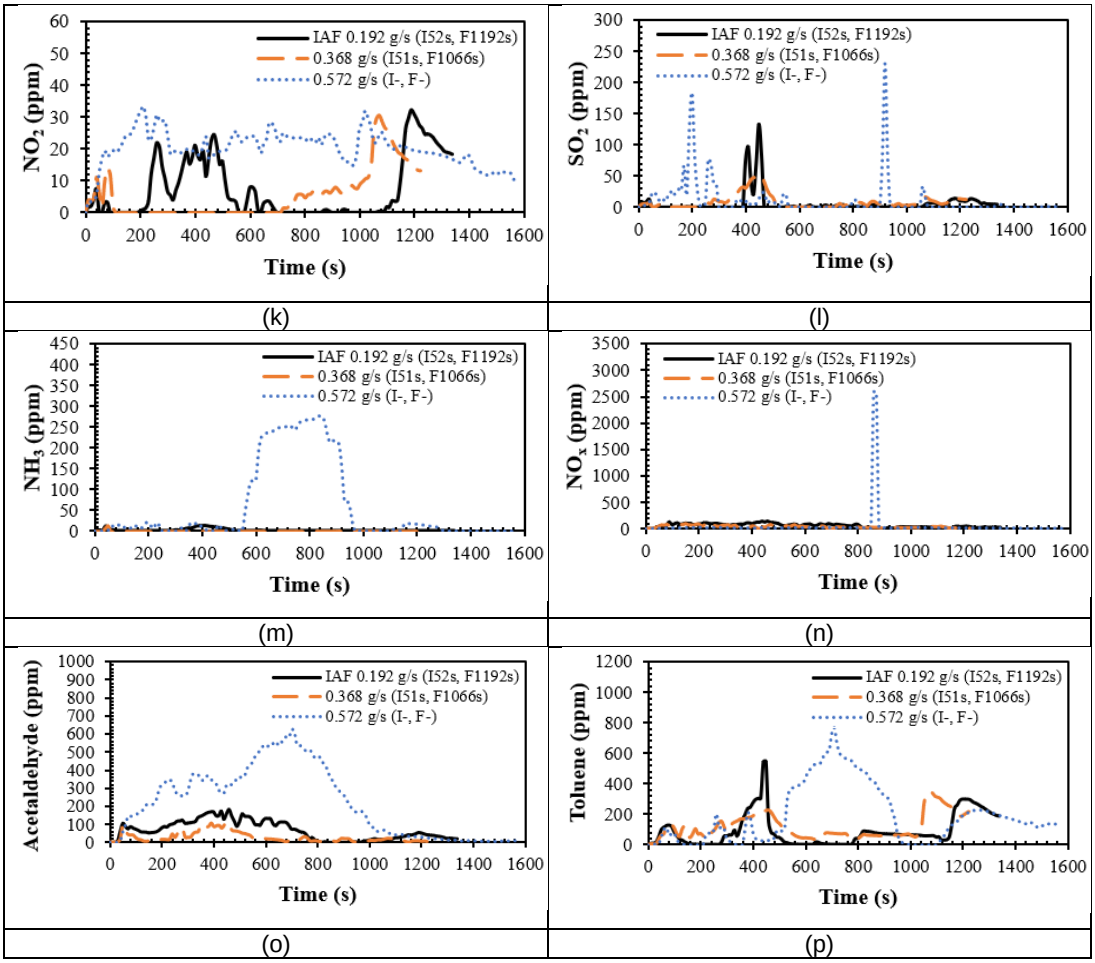


**Figure 4.9** Gas concentrations as a function of time for PVC Prysmian A electrical cable fires at 25 kW/m$^2$ and various ventilation rates.

Figure 4.10 showed concentration of gases for PVC Prysmian A electrical cable fires at heat flux of 35 kW/m$^2$ under four different ventilation rates. As shown in the following Figure 4.10, an increase in heat flux value, it gave an increase in emissions for most of toxic gases for these PVC Prysmian A cable fires. The highest CO concentration was about 19000 ppm. HCl concentration for PVC cable fire at 35 kW/m$^2$ irradiation level showed about 4000 ppm higher than the PVC cable fire at 25 kW/m$^2$ irradiation level. Toxic gas concentrations from PVC Prysmian A cable fire under free ventilation rate were lower than the cable fire under ventilation rates of 0.192 g/s (9.4 L/min) and 0.368 g/s (18 L/min).

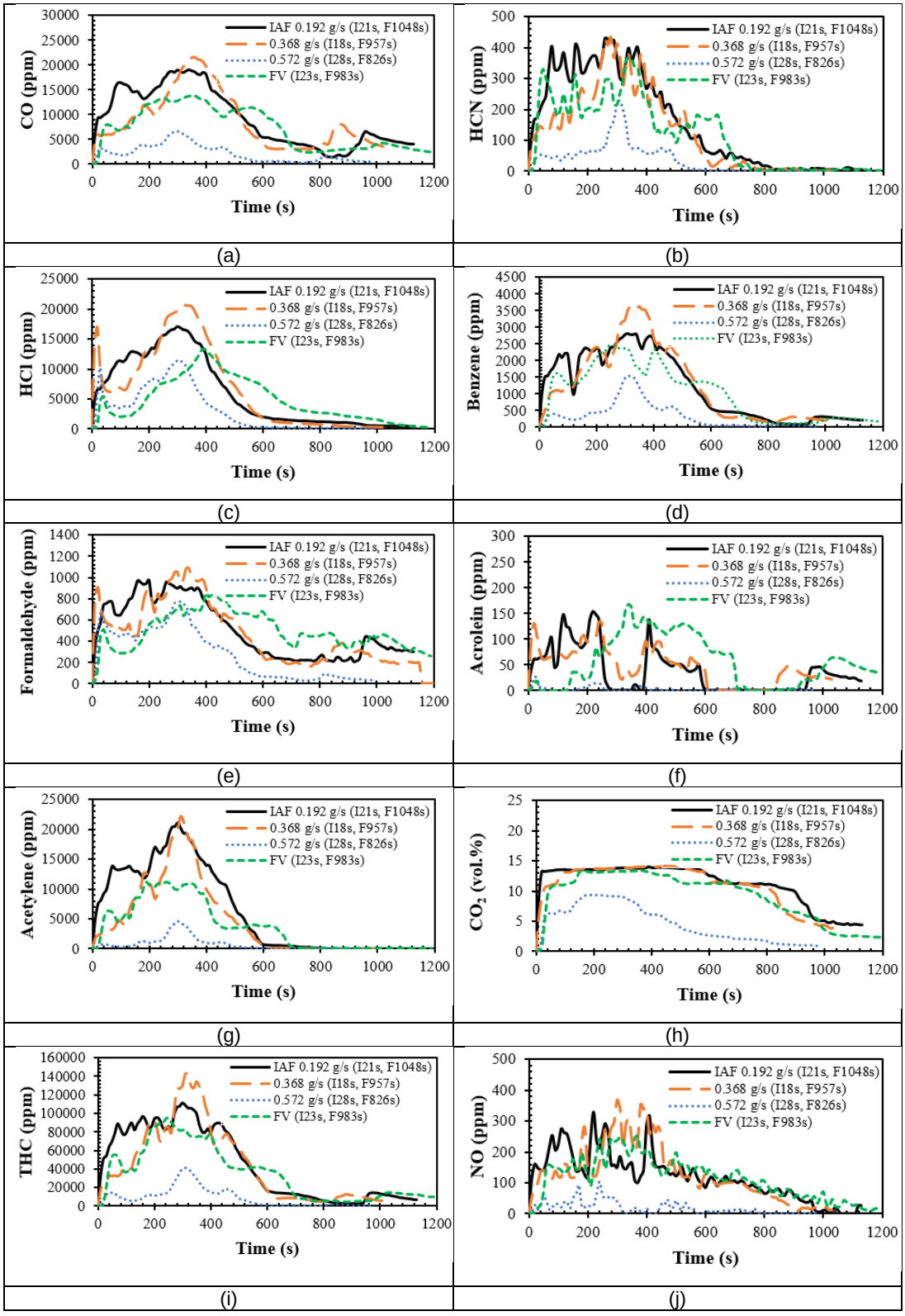
CO (ppm)
HCN (ppm)
HCl (ppm)
Benzene (ppm)
Formaldehyde (ppm)
Acrolein (ppm)
Acetylene (ppm)
CO2 (vol.%)
THC (ppm)
NO (ppm)
Time (s)
IAF 0.192 g/s (I21s, F1048s)
0.368 g/s (I18s, F957s)
0.572 g/s (I28s, F826s)
FV (I23s, F983s)
(a)
(b)
(c)
(d)
(e)
(f)
(g)
(h)
(i)
(j)

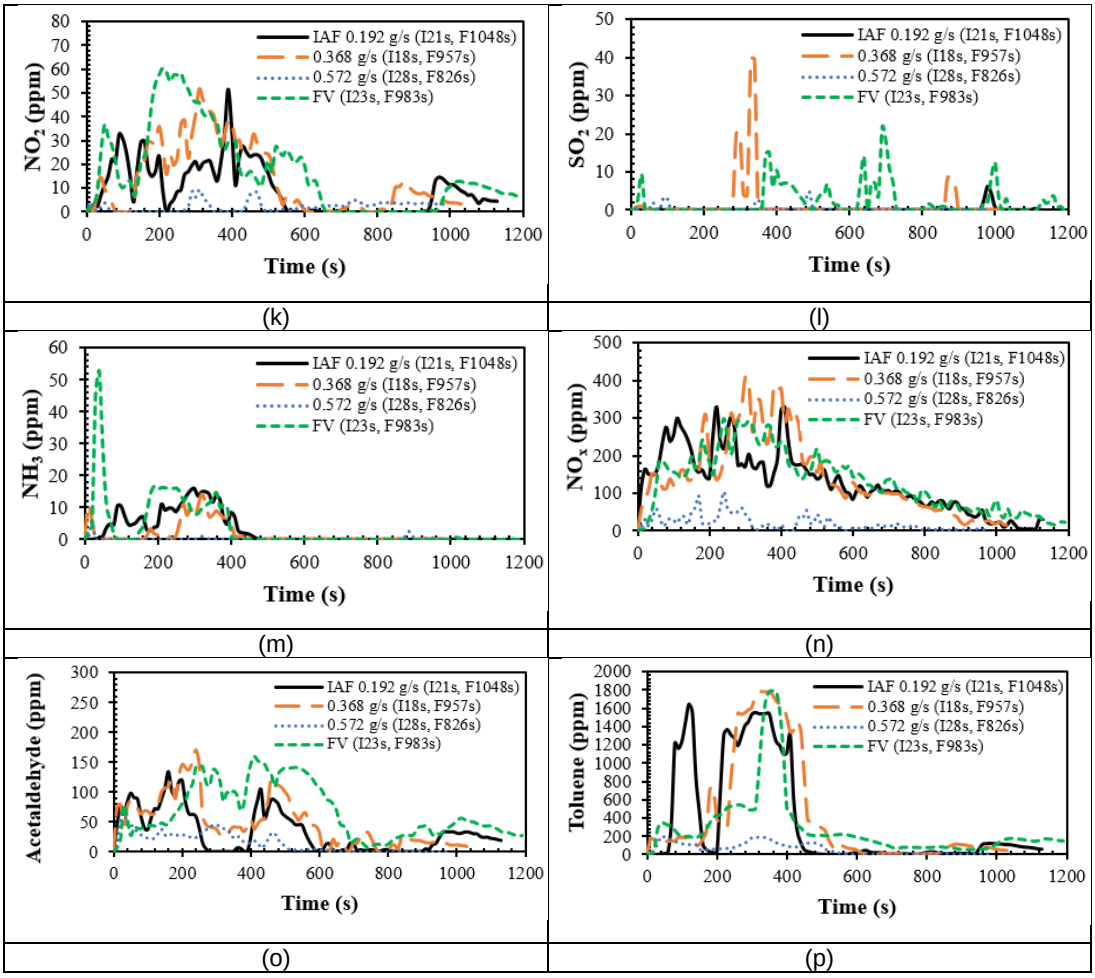


**Figure 4.10** Gas concentrations as a function of time for PVC Prysmian A electrical cable fires at 35 kW/m$^2$ and various ventilation rates.

At higher heat flux, the burning period for PVC Prysmian A cable fire had become shorter. Gas concentrations as a function of time for PVC Prysmian A electrical cable fires at 50 kW/m$^2$ and various ventilation rates were shown in Figure 4.11. At heat flux of 50 kW/m$^2$, PVC cable fire had shown to take a longer burning duration when ventilation rate was increased. Higher ventilation rate would decrease fire equivalence ratio and this would allow a longer burning duration for PVC Prysmian A cable fire and more toxic gases would be produced. CO gave the highest concentration of up to 65000 ppm for the cable fire at a higher ventilation rate of 0.572 g/s compared to <60000 ppm for cable fires at the lower ventilation rates. $CO_2$ concentrations for this cable fires for all three ventilation rates showed a maximum value of 14% by volume and this was the highest $CO_2$ emission level which was achieved by these PVC Prysmian A cable fires under various fire conditions.

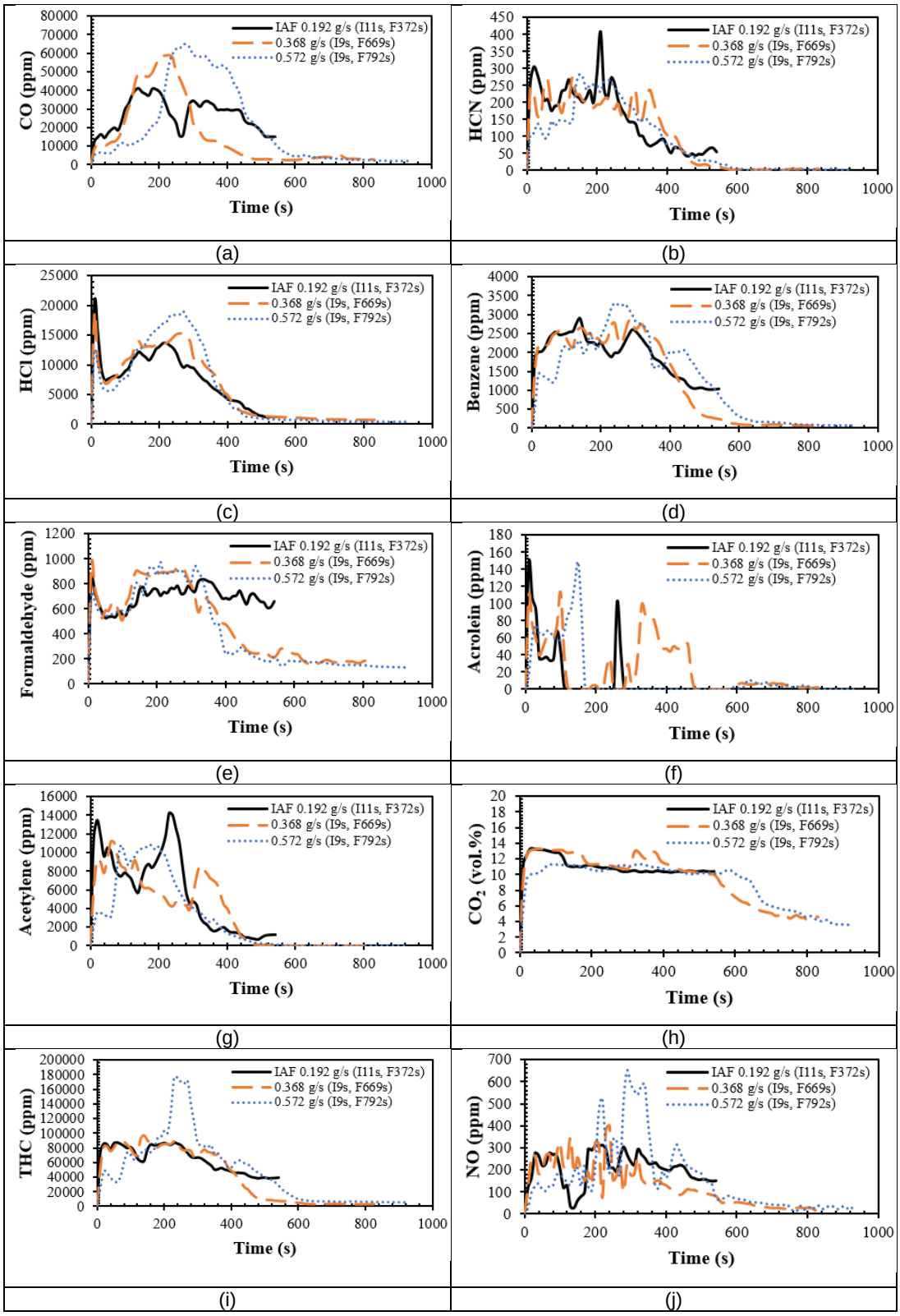
CO (ppm)
HCN (ppm)
HCl (ppm)
Benzene (ppm)
Formaldehyde (ppm)
Acrolein (ppm)
Acetylene (ppm)
CO2 (vol.%)
THC (ppm)
NO (ppm)
Time (s)
IAF 0.192 g/s (I11s, F372s)
0.368 g/s (I9s, F669s)
0.572 g/s (I9s, F792s)
(a)
(b)
(c)
(d)
(e)
(f)
(g)
(h)
(i)
(j)

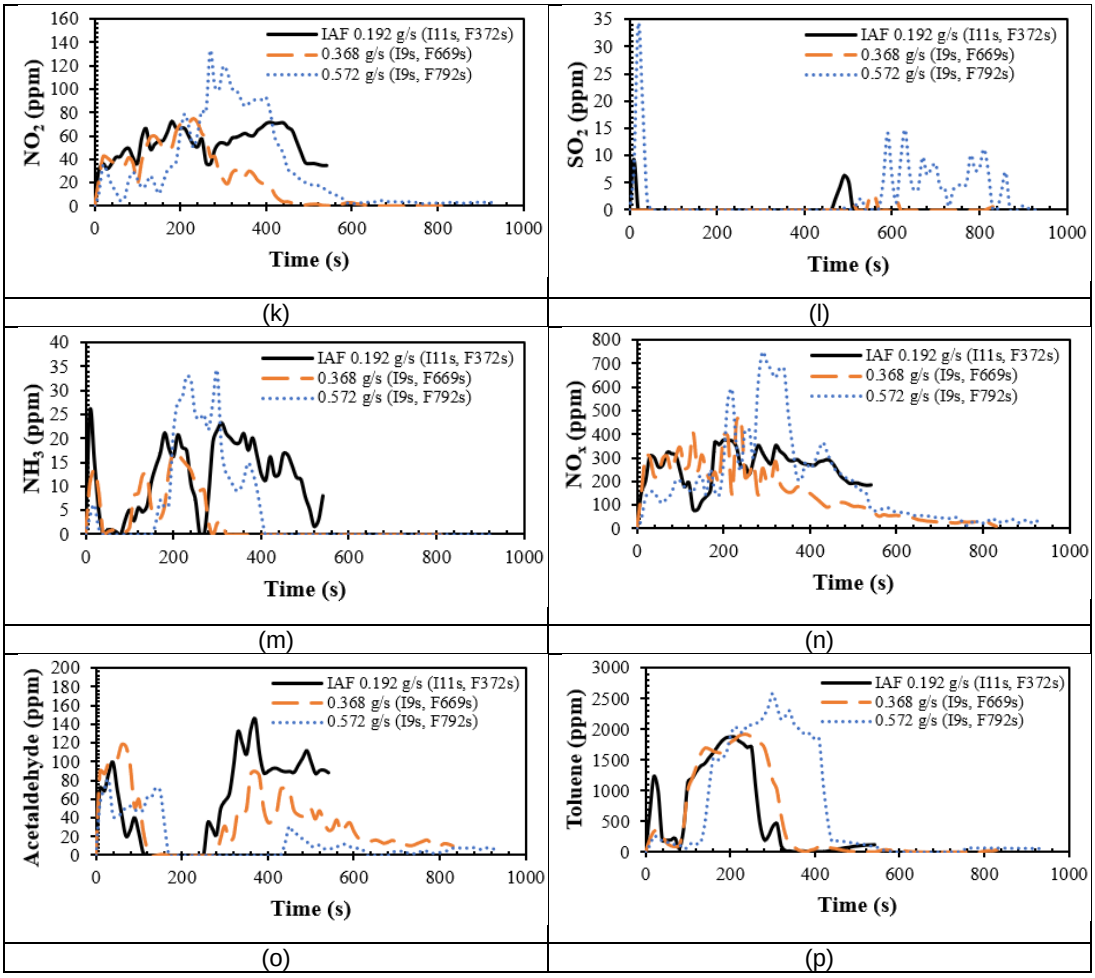


**Figure 4.11** Gas concentrations as a function of time for PVC Prysmian A electrical cable fires at 50 kW/m$^2$ and various ventilation rates.

### 4.3.2 Gas Concentrations for Other Electrical Cable Fires

Concentration of gases as a function of time for PVC electrical cable fires (PVC EC-GB 1 and PVC EC-GB 2 cable fires) under test conditions of 35 kW/m$^2$ irradiation level with free ventilation were shown in Figure 4.12. CO emission was higher for PVC EC-GB 2 fire (1200 ppm) compared to PVC EC-GB 1 fire (200 ppm). Concentrations for most of toxic species were higher for PVC EC-GB 2 cable fire than PVC EC-GB 1 cable fire except for $SO_2$ and $NO_x$ emissions. In comparison with other electrical cable fires, these electrical cable fires showed the lowest emission level for most of toxic gases. HCN concentration showed less than 15 ppm for both electrical cable fires. The highest concentration of HCl was about 500 ppm for PVC EC-GB 2 cable fire and none significant HCl emission was shown by PVC EC-GB 1 cable fire. From the low $CO_2$ concentration values less than 1.8% by volume in Figure

4.12 (g) and very low THC (total Hydrocarbons) value of less than 12000 ppm, it proved that these electrical cable samples had a very strong resistance to the growth of fire. Both cable samples were ignited fast which was less than half a minute and experienced the burning process of at least 20 minutes before extinguished with producing low emission of toxic species which the burning of these cables much more cleaner or less toxic than other cable fires.

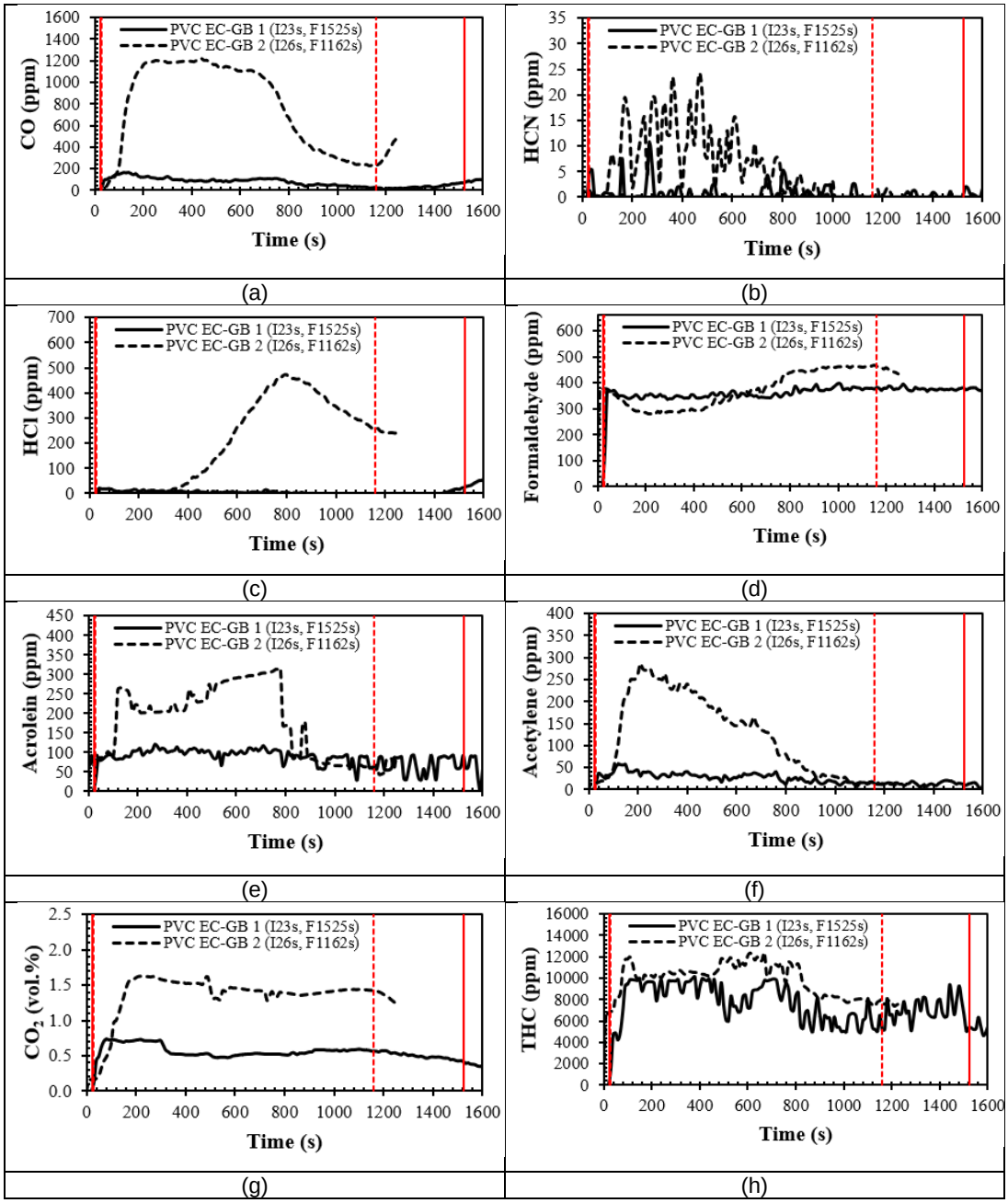

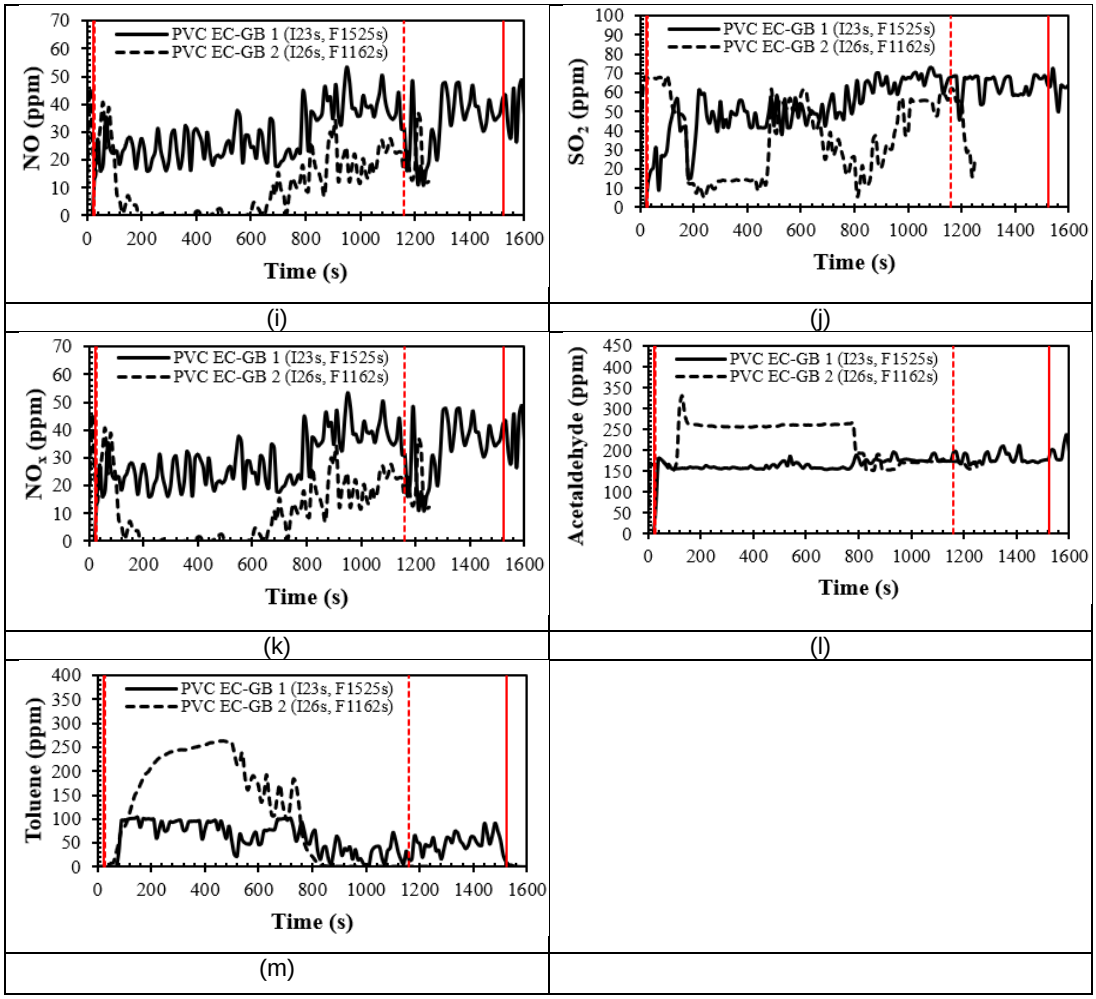


**Figure 4.12** Concentration of gases as a function of time from other PVC electrical cable fires at 35 kW/m$^2$ and free ventilation.

Two types of solar energy cables, HV1-4C and HV2-3C were compared. Figure 4.13 showed gas emissions against time from Solar Energy cable fires at 35 kW/m$^2$ and free ventilation condition. For each tested cables, the highest gas concentration peaks were observed after the ignition start where for HV1-4C was at 250 s and 600 s and for HV2-3C was at 1100 s. For HV2-3C, some gases such as HCl, Formaldehyde, Acrolein and $SO_2$ were giving a high peak at 200 s after test start before having an ignition at 1084 s. CO concentration for HV2-3C cable fire was 16000 ppm, at least 2.5 times higher than the CO concentration for HV1-4C cable fire. With HCl concentration up to 9000 ppm, it seemed that these cables contained halogenated fire retardants. From these Solar Energy cable fires, the production of $NO_2$ and $NH_3$ were too low and not really significant (<50 ppm) to be considered for further toxicity analysis. In comparison, the HV2-3C cable generally produced more toxic gases than the

HV1-4C. It can be said that the HV2-3C is more toxic than HV1-4C when burned.

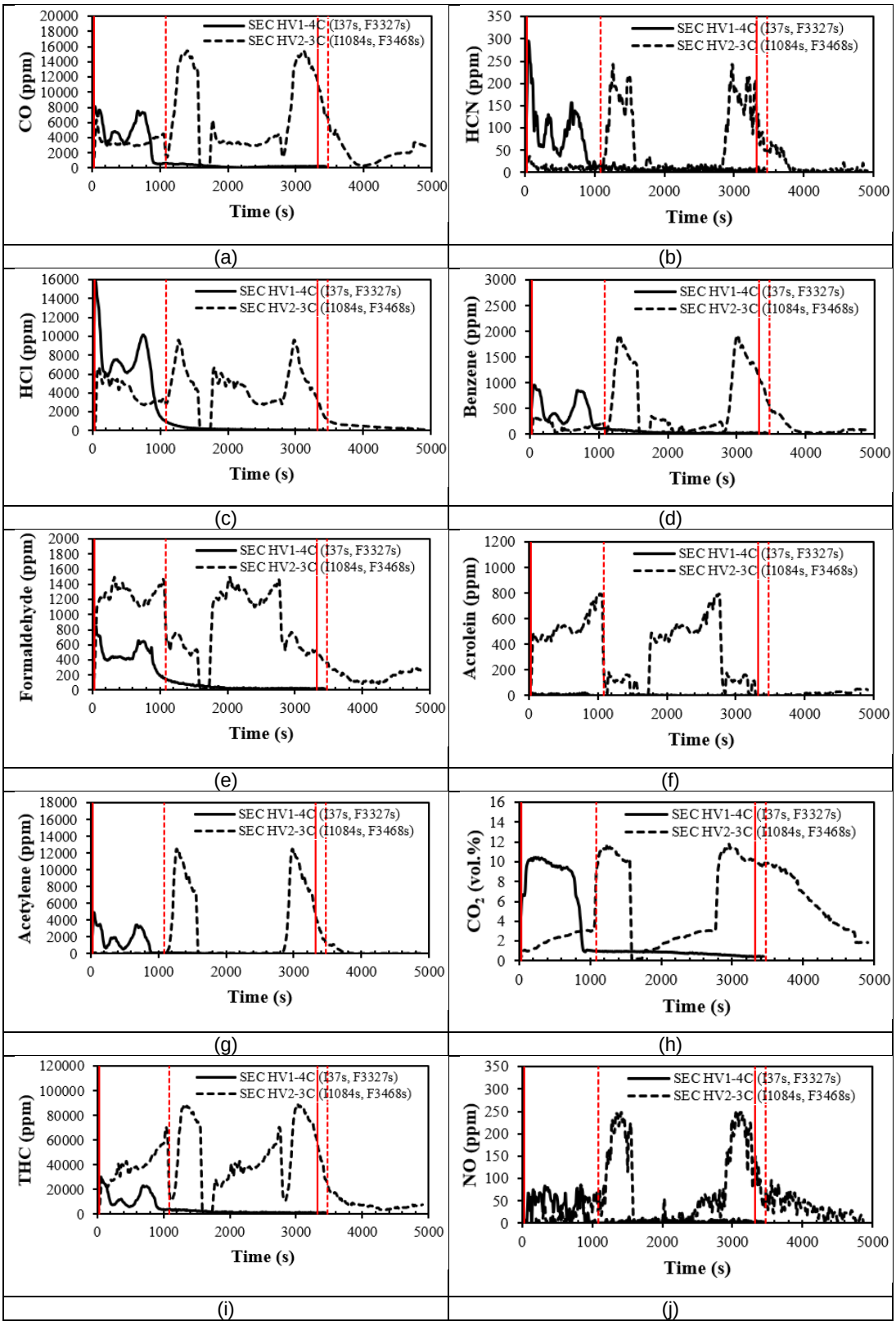

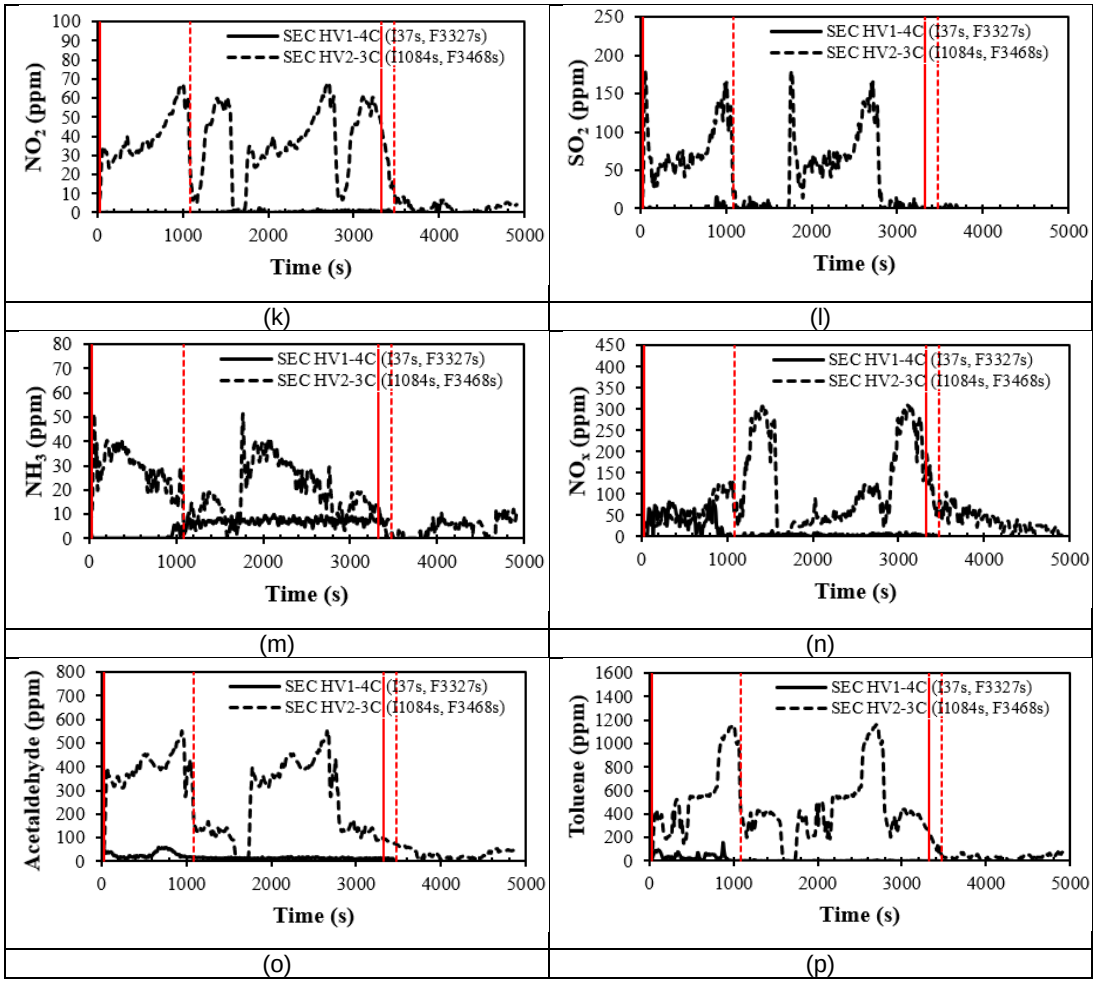


**Figure 4.13** Concentration of gases as a function of time from Solar Energy cable fires at 35 kW/m$^2$ and free ventilation.

Figure 4.14 showed gas emissions as a function of time for Siemens' Wind Turbine cable fires at 35 kW/m$^2$ and free ventilation. These Wind Turbine cables (AMI-G and AMI-B) were specified as Low Smoke Zero Halogens (LSZH) cables. From Figure 4.14 (a), both cable fires gave two CO concentration peaks with the first concentration peak lower than the second peak. The highest CO concentration for both cable fires was almost same, around 6000 ppm. In overall, emissions of HCN, Benzene, Acetylene, $CO_2$, NO and $NO_x$ were higher for AMI-G cable fire than AMI-B cable fire while emissions of other species such as Formaldehyde, Acrolein, THC, $SO_2$ and Toluene were higher for AMI-B cable fire than AMI-G cable fire. Concentration of halogenated products such as HCl, HF and HBr were insignificant and not presented. Even these electrical cable fires were free from emission of

halogenated products but the burnings were still having high emission of other toxic species as the results shown in Figure 4.14.

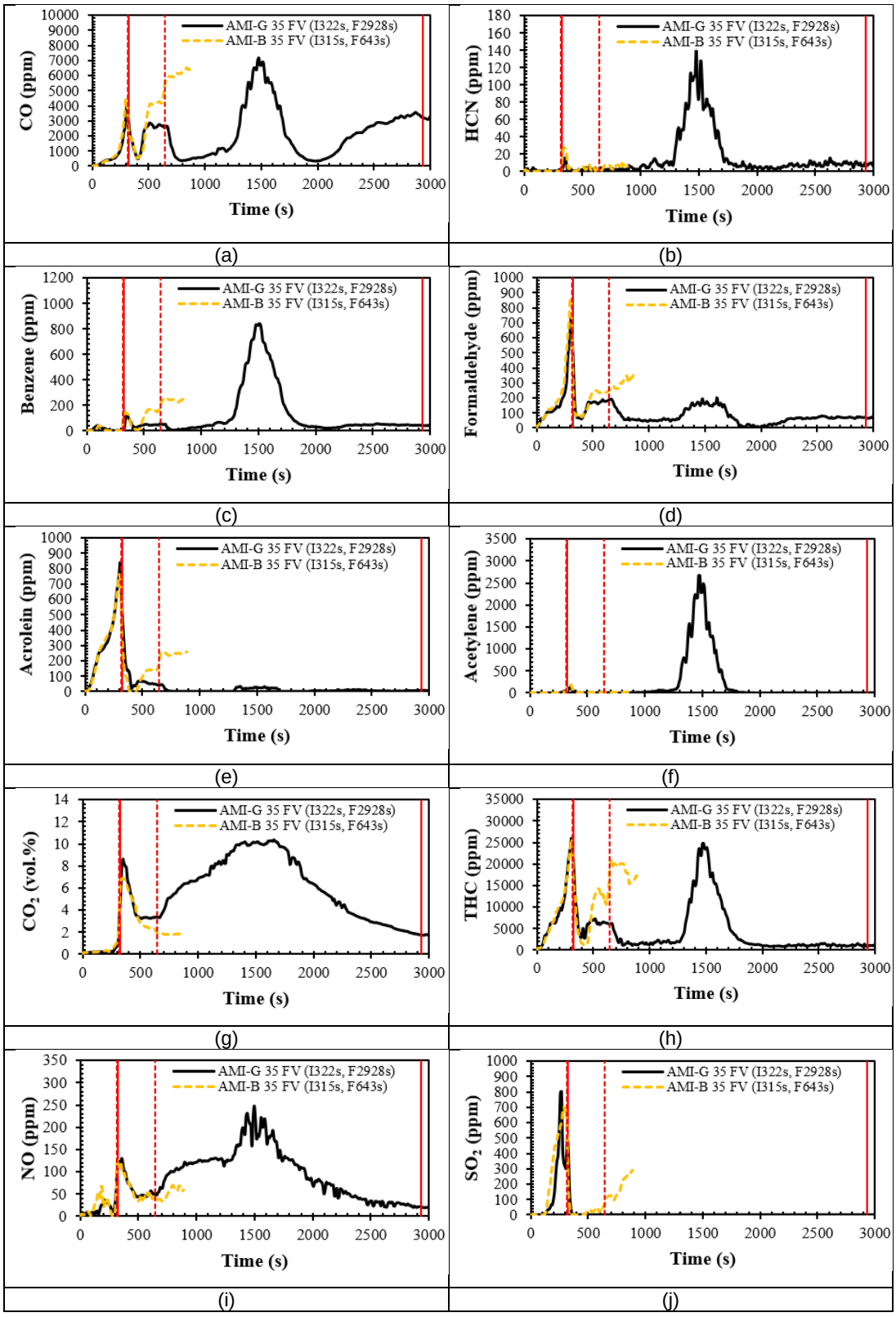

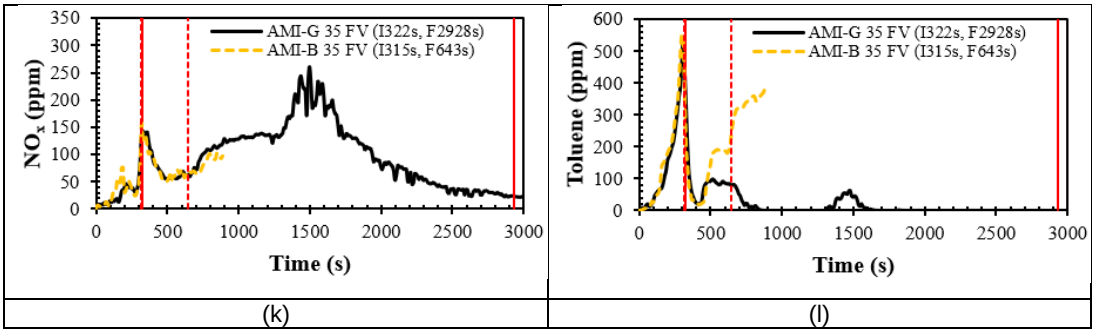


(k) (l)

**Figure 4.14** Concentration of gases as a function of time from Siemens' Wind Turbine cable fires at 35 kW/m$^2$ and free ventilation.

In this section, gas emission results for three other LSZH cables (Prysmian B, 6701B-W and TEC2-W cables) were presented and compared. Figure 4.15 showed concentration of gases as a function of time from LSZH electrical cable fires under several test conditions. For LSZH cable fires under test conditions of 35 kW/m$^2$ heat flux with free ventilation, TEC2-W cable fire gave the highest emission for most of toxic species if compared with PB and 6701B-W cable fires. For two LSZH cable fires under test conditions of 50 kW/m$^2$ heat flux with controlled ventilation (0.192 g/s or 9.4 L/min), both cable fires gave a high emission for most of toxic species. From Figure 4.15 (c), HCl emission was low and not more than 120 ppm for these electrical cable fires which the results were what had been initially expected for LSZH cable fires. $CO_2$ emissions were less than 10% by volume for these cable fires with a maximum total THC emission of about 200000 ppm. LSZH cable fires at a lower heat flux of 35 kW/m$^2$ produced less toxic gases than the cable fires at a higher heat flux of 50 kW/m$^2$. Between these three LSZH cable fires, 6701B-W cable fire showed the lowest emission for most of toxic gases. In comparison of initial weight, this 6701B-W cable sample was the lightest compared to another two LSZH cable samples and this could be a possible factor that caused low gas emissions by the 6701B-W cable fire.

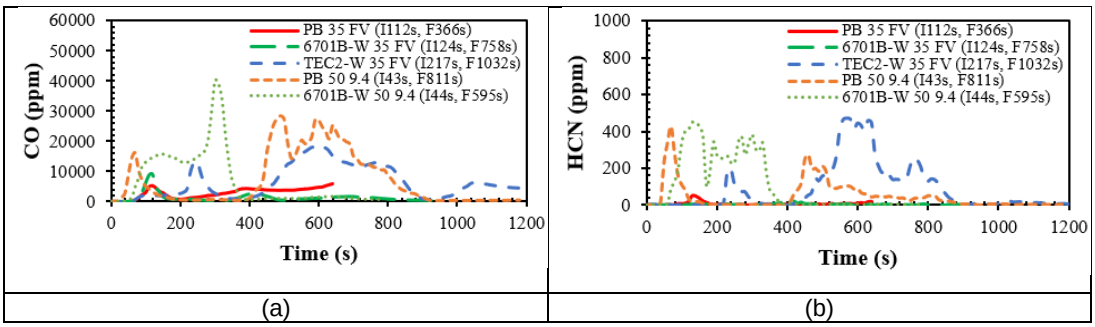


(a) (b)

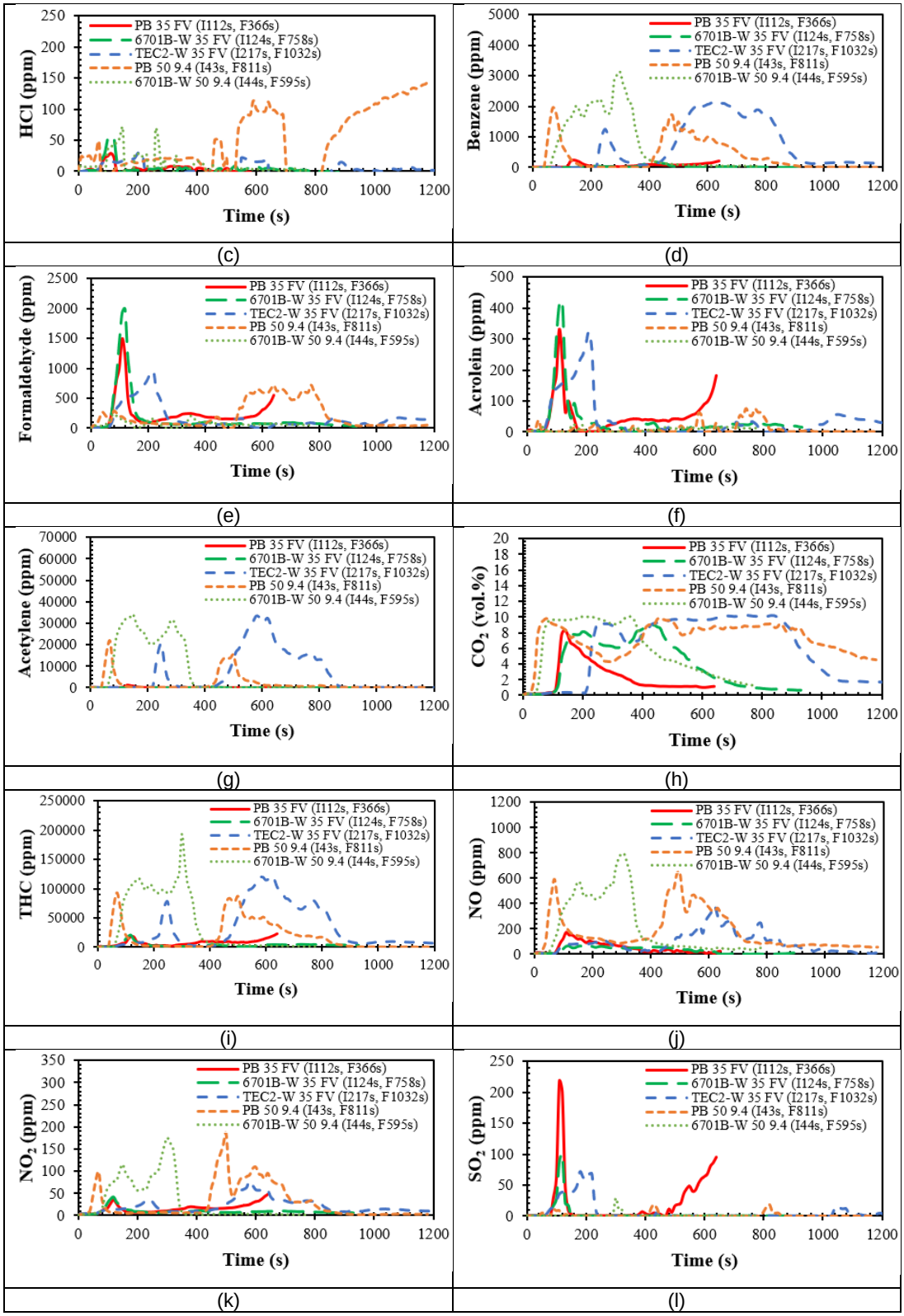
HCl (ppm)
Time (s)
PB 35 FV (I112s, F366s)
6701B-W 35 FV (I124s, F758s)
TEC2-W 35 FV (I217s, F1032s)
PB 50 9.4 (I43s, F811s)
6701B-W 50 9.4 (I44s, F595s)
(c)
Benzene (ppm)
Time (s)
(d)
Formaldehyde (ppm)
Time (s)
(e)
Acrolein (ppm)
Time (s)
(f)
Acetylene (ppm)
Time (s)
(g)
CO2 (vol.%)
Time (s)
(h)
THC (ppm)
Time (s)
(i)
NO (ppm)
Time (s)
(j)
NO2 (ppm)
Time (s)
(k)
SO2 (ppm)
Time (s)
(l)

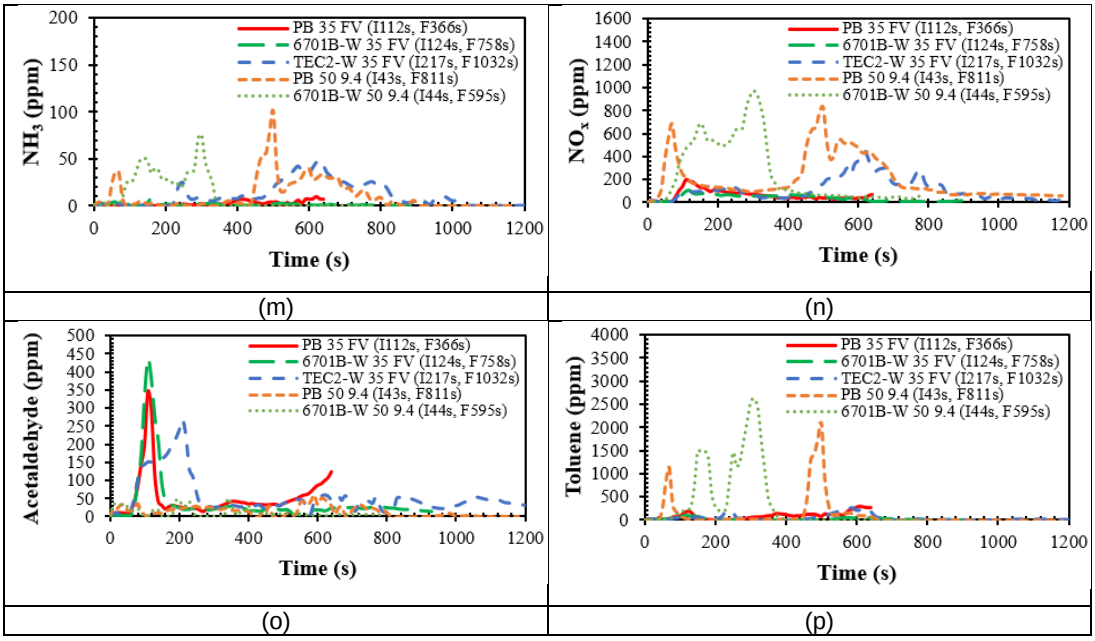


**Figure 4.15** Concentration of gases as a function of time from LSZH electrical cable fires under several test conditions.

Concentrations of various measured gases against time from FLEX1-BG and FLEX2-W electrical cable fires under test conditions of 35 kW/m2 heat flux and free ventilation were shown in the following Figure 4.16. FLEX1-BG electrical cable fire showed higher concentrations for most of toxic gases compared to FLEX2-W electrical cable fire except for some species like Acrolein, NO, $NH_3$, $NO_x$ and Acetaldehyde. FLEX1-BG had very high HCl emissions and this indicates that it was a PVC cable sheath. FLEX1-BG fire also gave the highest peak of CO concentration of 12000 ppm at 150 s, meanwhile FLEX2-W fire gave the highest peak of CO concentration of 7000 ppm at 600 s of burning time. From Figure 4.16, it can be seen that FLEX1-BG fire had the highest concentration at burning time less 200 s for most of produced toxic gases. These electrical cable samples were not initially classified under PVC cable type due to no specification details, but the high HCl concentration graph (Figure 4.16 (c)), shows that this cables was PVC which acts as a fire retardant. FLEX2-W fire had higher Acrolein concentrations compared to FLEX1-BG fire. It also gave higher concentrations of NO, $NH_3$ and $NO_x$. Presence of these species indicated that these cables were also initially made with an addition of Nitrogen compounds. The other reason of $NO_x$ presence could be due to a chemical reaction of the fuel with the Nitrogen element in the air [24]. Unlike FLEX1-BG fire, FLEX2-W

fire showed no production of $NO_2$ and $SO_2$ from its burning, indicating no fuel N or S compounds in the cable sheath.

All the toxic gases for FLEX1-BG were released very rapidly in the first 200s. This included high peaks in CO, HCN, HCl, Benzene, Formaldehyde and THC. This is dangerous as it indicates that in a fire these gases would be release early on in the fire evacuation procedures.

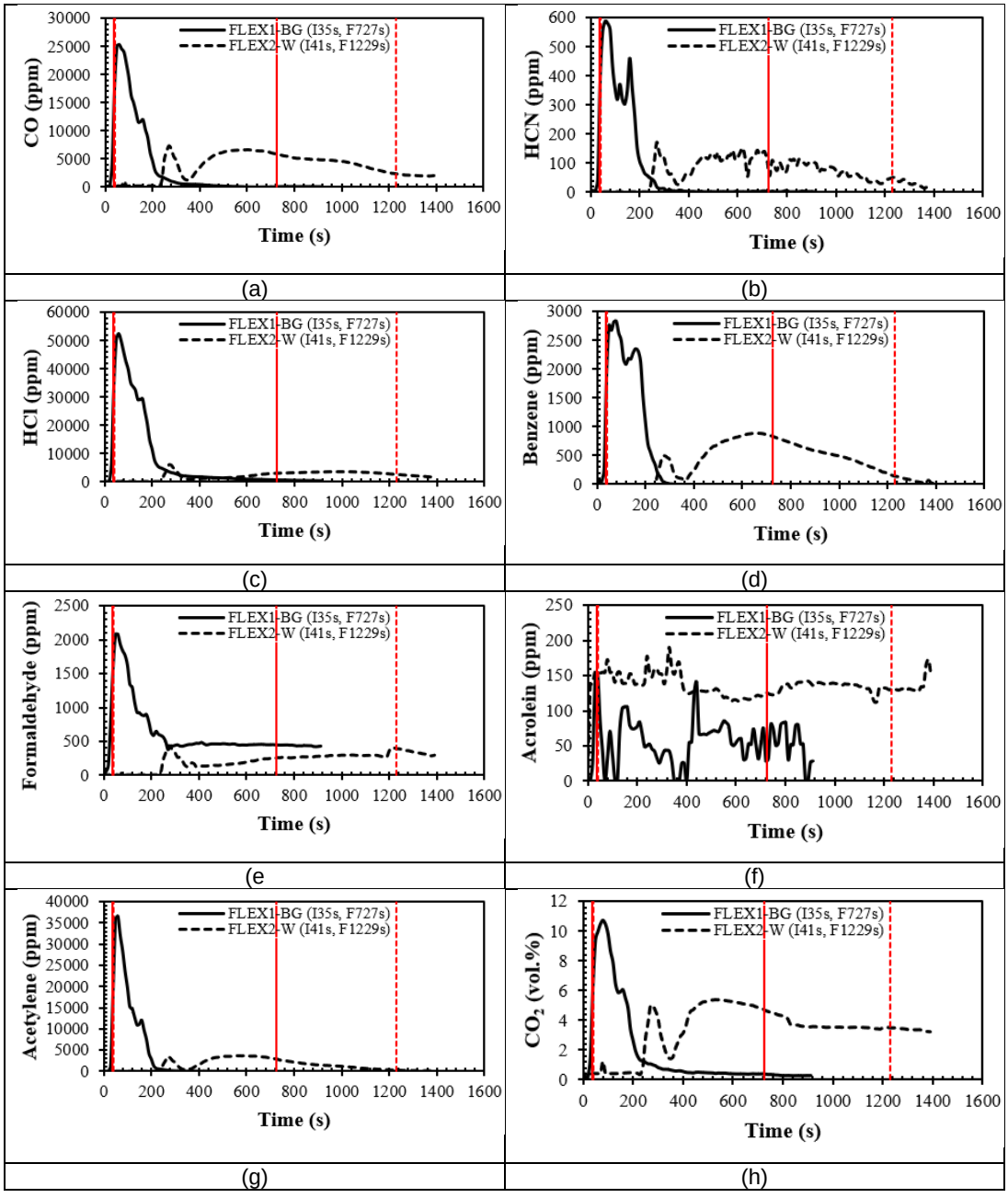

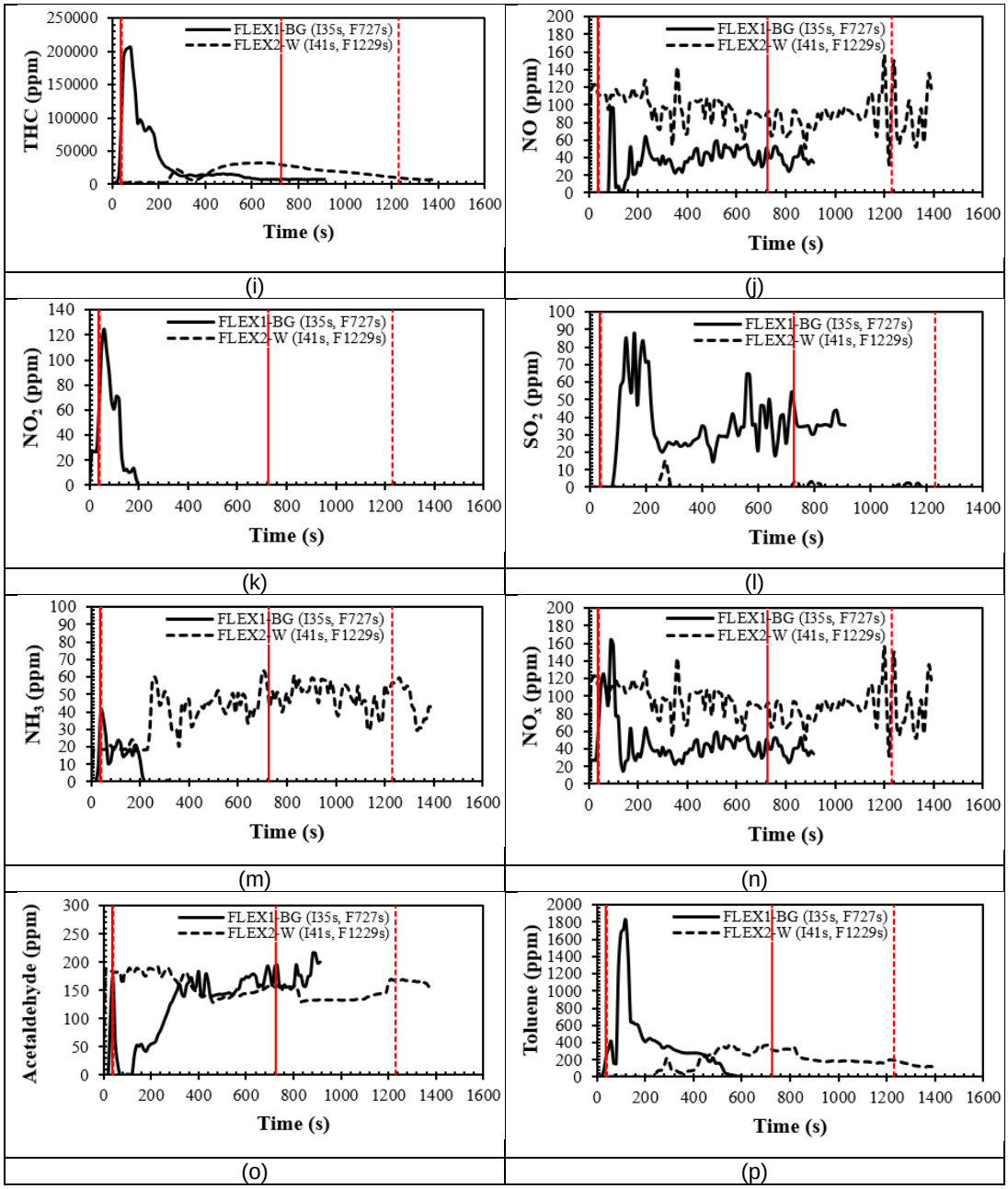


**Figure 4.16** Concentration of gases as a function of time from other Non-PVC electrical cable fires at 35 kW/m$^2$ and free ventilation.

### 4.3.3 Total Toxicity for PVC Prysmian A Cable Fires

Total LC50, COSHH15min and AEGL-2 indices for PVC Prysmian A electrical cable fires at heat flux of 25 kW/m$^2$ with three different air flow rates were shown in the following Figure 4.17. PVC Prysmian A cable fire at a higher air flowrate of 0.572 g/s (28 L/min) gave a non-flaming fire condition without indication of real flame during the burning process. It showed the lowest total LC50 and total $COSHH_{15min}$ at burning time of about 700 s in comparison to

PVC cable fires with lower air flowrates. Meanwhile, it gave higher toxicity values for AEGL-2 basis with the highest total AEGL-2 of 1500. Total toxicity peaks showed by these PVC cable fires at lower air flowrates (0.192 g/s and 0.368 g/s) were at about 450 s. The maximum total toxicities obtained for these PVC Prysmian cable fires were significant and high with LC50 of ~12, $COSHH_{15min}$ of ~6000 and AEGL-2 of up to 1500.

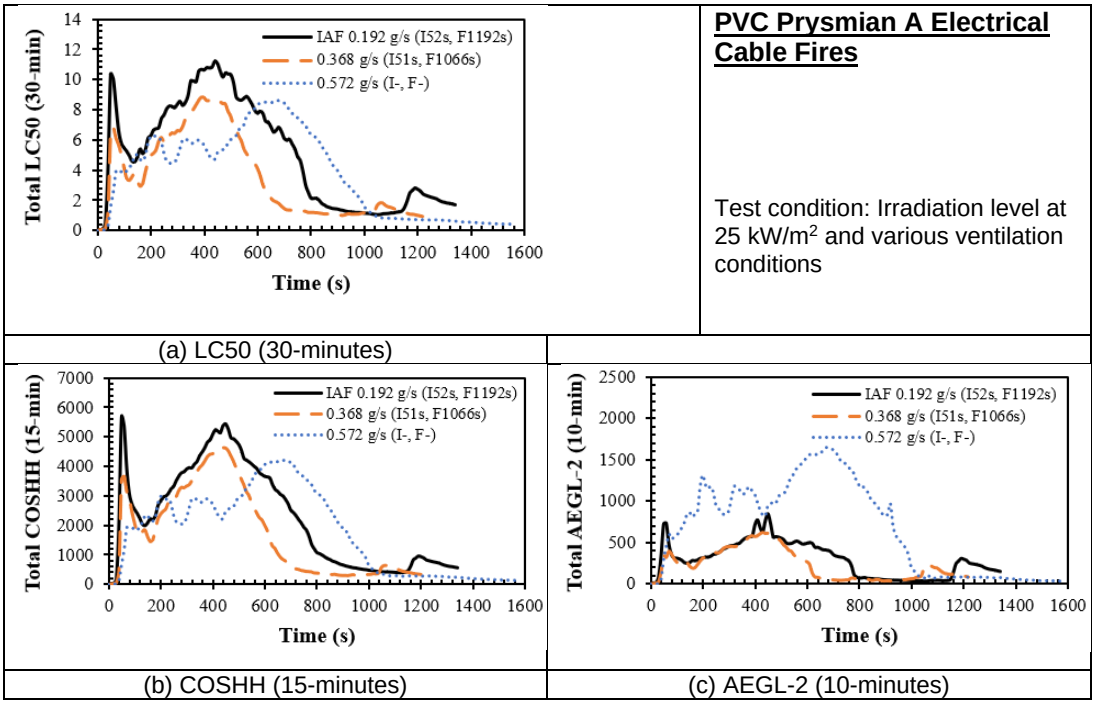


**Figure 4.17** Total toxicities indices for PVC Prysmian A electrical cable fires at 25 kW/m$^2$ with various air flow rates.

Figure 4.18 showed total toxicities for PVC Prysmian A electrical cable fires at irradiation level of 35 kW/m$^2$ with restricted and free ventilation rates. PVC Prysmian A cable fire with air flowrate of 0.368 g/s (18 L/min) gave the highest peak of total LC50 (~14) and total $COSHH_{15min}$ (6000). For AEGL-2 basis, the lowest total toxicity was shown by PVC Prysmian A cable fire with air flowrate of 0.572 g/s (28 L/min) while cables fires with lower flowrates and free ventilation rate had the same maximum peak of total AEGL-2 of about 600 at different burning time. PVC Prysmian A cable fire at a higher flowrate of 0.572 g/s was giving the lowest toxicity level for the three toxic assessment methods compared to other cable fires with lower air flowrates.

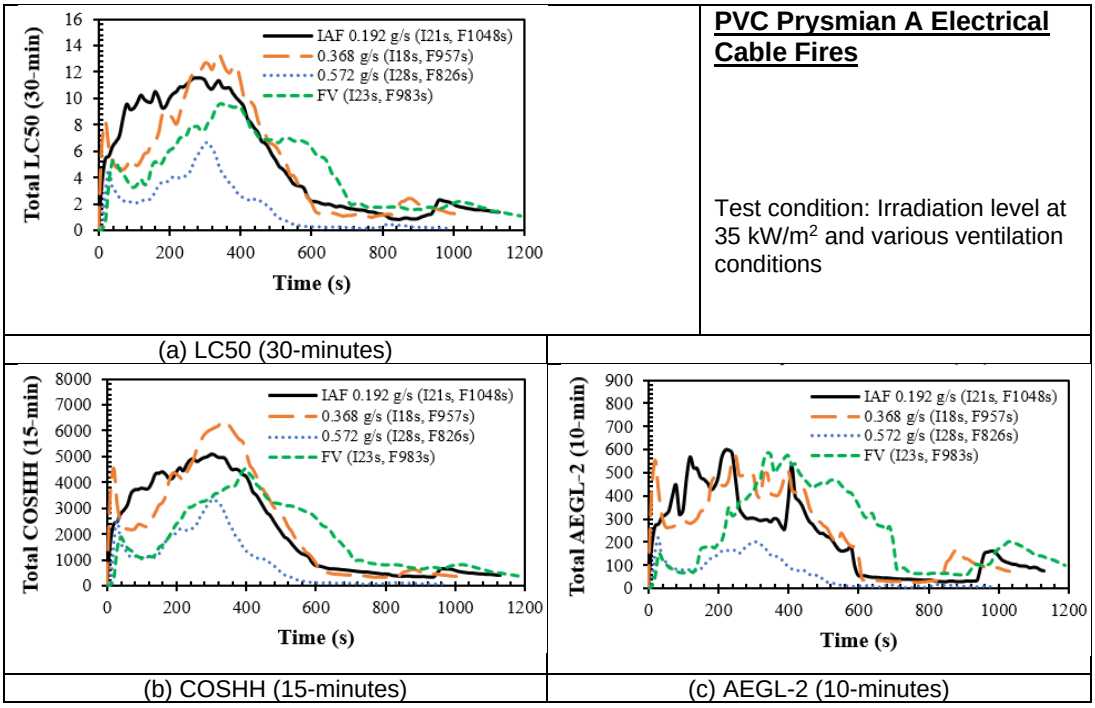


**Figure 4.18** Total toxicities for PVC Prysmian A electrical cable fires at 35 kW/m$^2$ with various air flow rates.

Figure 4.19 shows total toxicities for PVC Prysmian A electrical cable fires at 50 kW/m$^2$ with various air flow rates. For LC50 basis, PVC cable fire at air flowrate of 0.572 g/s had shown the highest total toxicity peak of about 20 compared to cable fires at lower air flowrates. Cable fires with 0.192 g/s and 0.572 g/s air flowrates gave the same maximum peak of $COSHH_{15min}$ total toxicity (6000). While for AEGL-2 basis, the cable fire with the lowest air flowrate of 0.192 g/s had given the highest total toxicity peak of about 600. After 100 s of the burning period, the average total toxicity value for all three toxic assessment methods was the lowest for the PVC cable fire at air flowrate of 0.192 g/s (9.4 L/min). However, all these cable fires were giving high and significant of total toxicity values.

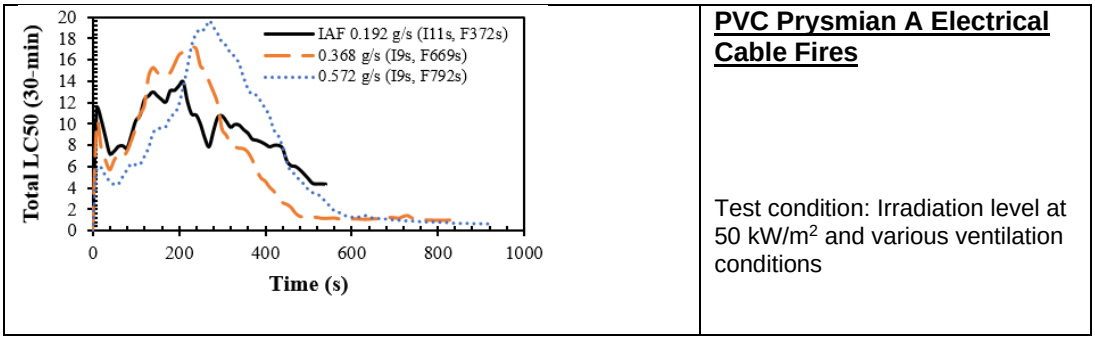

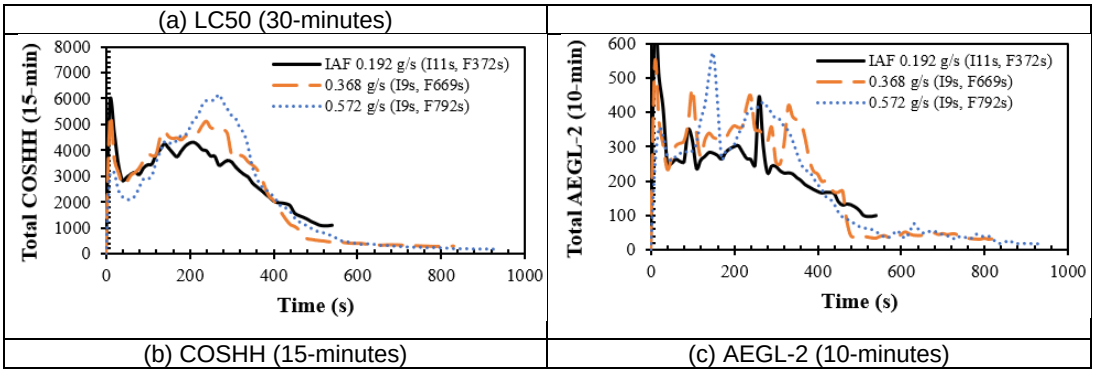


**Figure 4.19** Total toxicities for PVC Prysmian A electrical cable fires at 50 kW/m$^2$ with various air flow rates.

### 4.3.4 Total toxicity for Other Electrical Cable Fires

Figure 4.20 showed total toxicity against time for other PVC electrical cable fires at 35 kW/m$^2$ irradiation level and free ventilation condition. Compared with the total toxicities for other electrical cable fires, these PVC cable (PVC EC-GB 1 and PVC EC-GB 2) fires gave the lowest toxicity values. FEC LC50 values for these cable fires were not more than 3.5 while most of other cable fires that tested showed the FEC LC50 values higher than that. For all three toxic assessment methods, PVC EC-GB 2 gave higher total toxicities, more than double. Maximum total $COSHH_{15min}$ for PVC EC-GB 1 cable fire was ~ 600 while for PVC EC-GB 2 cable fire was ~1400. For LC50 basis, total toxicity for PVC EC-GB 2 cable fire gave the highest peak of 3.0 at 800 s and PVC EC-GB 1 cable fire gave a constant FEC LC50 profile with an average value of 1.3 during the whole burning period.

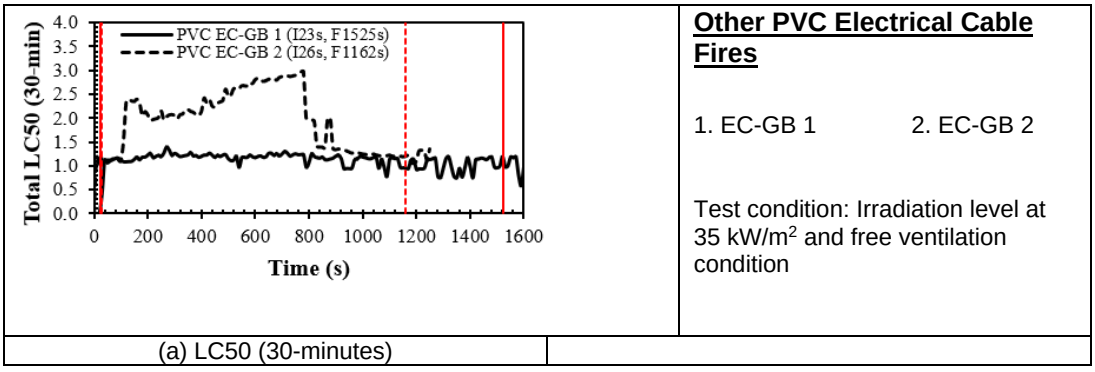

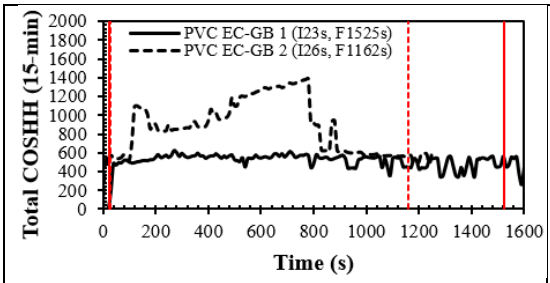


(b) COSHH (15-minutes)

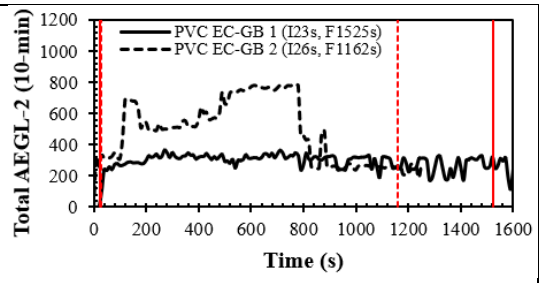


(c) AEGL-2 (10-minutes)

**Figure 4.20** Total toxicity for other PVC electrical cable fires at 35 kW/m$^2$ and free ventilation.

Total toxicity according to LC50, COSHH15min and AEGL-2 basis for Solar Energy cable fires at heat flux of 35 kW/m$^2$ and free ventilation were shown in Figure 4.21. From Figure 4.21, LC50 total toxicity for HV2-3C cable fire gave a higher maximum peak of 10 at time of ~1500 s while HV1-4C cable fire had a maximum peak of 6 at time of ~900 s. Total toxicity values for LC50, COSHH15min and AEGL-2 basis were higher for HV2-3C cable fire than HV1-4C cable fire. HV2-3C cable fire gave the highest total COSHH$_{15min}$ of about 4500, almost double than HV1-4C cable fire which showed the highest FEC COSHH$_{15min}$ below than 3000. Meanwhile, total AEGL-2 was much higher for HV2-3C cable fire showing a maximum toxicity level up to 2500 compared with HV1-4C cable fire that gave less than 200 of total AEGL-2. However, both cable fires showed very significant total toxicities with FEC values more than 1 which may impair people from escape safely during a fire.

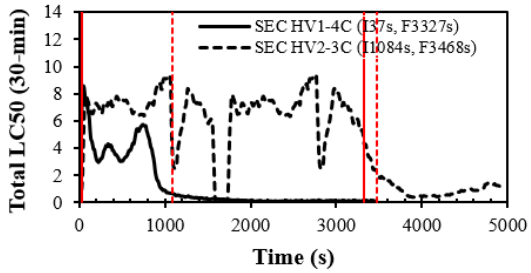


(a) LC50 (30-minutes)

**Solar Energy Cable Fires**

1. HV1-4C 2. HV2-3C

Test condition: Irradiation level at 35 kW/m$^2$ and free ventilation condition

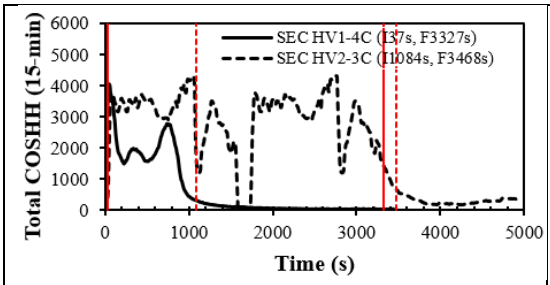


(b) COSHH (15-minutes)

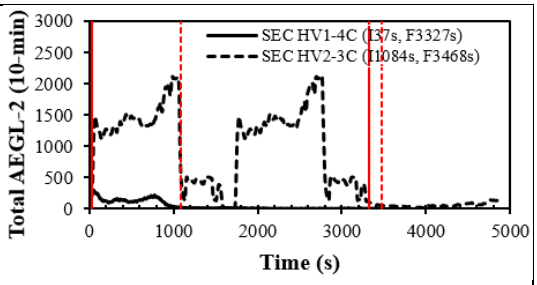


(c) AEGL-2 (10-minutes)

**Figure 4.21** Total toxicity for Solar Energy cable fires at 35 kW/m$^2$ and free ventilation.

Figure 4.22 showed total toxicity values for Siemens' Wind Turbine cable fires at 35 kW/m$^2$ irradiation level and free ventilation. Both cable samples were ignited almost at the same time, ~300 s (5 minutes) but giving a long gap of flame out time with AMI-G cable sample was burned longer which extinguished at 2928 s while AMI-B cable fire was extinguished at 643 s. Even AMI-G cable sample experienced a longer burning process than AMI-B cable sample, both cable fires had shown significant total toxicities before 1500 s of burning period where after that period, the values were insignificant. AMI-B cable fire was more toxic than AMI-G cable fire with giving higher total toxicity values for all three toxic assessment methods. The highest total LC50 shown by AMI-B cable fire was ~8 and the value was <3 for AMI-G cable fire. These cable fires gave the highest total $COSHH_{15min}$ of 3800 at 300 s for AMI-B cable fire and 1300 at 200 s for AMI-G cable fire. The maximum total AEGL-2 was ~2800 for AMI-B cable fire while it was less than 1000 for AMI-G cable fire. Both Wind Turbine cable fires gave two main peaks of total toxicity with the first peak at time before 500 s giving a higher value than the second peak at time after 500 s.

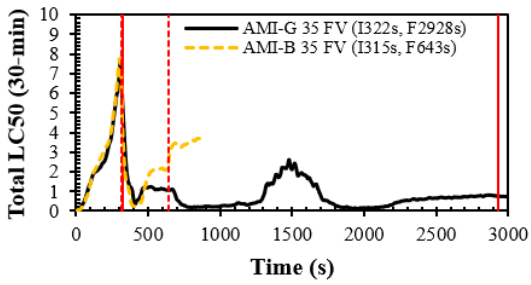


(a) LC50 (30-minutes)

**Siemens' Wind Turbine Cable Fires**

1. AMI-G
2. AMI-B

Test condition: Irradiation level at 35 kW/m$^2$ and free ventilation condition

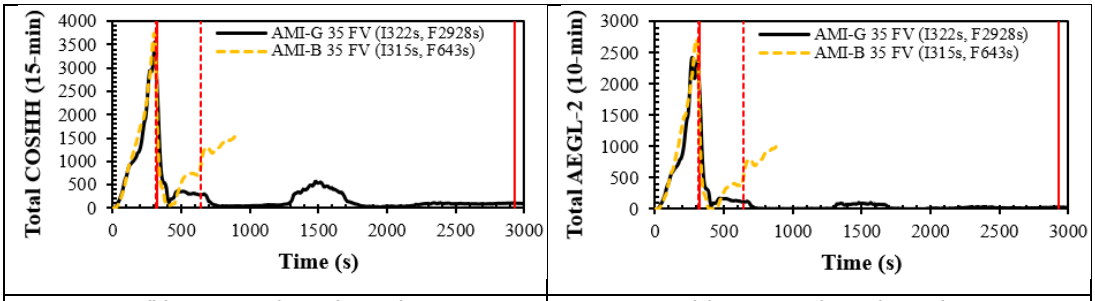


(b) COSHH (15-minutes) (c) AEGL-2 (10-minutes)

**Figure 4.22** Total toxicity for Siemens' Wind Turbine cable fires at 35 kW/m$^2$ and free ventilation.

Figure 4.23 showed total toxicity values based LC50, COSHH and AEGL-2 methods for LSZH electrical cable fires under several test conditions. At test conditions of 35 kW/m$^2$ heat flux and free ventilation, the highest total LC50 and $COSHH_{15min}$ was given by TEC2-W cable fire, followed by the second higher toxicity by Prysmian B cable fire and the lowest toxicity by 6701B-W cable fire. For AEGL-2 basis total toxicity, Prysmian B cable fire gave the highest peak of about 600 compared to TEC2-W (<500) and 6701B-W (<150) cable fires. Under fire conditions of 50 kW/m$^2$ heat flux and air flowrate of 0.192 g/s (9.4 L/min), total toxicity for both Prysmian B and 6701B-W cable fires were high with 6701B-W cable fire giving higher value of total LC50, $COSHH_{15min}$ and AEGL-2 than Prysmian B cable fire. Prysmian B cable burning showed two peaks of total toxicity for all three assessment methods with the first lower peak at burning time of ~150 s and the second higher peak at burning time of ~700 s.

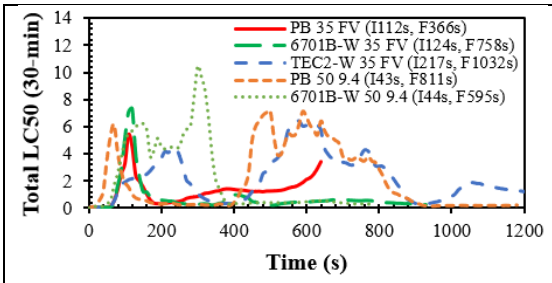


(a) LC50 (30-minutes)

**LSZH Electrical Cable Fires**

1. PB
2. 6701B-W
3. TEC2-W

Test condition: Various irradiation levels and ventilation conditions

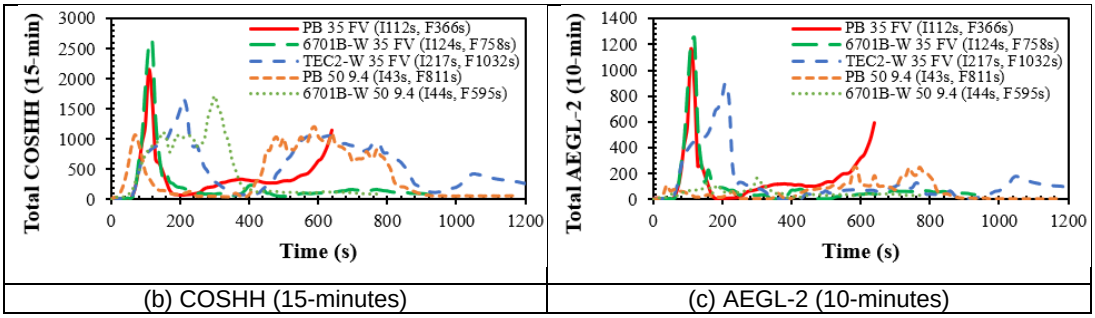


(b) COSHH (15-minutes) (c) AEGL-2 (10-minutes)

**Figure 4.23** Total toxicity values (LC50, COSHH and AEGL-2) for LSZH electrical cable fires under several test conditions.

Total toxicities based LC50, COSHH15min and AEGL-2 toxic assessment methods as a function of time for FLEX electrical cable fires were shown in Figure 4.24. From the graphs, it can be said that FLEX1-BG fire was more toxic than FLEX2-W fire by giving higher peaks of FEC values during the burning process. For LC50 basis, FLEX1-BG gave the highest total LC50 of 14 at 150 s meanwhile FLEX2-W gave a constant LC50 peak of 4 for a long burning period from 300 s to flame out time at 1200 s. Toxicity based FEC LC50 of FLEX1-BG fire was 3 times more than the FLEX2-W fire. FLEX1-BG fire gave the highest FEC $COSHH_{15min}$ of about 8000, 4 times higher than the highest FEC $COSHH_{15min}$ for FLEX2-W fire. For FEC AEGL-2 basis, FLEX2-W fire gave the highest total AEGL-2 value of 450 and FLEX1-BG gave the highest total AEGL-2 value of 700. In overall by comparing both electrical cable fire toxicity, before 300 s, total toxicity values were dominated by FLEX1-BG fire and after 300 s, it was dominated by FLEX2-W fire. The total toxicities for FLEX1-BG fire reduced to minimum after 300 s burning period until flame out and the values were lower or half than total toxicities of FLEX2-W fire.

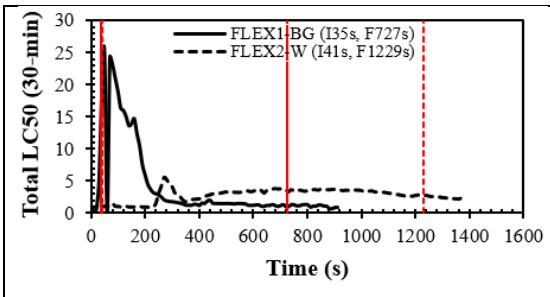


**FLEX Electrical Cable Fires**

1. FLEX1-BG 2. FLEX2-W

Test condition: Irradiation level at 35 kW/m$^2$ and free ventilation condition

(a) LC50 (30-minutes)

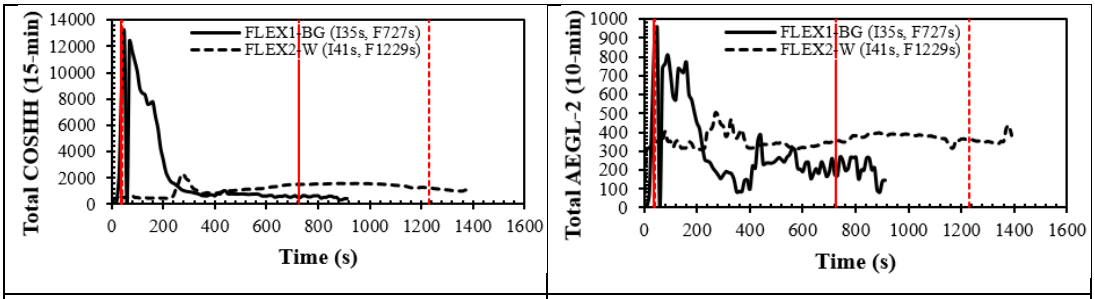


(b) COSHH (15-minutes) (c) AEGL-2 (10-minutes)

**Figure 4.24** Total toxicity for other Non-PVC electrical cable fires at 35 kW/m$^2$ and free ventilation.

### 4.3.5 Gas Yields for PVC Prysmian A Cable Fires

Under this heat flux exposure, the PVC cable fire produced maximum CO yield up to 0.12 g/g for air flowrate of 9.4 L/min (0.192 g/s) which was higher than the CO yields produced by the cable fires at higher air flowrates. CO yield would reduce with an increase in the air flowrate due to a more complete combustion was achieved which releasing less CO emissions. The HCl yield of these cable fires for three air flowrates was high and gave a similar highest peak of about 0.3 g/g. Gas yields for PVC Prysmian A electrical cable fires at 25 kW/m$^2$ and various ventilation conditions were shown in Figure 4.25. From Figure 4.25, the PVC cable fire at air flowrate of 0.192 g/s had given higher yields for most of major toxic species such as CO, HCN, HCl, Benzene and Acetylene compared to the cable fires at higher air flowrates. Yields for other species like Formaldehyde, Acrolein, NO, $NO_2$, $SO_2$, $NH_3$, $NO_x$, Acetaldehyde and Toluene were the highest for the cable fire at air flowrate of 0.572 g/s (28 L/min). $CO_2$ and THC yields for these cable fires were below 1.4 g/g and 0.15 g/g. In overall, yields of toxic gases produced from a combustion typically would decrease with the increasing of ventilation rate and heat flux value.

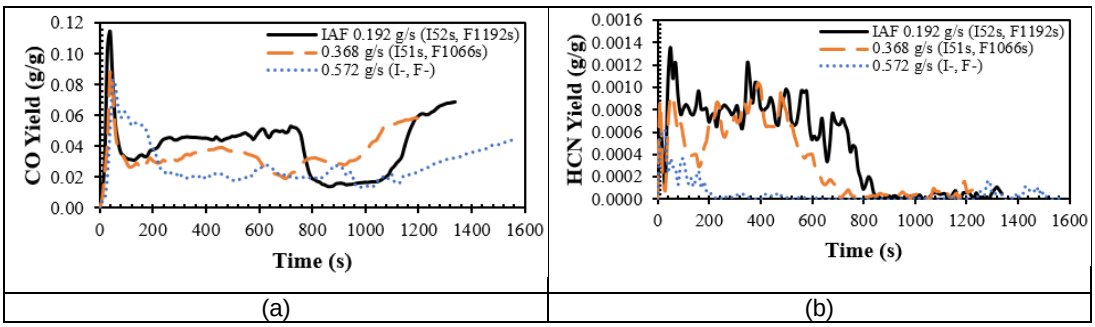


(a) (b)

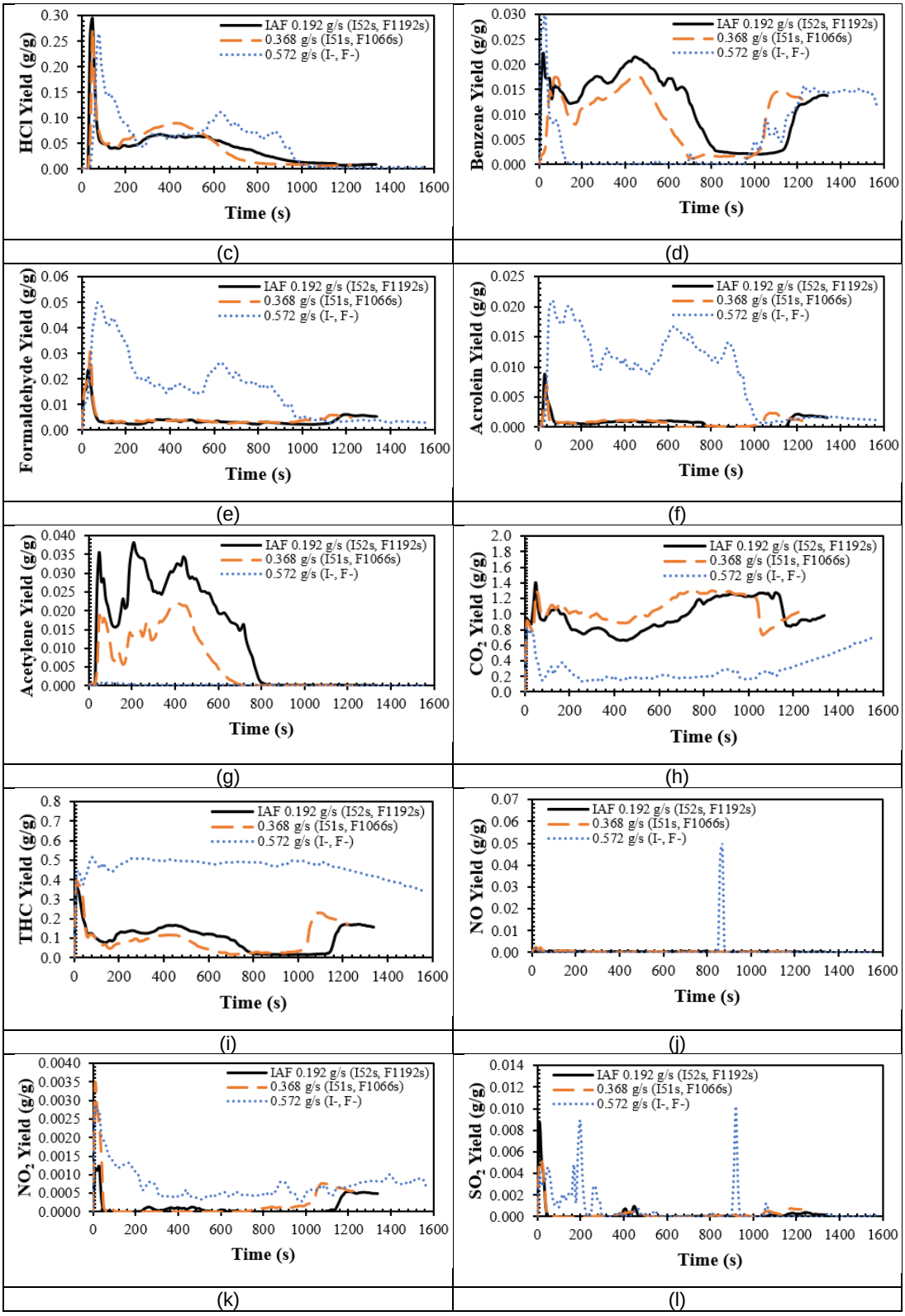
HCl Yield (g/g)
Time (s)
IAF 0.192 g/s (I52s, F1192s)
0.368 g/s (I51s, F1066s)
0.572 g/s (I-, F-)
(c)
Benzene Yield (g/g)
Time (s)
(d)
Formaldehyde Yield (g/g)
Time (s)
(e)
Acrolein Yield (g/g)
Time (s)
(f)
Acetylene Yield (g/g)
Time (s)
(g)
CO2 Yield (g/g)
Time (s)
(h)
THC Yield (g/g)
Time (s)
(i)
NO Yield (g/g)
Time (s)
(j)
NO2 Yield (g/g)
Time (s)
(k)
SO2 Yield (g/g)
Time (s)
(l)

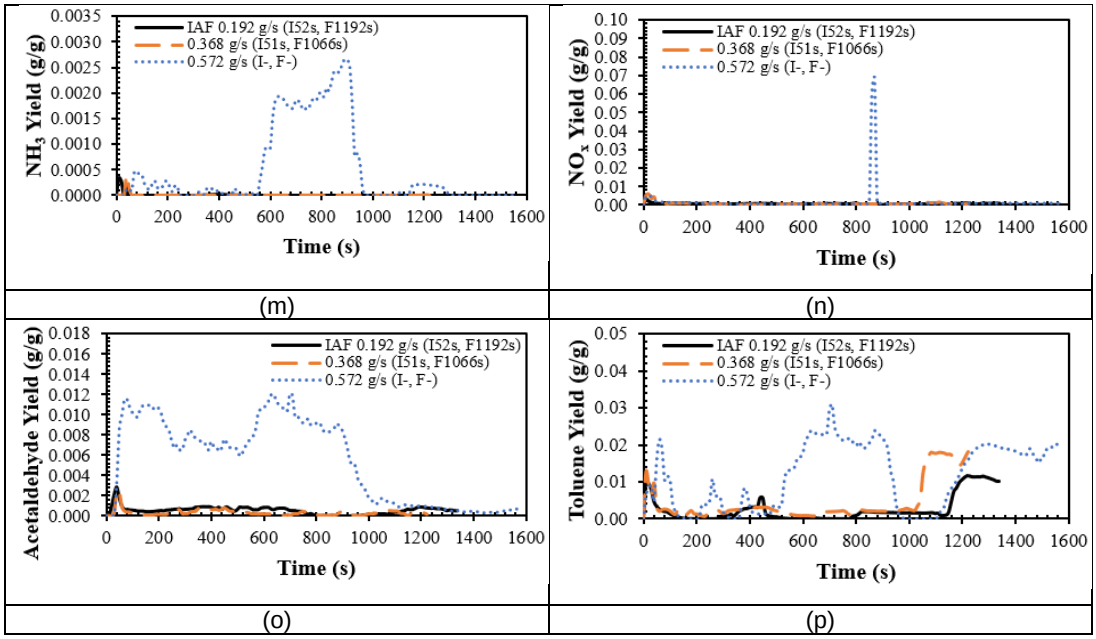


**Figure 4.25** Gas yields for PVC Prysmian A electrical cable fires at 25 kW/m$^2$ and various ventilation conditions.

Figure 4.26 shows combustion efficiency, ŋ as a function of time and equivalence ratio for PVC Prysmian A electrical cable fires at 25 kW/m$^2$ and various ventilation conditions. The combustion efficiency rate for cable fires at lower ventilation rates (9.4 and 18 L/min) were ~90%, about 40% higher than the cable fire at 28 L/min air flowrate. The cable fires at air flowrate of 9.4 and 18 L/min had experienced fuel rich burning or near stoichiometric fire condition while the cable fire at air flowrate of 28 L/min had a fuel lean burning with ER less than 0.4. Under well ventilated fire, the combustion of this PVC cable had produced higher yields of NO, $NO_2$, $NH_3$, $NO_x$ which the cable burning process was possibly involved some reactions with the supplied excess air [24].

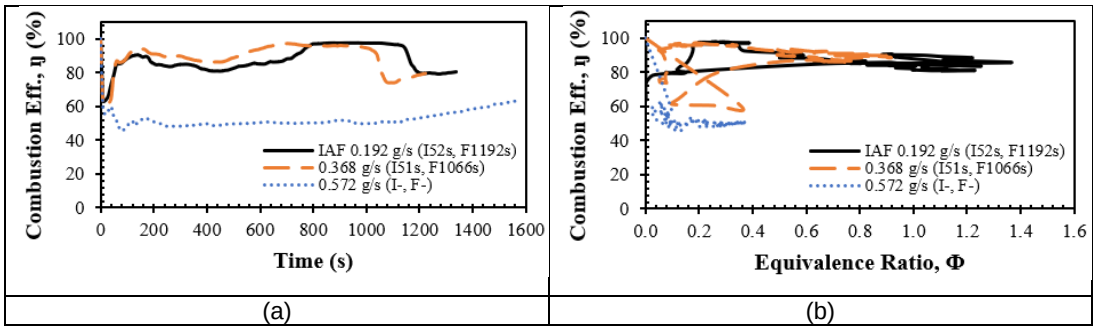


**Figure 4.26** Combustion efficiency, ŋ for PVC Prysmian A electrical cable fires at 25 kW/m$^2$ and various ventilation conditions.

Gas yields for PVC Prysmian A electrical cable fires at 35 kW/m$^2$ and various ventilation conditions are shown in following Figure 4.27. CO yields were below 0.1 g/g for these cable fires at four different air flowrates. The highest peak of HCl yield for cable fires at this heat flux were similar with the highest HCl yield obtained by the cable fires at a lower heat flux of 25 kW/m$^2$. With varying heat fluxes and air flowrates, the results showed that the maximum HCl yield given by the PVC Prysmian A fires was about 0.3 g/g or lower. $CO_2$ yields under these fire conditions were slightly higher than the cable fire at a lower heat flux. The THC yields for these cable fires were less than 0.3 g/g with free ventilation gave the highest peak of THC yield compared to other ventilation rates. These THC yields were lower than the THC yields produced from the cable burning at 25 kW/m$^2$ and various air flowrates. $NO_x$ emissions and yields were higher for the cable fires at these fire conditions.

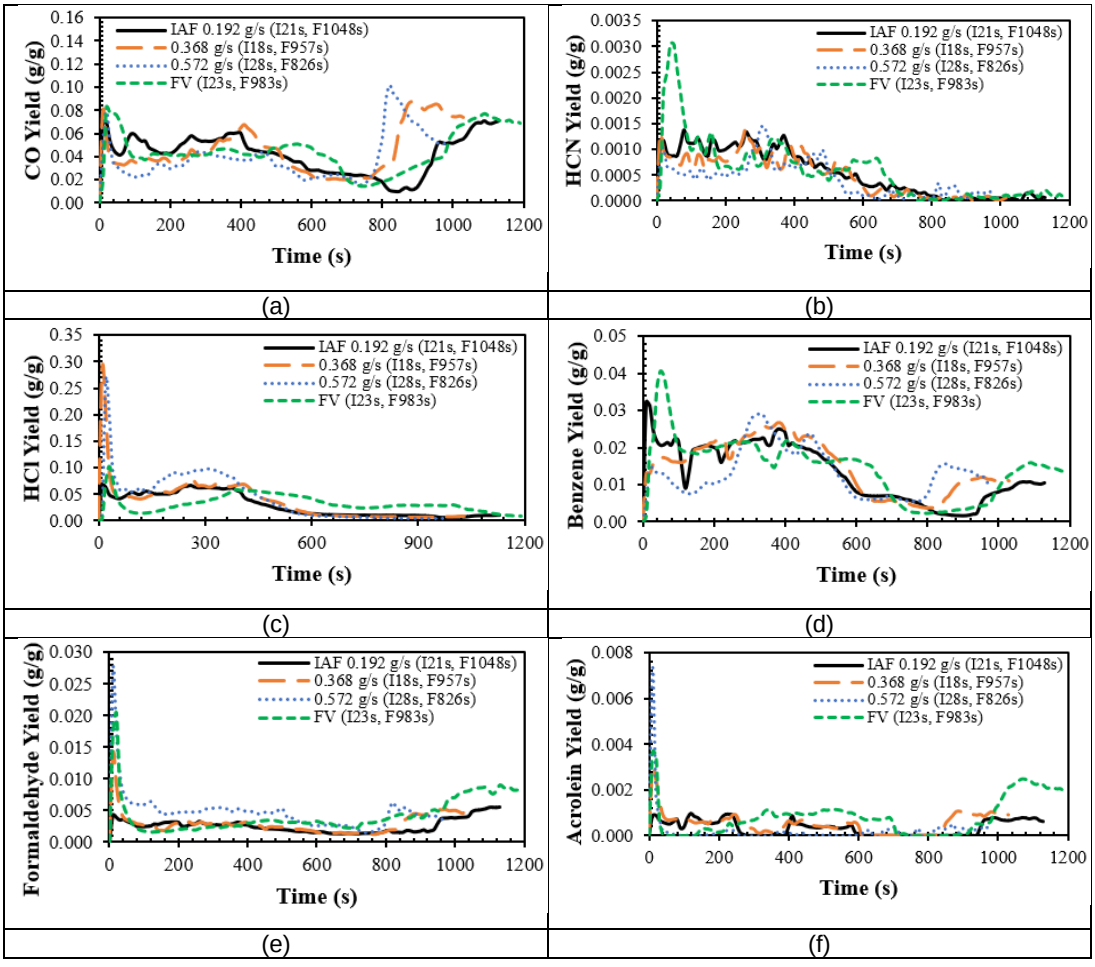

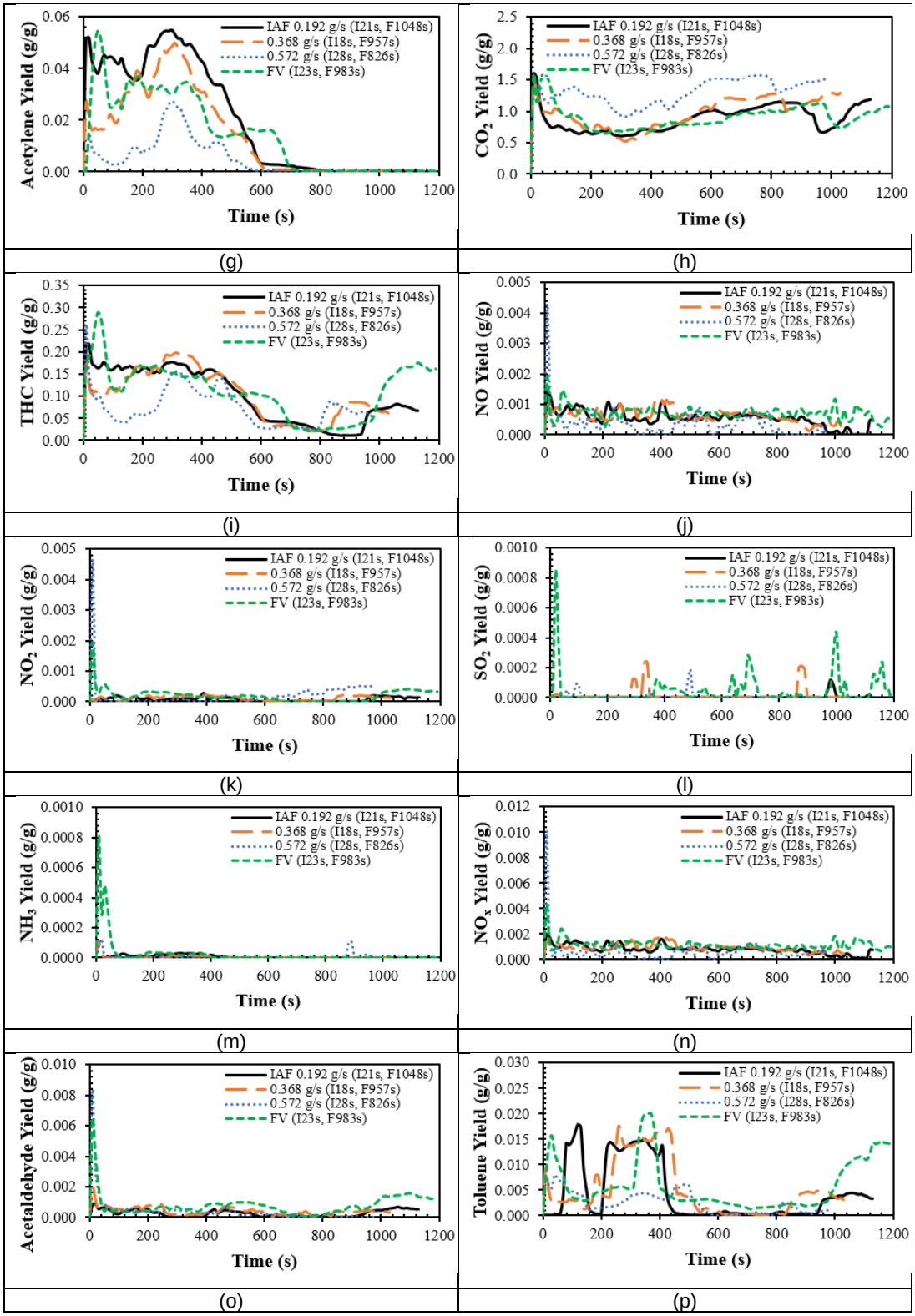


**Figure 4.27** Gas yields for PVC Prysmian A electrical cable fires at 35 kW/m$^2$ and various ventilation conditions.

The higher heat flux value, the higher combustion rate will be, hence this would contribute to a higher combustion efficiency rate. At this heat flux, the cable fires had shown the combustion efficiency above 80% for all different ventilation rates. Except for the cable fire with air flowrate of 0.572 g/s, other cable fires experienced the fuel rich burning or near stoichiometric condition with equivalence ratios about 1.0 and above. Even ER was less than 0.6 for the cable fire at 0.572 g/s, it had still achieved a high combustion efficiency rate of 90%. This is possibly because the effect of heat flux value that contributed to this higher efficiency rate. Figure 4.20 shows the combustion efficiency, ŋ for PVC Prysmian A electrical cable fires at 35 kW/m$^2$ and various ventilation conditions. From Figure 4.28 (a) and (b), cable fires with 0.192 g/s of restricted ventilation and free ventilation had shown a similar profile for general combustion properties. Combustion efficiency and equivalence ratio (ER) changes were almost same for these cable fires.

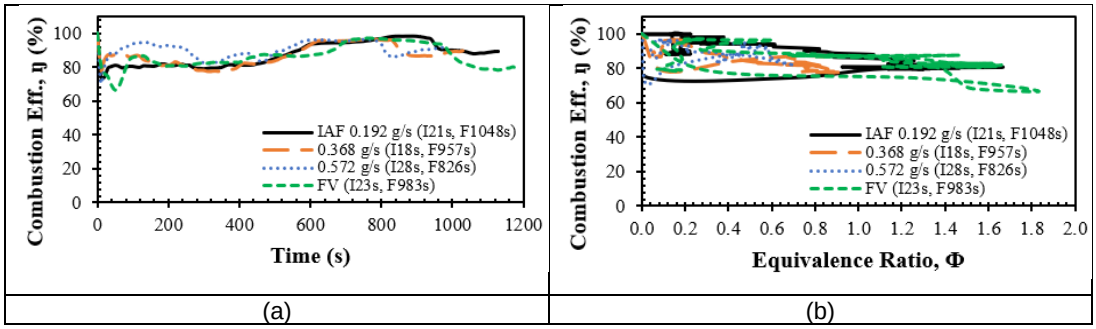


**Figure 4.28** Combustion efficiency, ŋ for PVC Prysmian A electrical cable fires at 35 kW/m$^2$ and various ventilation conditions.

The following Figure 4.29 shows gas yields for PVC Prysmian A electrical cable fires at 50 kW/m$^2$ and various ventilation conditions. CO yields produced from cable fires at this heat flux were about two (2) times higher than the cable fires at lower heat fluxes. With the higher heat flux exposure, other than reduced the time delay to the ignition, it would also shorten up the burning period. But, it had not affected much in the changes of fire equivalence ratios for this PVC cable burning. The unburnt fuel left at the end of combustion was lower with giving a higher CO yields. That was why the THC yields produced at this heat flux were lower than the cables fires that with lower heat fluxes. $CO_2$ yields produced for these cable fires were in a range from 1.4 to 1.8 g/g for all fire conditions. Yields for most of toxic species had reduced with the

increase of air flowrate for the cable fires at certain heat flux exposure. In overall comparison, HCN yields were the highest of about 0.002 g/g for these PVC cable fires with different heat fluxes and ventilation rates.

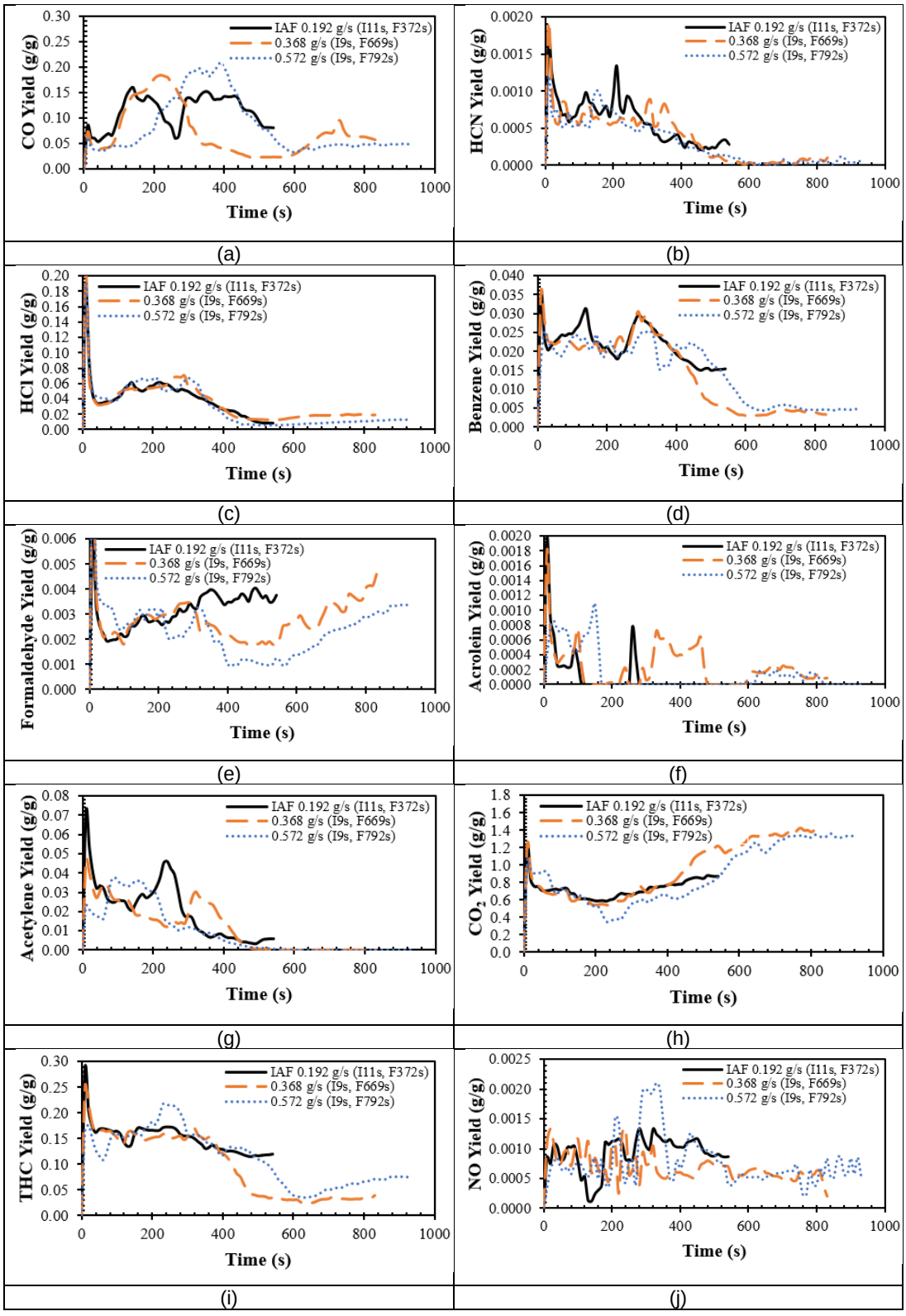

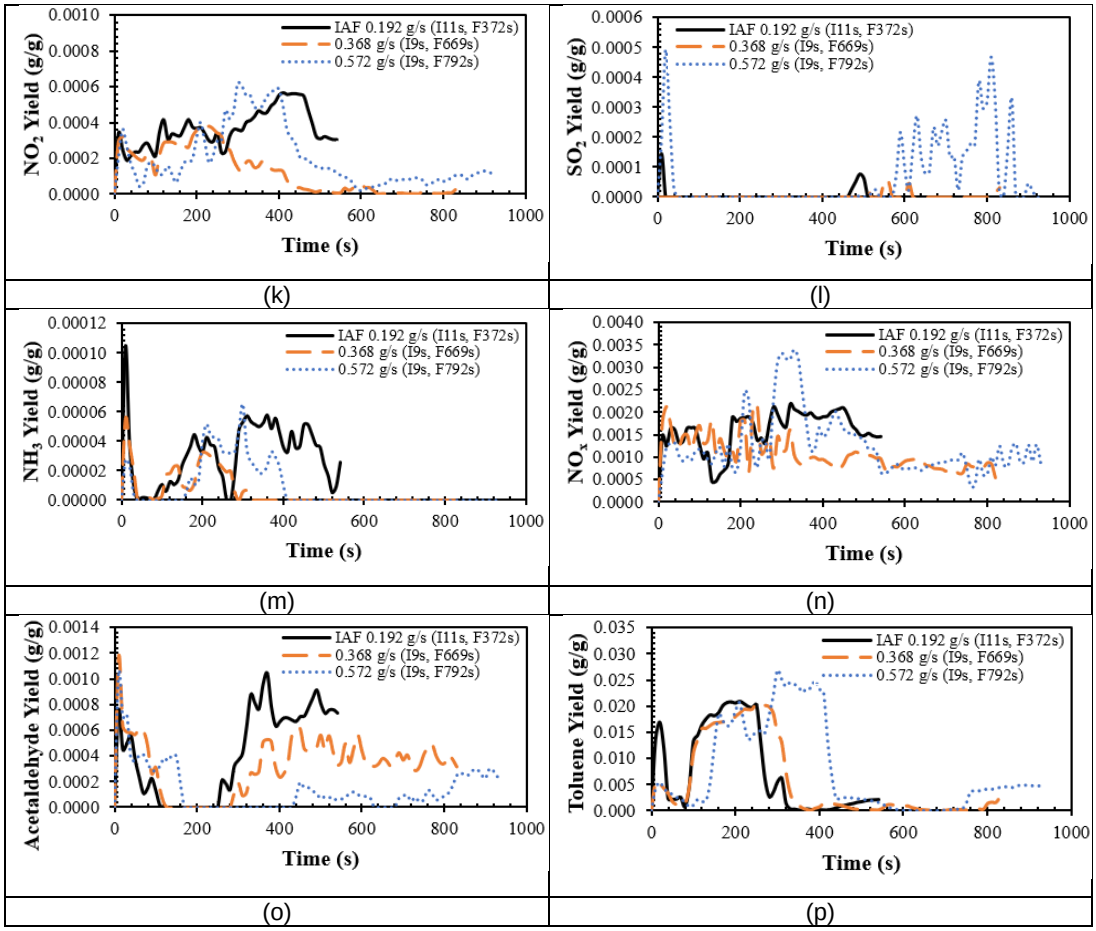


**Figure 4.29** Gas yields for PVC Prysmian A electrical cable fires at 50 kW/m$^2$ and various ventilation conditions.

The cable fires under this heat flux gave a combustion efficiency range from 70% up to 100% for all ventilation rates. Equivalence ratios had changed from lean to rich or near stoichiometric condition. ER less than 1.0 showed higher values of combustion efficiency rate for these cable fires. It showed that the cable fires were having a well ventilated condition with sufficient air supplied to assist the cable burning. The efficiency rates were slightly lower when the fire experiencing fuel rich condition with the ER values above 1.0. Following Figure 4.30 shows the combustion efficiency, ŋ for PVC Prysmian A electrical cable fires at 50 kW/m$^2$ and various ventilation conditions.

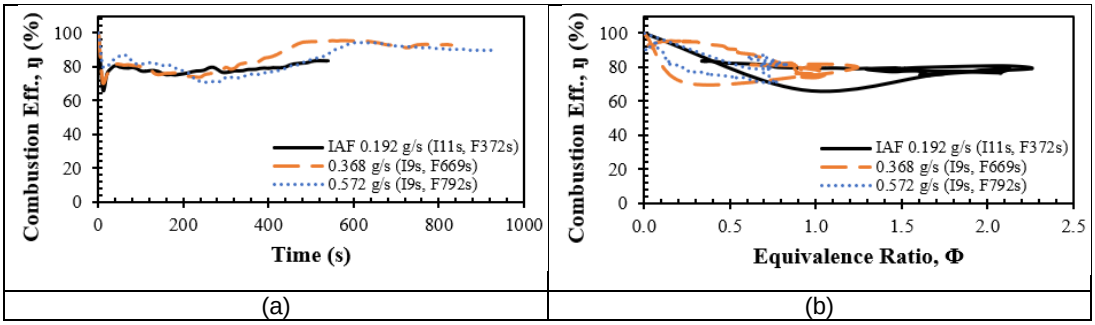


**Figure 4.30** Combustion efficiency, η for PVC Prysmian A electrical cable fires at 50 kW/m$^2$ and various ventilation conditions.

### 4.3.6 Gas Yields for Other Electrical Cable Fires

Following Figure 4.31 showed gas yields for other PVC electrical cable fires at heat flux of 35 kW/m$^2$ and free ventilation condition. CO yield (>0.03 g/g) for PVC EC-GB 2 cable fire was more than 3 times higher than CO yield (0.01 g/g) for PVC EC-GB 1 cable fire. PVC EC-GB 1 cable fire showed insignificant and lower HCl yield compared to PVC EC-GB 2 cable fire which the highest HCl yield given by PVC EC-GB 2 cable fire was ~0.02 g/g. Yields of other species like Acrolein, Acetylene, $CO_2$ and Toluene were higher for PVC EC-GB 2 cable fire compared to PVC EC-GB 1 fire. The highest Acrolein yield peak by PVC EC-GB 1 and PVC EC-GB 2 cable fires was same, ~0.02 g/g. Both electrical cable fires gave the maximum THC yield of ~0.4 g/g and each cable fire had the average $CO_2$ yield of 0.5 g/g (PVC EC-GB 1) and 0.7 g/g (PVC EC-GB 2). Yields of other species like Formaldehyde, NO, $SO_2$, $NO_x$ and Acetaldehyde indicated that PVC EC-GB 1 cable fire gave higher yield values than PVC EC-GB 2 cable fire. Benzene, $NO_2$ and HBr yields were zero and insignificant for both cable fires.

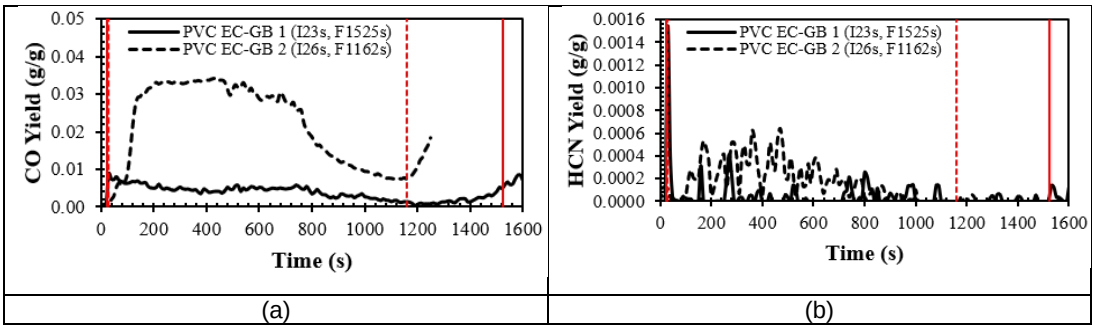

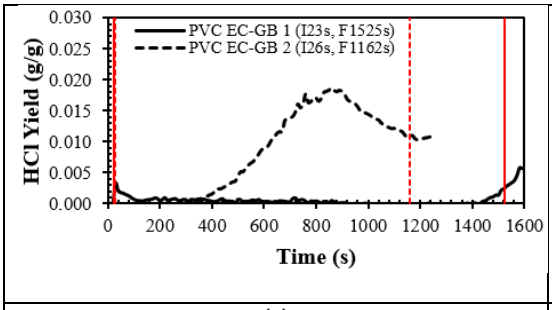
HCl Yield (g/g)
PVC EC-GB 1 (I23s, F1525s)
PVC EC-GB 2 (I26s, F1162s)
Time (s)

(c)

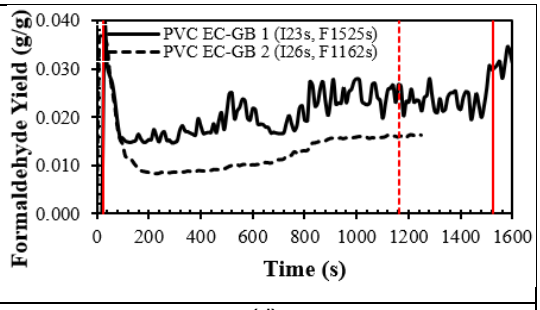
Formaldehyde Yield (g/g)
PVC EC-GB 1 (I23s, F1525s)
PVC EC-GB 2 (I26s, F1162s)
Time (s)

(d)

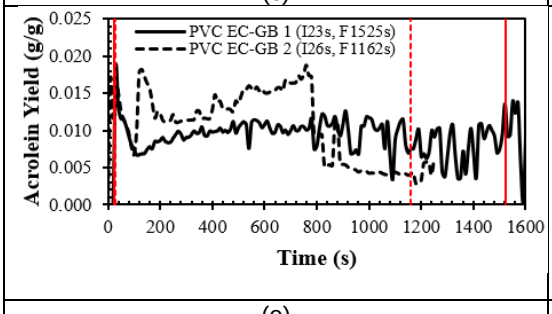
Acrolein Yield (g/g)
PVC EC-GB 1 (I23s, F1525s)
PVC EC-GB 2 (I26s, F1162s)
Time (s)

(e)

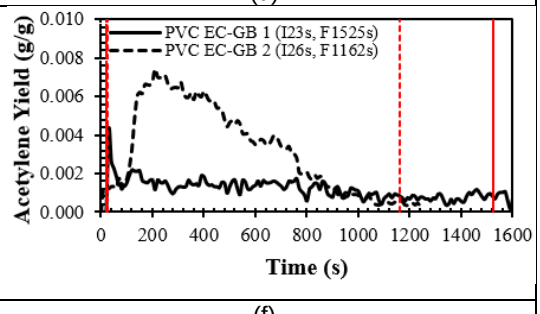
Acetylene Yield (g/g)
PVC EC-GB 1 (I23s, F1525s)
PVC EC-GB 2 (I26s, F1162s)
Time (s)

(f)

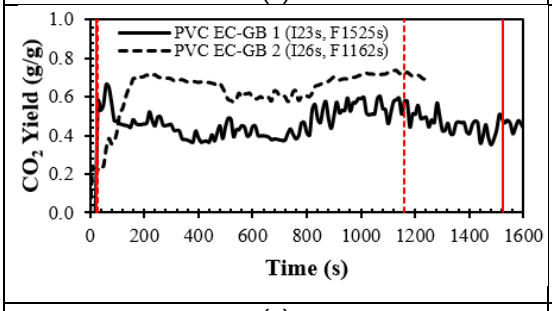
CO2 Yield (g/g)
PVC EC-GB 1 (I23s, F1525s)
PVC EC-GB 2 (I26s, F1162s)
Time (s)

(g)

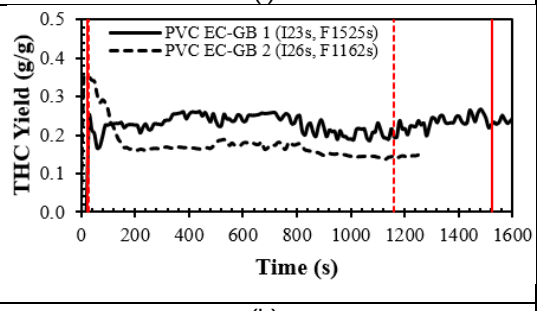
THC Yield (g/g)
PVC EC-GB 1 (I23s, F1525s)
PVC EC-GB 2 (I26s, F1162s)
Time (s)

(h)

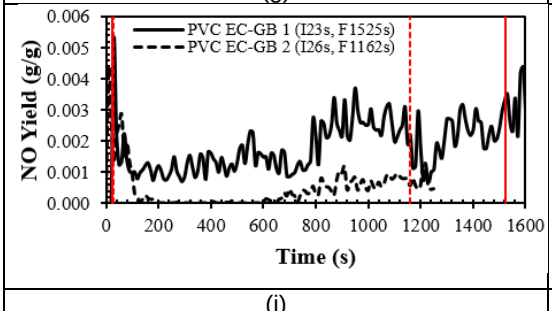
NO Yield (g/g)
PVC EC-GB 1 (I23s, F1525s)
PVC EC-GB 2 (I26s, F1162s)
Time (s)

(i)

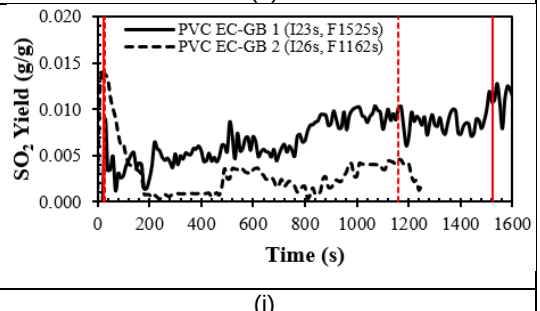
SO2 Yield (g/g)
PVC EC-GB 1 (I23s, F1525s)
PVC EC-GB 2 (I26s, F1162s)
Time (s)

(j)

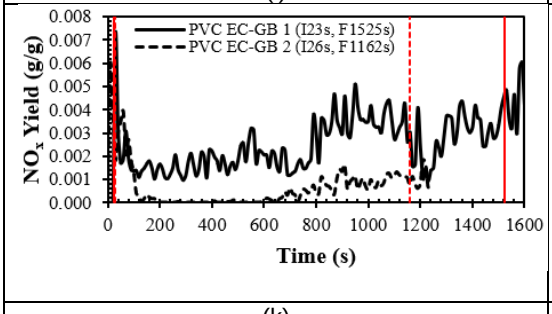
NOx Yield (g/g)
PVC EC-GB 1 (I23s, F1525s)
PVC EC-GB 2 (I26s, F1162s)
Time (s)

(k)

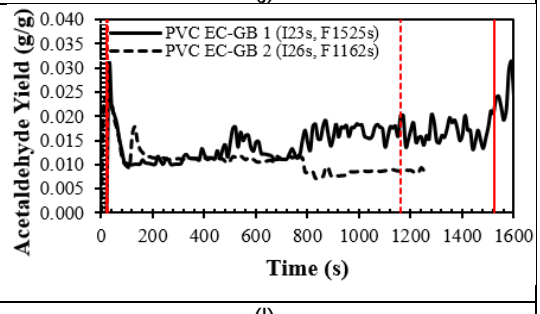
Acetaldehyde Yield (g/g)
PVC EC-GB 1 (I23s, F1525s)
PVC EC-GB 2 (I26s, F1162s)
Time (s)

(l)

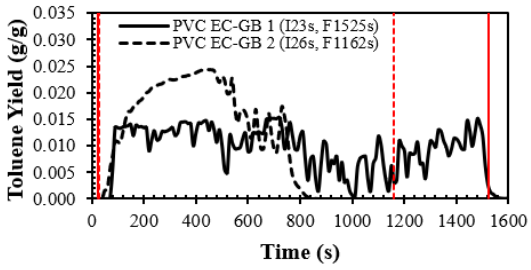


(m)

**Figure 4.31** Gas yields for other PVC electrical cable fires at 35 kW/m$^2$ and free ventilation.

Throughout the burning period, the efficiency rates for PVC EC-GB 1 and PVC EC-GB 2 cable fires were in a range between 60% to 80%. These combustion rates were lower compared to the PVC Prysmian A cable fires for the same test conditions. With these combustion efficiency profile, these cable fires were having fuel lean burning with fire equivalence ratios below than 0.2. PVC EC-GB 2 cable fire had a slightly higher efficiency rate than PVC EC-GB 1 cable fire with the richer equivalence ratios. The combustion efficiency, ŋ for PVC EC-GB 1 and PVC EC-GB 2 electrical cable fires at 35 kW/m$^2$ and free ventilation was shown in Figure 4.32. Having leaner fire equivalence ratios while burning, the PVC EC-GB 1 cable fire took longer time to burn before the flame extinguished at 1525 s if compared to the PVC EC-GB cable fire which the flame extinguished about 6 minutes earlier.

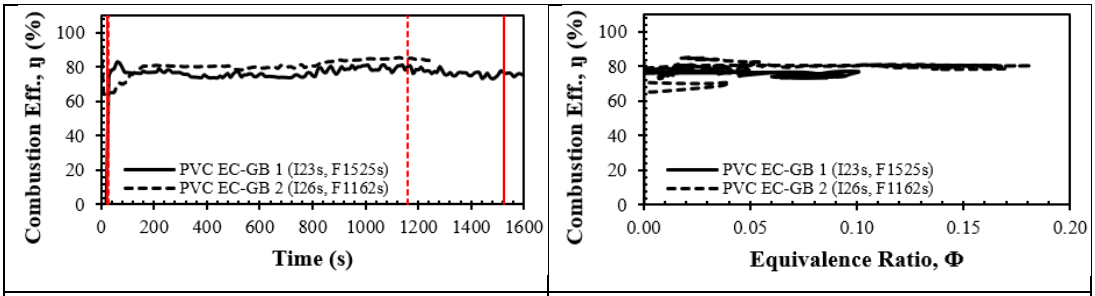


(a) (b)

**Figure 4.32** Combustion efficiency, ŋ for other PVC electrical cable fires at 35 kW/m$^2$ and free ventilation.

Under fire conditions of heat flux of 35 kW/m$^2$ and free ventilation, total burning period for Solar Energy cables such as HV1-4C and HV2-3C was more than 3000 s (>50 minutes). Gas yields for Solar Energy cable fires at irradiation

level of 35 kW/m$^2$ and free ventilation were shown in Figure 4.33. Gas yields showed by HV2-3C cable fire were much more higher than gas yields by HV1-4C cable fire for most of toxic species. The highest CO yield for HV2-3C was about 0.13 g/g and the yield values were higher than the HV1-4C cable fire. Yields of Formaldehyde, Acrolein, Acetylene, $SO_2$, Acetaldehyde and Toluene indicated lower values for HV1-4C cable fire while HV2-3C cable fire gave a high yield of these species. Both cable fires had an average CO2 yield ~0.8 g/g with HV2-3C cable fire gave the maximum yield peak of 1.4 g/g and HV1-4C gave the maximum peak of 1.2 g/g. The yields showed by these two Solar Energy cable fires after 2000 s of burning period were lower compared to the yields before that period for most of species. The maximum THC yield was about 0.3 g/g for HV2-3C cable fire and 0.15 g/g for HV1-4C cable fire.

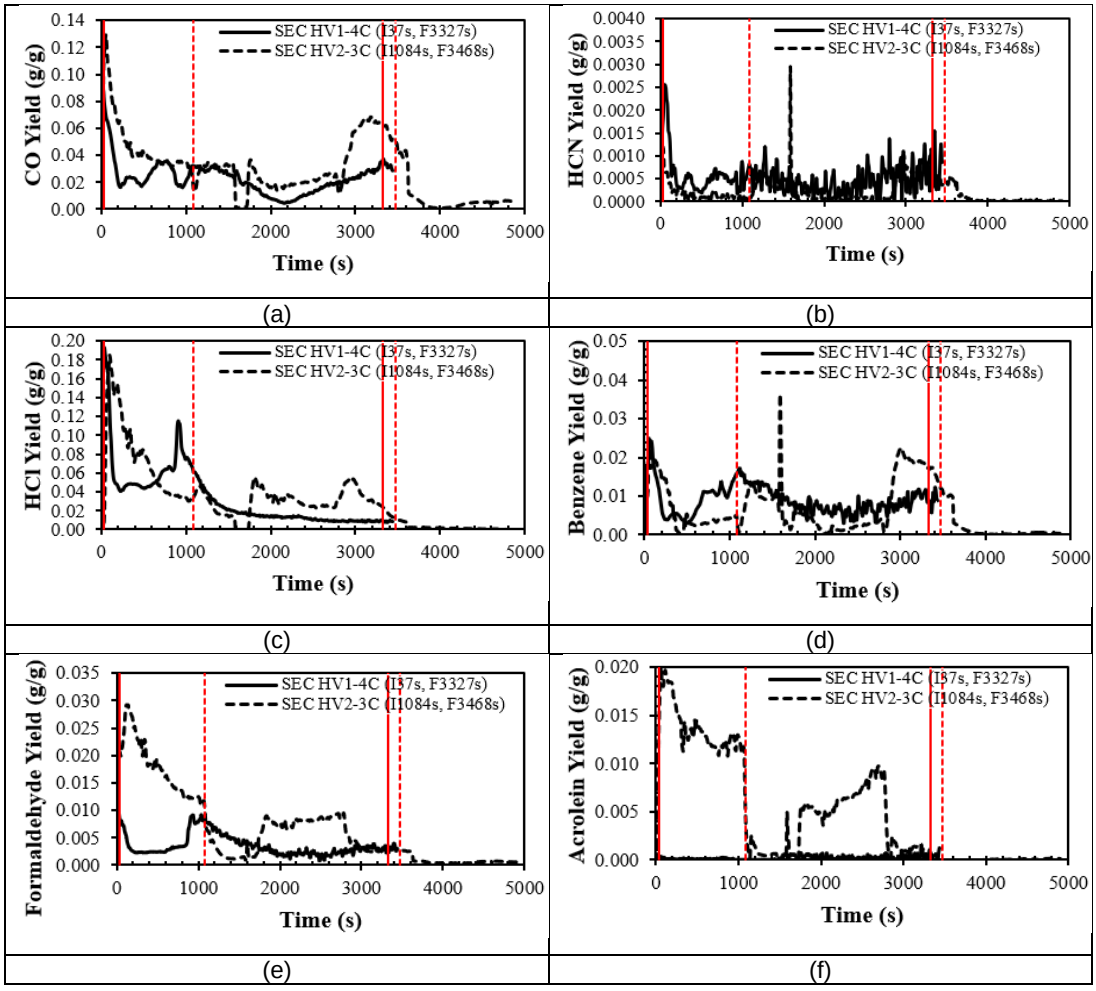

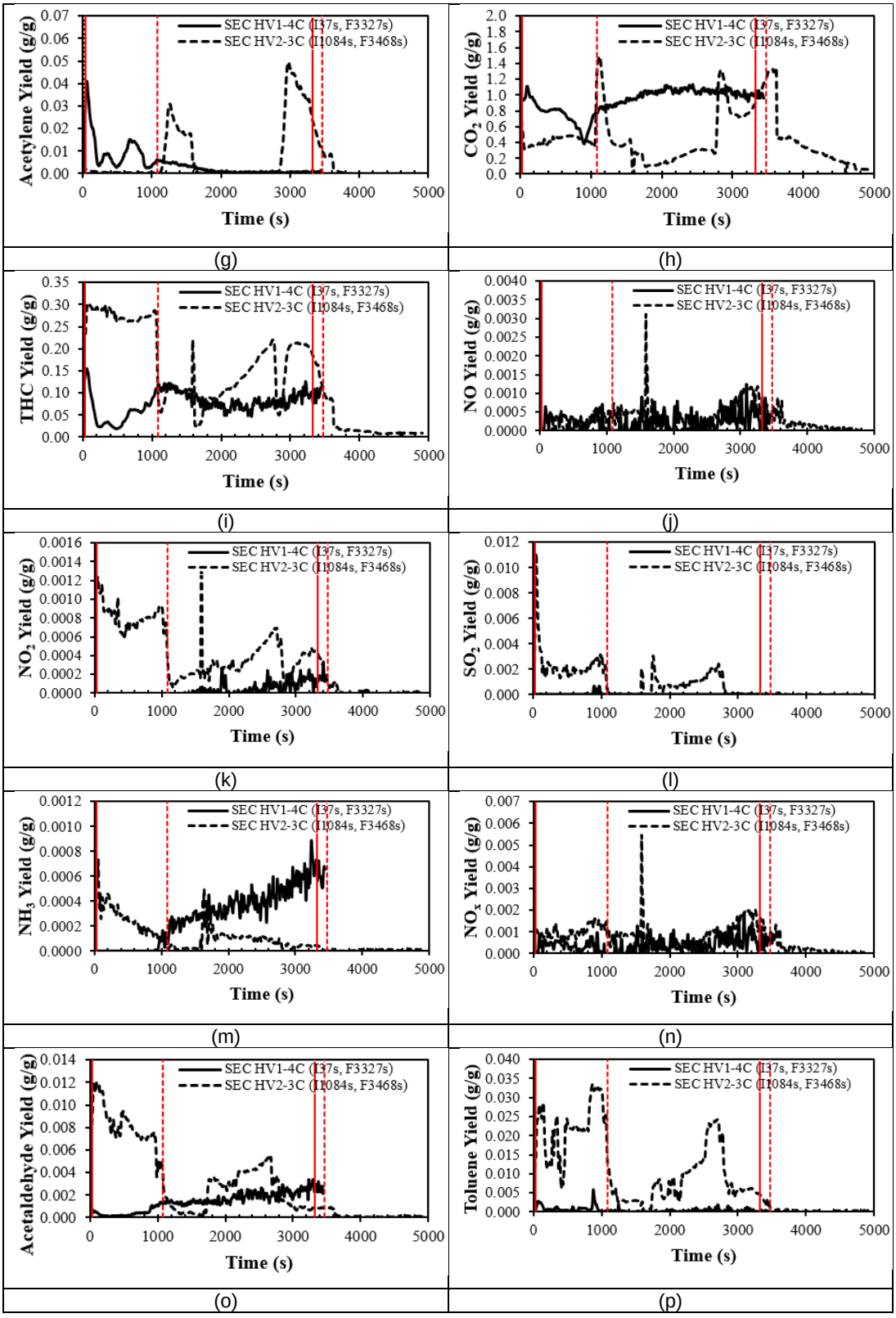


**Figure 4.33** Gas yields for Solar Energy cable fires at 35 kW/m$^2$ and free ventilation.

Combustion efficiency, ŋ for Solar Energy cable fires at 35 kW/m$^2$ and free ventilation was shown in Figure 4.34. The combustion efficiency for HV1-4C cable fire was almost 100% at initial stage of the combustion process then it had decreased slightly to 90% after 1000 s as shown in Figure 4.34. While HV2-3C cable fire showed the minimum combustion efficiency of ~70% at the start of ignition (~1084 s) before increased to the maximum efficiency peak of 95% while having a flaming fire condition. Fire equivalence ratios for PVC EC-GB 1 cable fire reached a maximum ER of 0.8 which was about double than the maximum ER shown by the PVC EC-GB 2 cable fire. Both cable fires had experienced fuel lean burning condition with the PVC EC-GB 2 cable fire which the ER much more leaner having a longer flaming condition than the PVC EC-GB 1 cable fire.

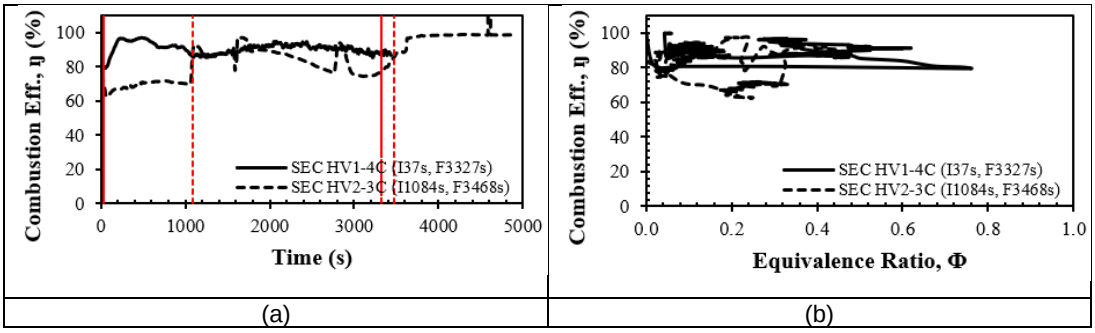


(a) (b)

**Figure 4.34** Combustion efficiency, ŋ for Solar Energy cable fires at 35 kW/m$^2$ and free ventilation.

Two types of Wind Turbine cable from Siemens were named as AMI-G and AMI-B cables. Figure 4.35 shows the gas yields for Siemens' Wind Turbine cable fires at 35 kW/m$^2$ and free ventilation. AMI-B cable sample had burned more than 4 times longer than the AMI-G cable sample. AMI-B cable fire had the highest CO yield of about 0.07 g/g at the start of ignition and at the flame out stage. Meanwhile, the AMI-G cable fire showed three peaks of CO yield at burning time of 500 s, 1500 s and 3000 s with each peak giving the CO yield value of 0.04 g/g, 0.02 g/g and 0.08 g/g. Toxic gas yields produced from the AMI-G cable fire were higher than the AMI-B cable fire. From Figure 4.35, it can be seen clearly that the gas yield profile for most of toxic species that produced from both cable fires have giving the same graph pattern for the first 300 s before the start of ignition. From the similar pattern of results, it could be said that both cables chemically had the same composition with the

different of cable mass and number of cores which these factors possibly differ the time taken while burning.

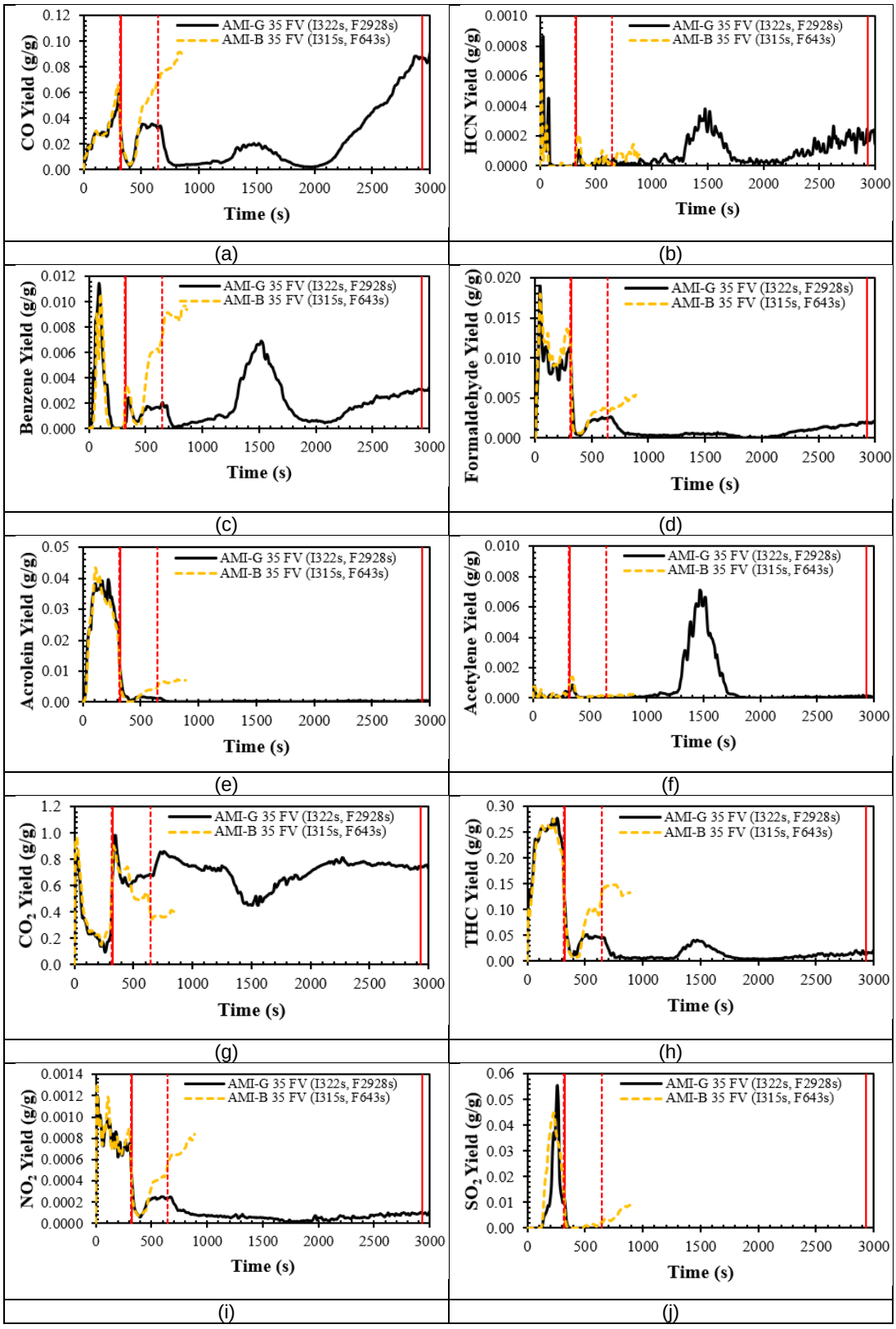

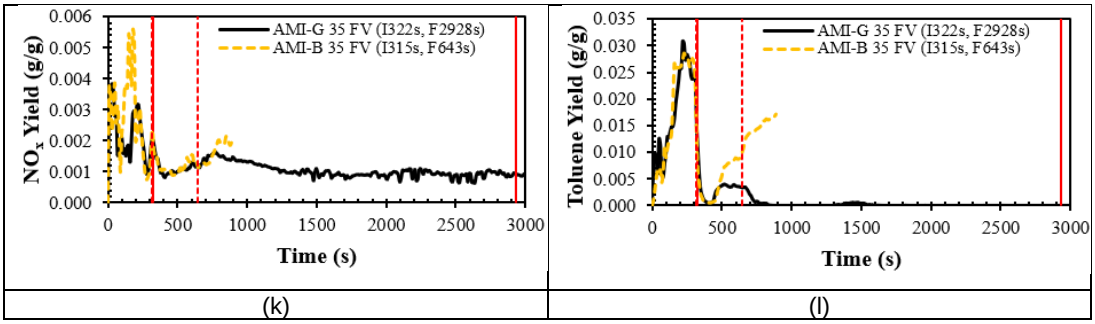


(k) (l)

**Figure 4.35** Gas yields for Siemens' Wind Turbine cable fires at 35 kW/m$^2$ and free ventilation.

As shown in Figure 4.36, the combustion efficiency rate values for these Wind Turbine cable fires were high, ranges from 70% up to 100%. The minimum efficiency rate for both cable fires was about 70% before the start of ignition and after that period the efficiency rate had increased to the maximum value before it decreased when the fires almost reached the flame out condition. Both cable fires showed a fuel lean fire condition with ER values below than 0.5. The ER values for AMI-G cable fire were higher than the AMI-B cable fire. Combustion efficiency, η as a function of time and equivalence ratio (ER) for Siemens' Wind Turbine cable fires at 35 kW/m$^2$ and free ventilation is shown in the following Figure 4.36. In overall, the combustion efficiency for both cable fires had shown an increase with the increase of fire equivalence ratio.

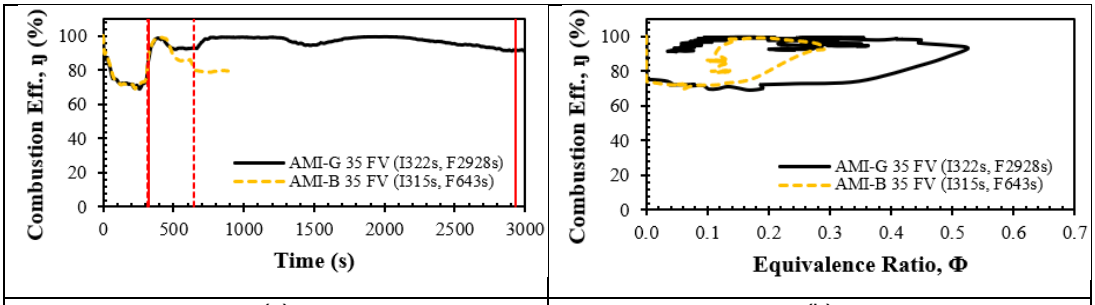


(a) (b)

**Figure 4.36** Combustion efficiency, η for Siemens' Wind Turbine cable fires at 35 kW/m$^2$ and free ventilation.

LSZH cable samples when burnt were expected to give lower yields of halogenated products like HCl, HF and HBr than non-LSZH cable samples. The following Figure 4.37 showed yield of gases as a function of time from the burning of LSZH electrical cable samples under two different heat fluxes (35

kW/m$^2$ and 50 kW/m$^2$) with free and restricted (0.192 g/s or 9.4 L/min) ventilations. As shown in Figure 4.15, toxic gas emissions were higher for LSZH cable fires at a higher heat flux of 50 kW/m$^2$ compared to the cable fires at a lower heat flux (35 kW/m$^2$). The result is relevant with gas yield values shown in the following Figure 4.37 where a higher gas emission has contributed to a higher gas yield. For LSZH cable fires under heat flux of 35 kW/m$^2$ and free ventilation, TEC2-W cable fire produced highest yields of HCN, Benzene, Acetylene and THC compared to Prysmian B and 6701B-W cable fires. This TEC2-W cable has not been tested at a higher heat flux of 50 kW/m$^2$ like other two cables, however from the result comparison of cable fires at a lower heat flux of 35 kW/m$^2$, it is expected to produce higher value of yields than the other two cables if burnt at a higher heat flux. From Figure 4.37 (h), the highest peak of $CO_2$ yield produced by LSZH cable fires for both heat flux values was 1.0 g/g. HCl yields was low as expected for LSZH cable fires which less than 0.01 g/g. Prysmian B (PB) cable fire seemed to produce higher $SO_2$ yields (up to 0.013 g/g), more than double compared to other two LSZH cable fires (less than 0.006 g/g).

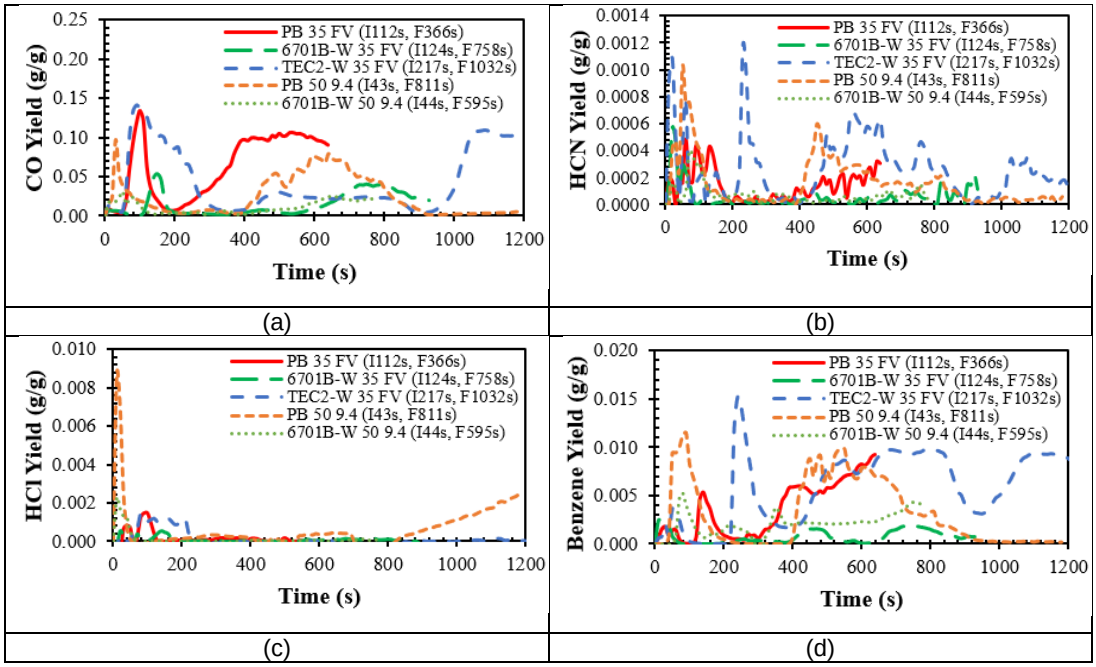

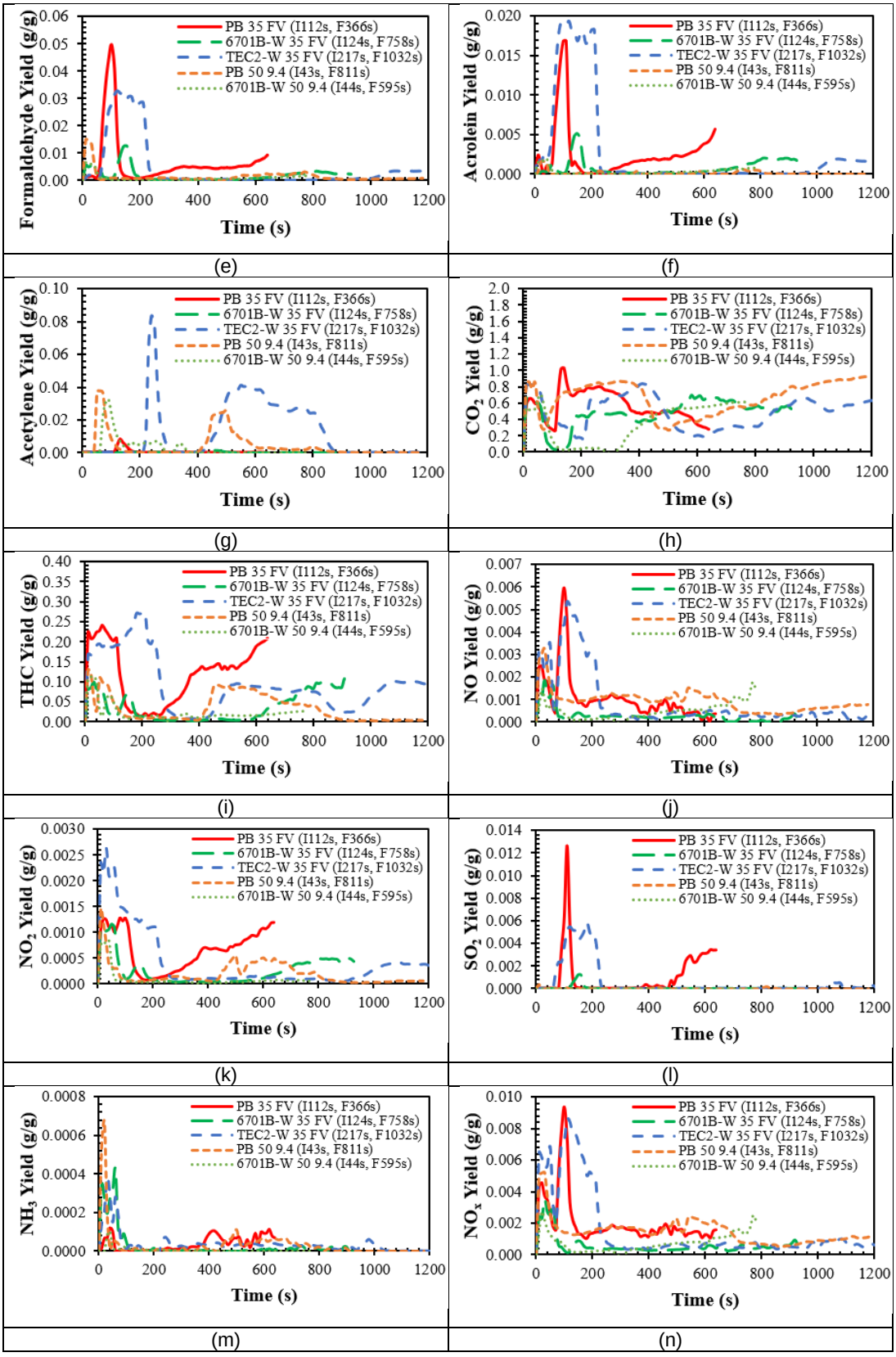
Formaldehyde Yield (g/g)
Time (s)
PB 35 FV (I112s, F366s)
6701B-W 35 FV (I124s, F758s)
TEC2-W 35 FV (I217s, F1032s)
PB 50 9.4 (I43s, F811s)
6701B-W 50 9.4 (I44s, F595s)
(e)
Acrolein Yield (g/g)
Time (s)
PB 35 FV (I112s, F366s)
6701B-W 35 FV (I124s, F758s)
TEC2-W 35 FV (I217s, F1032s)
PB 50 9.4 (I43s, F811s)
6701B-W 50 9.4 (I44s, F595s)
(f)
Acetylene Yield (g/g)
Time (s)
PB 35 FV (I112s, F366s)
6701B-W 35 FV (I124s, F758s)
TEC2-W 35 FV (I217s, F1032s)
PB 50 9.4 (I43s, F811s)
6701B-W 50 9.4 (I44s, F595s)
(g)
CO2 Yield (g/g)
Time (s)
PB 35 FV (I112s, F366s)
6701B-W 35 FV (I124s, F758s)
TEC2-W 35 FV (I217s, F1032s)
PB 50 9.4 (I43s, F811s)
6701B-W 50 9.4 (I44s, F595s)
(h)
THC Yield (g/g)
Time (s)
PB 35 FV (I112s, F366s)
6701B-W 35 FV (I124s, F758s)
TEC2-W 35 FV (I217s, F1032s)
PB 50 9.4 (I43s, F811s)
6701B-W 50 9.4 (I44s, F595s)
(i)
NO Yield (g/g)
Time (s)
PB 35 FV (I112s, F366s)
6701B-W 35 FV (I124s, F758s)
TEC2-W 35 FV (I217s, F1032s)
PB 50 9.4 (I43s, F811s)
6701B-W 50 9.4 (I44s, F595s)
(j)
NO2 Yield (g/g)
Time (s)
PB 35 FV (I112s, F366s)
6701B-W 35 FV (I124s, F758s)
TEC2-W 35 FV (I217s, F1032s)
PB 50 9.4 (I43s, F811s)
6701B-W 50 9.4 (I44s, F595s)
(k)
SO2 Yield (g/g)
Time (s)
PB 35 FV (I112s, F366s)
6701B-W 35 FV (I124s, F758s)
TEC2-W 35 FV (I217s, F1032s)
PB 50 9.4 (I43s, F811s)
6701B-W 50 9.4 (I44s, F595s)
(l)
NH3 Yield (g/g)
Time (s)
PB 35 FV (I112s, F366s)
6701B-W 35 FV (I124s, F758s)
TEC2-W 35 FV (I217s, F1032s)
PB 50 9.4 (I43s, F811s)
6701B-W 50 9.4 (I44s, F595s)
(m)
NOx Yield (g/g)
Time (s)
PB 35 FV (I112s, F366s)
6701B-W 35 FV (I124s, F758s)
TEC2-W 35 FV (I217s, F1032s)
PB 50 9.4 (I43s, F811s)
6701B-W 50 9.4 (I44s, F595s)
(n)

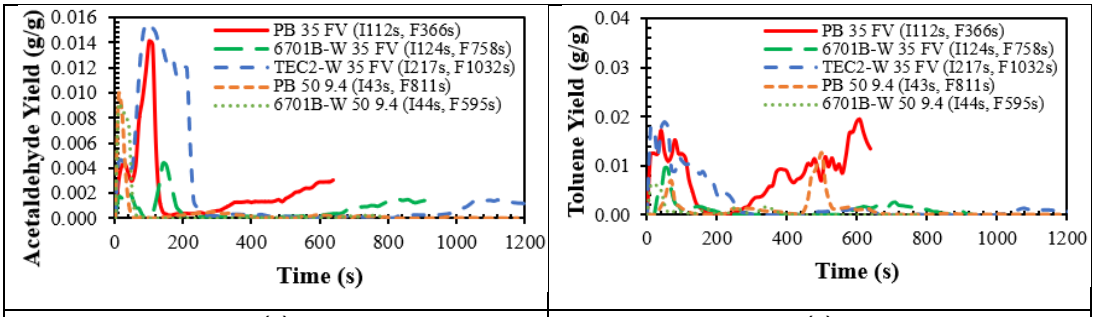


(o) (p)

**Figure 4.37** Gas yields for LSZH electrical cable fires at different heat fluxes and ventilation rates.

Combustion efficiency, ŋ for LSZH electrical cable fires at different heat fluxes and ventilation rates is shown in Figure 4.38. These LSZH cable fires gave a range of combustion efficiency from 70% to 100%. From Figure 4.38 (a), lower efficiency rates were obtained at initial and at the end of burning for most of these cable fires. At irradiation level of 35 kW/m$^2$ and free ventilation, between three different LSZH cable samples, only the TEC2-W cable sample had experienced the fuel rich burning condition with ER values up to 1.2 while other two cable fires gave fire equivalence ratios less than 0.3. For cable fires at irradiation level of 50 kW/m$^2$ and air flowrate of 9.4 L/min, the cable fires were having a fuel lean burning with ER values less than 1.0.

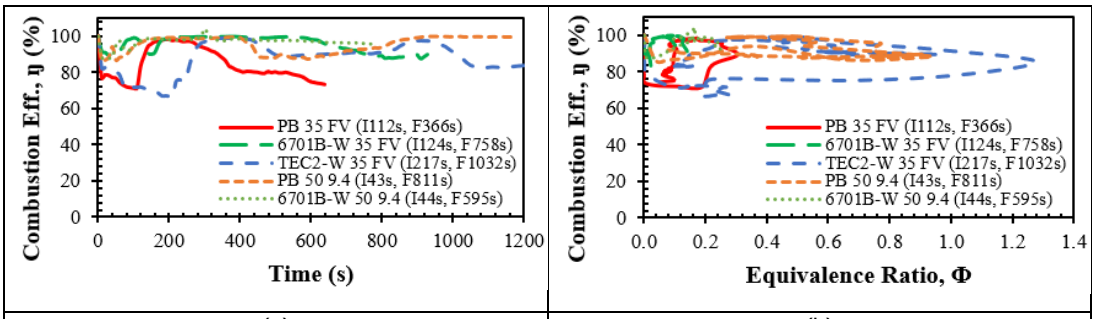


(a) (b)

**Figure 4.38** Combustion efficiency, ŋ for LSZH electrical cable fires at different heat fluxes and ventilation rates.

FLEX1-BG electrical cable fire produced a higher yield of toxic gases than FLEX2-W fire as shown in Figure 4.39 except for Acrolein, NO, $NH_3$ and $NO_x$. Yields for several toxic species produced from FLEX cable fires against time were shown in the following Figure 4.39. The highest yield of CO for FLEX2-

W fire was 0.08 g/g, about half than the highest CO yield produced from FLEX1-BG fire. The peak yields for several species like CO, HCN, HCl, Benzene and Acetylene were shown after 200 s of burning period for FLEX2-W fire. FLEX2-W fire showed the highest HCN yield of 0.002 g/g at 300 s while FLEX1-BG fire had the highest HCN yield of 0.0035 g/g at 35 s. FLEX1-BG fire gave the highest $NO_2$ yield of 0.02 g/g (before the ignition) and $SO_2$ yield of 0.012 g/g (at 750 s) with none $NO_2$ and $SO_2$ yields were shown by FLEX2-W fire. The highest 0.0015 g/g of $NH_3$ yield was given by FLEX2-W fire and no significant $NH_3$ yield was shown by FLEX1-BG fire. There was no indication of $NO_2$ and $SO_2$ production from FLEX2-W fire (see Figure 4.16 (k) and (l)) and less than 20 ppm of $NH_3$ production from FLEX1-BG fire (see Figure 4.16 (m)), this showed a good agreement with the yield data of these species.

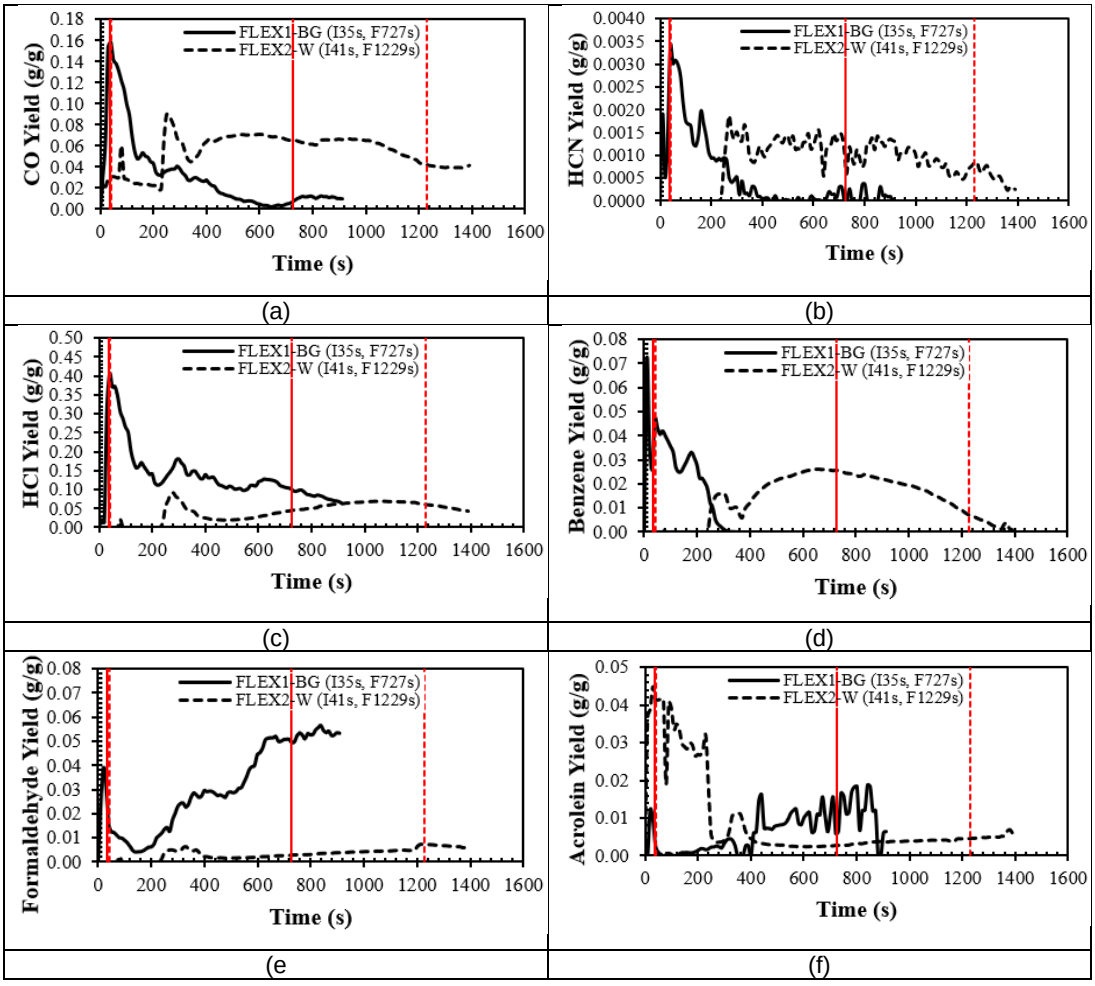

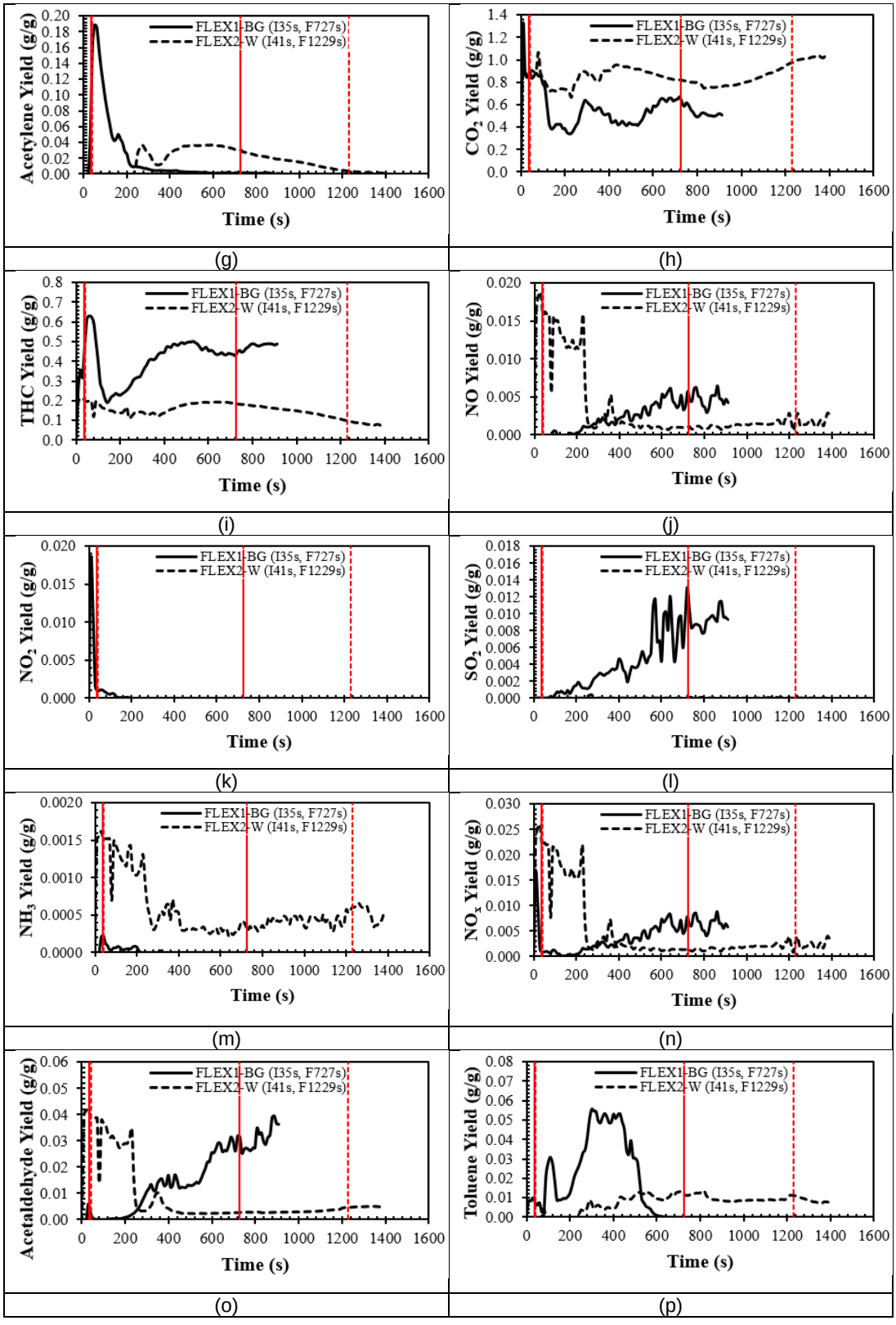


**Figure 4.39** Gas yields for other Non-PVC electrical cable fires at 35 kW/m$^2$ and free ventilation.

Figure 4.40 (a) and (b) showed combustion efficiency, ŋ as a function of time and equivalence ratio for FLEX electrical cable fires at 35 kW/m$^2$ and free ventilation. It showed that FLEX2-W electrical cable fire had a higher combustion efficiency, ŋ (~80%) throughout the burning period which was about 30% higher than FLEX1-BG cable fire. FLEX1-BG cable fire showed a rich burning with equivalence ratio more than 1.0 while FLEX2-W cable fire had a lean burning with ER less than 0.3. From the gas concentration graph in Figure 4.16 (h), $CO_2$ had reached the maximum peak of 10% before decreasing after 200 s for FLEX1-BG cable fire. This result had a good agreement with the combustion efficiency profile in Figure 4.40 (a) which showing a decrease in the value after that period. Table 4.5 (a), (b) and (c) include the summary of maximum and mean yields for 18 species from various electrical cable fires. Graphs for cumulative mass of CO produced from various electrical cable fires are also included in Appendix E.

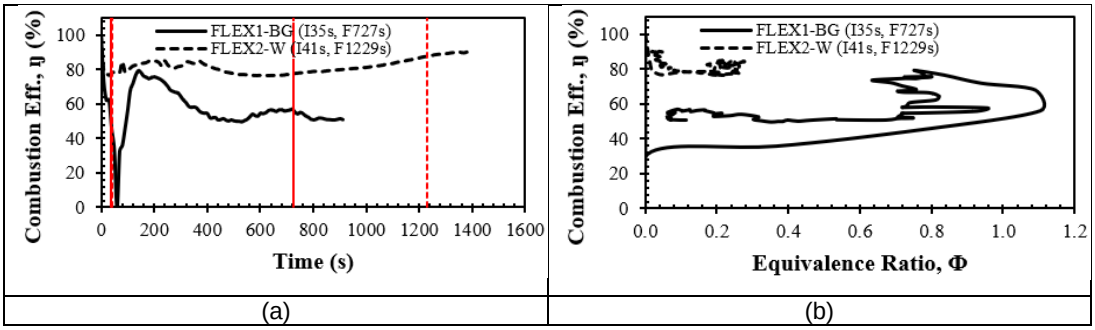


**Figure 4.40** Combustion efficiency, ŋ for other Non-PVC electrical cable fires at 35 kW/m$^2$ and free ventilation.

**Table 4.5 (a)** Maximum gas yields for electrical cable fires at various irradiation levels and ventilation rates.

| No. | Types of Cable Fire | Maximum Gas Yields (g/g) | | | | | | | | | | | | | | | | | |
|---|---|---|---|---|---|---|---|---|---|---|---|---|---|---|---|---|---|---|---|
| | | CO | HCN | HCl | HF | Benzene | Formaldehyde | Acrolein | Acetylene | $CO_2$ | THC | NO | $NO_2$ | $SO_2$ | $NH_3$ | $NO_x$ | HBr | Acetaldehyde | Toluene |
| 1 | PVC PA (25 9.4) | 0.1144 | 0.0014 | 0.2939 | 0.0001 | 0.0223 | 0.0233 | 0.0087 | 0.0381 | 1.4056 | 0.3614 | 0.0015 | 0.0012 | 0.0086 | 0.0003 | 0.0031 | 0.0000 | 0.0028 | 0.0116 |
| 2 | PVC PA (25 18) | 0.0880 | 0.0010 | 0.2733 | 0.0002 | 0.0174 | 0.0308 | 0.0070 | 0.0220 | 1.3221 | 0.3942 | 0.0023 | 0.0034 | 0.0053 | 0.0004 | 0.0057 | 0.0000 | 0.0024 | 0.0183 |
| 3 | PVC PA (25 28) | 0.0830 | 0.0006 | 0.2653 | 0.0002 | 0.0306 | 0.0497 | 0.0209 | 0.0011 | 0.8156 | 0.5154 | 0.0493 | 0.0029 | 0.0103 | 0.0027 | 0.0684 | 0.0000 | 0.0121 | 0.0308 |
| 4 | PVC PA (35 9.4) | 0.0705 | 0.0014 | 0.0675 | 0.0000 | 0.0323 | 0.0056 | 0.0010 | 0.0549 | 1.5979 | 0.2178 | 0.0014 | 0.0003 | 0.0001 | 0.0000 | 0.0019 | 0.0000 | 0.0009 | 0.0179 |
| 5 | PVC PA (35 18) | 0.0877 | 0.0014 | 0.2863 | 0.0000 | 0.0266 | 0.0140 | 0.0030 | 0.0498 | 1.4741 | 0.1965 | 0.0012 | 0.0002 | 0.0002 | 0.0001 | 0.0018 | 0.0000 | 0.0019 | 0.0175 |
| 6 | PVC PA (35 28) | 0.1014 | 0.0015 | 0.2631 | 0.0002 | 0.0292 | 0.0272 | 0.0073 | 0.0273 | 1.5692 | 0.2585 | 0.0043 | 0.0047 | 0.0002 | 0.0001 | 0.0101 | 0.0000 | 0.0083 | 0.0080 |
| 7 | PVC PA (35 FV) | 0.0825 | 0.0030 | 0.1025 | 0.0000 | 0.0406 | 0.0205 | 0.0037 | 0.0545 | 1.5856 | 0.2900 | 0.0019 | 0.0019 | 0.0008 | 0.0008 | 0.0043 | 0.0000 | 0.0064 | 0.0201 |
| 8 | PVC PA (50 9.4) | 0.1593 | 0.0017 | 0.1792 | 0.0000 | 0.0347 | 0.0061 | 0.0020 | 0.0715 | 1.1914 | 0.2858 | 0.0013 | 0.0006 | 0.0001 | 0.0001 | 0.0022 | 0.0000 | 0.0010 | 0.0209 |
| 9 | PVC PA (50 18) | 0.1842 | 0.0019 | 0.2012 | 0.0000 | 0.0357 | 0.0086 | 0.0018 | 0.0468 | 1.4316 | 0.2513 | 0.0013 | 0.0004 | 0.0001 | 0.0001 | 0.0022 | 0.0000 | 0.0012 | 0.0206 |
| 10 | PVC PA (50 28) | 0.2097 | 0.0012 | 0.1897 | 0.0000 | 0.0255 | 0.0093 | 0.0011 | 0.0375 | 1.3516 | 0.2164 | 0.0021 | 0.0006 | 0.0005 | 0.0001 | 0.0034 | 0.0000 | 0.0010 | 0.0269 |
| 11 | PVC EC-GB 1 (35 FV) | 0.0088 | 0.0015 | 0.0111 | 0.0025 | 0.0000 | 0.0391 | 0.0184 | 0.0043 | 0.6643 | 0.2673 | 0.0053 | 0.0000 | 0.0127 | 0.0001 | 0.0073 | 0.0000 | 0.0314 | 0.0154 |
| 12 | PVC EC-GB 2 (35 FV) | 0.0344 | 0.0006 | 0.0187 | 0.0003 | 0.0000 | 0.0372 | 0.0188 | 0.0074 | 0.7402 | 0.3522 | 0.0043 | 0.0000 | 0.0144 | 0.0000 | 0.0059 | 0.0000 | 0.0239 | 0.0243 |
| 13 | HV Power 1-4C (35 FV) | 0.1181 | 0.0026 | 0.1928 | 0.0006 | 0.0243 | 0.0119 | 0.0016 | 0.0409 | 1.1365 | 0.1552 | 0.0012 | 0.0003 | 0.0006 | 0.0009 | 0.0019 | 0.0000 | 0.0034 | 0.0057 |
| 14 | HV Power 2-3C (35 FV) | 0.1297 | 0.0030 | 0.1847 | 0.0023 | 0.0356 | 0.0293 | 0.0201 | 0.0497 | 1.4848 | 0.3031 | 0.0031 | 0.0013 | 0.0111 | 0.0015 | 0.0055 | 0.0000 | 0.0121 | 0.0333 |
| 15 | AMI-G (35 FV) | 0.1049 | 0.0009 | 0.0018 | 0.0004 | 0.0114 | 0.0189 | 0.0394 | 0.0071 | 0.9783 | 0.2769 | 0.0022 | 0.0012 | 0.0555 | 0.0004 | 0.0038 | 0.0000 | 0.0062 | 0.0307 |
| 16 | AMI-G (50 9.4) | 0.0570 | 0.0007 | 0.0009 | 0.0000 | 0.0104 | 0.0099 | 0.0059 | 0.0302 | 1.0096 | 0.1024 | 0.0028 | 0.0013 | 0.0002 | 0.0001 | 0.0050 | 0.0000 | 0.0114 | 0.0094 |
| 17 | AMI-B (35 FV) | 0.0915 | 0.0007 | 0.0015 | 0.0003 | 0.0106 | 0.0179 | 0.0433 | 0.0014 | 0.9668 | 0.2748 | 0.0036 | 0.0013 | 0.0450 | 0.0007 | 0.0056 | 0.0000 | 0.0061 | 0.0286 |
| 18 | Prysmian B (35 FV) | 0.1339 | 0.0005 | 0.0014 | 0.0003 | 0.0093 | 0.0495 | 0.0168 | 0.0083 | 1.0263 | 0.2409 | 0.0060 | 0.0013 | 0.0127 | 0.0001 | 0.0093 | 0.0000 | 0.0142 | 0.0194 |
| 19 | Prysmian B (50 9.4) | 0.0969 | 0.0010 | 0.0087 | 0.0001 | 0.0115 | 0.0150 | 0.0016 | 0.0376 | 0.9284 | 0.1297 | 0.0033 | 0.0014 | 0.0003 | 0.0007 | 0.0052 | 0.0000 | 0.0098 | 0.0125 |
| 20 | 6701B-W 2.5 (35 FV) | 0.0535 | 0.0006 | 0.0005 | 0.0002 | 0.0024 | 0.0128 | 0.0051 | 0.0015 | 0.8564 | 0.1510 | 0.0019 | 0.0012 | 0.0012 | 0.0004 | 0.0035 | 0.0000 | 0.0044 | 0.0095 |
| 21 | 6701B-W 2.5 (50 9.4) | 0.0315 | 0.0004 | 0.0023 | 0.0000 | 0.0053 | 0.0066 | 0.0020 | 0.0322 | 0.7021 | 0.1144 | 0.0018 | 0.0008 | 0.0000 | 0.0001 | 0.0027 | 0.0000 | 0.0091 | 0.0062 |
| 22 | TEC2-W (35 FV) | 0.1410 | 0.0012 | 0.0015 | 0.0003 | 0.0152 | 0.0328 | 0.0194 | 0.0834 | 0.8391 | 0.2728 | 0.0053 | 0.0026 | 0.0059 | 0.0004 | 0.0086 | 0.0000 | 0.0155 | 0.0189 |
| 23 | Flex 1 BG (35 FV) | 0.1586 | 0.0034 | 0.4058 | 0.0006 | 0.0719 | 0.0564 | 0.0188 | 0.1885 | 1.2991 | 0.6296 | 0.0064 | 0.0184 | 0.0131 | 0.0002 | 0.0165 | 0.0000 | 0.0393 | 0.0557 |
| 24 | Flex 2 W (35 FV) | 0.0891 | 0.0019 | 0.0900 | 0.0006 | 0.0259 | 0.0075 | 0.0448 | 0.0368 | 1.0623 | 0.2163 | 0.0188 | 0.0000 | 0.0004 | 0.0016 | 0.0258 | 0.0000 | 0.0419 | 0.0137 |

**Table 4.5 (b)** Mean gas yields for PVC Prysmian A electrical cable fires at various irradiation levels and ventilation rates.

| PVC PRYSMIAN A ELECTRICAL CABLE | | | | | | | | | | |
|---|---|---|---|---|---|---|---|---|---|---|
| **Test Condition** | **25 9.4** | **25 18** | **25 28** | **35 9.4** | **35 18** | **35 28** | **35 FV** | **50 9.4** | **50 18** | **50 28** |
| **Initial Mass (with Copper) (g)** | 150.72 | 153.25 | 151.96 | 152.74 | 152.35 | 151.87 | 152.46 | 152.50 | 152.70 | 154.59 |
| **Initial Mass (without Copper) (g)** | 63.92 | 66.45 | 65.16 | 65.94 | 65.55 | 65.07 | 65.66 | 65.70 | 65.90 | 67.79 |
| **Total Mass Loss (g)** | 31.51 | 37.15 | 33.45 | 33.27 | 34.63 | 34.28 | 35.99 | 30.01 | 33.22 | 34.68 |
| **Total Time (s)** | 1330 | 1180 | 1540 | 1130 | 1120 | 980 | 1190 | 540 | 830 | 930 |
| **Mean ER, Φ** | 1.10 | 0.75 | 0.29 | 1.35 | 1.28 | 0.32 | 1.03 | 1.52 | 1.18 | 1.26 |
| **Species** | **Mean Yields (g/g)** | | | | | | | | | |
| CO | 0.0409 | 0.0350 | 0.0248 | 0.0454 | 0.0430 | 0.0354 | 0.0449 | 0.1123 | 0.0911 | 0.0977 |
| HCN | 0.0007 | 0.0005 | 0.0000 | 0.0008 | 0.0007 | 0.0006 | 0.0009 | 0.0007 | 0.0006 | 0.0006 |
| HCl | 0.0512 | 0.0589 | 0.0654 | 0.0408 | 0.0508 | 0.0665 | 0.0374 | 0.0459 | 0.0451 | 0.0495 |
| HF | 0.0000 | 0.0000 | 0.0000 | 0.0000 | 0.0000 | 0.0000 | 0.0000 | 0.0000 | 0.0000 | 0.0000 |
| Benzene | 0.0146 | 0.0118 | 0.0022 | 0.0174 | 0.0189 | 0.0161 | 0.0188 | 0.0230 | 0.0208 | 0.0205 |
| Formaldehyde | 0.0033 | 0.0041 | 0.0180 | 0.0026 | 0.0028 | 0.0050 | 0.0031 | 0.0030 | 0.0027 | 0.0027 |
| Acrolein | 0.0007 | 0.0009 | 0.0108 | 0.0004 | 0.0005 | 0.0001 | 0.0006 | 0.0001 | 0.0003 | 0.0003 |
| Acetylene | 0.0214 | 0.0111 | 0.0002 | 0.0330 | 0.0261 | 0.0103 | 0.0247 | 0.0240 | 0.0188 | 0.0192 |
| $CO_2$ | 0.8914 | 1.0262 | 0.2304 | 0.7902 | 0.8217 | 1.1891 | 0.8683 | 0.7009 | 0.7387 | 0.6581 |
| THC | 0.1125 | 0.0955 | 0.4820 | 0.1337 | 0.1350 | 0.0889 | 0.1369 | 0.1559 | 0.1389 | 0.1553 |
| NO | 0.0004 | 0.0004 | 0.0007 | 0.0006 | 0.0007 | 0.0003 | 0.0007 | 0.0009 | 0.0008 | 0.0009 |
| $NO_2$ | 0.0001 | 0.0001 | 0.0006 | 0.0001 | 0.0001 | 0.0001 | 0.0002 | 0.0004 | 0.0002 | 0.0003 |
| $SO_2$ | 0.0001 | 0.0002 | 0.0006 | 0.0000 | 0.0000 | 0.0000 | 0.0000 | 0.0000 | 0.0000 | 0.0000 |
| $NH_3$ | 0.0000 | 0.0000 | 0.0007 | 0.0000 | 0.0000 | 0.0000 | 0.0000 | 0.0000 | 0.0000 | 0.0000 |
| $NO_x$ | 0.0005 | 0.0006 | 0.0016 | 0.0009 | 0.0011 | 0.0005 | 0.0012 | 0.0016 | 0.0012 | 0.0015 |
| HBr | 0.0000 | 0.0000 | 0.0000 | 0.0000 | 0.0000 | 0.0000 | 0.0000 | 0.0000 | 0.0000 | 0.0000 |
| Acetaldehyde | 0.0006 | 0.0003 | 0.0074 | 0.0003 | 0.0004 | 0.0004 | 0.0007 | 0.0003 | 0.0002 | 0.0002 |
| Toluene | 0.0013 | 0.0033 | 0.0119 | 0.0062 | 0.0073 | 0.0033 | 0.0064 | 0.0090 | 0.0094 | 0.0117 |

**Table 4.5 (c)** Mean gas yields for other electrical cable fires at several irradiation levels and ventilation rates.

| Cable Type | EC-GB 1 | EC-GB 2 | HV1-4C | HV2-3C | AMI-G | AMI-G | AMI-B | Prysmian B | Prysmian B | 6701B-W | 6701B-W | TEC2-W | FLEX1-BG | FLEX2-W |
|---|---|---|---|---|---|---|---|---|---|---|---|---|---|---|
| **Test Condition** | 35 FV | 35 FV | 35 FV | 35 FV | 35 FV | 50 9.4 | 35 FV | 35 FV | 50 9.4 | 35 FV | 50 9.4 | 35 FV | 35 FV | 35 FV |
| **Initial Mass (with Copper) (g)** | 219.33 | 181.05 | 318.83 | 354.71 | 210.08 | 207.62 | 224.60 | 113.50 | 113.68 | 83.45 | 82.31 | 111.00 | 76.52 | 145.58 |
| **Initial Mass (without Copper) (g)** | | | 117.23 | 134.91 | 147.78 | 145.32 | 162.30 | 62.80 | 62.98 | 24.05 | 22.91 | | | |
| **Total Mass Loss (g)** | 40.80 | 39.47 | 57.35 | 62.02 | 66.52 | 84.24 | 20.38 | 11.22 | 62.45 | 17.16 | 16.90 | 25.34 | 41.53 | 54.76 |
| **Total Time (s)** | 1610 | 540 | 3440 | 3630 | 2970 | 1060 | 890 | 640 | 820 | 940 | 760 | 1220 | 890 | 1390 |
| **Mean ER, Φ** | 0.03 | 0.06 | 0.15 | 0.60 | 0.32 | 2.73 | 0.16 | 0.16 | 0.95 | 0.11 | 0.12 | 1.33 | 0.34 | 0.22 |
| **Species** | **Mean Yields (g/g)** | | | | | | | | | | | | | |
| CO | 0.0043 | 0.0283 | 0.0278 | 0.0344 | 0.0171 | 0.0148 | 0.0477 | 0.0583 | 0.0381 | 0.0116 | 0.0073 | 0.0454 | 0.0363 | 0.0561 |
| HCN | 0.0000 | 0.0002 | 0.0006 | 0.0002 | 0.0001 | 0.0002 | 0.0001 | 0.0001 | 0.0002 | 0.0000 | 0.0001 | 0.0008 | 0.0006 | 0.0009 |
| HCl | 0.0005 | 0.0061 | 0.0552 | 0.0450 | 0.0001 | 0.0000 | 0.0002 | 0.0001 | -0.0002 | 0.0001 | 0.0000 | 0.0408 | 0.1482 | 0.0320 |
| HF | 0.0001 | 0.0001 | 0.0000 | 0.0000 | 0.0000 | 0.0000 | 0.0000 | 0.0000 | 0.0000 | 0.0000 | 0.0000 | 0.0000 | 0.0001 | 0.0001 |
| Benzene | 0.0000 | 0.0000 | 0.0101 | 0.0069 | 0.0019 | 0.0055 | 0.0045 | 0.0034 | 0.0040 | 0.0005 | 0.0017 | 0.0174 | 0.0109 | 0.0142 |
| Formaldehyde | 0.0203 | 0.0106 | 0.0043 | 0.0096 | 0.0012 | 0.0002 | 0.0044 | 0.0070 | 0.0019 | 0.0021 | 0.0003 | 0.0026 | 0.0213 | 0.0027 |
| Acrolein | 0.0099 | 0.0125 | 0.0001 | 0.0071 | 0.0019 | 0.0000 | 0.0082 | 0.0026 | 0.0003 | 0.0008 | 0.0001 | 0.0004 | 0.0040 | 0.0102 |
| Acetylene | 0.0013 | 0.0045 | 0.0080 | 0.0066 | 0.0010 | 0.0086 | 0.0003 | 0.0012 | 0.0052 | 0.0002 | 0.0078 | 0.0330 | 0.0205 | 0.0207 |
| $CO_2$ | 0.4400 | 0.6526 | 0.8342 | 0.4580 | 0.6659 | 0.2500 | 0.5063 | 0.6331 | 0.5623 | 0.4093 | 0.1662 | 0.7902 | 0.5115 | 0.8486 |
| THC | 0.2380 | 0.1701 | 0.0724 | 0.1758 | 0.0303 | 0.0437 | 0.1117 | 0.0916 | 0.0460 | 0.0204 | 0.0213 | 0.1337 | 0.3724 | 0.1608 |
| NO | 0.0016 | 0.0002 | 0.0002 | 0.0003 | 0.0007 | 0.0007 | 0.0008 | 0.0011 | 0.0007 | 0.0002 | 0.0003 | 0.0006 | 0.0017 | 0.0040 |
| $NO_2$ | 0.0000 | 0.0000 | 0.0000 | 0.0005 | 0.0001 | 0.0001 | 0.0005 | 0.0005 | 0.0002 | 0.0001 | 0.0001 | 0.0001 | 0.0001 | 0.0000 |
| $SO_2$ | 0.0065 | 0.0020 | 0.0000 | 0.0012 | 0.0012 | 0.0000 | 0.0070 | 0.0013 | 0.0000 | 0.0001 | 0.0000 | 0.0000 | 0.0030 | 0.0000 |
| $NH_3$ | 0.0000 | 0.0000 | 0.0001 | 0.0001 | 0.0000 | 0.0000 | 0.0000 | 0.0000 | 0.0000 | 0.0000 | 0.0000 | 0.0000 | 0.0000 | 0.0006 |
| $NO_x$ | 0.0022 | 0.0002 | 0.0003 | 0.0009 | 0.0011 | 0.0011 | 0.0015 | 0.0020 | 0.0011 | 0.0004 | 0.0004 | 0.0009 | 0.0024 | 0.0055 |
| HBr | 0.0000 | 0.0000 | 0.0000 | 0.0000 | 0.0000 | 0.0000 | 0.0000 | 0.0000 | 0.0000 | 0.0000 | 0.0000 | 0.0000 | 0.0000 | 0.0000 |
| Acetaldehyde | 0.0139 | 0.0108 | 0.0009 | 0.0043 | 0.0002 | 0.0000 | 0.0009 | 0.0022 | 0.0001 | 0.0007 | 0.0002 | 0.0003 | 0.0096 | 0.0096 |
| Toluene | 0.0106 | 0.0161 | 0.0007 | 0.0129 | 0.0019 | 0.0014 | 0.0111 | 0.0060 | 0.0008 | 0.0006 | 0.0005 | 0.0062 | 0.0297 | 0.0070 |

### 4.3.7 Major Gases Contribution for PVC Prysmian A Cable Fires

In determination of fire toxicity of the burned material, aside from toxic gas concentrations, gas yields and total toxicities, contribution of major toxic gases could also be determined. From the plotted major gas contribution graphs, the major toxic species were identified clearly. As in Figure 4.31, the graphs show the major toxic species based on LC50 toxic assessment that produced from the PVC Prysmian A electrical cable fire at 25 kW/m$^2$ under different initial air flowrates (9.4, 18 and 28 L/min (LPM)). PVC type of material would produce HCl as one of the main combustion products. For this PVC electrical cable fire, it proved the same fact. Other than HCl, other species like CO, HCN, Formaldehyde and Acrolein were also the main contributors of fire toxicity. These toxic species especially CO and HCl (asphyxiants) could be the cause of fire death in the similar fire condition.

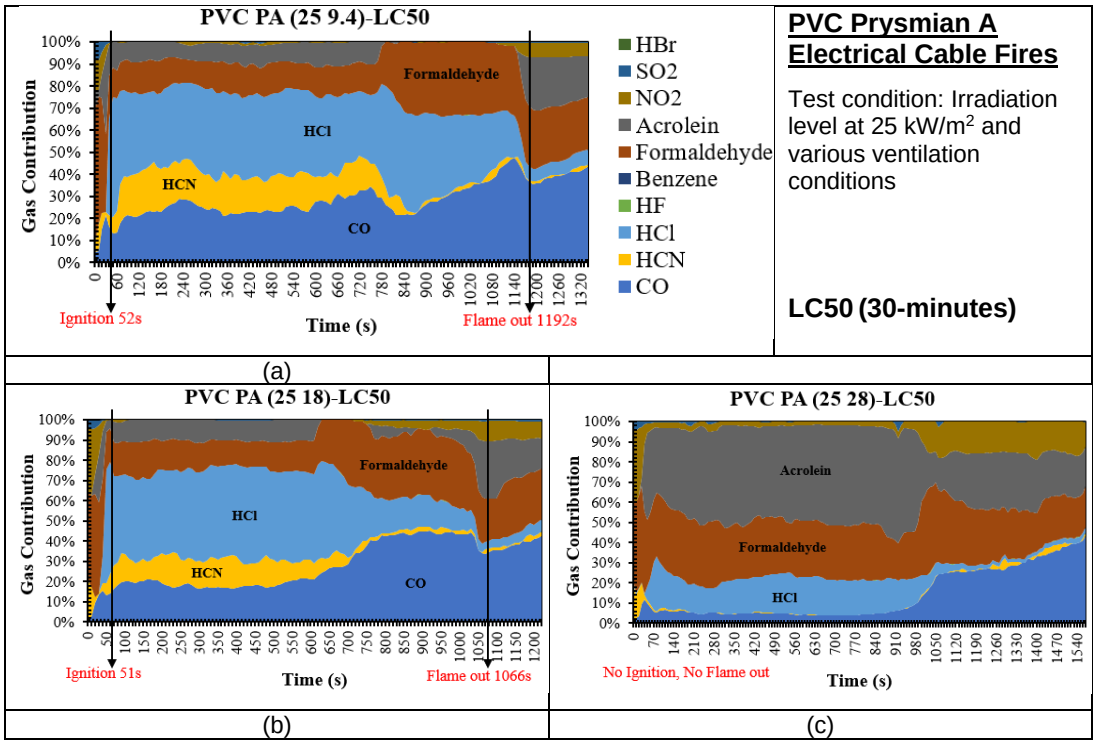


**Figure 4.41** Contribution of major toxic gases (based $LC50_{30min}$) for PVC Prysmian A electrical cable fires at 25 kW/m$^2$ with various air flow rates.

Based on $COSHH_{15min}$, contribution of CO and HCN was not really significant and it was not the main contributor to fire toxicity of the PVC Prysmian A electrical cable fire at the stated fire conditions. From Figure 4.32, it can be

clearly seen that HCl, Formaldehyde, Acrolein and Benzene were the major toxic gases. These species which are irritants can cause impairment of escape to humans who have exposed to them. The contribution of HCl and Benzene had decreased when increasing of initial air flowrate value and the contribution of Formaldehyde and Acrolein had decreased when increasing of the air flowrate. For this PVC cable fire, it look like Formaldehyde ($CH_2O$) and Acrolein ($C_3H_4O$) were produced more as the major toxic species in fuel lean fire condition with more air compared to fuel rich condition with less air.

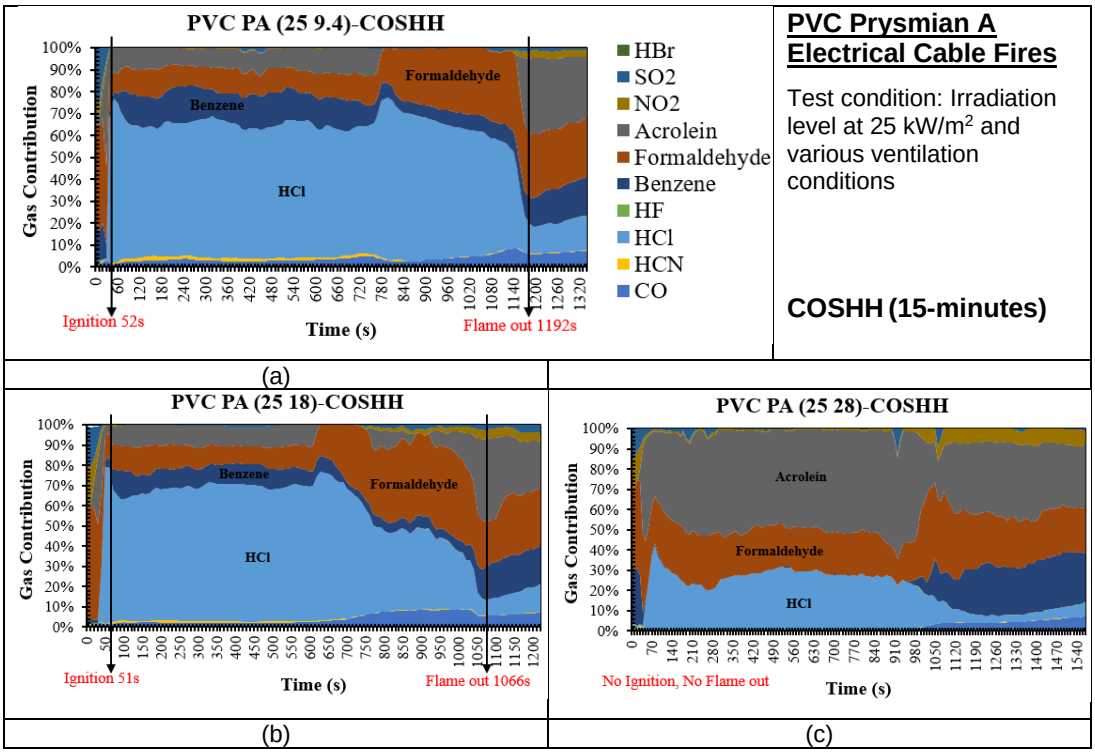


**Figure 4.42** Contribution of major toxic gases (based $COSHH_{15min}$) for PVC Prysmian A electrical cable fires at 25 kW/m$^2$ with various air flow rates.

Figure 4.33 showed the contribution of major toxic gases based on AEGL-2 toxicity assessment against test time for PVC Prysmian A electrical cable fires at 25 kW/m$^2$ with various air flow rates. Compared to $COSHH_{15min}$, AEGL-2 based major gas contributions were same with HCl, Formaldehyde and Acrolein as the main toxic species except only for Benzene. This is because the limit concentration value for Benzene by the AEGL-2 is 2000 ppm, hundred times higher than the limit concentration value for Benzene (3 ppm) by the $COSHH_{15min}$. CO contribution was shown more significant for AEGL-2

based when compared to $COSHH_{15min}$ based toxic assessment. Even the contribution of $SO_2$ could be clearly identified from the graphs.

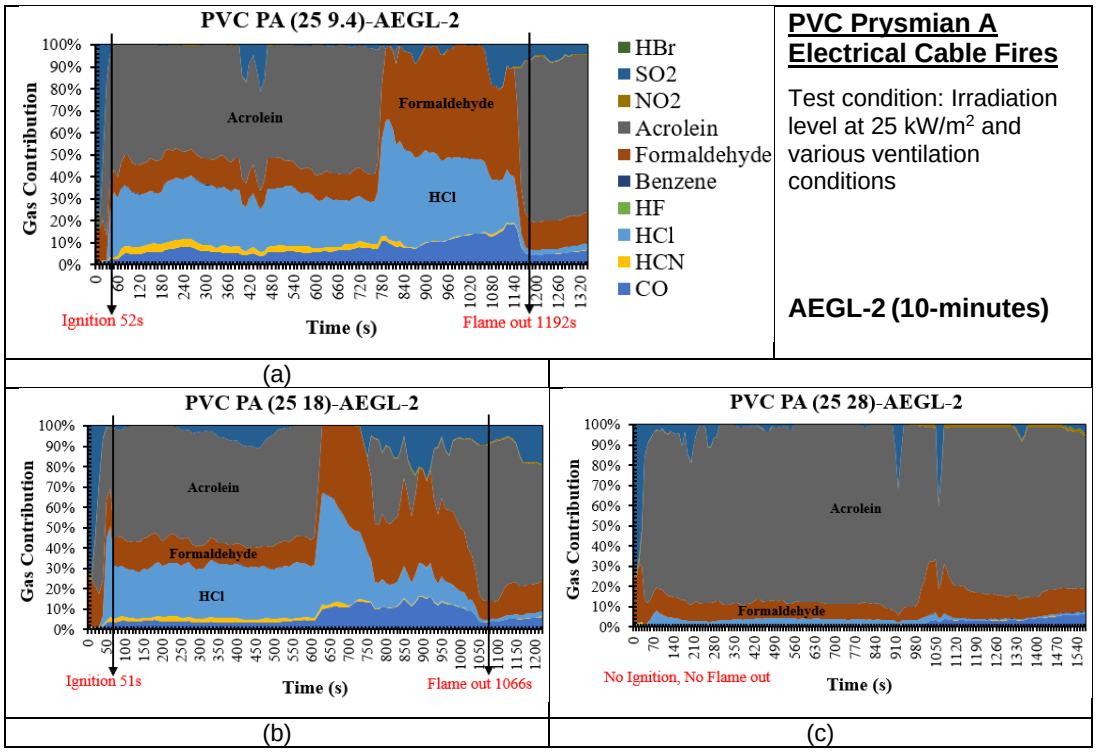


**Figure 4.43** Contribution of major toxic gases (based AEGL-$2_{10min}$) for PVC Prysmian A electrical cable fires at 25 kW/m$^2$ with various air flow rates.

By increasing the irradiation level, it would increase the burning rate of the burned materials. Hence, may also reduce the production of certain toxic gases. In Figure 4.34, for LC50 based major gas contribution, CO contribution was increased for 35 kW/m$^2$ irradiation level fires. Obviously it also could be seen that Acrolein contribution had reduced much for PVC cable fire at 35 kW/m$^2$ compared to PVC cable fire at 25 kW/m$^2$ in comparison at the same air flowrate. From Figure 4.34, with the increasing of the air flowrate, it decreased the CO contribution to fire toxicity. If free ventilation condition test was compared with the restricted ventilation tests for PVC cable fires, CO contribution would be higher for the restricted fires. This could be due to a more complete combustion caused by the free-ventilated fire that had produced less CO.

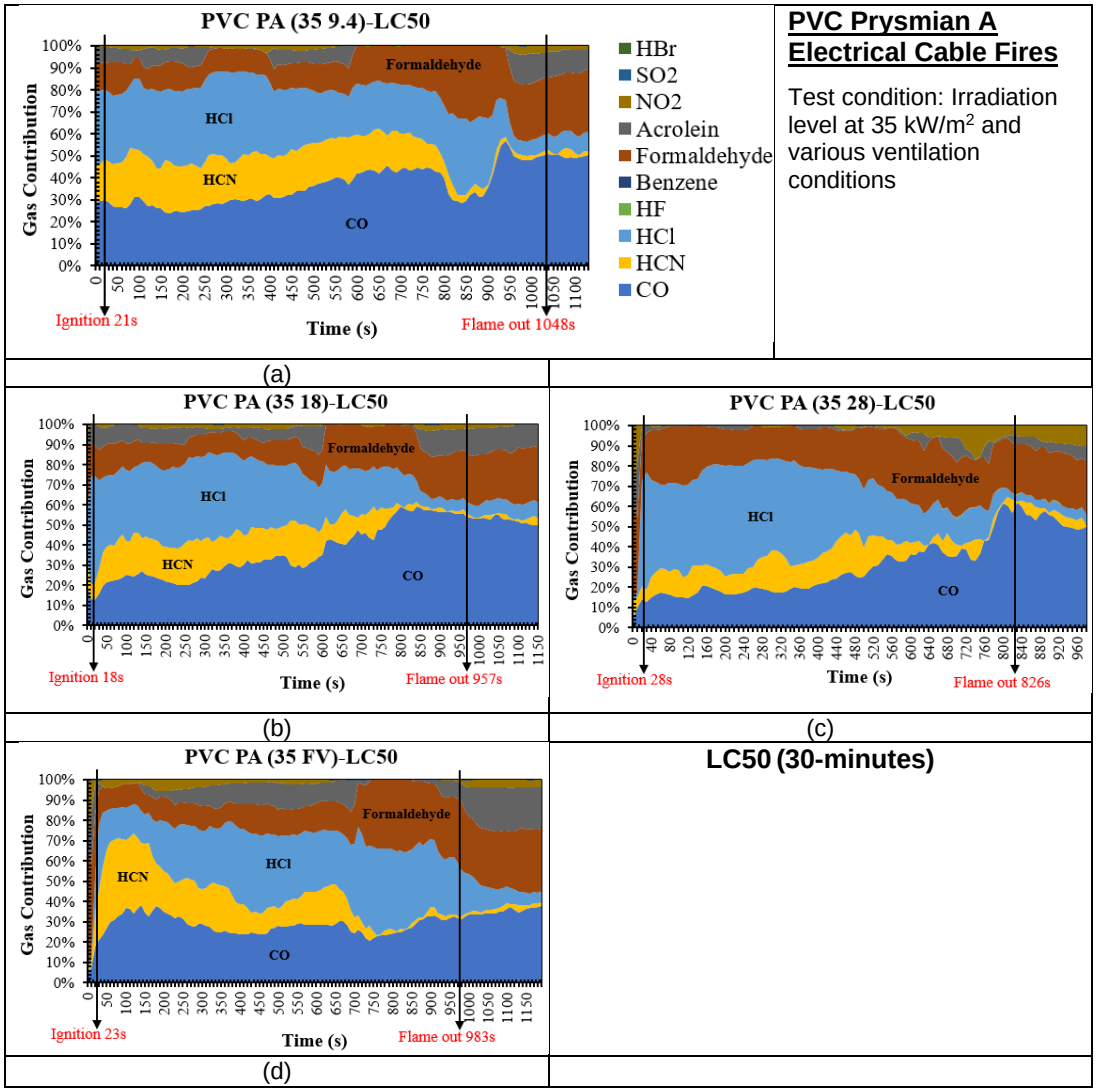


**Figure 4.44** Contribution of major toxic gases (based $LC50_{30min}$) for PVC Prysmian A electrical cable fires at 35 kW/m$^2$ with various air flow rates.

At 35 kW/m$^2$, even the major toxic species based $COSHH_{15min}$ identified were still same but HCl contributions were much more higher compared to its contribution at 25 kW/m$^2$ test condition. From Figure 4.34, contributions of Formaldehyde, Acrolein and Benzene were not differ so much with increasing the ventilation rate, only for HCl the different in pattern could be seen with slightly decreasing in contribution's percentage.

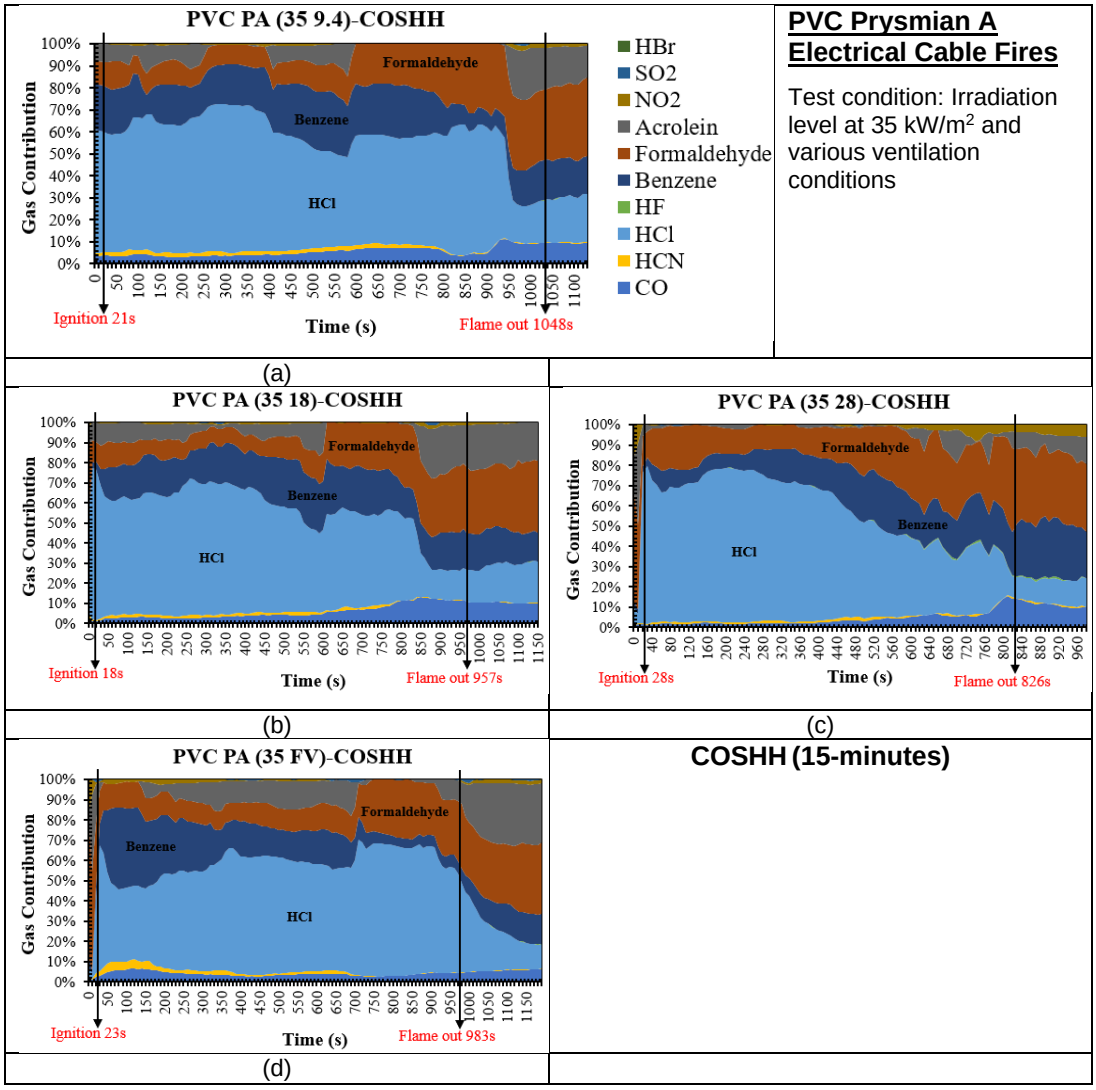


**Figure 4.45** Contribution of major toxic gases (based $COSHH_{15min}$) for PVC Prysmian A electrical cable fires at 35 kW/m$^2$ with various air flow rates.

For AEGL-2 based major gas contribution, Acrolein contribution were high for PVC cable fires at 35 kW/m$^2$ with various air flow rates (9.4, 18 and 28 L/min and free ventilation condition) as shown in Figure 4.36. Formaldehyde contribution also gave a higher percentage for the tests at 35 kW/m$^2$ irradiation level if compared with the tests at 25 kW/m$^2$. Meanwhile HCN contributions were identified decreasing with increasing the irradiation level. HCl maintained as the first major species from these PVC electrical cable fires with those specified test conditions.

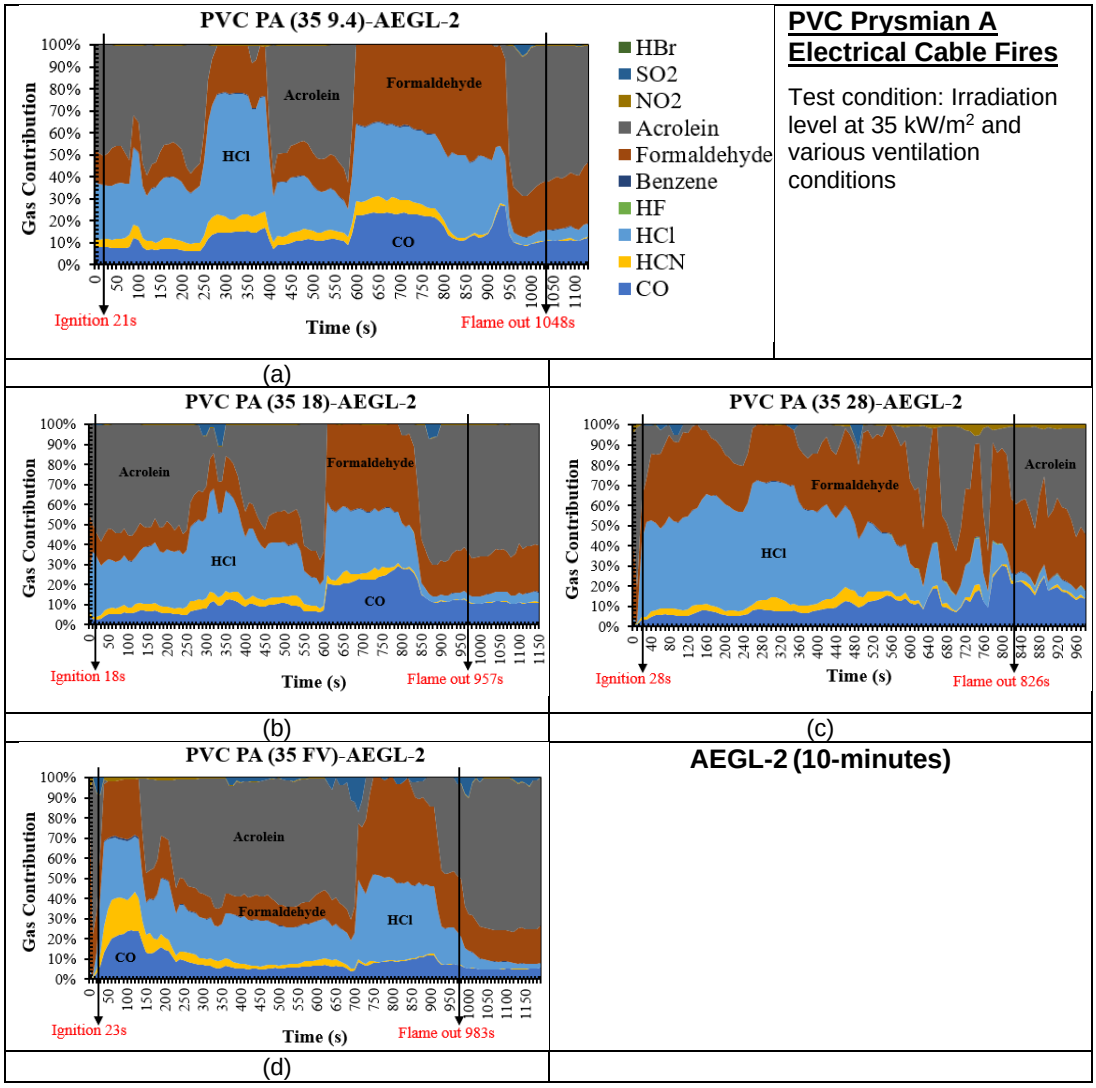


**Figure 4.46** Contribution of major toxic gases (based AEGL-$2_{10min}$) for PVC Prysmian A electrical cable fires at 35 kW/m$^2$ with various air flow rates.

For the PVC cable tests at 50 kW/m$^2$ under three different air flowrates (9.4, 18 and 28 L/min), the first major species that determined based on LC50 toxic assessment was not HCl but CO. It showed in Figure 4.37 that CO contribution's percentage was about 60% in average, was double than the contribution's percentage of HCl. It can be said that the HCl contributions had decreased (from 60% to 30%) with increasing the irradiation level (from 25 kW/m$^2$ to 50 kW/m$^2$). In this case, CO is the major species that would be the first contributor to fire death followed by HCl, Formaldehyde and HCN. In comparison of major gas contribution data for LC50 at 25 kW/m$^2$ and 50 kW/m$^2$ test conditions, lower heat irradiation used to burn the PVC cables would contribute to higher HCl contribution's percentage. The increasing in

heating value would reduce the HCl production and hence would also reduce the HCl contribution's percentage. Unlike CO, it was opposite with the HCl contribution profile, the CO gas contribution profile showed an increase in percentage with the increasing of heat irradiation.

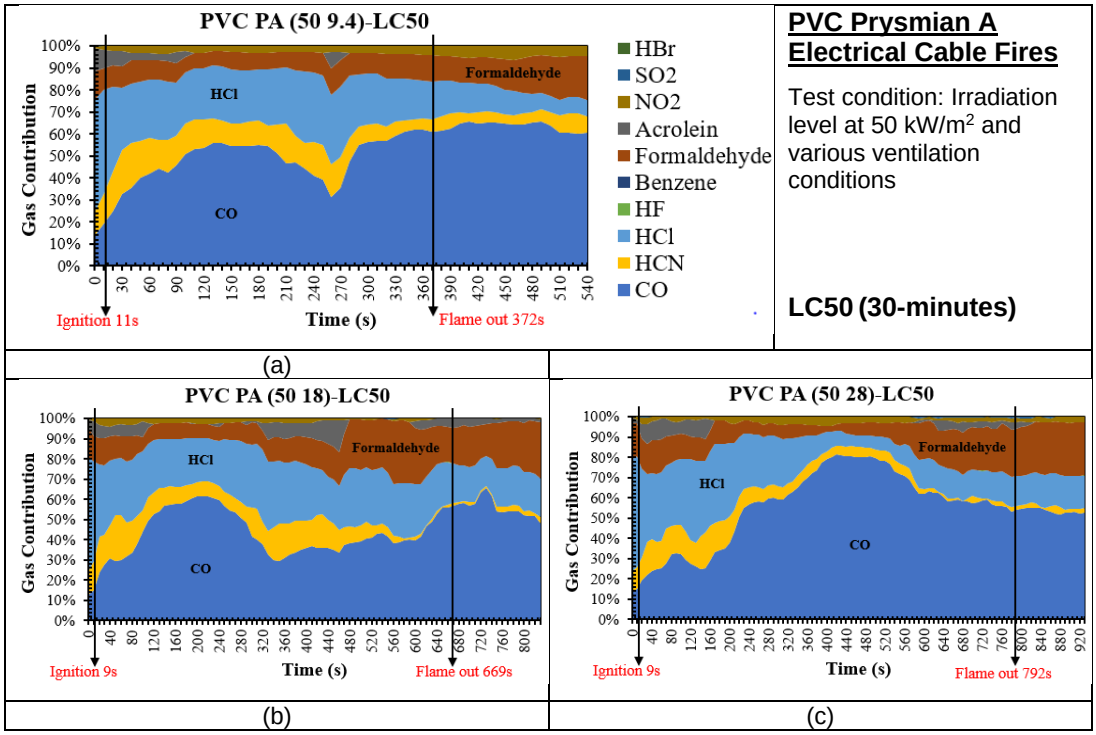


**Figure 4.47** Contribution of major toxic gases (based $LC50_{30min}$) for PVC Prysmian A electrical cable fires at 50 kW/m$^2$ with various air flow rates.

Based on $COSHH_{15min}$ toxic assessment, HCl was the first contributor to fire toxicity followed by Benzene, Formaldehyde, CO and Acrolein as can be seen clearly in Figure 4.38. HCN contribution was small and almost unidentified from the graphs in Figure 4.38. In general, for the PVC Prysmian A electrical cable fires at these test conditions, irritant like HCl would be the first major species that would impair humans from escape.

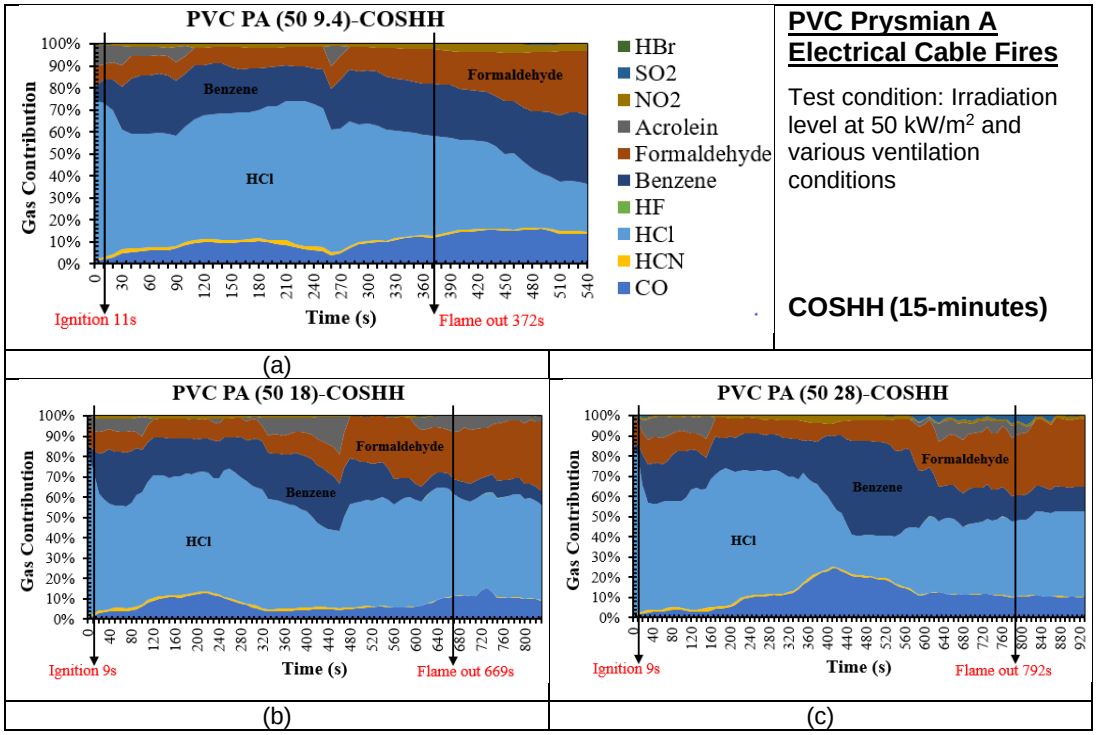


**Figure 4.48** Contribution of major toxic gases (based $COSHH_{15min}$) for PVC Prysmian A electrical cable fires at 50 kW/m$^2$ with various air flow rates.

For PVC Prysmian A electrical cable fires at 50 kW/m$^2$ with various air flow rates, the contribution's percentage for each major gas such as CO, HCl, Formaldehyde and Acrolein were not much different for AEGL-2 based fire toxic assessment. In Figure 4.39, it was clearly identified that CO percentage had increased with the increasing of air flowrate, meanwhile Formaldehyde percentage had decreased with the increasing of air flowrate. As can be seen in Figure 4.39, Acrolein pattern was not certain but still a major species in this case for all three ventilation rates. HCN contribution was the least significant compared to CO, HCl, Formaldehyde and Acrolein contributions at high irradiation heat of test conditions. The following Table 4.6 shows the summary of the six major species for PVC Prysmian A electrical cable fires.

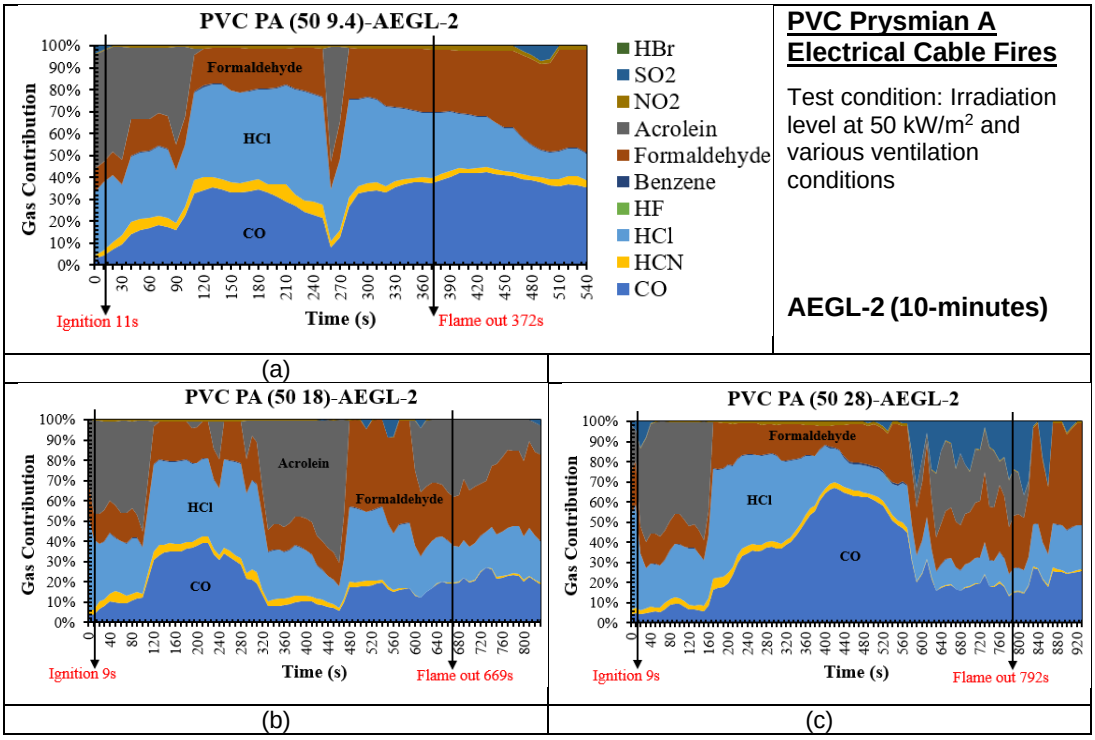


**Figure 4.49** Contribution of major toxic gases (based AEGL-$2_{10min}$) for PVC Prysmian A electrical cable fires at 50 kW/m$^2$ with various air flow rates.

**Table 4.6** First six major species for PVC Prysmian A electrical cable fires.

| PVC PRYSMIAN A ELECTRICAL CABLE FIRES | | | | | | | | | | | | |
|---|---|---|---|---|---|---|---|---|---|---|---|---|
| **Test** | **Test Details** | **Mean ER, Φ (Chan)** | **Time (s)** | **Fire Stage** | | **Major Species** | | | | | | |
| | | | | | | **1** | **2** | **3** | **4** | **5** | **6** |
| 1 | 25 9.4 | 1.1 | <52 | Ignition | **LC50** | Formaldehyde | HCl | Acrolein | CO | HCN | $NO_2$ |
| | I = 52 s | 1.6 | 52 - 800 | SS Flaming | | HCl | CO | HCN | Formaldehyde | Acrolein | $NO_2$ |
| | F = 1192 s | 0.8 | 800 - 1192 | Flaming | | HCl | CO | Formaldehyde | HCN | Acrolein | $NO_2$ |
| | | 0.5 | >1192 | Post-flaming | | CO | Formaldehyde | Acrolein | HCl | $NO_2$ | HCN |
| | | 1.1 | <52 | Ignition | **COSHH** | Formaldehyde | HCl | Acrolein | $SO_2$ | Benzene | CO |
| | | 1.6 | 52 - 800 | SS Flaming | | HCl | Benzene | Acrolein | Formaldehyde | CO | HCN |
| | | 0.8 | 800 - 1192 | Flaming | | HCl | Formaldehyde | Benzene | CO | Acrolein | HCN |
| | | 0.5 | >1192 | Post-flaming | | Acrolein | Formaldehyde | HCl | Benzene | CO | $NO_2$ |
| | | 1.1 | <52 | Ignition | **AEGL-2** | Acrolein | $SO_2$ | Formaldehyde | HCl | CO | HCN |
| | | 1.6 | 52 - 800 | SS Flaming | | Acrolein | HCl | Formaldehyde | CO | HCN | $SO_2$ |
| | | 0.8 | 800 - 1192 | Flaming | | Formaldehyde | HCl | CO | $SO_2$ | Acrolein | HCN |
| | | 0.5 | >1192 | Post-flaming | | Acrolein | Formaldehyde | $SO_2$ | CO | HCl | HCN |
| 2 | 25 18 | 0.9 | <51 | Ignition | **LC50** | Formaldehyde | HCl | Acrolein | $NO_2$ | CO | HCN |
| | I = 51 s | 1.2 | 51 - 620 | SS Flaming | | HCl | CO | Formaldehyde | HCN | Acrolein | $NO_2$ |
| | F = 1066 s | 0.7 | 620 - 1066 | Flaming | | CO | Formaldehyde | HCl | Acrolein | HCN | $NO_2$ |
| | | 0.4 | >1066 | Post-flaming | | CO | Formaldehyde | Acrolein | $NO_2$ | HCl | HCN |
| | | 0.9 | <51 | Ignition | **COSHH** | Formaldehyde | HCl | Acrolein | $SO_2$ | $NO_2$ | CO |
| | | 1.2 | 51 - 620 | SS Flaming | | HCl | Benzene | Formaldehyde | Acrolein | CO | HCN |
| | | 0.7 | 620 - 1066 | Flaming | | HCl | Formaldehyde | Acrolein | Benzene | CO | $NO_2$ |
| | | 0.4 | >1066 | Post-flaming | | Acrolein | Formaldehyde | Benzene | HCl | CO | $NO_2$ |

| | | | | | | | | | | | |
|---|---|---|---|---|---|---|---|---|---|---|---|
| | | 0.9 | <51 | Ignition | **AEGL-2** | Acrolein | $SO_2$ | Formaldehyde | HCl | CO | HCN |
| | | 1.2 | 51 - 620 | SS Flaming | | Acrolein | HCl | Formaldehyde | $SO_2$ | CO | HCN |
| | | 0.7 | 620 - 1066 | Flaming | | Formaldehyde | Acrolein | HCl | CO | $SO_2$ | HCN |
| | | 0.4 | >1066 | Post-flaming | | Acrolein | Formaldehyde | $SO_2$ | CO | HCl | $NO_2$ |
| 3 | 25 28 | 0.1 | <30 | - | **LC50** | Formaldehyde | $NO_2$ | HCN | CO | $SO_2$ | HCl |
| | I = No | 0.3 | 30 - 930 | SS | | Acrolein | Formaldehyde | HCl | CO | $NO_2$ | HCN |
| | F = No | 0.3 | >930 | Post-SS | | Acrolein | Formaldehyde | CO | $NO_2$ | HCl | HCN |
| | | 0.1 | <30 | - | **COSHH** | Formaldehyde | Benzene | Acrolein | $SO_2$ | $NO_2$ | HCl |
| | | 0.3 | 30 - 930 | SS | | Acrolein | HCl | Formaldehyde | $SO_2$ | $NO_2$ | Benzene |
| | | 0.3 | >930 | Post-SS | | Acrolein | Formaldehyde | Benzene | $NO_2$ | HCl | CO |
| | | 0.1 | <30 | - | **AEGL-2** | SO2 | Formaldehyde | Acrolein | HCN | HCl | - |
| | | 0.3 | 30 - 930 | SS | | Acrolein | Formaldehyde | HCl | $SO_2$ | - | - |
| | | 0.3 | >930 | Post-SS | | Acrolein | Formaldehyde | CO | $NO_2$ | $SO_2$ | HCl |
| 4 | 35 9.4 | 0.8 | <21 | Ignition | **LC50** | HCl | CO | HCN | Formaldehyde | Acrolein | $NO_2$ |
| | I = 21 s | 1.8 | 21 - 580 | SS Flaming | | HCl | CO | HCN | Formaldehyde | Acrolein | $NO_2$ |
| | F = 1048 s | 0.9 | 580 - 1048 | Flaming | | CO | HCl | Formaldehyde | HCN | Acrolein | $NO_2$ |
| | | 0.3 | >1048 | Post-flaming | | CO | Formaldehyde | Acrolein | HCl | HCN | $NO_2$ |
| | | 0.8 | <21 | Ignition | **COSHH** | HCl | Benzene | Formaldehyde | Acrolein | CO | HCN |
| | | 1.8 | 21 - 580 | SS Flaming | | HCl | Benzene | Formaldehyde | Acrolein | CO | HCN |
| | | 0.9 | 580 - 1048 | Flaming | | HCl | Formaldehyde | Benzene | CO | Acrolein | HCN |
| | | 0.3 | >1048 | Post-flaming | | Formaldehyde | HCl | Acrolein | Benzene | CO | $NO_2$ |
| | | 0.8 | <21 | Ignition | **AEGL-2** | Acrolein | HCl | Formaldehyde | CO | HCN | - |
| | | 1.8 | 21 - 580 | SS Flaming | | Acrolein | HCl | Formaldehyde | CO | HCN | $NO_2$ |
| | | 0.9 | 580 - 1048 | Flaming | | Formaldehyde | HCl | CO | Acrolein | HCN | $NO_2$ |
| | | 0.3 | >1048 | Post-flaming | | Acrolein | Formaldehyde | CO | HCl | HCN | $NO_2$ |

| | | | | | | | | | | | |
|---|---|---|---|---|---|---|---|---|---|---|---|
| 5 | 35 18 | 0.5 | <18 | Ignition | **LC50** | HCl | Formaldehyde | CO | Acrolein | HCN | $NO_2$ |
| | I = 18 s | 2.0 | 18 - 580 | SS Flaming | | HCl | CO | HCN | Formaldehyde | Acrolein | $NO_2$ |
| | F = 957 s | 0.7 | 580 - 957 | Flaming | | CO | Formaldehyde | HCl | HCN | Acrolein | $NO_2$ |
| | | 0.3 | >957 | Post-flaming | | CO | Formaldehyde | Acrolein | HCl | HCN | $NO_2$ |
| | | 0.5 | <18 | Ignition | **COSHH** | HCl | Formaldehyde | Acrolein | CO | HCN | Benzene |
| | | 2.0 | 18 - 580 | SS Flaming | | HCl | Benzene | Formaldehyde | Acrolein | CO | HCN |
| | | 0.7 | 580 - 957 | Flaming | | HCl | Formaldehyde | Benzene | CO | Acrolein | HCN |
| | | 0.3 | >957 | Post-flaming | | Formaldehyde | Acrolein | HCl | Benzene | CO | $NO_2$ |
| | | 0.5 | <18 | Ignition | **AEGL-2** | Acrolein | HCl | Formaldehyde | CO | HCN | - |
| | | 2.0 | 18 - 580 | SS Flaming | | Acrolein | HCl | Formaldehyde | CO | HCN | $SO_2$ |
| | | 0.7 | 580 - 957 | Flaming | | Formaldehyde | HCl | CO | Acrolein | HCN | $SO_2$ |
| | | 0.3 | >957 | Post-flaming | | Acrolein | Formaldehyde | CO | HCl | HCN | $NO_2$ |
| 6 | 35 28 | 0.3 | <28 | Ignition | **LC50** | Formaldehyde | HCl | Acrolein | $NO_2$ | CO | HCN |
| | I = 28 s | 0.6 | 28 - 500 | SS Flaming | | HCl | Formaldehyde | CO | HCN | Acrolein | $NO_2$ |
| | F = 826 s | 0.2 | 500 - 826 | Flaming | | CO | Formaldehyde | HCN | HCN | $NO_2$ | Acrolein |
| | | 0.1 | >826 | Post-flaming | | CO | Formaldehyde | $NO_2$ | Acrolein | HCl | HCN |
| | | 0.3 | <28 | Ignition | **COSHH** | HCl | Formaldehyde | Acrolein | $NO_2$ | CO | HCN |
| | | 0.6 | 28 - 500 | SS Flaming | | HCl | Formaldehyde | Benzene | CO | Acrolein | HCN |
| | | 0.2 | 500 - 826 | Flaming | | HCl | Formaldehyde | Benzene | CO | Acrolein | $NO_2$ |
| | | 0.1 | >826 | Post-flaming | | Formaldehyde | Benzene | HCl | CO | Acrolein | $NO_2$ |
| | | 0.3 | <28 | Ignition | **AEGL-2** | Acrolein | Formaldehyde | HCl | $NO_2$ | HCN | CO |
| | | 0.6 | 28 - 500 | SS Flaming | | HCl | Formaldehyde | Acrolein | CO | HCN | $SO_2$ |
| | | 0.2 | 500 - 826 | Flaming | | Formaldehyde | HCl | Acrolein | CO | HCN | $NO_2$ |
| | | 0.1 | >826 | Post-flaming | | Acrolein | Formaldehyde | CO | HCl | $NO_2$ | HCN |

| | | | | | | | | | | | | |
|---|---|---|---|---|---|---|---|---|---|---|---|---|
| 7 | 35 FV | 0.9 | <23 | Ignition | **LC50** | Formaldehyde | Acrolein | HCl | $NO_2$ | HCN | CO |
| | I = 23 s | 1.4 | 23 - 700 | SS Flaming | | CO | HCl | HCN | Formaldehyde | Acrolein | $NO_2$ |
| | F = 983 s | 0.5 | 700 - 983 | Flaming | | HCl | Formaldehyde | CO | Acrolein | HCN | $NO_2$ |
| | | 0.2 | >983 | Post-flaming | | CO | Formaldehyde | Acrolein | HCl | $NO_2$ | HCN |
| | | 0.9 | <23 | Ignition | **COSHH** | Formaldehyde | Acrolein | HCl | $NO_2$ | HCN | CO |
| | | 1.4 | 23 - 700 | SS Flaming | | HCl | Benzene | Formaldehyde | Acrolein | CO | HCN |
| | | 0.5 | 700 - 983 | Flaming | | HCl | Formaldehyde | Benzene | Acrolein | CO | HCN |
| | | 0.2 | >983 | Post-flaming | | Formaldehyde | HCl | Acrolein | Benzene | CO | $NO_2$ |
| | | 0.9 | <23 | Ignition | **AEGL-2** | Formaldehyde | Acrolein | HCl | $NO_2$ | HCN | CO |
| | | 1.4 | 23 - 700 | SS Flaming | | CO | HCl | HCN | Formaldehyde | Acrolein | $NO_2$ |
| | | 0.5 | 700 - 983 | Flaming | | HCl | Formaldehyde | CO | Acrolein | HCN | $NO_2$ |
| | | 0.2 | >983 | Post-flaming | | CO | Formaldehyde | Acrolein | HCl | $NO_2$ | HCN |
| 8 | 50 9.4 | 0.5 | <11 | Ignition | **LC50** | HCl | CO | HCN | Formaldehyde | Acrolein | $NO_2$ |
| | I = 11 s | 1.8 | 11 - 260 | SS Flaming | | CO | HCl | HCN | Formaldehyde | $NO_2$ | Acrolein |
| | F = 372 s | 1.5 | 260 - 372 | Flaming | | CO | HCl | Formaldehyde | HCN | $NO_2$ | Acrolein |
| | | 1.3 | >372 | Post-flaming | | CO | Formaldehyde | HCl | HCN | $NO_2$ | - |
| | | 0.5 | <11 | Ignition | **COSHH** | HCl | Benzene | Formaldehyde | Acrolein | CO | HCN |
| | | 1.8 | 11 - 260 | SS Flaming | | HCl | Benzene | Formaldehyde | CO | Acrolein | $NO_2$ |
| | | 1.5 | 260 - 372 | Flaming | | HCl | Benzene | Formaldehyde | CO | $NO_2$ | HCN |
| | | 1.3 | >372 | Post-flaming | | HCl | Benzene | Formaldehyde | CO | $NO_2$ | HCN |
| | | 0.5 | <11 | Ignition | **AEGL-2** | Acrolein | HCl | Formaldehyde | CO | HCN | $SO_2$ |
| | | 1.8 | 11 - 260 | SS Flaming | | HCl | CO | Acrolein | Formaldehyde | HCN | $NO_2$ |
| | | 1.5 | 260 - 372 | Flaming | | HCl | CO | Formaldehyde | Acrolein | HCN | $NO_2$ |
| | | 1.3 | >372 | Post-flaming | | CO | Formaldehyde | HCl | HCN | $NO_2$ | $SO_2$ |

| | | | | | | | | | | | |
|---|---|---|---|---|---|---|---|---|---|---|---|
| 9 | 50 18 | 0.4 | <9 | Ignition | **LC50** | HCl | Formaldehyde | CO | HCN | Acrolein | $NO_2$ |
| | I = 9 s | 2.0 | 9 - 460 | SS Flaming | | CO | HCl | Formaldehyde | HCN | Acrolein | $NO_2$ |
| | F = 669 s | 0.8 | 460 - 669 | Flaming | | CO | HCl | Formaldehyde | HCN | Acrolein | $NO_2$ |
| | | 0.3 | >669 | Post-flaming | | CO | Formaldehyde | HCl | Acrolein | HCN | - |
| | | 0.4 | <9 | Ignition | **COSHH** | HCl | Formaldehyde | Benzene | Acrolein | CO | HCN |
| | | 2.0 | 9 - 460 | SS Flaming | | HCl | Benzene | Formaldehyde | CO | Acrolein | HCN |
| | | 0.8 | 460 - 669 | Flaming | | HCl | Formaldehyde | Benzene | CO | Acrolein | HCN |
| | | 0.3 | >669 | Post-flaming | | HCl | Formaldehyde | Benzene | CO | Acrolein | HCN |
| | | 0.4 | <9 | Ignition | **AEGL-2** | HCl | Acrolein | Formaldehyde | CO | HCN | $NO_2$ |
| | | 2.0 | 9 - 460 | SS Flaming | | HCl | Acrolein | CO | Formaldehyde | HCN | $NO_2$ |
| | | 0.8 | 460 - 669 | Flaming | | Formaldehyde | HCl | CO | Acrolein | HCN | $SO_2$ |
| | | 0.3 | >669 | Post-flaming | | Formaldehyde | Acrolein | CO | HCl | HCN | $SO_2$ |
| 10 | 50 28 | 0.5 | <9 | Ignition | **LC50** | HCl | Formaldehyde | CO | HCN | Acrolein | $NO_2$ |
| | I = 9 s | 2.5 | 9 - 600 | SS Flaming | | CO | HCl | Formaldehyde | HCN | $NO_2$ | Acrolein |
| | F = 792 s | 0.7 | 600 - 792 | Flaming | | CO | Formaldehyde | HCl | Acrolein | HCN | $NO_2$ |
| | | 0.3 | >792 | Post-flaming | | CO | Formaldehyde | HCl | HCN | $NO_2$ | Acrolein |
| | | 0.5 | <9 | Ignition | **COSHH** | HCl | Formaldehyde | Benzene | Acrolein | CO | HCN |
| | | 2.5 | 9 - 600 | SS Flaming | | HCl | Benzene | CO | Formaldehyde | Acrolein | $NO_2$ |
| | | 0.7 | 600 - 792 | Flaming | | HCl | Formaldehyde | Benzene | CO | Acrolein | $SO_2$ |
| | | 0.3 | >792 | Post-flaming | | HCl | Formaldehyde | Benzene | CO | $SO_2$ | Acrolein |
| | | 0.5 | <9 | Ignition | **AEGL-2** | HCl | Formaldehyde | Acrolein | $SO_2$ | CO | HCN |
| | | 2.5 | 9 - 600 | SS Flaming | | CO | HCl | Formaldehyde | Acrolein | HCN | $NO_2$ |
| | | 0.7 | 600 - 792 | Flaming | | Acrolein | Formaldehyde | $SO_2$ | CO | HCl | HCN |
| | | 0.3 | >792 | Post-flaming | | Formaldehyde | CO | HCl | $SO_2$ | Acrolein | HCN |

### 4.3.8 Major Gases Contribution for Other Electrical Cable Fires

Other than PVC Prysmian A electrical cable, other PVC electrical cables such as PVC EC-GB 1 and PVC EC-GB 2 were also tested in the Cone Calorimeter fire tests. Unexpectedly, these two PVC cables gave different results in the contribution of major species, not similar with the PVC Prysmian A electrical cable fires. HCl contribution was not high for these two PVC cables especially for PVC EC-GB 1. Figure 4.40 showed major gases contribution (based LC50, $COSHH_{15min}$ and AEGL-2) for PVC EC-GB 1 and PVC EC-GB 2 electrical cable fires at 35 kW/m2 under free ventilation test condition. For PVC EC-GB 1 cable fire, based on LC50 assessment, Acrolein (50%) and Formaldehyde (40%) were the main major species giving a high contribution's percentage. According to $COSHH_{15min}$, Formaldehyde contribution (35%) had slightly decreased compared to LC50 based assessment with another two major species like Acrolein and $SO_2$ had contributed to 50% and 10% each. From AEGL-2 toxic assessment, Acrolein contribution's percentage was the highest which was about 70%, followed by 20% $SO_2$ and 10% Formaldehyde. HCl contribution was insignificant for this PVC EC-GB 1 electrical cable fire.

For PVC EC-GB 2 electrical cable fire, Acrolein was also the first major toxic species like the PVC EC-GB 1 electrical cable fire, followed by Formaldehyde and $SO_2$. In comparison with PVC EC-GB 1 cable fire, the PVC EC-GB 2 fire gave a higher contribution's percentage of Acrolein and a slightly lower in Formaldehyde contribution's percentage. HCl contribution was also identified for LC50 and $COSHH_{15min}$ assessments even only in small percentage. CO contribution was only identified for LC50 based assessment method for PVC EC-GB 2 cable fire with less than 10% of contribution only. In overall, it could be expected that for these types of PVC cable fires, the two main toxic species were Acrolein and Formaldehyde. For future fire toxicity tests under the similar test conditions, other significant species that can be expected will be produced from PVC electrical cable fires are CO, HCl, HCN and also Benzene.

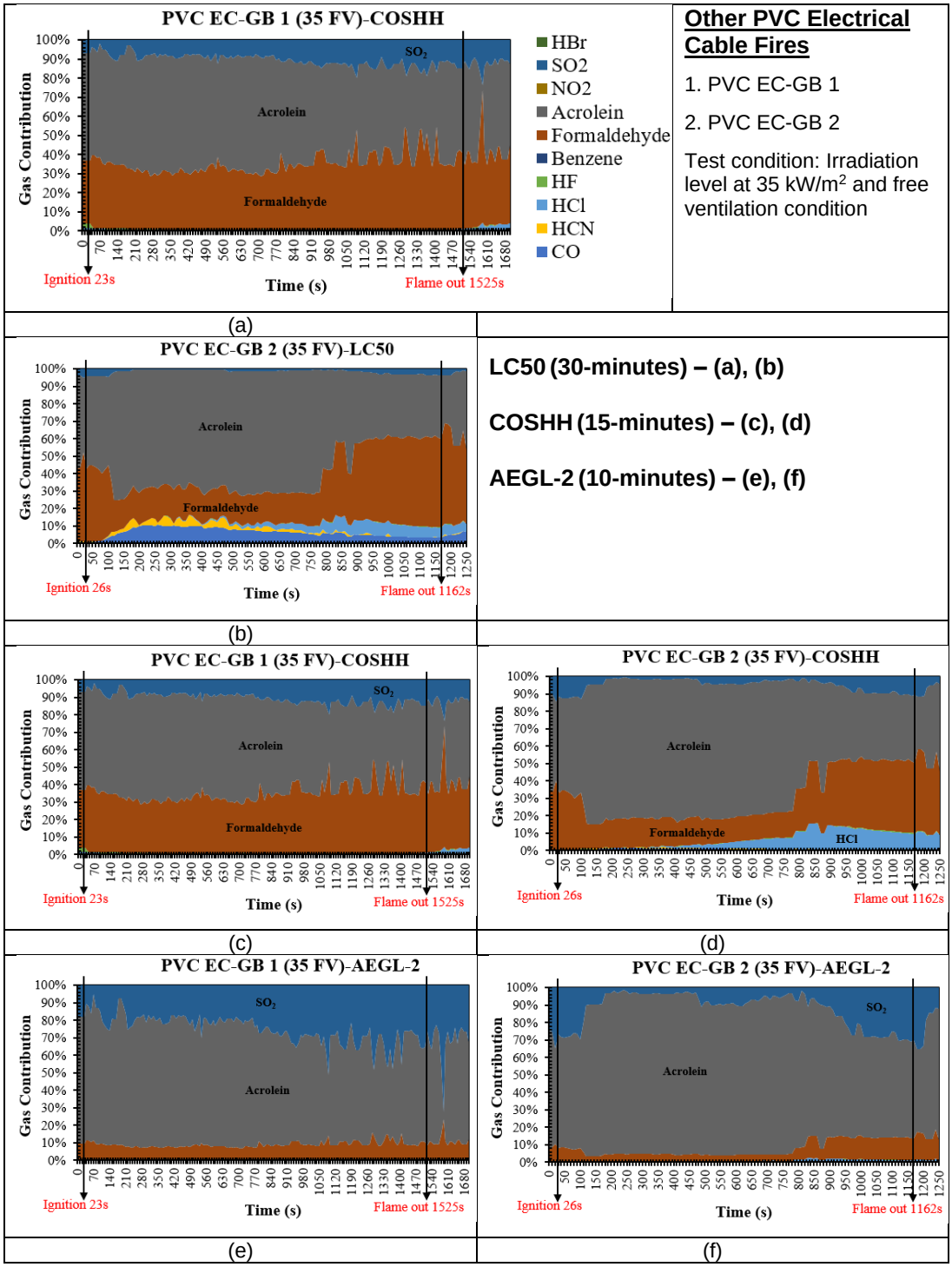


**Figure 4.50** Major gases contribution (based $LC50_{30min}$, $COSHH1_{5min}$ and $AEGL\text{-}2_{10min}$) for other PVC electrical cable fires at 35 kW/m$^2$ and free ventilation.

Solar Energy cables such as HV1-4C and HV2-3C were grouped in the non-PVC cable group based on the information stated on their physical bodies. They were not clearly described as PVC type of cables. As shown in Figure

4.41 for test conditions at 35 kW/m$^2$ and free ventilation, HCl contribution's percentage for those two cable fires are high for non-PVC materials and obviously they were actually PVC type of cables. As previously indicated by PVC Prysmian A, PVC EC-GB 1 and PVC EC-GB 2 electrical cable fires, HV1-4C and HV2-3C cable fires had the same major toxic species indicated which were CO, HCl, Formaldehyde, Acrolein, HCN and Benzene. HCl contribution for HV1-4C cable fire was higher than HV2-3C cable fire for all three ($LC50_{30min}$, $COSHH_{15min}$ and $AEGL\text{-}2_{10min}$) toxic assessments. Same happened to the Formaldehyde contribution's profile when comparing both Solar Energy cables with HV2-3C cable fire showed a lower percentage contribution than the HV1-4C cable fire. Unlike Acrolein contribution, HV1-4C cable fire indicated a much lower percentage compared to HV2-3C cable fire. CO, HCN and Benzene profiles were almost similar for both Solar Energy cable fires. In overall, HCl and Formaldehyde were the main toxic species for HV1-4C cable fire and Acrolein was the first main toxic species for HV2-3C cable fire.

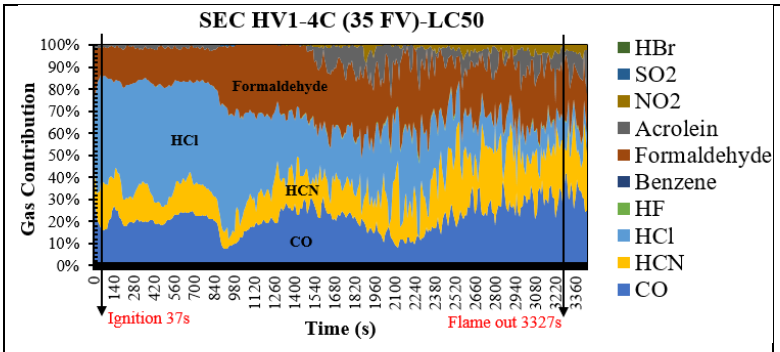


(a)

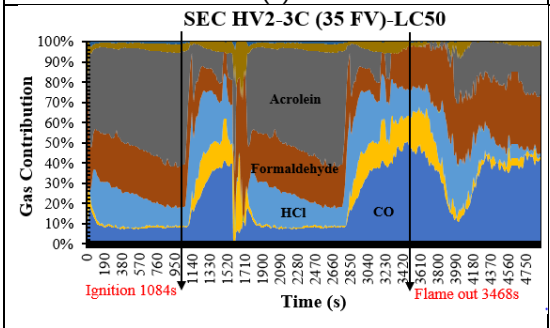


(b)

**Solar Energy Cable Fires**

1. SEC HV1-4C
2. SEC HV2-3C

Test condition: Irradiation level at 35 kW/m$^2$ and free ventilation condition

**LC50 (30-minutes) – (a), (b)**

**COSHH (15-minutes) – (c), (d)**

**AEGL-2 (10-minutes) – (e), (f)**

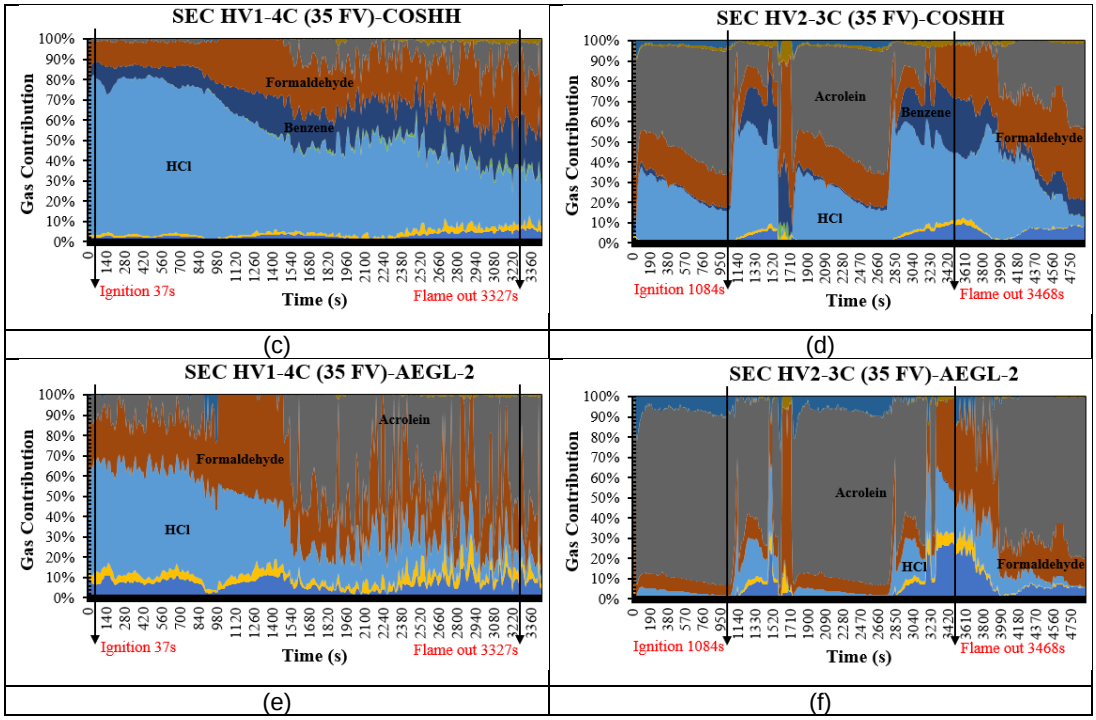


**Figure 4.51** Major gases contribution (based $LC50_{30min}$, $COSHH1_{5min}$ and $AEGL\text{-}2_{10min}$) for Solar Energy cable fires at 35 kW/m$^2$ and free ventilation.

Wind Turbine cables such as AMI-G and AMI-B were classified and grouped under Low Smoke Zero Halogens (LSZH) cable group as described clearly in the cable specification's information. According to LC50 toxic assessment in Figure 4.42, CO was the highest percentage's contributor for AMI-G cable fire meanwhile, Acrolein was the highest percentage's contributor for AMI-B cable fire. HCN contribution were very high for both AMI-G and AMI-B cable fires. These Wind Turbine cables possibly were nitrogen contained cables. Even $NO_2$ which was one of common main products for nitrogen based material fires, was one of the major toxic species for these Wind Turbine cable fires as clearly illustrated in Figure 4.42. From comparison between two different test conditions (35 kW/m$^2$ with free ventilation and 50 kW/m$^2$ with restricted ventilation) for AMI-G cable fires, CO and Formaldehyde contributions were lower under 50 kW/m$^2$ with restricted ventilation condition than under 35 kW/m$^2$ with free ventilation.

From major gas contribution graphs based on $COSHH_{15min}$ in Figure 4.42 with considering the AMI-G and AMI-B fire tests at 35 kW/m$^2$ and free ventilation, the first two main species for AMI-G cable fire were Benzene and Formaldehyde and the first two main species for AMI-B cable fire were

Acrolein and Formaldehyde. Benzene contribution was much higher for AMI-G cable fire under 50 kW/m$^2$ with restricted ventilation condition compared to AMI-G cable fire under 35 kW/m$^2$ with free ventilation.

Based on AEGL-2 assessment, under the same test conditions of 35 kW/m$^2$ and free ventilation, combination of Acrolein and Formaldehyde total percentage's contribution for both cable fires were almost same, about 80%. Other major species like $SO_2$ had also contributed to the percentage for AMI-B cable fire. CO which is the common product of incomplete combustion under restricted ventilation test. Its contribution as the major species for AMI-G cable fire with 50 kW/m$^2$ irradiation heat and under restricted ventilation condition showed a good agreement.

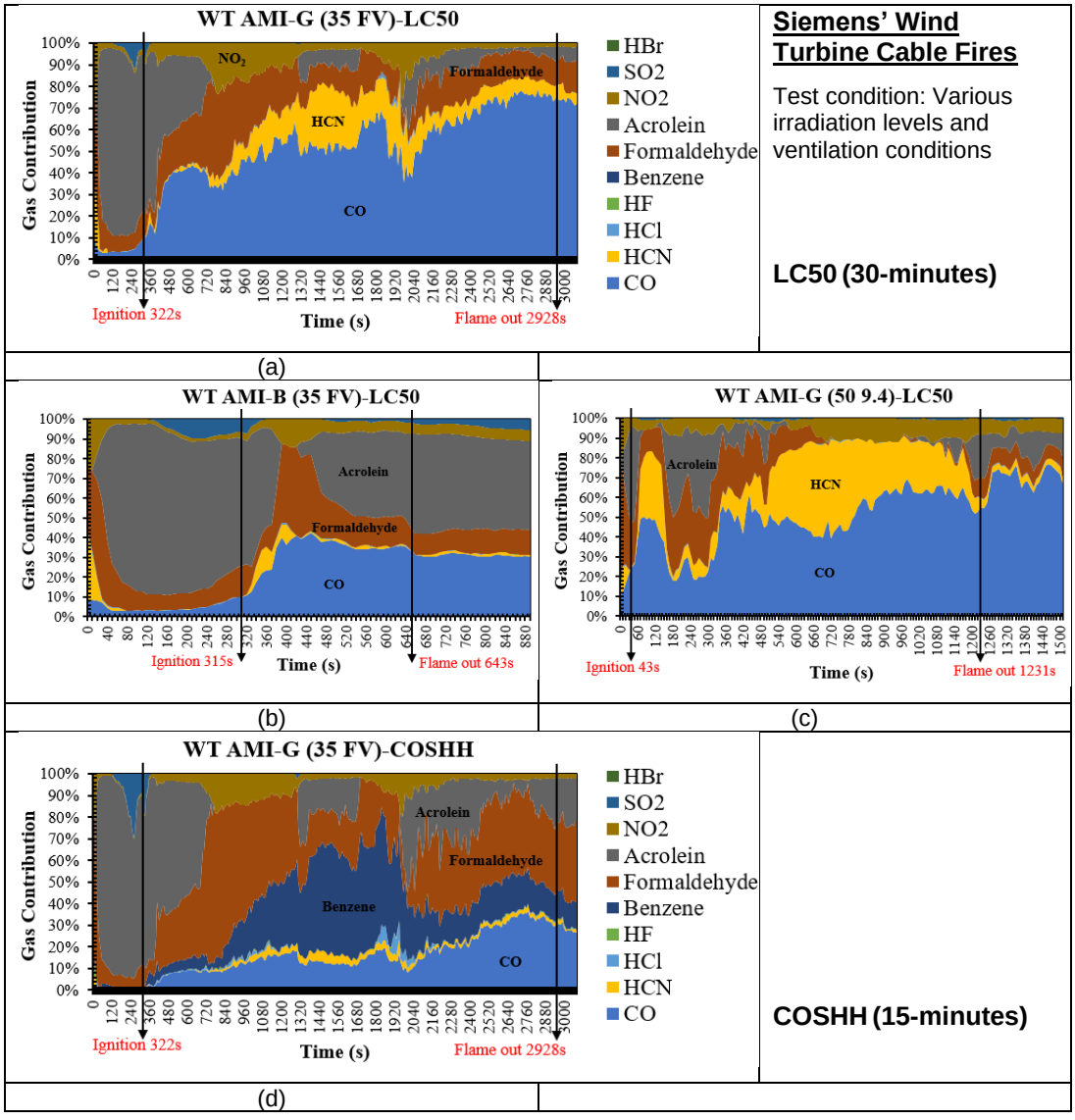

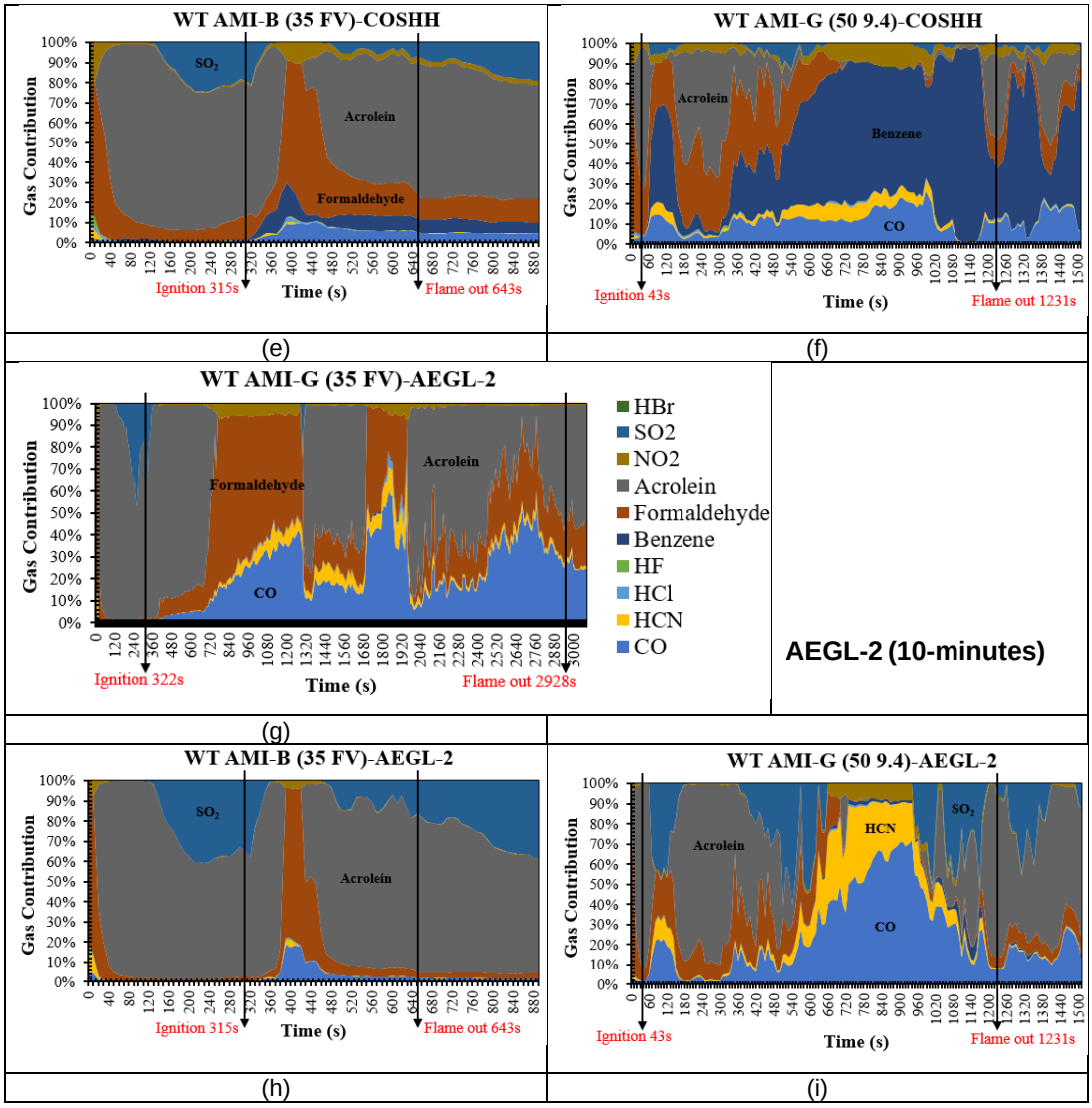


**Figure 4.52** Major gases contribution (based $LC50_{30min}$, $COSHH1_{5min}$ and $AEGL\text{-}2_{10min}$) for Siemens' Wind Turbine cable fires at 35 kW/m$^2$ and free ventilation.

CO, Formaldehyde, Acrolein and Benzene were found to be the usual major species for most of conducted electrical cable fires that presented and discussed previously. Similar results were shown in Figure 4.50 by other LSZH electrical cable fires. Other than these usual species, HCN and $NO_2$ also the main contributor for nitrogen contained materials. For fire tests at 35 kW/m$^2$ and free ventilation, TEC2-W cable fire had contributed to the highest percentage of CO and HCN contributions compared to Prysmian B and 6701B-W cable fires according to LC50 assessment. Major gas contribution profiles for both Prysmian B and 6701B-W cable fires based LC50 under both test conditions (35 kW/m$^2$ with free ventilation and 50 kW/m$^2$ with restricted

ventilation) were not much different to each other. Prysmian B and 6701B-W cable fires under 50 kW/m$^2$ and restricted ventilation condition seemed to have higher CO and HCN contributions than the cable fires under 35 kW/m$^2$ and free ventilation condition. From $COSHH_{15min}$ assessment method, the contribution's influence by CO and HCN was low with Formaldehyde, Acrolein and Benzene had become the major species. TEC2-W cable fire contributed to the highest percentage of Benzene (about 60%) compared to Prysmian B and 6701B-W cable fires. From AEGL-2 based of toxic assessment, Acrolein was the first major species obviously indicated for these LSZH electrical cable fires, followed by CO and Formaldehyde.

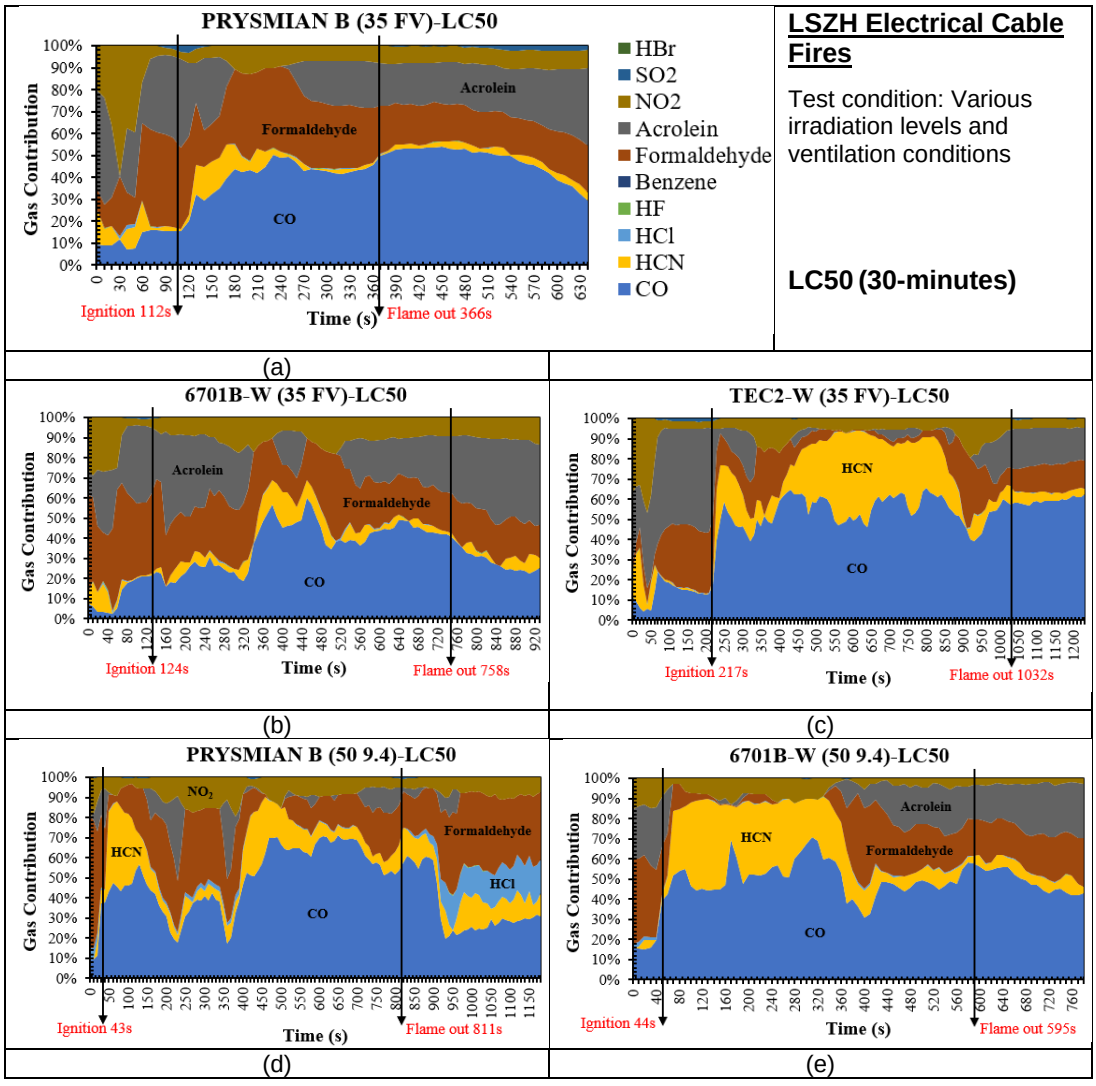

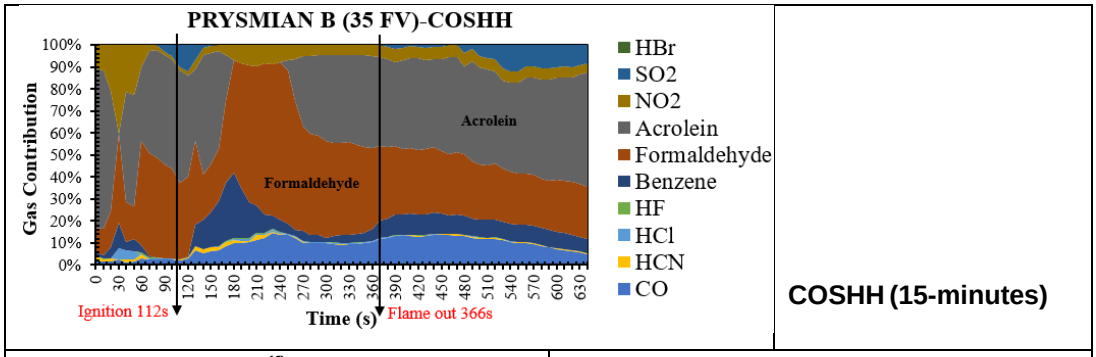
PRYSMIAN B (35 FV)-COSHH
Gas Contribution
Time (s)
Ignition 112s
Flame out 366s
Acrolein
Formaldehyde
HBr
SO2
NO2
Acrolein
Formaldehyde
Benzene
HF
HCl
HCN
CO
COSHH (15-minutes)

(f)

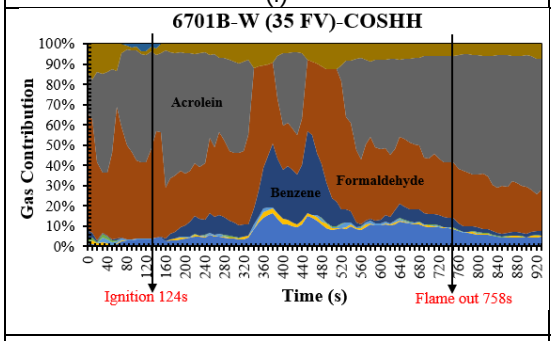
6701B-W (35 FV)-COSHH
Gas Contribution
Time (s)
Ignition 124s
Flame out 758s
Acrolein
Benzene
Formaldehyde

(g)

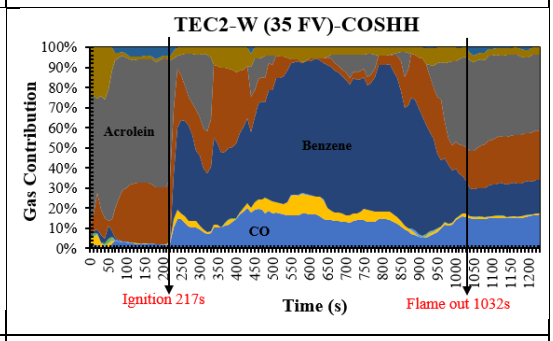
TEC2-W (35 FV)-COSHH
Gas Contribution
Time (s)
Ignition 217s
Flame out 1032s
Acrolein
Benzene
CO

(h)

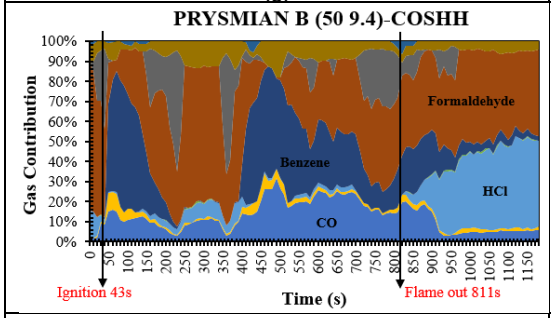
PRYSMIAN B (50 9.4)-COSHH
Gas Contribution
Time (s)
Ignition 43s
Flame out 811s
Formaldehyde
Benzene
HCl
CO

(i)

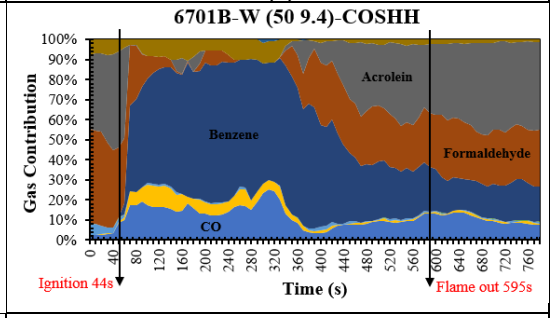
6701B-W (50 9.4)-COSHH
Gas Contribution
Time (s)
Ignition 44s
Flame out 595s
Acrolein
Benzene
Formaldehyde
CO

(j)

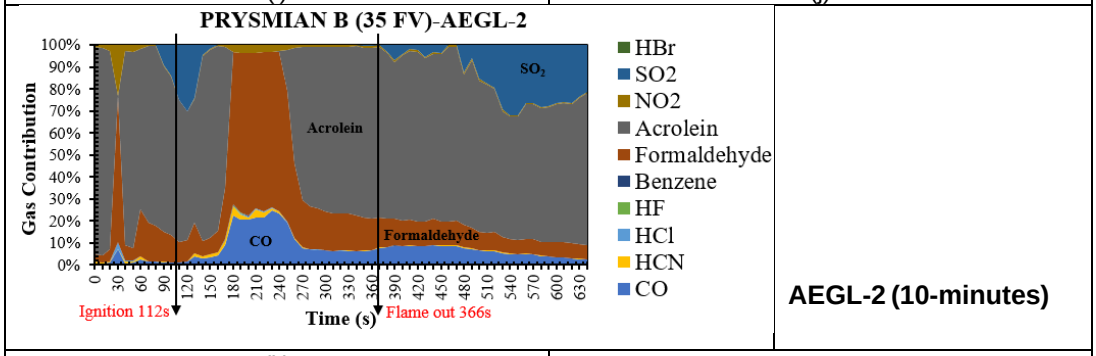
PRYSMIAN B (35 FV)-AEGL-2
Gas Contribution
Time (s)
Ignition 112s
Flame out 366s
Acrolein
Formaldehyde
CO
SO2
HBr
SO2
NO2
Acrolein
Formaldehyde
Benzene
HF
HCl
HCN
CO
AEGL-2 (10-minutes)

(k)

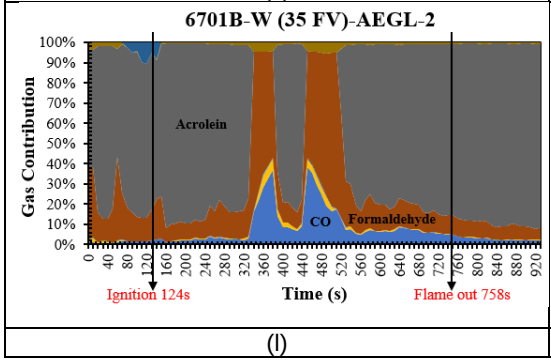
6701B-W (35 FV)-AEGL-2
Gas Contribution
Time (s)
Ignition 124s
Flame out 758s
Acrolein
CO
Formaldehyde

(l)

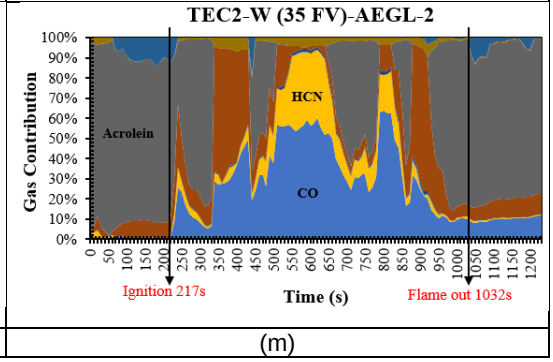
TEC2-W (35 FV)-AEGL-2
Gas Contribution
Time (s)
Ignition 217s
Flame out 1032s
Acrolein
HCN
CO

(m)

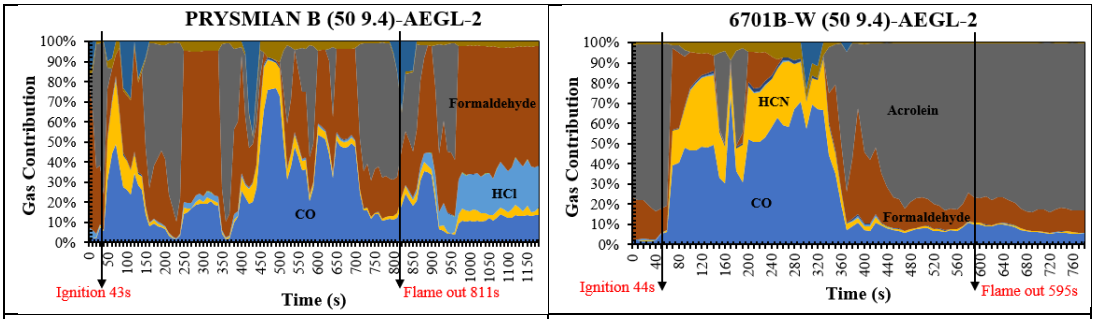


**Figure 4.53** Major gases contribution (based $LC50_{30min}$, $COSHH1_{5min}$ and $AEGL\text{-}2_{10min}$) for LSZH electrical cable fires at different heat fluxes and ventilation rates.

At the initial stage of pre analysis work, FLEX1-BG and FLEX2-W electrical cables were grouped under the non-PVC cable group due to insufficient information provided about the cable specifications. As HCl was one of the major species as shown in Figure 4.51, it was confirmed that these two cables were PVC type or fire retarded cables containing the Chlorin (Cl) element. Other than HCl, Acrolein and Formaldehyde contributions were also high. According to FEC LC50 basis in Figure 4.51 (a) and (b), Acrolein contribution as the significant major species was realised after 100 s of burning period for FLEX-1 BG fire and its contribution was very high (>90%) from the start of burning up to 200 s for FLEX2-W fire. From Figure 4.51 (e), $SO_2$ contribution was realised for FLEX1-BG cable fire for AEGL-2 assessment based and none was found for FLEX2-W cable fire. At the initial stage of fire growth, HCl was seen to be the first major species for FLEX1-BG cable fire with Acrolein was dominating the contribution percentage with 60% after 400 s until the fire extinguished at 727 s. Acrolein was shown to be the first major species for FLEX2-W cable fire with at least 80% from total contribution for the whole burning process under 35 $kW/m^2$ radiant heat and free ventilation test conditions. The summary of first six major species for various electrical cable fires is shown in Table 4.7.

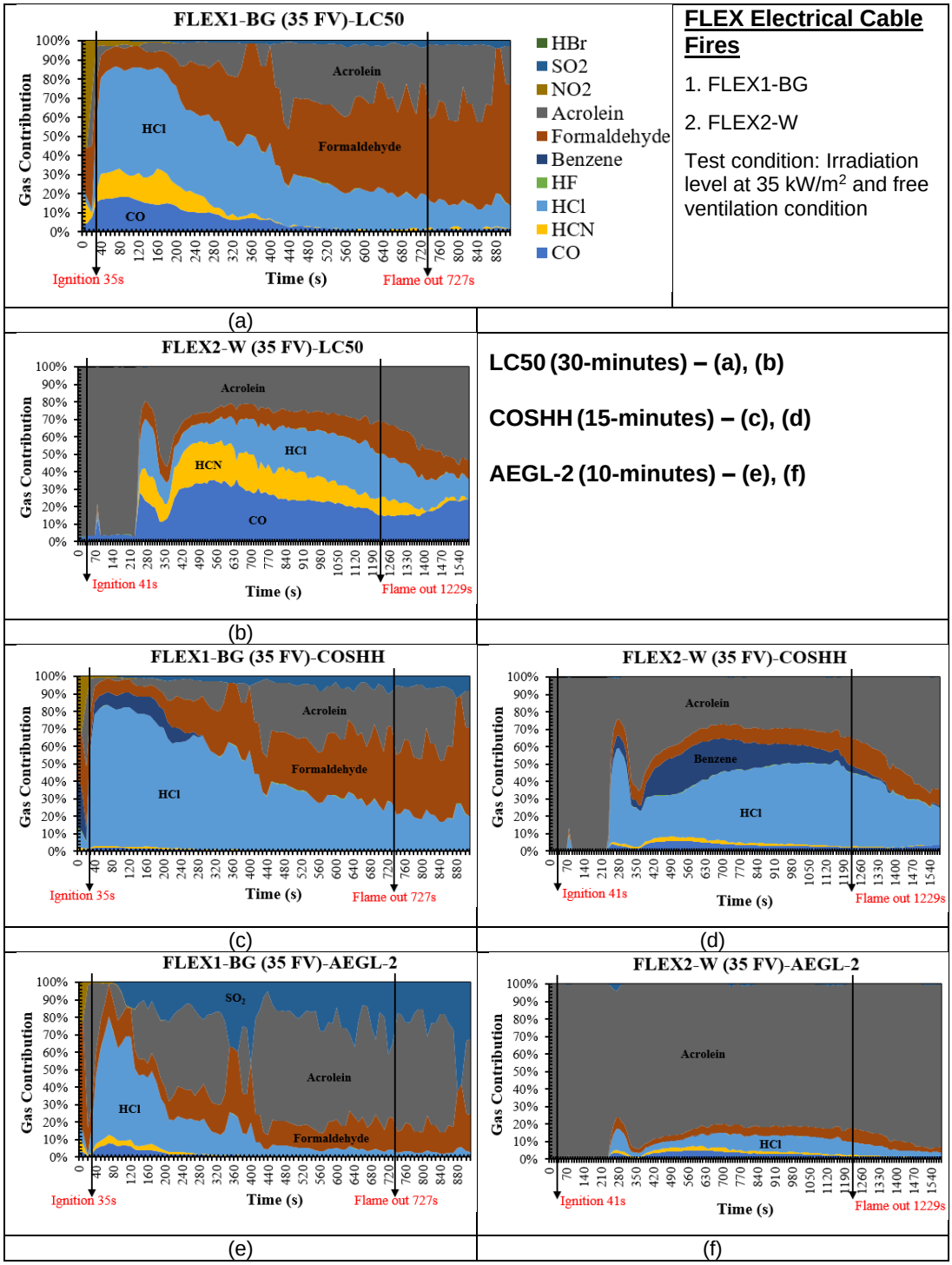


**Figure 4.54** Major gases contribution (based $LC50_{30min}$, $COSHH1_{5min}$ and $AEGL\text{-}2_{10min}$) for Non-PVC electrical cable fires at 35 kW/m$^2$ and free ventilation.

**Table 4.7** First six major species for various electrical cable fires.

| Test | Test Details | Mean ER, Φ (Chan) | Time (s) | Fire Stage | TT | Major Species | | | | | |
|---|---|---|---|---|---|---|---|---|---|---|---|
| | | | | | | 1 | 2 | 3 | 4 | 5 | 6 |
| 1 | PVC EC-GB 1 | 0.02 | <23 | Ignition | LC50 | Acrolein | Formaldehyde | HCN | $SO_2$ | - | - |
| | 35 FV | 0.04 | 23 - 1525 | SS Flaming | | Acrolein | Formaldehyde | $SO_2$ | HCN | CO | - |
| | I = 23 s | 0.02 | >1525 | Post-flaming | | Formaldehyde | Acrolein | $SO_2$ | HCl | HCN | CO |
| | F = 1525 s | 0.02 | <23 | Ignition | COSHH | Acrolein | Formaldehyde | $SO_2$ | HBr | - | - |
| | | 0.04 | 23 - 1525 | SS Flaming | | Acrolein | Formaldehyde | $SO_2$ | HBr | - | - |
| | | 0.02 | >1525 | Post-flaming | | Acrolein | Formaldehyde | $SO_2$ | HCl | - | - |
| | | 0.02 | <23 | Ignition | AEGL-2 | Acrolein | $SO_2$ | Formaldehyde | - | - | - |
| | | 0.04 | 23 - 1525 | SS Flaming | | Acrolein | $SO_2$ | Formaldehyde | - | - | - |
| | | 0.02 | >1525 | Post-flaming | | Acrolein | $SO_2$ | Formaldehyde | - | - | - |
| 2 | PVC EC-GB 2 | 0.02 | <26 | Ignition | LC50 | Acrolein | Formaldehyde | $SO_2$ | HCN | - | - |
| | 35 FV | 0.07 | 26 - 800 | SS Flaming | | Acrolein | Formaldehyde | CO | HCN | HCl | $SO_2$ |
| | I = 26 s | 0.07 | 800 - 1162 | Flaming | | Formaldehyde | Acrolein | HCl | CO | $SO_2$ | HCN |
| | F = 1162 s | 0.06 | >1162 | Post-flaming | | Formaldehyde | Acrolein | HCl | CO | $SO_2$ | HCN |
| | | 0.02 | <26 | Ignition | COSHH | Acrolein | Formaldehyde | $SO_2$ | - | - | - |
| | | 0.07 | 26 - 800 | SS Flaming | | Acrolein | Formaldehyde | $SO_2$ | HCl | - | - |
| | | 0.07 | 800 - 1162 | Flaming | | Acrolein | Formaldehyde | HCl | $SO_2$ | - | - |
| | | 0.06 | >1162 | Post-flaming | | Acrolein | Formaldehyde | HCl | $SO_2$ | - | - |
| | | 0.02 | <26 | Ignition | AEGL-2 | Acrolein | $SO_2$ | Formaldehyde | - | - | - |
| | | 0.07 | 26 - 800 | SS Flaming | | Acrolein | $SO_2$ | Formaldehyde | - | - | - |
| | | 0.07 | 800 - 1162 | Flaming | | Acrolein | $SO_2$ | Formaldehyde | HCl | - | - |
| | | 0.06 | >1162 | Post-flaming | | Acrolein | $SO_2$ | Formaldehyde | HCl | - | - |

| | | | | | | | | | | | |
|---|---|---|---|---|---|---|---|---|---|---|---|
| 3 | SEC HV1-4C | 0.3 | <37 | Ignition | **LC50** | HCl | CO | Formaldehyde | HCN | Acrolein | - |
| | 35 FV | 0.6 | 37 - 900 | SS Flaming | | HCl | CO | Formaldehyde | HCN | Acrolein | - |
| | I = 37 s | 0.1 | 900 - 3327 | Flaming | | HCl | Formaldehyde | CO | HCN | Acrolein | $NO_2$ |
| | F = 3327 s | 0.1 | >3327 | Post-flaming | | CO | HCN | Formaldehyde | HCl | Acrolein | $NO_2$ |
| | | 0.3 | <37 | Ignition | **COSHH** | HCl | Formaldehyde | Benzene | HCN | Acrolein | CO |
| | | 0.6 | 37 - 900 | SS Flaming | | HCl | Formaldehyde | Benzene | Acrolein | HCN | CO |
| | | 0.1 | 900 - 3327 | Flaming | | HCl | Formaldehyde | Benzene | Acrolein | CO | HCN |
| | | 0.1 | >3327 | Post-flaming | | HCl | Formaldehyde | Benzene | Acrolein | CO | HCN |
| | | 0.3 | <37 | Ignition | **AEGL-2** | HCl | Formaldehyde | Acrolein | CO | HCN | $SO_2$ |
| | | 0.6 | 37 - 900 | SS Flaming | | HCl | Formaldehyde | Acrolein | CO | HCN | $SO_2$ |
| | | 0.1 | 900 - 3327 | Flaming | | Acrolein | Formaldehyde | HCl | CO | HCN | $NO_2$ |
| | | 0.1 | >3327 | Post-flaming | | Acrolein | Formaldehyde | HCl | CO | HCN | $NO_2$ |
| 4 | SEC HV2-3C | 0.3 | <1084 | Ignition | **LC50** | Acrolein | Formaldehyde | HCl | CO | $NO_2$ | HCN |
| | 35 FV | 2.5 | 1084 - 1600 | Flaming | | CO | HCl | HCN | Formaldehyde | Acrolein | $NO_2$ |
| | I = 1084 s | 0.7 | 1600 - 2850 | SS Flaming | | Acrolein | Formaldehyde | HCl | CO | $NO_2$ | HCN |
| | F = 3468 s | 0.8 | 2850 - 3468 | Flaming | | CO | HCl | HCN | Formaldehyde | Acrolein | $NO_2$ |
| | | 1.3 | >3468 | Post-flaming | | CO | Formaldehyde | HCl | Acrolein | HCN | $NO_2$ |
| | | 0.3 | <1084 | Ignition | **COSHH** | Acrolein | HCl | Formaldehyde | $SO_2$ | Benzene | $NO_2$ |
| | | 2.5 | 1084 - 1600 | Flaming | | HCl | Acrolein | Benzene | Formaldehyde | CO | $NO_2$ |
| | | 0.7 | 1600 - 2850 | SS Flaming | | Acrolein | HCl | Formaldehyde | $SO_2$ | Benzene | $NO_2$ |
| | | 0.8 | 2850 - 3468 | Flaming | | HCl | Benzene | Formaldehyde | Acrolein | CO | $NO_2$ |
| | | 1.3 | >3468 | Post-flaming | | HCl | Formaldehyde | Acrolein | Benzene | CO | $NO_2$ |
| | | 0.3 | <1084 | Ignition | **AEGL-2** | Acrolein | $SO_2$ | Formaldehyde | HCl | - | - |
| | | 2.5 | 1084 - 1600 | Flaming | | Acrolein | Formaldehyde | HCl | CO | $SO_2$ | HCN |
| | | 0.7 | 1600 - 2850 | SS Flaming | | Acrolein | $SO_2$ | Formaldehyde | HCl | - | - |
| | | 0.8 | 2850 - 3468 | Flaming | | Acrolein | HCl | Formaldehyde | CO | HCN | $SO_2$ |
| | | 1.3 | >3468 | Post-flaming | | Acrolein | Formaldehyde | HCl | CO | HCN | $SO_2$ |

| | | | | | | | | | | | | |
|---|---|---|---|---|---|---|---|---|---|---|---|---|
| 5 | WT AMI-G | 0.1 | <322 | Ignition | **LC50** | Acrolein | Formaldehyde | $NO_2$ | $SO_2$ | CO | HCN |
| | 35 FV | 0.8 (max. 1.3) | 322 - 1980 | SS Flaming | | CO | Formaldehyde | HCN | $NO_2$ | Acrolein | $SO_2$ |
| | I = 322 s | 0.2 | 1980 - 2928 | Flaming | | CO | Formaldehyde | HCN | Acrolein | $NO_2$ | - |
| | F = 2928 s | 0.1 | >2928 | Post-flaming | | CO | Formaldehyde | Acrolein | HCN | $NO_2$ | - |
| | | 0.1 | <322 | Ignition | **COSHH** | Acrolein | Formaldehyde | $SO_2$ | $NO_2$ | CO | - |
| | | 0.8 (max. 1.3) | 322 - 1980 | SS Flaming | | Benzene | Formaldehyde | Acrolein | CO | $NO_2$ | HCN |
| | | 0.2 | 1980 - 2928 | Flaming | | Formaldehyde | CO | Acrolein | Benzene | $NO_2$ | HCN |
| | | 0.1 | >2928 | Post-flaming | | Formaldehyde | CO | Acrolein | Benzene | $NO_2$ | HCN |
| | | 0.1 | <322 | Ignition | **AEGL-2** | Acrolein | Formaldehyde | $NO_2$ | $SO_2$ | CO | HCN |
| | | 0.8 (max. 1.3) | 322 - 1980 | SS Flaming | | CO | Formaldehyde | HCN | $NO_2$ | Acrolein | $SO_2$ |
| | | 0.2 | 1980 - 2928 | Flaming | | CO | Formaldehyde | HCN | Acrolein | $NO_2$ | - |
| | | 0.1 | >2928 | Post-flaming | | CO | Formaldehyde | HCN | Acrolein | $NO_2$ | - |
| 6 | WT AMI-G | 0.1 | <43 | Ignition | **LC50** | Formaldehyde | Acrolein | CO | $NO_2$ | HCN | - |
| | 50 9.4 | 0.6 | 43 - 500 | SS Flaming | | CO | Formaldehyde | Acrolein | HCN | $NO_2$ | $SO_2$ |
| | I = 43 s | 5.0 | 500 - 1231 | Flaming | | CO | HCN | $NO_2$ | Formaldehyde | Acrolein | $SO_2$ |
| | F = 1231 s | - | >1231 | Post-flaming | | CO | Acrolein | Formaldehyde | $NO_2$ | HCN | $SO_2$ |
| | | 0.1 | <43 | Ignition | **COSHH** | Formaldehyde | Acrolein | $NO_2$ | CO | HCN | HCl |
| | | 0.6 | 43 - 500 | SS Flaming | | Formaldehyde | Acrolein | Benzene | CO | $NO_2$ | HCN |
| | | 5.0 | 500 - 1231 | Flaming | | Benzene | CO | Formaldehyde | $NO_2$ | HCN | Acrolein |
| | | - | >1231 | Post-flaming | | Benzene | Acrolein | CO | Formaldehyde | $NO_2$ | $SO_2$ |
| | | 0.1 | <43 | Ignition | **AEGL-2** | Acrolein | Formaldehyde | $NO_2$ | CO | HCN | - |
| | | 0.6 | 43 - 500 | SS Flaming | | Acrolein | Formaldehyde | $SO_2$ | CO | HCN | $NO_2$ |
| | | 5.0 | 500 - 1231 | Flaming | | CO | HCN | $SO_2$ | Acrolein | Formaldehyde | $NO_2$ |
| | | - | >1231 | Post-flaming | | Acrolein | CO | SO2 | Formaldehyde | $NO_2$ | HCN |

| | | | | | | | | | | | | |
|---|---|---|---|---|---|---|---|---|---|---|---|---|
| 7 | WT AMI-B | 0.2 | <315 | Ignition | **LC50** | Acrolein | Formaldehyde | $NO_2$ | $SO_2$ | CO | HCN |
| | 35 FV | 0.4 | 315 - 380 | SS Flaming | | Acrolein | CO | Formaldehyde | HCN | $NO_2$ | $SO_2$ |
| | I = 315 s | 0.2 | 380 - 643 | Flaming | | CO | Acrolein | Formaldehyde | $NO_2$ | HCN | $SO_2$ |
| | F = 643 s | 0.2 | >643 | Post-flaming | | Acrolein | CO | Formaldehyde | $NO_2$ | $SO_2$ | HCN |
| | | 0.2 | <315 | Ignition | **COSHH** | Acrolein | Formaldehyde | $SO_2$ | $NO_2$ | Benzene | HCN |
| | | 0.4 | 315 - 380 | SS Flaming | | Acrolein | Formaldehyde | Benzene | $SO_2$ | CO | $NO_2$ |
| | | 0.2 | 380 - 643 | Flaming | | Acrolein | Formaldehyde | CO | Benzene | $NO_2$ | $SO_2$ |
| | | 0.2 | >643 | Post-flaming | | Acrolein | $SO_2$ | Formaldehyde | Benzene | CO | $NO_2$ |
| | | 0.2 | <315 | Ignition | **AEGL-2** | Acrolein | $SO_2$ | Formaldehyde | $NO_2$ | HCN | CO |
| | | 0.4 | 315 - 380 | SS Flaming | | Acrolein | $SO_2$ | Formaldehyde | CO | $NO_2$ | HCN |
| | | 0.2 | 380 - 643 | Flaming | | Acrolein | Formaldehyde | SO2 | CO | $NO_2$ | HCN |
| | | 0.2 | >643 | Post-flaming | | Acrolein | $SO_2$ | Formaldehyde | CO | - | - |
| 8 | PRYSMIAN B | 0.06 | <112 | Ignition | **LC50** | Acrolein | Formaldehyde | $NO_2$ | CO | HCN | HCl |
| | 35 FV | 0.45 | 112 - 170 | SS Flaming | | CO | Formaldehyde | Acrolein | HCN | $NO_2$ | $SO_2$ |
| | I = 112 s | 0.30 | 170 - 366 | Flaming | | CO | Formaldehyde | Acrolein | $NO_2$ | HCN | - |
| | F = 366 s | 0.15 | >366 | Post-flaming | | CO | Acrolein | Formaldehyde | $NO_2$ | HCN | $SO_2$ |
| | | 0.06 | <112 | Ignition | **COSHH** | Acrolein | Formaldehyde | $NO_2$ | Benzene | CO | HCl |
| | | 0.45 | 112 - 170 | SS Flaming | | Formaldehyde | Acrolein | Benzene | CO | $NO_2$ | $SO_2$ |
| | | 0.30 | 170 - 366 | Flaming | | Formaldehyde | Acrolein | CO | Benzene | $NO_2$ | HCl |
| | | 0.15 | >366 | Post-flaming | | Acrolein | Formaldehyde | CO | Benzene | $SO_2$ | $NO_2$ |
| | | 0.06 | <112 | Ignition | **AEGL-2** | Acrolein | Formaldehyde | $NO_2$ | $SO_2$ | CO | HCN |
| | | 0.45 | 112 - 170 | SS Flaming | | Acrolein | Formaldehyde | $SO_2$ | CO | HCN | $NO_2$ |
| | | 0.30 | 170 - 366 | Flaming | | Acrolein | Formaldehyde | CO | $NO_2$ | HCN | - |
| | | 0.15 | >366 | Post-flaming | | Acrolein | $SO_2$ | Formaldehyde | CO | - | - |

| | | | | | | | | | | | | |
|---|---|---|---|---|---|---|---|---|---|---|---|---|
| 9 | PRYSMIAN B | 1.0 | <43 | Ignition | **LC50** | Formaldehyde | CO | $NO_2$ | Acrolein | HCN | HCl |
| | 50 9.4 | 2.0 | 43 - 350 | SS Flaming | | CO | Formaldehyde | HCN | $NO_2$ | Acrolein | HCl |
| | I = 43 s | 2.0 | 350 - 811 | Flaming | | CO | Formaldehyde | HCN | $NO_2$ | Acrolein | HCl |
| | F = 811 s | 0.5 | >811 | Post-flaming | | CO | Formaldehyde | HCl | HCN | $NO_2$ | Acrolein |
| | | 1.0 | <43 | Ignition | **COSHH** | Formaldehyde | Acrolein | HCl | $NO_2$ | CO | $SO_2$ |
| | | 2.0 | 43 - 350 | SS Flaming | | Formaldehyde | Benzene | CO | Acrolein | $NO_2$ | HCl |
| | | 2.0 | 350 - 811 | Flaming | | Formaldehyde | Benzene | CO | Acrolein | $NO_2$ | HCl |
| | | 0.5 | >811 | Post-flaming | | Formaldehyde | HCl | Benzene | CO | $NO_2$ | Acrolein |
| | | 1.0 | <43 | Ignition | **AEGL-2** | Formaldehyde | Acrolein | $SO_2$ | CO | HCl | $NO_2$ |
| | | 2.0 | 43 - 350 | SS Flaming | | Formaldehyde | CO | Acrolein | HCN | $SO_2$ | $NO_2$ |
| | | 2.0 | 350 - 811 | Flaming | | CO | Acrolein | Formaldehyde | HCN | $NO_2$ | $SO_2$ |
| | | 0.5 | >811 | Post-flaming | | Formaldehyde | CO | HCl | Acrolein | $NO_2$ | $SO_2$ |
| 10 | 6701B-W | 0.05 | <124 | Ignition | **LC50** | Formaldehyde | Acrolein | $NO_2$ | CO | HCN | $SO_2$ |
| | 35 FV | 0.20 | 124 - 340 | SS Flaming | | Formaldehyde | Acrolein | CO | $NO_2$ | HCN | - |
| | I = 124 s | 0.25 | 340 - 758 | Flaming | | CO | Formaldehyde | Acrolein | $NO_2$ | HCN | - |
| | F = 758 s | 0.03 | >758 | Post-flaming | | Acrolein | CO | Formaldehyde | $NO_2$ | HCN | - |
| | | 0.05 | <124 | Ignition | **COSHH** | Formaldehyde | Acrolein | $NO_2$ | $SO_2$ | CO | - |
| | | 0.20 | 124 - 340 | SS Flaming | | Acrolein | Formaldehyde | Benzene | $NO_2$ | CO | HCN |
| | | 0.25 | 340 - 758 | Flaming | | Formaldehyde | Acrolein | Benzene | CO | $NO_2$ | HCN |
| | | 0.03 | >758 | Post-flaming | | Acrolein | Formaldehyde | $NO_2$ | CO | Benzene | HCN |
| | | 0.05 | <124 | Ignition | **AEGL-2** | Acrolein | Formaldehyde | $SO_2$ | $NO_2$ | CO | HCN |
| | | 0.20 | 124 - 340 | SS Flaming | | Acrolein | Formaldehyde | CO | $NO_2$ | $SO_2$ | HCN |
| | | 0.25 | 340 - 758 | Flaming | | Acrolein | Formaldehyde | CO | $NO_2$ | HCN | - |
| | | 0.03 | >758 | Post-flaming | | Acrolein | Formaldehyde | CO | $NO_2$ | HCN | - |

| | | | | | | | | | | | |
|---|---|---|---|---|---|---|---|---|---|---|---|
| 11 | 6701B-W | 0.1 | <44 | Ignition | **LC50** | Formaldehyde | Acrolein | CO | $NO_2$ | HCN | HCl |
| | 50 9.4 | 1.2 (peak) | 44 - 340 | SS Flaming | | CO | HCN | $NO_2$ | Formaldehyde | Acrolein | - |
| | I = 44 s | - | 340 - 595 | Flaming | | CO | Formaldehyde | Acrolein | HCN | $NO_2$ | HCl |
| | F = 595 s | - | >595 | Post-flaming | | CO | Acrolein | Formaldehyde | HCN | $NO_2$ | - |
| | | 0.1 | <44 | Ignition | **COSHH** | Formaldehyde | Acrolein | $NO_2$ | HCl | CO | HCN |
| | | 1.2 (peak) | 44 - 340 | SS Flaming | | Benzene | CO | $NO_2$ | HCN | Formaldehyde | Acrolein |
| | | - | 340 - 595 | Flaming | | Benzene | Acrolein | Formaldehyde | CO | $NO_2$ | HCN |
| | | - | >595 | Post-flaming | | Acrolein | Formaldehyde | Benzene | CO | $NO_2$ | HCN |
| | | 0.1 | <44 | Ignition | **AEGL-2** | Acrolein | Formaldehyde | CO | $NO_2$ | HCl | - |
| | | 1.2 (peak) | 44 - 340 | SS Flaming | | CO | HCN | Acrolein | Formaldehyde | $NO_2$ | $SO_2$ |
| | | - | 340 - 595 | Flaming | | Acrolein | Formaldehyde | CO | HCN | $NO_2$ | $SO_2$ |
| | | - | >595 | Post-flaming | | Acrolein | Formaldehyde | CO | HCN | - | - |
| 12 | TEC2-W | 0.1 | <217 | Ignition | **LC50** | Acrolein | Formaldehyde | $NO_2$ | CO | HCN | $SO_2$ |
| | 35 FV | 1.0 | 217 - 330 | SS Flaming | | CO | HCN | Formaldehyde | Acrolein | $NO_2$ | $SO_2$ |
| | I = 217 s | 5.0 (max. 9.0) | 330 - 1032 | Flaming | | CO | HCN | Formaldehyde | $NO_2$ | Acrolein | - |
| | F = 1032 s | 0.2 | >1032 | Post-flaming | | CO | Acrolein | Formaldehyde | HCN | NO2 | $SO_2$ |
| | | 0.1 | <217 | Ignition | **COSHH** | Acrolein | Formaldehyde | $NO_2$ | $SO_2$ | CO | HCN |
| | | 1.0 | 217 - 330 | SS Flaming | | Benzene | CO | Formaldehyde | Acrolein | $NO_2$ | HCN |
| | | 5.0 (max. 9.0) | 330 - 1032 | Flaming | | Benzene | CO | Formaldehyde | Acrolein | $NO_2$ | HCN |
| | | 0.2 | >1032 | Post-flaming | | Acrolein | Formaldehyde | CO | Benzene | $NO_2$ | $SO_2$ |
| | | 0.1 | <217 | Ignition | **AEGL-2** | Acrolein | $SO_2$ | Formaldehyde | $NO_2$ | HCN | CO |
| | | 1.0 | 217 - 330 | SS Flaming | | Acrolein | CO | Formaldehyde | HCN | $NO_2$ | $SO_2$ |
| | | 5.0 (max. 9.0) | 330 - 1032 | Flaming | | CO | Acrolein | Formaldehyde | HCN | $NO_2$ | $SO_2$ |
| | | 0.2 | >1032 | Post-flaming | | Acrolein | CO | Formaldehyde | $SO_2$ | HCN | - |

| | | | | | | | | | | | | |
|---|---|---|---|---|---|---|---|---|---|---|---|---|
| 13 | FLEX1-BG | 0.6 | <35 | Ignition | **LC50** | $NO_2$ | Formaldehyde | Acrolein | HCl | HCN | CO |
| | 35 FV | 0.9 (max. 1.8) | 35 - 440 | SS Flaming | | HCl | Formaldehyde | CO | Acrolein | HCN | $NO_2$ |
| | I = 35 s | 0.2 | 440 - 727 | Flaming | | Formaldehyde | Acrolein | HCl | $SO_2$ | CO | HCN |
| | F = 727 s | 0.1 | >727 | Post-flaming | | Formaldehyde | Acrolein | HCl | $SO_2$ | CO | HCN |
| | | 0.6 | <35 | Ignition | **COSHH** | Formaldehyde | Acrolein | $NO_2$ | HCl | Benzene | HCN |
| | | 0.9 (max. 1.8) | 35 - 440 | SS Flaming | | HCl | Formaldehyde | Acrolein | Benzene | $SO_2$ | CO |
| | | 0.2 | 440 - 727 | Flaming | | HCl | Formaldehyde | Acrolein | $SO_2$ | - | - |
| | | 0.1 | >727 | Post-flaming | | Formaldehyde | Acrolein | HCl | $SO_2$ | - | - |
| | | 0.6 | <35 | Ignition | **AEGL-2** | Acrolein | Formaldehyde | $NO_2$ | HCl | HCN | CO |
| | | 0.9 (max. 1.8) | 35 - 440 | SS Flaming | | HCl | Acrolein | $SO_2$ | Formaldehyde | CO | HCN |
| | | 0.2 | 440 - 727 | Flaming | | Acrolein | $SO_2$ | Formaldehyde | HCl | - | - |
| | | 0.1 | >727 | Post-flaming | | Acrolein | $SO_2$ | Formaldehyde | HCl | - | - |
| 14 | FLEX2-W | 0.05 | <41 | Ignition | **LC50** | Acrolein | - | - | - | - | - |
| | 35 FV | 0.20 (max. 0.35) | 41 - 350 | SS Flaming | | Acrolein | HCl | CO | HCN | Formaldehyde | - |
| | I = 41 s | 0.4 (peak) | 350 - 1229 | Flaming | | CO | Acrolein | HCl | HCN | Formaldehyde | - |
| | F = 1229 s | 0.20 | >1229 | Post-flaming | | Acrolein | CO | HCl | Formaldehyde | HCN | - |
| | | 0.05 | <41 | Ignition | **COSHH** | Acrolein | - | - | - | - | - |
| | | 0.20 (max. 0.35) | 41 - 350 | SS Flaming | | Acrolein | HCl | Formaldehyde | Benzene | CO | HCN |
| | | 0.4 (peak) | 350 - 1229 | Flaming | | HCl | Acrolein | Benzene | Formaldehyde | CO | HCN |
| | | 0.20 | >1229 | Post-flaming | | Acrolein | HCl | Formaldehyde | Benzene | CO | HCN |
| | | 0.05 | <41 | Ignition | **AEGL-2** | Acrolein | - | - | - | - | - |
| | | 0.20 (max. 0.35) | 41 - 350 | SS Flaming | | Acrolein | HCl | Formaldehyde | CO | HCN | $SO_2$ |
| | | 0.4 (peak) | 350 - 1229 | Flaming | | Acrolein | HCl | Formaldehyde | CO | HCN | $SO_2$ |
| | | 0.20 | >1229 | Post-flaming | | Acrolein | HCl | Formaldehyde | CO | HCN | - |

## 4.4 Particle Number and Mass Distributions for Electrical Cable Fires

### 4.4.1 Particle Number Distributions for PVC Prysmian A Cable Fires at Various Heat Fluxes and Ventilation Rates

Particle number distributions from the burning of PVC Prysmian A cable at heat flux of 25 kW/m$^2$ and various air flowrates were shown in Figure 4.55. Most of these cable fires showed a similar profile of particle numbers with giving two different peaks. For PVC Prysmian cable fire with 9.4 L/min air flowrate, it gave two peaks with the first peak representing the smaller particles (~10 nm) and the second peak representing the bigger particles (>100 nm). PVC Prysmian cable fire with 18 L/min air flowrate also gave two particle number peaks with the second peak of bigger particles more than 100 nm giving a lower particle number than the first peak of smaller particles. A non-flaming cable fire at 28 L/min showed the highest particle number peak of 1.0E+10 p/cm$^3$ compared to the flaming cable fires with lower air flowrates. The flaming cable fires had a higher HRR and released more nanoparticles less than 10 nm than the non-flaming cable fire. During pyrolysis for cable fires with lower air flowrates, it showed a lower particle number distribution at 50 s before ignition took place compared to the cable fire with 28 L/min air flowrate and after that period, the particle number distributions had increased. Smaller particles less than 100 nm had higher particle number peaks than bigger particles for these cable fires. As shown in Figure 4.55 (d) to (f), the cable fires with 9.4 and 18 L/min air flowrates gave a higher number of 10 nm particles than 100 nm particles while the cable fire with 28 L/min gave a lower number of 10 nm particles than 100 nm particles. Non-flaming cable fire would have a lower temperature profile and this would expedite the agglomeration of particles to form larger particles.

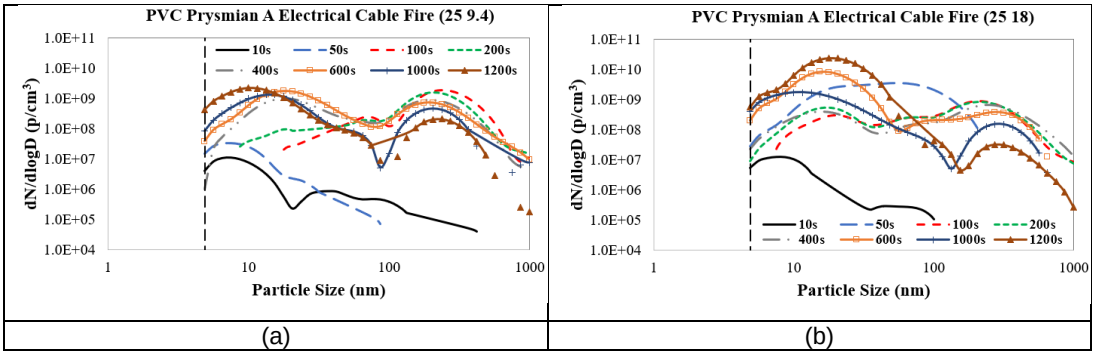


(a) (b)

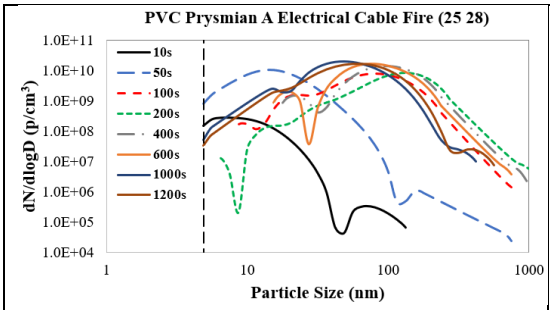
PVC Prysmian A Electrical Cable Fire (25 28)
dN/dlogD (p/cm³)
1.0E+11
1.0E+10
1.0E+09
1.0E+08
1.0E+07
1.0E+06
1.0E+05
1.0E+04
10s
50s
100s
200s
400s
600s
1000s
1200s
1
10
100
1000
Particle Size (nm)

(c)

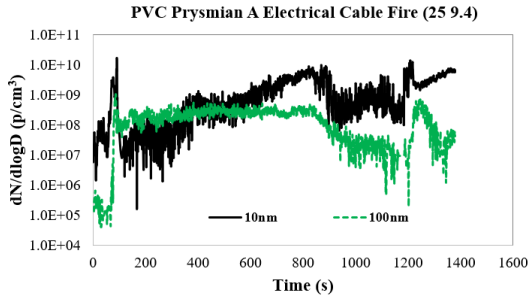
PVC Prysmian A Electrical Cable Fire (25 9.4)
dN/dlogD (p/cm³)
1.0E+11
1.0E+10
1.0E+09
1.0E+08
1.0E+07
1.0E+06
1.0E+05
1.0E+04
10nm
100nm
0
200
400
600
800
1000
1200
1400
1600
Time (s)

(d)

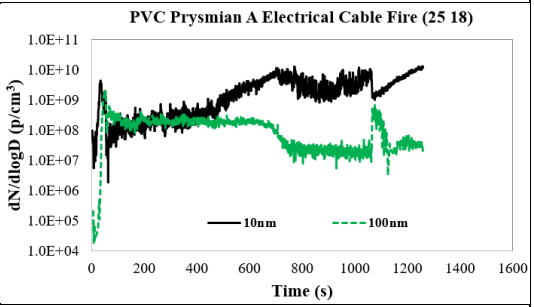
PVC Prysmian A Electrical Cable Fire (25 18)
dN/dlogD (p/cm³)
1.0E+11
1.0E+10
1.0E+09
1.0E+08
1.0E+07
1.0E+06
1.0E+05
1.0E+04
10nm
100nm
0
200
400
600
800
1000
1200
1400
1600
Time (s)

(e)

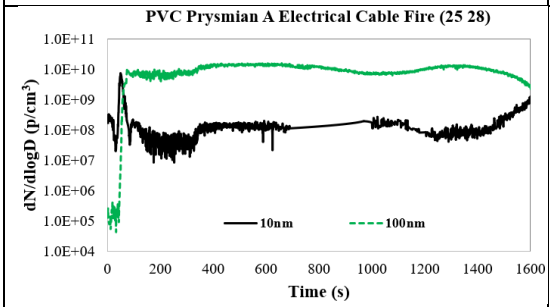
PVC Prysmian A Electrical Cable Fire (25 28)
dN/dlogD (p/cm³)
1.0E+11
1.0E+10
1.0E+09
1.0E+08
1.0E+07
1.0E+06
1.0E+05
1.0E+04
10nm
100nm
0
200
400
600
800
1000
1200
1400
1600
Time (s)

(f)

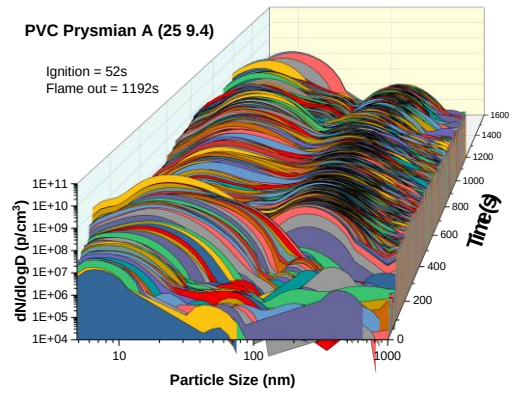
PVC Prysmian A (25 9.4)
Ignition = 52s
Flame out = 1192s
dN/dlogD (p/cm³)
1E+11
1E+10
1E+09
1E+08
1E+07
1E+06
1E+05
1E+04
10
100
1000
Particle Size (nm)
Time (s)
0
200
400
600
800
1000
1200
1400
1600

(g)

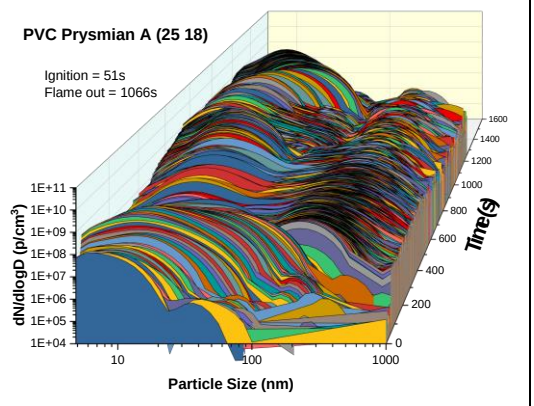
PVC Prysmian A (25 18)
Ignition = 51s
Flame out = 1066s
dN/dlogD (p/cm³)
1E+11
1E+10
1E+09
1E+08
1E+07
1E+06
1E+05
1E+04
10
100
1000
Particle Size (nm)
Time (s)
0
200
400
600
800
1000
1200
1400
1600

(h)

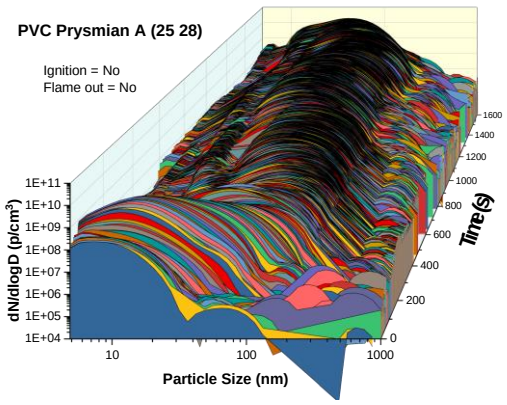


(i)

**Figure 4.55** Particle number distributions from the burning of PVC Prysmian A cable at 25 kW/m$^2$ and various air flow rates.

The particle size results in as a function of time in Figure 4.56 show that the size distribution changes with time. There are at least 3 phases in the fire which are non-flaming, flaming and flame out conditions [45]. There are two peaks observed: the first peak represents 10nm particles (nucleation mode) and the second peak represents 100nm particles (cumulative mode). The first peak shows the presence of Hydrocarbon aerosol in the initial fire development caused by the devolatilization of the electrical cable with no ignition. The second peak is due to the formation of carbon in the flaming combustion phase. The reason for the decrease in number of the agglomerative particles in the 100 nm size range is the oxidation of carbon particles as the fire temperature increases in the cone calorimeter. Near the end of the test there was a sudden change in the size distribution and a loss of the nuclei mode and a sudden growth in a particle mode in the size range around 50 nm. This occurs in the time when it was observed that the flaming combustion ceased and there was a transition to char burning. The flaming combustion is responsible for the production of the nuclei mode 10nm particles and these were only generated by flaming combustion.

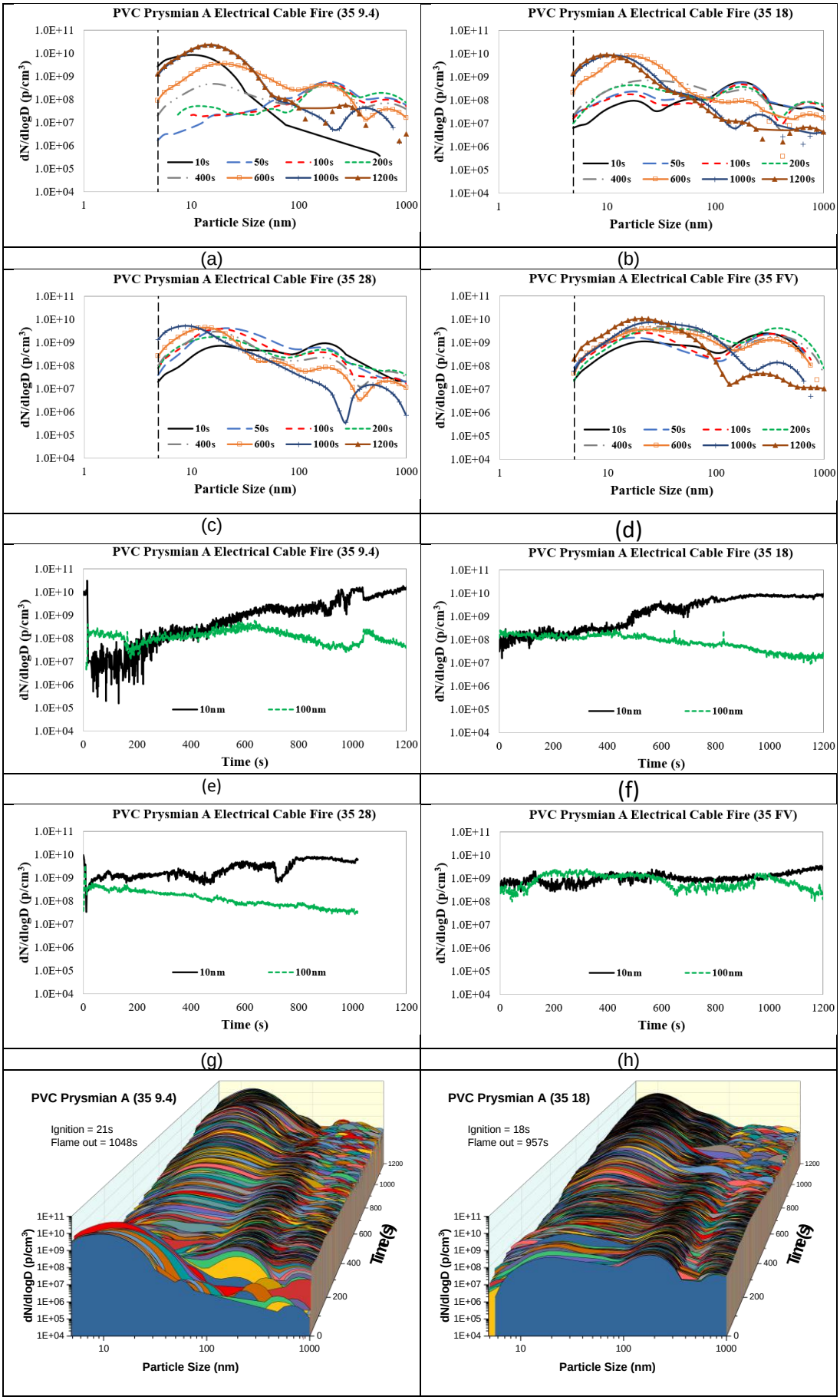
PVC Prysmian A Electrical Cable Fire (35 9.4)
dN/dlogD (p/cm³)
Particle Size (nm)
10s 50s 100s 200s 400s 600s 1000s 1200s
(a)
PVC Prysmian A Electrical Cable Fire (35 18)
dN/dlogD (p/cm³)
Particle Size (nm)
10s 50s 100s 200s 400s 600s 1000s 1200s
(b)
PVC Prysmian A Electrical Cable Fire (35 28)
dN/dlogD (p/cm³)
Particle Size (nm)
10s 50s 100s 200s 400s 600s 1000s 1200s
(c)
PVC Prysmian A Electrical Cable Fire (35 FV)
dN/dlogD (p/cm³)
Particle Size (nm)
10s 50s 100s 200s 400s 600s 1000s 1200s
(d)
PVC Prysmian A Electrical Cable Fire (35 9.4)
dN/dlogD (p/cm³)
Time (s)
10nm 100nm
(e)
PVC Prysmian A Electrical Cable Fire (35 18)
dN/dlogD (p/cm³)
Time (s)
10nm 100nm
(f)
PVC Prysmian A Electrical Cable Fire (35 28)
dN/dlogD (p/cm³)
Time (s)
10nm 100nm
(g)
PVC Prysmian A Electrical Cable Fire (35 FV)
dN/dlogD (p/cm³)
Time (s)
10nm 100nm
(h)
PVC Prysmian A (35 9.4)
Ignition = 21s
Flame out = 1048s
dN/dlogD (p/cm³)
Time (s)
Particle Size (nm)
PVC Prysmian A (35 18)
Ignition = 18s
Flame out = 957s
dN/dlogD (p/cm³)
Time (s)
Particle Size (nm)

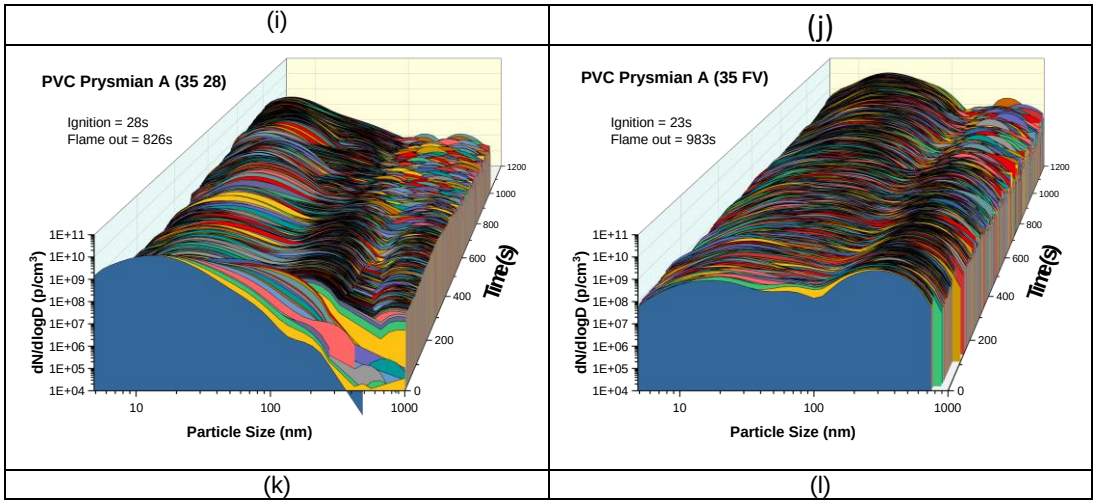


**Figure 4.56** Particle number distributions from the burning of PVC Prysmian A cable at 35 kW/m$^2$ and various air flow rates.

Particle number distributions from the burning of PVC Prysmian A cable at 50 kW/m$^2$ and various air flow rates are shown in Figure 4.57. Number of particles (1.0E+10 p/cm$^3$, < 50 nm) released was higher for time less than 50 s for PVC Prysmian A electrical cable fire at air flowrate of 28 L/min compared to lower air flowrates. At lower air flowrates, the cable fires gave highest particle numbers with the particle sizes were below 100 nm after 400 s of burning time. As shown in Figure 4.57 (d) to (f), number distributions for 10 nm and 100 nm particles were same for PVC cable fire at air flowrate of 9.4 L/min while at higher flowrates, it showed that the number distribution of 10 nm particles were higher than 100 nm particles. The number distributions for bigger particles had decreased with the increasing of air flowrate after 400 s. 3D graphs clearly showed that number concentration peak for smaller particles with size below than 100 nm were higher than the bigger particles especially for cable fire at air flowrate of 28 L/min. The number concentrations of particle size below 100nm were slightly lower than larger particles at initial burning before increased after 400 s for cable fires with 9.4 and 18 L/min air flowrates.

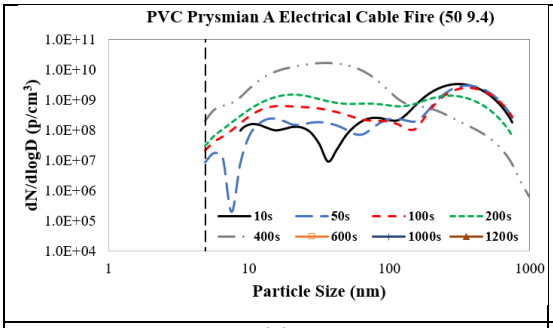
PVC Prysmian A Electrical Cable Fire (50 9.4)
dN/dlogD (p/cm³)
1.0E+11
1.0E+10
1.0E+09
1.0E+08
1.0E+07
1.0E+06
1.0E+05
1.0E+04
1
10
100
1000
Particle Size (nm)
10s
50s
100s
200s
400s
600s
1000s
1200s

(a)

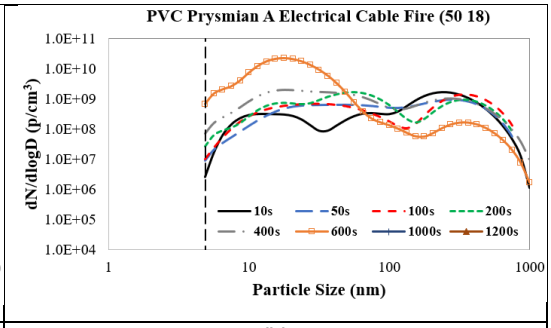
PVC Prysmian A Electrical Cable Fire (50 18)
dN/dlogD (p/cm³)
1.0E+11
1.0E+10
1.0E+09
1.0E+08
1.0E+07
1.0E+06
1.0E+05
1.0E+04
1
10
100
1000
Particle Size (nm)
10s
50s
100s
200s
400s
600s
1000s
1200s

(b)

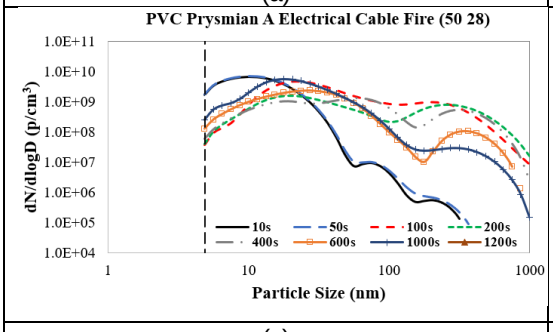
PVC Prysmian A Electrical Cable Fire (50 28)
dN/dlogD (p/cm³)
1.0E+11
1.0E+10
1.0E+09
1.0E+08
1.0E+07
1.0E+06
1.0E+05
1.0E+04
1
10
100
1000
Particle Size (nm)
10s
50s
100s
200s
400s
600s
1000s
1200s

(c)

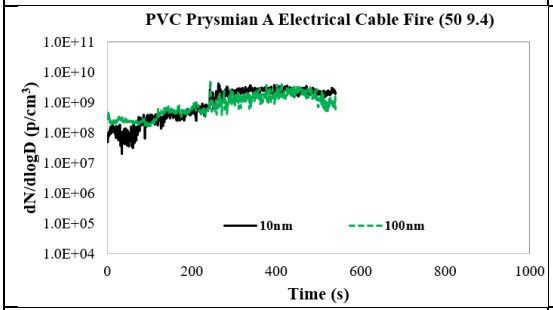
PVC Prysmian A Electrical Cable Fire (50 9.4)
dN/dlogD (p/cm³)
1.0E+11
1.0E+10
1.0E+09
1.0E+08
1.0E+07
1.0E+06
1.0E+05
1.0E+04
0
200
400
600
800
1000
Time (s)
10nm
100nm

(d)

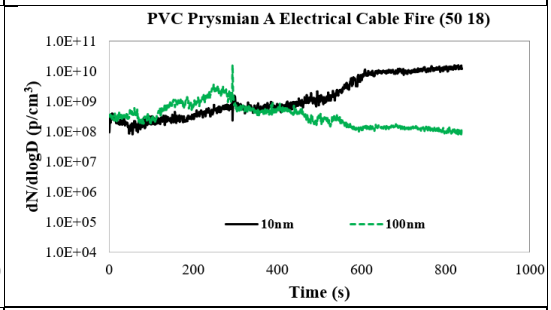
PVC Prysmian A Electrical Cable Fire (50 18)
dN/dlogD (p/cm³)
1.0E+11
1.0E+10
1.0E+09
1.0E+08
1.0E+07
1.0E+06
1.0E+05
1.0E+04
0
200
400
600
800
1000
Time (s)
10nm
100nm

(e)

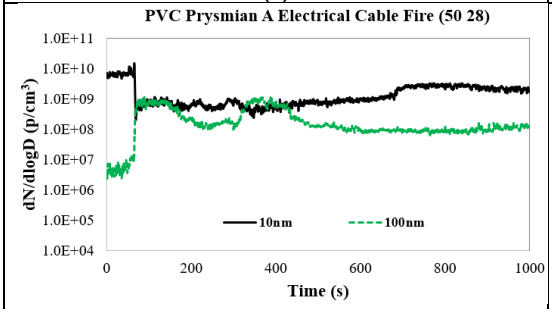
PVC Prysmian A Electrical Cable Fire (50 28)
dN/dlogD (p/cm³)
1.0E+11
1.0E+10
1.0E+09
1.0E+08
1.0E+07
1.0E+06
1.0E+05
1.0E+04
0
200
400
600
800
1000
Time (s)
10nm
100nm

(f)

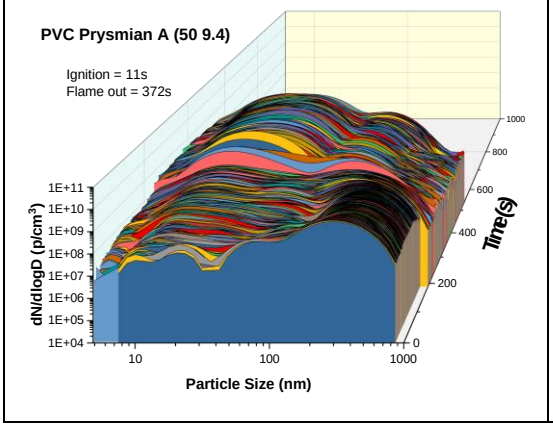
PVC Prysmian A (50 9.4)
Ignition = 11s
Flame out = 372s
dN/dlogD (p/cm³)
1E+11
1E+10
1E+09
1E+08
1E+07
1E+06
1E+05
1E+04
10
100
1000
Particle Size (nm)
0
200
400
600
800
1000
Time(s)

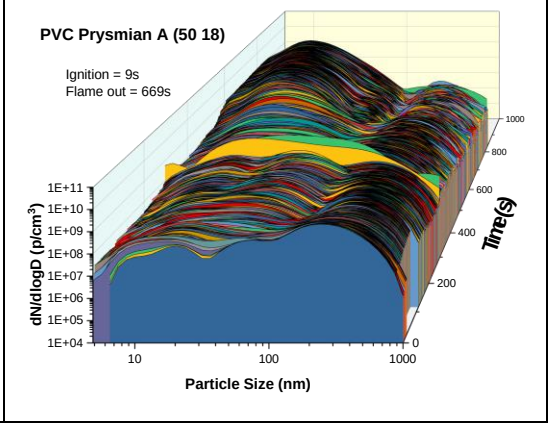
PVC Prysmian A (50 18)
Ignition = 9s
Flame out = 669s
dN/dlogD (p/cm³)
1E+11
1E+10
1E+09
1E+08
1E+07
1E+06
1E+05
1E+04
10
100
1000
Particle Size (nm)
0
200
400
600
800
1000
Time(s)

| (g) | (h) |
|---|---|
| 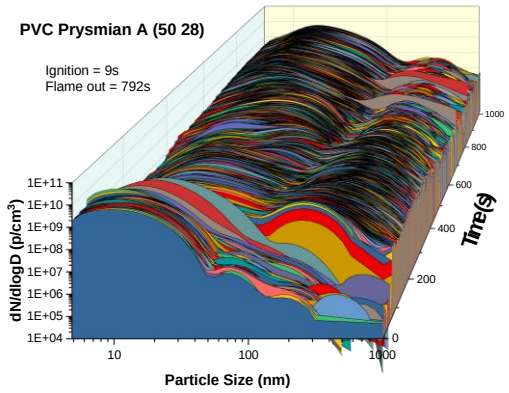 | |
| (i) | |

**Figure 4.57** Particle number distributions from the burning of PVC Prysmian A cable at 50 kW/m$^2$ and various air flow rates.

### 4.4.2 Particle Mass Distributions for PVC Prysmian A Cable Fires at Various Heat Fluxes and Ventilation Rates

For the same particle numbers, larger particles were usually heavier and contributed to a higher mass than the smaller particles. Smaller particles may agglomerate to form larger particles. Figure 4.58 shows particle mass distributions from the burning of PVC Prysmian A cable at 25 kW/m$^2$ and various air flow rates. For all three air flowrates, particle mass for larger particles with particle size above 100 nm was much more higher than the smaller particles. At initial burning with time less than 50 s, particle mass for cable fire at 28 L/min air flowrate was about 1.0E-2 g/cm$^3$, lower than the cable fires at lower air flowrates. This is possibly because at early burning, smaller particles are produced more than the larger particles due to an increase in the temperature profile. A high temperature would slow down the agglomeration process of the particles. From Figure 4.58 (f), the 3D Waterfall plot for PVC cable fire at air flowrate of 28 L/min shows a higher particle mass distribution compared to the cable fires at lower air flowrates. Other than increasing the burning of the fuel, the higher air flowrate would also reduce the development of burning temperature especially when the combustion was reaching the flame out condition. This would increase the agglomeration of particles to form larger particles, hence increased the particle mass. The highest particle mass distributions for PVC Prysmian A cable fires at heat flux of 25 kW/m$^2$ and different air flowrates were up to 1.0E+2 g/cm$^3$.

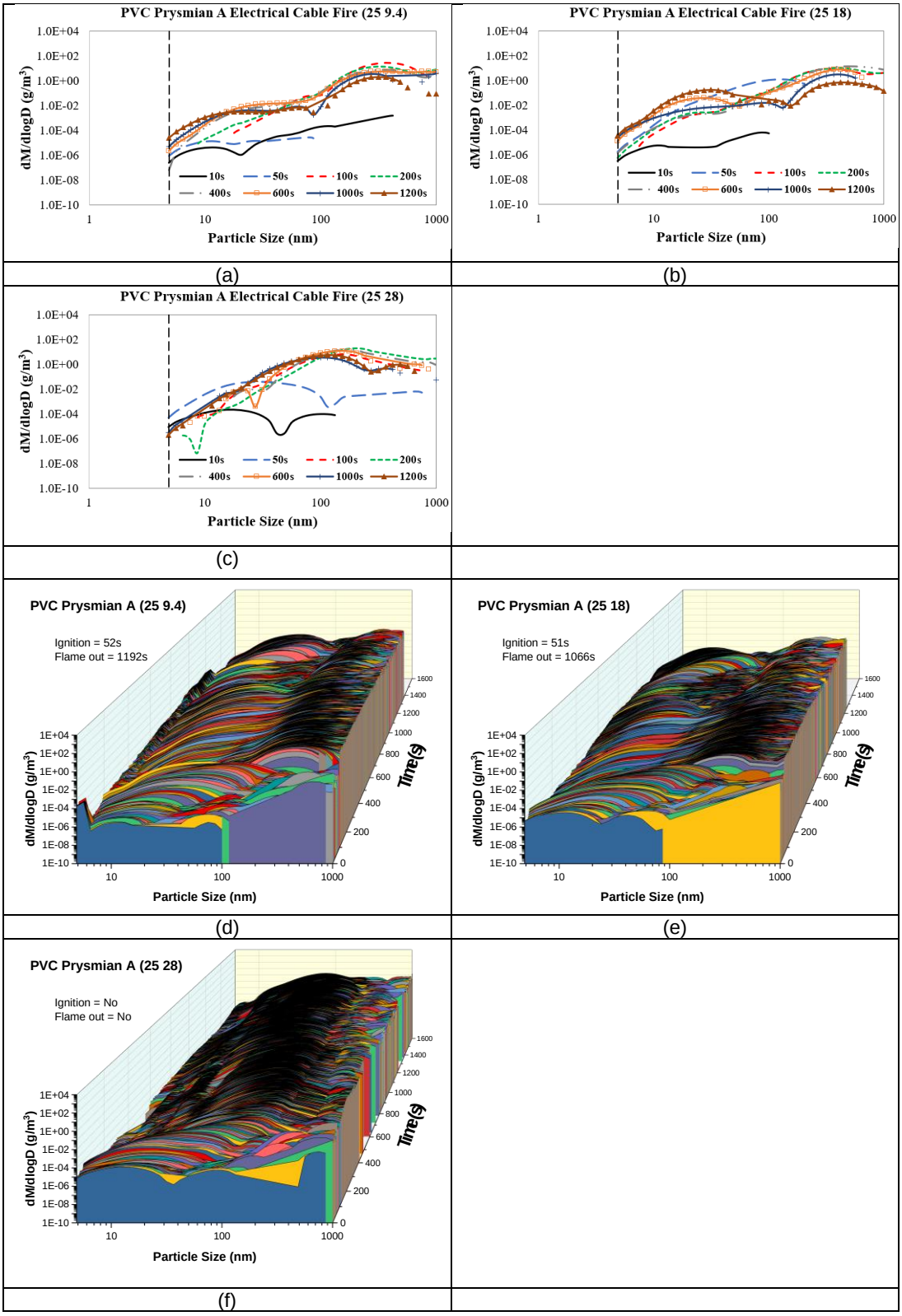


**Figure 4.58** Particle mass distributions from the burning of PVC Prysmian A cable at 25 kW/m$^2$ and various air flow rates.

Figure 4.59 shows size distributions for 10 nm and 100 nm particles from PVC Prysmian A cable fires at 25 kW/m$^2$ and various air flow rates. 100 nm particles gave a higher mass distribution than 10 nm particles for all three air flowrates. The gap in mass distribution between 10 nm and 100 nm particles were high and the highest for the cable fire at air flowrate of 28 L/min compared to the lower air flowrates. In comparison with lower air flowrates of 9.4 and 18 L/min, smoke obscuration was lower for the cable fire at a higher air flowrate of 28 L/min. It can be concluded that the higher ventilation rate, the lower smoke obscuration will be. The possible reason is excess air would disperse and dilute the particles in smoke, hence decreased the obscuration level caused by the smoke. In terms of escape capability, well ventilated fires provide more chance of escape compared to under ventilated fires because it give a lower smoke obscuration level. The average particle mass concentration for 10 nm particles was 1.0E-4 g/cm$^3$ and for 100 nm particles was about 1.0E+0 g/cm$^3$.

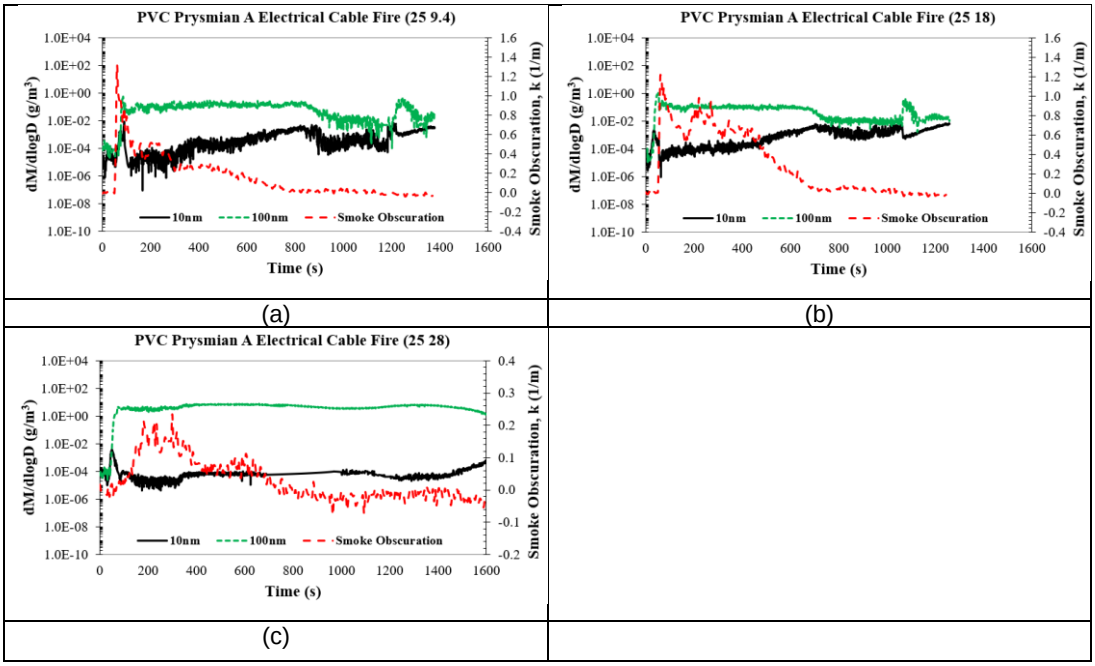


**Figure 4.59** Size distributions for 10 nm and 100 nm particles from PVC Prysmian A cable fires at 25 kW/m$^2$ and various air flow rates.

Particulate cumulative mass for PVC Prysmian A cable fires at 25 kW/m$^2$ and various air flow rates is shown in the following Figure 4.60.The calculated cumulative mass of particulate was the highest for PVC Prysmian A cable fire at the highest air flowrate of 28 L/min with the value of >20000 g/m$^3$. The cable

fires at lower air flowrates gave the maximum particulate cumulative mass of about 15000 g/m$^3$. It showed that well ventilated fires produced more nanoparticles with particle size <300 nm than under ventilated fires. As shown in Figure 4.60, the cumulative mass was peak for 200 nm particles for PVC cable fire at air flowrate of 28 L/min. At air flowrate of 18 L/min, 400 nm particles gave the highest peak of cumulative mass while the highest cumulative peak for cable fire at air flowrate of 9.4 L/min was shown by 300 nm particles. Cumulative mass values for particle sizes above 600 nm were low for these cable fires.

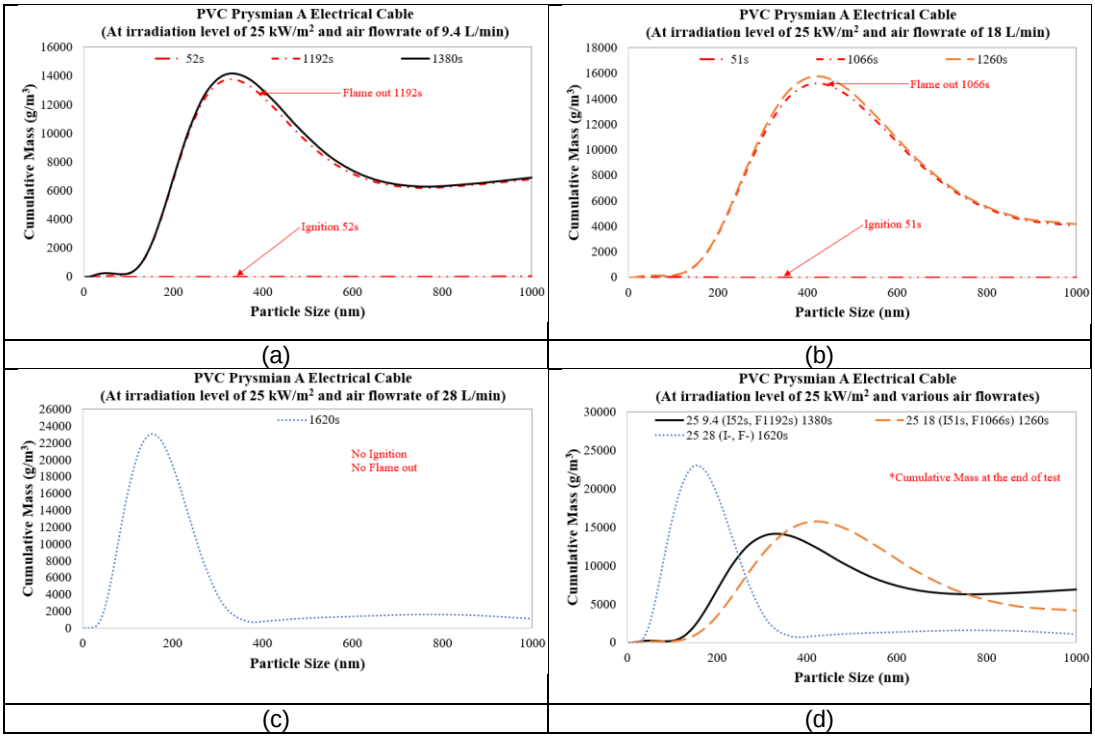


**Figure 4.60** Particulate cumulative mass for PVC Prysmian A cable fires at 25 kW/m$^2$ and various air flow rates.

Particle mass distributions for PVC Prysmian A cable fires at irradiation level of 35 kW/m$^2$ with various air flowrates as shown in Figure 4.61 gave a range from 1.0E-7 g/cm$^3$ and 1.0E+2 g/cm$^3$. For these cable fires, the particle mass had decreased with the increase of particle size with larger particles were giving a higher mass concentration. At this heat flux, the varying air flowrates did not show an obvious difference in the particle mass results. However, it was still identified that the free ventilation fire had given a slightly higher mass distribution for larger particles (1000 nm) compared to the restricted fires.

There were three particle mass peaks observed for cable fires at air flowrates of 9.4 and 18 L/min while for cable fires at other air flowrate of 28 L/min and free ventilation, there were only two particle mass peaks observed. All these peaks represented different size of particles.

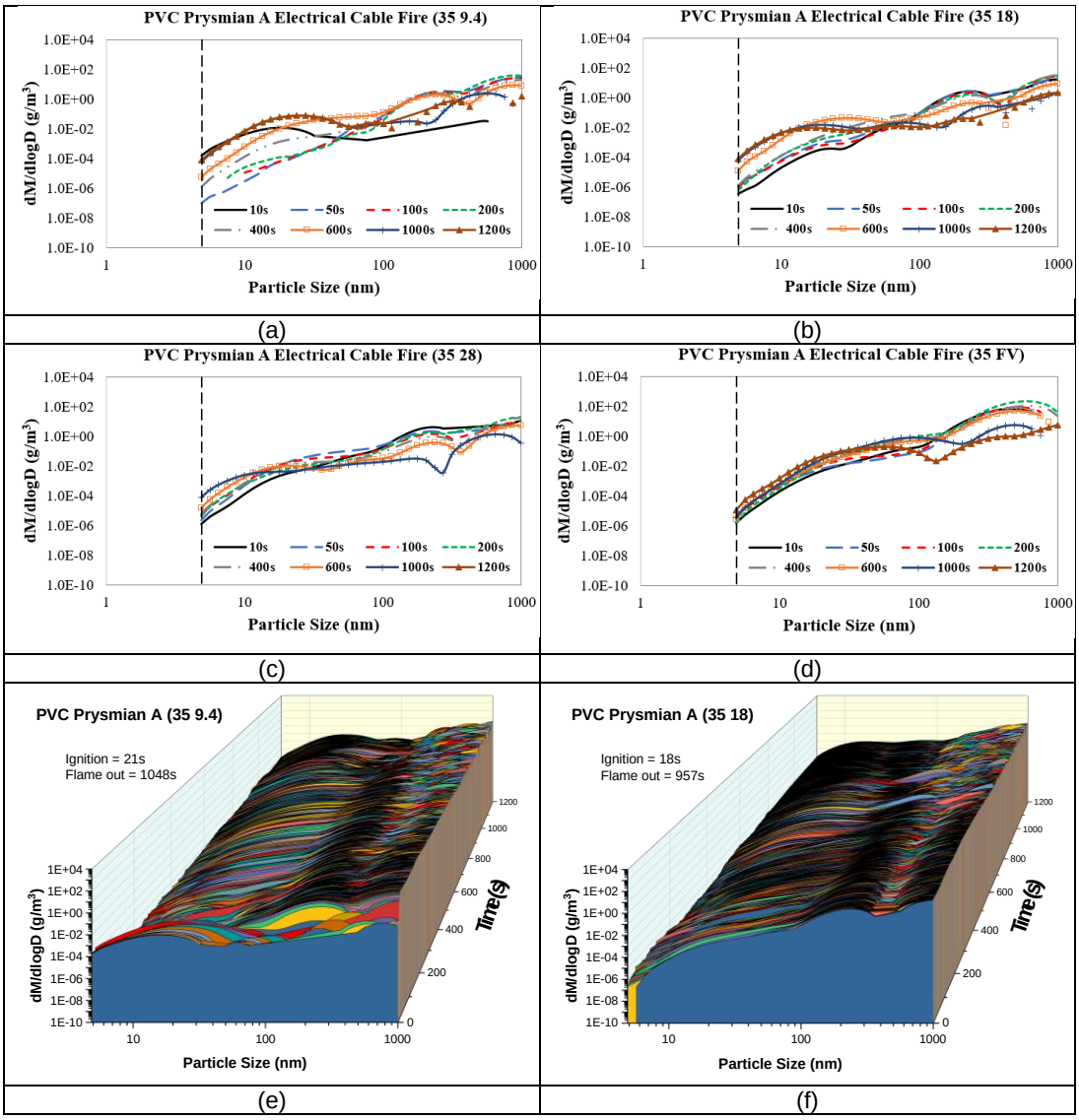

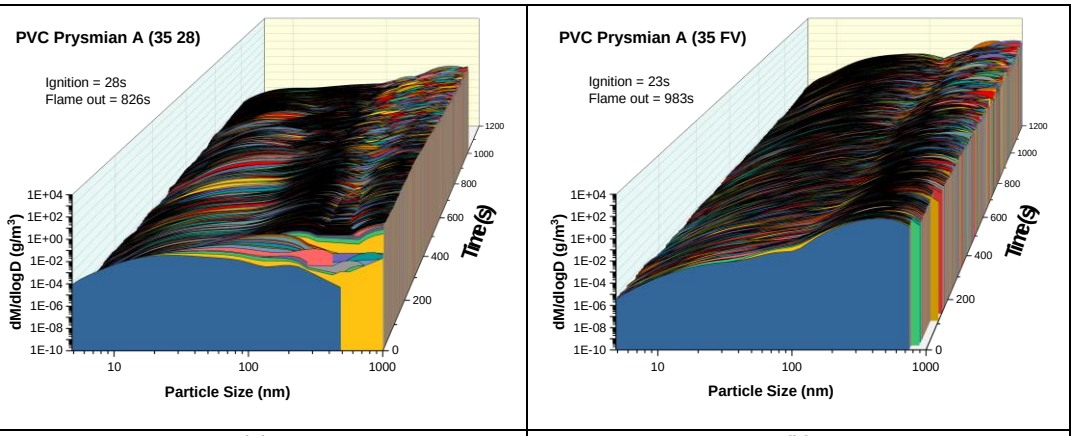


(g) (h)

**Figure 4.61** Particle mass distributions from the burning of PVC Prysmian A cable at 35 kW/m$^2$ and various air flow rates.

Figure 4.62 shows size distributions for 10 nm and 100 nm particles from PVC Prysmian A cable fires at 35 kW/m$^2$ and various air flow rates. Free ventilation fire showed higher particle mass distributions for both 10 nm and 100 nm particle sizes than restricted fires. 100 nm particles were giving a higher mass concentration compared to 10 nm particles for these cable fires. For 10 nm particles, the minimum mass distribution level was lowest for cable fire at air flowrate of 9.4 L/min which was about 1.0E-6 g/cm$^3$ with other air flowrates gave a minimum mass distribution level of about 1.0E-4 g/cm$^3$. Free ventilation fire showed the lowest smoke obscuration level compared to other three restricted fires. For restricted fires under exposure to this 35 kW/m$^2$ of heat flux, the smoke obscuration level had shown an increase with the increasing of air flowrate value. At discussed earlier for cable fires at lower heat flux (25 kW/m$^2$), the higher air flowrate value would reduce the smoke obscuration level. But for cable fires at heat flux of 35 kW/m$^2$, it gave opposite results where the higher air flowrate value, the higher smoke obscuration level. The results showed that the exposure temperature played an important role in reducing the agglomeration process of smoke particulates. It can be said that smaller particles would contribute to a higher obscuration level than the larger particles. In this case for the flaming restricted fires, the increasing air flowrate did not help much or insufficient in reducing the temperature or expediting the particle agglomeration. Hence, it increased the smoke obscuration level.

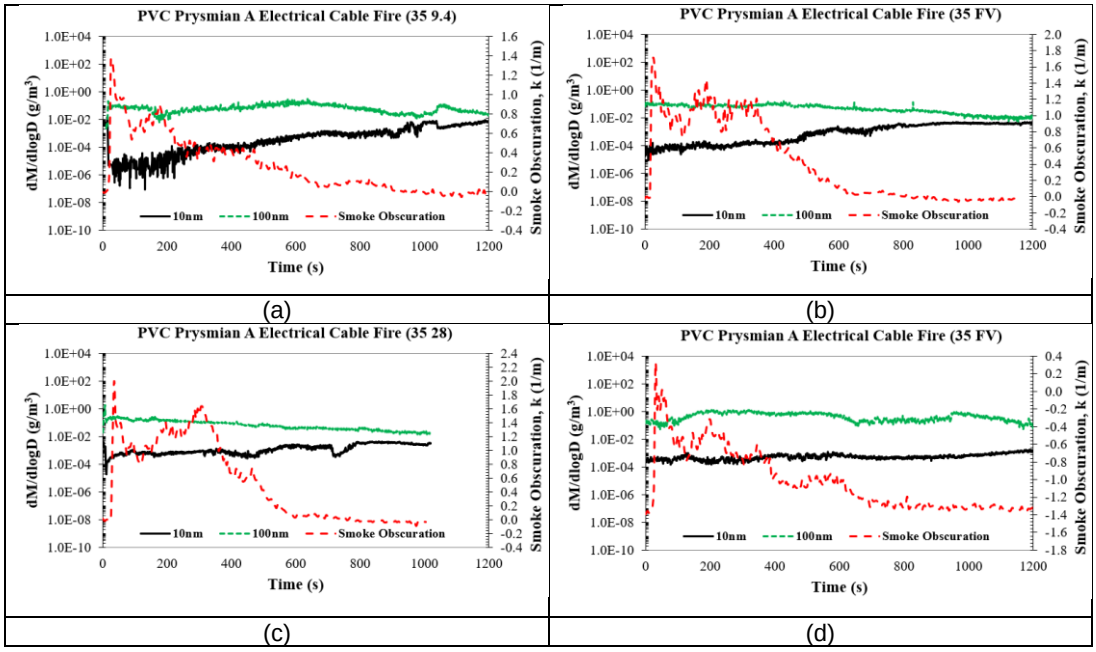


**Figure 4.62** Size distributions for 10 nm and 100 nm particles from PVC Prysmian A cable fires at 35 kW/m$^2$ and various air flow rates.

From Figure 4.63, with an increase in heat flux value, it showed an increase in particulate cumulative mass values. Particulate cumulative mass for PVC Prysmian A cable fires at 35 kW/m$^2$ and various air flow rates is shown in Figure 4.63. Cumulative mass for larger particles (>200 nm) was higher for all cable fires. For particle size less than 200 nm, the cumulative mass was below 5000 g/m$^3$. The free-ventilated cable fire gave the highest particulate cumulative mass with the maximum cumulative mass >4 times higher compared to these cable fires under restricted ventilation. Figure 4.63 shows that the cable fires with restricted ventilation condition have a higher number of particles larger than 1000 nm which are not measured directly by the particle sizer in the present work.

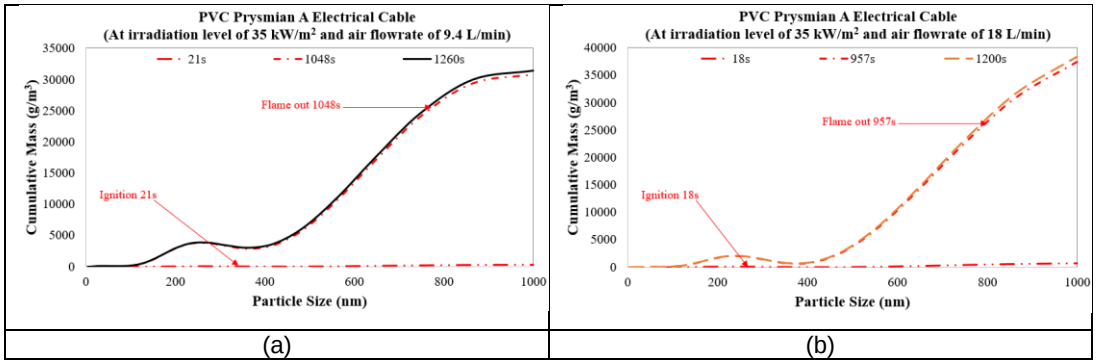

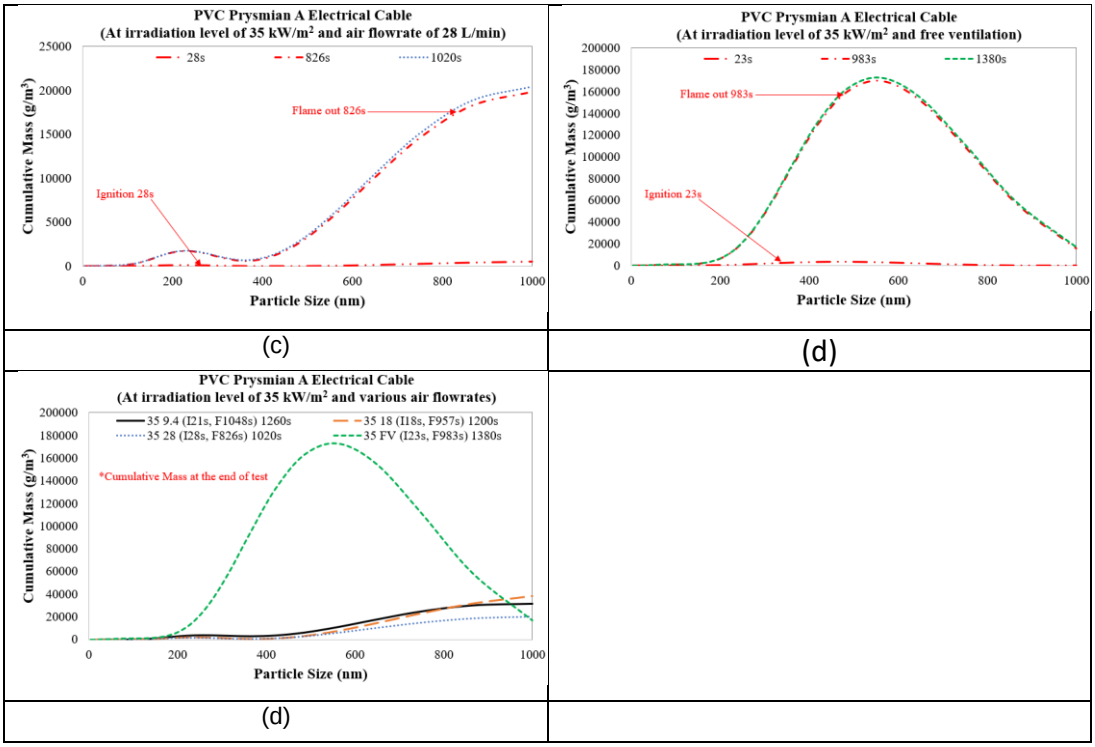


**Figure 4.63** Particulate cumulative mass for PVC Prysmian A cable fires at 35 kW/m$^2$ and various air flow rates.

At initial fire stage with burning time less than 50 s, there were three particle mass peak observed and after that period, only two particle mass peak were observed. Figure 4.64 shows particle mass distributions from the burning of PVC Prysmian A cable at 50 kW/m$^2$ and various air flow rates. At this irradiation level, the highest particle mass distribution was shown by the cable fire at air flowrate of 9.4 L/min. For this cable fire, particle mass concentration for larger particles were higher than other two cable fires at higher air flowrates. It showed that at air flowrate of 9.4 L/min, the amount of unburnt fuel was higher than at higher flowrates. Cable fires at this heat flux experienced a longer burning period with the increasing of air flowrate. With a lower air flowrate, the burning of the cable would reach the flame out state quicker due to insufficient air. This would be the reason of the higher particle mass value for the cable fire at air flowrate of 9.4 L/min.

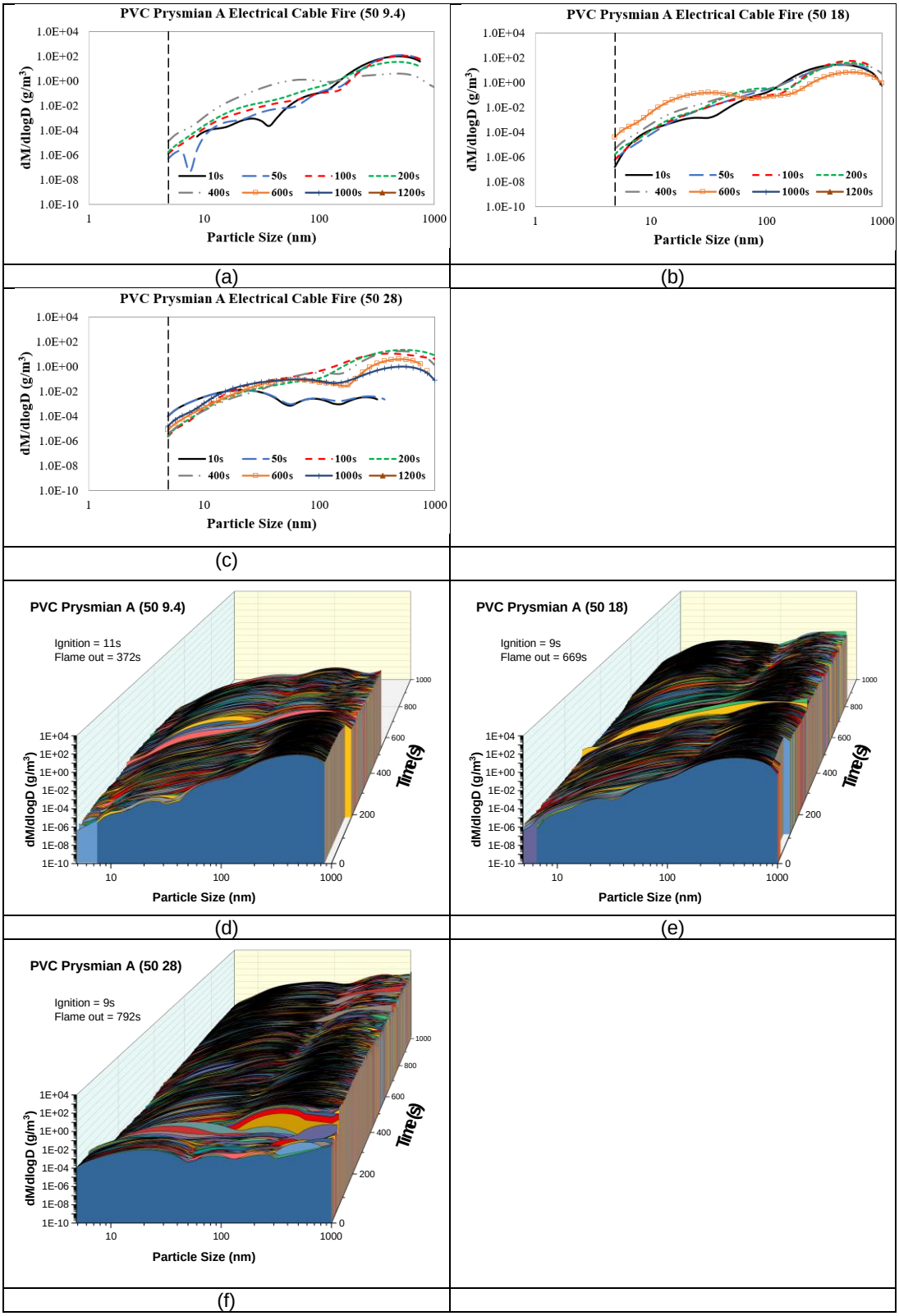


**Figure 4.64** Particle mass distributions from the burning of PVC Prysmian A cable at 50 kW/m$^2$ and various air flow rates.

Size distributions for 10 nm and 100 nm particles from PVC Prysmian A cable fires at 50 kW/m$^2$ and various air flow rates is shown in the following Figure 4.65. At this heat flux, particle mass distributions for these cable fires were range between 1.0E-5 g/cm$^3$ and 1.0E+0 g/cm$^3$ for these size of particles. Compared with the lower heat fluxes, mass concentration for 10 nm particles were higher for this heat flux. From Figure 4.65, 100 nm particles gave a higher particle mass concentration than 10 nm particles for these cable fires. Smoke obscuration level for cable fires at this heat flux increased with the increase of air flowrate. There were two peaks of smoke obscuration observed for cable fire at air flowrate of 18 L/min. The first peak after the start of ignition and the second peak at about 400 s. For this cable fire, the smoke obscuration level had decreased after 200 s before increased back at 300 s to reach the second peak. The highest smoke obscuration level, k was about 2.5 1/m which given by the cable fire at air flowrate of 28 L/min with other two cable fires were given k below 2.4 1/m.

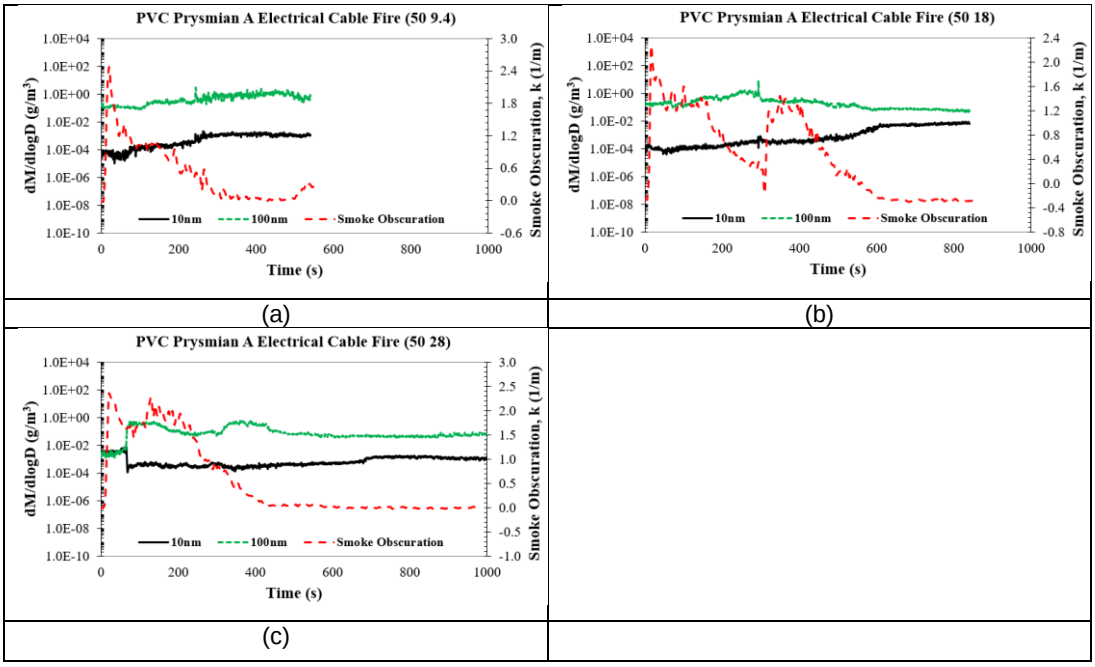


**Figure 4.65** Size distributions for 10 nm and 100 nm particles from PVC Prysmian A cable fires at 50 kW/m$^2$ and various air flow rates.

With a shorter burning period of <400 s and insufficient air, the cable fire at air flowrate of 9.4 L/min gave the highest peak of particulate cumulative mass which about 45000 g/m$^3$ if compared to the cable fires at higher air flowrates.

The other two air flowrates had shown the cumulative mass <35000 g/m$^3$. The higher value of cumulative mass by this cable fire is possibly due to a higher amount of unburnt fuel still left at the end of fire. While the cable fires at higher air flowrates contributed to a lower cumulative mass due to less unburnt fuel left from the combustion process. Following Figure 4.66 shows particulate cumulative mass for PVC Prysmian A cable fires at 50 kW/m$^2$ and various air flow rates. 500 nm particles had dominated the cumulative mass for these cable fires for all four air flowrates.

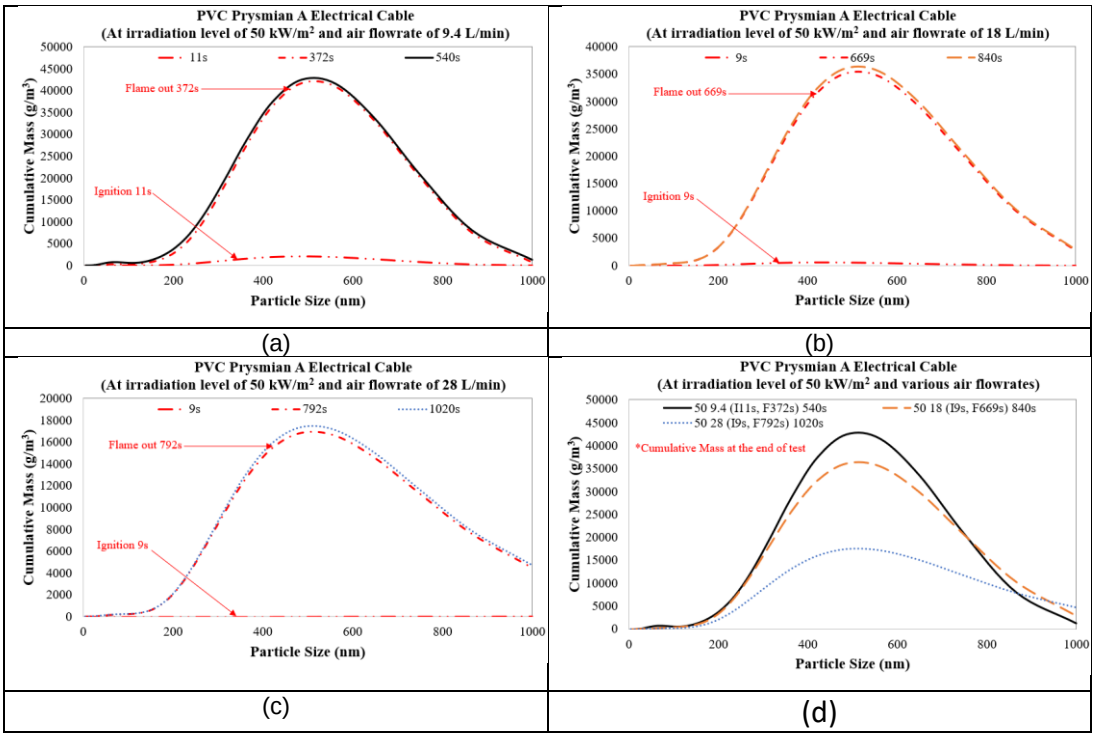


**Figure 4.66** Particulate cumulative mass for PVC Prysmian A cable fires at 50 kW/m$^2$ and various air flow rates.

### 4.4.3 Particle Size Distributions for Wind Turbine Cable Fires at Irradiation Level of 35 kW/m2 and Free Ventilation

Particle number distributions from the burning of Wind Turbine cables at 35 kW/m$^2$ and free ventilation are shown in Figure 4.67. AMI-G cable fire produced higher number concentration of larger particles compared to AMI-B cable fire. AMI-B cable fire produced no particles which were larger than 500 nm. AMI-G cable sample burned about 3 times longer (~3000 s) than AMI-B cable sample (~1000 s). This could be a reason why AMI-G cable fire had produced more larger particles than AMI-B cable fire. Under free ventilation

condition, especially at the end of combustion process when the fire had almost reached the flame out state, the supplied air would dilute the area and reduce the hot area surrounding and this would allow the particles to agglomerate to form larger particles. From Figure 4.67 (c), it showed that number concentration for 10 nm particles were higher than 100 nm particles for AMI-G cable fire. Meanwhile for AMI-B cable fire, number concentration for 10 nm particles were higher compared to 100 nm particles at burning time up to 100 s and from 400 s to 700 s of burning period. From 3D Waterfall plot, it is obviously shown that AMI-G cable fire has produced large number of particles with size range from 100 to 1000 nm, unlike AMI-B cable fire which has produced no particles larger than 500 nm.

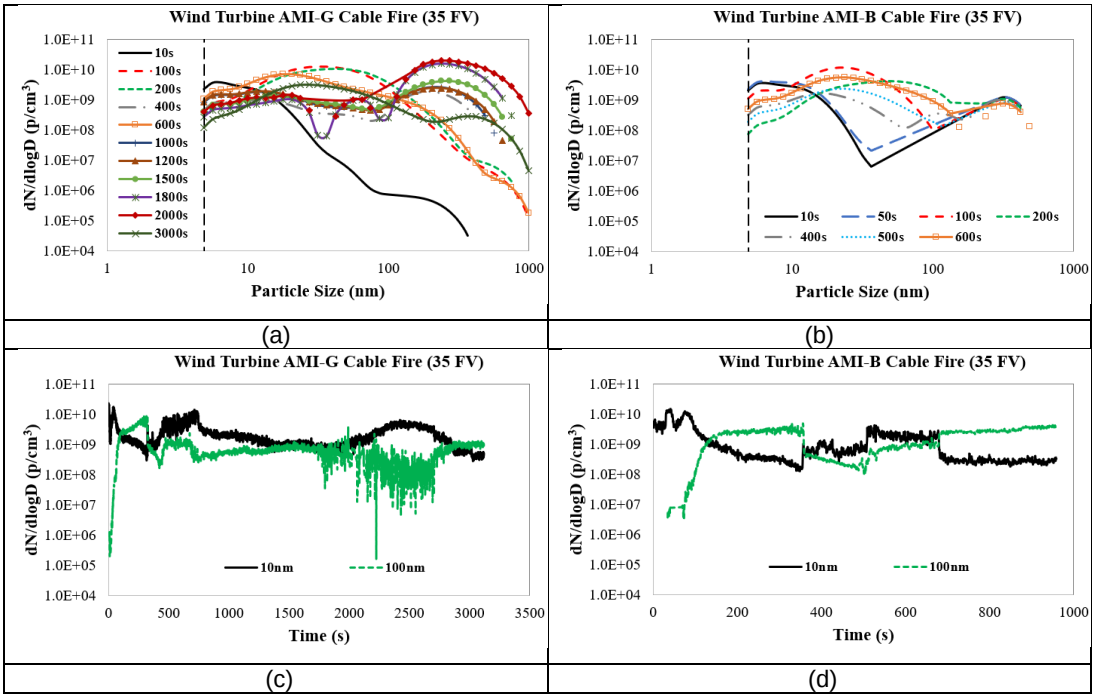

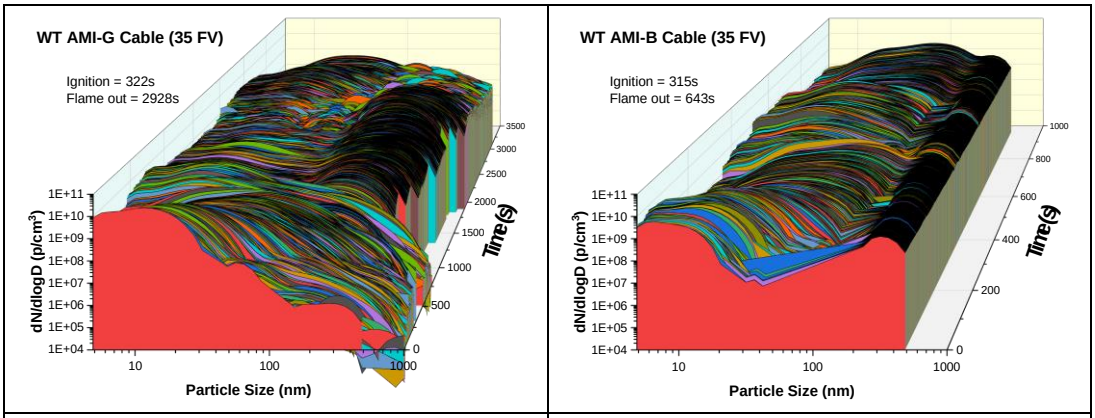


(e) (f)

**Figure 4.67** Particle number distributions from the burning of Wind Turbine cables at 35 kW/m$^2$ and free ventilation.

The highest particle mass concentration of about 1.0E+3 g/cm$^3$ was shown by AMI-G cable fire while the particle mass concentration for AMI-B cable fire was below than 1.0E+2 g/cm$^3$. The large different in particle mass distribution between both cable fires was due to higher number of larger particles produced by AMI-G cable fire compared to AMI-B cable fire which contributed to a higher particle mass concentration. The following Figure 4.68 shows particle mass distributions from the burning of Wind Turbine cables at 35 kW/m$^2$ and free ventilation. From Figure 4.68 (c) and (d), the particle mass distributions for 10 nm and 100 nm particles for both fires were in a range from 1.0E-4 g/cm$^3$ and 1.0E+0 g/cm$^3$. For particle sizes below than 100 nm, both fires showed a similar high particle number and mass distributions. But, for particles larger than 100 nm, there was a huge different in particle number and mass distributions for both cable fires. The different could be seen clearly from the 3D Waterfall plot in Figure 4.68 (e) and (f) which AMI-G cable fire had shown a higher particle mass concentration than AMI-B cable fire.

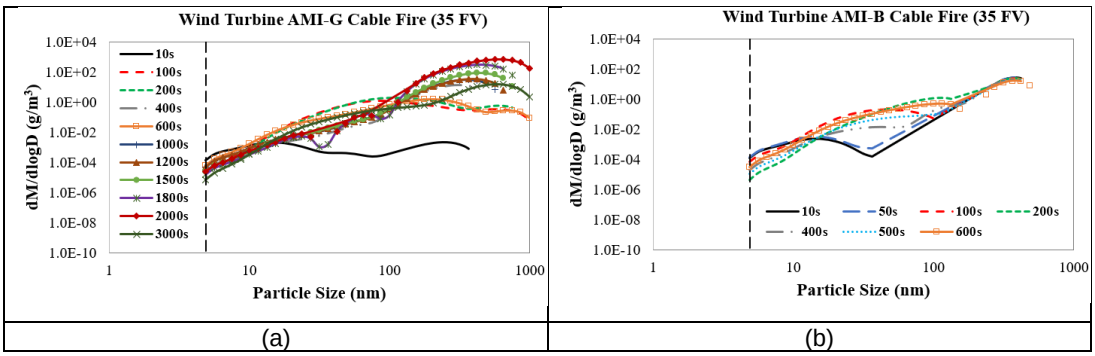


(a) (b)

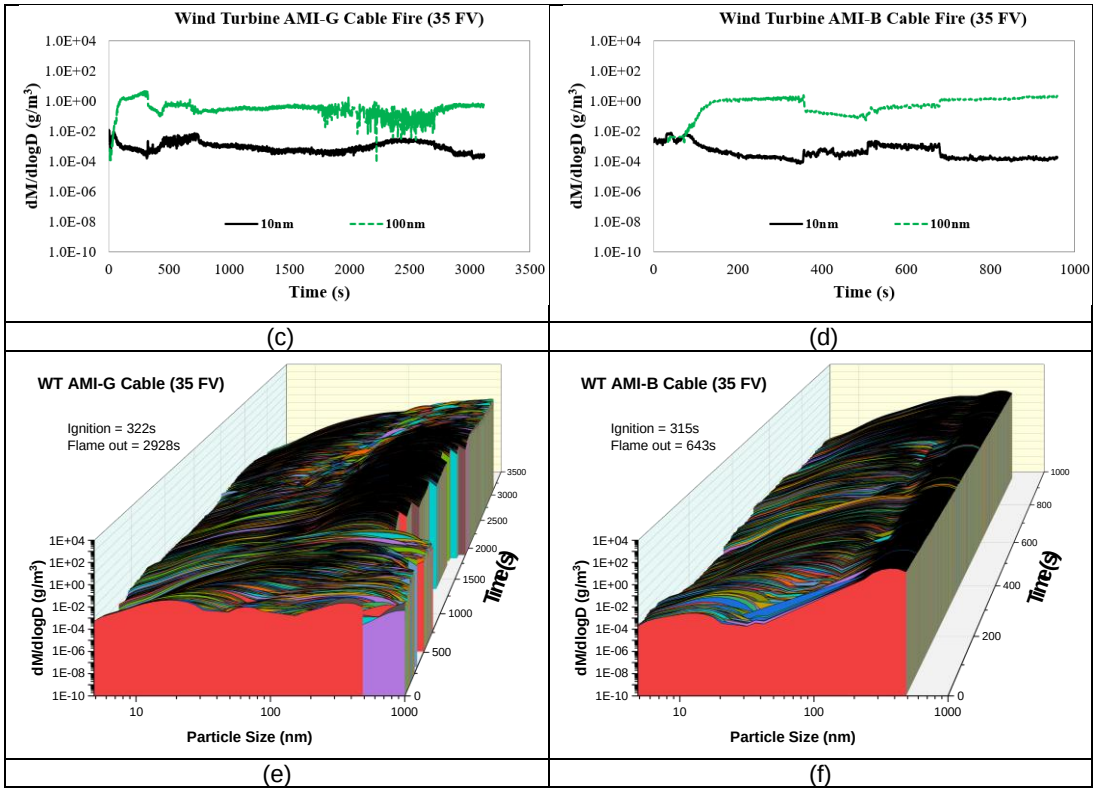


**Figure 4.68** Particle mass distributions from the burning of Wind Turbine cables at 35 kW/m$^2$ and free ventilation.

Figure 4.69 shows particulate cumulative mass in g/m$^3$ from the burning of Wind Turbine cables at 35 kW/m$^2$ and free ventilation. From particulate cumulative mass plots in Figure 4.69, the highest cumulative mass of ~600000 g/m$^3$ was given by AMI-G cable fire for 400 nm particles, >6 times higher than the cumulative mass of 400 nm particles shown by AMI-B cable fire. The cumulative mass for AMI-G cable fire was higher than AMI-B cable fire for particle size ranges from 100 to 1000 nm. For particle size larger than 500 nm, AMI-G cable fire had lower cumulative mass values. The highest cumulative mass for AMI-G cable fire was about 300000 g/m$^3$ for particle size of 1000 nm. It is shown that for AMI-G cable fire, particles larger than 1000 nm are in a high amount even it is out from the measurement scale of the particle sizer used in the present work. For AMI-B cable fire, no particles larger than 600 nm produced and measured in the present work.

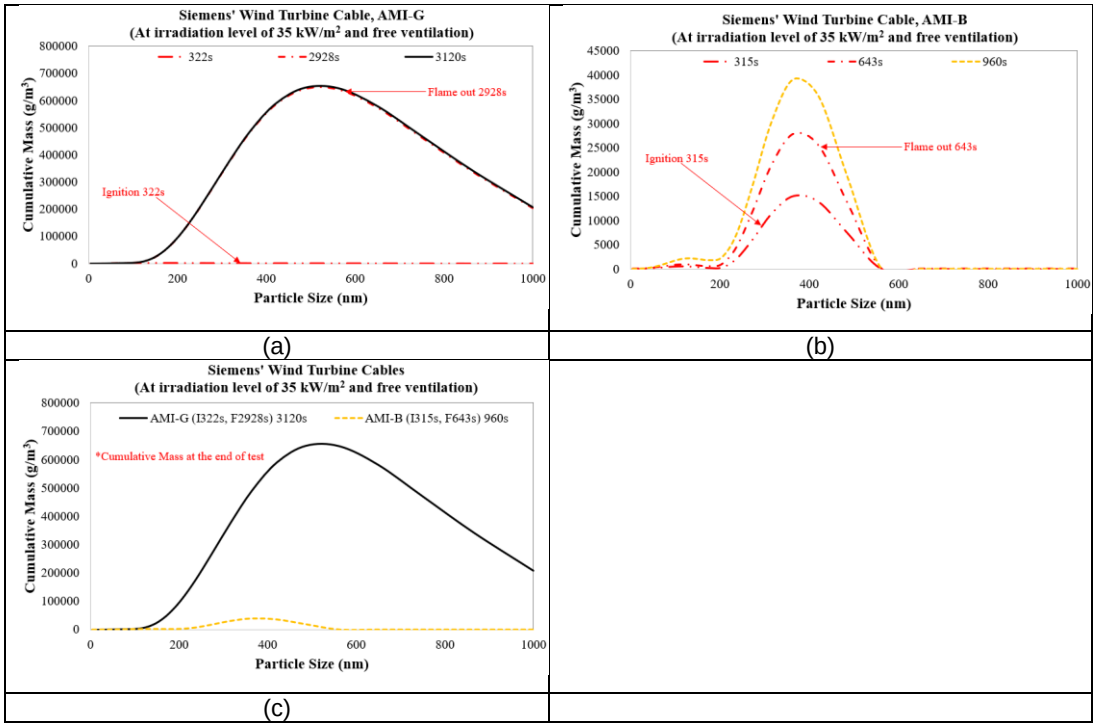


**Figure 4.69** Particulate cumulative mass from the burning of Wind Turbine cables at 35 kW/m$^2$ and free ventilation.

### 4.4.4 Particle Size Distributions for Other LSZH Cable Fires at Irradiation Level of 35 kW/m2 and Free Ventilation

Figure 4.70 shows particle number distributions from the burning of other LSZH cables at 35 kW/m$^2$ and free ventilation. Particle number concentrations for these LSZH cable fires were higher for particle size of 100 nm and below compared to particle size above 100 nm. In comparison between 10 nm and 100 nm particles, 10 nm particles gave a higher number distribution than 100 nm particles for both LSZH cable fires. 6701B-W cable fires gave a higher maximum particle number concentration with the value of about 5.0E+10 p/cm$^3$ compared to Prysmian B cable fire with the maximum particle number concentration of about 1.0E+10 p/cm$^3$. Prysmian B cable fire had reached the flame out condition at 366 s and after that period the particle number concentration for larger particles had decreased. This is possibly due to agglomeration occurrence of smaller particles that forms larger particles. For 6701B-W cable fire, it reached the flame out condition at 758 s. For this cable fire, within burning period between 200 s to 600 s, the 3D Waterfall plot as in Figure 5.70 (f) shows a high particle number concentration for particle size

above 100 nm. During this burning period, there could be due to the presence of liquid droplets which contributing to the larger size of particles.

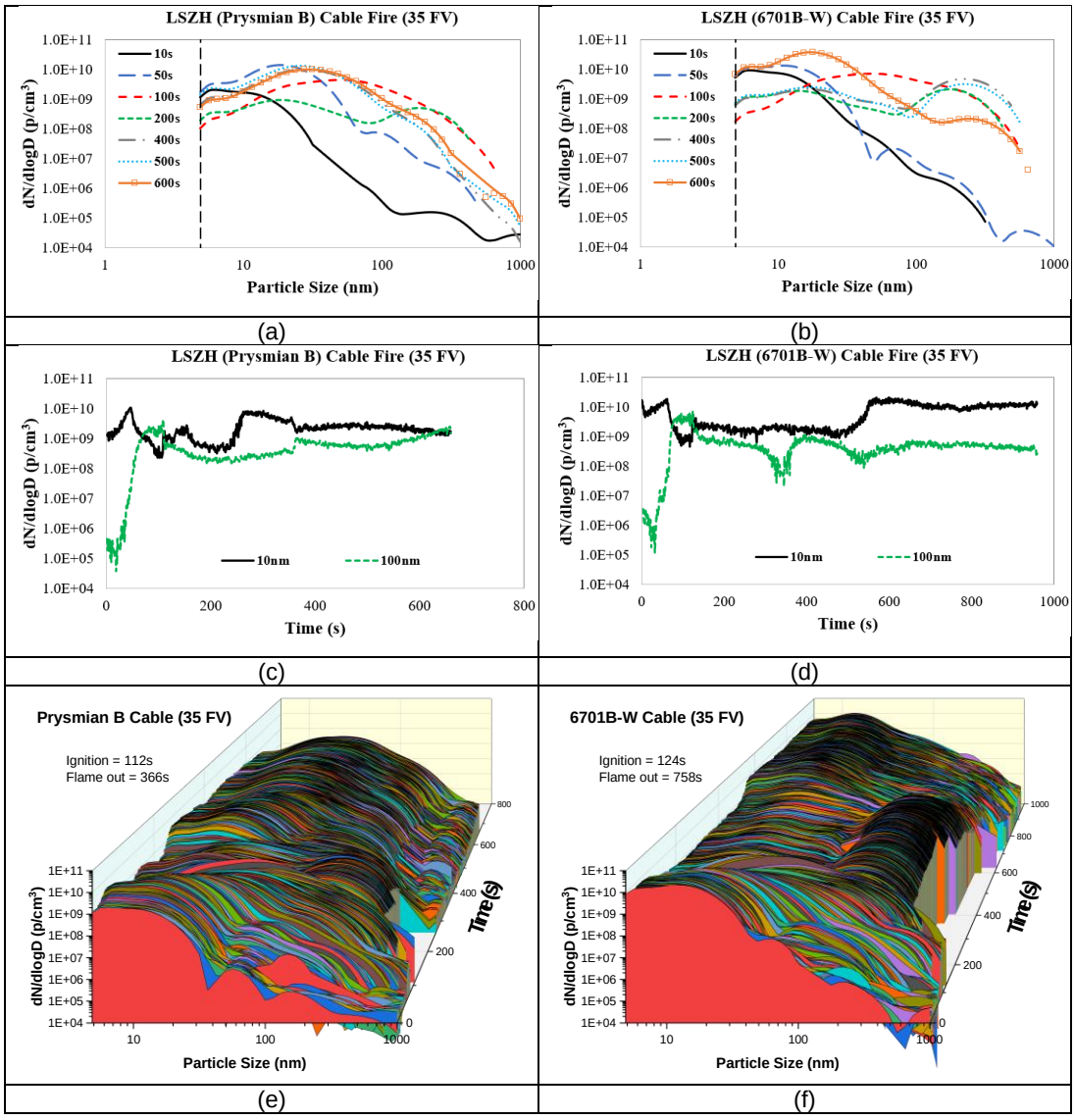


**Figure 4.70** Particle number distributions from the burning of other LSZH cables at 35 kW/m$^2$ and free ventilation.

The following Figure 6.71 shows particle mass distributions from the burning of other LSZH cables at 35 kW/m$^2$ and free ventilation. Particle mass concentration for 6701B-W cable fire was higher than Prysmian B cable fire for particle size above 100 nm. Particle mass concentration of 10 nm particles was higher than particle mass concentration of 100 nm particles for both cable fires. In general, particle mass concentration had increased with the increase of particle size for most of fires. For these cable fires, the particle mass

distribution ranges from 1.0E-6 g/cm$^3$ to 1.0E+2 g/cm$^3$. Particle mass concentration for particle size lower than 100 nm was less than 1.0E+0 g/cm$^3$ while for particle size larger than 100 nm, the particle mass concentration was more than 1.0E+0 g/cm$^3$. From Figure 6.71 (f), it showed a high particle mass concentration for 6701B-W cable fire within the burning period from 200 s to 600 s for particle size above 100 nm. This was due to a large number of bigger particles produced during that period which contributed to a higher particle mass value. From the 3D plots, the empty spaces showed that particles with certain sizes were not produced for both cable fires, hence number and mass concentration for those particles were none or zero.

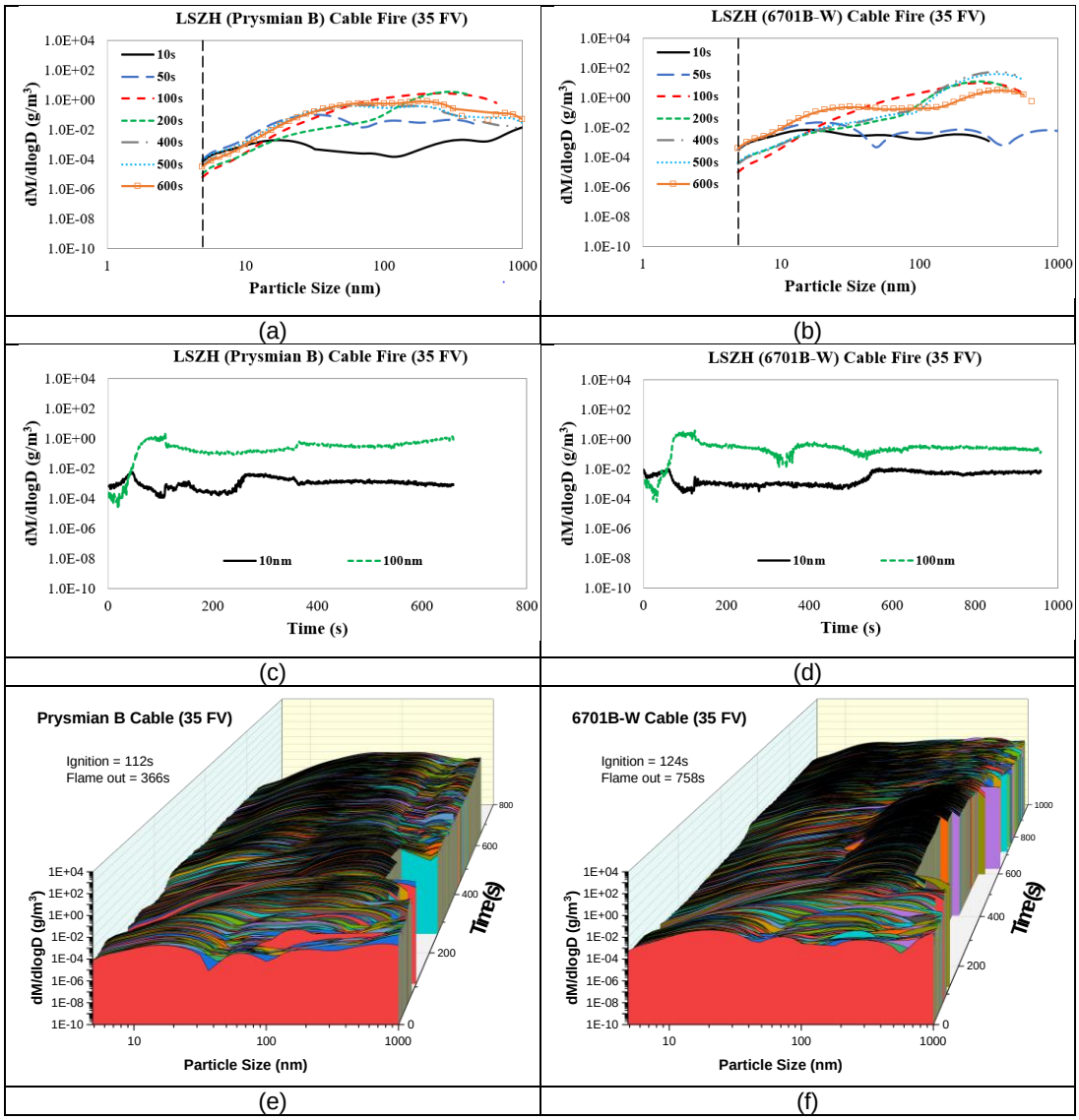


**Figure 4.71** Particle mass distributions from the burning of other LSZH cables at 35 kW/m$^2$ and free ventilation.

Particulate cumulative mass from the burning of other LSZH cables at 35 kW/m$^2$ and free ventilation is shown in Figure 4.72. For particle size from 100 nm to 700 nm, the particulate cumulative mass was higher for 6701B-W cable fire compared to Prysmian B cable fire. The highest cumulative mass of 30000 g/m$^3$ was given by 6701B-W cable fire for ~400 nm particles which in a factor of 12 at least compared to the cumulative mass by Prysmian B cable fire for the same size of particles. These cable fires showed insignificant mass value for particles larger than 700 nm. As shown in Figure 4.72 (a), the cumulative mass of 100 nm particles had increased in a factor of 2 from the start of ignition until the flame out state.

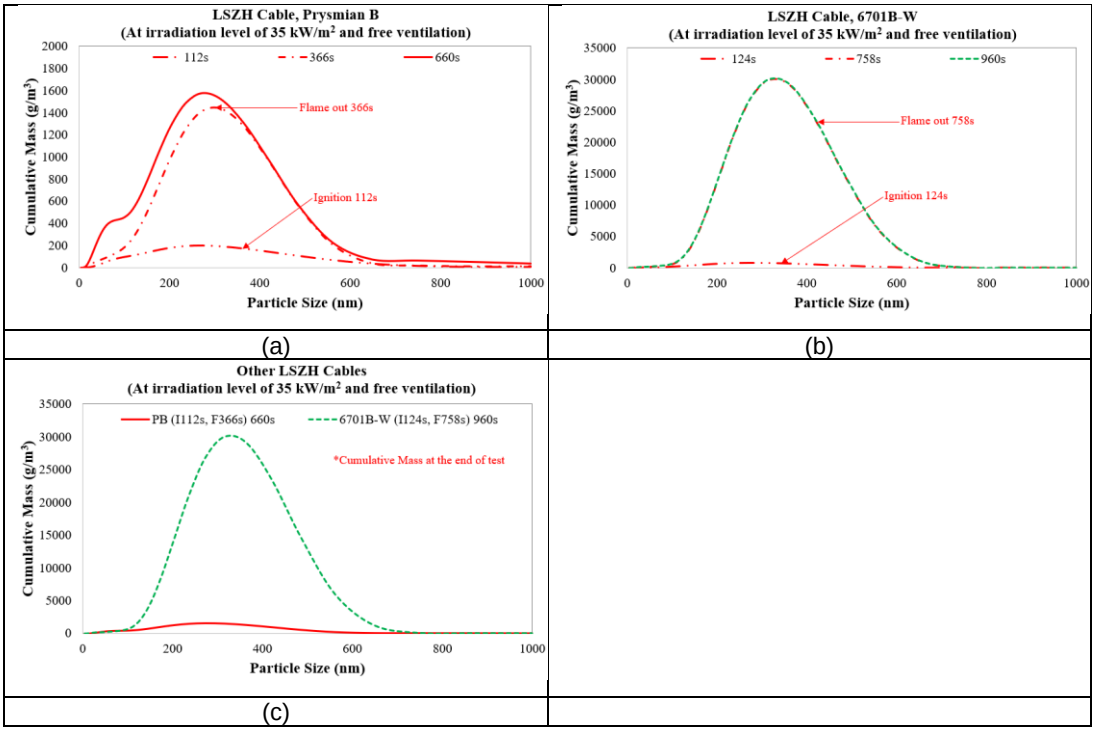


**Figure 4.72** Particulate cumulative mass from the burning of other LSZH cables at 35 kW/m$^2$ and free ventilation.

### 4.4.5 Particulate Yields for PVC Prysmian A Cable Fires at Various Heat Fluxes and Ventilation Rates

Particulate yields as a function of time for 10 nm and 100 nm particles for PVC Prysmian A cable fires at 25 kW/m$^2$ and various air flow rates are shown in Figure 4.73. At the same heat flux, the higher air flowrate value of these cable

fires showed the higher values of particulate yield. At the lowest air flowrate of 9.4 L/min, the yields of 10 nm and 100 nm particles were in a range from 1.0E-07 g/g to 1.0E-02 g/g, the results showed the smallest different in yields of both particulate sizes compared to the cable fires at the higher air flowrates. As shown in Figure 4.73 (e), the 100 nm particles had given an average yield of 1.0E-01 g/g which was much more higher than the average yield for 10 nm particles (1.0E-04 g/g) for a non-flaming PVC cable fire at heat flux of 25 kW/m2 and air flowrate of 28 L/min. A richer fire condition with equivalence ratio values over 1.5 was shown by the PVC Prysmian A cable fires at air flowrates of 9.4 L/min and 18 L/min compared to the cable fire at a higher air flowrate of 28 L/min. Lower air flowrates with a rich fire condition are expected to give higher yields of larger particles (>100 nm) due to a higher amount of unburned fuel or soot formation. Figure 4.73 (f) showed that a higher ventilation rate would cause a leaner cable burning which releasing more smaller particles (<100 nm) compared to the cable fires at lower ventilation rates.

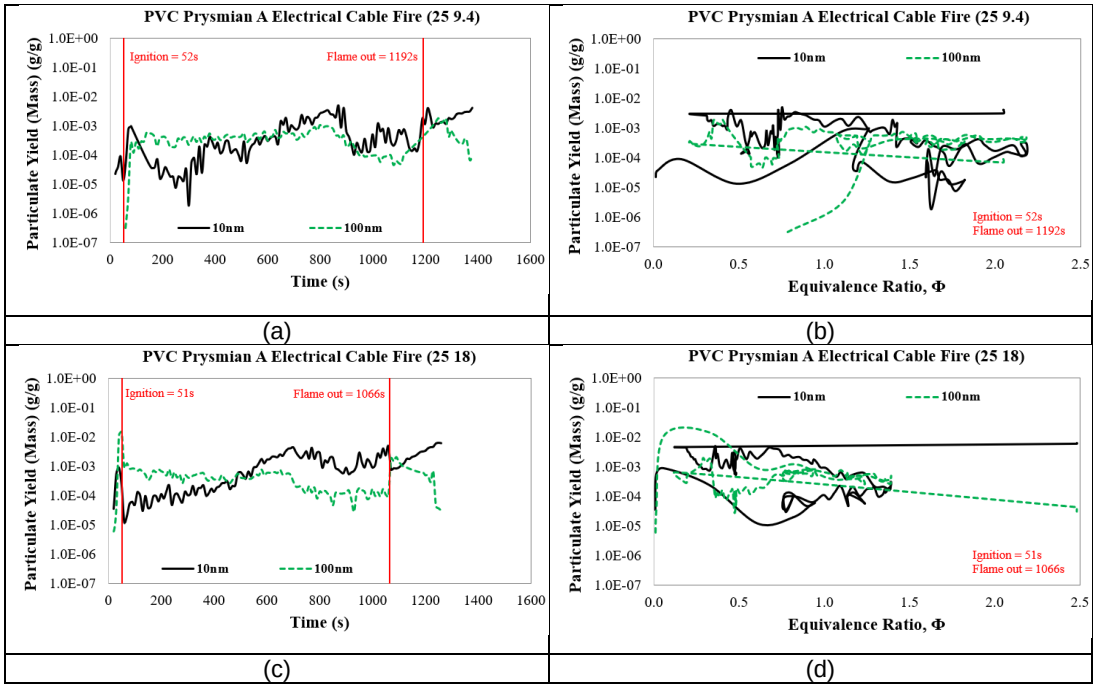

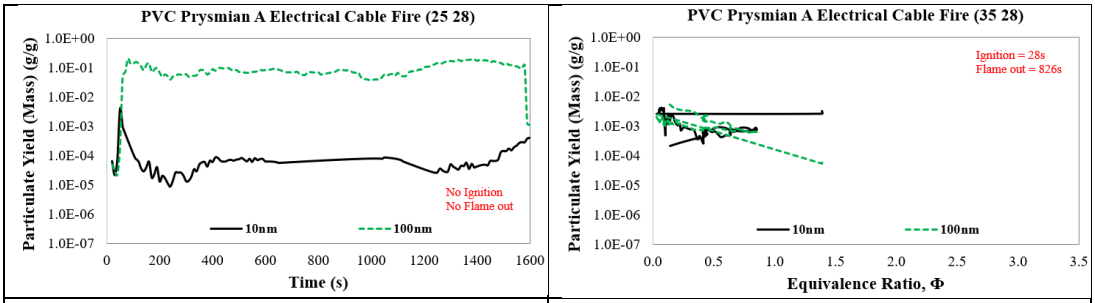


**Figure 4.73** Particulate yields for PVC Prysmian A cable fires at 25 kW/m$^2$ and various air flow rates.

With increasing of air flowrate value, it showed a higher gap in yields of 10 nm and 100 nm particles. Yields of 100 nm particles were higher than 10 nm particles for the burning period less than 600 s for most of these cable fires except for the highest air flowrate of 28 L/min. At air flowrate of 28 L/min (0.572 g/s), yields of 100 nm particles were higher than the yields of 10 nm particles throughout the overall cable burning. Formation of soot was the lowest for the cable fire at air flowrate of 28 L/min which showing a leaner fire condition with ER less than 1.5 compared to the cable fires at lower air flowrates and free ventilation which giving ER above 2.5. In comparison with the cable fires at a lower heat flux of 25 kW/m$^2$, the cable fires at this heat flux had shown lower yield values for 10 nm and 100 nm particles. Following Figure 4.74 shows particulate yields for PVC Prysmian A cable fires at heat flux of 35 kW/m$^2$ and various air flow rates.

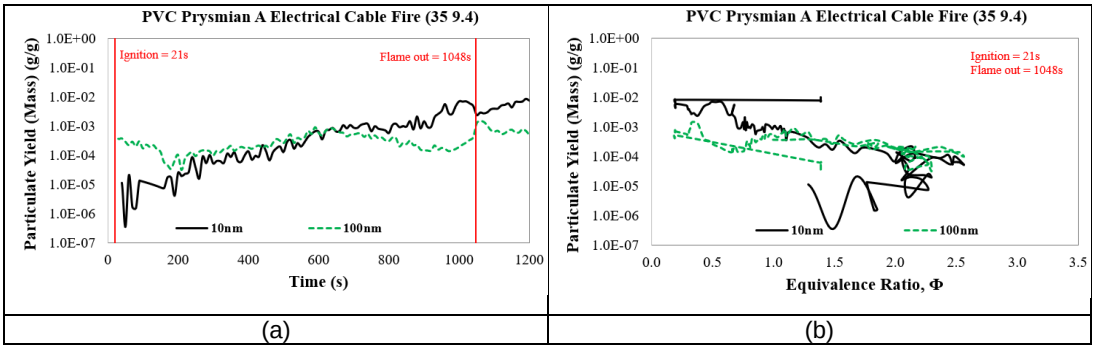

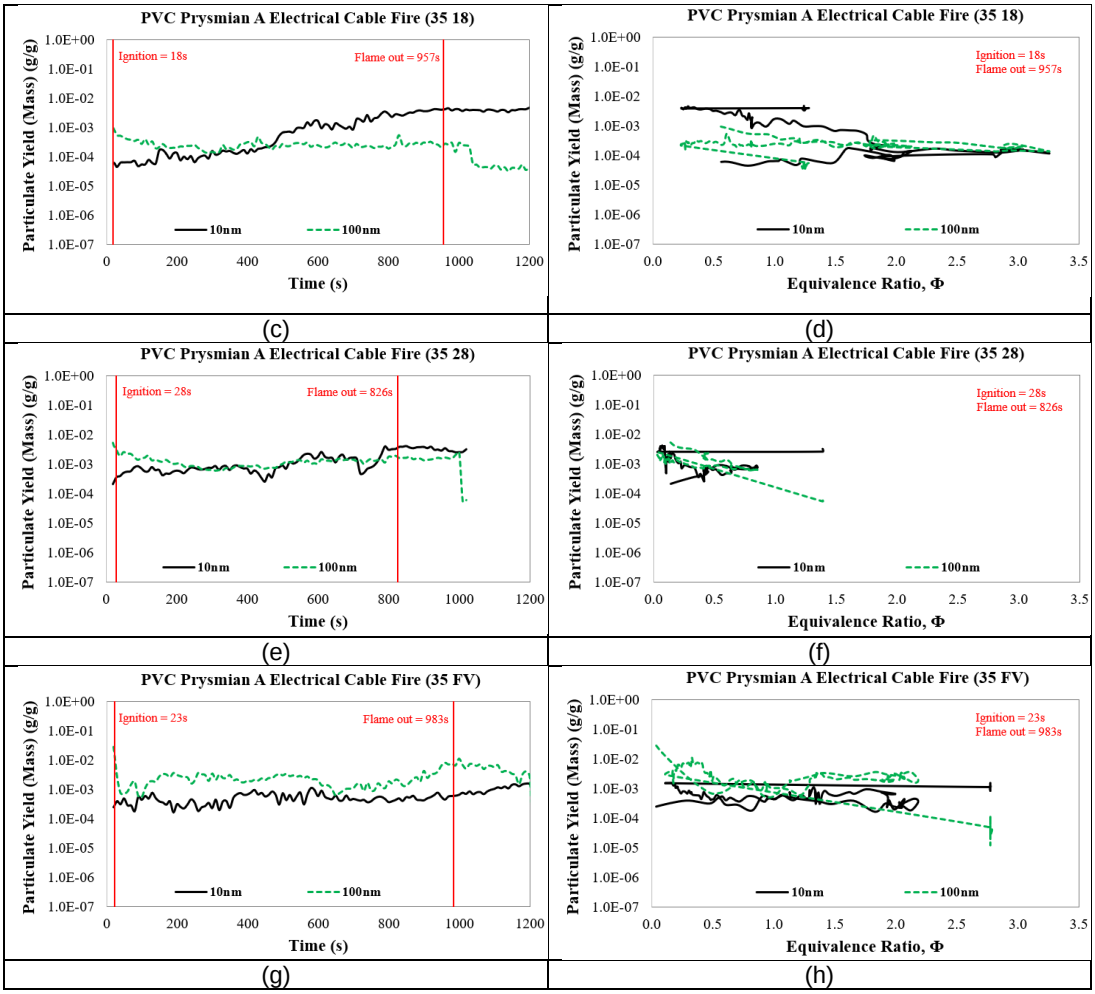


**Figure 4.74** Particulate yields for PVC Prysmian A cable fires at 35 kW/m$^2$ and various air flow rates.

Figure 4.75 shows particulate yield values for PVC Prysmian A cable fires at 50 kW/m$^2$ and various air flow rates. Yields of particulate from these cable fires at a higher heat flux of 50 kW/m$^2$ had shown an insignificant different if compared with 35 kW/m$^2$. In general, the higher of the heat flux, the shorter the burning period of the fuel will be. At this heat flux, an increase in air supply had given a richer fire equivalence ratio. PVC Prysmian A cable fire with the highest air flowrate of 28 L/min showed a richer fire condition with equivalence ratios up to 4.0 while the cable fires at lower air flowrates had given fire equivalence ratios less than 2.5. Most of these cable fires had reached a rich burning condition (ER>1.0) where it could be expected that the process would produce a high amount of soot in the end.

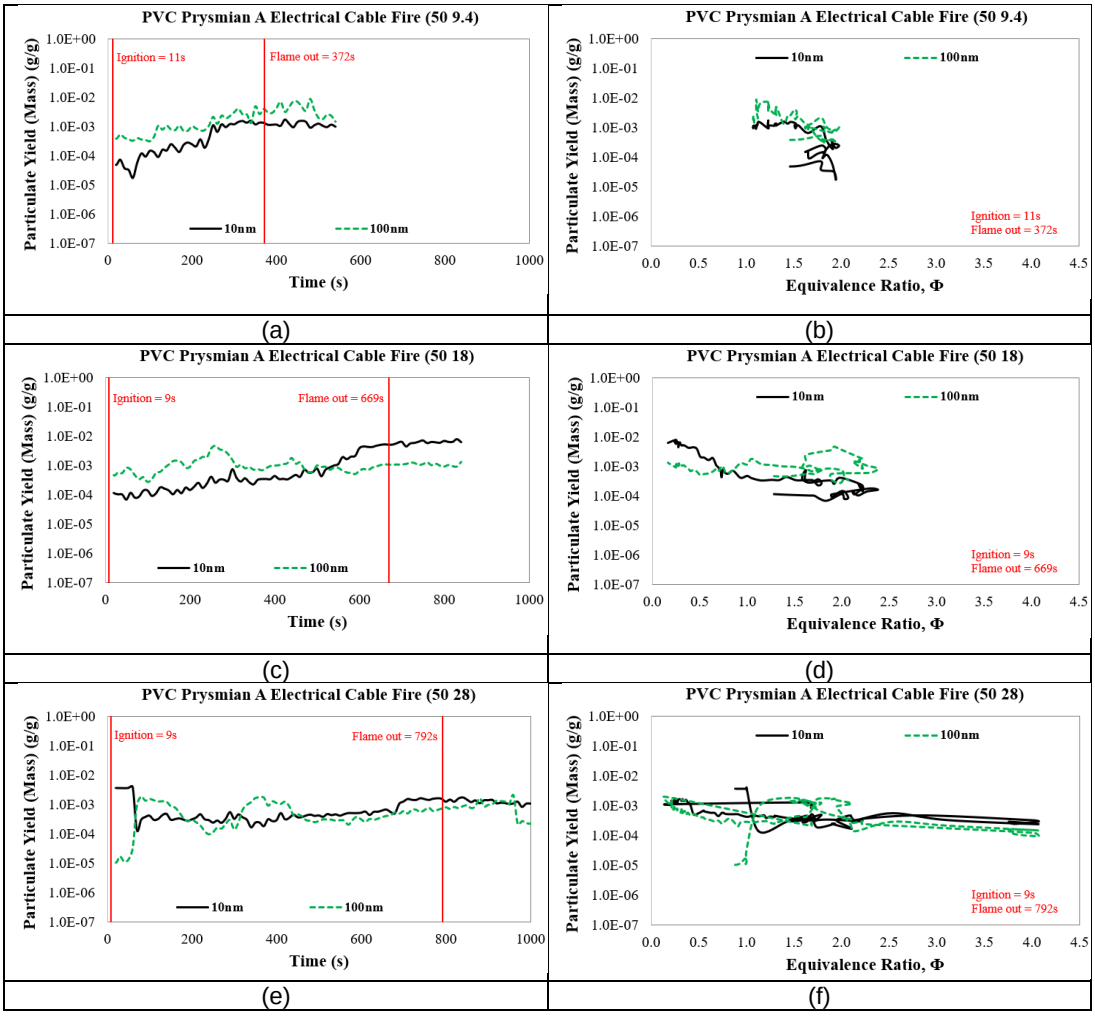


**Figure 4.75** Particulate yields for PVC Prysmian A cable fires at 50 kW/m$^2$ and various air flow rates.

### 4.4.6 Particulate Yields for Siemens' Wind Turbine Cable Fires at Heat Flux of 35 kW/m$^2$ and Free Ventilation

Particulate yields (number and mass) for two Wind Turbine cable fires at 35 kW/m$^2$ and free ventilation are shown in following Figure 4.76. Number yields for 10 nm particles was higher for AMI-G cable fire compared to AMI-B cable fire while for 100 nm particles, the number yields for both cable fires were giving a similar average of 1.0E+04 p/kg. AMI-G cable burning had shown a richer burning condition with ER>1.0 while AMI-B cable fire had a leaner fire condition with ER<0.4. For 10 nm and 100 nm particles, the difference in yield values is not really realised and identifiable but for larger size of particles (>100 nm), AMI-G cable fire is expected to give higher yield values than the AMI-B cable fire. However, the main focus of the present work is on the

particle sizes less than 100 nm which it could cause more severe effects (short or long term) than the larger size of particles. AMI-G and AMI-B cables were classified as Low Smoke Zero Halogen (LSZH) cables. But if compared these cable fires with the PVC Prysmian cable fire at the same fire conditions (irradiation level of 35 kW/m2 and free ventilation) as shown in Figure 7.44 (g), mass yields of 10 nm and 100 nm particles were higher for these LSZH cable fires. This is possibly because the richer fire condition (ER~3.0) experienced by PVC Prysmian A cable fire which has produced more soot or larger size of particles than the smaller size of particles (<100 nm) compared to the leaner AMI-G and AMI-B cable fires.

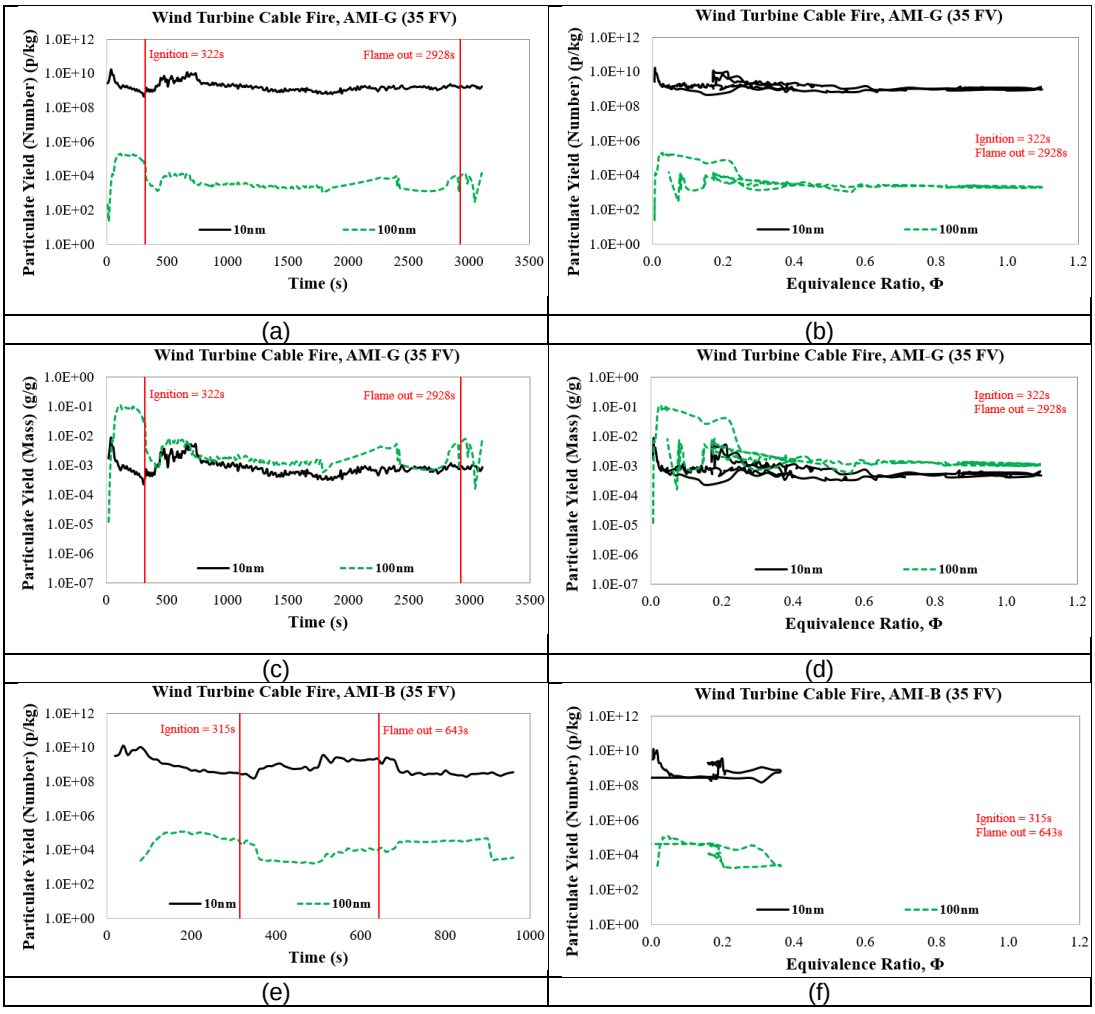

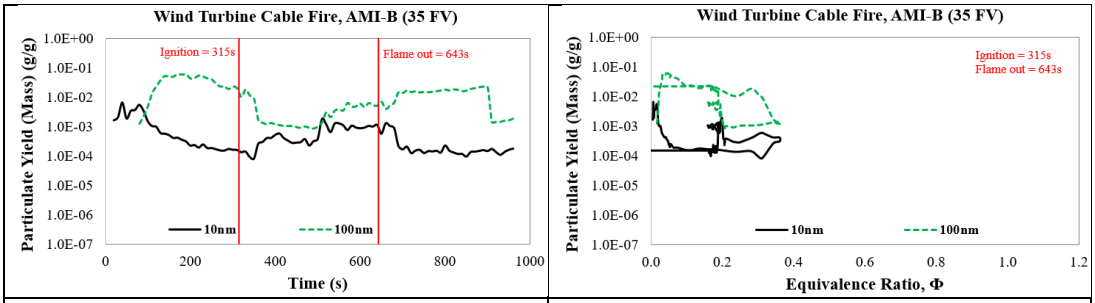


**Figure 4.76** Particulate yields (number and mass) for Wind Turbine cable fires at 35 kW/m$^2$ and free ventilation.

### 4.4.7 Particulate Yields for Other LSZH Cable Fires at Heat Flux of 35 kW/m$^2$ and Free Ventilation

The average number and mass yields of 10 nm particles for other LSZH cable fires such as Prysmian B and 6701B-W were 1.0E+10 p/kg and 1.0E-03 g/g. Meanwhile for 100 nm particles, the average number and mass yields for these cable fires were 1.0E+4 p/kg and 1.0E-02 g/g. These yield values were similar with the average values for Wind Turbine cable fires. The fire equivalence ratios for these Prysmian B and 6701B-W cable fires were less than 0.5 (lean fires). Between these four LSZH cable fires, only AMI-G had experienced a rich burning condition with ER>1.0. So, the burning of AMI-G cable would produce more soot or large particles under these fire conditions compared to other LSZH cable fires. 10 nm particles had shown higher values of number yields (p/kg) and lower mass yields (g/g) compared to 100 nm particles.

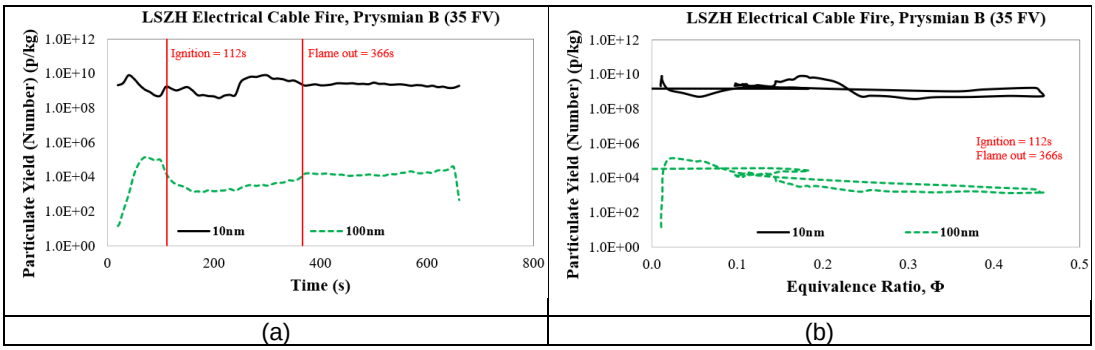

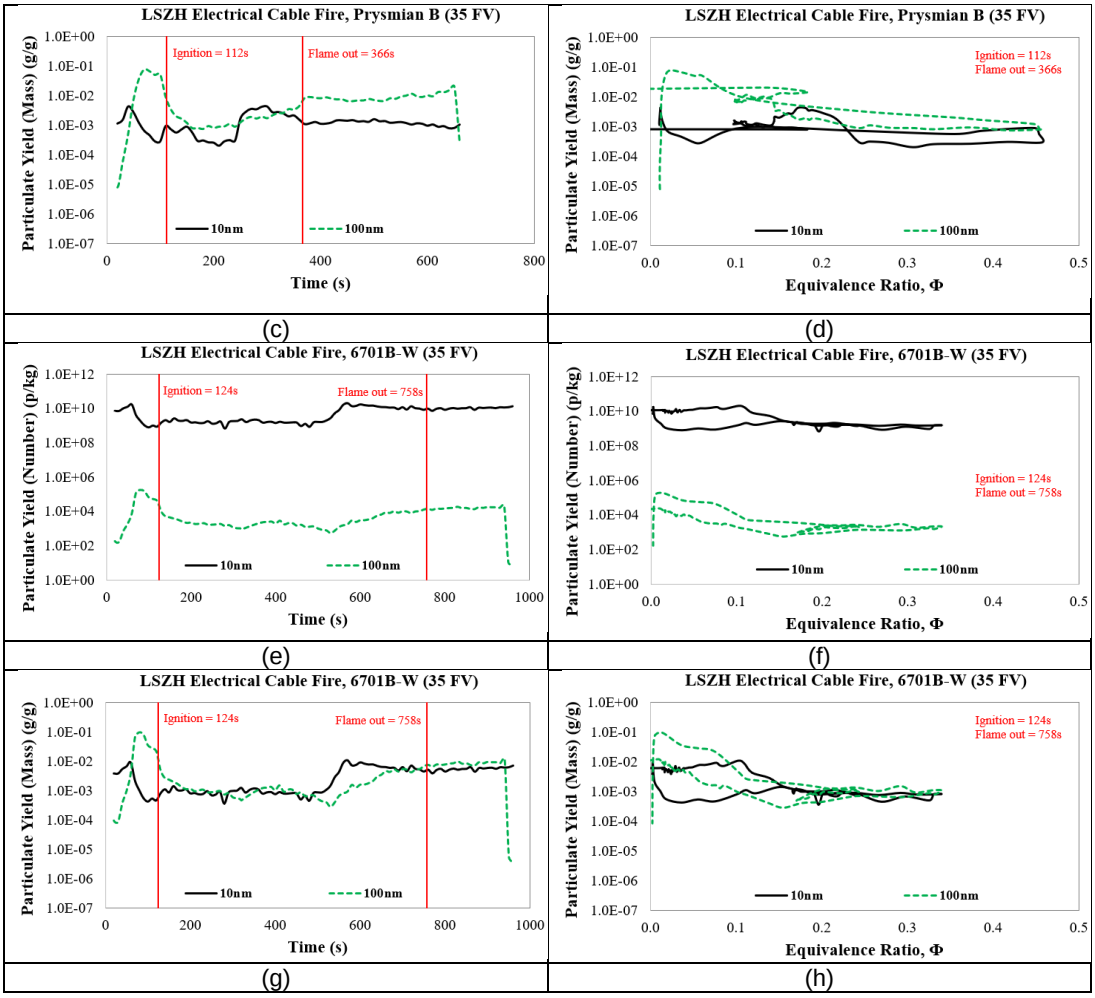


**Figure 4.77** Particulate yields (number and mass) for other LSZH cable fires at 35 kW/m$^2$ and free ventilation.

## 4.5 Findings and Conclusion from Electrical Cable Fire Tests

Main findings from various conducted electrical cable fires are as follow:

- PVC electrical cable fires such as PVC Prysmian A and FLEX1-BG produced HCl as the major product in the present work. The PVC Prysmian A cable fires under various heat fluxes and ventilation rates had resulted in a high emission of HCl which >20,000 ppm. The FLEX1-BG cable was not initially specified as a PVC cable due to insufficient information provided for the cable, but the result showed a high production of HCl (~50000 ppm) from its burning which was higher than the PVC Prysmian A cable fires. HCl emissions for Solar Energy cable fires (HV1-4C and HV2-3C) were also high and significant which were

up to 16000 ppm even the concentrations were lower than the HCl concentration released from the PVC Prysmian A cable fires. Other PVC cables like PVC EC-GB 1 and PVC EC-GB 2 had given HCl concentrations <1000 ppm. The emissions of HCl were lower for most of LSZH cable fires including the Wind Turbine cable fires.

- The FEC LC50 total toxicity had shown a higher average peak value from 10 to 12 with the increase of radiant heat from 25 kW/m$^2$ to 50 kW/m$^2$ for PVC Prysmian A cable fires. The highest LC50 value of 25 had been contributed by the FLEX1-BG cable fire compared to other electrical cable fires. Other electrical cables gave LC50 total toxicities <10 with PVC EC-GB1 and PVC EC-GB2 had resulted in the lowest LC50 total toxicities which were lower than 4. For $COSHH_{15min}$ total toxicity, the FLEX1-BG cable fire had the maximum value of ~16000 while most of PVC Prysmian A cable fires had given the maximum FEC $COSHH_{15min}$ of ~6000. Other cable fires gave lower values of the FEC $COSHH_{15min}$ (<4000). The determined AEGL-2 based total toxicities for all electrical cable fires were less than 3000 which most of these cable fires had shown the FEC AEGL-2 total toxicity values <1000.
- As summarised in Table 4.5, the highest CO yield of ~0.2 g/g had given by the PVC Prysmian A cable fire at heat flux of 50 kW/m$^2$ and air flowrate of 28 L/min. For all conducted electrical cable fires, $CO_2$ yields determined were less than 2.0 g/g. The maximum HCl yield of >0.4 g/g was given by the FLEX1-BG cable fire while the maximum HCl yield for PVC Prysmian A cable fires was ~3.0 g/g. LSZH electrical cable fires gave the lowest maximum HCl yields (<0.009 g/g) compared to other group of cable fires.
- Generally from the findings, it can be concluded that CO, Formaldehyde, Acrolein and Benzene were the main four species for most of electrical cable fires. HCl had also been the major toxic species for halogen (Cl) contained or fire retarded cable fires especially PVC Prysmian A, FLEX1-BG and Solar Energy cable fires. Then, indication of $NO_2$ as a major species was also realised for most of these cable fires especially before the point of ignition and during the post-flaming stage. $NO_2$ contribution as one of the major species had increased with the increase of ventilation rate. Most of these electrical cable samples are not a Nitrogen contained cable according to the elemental analysis results in Table 3.11. However the presence of $NO_2$ and HCN as one of major species from these cable fires could be due to the reaction of

the fuel with the Nitrogen in air. Some of the conducted electrical cable fires had also given $SO_2$ as one of the major toxic species.

- Fine particles are a toxic hazards in fires and must be measured for all materials used in fires and regulations need to be changed to make this compulsory. Particles below 100nm are a health hazard and the results from the present study show that these dominate the number of particles in PVC electrical cable fires. For most of electrical cable fires, the 10 nm particles were giving a higher number concentration than 100 nm particles. Larger particles had contributed to a higher value of mass concentration than the smaller particles (<100 nm). Particle mass distributions for 10 nm and 100 nm particles of all these cable fires were in a range from 1.0E-06 g/$m^3$ to 1.0E+00 g/$m^3$. Among all cable fires, the determined cumulative mass in g/m3 was the highest for 600 nm particles for PVC Prysmian A cable fire at heat flux of 35 kW/$m^2$ and free ventilation condition.
- Particles released from burning materials during fires include condensed droplets of various organic products but mainly of carbonaceous soot particles. Soot particles are mainly elemental carbon, but a variety of acid gases and organic vapours become adsorbed onto them. Mineral particles and fibres can also be released in building fires. Particles released from burning materials cover a wide size range from nanometre diameters up to 50-100 micrometres. Even larger particles on mm diameter scales are released in fires. From a toxicity perspective those measured historically have been in the inhalable (~10-100 microns) and respirable ranges depositing in the airways and alveolar regions of the lung (0.5-10 microns). Studies of combustion products have shown a high proportion of smoke particulates to be in the respirable range, exerting both acute and chronic effects on the airways (acute inflammation and chronic obstructive pulmonary disease) and lung (acute inflammation and chronic emphysema or fibrosis). More recently, especially with the development of measurement technology, interest has extended to fine and ultrafine (nanometre) particles in up to pm 2.5 microns. The smaller particles have been shown to be important components of air pollutants, mostly from combustion sources (especially vehicle emissions). The have also been shown to be capable of affecting not just the lungs, but also of penetrating and circulating in the bloodstream, causing a variety of systemic toxic effects (for example

promoting blood vessel atherosclerosis and clotting, or by carrying carcinogenic substances to different target organs).

- For this study I have therefore examined the extent to which burning cable materials products particles in the ultrafine range from 5-1000 nanometers. The results have shown that all materials tested produced very large numbers of particles over this size range, with a significant mass across the range. The implication of these findings is that smoke released when these materials may present a significant toxic health hazard when inhaled.

# Chapter 5
# Solid Foam Fires with Free Ventilation in the Cone Calorimeter Test

## 5.1 General Combustion Properties of Various Foam Fires

Polyurethane (PU) and Polyisocyanurate (PIR) foams such as Polyurethane foam from spray can (PU-FSC) and Polyisocyanurate insulation foam were investigated, similar to those used at Grenfell Towers. The results were compared with two other materials made from PU which were Polyurethane floor mat (PU-FM) and black foam used as packaging material (PU-FB) using the Cone Calorimeter with heated Gasmet FTIR analysis of toxic gases. The black packaging foam were identified as Polyurethane according to the obtained GCV value of 32 MJ/kg from ultimate analysis with the Bomb Calorimeter. PU-FSC and PIR-F GT were part of the fire load at Grenfell Towers Fire in London (2017). The PVC window frames were badly fitted and spray can polyurethane (PU) foam was used to fill the air gaps around the windows. It was a significant source of the fuel load in the external cladding fire spread. Two other PU foams were tested, the first was a door mat (PU-FM) and the second was packaging foam protection (PU-FB). The PIR foam (PIR-F GT) was the thermal insulating material used in the external cladding, which was the main source of the external spread of the fire. The materials were investigated using the Cone Calorimeter with 100 mm square sample size and each sample had different thickness. The Cone Calorimeter was operated in various irradiation modes for PIR-F GT fire tests (see Table 5.1) and for other foams, the tests were conducted at heat flux of 35 kW/m$^2$, in free ventilation condition for all solid foam tests. These cone tests were done with a raw heating sample gas taken from a chimney placed on the cone outlet. A heated Gasmet FTIR, calibrated for all species of interest in fire toxicity.

Test details for PIR foam fires (Grenfell Tower) at various irradiation levels with free ventilation were shown in Table 5.1 and test details for PU and PIR foam fires at 35 kW/m$^2$ irradiation level with free ventilation were shown in Table 5.2. PIR-F GT fires at lower heat fluxes (25 and 28 kW/m$^2$) showed no ignition. For tests at higher heat fluxes, all tests gave a flaming condition with an increase in heat irradiation value had given a decrease in ignition time delay. In comparison with other lower heat fluxes, the PIR-F GT fire test at the highest heat flux of 50 kW/m$^2$ took the longest time to burn before it reached the flame out at 567 s. From foam tests conducted at 35 kW/m$^2$ and free

ventilation, PIR-F GT fire was the earliest achieving an ignition (3 s), followed by PU-FSC (7 s), PU-FM (14 s) and PU-FB (19 s) fires. High density of PU-FM floor mat had taken the longest burning period compared to other foam fires with a lower density or mass before the flame extinguished at 434 s. PU-FSC was the lightest foam and its burning period was the shortest about 104 s from the start test.

.

**Table 5.1** Test details for PIR foam (Grenfell Tower) fires at various irradiation levels with free ventilation.

| Test | Radiant heat ($kW/m^2$) | Initial Mass (g) | Ignition (s) | Flame out (s) |
|---|---|---|---|---|
| 1 | 25 | 7.5 | No | No |
| 2 | 28 | 7.9 | No | No |
| 3 | 30 | 7.4 | 21 | 164 |
| 4 | 35 | 7.4 | 3 | 159 |
| 5 | 50 | 7.6 | 2 | 567 |

**Table 5.2** Test details for PU and PIR foam (Grenfell Tower) fires at 35 $kW/m^2$ irradiation level with free ventilation.

| Test | Foam Type | Thickness (mm) | Initial Mass (g) | Ignition (s) | Flame out (s) |
|---|---|---|---|---|---|
| 1 | PU-FSC | 25 | 6.7 | 7 | 104 |
| 2 | PU-FM | 20 | 39.6 | 14 | 434 |
| 3 | PIR-F GT | 25 | 7.4 | 3 | 159 |
| 4 | PU-FB | 27 | 7.1 | 19 | 178 |

### 5.1.1 Mass Loss Rates, Equivalence Ratios and Heat Release Rates for PIR Foam Fires

General combustion properties against time for PIR foam fires under various heat fluxes and free ventilation were included in Figure 5.1. In overall, total normalised mass loss increased with an increase of heat flux value for most of PIR foam fires. At low heat fluxes (25 28 $kW/m^2$ and 28 $kW/m^2$), PIR foam burning showed a non-flaming fire condition. With an increase in heat flux value, it had decreased time delay for an ignition for PIR foam fires with high heat fluxes (35 $kW/m^2$ and 50 $kW/m^2$) took only less than 5 s to reach an ignition. For irradiation levels below than 35 $kW/m^2$, maximum total mass loss achieved by PIR foam fires was about 30%. For irradiation level at 50 $kW/m^2$, total mass loss was high (up to 90%). From Figure 5.1 (b), Oxygen

consumption by PIR foam fires increased with an increase in heat flux value. PIR foam fire with heat flux at 50 kW/m$^2$ showed the highest $O_2$ consumption, about 8% and for non-flaming fires at low heat fluxes (25 kW/m$^2$ and 28 kW/m$^2$), it consumed very minimum $O_2$ which less than 1%. A higher mass loss would give a higher mass loss rate (MLR). The highest MLR peak shown by PIR foam fire was 0.025 g/s at heat flux of 50 kW/m$^2$. At about below 100 s of burning period, most of PIR foam fires under various irradiation levels showed a MLR peak less than 0.014 g/s with the highest peak of 0.014 g/s was given by PIR foam fire at 50 kW/m$^2$ followed by 35 kW/m$^2$ (0.01 g/s), 30 kW/m2 (0.008 g/s), 28 kW/m$^2$ (0.006 g/s) and 25 kW/m$^2$ (0.007 g/s). All these PIR foam fires had experienced a lean burning condition with giving fire equivalence ratio (ER) less than 0.4. ER profile decreased with a decrease in heat flux value. Heat release rates for PIR foam fires were low, less than 60 kW/m$^2$. This PIR foam sample had a GCV value of 26.36 MJ/kg (refer Table 3.6 in Chapter 3). For total HRR based MLR in Figure 5.1 (e), most HRR peaks were observed at 70 s of burning while for total HRR based OC in Figure 5.1 (f), the HRR peak for each PIR foam fire was at different burning time with following the $O_2$ consumption pattern. These PIR foam fires also gave primary HRR of <60 kW/m$^2$ and secondary HRR of <7 kW/m$^2$.

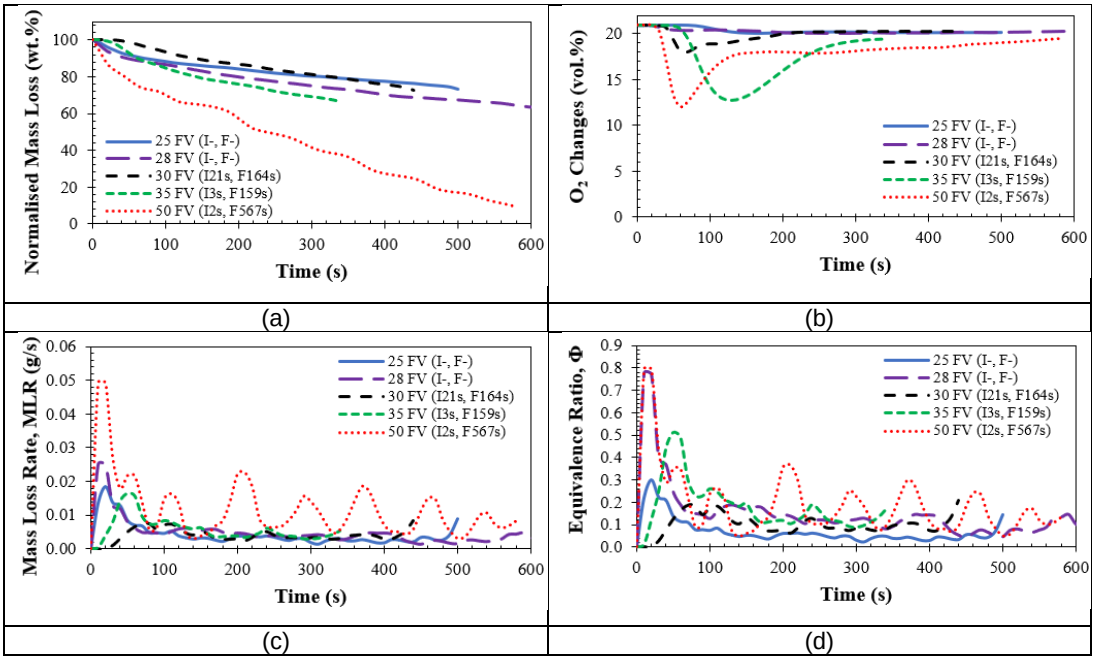

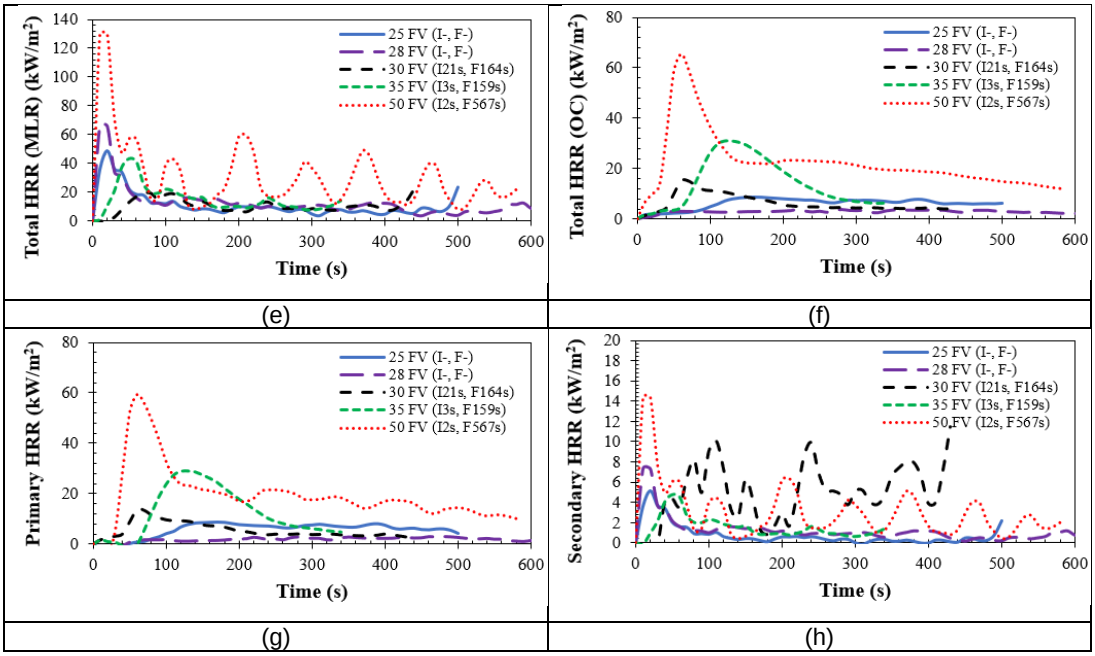


**Figure 5.1** Combustion properties for Polyisocyanurate foam fires at various heat fluxes with free ventilation.

### 5.1.2 Mass Loss Rates, Equivalence Ratios and Heat Release Rates for PU and PIR Foam Fires

Figure 5.2 showed general combustion properties as a function of time for four Polyurethane (PU) and Polyisocyanurate (PIR) foam fires at heat flux of 35 kW/m$^2$ and free ventilation. Ignition time for each of these solid foam fires was less than 20 s and the longest burning period was about 434 s (<8 minutes) given by PU-FM fire. The density of PU-FM sample was the highest compared to other three foam samples and this could be the reason why it took the longest burning duration before extinguished. In comparison between four foam fires, the lowest normalised mass loss of 30% was shown by PIR-F GT fire. Meanwhile, PU-FSC and PU-FB fires gave the highest mass loss of ~100% and PU-FM fire gave maximum 90% of normalised mass loss. From Figure 5.2 (b), it can be seen that PU-FM burning has the highest $O_2$ consumption which the fire has fully consumed all $O_2$. PU-FB fire had consumed 14% of $O_2$, meanwhile $O_2$ consumption by PU-FSC fire was 11% and PIR-F GT fire was 8%. Mass loss rate (MLR) for PU-FM fire was the highest (0.3 g/s) and much more higher compared with the MLR of other three foam fires which the MLR values were less than 0.05 g/s. PU-FM fire gave the highest MLR peak at 150 s with rich fire equivalence ratio of 1.2 and other foam fires gave a MLR peak at about 70 s with lean fire equivalence ratio of

less than 0.9. The high density of PU-FM sample contributed to a high burning rate of PU-FM foam fire, hence giving a high heat release rate (HRR) value. The highest HRR based MLR of about 900 kW/m$^2$ was given by the PU-FM foam fire with primary HRR was 700 kW/m$^2$ and secondary HRR was 90 kW/m$^2$. Meanwhile, other foam fires showed maximum heat release rates (HRRs) less than 200 kW/m$^2$.

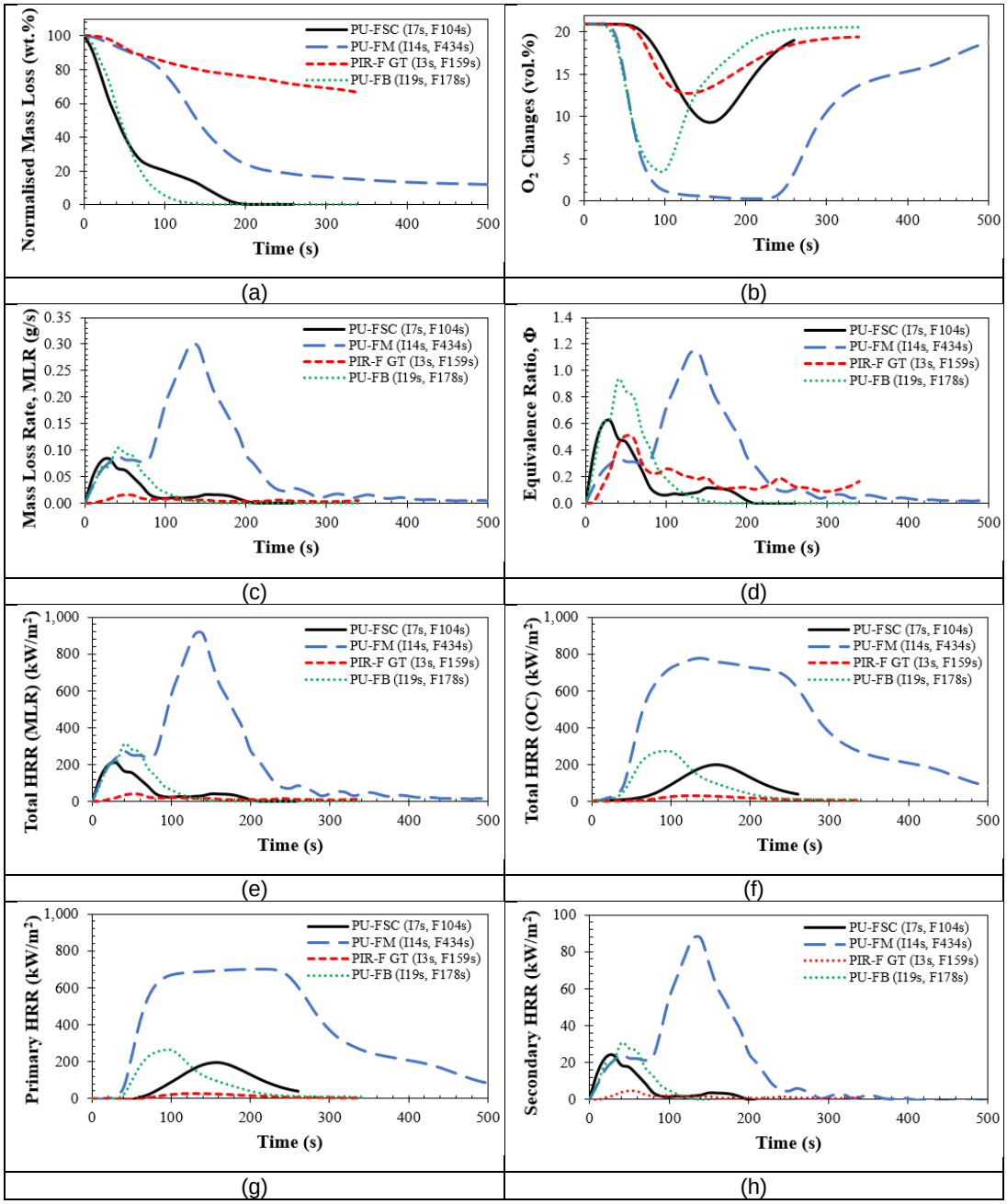


**Figure 5.2** Combustion properties for Polyurethane and Polyisocyanurate foam fires at 35 kW/m2 with free ventilation.

## 5.2 Toxicity from PU and PIR Foam Fires

Toxicity of certain material fire depended to concentration of toxic gases produced and referred toxic limit concentrations by certain assessment methods. The higher the value of toxic gas concentration would give the higher total toxicity value. There are three toxic assessment methods used in the present work which are $LC50_{30min}$, $COSHH_{15min}$ and $AEGL\text{-}2_{10min}$. Limit concentrations for each major toxic species for all three methods were summarised in Table 2.3 in Chapter 2 as reference.

### 5.2.1 Gas Concentrations for PIR Foam Fires at Various Irradiation Levels with Free Ventilation

Concentration of toxic gases as a function of time for various PIR foam fires was shown in the following Figure 5.3. PIR-F GT foam sample is nitrogen containing material which its burning is expected to give high HCN and $NO_x$ emissions. CO concentration was high for all PIR-F GT foam fires with higher heat fluxes (35 kW/m$^2$ and 50 kW/m$^2$) gave the highest CO concentration of about 6000 ppm and lower heat fluxes (25 kW/m$^2$, 28 kW/m$^2$ and 30 kW/m$^2$) gave CO concentration of 4000 ppm or less. HCN concentration was not more than 300 ppm for all PIR-F GT foam fires. From Figure 5.3 (c), (e), (g) and (h), it could been clearly seen that HCl, CO2, NO and $NO_x$ concentrations were the highest for PIR foam fire at irradiation level of 35 kW/m$^2$ (heating temperature of 695$^o$C). PIR foam fire at irradiation level of 25 kW/m$^2$ showed the highest peak of Formaldehyde (~1500 ppm) and THC (45000 ppm) at 50 s of burning time. The highest Toluene concentration was given by PIR foam fire at irradiation level of 28 kW/m$^2$. It can be said that most of toxic species are produced higher at lower heat fluxes than the higher heat fluxes for these PIR-F GT foam fires. HCl concentration had given a maximum value of 400 ppm as shown in Figure 5.3 (c) proved that this PIR foam sample was also a fire retarded (halogen based) material. That was why the heat release rate (HRR) values as discussed earlier for these PIR-F GT foam fires were very low compared to other foam fires which giving much more higher of HRR values.

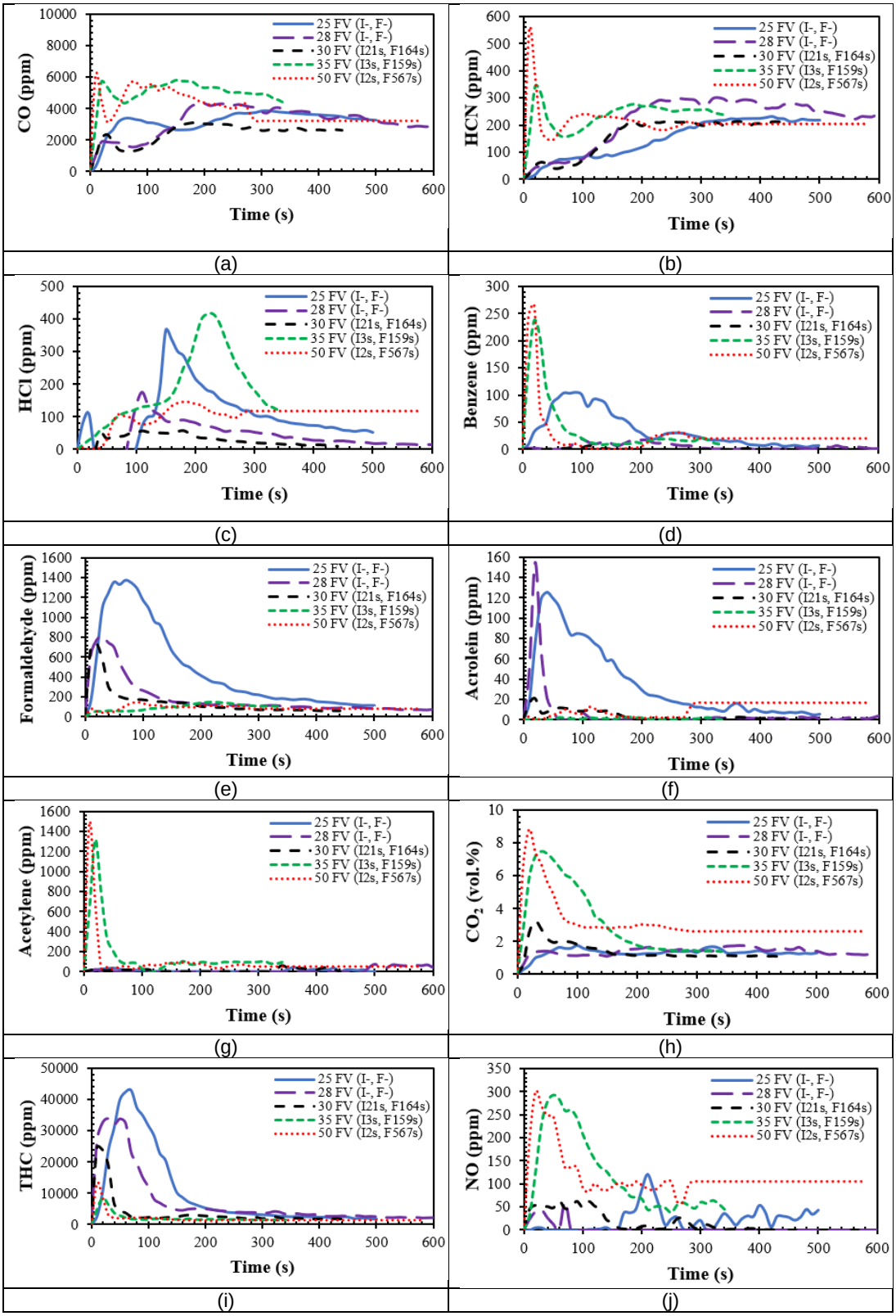
CO (ppm)
Time (s)
25 FV (I-, F-)
28 FV (I-, F-)
30 FV (I21s, F164s)
35 FV (I3s, F159s)
50 FV (I2s, F567s)
(a)
HCN (ppm)
Time (s)
(b)
HCl (ppm)
Time (s)
(c)
Benzene (ppm)
Time (s)
(d)
Formaldehyde (ppm)
Time (s)
(e)
Acrolein (ppm)
Time (s)
(f)
Acetylene (ppm)
Time (s)
(g)
CO2 (vol.%)
Time (s)
(h)
THC (ppm)
Time (s)
(i)
NO (ppm)
Time (s)
(j)

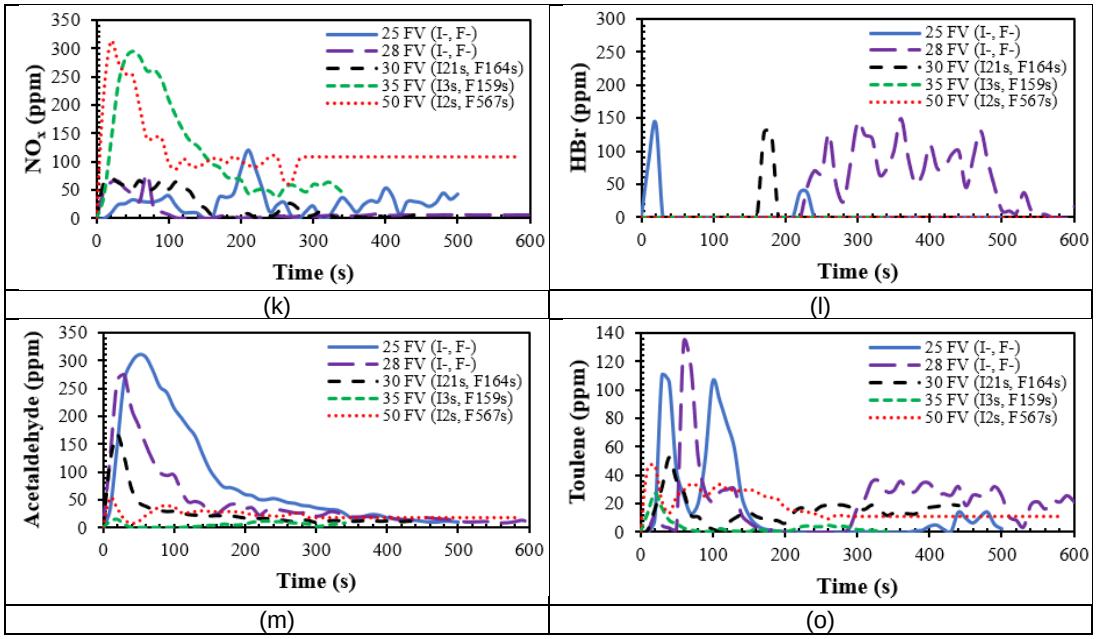


**Figure 5.3** Concentration of toxic gases as a function of time for various PIR foam fires.

### 5.2.2 Gas Concentrations for PU and PIR Foam Fires at 35 kW/m$^2$ Irradiation Level with Free Ventilation

Figure 5.4 showed concentration of toxic gases as a function of time for PU and PIR foam fires at 35 kW/m$^2$ and free ventilation. PU-FM foam fire showed the highest concentration of HCN, Benzene, Acrolein, CO2, $NH_3$, Acetaldehyde and Toluene within burning period up to 200 s if compared to other three foam fires. Concentrations of HCl, HF, Formaldehyde and HBr were the highest at 70 s of burning time for PU-FSC foam fire, meanwhile the highest concentration of Acetylene, THC, NO, NO2, $SO_2$ and $NO_x$ were given by PU-FB foam fire. Toxic gases such as HF (<50 ppm), Formaldehyde (<300 ppm), Acrolein (<150 ppm), NO2 (<200 ppm) and SO2 (<100 ppm) gave a lower concentration than the other toxic gases which presented in Figure 5.4 for all four foam fires. In comparison between these solid foam fires, PIR-GT foam fire gave the lowest concentration for most of toxic species. PU-FM and PU-FB fires had the maximum CO emission peak of 5000 ppm and HCN peak of 3000 ppm. There were two peaks of HBr emission observed for PU-FSC foam fire with the first highest peak gave a concentration value of 300 ppm at 70 s and the second lower peak gave a concentration value of 250 ppm at 200 s with no significant HBr concentration were shown by other foam fires. Other than PU-FSC foam fire that showed the maximum value of HCl

concentration (2000 ppm), PIR-F GT foam fire also gave a HCl peak of 500 ppm after 200 s of its burning while other two foam fires (PU-FM and PU-FB fires) had shown no significant HCl emission. From Figure 5.4 (i), these foam fires gave a $CO_2$ emission peak at burning time of 70 s with PU-FM fire had the highest $CO_2$ concentration of 15% by volume.

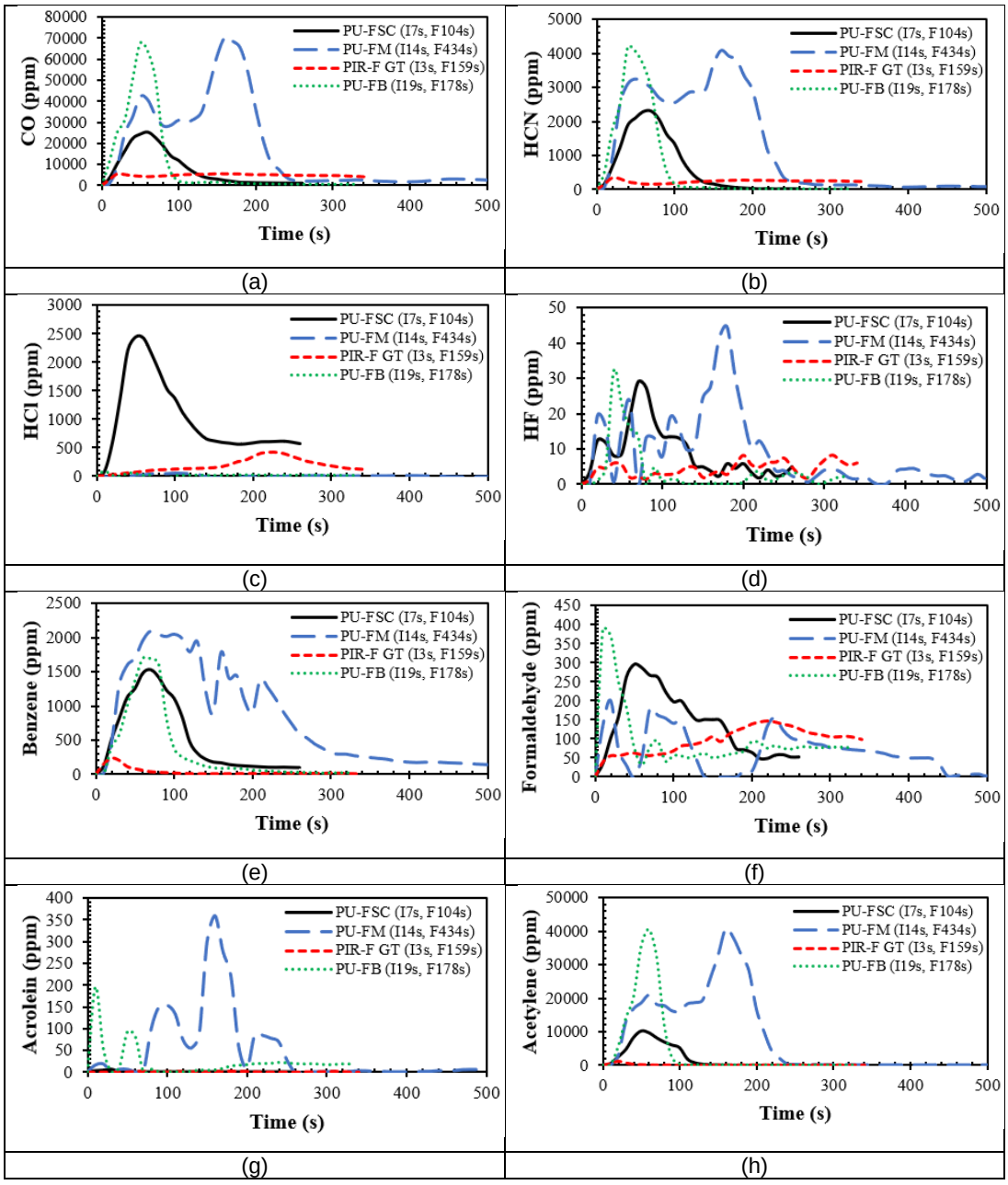

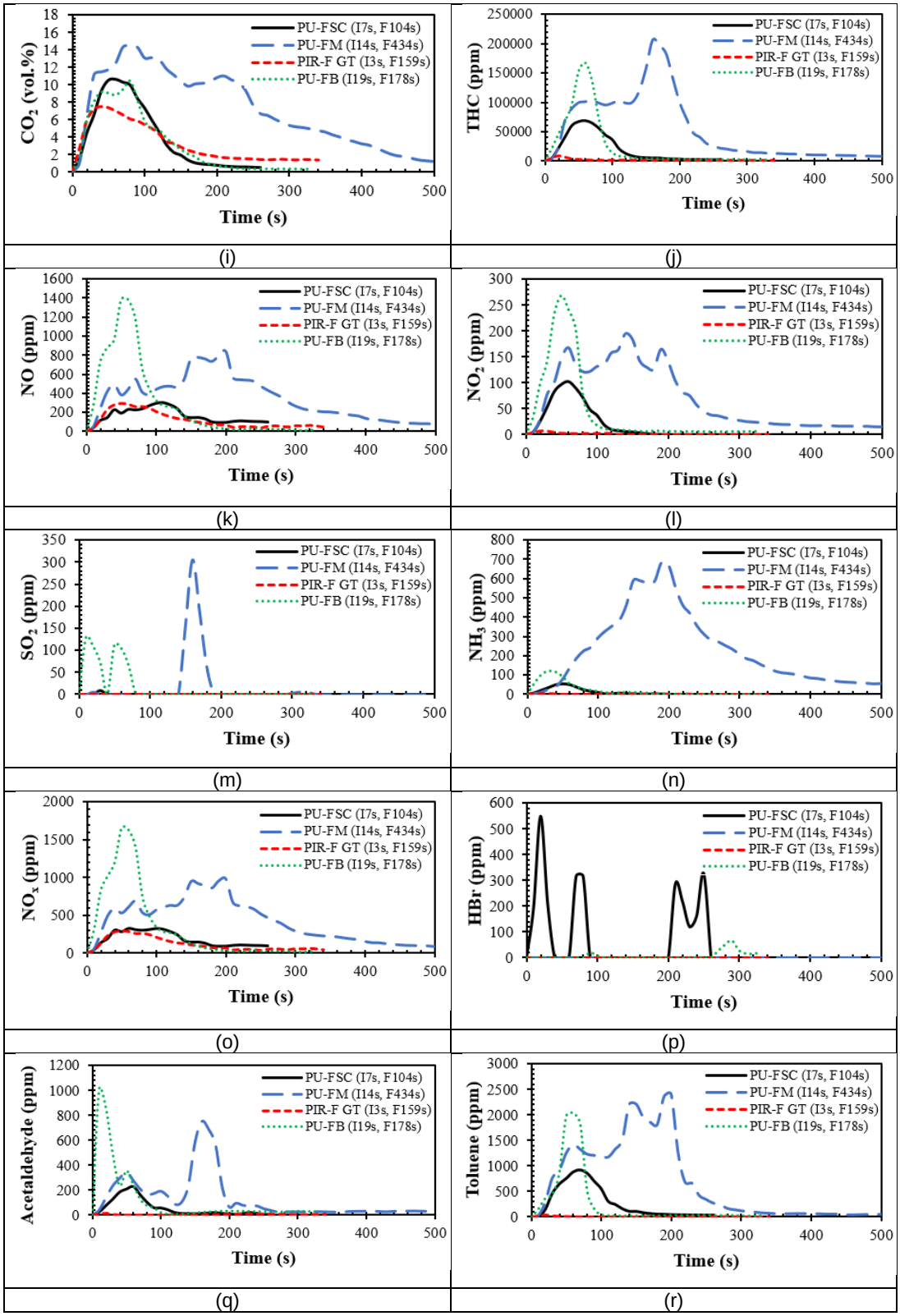


**Figure 5.4** Concentration of toxic gases as a function of time for PU and PIR foam fires at 35 kW/m$^2$ and free ventilation.

### 5.2.3 Gas Yields for PIR Foam Fires at Various Irradiation Levels with Free Ventilation

Yield of gases as a function of time for various PIR foam fires under various heat fluxes and free ventilation were shown in the following Figure 5.5. PIR-F GT foam fire at 25 kW/m$^2$ heat flux showed the highest yield value for most of presented toxic species like HCN, Formaldehyde, Acrolein, NO, $NO_x$, HBr, Acetaldehyde and Toluene. Yields for most of toxic species were the lowest for PIR-F GT foam fire at the highest heat flux of 50 kW/m$^2$. High gas yields were given by a material burning at low heat fluxes was in a good agreement with the theory where a fire at low heat flux would have low burning rate and produce more toxic gases which were the common products for an incomplete combustion, hence it would also contribute to a high yield of gases. CO yields for these foam fires were <0.4 g/g. This value >2 times higher than the CO yield reported for a Nitrogen containing polymer (Polyamide-6) fire [136].

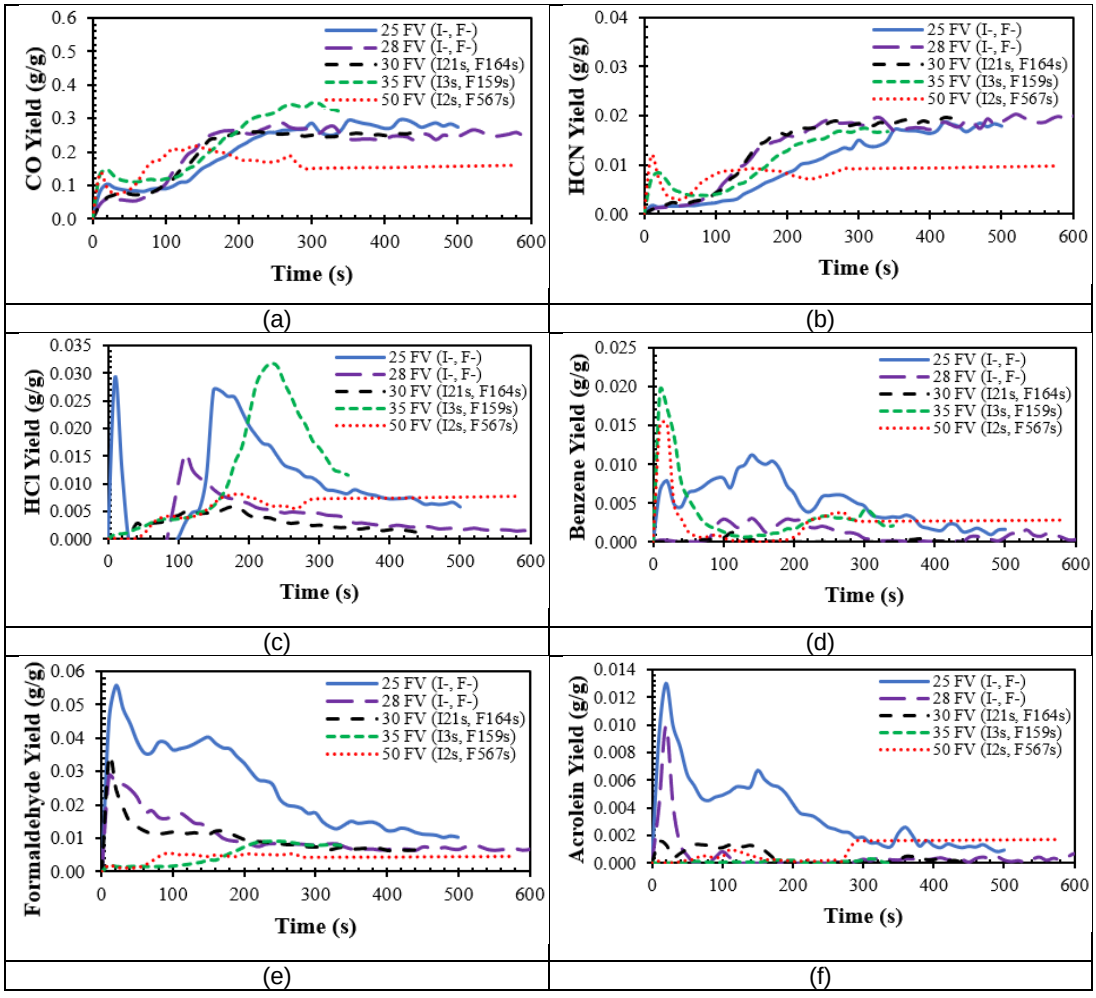

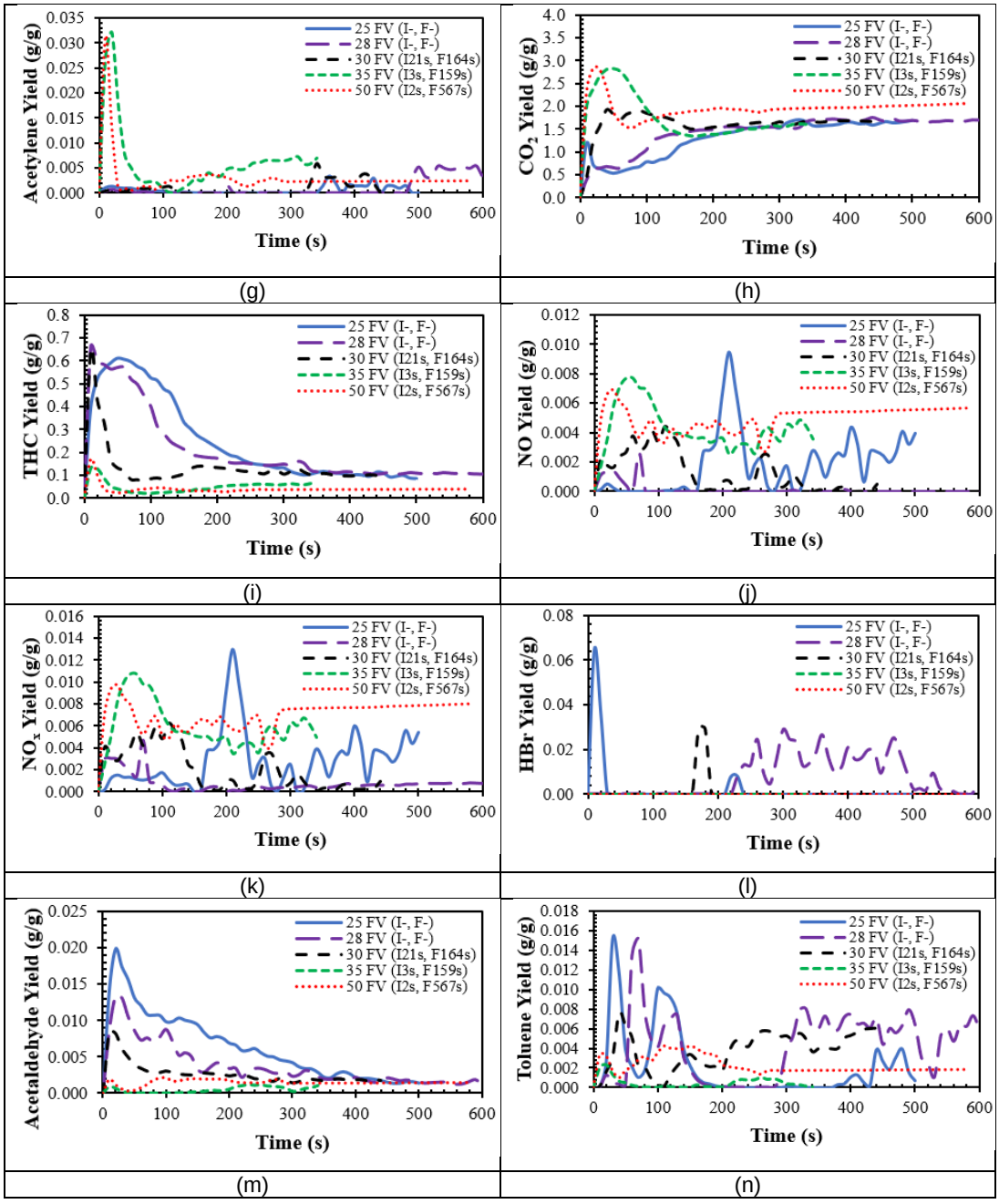


**Figure 5.5** Yield of gases as a function of time for various PIR foam fires.

Combustion efficiency rate would reduce with an increase in CO yield value where high CO formation represented an incomplete combustion of certain material. Compared to PIR-F GT foam fires with higher heat fluxes, PIR-F GT foam fires with lower heat fluxes (25 kW/m$^2$ and 28 kW/m$^2$) gave lower combustion efficiency (<80%). PIR-F GT foam fire at 25 kW/m2 started to show a significant increase in combustion efficiency rate after 200 s of burning period as shown in the following Figure 5.6 (a) where before 200 s, the

efficiency rate at the minimum. Figure 5.6 showed combustion efficiency, ŋ as a function of time and equivalence ratio for various PIR foam fires. As shown in Figure 5.6 (b), fire equivalence ratios (ER) for these PIR-F GT foam fires had shown the lean burning condition with ER values less than 0.8.

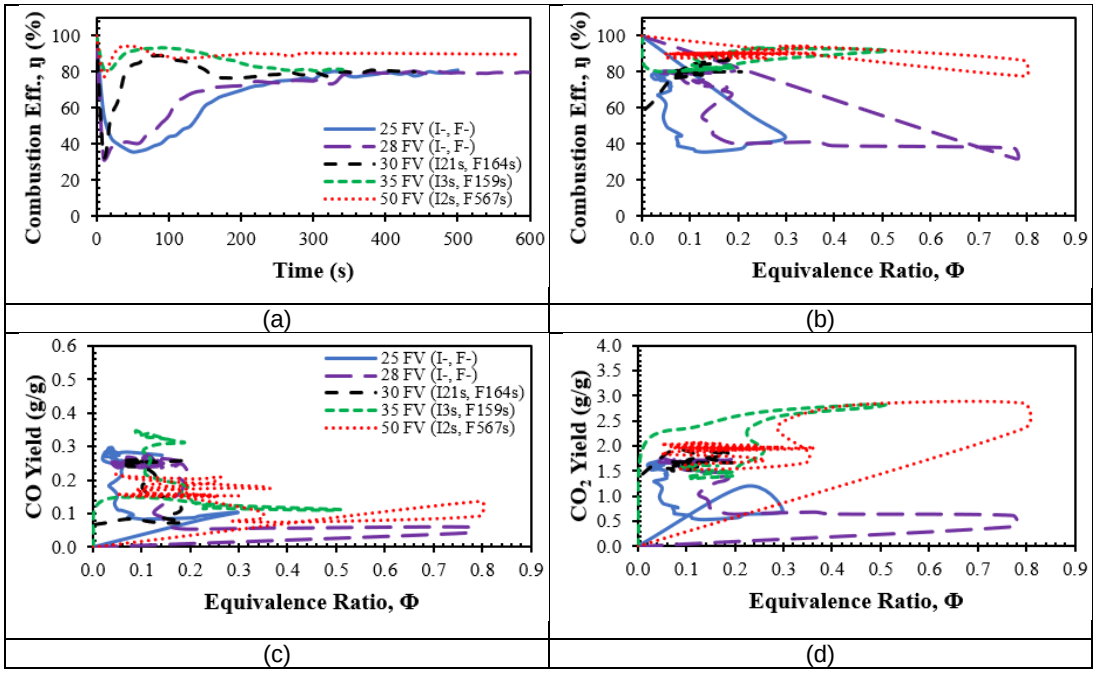


**Figure 5.6** Combustion efficiency, ŋ as a function of time for various PIR foam fires.

### 5.2.4 Gas Yields for PU and PIR Foam Fires at 35 kW/m$^2$ Irradiation Level with Free Ventilation

The following Figure 5.7 showed the yield of gases as a function of time for PU and PIR foam fires at 35 kW/m$^2$ and free ventilation. From Figure 5.7 (c), (d) and (p), HCl, HBr and HF were measured in the product gases especially for PU-FSC foam fire indicating that halogenated fire retardants were used and contained by these solid foam materials in order to reduce the risk of ignition and to reduce the rate of fire propagation. However, once the fire grew at Grenfell Towers the fire retardants became ineffective, but could potentially add to the toxic gas yields and total toxicity values. For most of foam fires, PU-FM and PU-FB foam fires gave the highest toxic gas yields except for Benzene, HCl and HBr yields which PU-FSC foam fire had dominated. The shortest burning period of PU-FSC foam fire had shown that the maximum yield for most of species for this foam fire was achieved at time less than 200

s. PIR-F GT fire showed the lowest gas yields compared to other three foam fires except for several toxic species like HCl, HF, Formaldehyde and $CO_2$. The gas yields from PU-FB foam fire were the highest and most significant for most of toxic species before 100 s of burning period compared to the gas yields produced from PU-FSC, PU-FM and PIR-F GT foam fires.

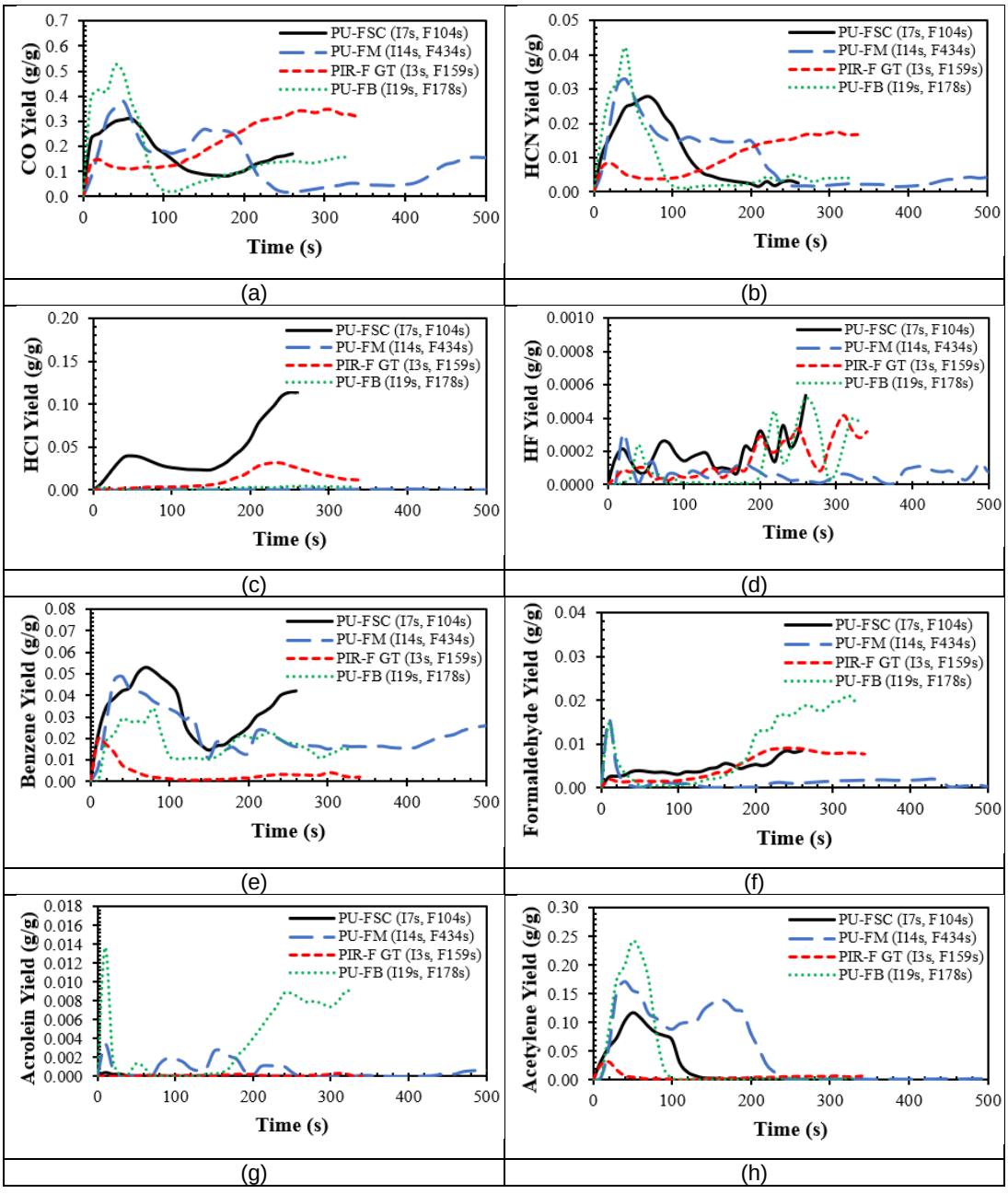

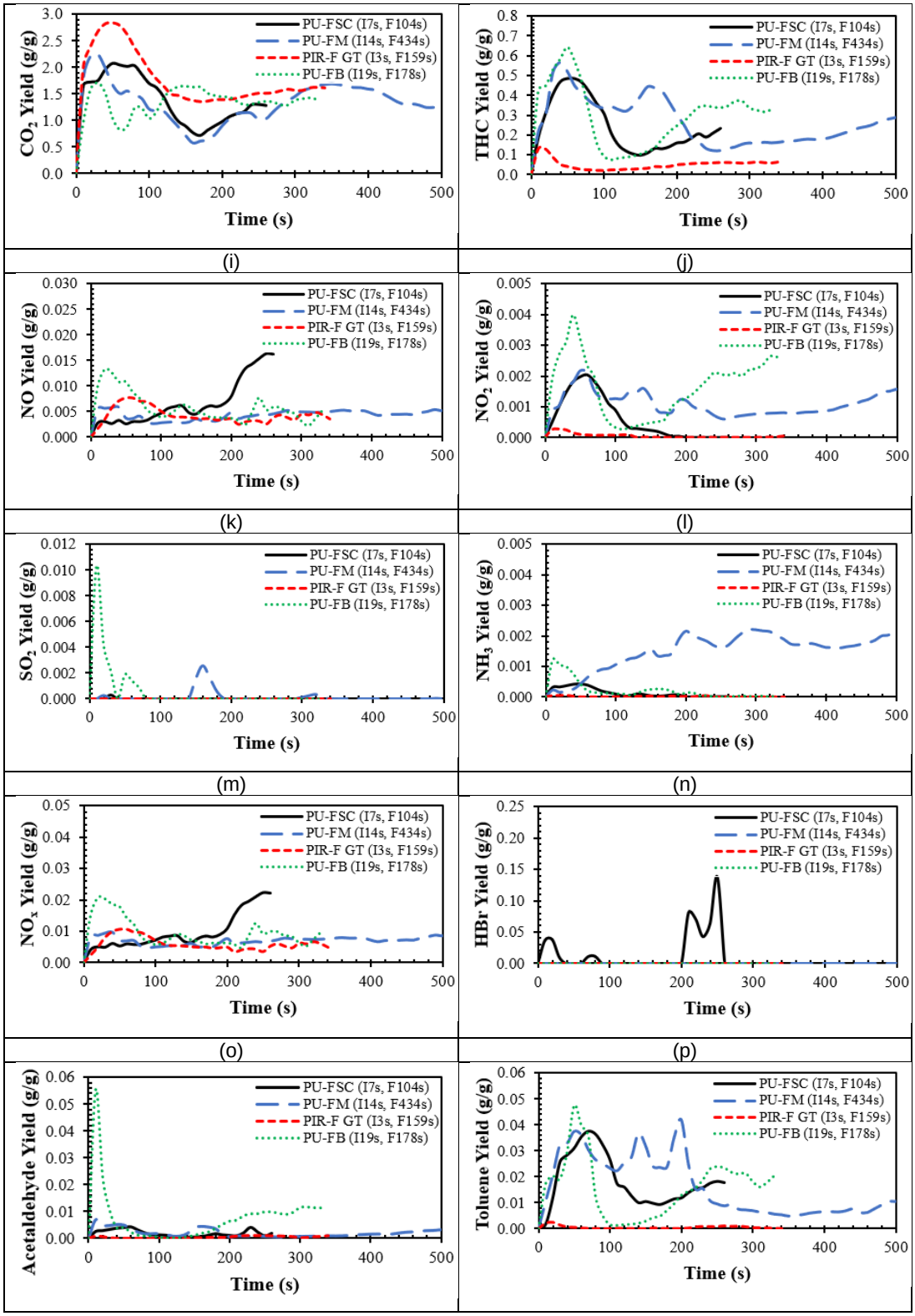


**Figure 5.7** Yield of gases as a function of time for PU and PIR foam fires at 35 kW/m$^2$ and free ventilation.

Figure 5.8 showed combustion efficiency, ŋ as a function of time and equivalence ratio for PU and PIR foam fires at 35 kW/m$^2$ and free ventilation. PIR-F GT foam fire had shown a high combustion efficiency values from 80% to 100% within the whole burning period. PU-FSC, PU-FM and PU-FB foam fires had the combustion efficiency <50% at 50 s before the efficiency rate increased up to 80% after 100 s. From these combustion efficiency results, between these four foam fires, it could be concluded that PU-FM fire was the most toxic and PIR-F GT was the least toxic. In general, high gas yields produced from the foam burning would decrease the combustion efficiency rate, ŋ and contributed to high total toxicity values. The combustion efficiency of <30% that given by the PU-FM fire was at rich burning equivalence ratio of 1.1 with higher combustion efficiency values by other foam fires were at a leaner burning equivalence ratio, less than 0.9.

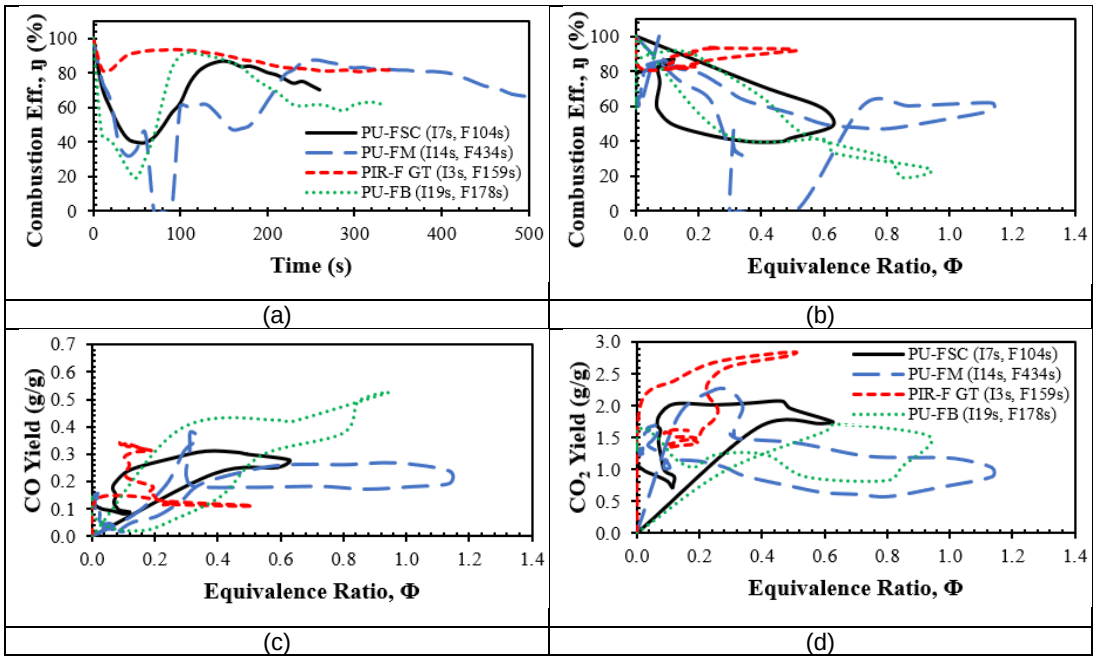


**Figure 5.8** Combustion efficiency, ŋ as a function of time for PU and PIR foam fires at 35 kW/m$^2$ and free ventilation.

### 5.2.5 Total Toxicity for PIR Foam Fires at Various Irradiation Levels with Free Ventilation

Figure 5.9 showed the $LC50_{30min}$, $COSHH_{15min}$ and $AEGL\text{-}2_{10min}$ total relative toxicity for various PIR foam fires. From Figure 5.9, it showed that the highest total toxicity was given by PIR foam fire at heat flux of 25 kW/m$^2$ and at 70 s

of burning time for all three toxic assessment methods. The highest total FEC LC50 was about 3.7, while the highest total FEC by $COSHH_{15min}$ and AEGL-2 methods were ~1200 and ~350. Most of PIR-F GT foam fires either it gave a non-flaming or flaming fire, the total LC50 values were all significant which more than 2.0 for the whole burning period. Toxic species such as Benzene, Formaldehyde, Acrolein, $NH_3$ and Acetaldehyde (see Figure 5.3 and Figure 5.5) were seen to be the main contributors for the overall total toxicity of these PIR foam fires. Based on COSHH15min and AEGL-2 toxic assessments, total toxicity for PIR-F GT foam fires were high within 200 s of burning period then it decreased to the minimum values until the flame out state. The summary of maximum and mean gas yields for solid foam fires at various irradiation levels with free ventilation are included in Table 5.3 and Table 5.4. Appendix E includes the cumulative mass of CO produced for these foam fires.

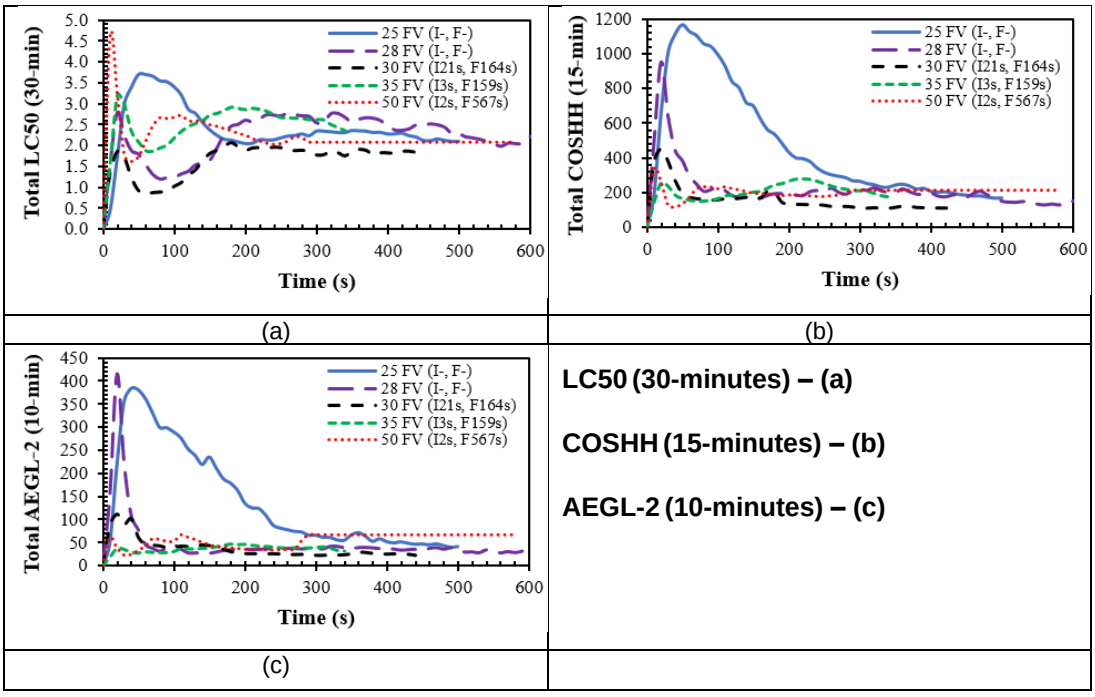


**Figure 5.9** The $LC50_{30min}$, $COSHH_{15min}$ and $AEGL\text{-}2_{10min}$ total relative toxicity for various PIR foam fires.

**Table 5.3** Maximum gas yields for solid foam fires at various irradiation levels with free ventilation.

| **Foam Type** | **PIR-F GT** | | | | | **PU-FSC** | **PU-FM** | **PU-FB** |
|---|---|---|---|---|---|---|---|---|
| **Test Condition** | **25 FV** | **28 FV** | **30 FV** | **35 FV** | **50 FV** | **35 FV** | **35 FV** | **35 FV** |
| **Species** | **Maximum Yields (g/g)** | | | | | | | |
| CO | 0.2938 | 0.2854 | 0.2609 | 0.3460 | 0.2192 | 0.3125 | 0.3825 | 0.5239 |
| HCN | 0.0187 | 0.0213 | 0.0200 | 0.0175 | 0.0119 | 0.0278 | 0.0328 | 0.0423 |
| HCl | 0.0290 | 0.0154 | 0.0058 | 0.0317 | 0.0081 | 0.1134 | 0.0007 | 0.0046 |
| HF | 0.0003 | 0.0005 | 0.0003 | 0.0004 | 0.0004 | 0.0005 | 0.0003 | 0.0005 |
| Benzene | 0.0111 | 0.0031 | 0.0012 | 0.0195 | 0.0153 | 0.0531 | 0.0490 | 0.0340 |
| Formaldehyde | 0.0558 | 0.0288 | 0.0339 | 0.0092 | 0.0053 | 0.0086 | 0.0157 | 0.0211 |
| Acrolein | 0.0129 | 0.0099 | 0.0015 | 0.0004 | 0.0017 | 0.0004 | 0.0034 | 0.0137 |
| Acetylene | 0.0034 | 0.0063 | 0.0059 | 0.0320 | 0.0312 | 0.1177 | 0.1720 | 0.2418 |
| $CO_2$ | 1.7377 | 1.7681 | 1.9175 | 2.8387 | 2.8439 | 2.0676 | 2.2441 | 1.7104 |
| THC | 0.6120 | 0.6641 | 0.6446 | 0.1301 | 0.1709 | 0.4830 | 0.5643 | 0.6412 |
| NO | 0.0094 | 0.0026 | 0.0044 | 0.0077 | 0.0069 | 0.0162 | 0.0084 | 0.0133 |
| $NO_2$ | 0.0020 | 0.0016 | 0.0012 | 0.0003 | 0.0006 | 0.0021 | 0.0022 | 0.0040 |
| $SO_2$ | 0.0044 | 0.0006 | 0.0041 | 0.0000 | 0.0000 | 0.0003 | 0.0026 | 0.0103 |
| $NH_3$ | 0.0013 | 0.0008 | 0.0006 | 0.0000 | 0.0003 | 0.0004 | 0.0028 | 0.0012 |
| $NO_x$ | 0.0130 | 0.0047 | 0.0063 | 0.0107 | 0.0098 | 0.0223 | 0.0134 | 0.0207 |
| HBr | 0.0648 | 0.0288 | 0.0294 | 0.0000 | 0.0000 | 0.1385 | 0.0000 | 0.0000 |
| Acetaldehyde | 0.0197 | 0.0133 | 0.0085 | 0.0011 | 0.0021 | 0.0044 | 0.0068 | 0.0555 |
| Toluene | 0.0151 | 0.0151 | 0.0076 | 0.0024 | 0.0042 | 0.0377 | 0.0417 | 0.0473 |

**Table 5.4** Mean gas yields for solid foam fires at various irradiation levels with free ventilation.

| Foam Type | PIR-F GT | | | | | PU-FSC | PU-FM | PU-FB |
|---|---|---|---|---|---|---|---|---|
| **Test Condition** | **25 FV** | **28 FV** | **30 FV** | **35 FV** | **50 FV** | **35 FV** | **35 FV** | **35 FV** |
| **Initial Mass (g)** | 7.91 | 7.94 | 6.46 | 5.94 | 7.53 | 5.73 | 39.68 | 6.47 |
| **Total Mass Loss (g)** | 2.84 | 3.37 | 1.79 | 2.00 | 6.82 | 5.73 | 35.39 | 6.47 |
| **Total Time (s)** | 510 | 720 | 440 | 340 | 580 | 210 | 660 | 160 |
| **Mean ER, Φ** | 0.13 | 0.11 | 0.10 | 0.20 | 0.18 | 0.40 | 0.79 | 0.81 |
| **Species** | **Mean Yields (g/g)** | | | | | | | |
| CO | 0.1934 | 0.1852 | 0.1970 | 0.1908 | 0.1505 | 0.2400 | 0.2069 | 0.3615 |
| HCN | 0.0099 | 0.0123 | 0.0128 | 0.0087 | 0.0083 | 0.0181 | 0.0148 | 0.0239 |
| HCl | 0.0078 | 0.0012 | 0.0032 | 0.0096 | 0.0050 | 0.0293 | 0.0001 | 0.0003 |
| HF | 0.0001 | 0.0001 | 0.0001 | 0.0001 | 0.0002 | 0.0002 | 0.0001 | 0.0001 |
| Benzene | 0.0045 | 0.0008 | 0.0002 | 0.0037 | 0.0041 | 0.0364 | 0.0251 | 0.0239 |
| Formaldehyde | 0.0266 | 0.0135 | 0.0095 | 0.0041 | 0.0037 | 0.0035 | 0.0007 | 0.0025 |
| Acrolein | 0.0043 | 0.0015 | 0.0006 | 0.0001 | 0.0008 | 0.0001 | 0.0012 | 0.0012 |
| Acetylene | 0.0005 | 0.0013 | 0.0010 | 0.0050 | 0.0050 | 0.0668 | 0.0999 | 0.1501 |
| $CO_2$ | 1.2799 | 1.2966 | 1.6892 | 2.0078 | 2.0584 | 1.6893 | 1.1242 | 1.2412 |
| THC | 0.2808 | 0.2846 | 0.1081 | 0.0445 | 0.0507 | 0.3403 | 0.3506 | 0.4701 |
| NO | 0.0020 | 0.0003 | 0.0015 | 0.0051 | 0.0051 | 0.0035 | 0.0036 | 0.0095 |
| $NO_2$ | 0.0004 | 0.0008 | 0.0002 | 0.0001 | 0.0003 | 0.0012 | 0.0013 | 0.0025 |
| $SO_2$ | 0.0004 | 0.0000 | 0.0001 | 0.0000 | 0.0000 | 0.0000 | 0.0004 | 0.0017 |
| $NH_3$ | 0.0003 | 0.0002 | 0.0001 | 0.0000 | 0.0002 | 0.0003 | 0.0013 | 0.0005 |
| $NO_x$ | 0.0032 | 0.0011 | 0.0023 | 0.0071 | 0.0073 | 0.0059 | 0.0060 | 0.0152 |
| HBr | 0.0056 | 0.0049 | 0.0010 | 0.0000 | 0.0000 | 0.0113 | 0.0000 | 0.0000 |
| Acetaldehyde | 0.0072 | 0.0049 | 0.0024 | 0.0003 | 0.0014 | 0.0029 | 0.0024 | 0.0080 |
| Toluene | 0.0027 | 0.0037 | 0.0038 | 0.0004 | 0.0023 | 0.0217 | 0.0258 | 0.0266 |

### 5.2.6 Total toxicity for PU and PIR Foam Fires at 35 kW/m² Irradiation Level with Free Ventilation

The FEC method of toxicity analysis was used with each of the 60 toxic gases measured divided by the toxic limit to give an N factor and the N for each species was summated to give the total toxic hazard, as shown below for LC50 and $COSHH_{15min}$ impairment of escape toxic assessments. Both methods of toxic gas assessment showed very high toxicity for all foams. HCN and CO emissions were dominant in the toxic assessment. The PIR foam had the lowest toxicity, but burned over a longer period.

The HCl levels in Figure 5.4 were up to 2500 ppm for the PU spray foam, but this was less than the LC50 of 3800 ppm. This shows that the halogen fire retardants were not the major source of toxic gases. Figure 5.10 (a) shows the normalised total toxicity, FEC, for the four foams. This shows that the PU

floor mat had the highest toxicity, but that all the foams had high toxicity with the LC50 FEC well above 1. For impairment of escape the COSHH 15 minute exposure data is relevant and the FEC on this basis is shown in Figure 5.10 (b), which is similar in shape to Figure 5.10 (a). PU-FSC, PU-FM and PU-FB gave about 2000 times of $COSHH1_{5min}$ FEC. From AEGL-2 total toxicity, the FEC values for all foam fires were below than 500 with PU-FM fire gave the highest total toxicity. PIR-F GT showed the lowest total toxicity for all three toxic assessment methods but the values were still significant and could still cause an impairment of escape.

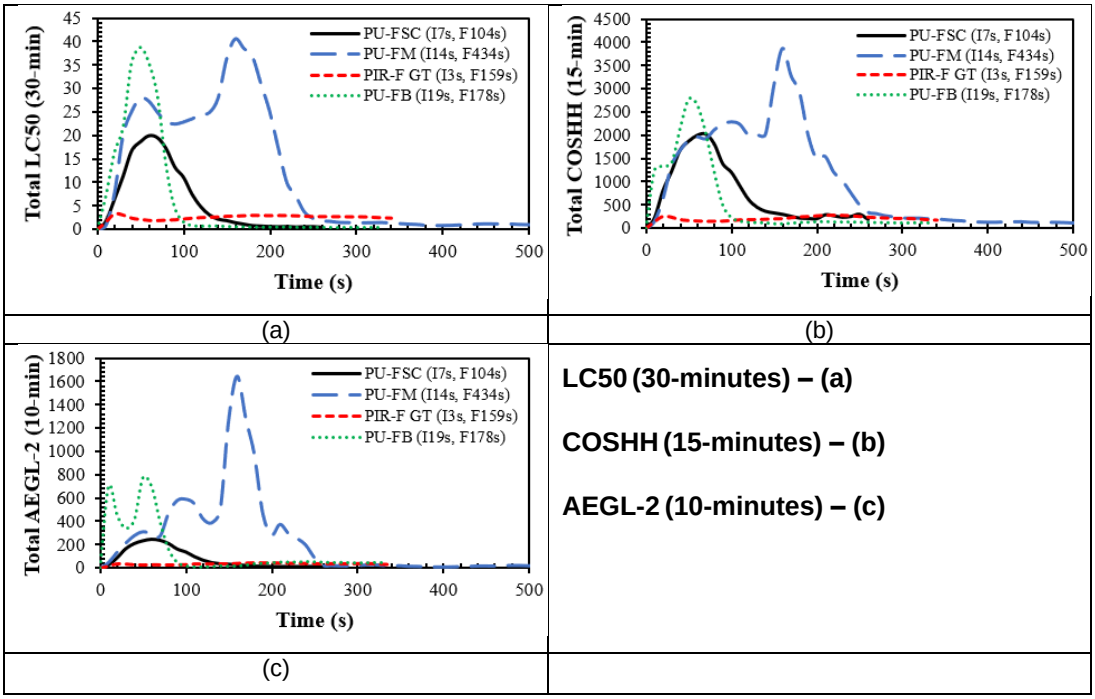


**Figure 5.10** The $LC50_{30min}$, $COSHH_{15min}$ and $AEGL\text{-}2_{10min}$ total relative toxicity for PU and PIR foam fires at 35 kW/m$^2$ and free ventilation.

### 5.2.7 Major Gases Contribution for PIR Foam Fires at Various Irradiation Levels with Free Ventilation

Polyisocyanurate (PIR) foam like PIR-F GT contained nitrogen elements in its chemical structure and would release HCN as one of the major toxic species other than CO, Formaldehyde and Acrolein. Figure 5.11 showed the contribution of major gases for LC50 basis from various PIR-F GT foam fires. HCN contribution on toxicity was at the highest with the contribution percentage range from 40% to 60% from the total contribution by all 10

considered main gases. The gas contribution graphs (Figure 5.11 (a, b and c)) showed that PIR-F GT fires at lower heat fluxes giving a higher percentage of HCN contribution than the fires at higher heat fluxes. The second major species that contributing to the total toxicity of PIR-F GT fires was CO which percentage range from 20% to 40% with tests at a higher irradiation level were giving a higher percentage of fire toxicity. In general, the decreasing order of major gas contribution for PIR-F GT fire based on LC50 assessment method was dominate by HCN and followed by CO, Formaldehyde and Acrolein. Only small percentage were contributed by other species such as HCl, $NO_2$ and $SO_2$ as illustrated in Figure 5.11.

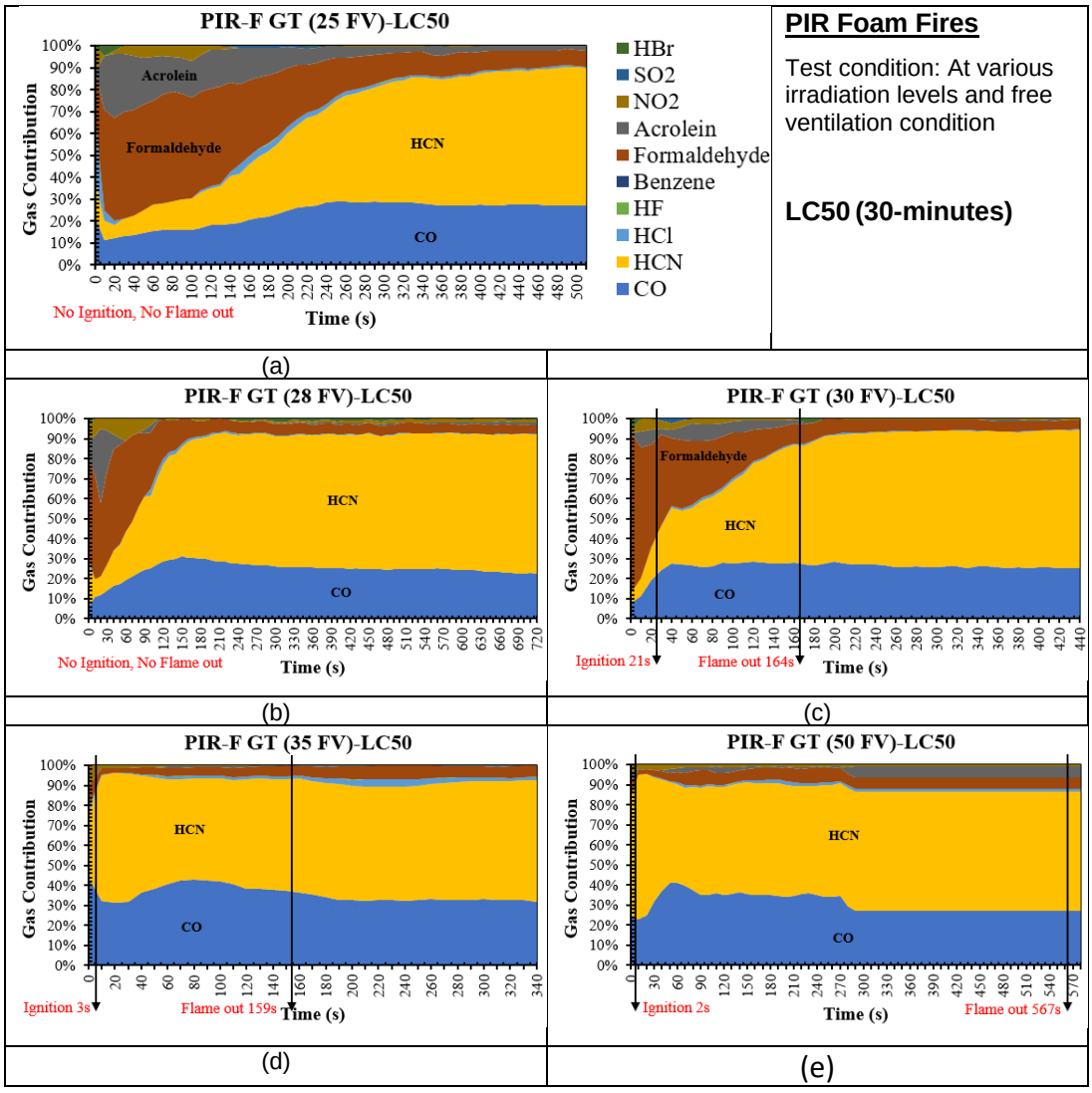


**Figure 5.11** Contribution of major gases (based $LC50_{30min}$) for various PIR foam fires.

From $COSHH_{15min}$ based toxic assessment method as in Figure 5.12, it could be seen that Formaldehyde had given the highest contribution to the total toxicity especially for PIR-F GT fires with lower irradiation levels (below 30 kW/m$^2$). Formaldehyde contribution had shown a decrement throughout the burning period for all PIR-F GT fires. The contribution of HCl and Acrolein was higher than LC50 basis and more significant. HCN and CO were also dominant toxic species and their contributions to toxicity were also high. HBr contribution was also realised under this COSHH15min basis for PIR-F GT fires at 28 and 30 kW/m$^2$ of heat irradiation even the contribution value was small. Irritants seemed to dominate the fire toxicity in the early start of fire which might cause an impairment of escape to the people.

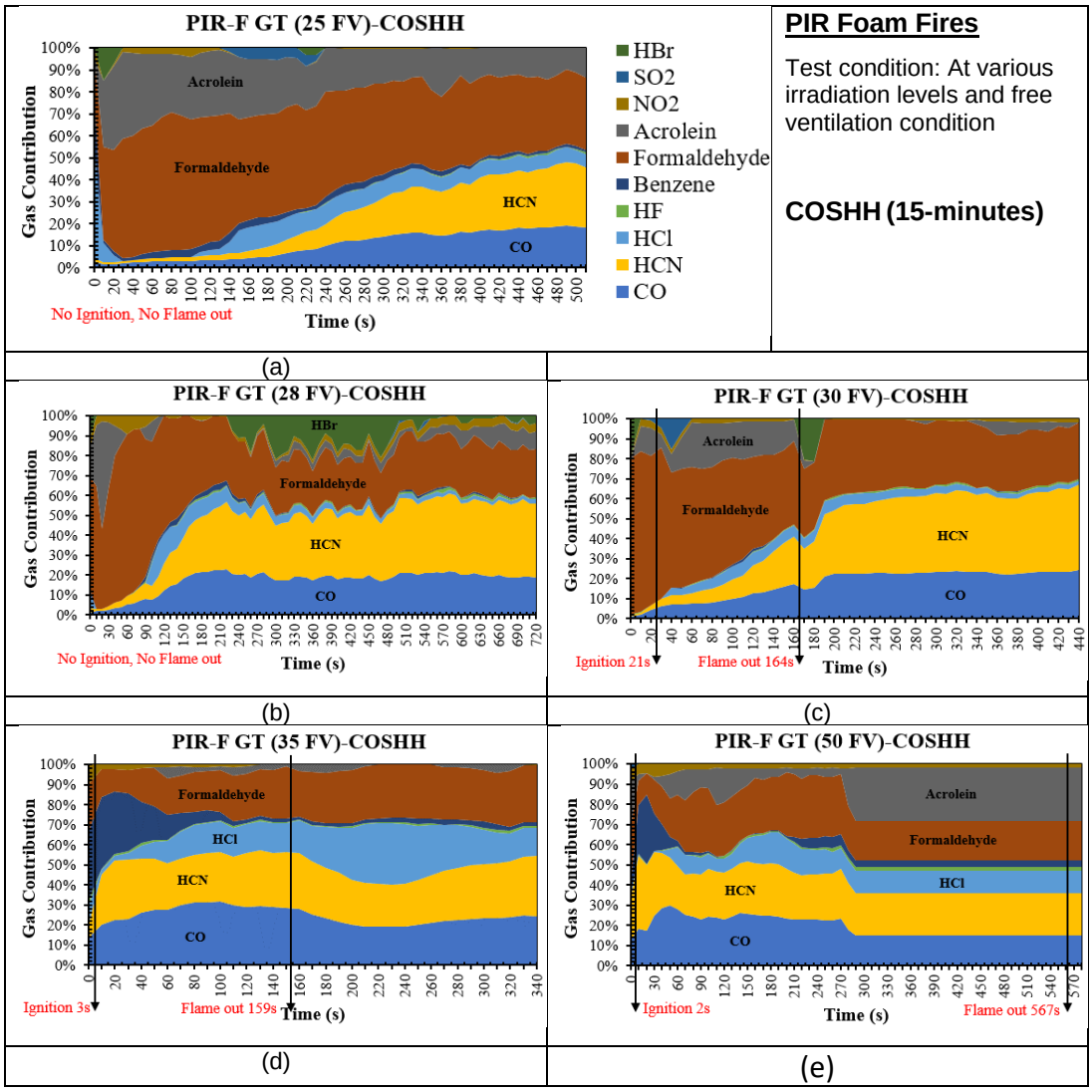


**Figure 5.12** Contribution of major gases (based $COSHH_{15min}$) for various PIR foam fires.

For AEGL-2 basis, Acrolein contribution was high especially for PIR-F GT foam fires at test conditions of 25 kW/m$^2$ and 50 kW/m$^2$ heat fluxes with free ventilation condition. HCN contribution showed an increment during the burning period for most of conducted PIR-F fires. CO had shown a higher contribution for tests at a higher heat flux exposure. The same four major species (CO, HCN, Formaldehyde and Acrolein) were observed to be main contributors to the total toxicity for all conducted PIR-F fires either the fire experienced a flaming condition or not, even with varying heat fluxes. The formation of HCl and its toxicity contribution could confirm that this PIR-F foam was fire retardant type. For PIR-F GT foam fire at 50 kW/m2 and free ventilation, it showed a decrease in CO, HCN, HCl and Formaldehyde contribution after 300 s while Acrolein contribution showed an increase after that period with more than 50% of contribution from the total toxicity.

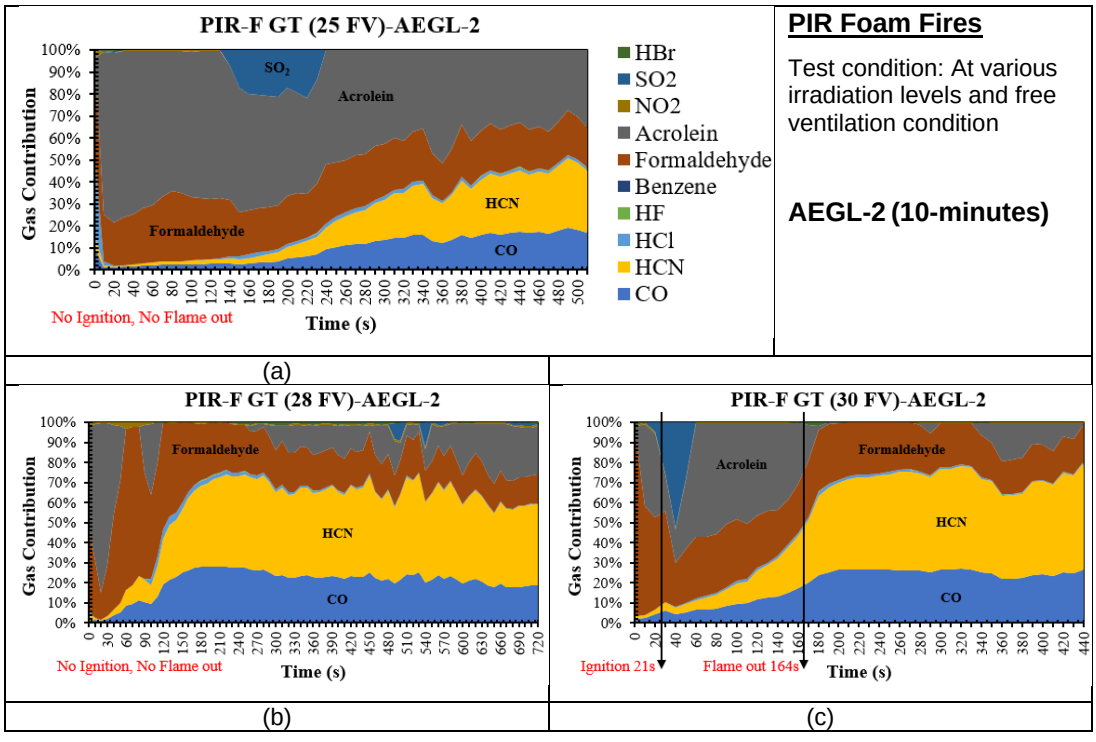

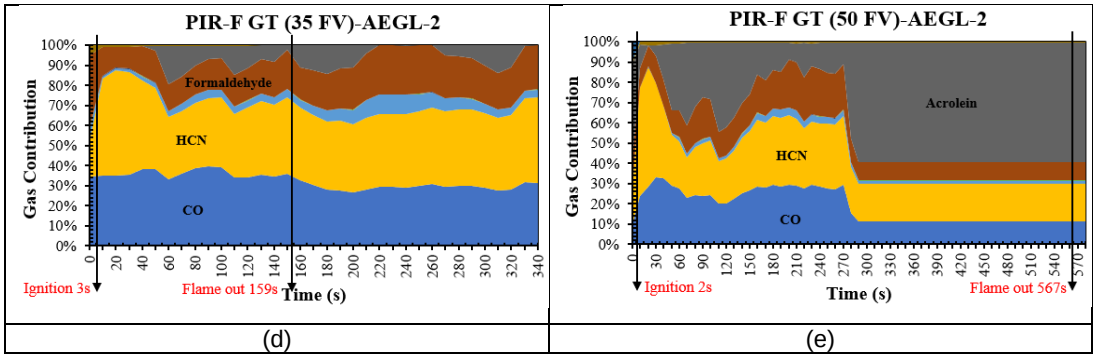


(d) (e)

**Figure 5.13** Contribution of major gases (based AEGL-$2_{10min}$) for various PIR foam fires.

## 5.2.8 Major Gases Contribution for PU and PIR Foam Fires at 35 kW/m² Irradiation Level with Free Ventilation

Major gas contribution based LC50 method as a function of time for four Polyurethane (PU) and a Polyisocyanurate (PIR) foam fires was shown in Figure 5.14. For most of these PU and PIR foam fires, CO and HCN were the main two toxic species with the highest contribution percentage, followed by other species such as Formaldehyde, Acrolein, HCl, HBr and $NO_2$. PU-FSC fire gave the highest HCN contribution with 40% to 70% from total contribution compared to other three foam fires with maximum less than 60% of contribution as major species. For PIR-F GT foam fire, CO showed 40% of contribution and HCN showed about 50% of contribution with another 10% contributed by Formaldehyde, HCl and $NO_2$ species.

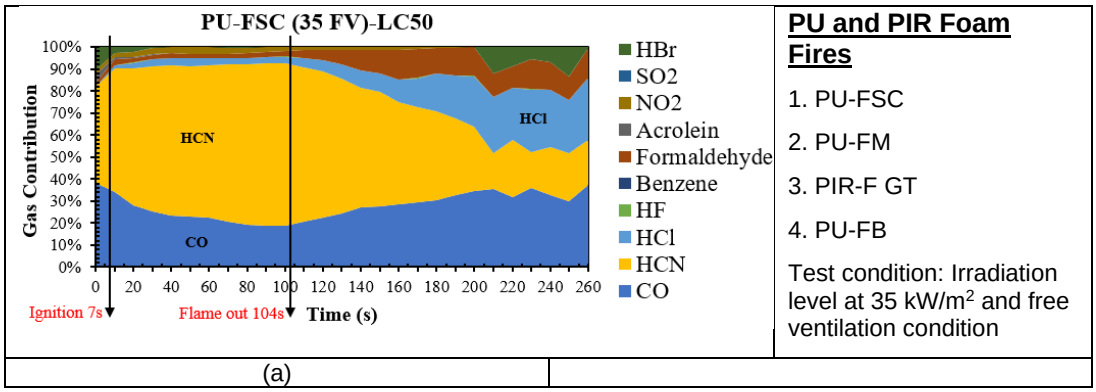


(a)

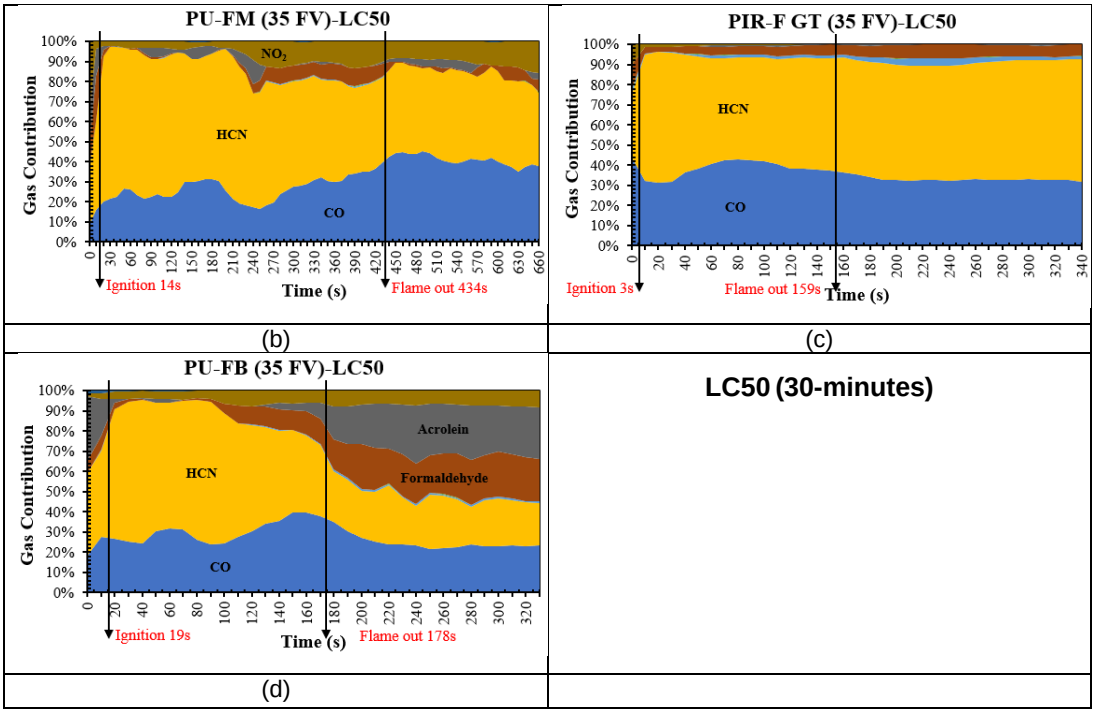


**Figure 5.14** Contribution of major gases (based $LC50_{30min}$) for PU and PIR foam fires at 35 kW/m$^2$ and free ventilation.

For major gas contribution based on $COSHH_{15min}$ method (see Figure 5.15), Benzene contribution for these foam fires were significant with PU-FM fire dominated the highest contribution of this species. HBr's contribution as a major species was identified within 50 s of PU-FSC foam fire with about 25% of percentage contribution, where other foam fires showed no significant HBr contribution from their burning. HCl contributions were high for PU-FSC and PIR-F GT foam fires according to this $COSHH_{15min}$ assessment method. PU-FB fire indicated the highest contribution of Acrolein at the start of burning and at the end of burning. For the first 50 s of PU-FB burning, the dominant species were Acrolein, CO and HCN and after that period, the highest percentage was dominated by Benzene and Formaldehyde. As in Figure 5.15 (b), the same species, Benzene and Formaldehyde had contributed to the highest percentage contribution as major species for PU-FM foam fire after 250 s of burning till the end of fire.

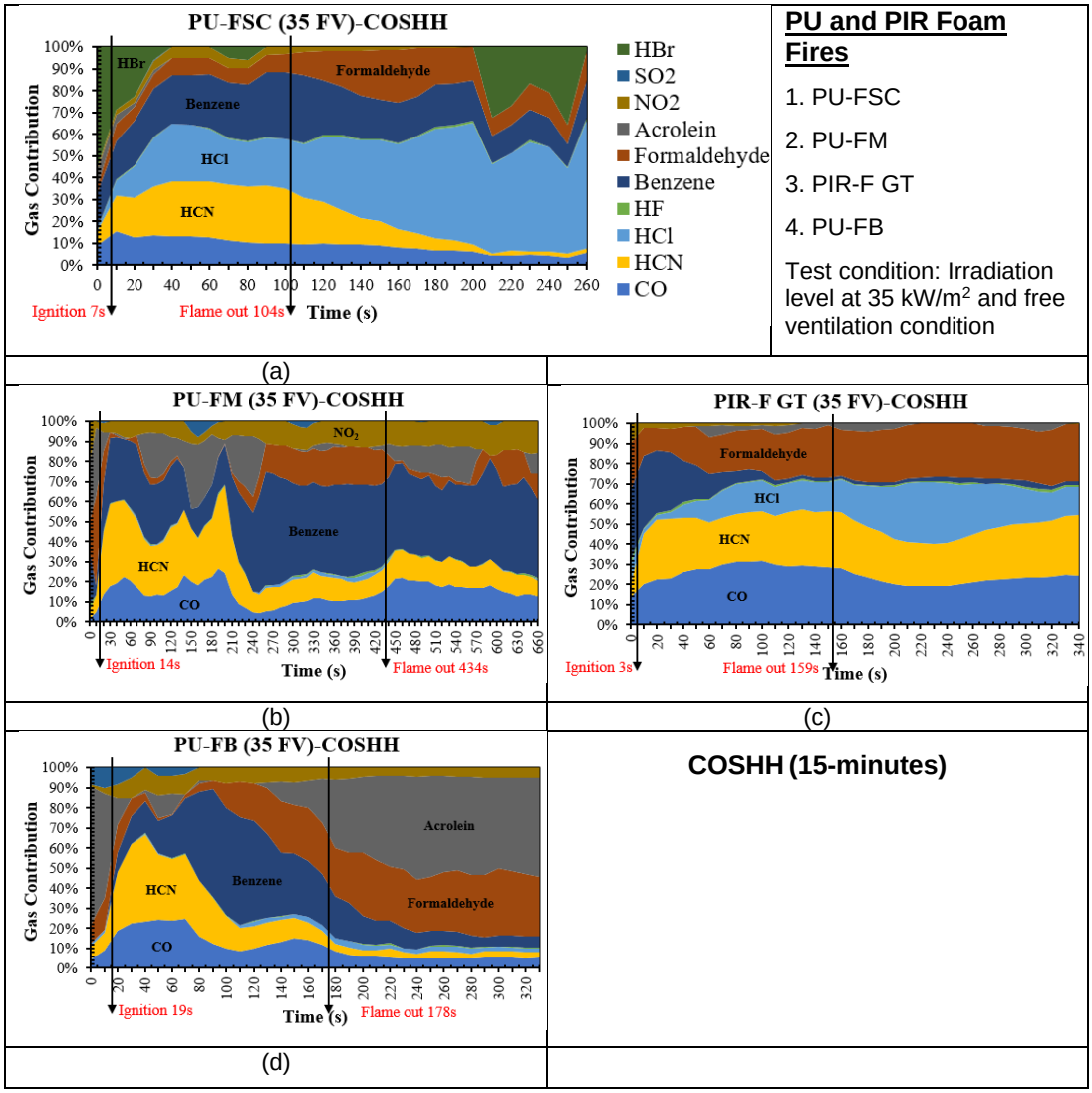


**Figure 5.15** Contribution of major gases (based $COSHH_{15min}$) for PU and PIR foam fires at 35 kW/m$^2$ and free ventilation.

Figure 5.16 showed contribution of major species based AEGL-2 method against time for PU and PIR foam fires.CO contribution was the highest for PIR-F GT foam fire compared to other three foam fires. Two HCN contribution peaks were observed for PU-FM foam fires with the first peak at 50 s and the second peak at 200 s. Acrolein had been the first major species for PU-FM and PU-FB foam fires with more than 50% percentage contribution. $SO_2$ contribution as a major species was also realised for PU-FM and PU-FB foam fires but no significant contribution was shown by PU-FSC and PIR-F GT foam fires. The percentage contribution of CO, HCN, HCl and Formaldehyde were shown a constant contribution profile after 50 s from the start of test until the flame out state for both PU-FSC and PIR-F GT foam fires. In general, it could

be concluded that CO, HCN, Formaldehyde, Acrolein and Benzene were the first five major species for PU and PIR foam fires that contributing to the total fire toxicity. The following Table 5.5 shows the first six major species for various solid foam fires.

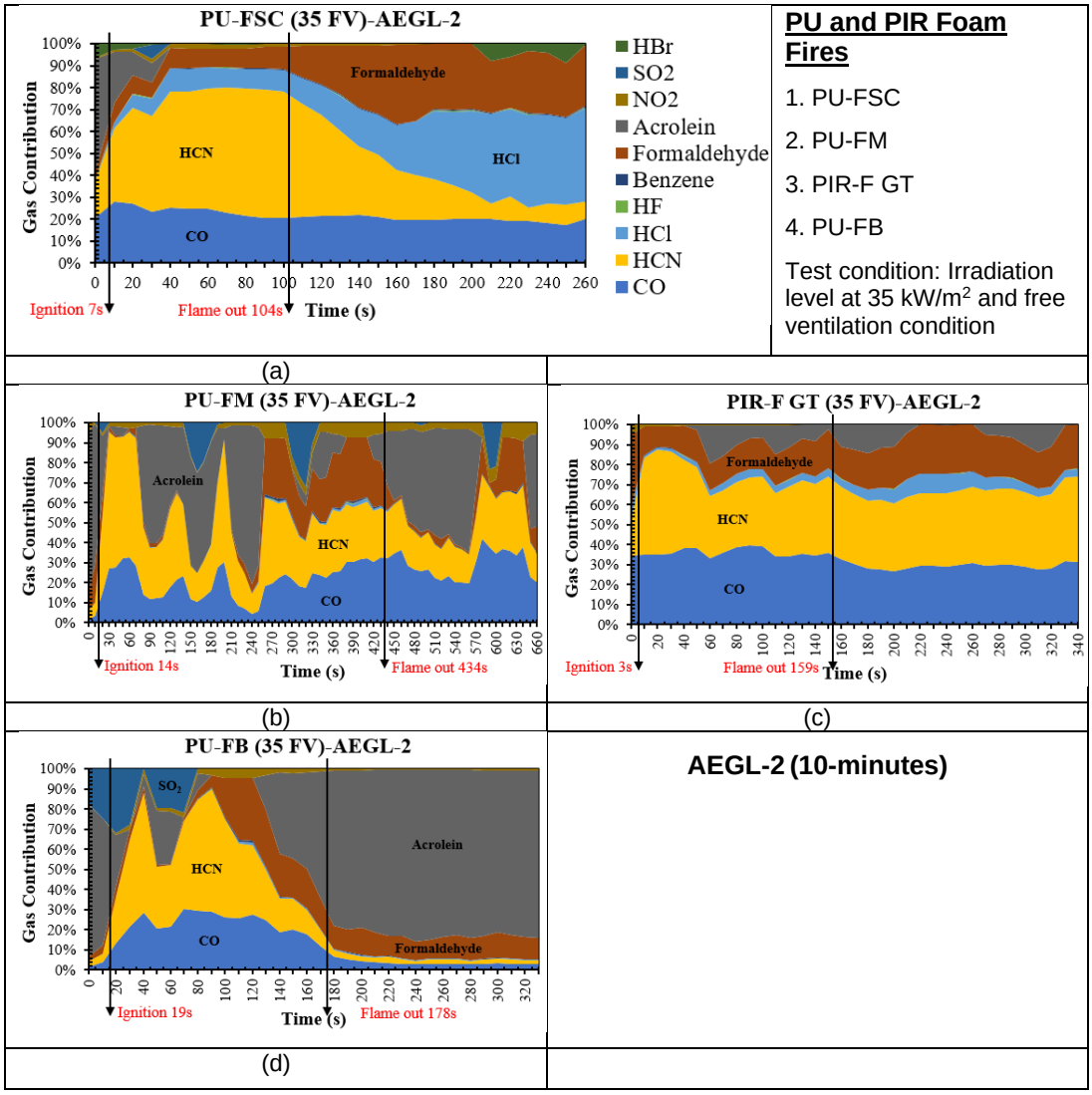


**Figure 5.16** Contribution of major gases (based AEGL-$2_{10min}$) for PU and PIR foam fires at 35 kW/m$^2$ and free ventilation.

**Table 5.5** First six major species for various solid foam fires.

| PIR SOLID FOAM GT FIRES | | | | | | | | | | | | |
|---|---|---|---|---|---|---|---|---|---|---|---|---|
| **Test** | **Test Details** | **Mean ER, Φ (Chan)** | **Time (s)** | **Fire Stage** | **TT** | **Major Species** | | | | | | |
| | | | | | | **1** | **2** | **3** | **4** | **5** | **6** |
| 1 | PIR-F GT | 0.03 | <10 | - | LC50 | Formaldehyde | HCl | Acrolein | CO | HCN | $NO_2$ |
| | 25 FV | 0.30 (peak) | 10 - 140 | SS 1 | | Formaldehyde | Acrolein | CO | HCN | $NO_2$ | HCl |
| | I = No | 0.10 | >140 | SS 2 | | HCN | CO | Formaldehyde | Acrolein | HCl | - |
| | F = No | 0.03 | <10 | - | COSHH | HCl | Formaldehyde | Acrolein | HBr | CO | HCN |
| | | 0.30 (peak) | 10 - 140 | SS 1 | | Formaldehyde | Acrolein | CO | Benzene | $NO_2$ | HCN |
| | | 0.10 | >140 | SS 2 | | Formaldehyde | Acrolein | HCN | CO | HCl | Benzene |
| | | 0.03 | <10 | - | AEGL-2 | Acrolein | Formaldehyde | HCl | CO | HCN | $NO_2$ |
| | | 0.30 (peak) | 10 - 140 | SS 1 | | Acrolein | Formaldehyde | CO | HCN | $SO_2$ | $NO_2$ |
| | | 0.10 | >140 | SS 2 | | Acrolein | Formaldehyde | HCN | CO | $SO_2$ | HCl |
| 2 | PIR-F GT | 0.10 | <15 | - | LC50 | Formaldehyde | Acrolein | HCN | CO | $NO_2$ | - |
| | 28 FV | 0.25 (peak) | 15 - 100 | - | | Formaldehyde | HCN | CO | Acrolein | $NO_2$ | HCl |
| | I = No | 0.12 | >100 | SS | | HCN | CO | Formaldehyde | $NO_2$ | HCl | HBr |
| | F = No | 0.10 | <15 | - | COSHH | Formaldehyde | Acrolein | $NO_2$ | HCl | - | - |
| | | 0.25 (peak) | 15 - 100 | - | | Formaldehyde | CO | HCN | Acrolein | $NO_2$ | HCl |
| | | 0.12 | >100 | SS | | HCN | Formaldehyde | CO | HBr | HCl | Acrolein |
| | | 0.10 | <15 | - | AEGL-2 | Acrolein | Formaldehyde | $NO_2$ | HCN | CO | HCl |
| | | 0.25 (peak) | 15 - 100 | - | | Formaldehyde | Acrolein | HCN | CO | HCl | $NO_2$ |
| | | 0.12 | >100 | SS | | HCN | Formaldehyde | CO | Acrolein | HCl | $SO_2$ |
| 3 | PIR-F GT | 0.15 | <21 | Ignition | LC50 | Formaldehyde | HCN | CO | Acrolein | $NO_2$ | HBr |
| | 30 FV | 0.24 (peak) | 21 - 40 | Flaming | | Formaldehyde | HCN | CO | Acrolein | $NO_2$ | $SO_2$ |
| | I = 21 s | 0.12 | 40 - 164 | SS Flaming | | HCN | CO | Formaldehyde | Acrolein | $NO_2$ | $SO_2$ |
| | F = 164 s | 0.08 | >164 | Post-flaming | | HCN | CO | Formaldehyde | $NO_2$ | HBr | - |

| | | | | | | | | | | | |
|---|---|---|---|---|---|---|---|---|---|---|---|
| | | 0.15 | <21 | Ignition | **COSHH** | Formaldehyde | Acrolein | $NO_2$ | HCN | HBr | CO |
| | | 0.24 (peak) | 21 - 40 | Flaming | | Formaldehyde | Acrolein | CO | HCN | $SO_2$ | $NO_2$ |
| | | 0.12 | 40 - 164 | SS Flaming | | Formaldehyde | Acrolein | HCN | CO | HCl | $NO_2$ |
| | | 0.08 | >164 | Post-flaming | | HCN | Formaldehyde | CO | HCl | Acrolein | HBr |
| | | 0.15 | <21 | Ignition | **AEGL-2** | Formaldehyde | Acrolein | HCN | CO | $SO_2$ | $NO_2$ |
| | | 0.24 (peak) | 21 - 40 | Flaming | | Formaldehyde | $SO_2$ | Acrolein | CO | HCN | - |
| | | 0.12 | 40 - 164 | SS Flaming | | Acrolein | Formaldehyde | HCN | CO | $SO_2$ | HCl |
| | | 0.08 | >164 | Post-flaming | | HCN | CO | Formaldehyde | Acrolein | HCl | - |
| 4 | PIR-F GT | 0.07 | <3 | Ignition | **LC50** | HCN | CO | Formaldehyde | $NO_2$ | - | - |
| | 35 FV | 0.18 | 3 - 10 | Flaming | | HCN | CO | Formaldehyde | $NO_2$ | - | - |
| | I = 3 s | 0.30 | 10 - 159 | SS Flaming | | HCN | CO | Formaldehyde | HCl | $NO_2$ | - |
| | F = 159 s | 0.15 | >159 | Post-flaming | | HCN | CO | Formaldehyde | HCl | - | - |
| | | 0.07 | <3 | Ignition | **COSHH** | Benzene | Formaldehyde | CO | HCN | HCl | $NO_2$ |
| | | 0.18 | 3 - 10 | Flaming | | CO | HCN | Formaldehyde | Benzene | HCl | Acrolein |
| | | 0.30 | 10 - 159 | SS Flaming | | Benzene | HCN | CO | Formaldehyde | HCl | $NO_2$ |
| | | 0.15 | >159 | Post-flaming | | Formaldehyde | HCl | CO | HCN | Acrolein | Benzene |
| | | 0.07 | <3 | Ignition | **AEGL-2** | CO | HCN | Formaldehyde | HCl | $NO_2$ | - |
| | | 0.18 | 3 - 10 | Flaming | | HCN | CO | Formaldehyde | $NO_2$ | HCl | - |
| | | 0.30 | 10 - 159 | SS Flaming | | CO | HCN | Formaldehyde | Acrolein | HCl | $NO_2$ |
| | | 0.15 | >159 | Post-flaming | | HCN | CO | Formaldehyde | Acrolein | HCl | - |
| 5 | PIR-F GT | 0.15 | <2 | Ignition | **LC50** | HCN | CO | Formaldehyde | $NO_2$ | Acrolein | - |
| | 50 FV | 0.35 (peak) | 2 - 290 | SS Flaming 1 | | HCN | CO | Formaldehyde | $NO_2$ | HCl | Acrolein |
| | I = 2 s | 0.15 | 290 - 567 | SS Flaming 2 | | HCN | CO | Acrolein | Formaldehyde | HCl | $NO_2$ |
| | F = 567 s | 0.15 | >567 | Post-flaming | | HCN | CO | Acrolein | Formaldehyde | HCl | $NO_2$ |

| | | | | | | | | | | | |
|---|---|---|---|---|---|---|---|---|---|---|---|
| | | 0.15 | <2 | Ignition | **COSHH** | Formaldehyde | HCN | Acrolein | CO | Benzene | $NO_2$ |
| | | 0.35 (peak) | 2 - 290 | SS Flaming 1 | | Formaldehyde | CO | HCN | HCl | Acrolein | Benzene |
| | | 0.15 | 290 - 567 | SS Flaming 2 | | Acrolein | HCN | Formaldehyde | CO | HCl | Benzene |
| | | 0.15 | >567 | Post-flaming | | Acrolein | HCN | Formaldehyde | CO | HCl | Benzene |
| | | 0.15 | <2 | Ignition | **AEGL-2** | Acrolein | HCN | Formaldehyde | CO | $SO_2$ | - |
| | | 0.35 (peak) | 2 - 290 | SS Flaming 1 | | HCN | CO | Acrolein | Formaldehyde | HCl | $NO_2$ |
| | | 0.15 | 290 - 567 | SS Flaming 2 | | Acrolein | HCN | CO | Formaldehyde | HCl | - |
| | | 0.15 | >567 | Post-flaming | | Acrolein | HCN | CO | Formaldehyde | HCl | - |
| **PU SOLID FOAM FIRES** | | | | | | | | | | | |
| 6 | PU-FSC | 0.06 | <7 | Ignition | **LC50** | HCN | CO | HBr | $NO_2$ | Formaldehyde | Acrolein |
| | 35 FV | 0.70 (peak) | 7 - 104 | SS Flaming | | HCN | CO | $NO_2$ | HCl | Formaldehyde | HBr |
| | I = 7 s | 0.30 | 104 - 200 | Post-flaming 1 | | HCN | CO | HCl | Formaldehyde | $NO_2$ | - |
| | F = 104 s | 0.10 | >200 | Post-flaming 2 | | CO | HCl | HCN | Formaldehyde | HBr | - |
| | | 0.06 | <7 | Ignition | **COSHH** | HBr | Benzene | HCN | CO | HCl | Formaldehyde |
| | | 0.70 (peak) | 7 - 104 | SS Flaming | | HCN | Benzene | HCl | CO | Formaldehyde | HBr |
| | | 0.30 | 104 - 200 | Post-flaming 1 | | HCl | Benzene | Formaldehyde | HCN | CO | $NO_2$ |
| | | 0.10 | >200 | Post-flaming 2 | | HCl | HBr | Benzene | Formaldehyde | CO | HCN |
| | | 0.06 | <7 | Ignition | **AEGL-2** | Acrolein | HCN | CO | HBr | Formaldehyde | HCl |
| | | 0.70 (peak) | 7 - 104 | SS Flaming | | HCN | CO | HCl | Formaldehyde | Acrolein | $NO_2$ |
| | | 0.30 | 104 - 200 | Post-flaming 1 | | Formaldehyde | HCN | HCl | CO | $NO_2$ | - |
| | | 0.10 | >200 | Post-flaming 2 | | HCl | Formaldehyde | CO | HCN | HBr | - |
| 7 | PU-FM | 0.5 | <14 | Ignition | **LC50** | HCN | Formaldehyde | Acrolein | CO | $NO_2$ | - |
| | 35 FV | 3.0 (peak) | 14 - 250 | SS Flaming 1 | | HCN | CO | $NO_2$ | Acrolein | Formaldehyde | - |
| | I = 14 s | 1.0 | 250 - 434 | SS Flaming 2 | | HCN | CO | $NO_2$ | Formaldehyde | Acrolein | - |
| | F = 434 s | 0.3 | >434 | Post-flaming | | CO | HCN | $NO_2$ | Acrolein | Formaldehyde | - |

| | | | | | | | | | | | |
|---|---|---|---|---|---|---|---|---|---|---|---|
| | | 0.5 | <14 | Ignition | **COSHH** | Formaldehyde | Acrolein | HCN | Benzene | $NO_2$ | CO |
| | | 3.0 (peak) | 14 - 250 | SS Flaming 1 | | HCN | Benzene | CO | Acrolein | $NO_2$ | Formaldehyde |
| | | 1.0 | 250 - 434 | SS Flaming 2 | | Benzene | Formaldehyde | HCN | CO | $NO_2$ | HCl |
| | | 0.3 | >434 | Post-flaming | | Benzene | CO | $NO_2$ | HCN | Acrolein | Formaldehyde |
| | | 0.5 | <14 | Ignition | **AEGL-2** | Acrolein | Formaldehyde | HCN | CO | $NO_2$ | - |
| | | 3.0 (peak) | 14 - 250 | SS Flaming 1 | | HCN | Acrolein | CO | $NO_2$ | $SO_2$ | Formaldehyde |
| | | 1.0 | 250 - 434 | SS Flaming 2 | | HCN | CO | Formaldehyde | $NO_2$ | $SO_2$ | Acrolein |
| | | 0.3 | >434 | Post-flaming | | Acrolein | CO | HCN | Formaldehyde | $NO_2$ | $SO_2$ |
| 8 | PU-FB | 0.4 | <19 | Ignition | **LC50** | HCN | Acrolein | CO | Formaldehyde | $NO_2$ | $SO_2$ |
| | 35 FV | 0.8 (peak) | 19 - 130 | SS Flaming 1 | | HCN | CO | $NO_2$ | Formaldehyde | Acrolein | - |
| | I = 19 s | 0.3 | 130 - 178 | SS Flaming 2 | | HCN | CO | Formaldehyde | $NO_2$ | Acrolein | - |
| | F = 178 s | 0.1 | >78 | Post-flaming | | CO | Acrolein | HCN | Formaldehyde | $NO_2$ | HCl |
| | | 0.40 | <19 | Ignition | **COSHH** | Acrolein | Formaldehyde | HCN | $SO_2$ | CO | $NO_2$ |
| | | 0.8 (peak) | 19 - 130 | SS Flaming 1 | | Benzene | HCN | CO | Formaldehyde | $NO_2$ | Acrolein |
| | | 0.30 | 130 - 178 | SS Flaming 2 | | Benzene | Formaldehyde | Acrolein | CO | HCN | $NO_2$ |
| | | 0.10 | >78 | Post-flaming | | Acrolein | Formaldehyde | Benzene | CO | $NO_2$ | HCN |
| | | 0.40 | <19 | Ignition | **AEGL-2** | Acrolein | $SO_2$ | HCN | Formaldehyde | CO | - |
| | | 0.8 (peak) | 19 - 130 | SS Flaming 1 | | HCN | CO | Acrolein | $SO_2$ | Formaldehyde | $NO_2$ |
| | | 0.30 | 130 - 178 | SS Flaming 2 | | Acrolein | Formaldehyde | HCN | CO | $NO_2$ | - |
| | | 0.10 | >78 | Post-flaming | | Acrolein | Formaldehyde | CO | HCN | $NO_2$ | - |

## 5.3 Particle Size Distributions for PIR Foam Fires with Varied Irradiation Levels

### 5.3.1 Particle Number and Mass Distributions for PIR Foam Fires

The particle number distributions for several times in the fire are shown in Figure 5.17 for five radiant heating levels. The peak particle number was highest for the higher radiant heating, which gives higher foam temperatures. Most radiant heat levels except for 25 kW/m$^2$, ultra-fine particles were generated at 1.0E+10 particles/cm$^3$ and these are incredibly high fine particle emissions, much higher than in the raw exhaust from old dirty diesel engines. This was the cause of the black particles in the lungs of survivors at Grenfell Towers. Doctors reported that they had to develop methods to flush the fine particles out of the lungs to prevent deaths. Bigger particles (>100 nm) had shown a lower number distribution compared to smaller particles for these foam fires.

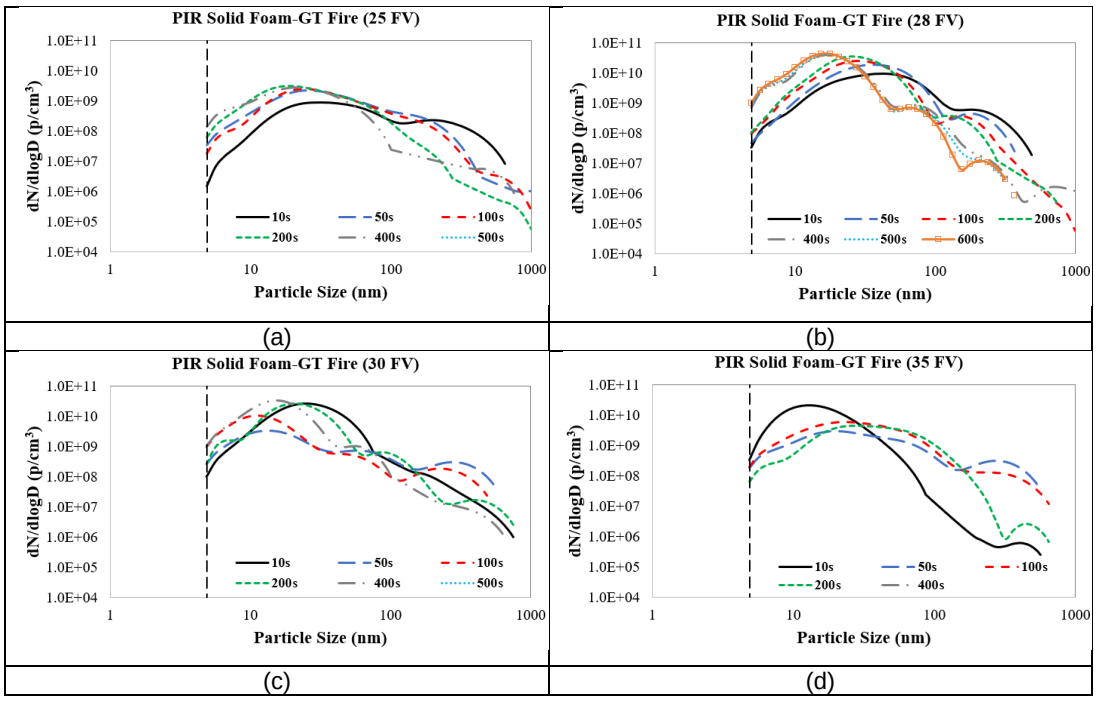

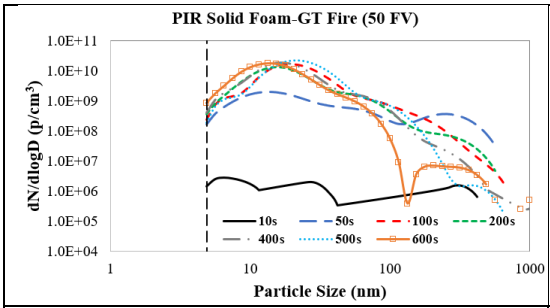


(e)

**Figure 5.17** Particle size (number) distribution for PIR foam fire at various heat fluxes and free ventilation.

Particle mass distribution for PIR foam fire at various heat fluxes and free ventilation is shown in Figure 5.18. These foam fires had shown mass concentration in a range from 1.0E-07 to 1.0E+01 g/m$^3$. In overall, the mass distribution graphs showed a higher mass concentration for larger particles than the smaller particles which the size below 100 nm. In early stage of burning at 10 s, larger particles were produced higher for lower heat fluxes of 25 kW/m$^2$ and 28 kW/m$^2$ compared to the higher heat fluxes. It showed that at lower temperature, the pyrolysis rate of the fuel was low and this reduced the formation of smaller particulates such as gases or aerosols which larger particles were produced more in this condition. Particle mass concentration values had increased with the increase in the size of particles produced from the combustion of this PIR-F GT foams.

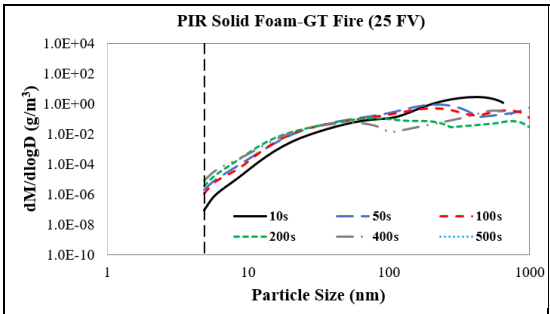


(a)

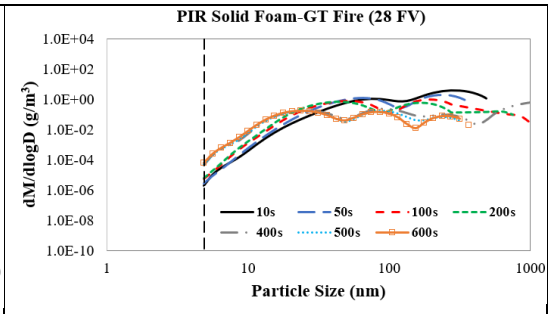


(b)

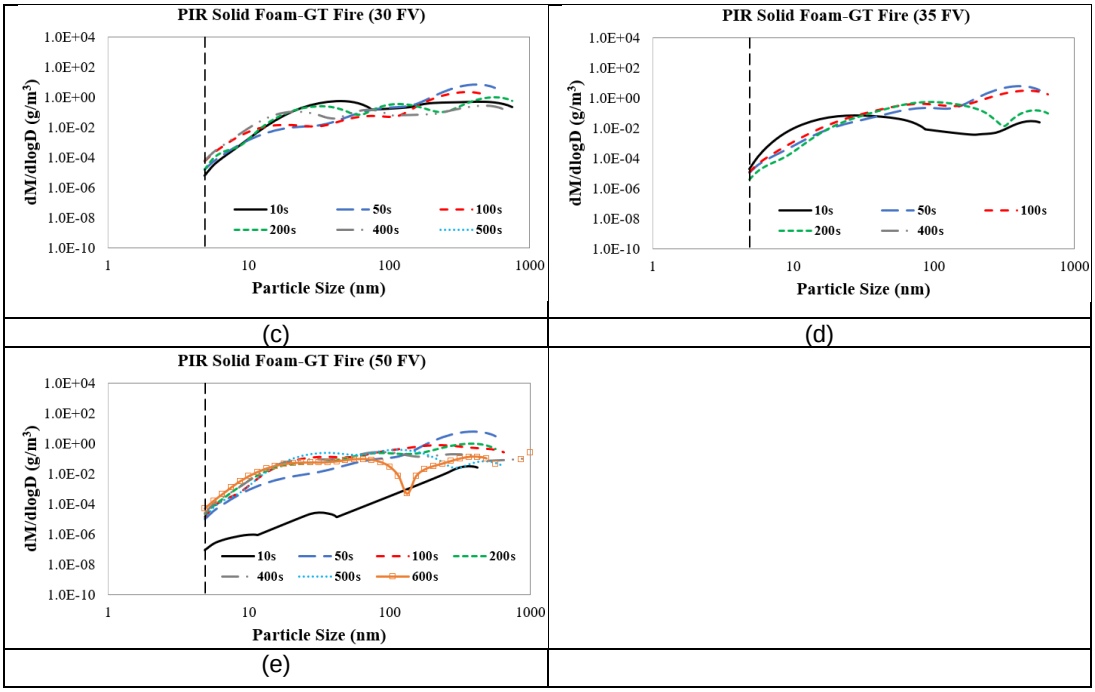


**Figure 5.18** Particle size (mass) distribution for PIR foam fire at various heat fluxes and free ventilation.

The health effect of smaller particles (<100 nm) is typically more critical than larger particles. These ultra-fine particles could act as carriers to toxic species which could enter human's body and bloodline through inhalation. which some of those toxic species were irritants and could cause irritations and damages to the internal organs while a toxic species like Benzene was carcinogenic and could cause cancers. These kind of fire hazards are not only giving short term effects but may also cause long term effects. In example, the World Trade Centre fire in New York in 2001, there were three firefighters who gave services as the first responders in the rescue process during the incident died on the same day due to different cancer deceases after 13$^{th}$ years of anniversary of the incident [17]. Figure 5.19 shows number and mass distributions for 10nm, 50nm and 100nm particles from PIR foam fire at various heat fluxes and free ventilation. For PIR-F GT foam fires, the highest particle number and mass concentrations were up to 1.0E+11 p/cm$^3$ and 1.0E+00 g/m$^3$. Number concentration of 10 nm, 50 nm and 100 nm particles were all high while 50 nm and 100 nm particles showed the higher mass concentration values than 10 nm particles.

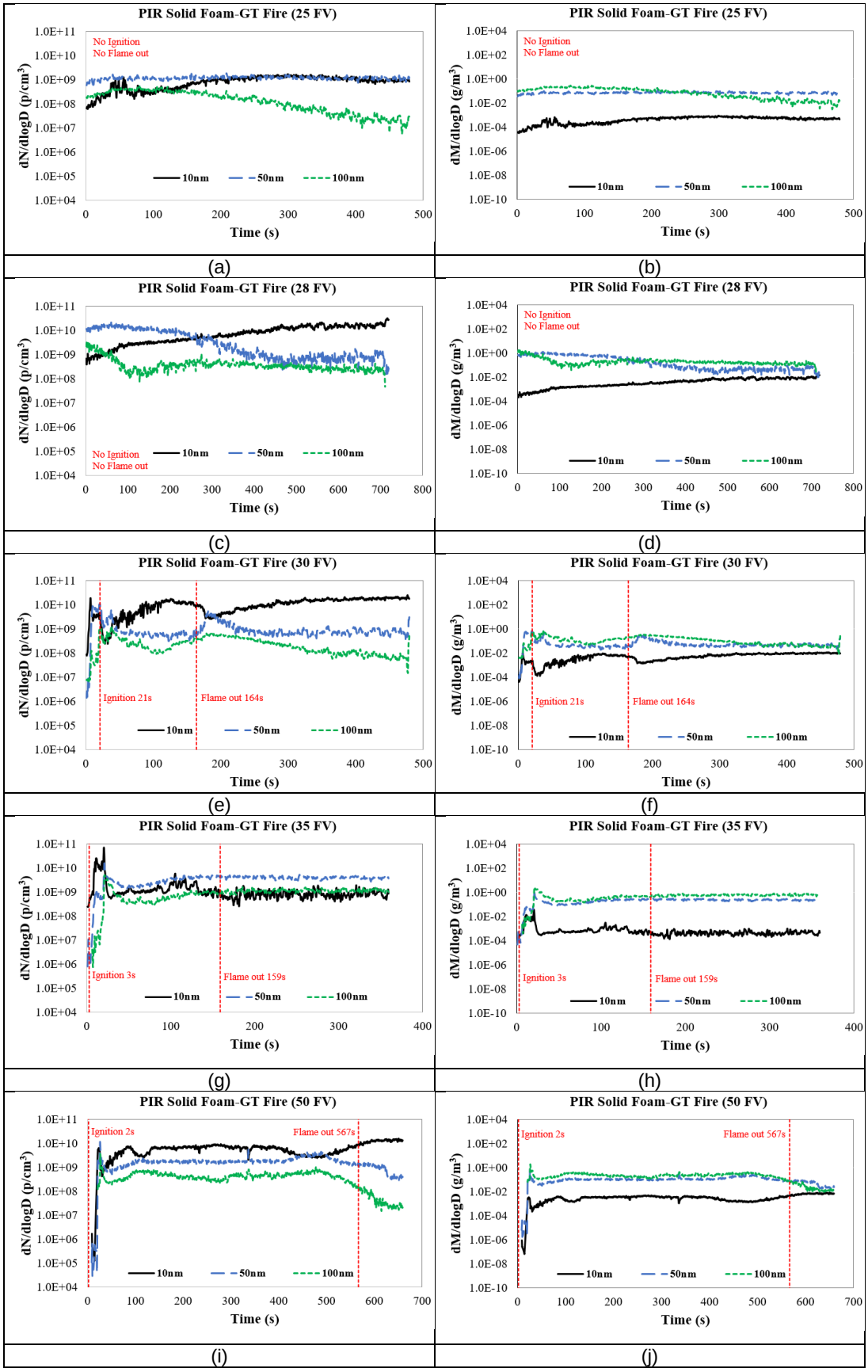


**Figure 5.19** Number and mass distributions for 10 nm, 50 nm and 100 nm particles from PIR foam fire at various heat fluxes and free ventilation.

From the 3D Waterfall plots, it could be seen clearly that the highest number concentration of <100 nm particles was given by PIR-F GT foam fire at heat flux of 28 kW/m$^2$. At this heat flux, the number concentration for ~200 nm particles was also high similar to foam fires at the higher heat fluxes. For heat fluxes from 28 kW/m$^2$ to 50 kW/m$^2$, the 3D plot profiles had given more than two peaks of the number concentration which each peak represented different sizes of particle. The same number of peaks were shown by the 3D mass distribution graphs especially for foam fires at heat fluxes of 28 kW/m$^2$ and 30 kW/m$^2$. Particle mass concentration had shown an increasing pattern with the increasing of particle size. For non-flaming foam fires at heat flux of 28 kW/m$^2$, it could be concluded that smaller particles (<100 nm) were produced more than the flaming foam fires at the higher heat fluxes. But, when the heating temperature was lower than 28 kW/m$^2$ (i.e. 25 kW/m$^2$), the production of particles was much more lower. It is possibly because the low rate of pyrolysis of the foam sample occurred at this temperature exposure which released low number of particles. Particle size (number and mass) distributions in 3D Waterfall plot for PIR foam fire at various heat fluxes and free ventilation is shown in the following Figure 5.20.

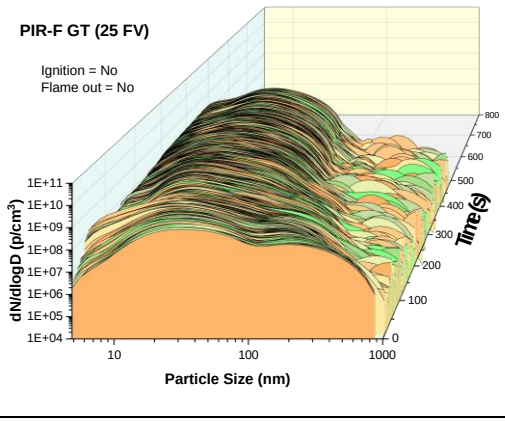
PIR-F GT (25 FV)
Ignition = No
Flame out = No
dN/dlogD (p/cm³)
Particle Size (nm)
Time(s)

(a)

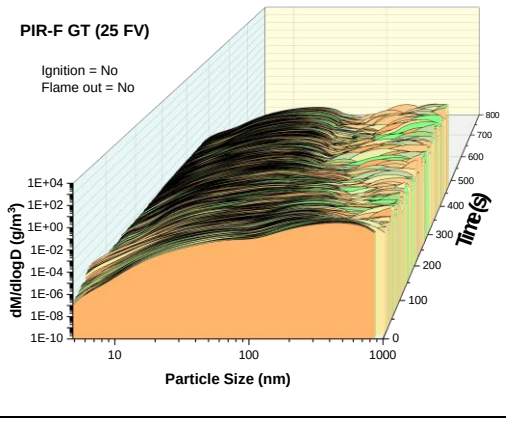
PIR-F GT (25 FV)
Ignition = No
Flame out = No
dM/dlogD (g/m³)
Particle Size (nm)
Time(s)

(b)

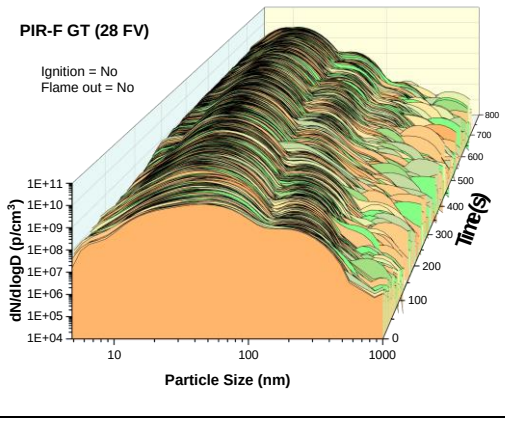
PIR-F GT (28 FV)
Ignition = No
Flame out = No
dN/dlogD (p/cm³)
Particle Size (nm)
Time(s)

(c)

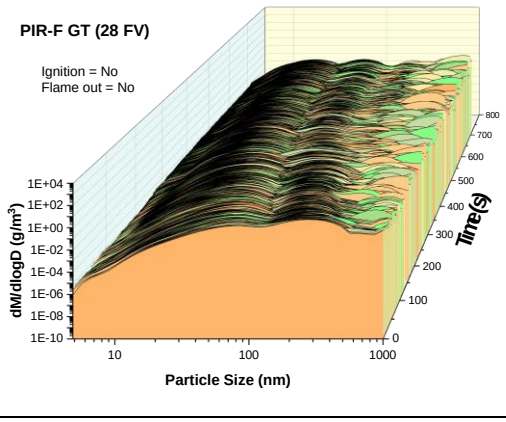
PIR-F GT (28 FV)
Ignition = No
Flame out = No
dM/dlogD (g/m³)
Particle Size (nm)
Time(s)

(d)

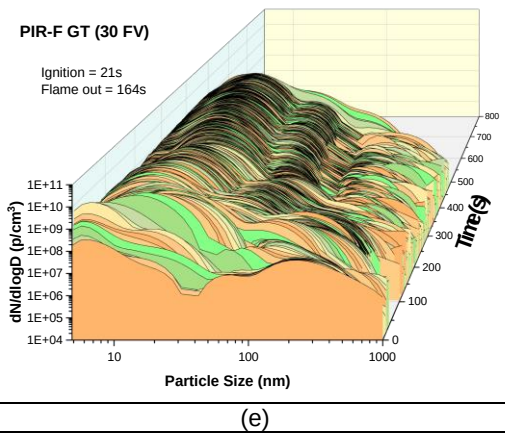
PIR-F GT (30 FV)
Ignition = 21s
Flame out = 164s
dN/dlogD (p/cm³)
Particle Size (nm)
Time(s)

(e)

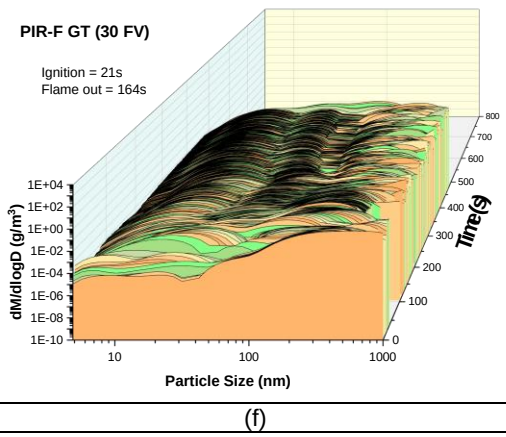
PIR-F GT (30 FV)
Ignition = 21s
Flame out = 164s
dM/dlogD (g/m³)
Particle Size (nm)
Time(s)

(f)

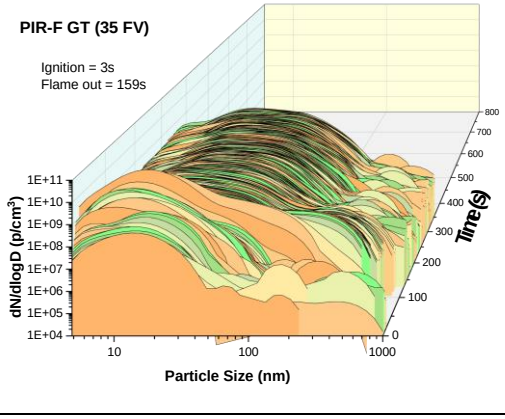
PIR-F GT (35 FV)
Ignition = 3s
Flame out = 159s
dN/dlogD (p/cm³)
Particle Size (nm)
Time(s)

(g)

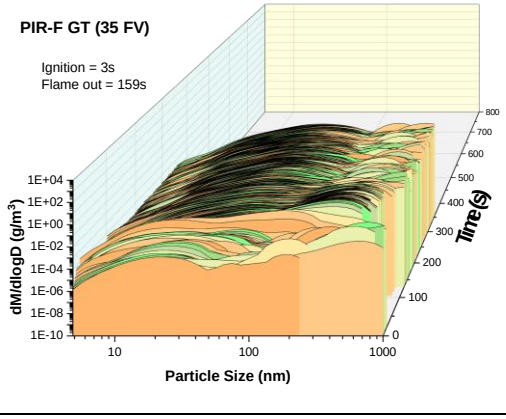
PIR-F GT (35 FV)
Ignition = 3s
Flame out = 159s
dM/dlogD (g/m³)
Particle Size (nm)
Time(s)

(h)

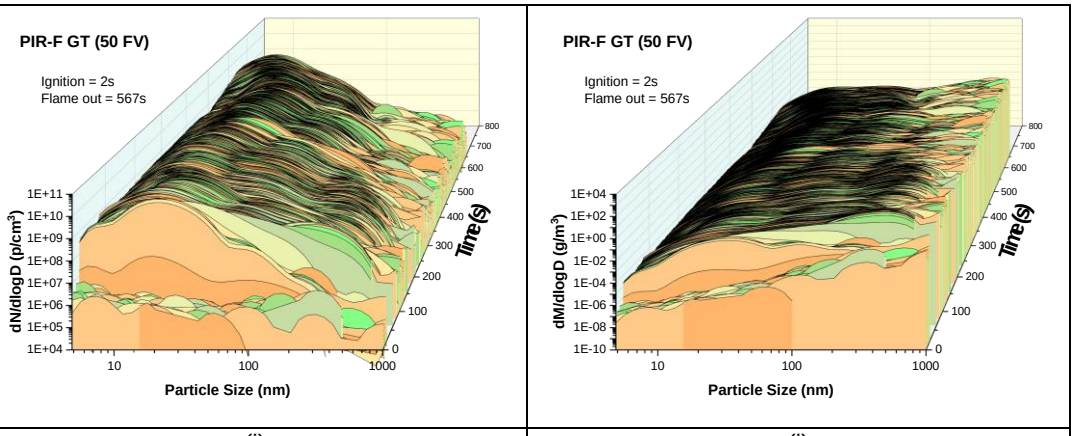


(i) (j)

**Figure 5.20** Particle size distributions in 3D Waterfall plot for PIR foam fire at various heat fluxes and free ventilation.

PIR foam fires at irradiation levels of 25 kW/m$^2$ and 28 kW/m$^2$ with free ventilation had shown a non-flaming fire condition. Following Figure 5.21 shows the cumulative mass at the end of each test as a function of particle size for PIR foam fire at various heat fluxes and free ventilation. For non-flaming PIR-F GT fires, the foam fire at heat flux of 28 kW/m$^2$ gave a higher cumulative mass of >600 g/m$^3$ compared to the foam fire at 25 kW/m$^2$ which <250 g/m$^3$. There were two peaks of cumulative mass shown by the foam fire at 28 kW/m$^2$ heat flux with the first and the second peaks were showing the cumulative mass of ~400 g/m$^3$ for 50 nm particles and ~600 g/m$^3$ for 200 nm particles. The cumulative mass values had increased with the increase of heat flux values for most of these foam fires. In comparison between the flaming and non-flaming fires, the flaming PIR-F GT foam fires gave a higher cumulative mass, at least double than the non-flaming PIR-F GT foam fires. This is possibly due to the higher number of larger size particles released which are mostly >400 nm from these flaming foam fires compared to the non-flaming foam fires. The higher heat flux value, the higher burning rate of these foam fires will be because more fuel is burned to form aerosols, hence it will produce more nano particles. The case was different for non-flaming fire condition where less fuel was burned without consuming the air due to insufficient energy to start the flaming combustion and the aerosols were only released during the pyrolysis only in a small amount.

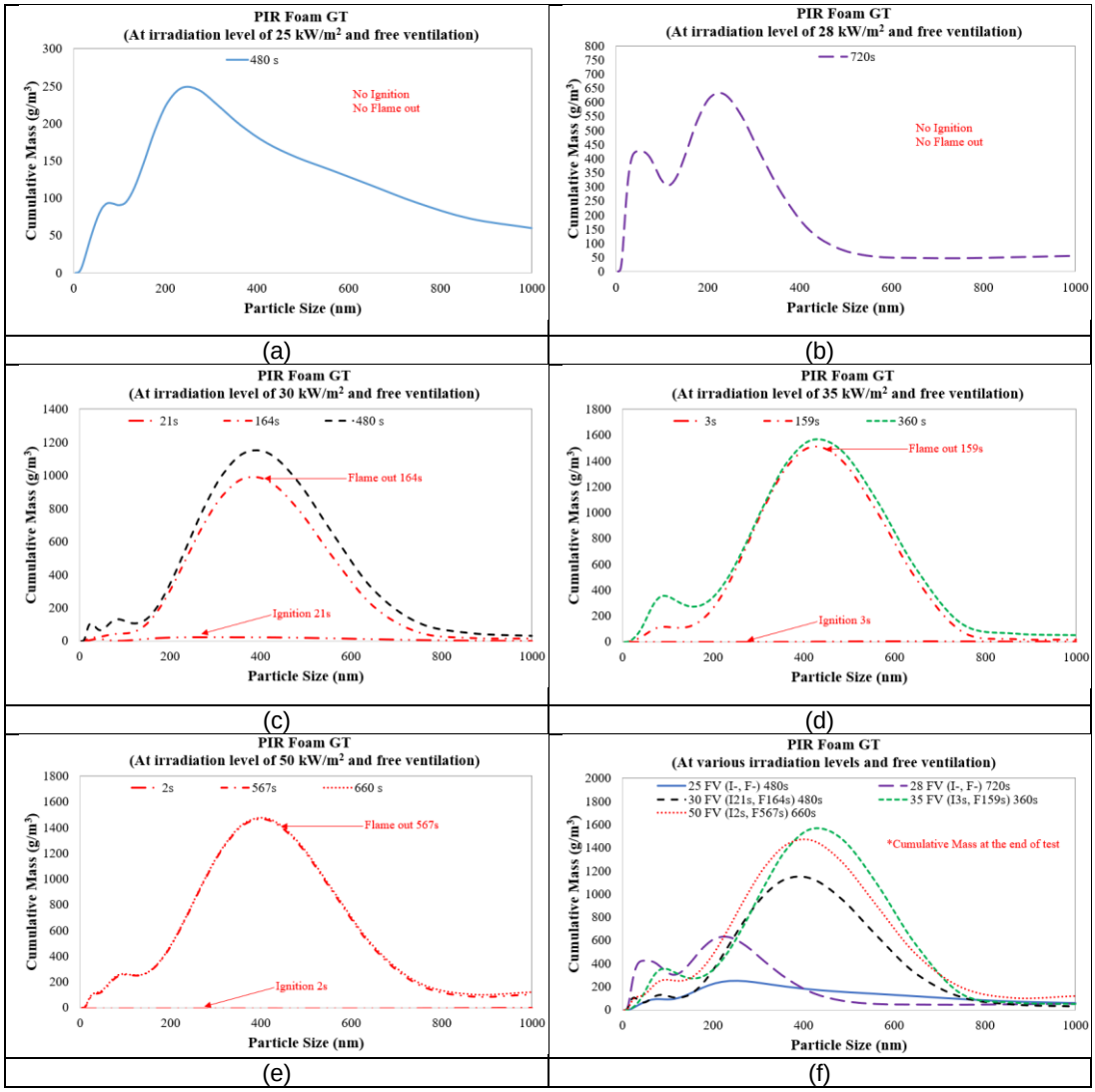


**Figure 5.21** Cumulative mass as a function of particle size for PIR foam fire at various heat fluxes and free ventilation.

## 5.3.2 Particulate Yields for PIR Foam Fires

PIR foam fire at heat flux of 25 kW/m$^2$ had given a maximum particulate mass yield of about 1.0E-02 g/g, this value was lower compared to PIR foam fires at higher heat fluxes which giving the mass yields >1.0E-02 g/g. Figure 5.22 shows the particulate yields in g/g for three sizes of particles (10 nm, 50 nm and 100 nm) as a function of time and fire equivalence ratio for PIR foam fire at various heat fluxes and free ventilation. For most of PIR foam fires, mass yields for 50 nm and 100 nm particles were higher than 10 nm particles. These solid foam fires had shown a lean burning condition with ER less than 0.4 with contributing to the almost same average level of mass yield for 10 nm, 50 nm and 100 nm particles except for PIR foam fires at heat fluxes of 25 kW/m$^2$ and

35 kW/m$^2$ which showing a larger different in the mass yield average. In overall, the increase in heat flux value had shown an increase in fire equivalence ratio value for this solid foam fires. By increasing the irradiation level, it would increase the burning rate and more fuel was burned and this would make the fire condition richer. As shown in Figure 5.22 (i), the mass yields were slightly increased with the increasing of size of particle.

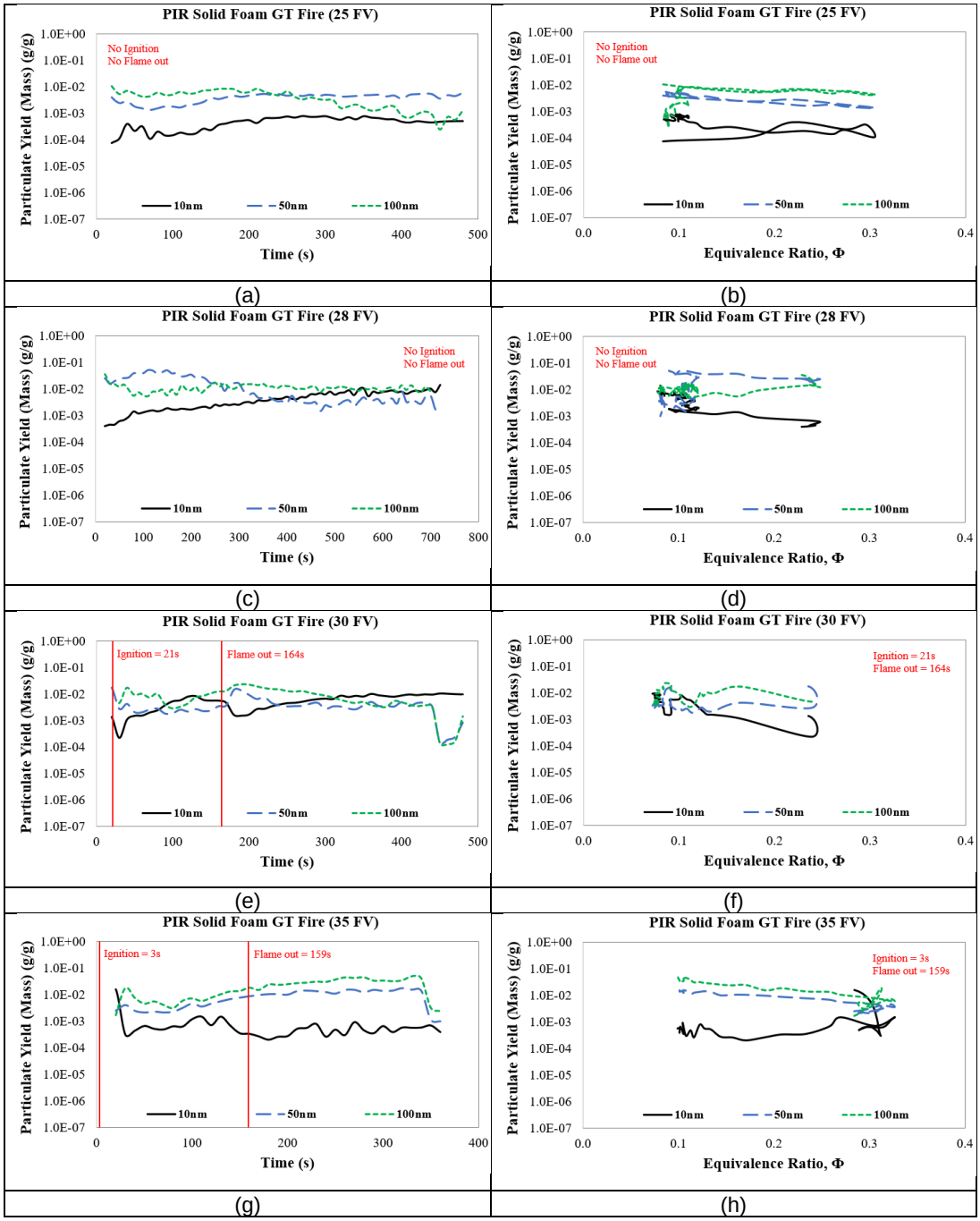

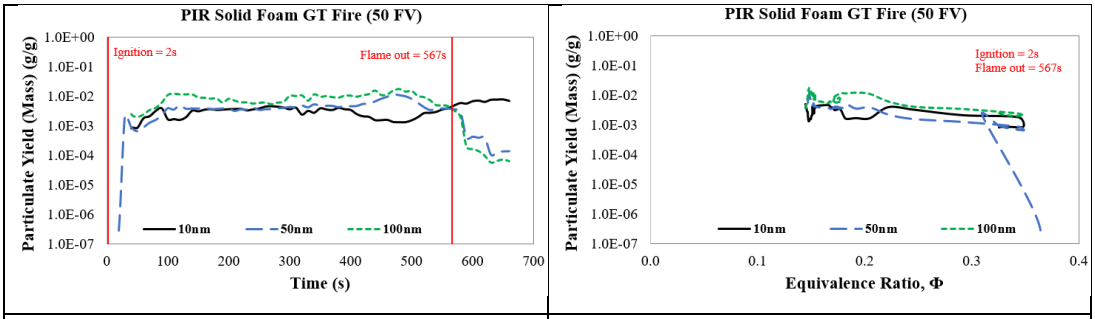


(i) (j)

**Figure 5.22** Particulate yields for PIR foam fire at various heat fluxes and free ventilation.

## 5.4 Findings and Conclusion from Solid Foam Fire Tests

### 5.4.1 PIR Foam Fires at Various Irradiation Levels

The PIR foam fire tests in the Cone Calorimeter with varying heat fluxes and with free ventilation condition resulted in the following findings:

- The burning rate of this PIR foam sample increased with the increase of heat flux value. The higher heat flux value exposed to the sample, the higher will be the mass loss. The result of these PIR foam fires showed that the highest mass loss and Oxygen consumption was given by the foam fire at the highest heat flux of 50 kW/m$^2$ compared to the lower heat fluxes. The HRR values released from this foam fire were also higher at the higher heat flux exposure to these PIR-F GT foam samples with the maximum peak of HRR value of ~140 kW/m$^2$ at heat flux of 50 kW/m$^2$. Compared with the lower heat fluxes (25 kW/m$^2$, 28 kW/m$^2$, 30 kW/,m$^2$ and 35 kW/m$^2$) the peak HRR at this heat flux for PIR foam fire was about double. Most of these foam fires had shown a fuel lean burning condition with fire equivalence ratios, ER<0.8.
- PIR foam fires at higher heat fluxes of 35 kW/m$^2$ and 50 kW/m$^2$ with free ventilation rate produced higher concentration of toxic gases such as CO, HCN, Benzene, Acetylene, $CO_2$, NO and $NO_x$ compared to the PIR foam fires at lower heat fluxes (25 kW/m$^2$ and 28 kW/m$^2$).
- Emissions of species (mainly Hydrocarbons) like Formaldehyde, Acrolein, THC, Acetaldehyde and Toluene were higher for PIR foam fires at lower heat fluxes of 25 kW/m$^2$ and 28 kW/m$^2$ than the PIR foam fires at the higher heat fluxes (35 kW/m$^2$ and 50 kW/m$^2$).

- Halogenated species like HCl and HBr were also released from these foam fires with each species gave a maximum concentration less than 500 ppm and 200 ppm.
- Maximum CO yields from the burning of these PIR foam samples were in a value range from 0.20 g/g to 0.35 g/g with the foam fire at heat flux of 35 kW/m$^2$ giving the highest maximum yield of ~0.35 g/g. The average of HCN yields was ~ 0.02 g/g for most of these PIR foam fires except for the foam fire with the heat flux value of 50 kW/m$^2$ which had shown the average HCN yield of ~0.01 g/g, half than the average HCN yield produced from other three foam fires.
- At higher heat fluxes of 35 kW/m$^2$ and 50 kW/m$^2$, the efficiency rate were higher for these PIR foam fires compared to the lower heat flux foam fires. It showed that the combustion efficiency increased when the heat flux value was increased. Most of these foam fires experienced a lean burning condition with equivalence ratios less than 1.0.
- Total toxicities based on LC50, COSHH$_{15min}$ and AEGL-2 assessments for these foam fires were <5, <1200 and <500. Compared to PIR burning at higher heat fluxes, the lower heat fluxes contributed to a higher total toxicity for COSHH$_{15min}$ and AEGL-2 basis.
- The six main toxic species that contributing to the fire toxicity from these PIR foam fires were CO, Benzene, Formaldehyde, Acrolein, HCN and $NO_2$. The presence, formation and production of HCN and $NO_2$ are as what initially expected from these Nitrogen contained Polyisocyanurate materials.
- The particulate cumulative mass in g/m$^3$ increased with the increase of heat irradiation. Larger particles (>200 nm) contributed to higher cumulative mass values compared to the smaller particles (<200 nm) for these PIR foam fires. For the two lower heat fluxes (25 kW/m$^2$ and 28 kW/m$^2$), the cumulative mass for 200 nm particles was about double than 100 nm particles while for the higher heat fluxes (30 kW/m$^2$, 35 kW/m$^2$ and 50 kW/m$^2$), the cumulative mass of 200 nm particles was about 4 times higher compared to 100 nm particles.

### 5.4.2 PIR and PU Foam Fires at 35 kW/m$^2$ with Free Ventilation

The main findings and comparison of results for four types of foam fires at irradiation level of 35 kW/m$^2$ and free ventilation as follow:

- PU-FM foam fire had the highest Oxygen consumption and contributed to the highest MLR value of 0.3 g/s. Other foam fires gave MLR values <0.1 g/s, were lower in a factor of 3 compared to the PU-FM foam fire. The PU-FM foam fire showed a rich burning condition with equivalence ratios (ER) up to 1.2 while other foam fires had shown a lean burning condition with ER<1.0.
- The Polyurethane floor mat (PU-FM) and packaging material (PU-FB) fires gave higher concentrations for most of considered toxic species compared to PU-FSC and PIR-F GT foam fires. CO emissions were about 70000 ppm maximum for both PU-FM and PU-FB foam fires, <3000 ppm for PU-FSC foam fire and about 5000 ppm maximum for PIR-F GT foam fire.
- Concentration of irritants such as HCl were the highest for PU-FSC foam fires compared to other three foam fires which giving a maximum HCl peak up to 2500 ppm while other foam fires gave less than 500 ppm of HCl concentrations.
- If compared between both PU and PIR foam fires, the PIR foam fire had shown a much lower of HCN emission which was <500 ppm. The HCN concentration for PU foam fires were several times higher than PIR foam fire and peaked at above 2000 ppm up to 4000 ppm.
- $CO_2$ and THC yields for these foam fires were <3.0 g/g and <0.7 g/g with PIR-F GT foam fire gave the highest $CO_2$ yield peak (~2.8 g/g) and the lowest THC yield peak (~0.15 g/g). Between the four foams, the PU-FB foam fire gave the highest maximum CO yield of >0.5 g/g while other foam fires showed lower yields of CO with <0.4 g/g. The PU-FB burning also produced a higher HCN yield of ~0.04 g/g compared to other three foam burnings which produced lower HCN yields.
- HCl yield was the highest for PU-FSC foam fire which ~0.13 g/g where PU-FM, PIR-F GT and PU-FB gave lower HCl yields (<0.03 g/g).
- For LC50 total relative toxicity, PIR foam fire had the FEC LC50 <5.0 which showing a lower toxicity level than the PU foam fires which with up to 40 of LC50 values. Under $COSHH_{15min}$ toxic assessment method, PU-FM foam fire gave the highest total toxicity of 4000, followed by PU-FB (~3000), PU-FSC (~2000) and PIR-F GT (<300). For AEGL-2 basis, PU-FM foam fire had shown the maximum peak of total toxicity of up to 1700 while other foam fires gave the total toxicity values <800.
- CO, Benzene, Formaldehyde, Acrolein, HCN and $NO_2$ were the major toxic species that dominating the total toxicity of these foam fires. Other

toxic species such as HCl, HBr and $SO_2$ were also presence and contributing to the overall fire toxicity but the contribution was less significant for these PU and PIR foam fires.

# Chapter 6
# Polyethylene Fires with Free Ventilation in the Cone Calorimeter Test

## 6.1 Introduction

Polyethylene was a key feature of the fire load at Grenfell Towers as the Aluminium outer cladding was lined by a thin layer of Polyethylene. Although samples of this cladding material were not included in this study, the toxic emissions from other Polyethylene samples would be similar. The present work was carried out under free ventilation conditions using the Cone Calorimeter. It is shown that the gases discharged from the cone through the chimney, added to enable gas sampling, were fuel rich for most of the fires. In the Grenfell Towers fire the Polyethylene was inside the Aluminium outer cover with an air gap to the insulating foam. This was a restricted ventilation condition and it is likely that locally the burning was richer than stoichiometric, in spite of the surrounding air. The Cone Calorimeter with its rich local combustion is thus considered to be a reasonable approximation to the burning conditions of PE at Grenfell Towers.

Polyethylene (PE) is used in industry for many purposes and five commercial PE samples were investigated. Three of the PE samples were used for portable bunding for flammable materials. Potentially PE bunding can increase the risk of a flammable liquid fire as PE is flammable and easily ignited. This work was carried out to determine the risk of ignition of PE bunds and the toxic products released if the bund material burnt in a fire. This was part of an industrial risk assessment of the fire hazards of these portable bunds (Neil Duddy). Three suppliers of commercial bunds were used for the samples in the Cone Calorimeter tests. The supplier PE codes were Denios 136403W (blue), Yellow Shield IBC (yellow) and Darcy 1840/NPIBC (black). They are referred to in this work by their colour (PE-Y, PE-Blue and PE-Black). A Glass Reinforced Plastic (GRP-Blue) bund was also investigated from SuiGeneris GRP code SG101. In addition, a common storage box for commercial paper document storage was investigated (this was a purple colour) and was referred to as a Polyethylene storage box (SB-P Purple storage box), the manufacturer was unknown but this type of large storage box is in common usage and were purchased from Wilko’s. A fifth PE material was PE water pipes (PE-Pipe or PEP-White) that are in common use in

household and commercial water plumbing circuits and were purchased from Homebase.

The elemental analysis of these materials (items 32 – 37 in Table 3.11) showed that the three bund materials were close to PE with H/C of 2.24 (PE-Blue), 2.36 (PE-Black) and 2.1 (PE-Yellow) compared with a H/C of 2.0 for pure Polyethylene. The purple storage box had a H/C of 1.51 and O/C of 0.13 and the PE pipe had a H/C of 1.01 and O/C of 0.57. It is clear that the last two materials may have been described as Polyethylene, but they had other oxygenated polymers in the composition. The first two PE bunds were also significantly different from pure PE.

The three of these PE that were used as flammable liquid bunds were also investigated for the minimum radiant ignition energy and the time to ignition, as this was related to their fire risk analysis safety case. Figure 6.1 shows the types of bunds used in industry.

## 6.2 General Combustion Properties for Different Types of Polyethylene Fires

Five samples of Polyethylene (PE) were investigated in the present work which were PE-Yellow (PE-Y), PE-Blue, PE-Black, purple storage box (SB-P) and PE pipe (PEP). GCV values (Table 3.11) for all Polyethylene samples obtained from ultimate analysis by the Bomb Calorimeter were almost same (~47 MJ/kg) except for PE pipe with a GCV of 44.42 MJ/kg). All five Polyethylene samples were tested in the Cone Calorimeter for assessments of fire toxicity at heat irradiation of 35 kW/m$^2$ under free ventilation condition.

Observations during the fire tests showed that most of the Polyethylene samples when exposed to the cone heater first produced a cracking sound before ignition. The PE melted in the fires and formed a liquid pool fire. The test details for Polyethylene fires are summarised in Table 6.1. Among these Polyethylene fires, the PE-Blue sample had the longest time delay before ignition at 114 s. SB-P and PEP samples had an ignition delay of 62 s. This different was significant and there was no obvious reason for this difference apart from the inclusion of a fire retardant in the composition. It is shown later that HBr was very high in all three PE bund materials, but was significantly higher for PE-Blue. There was low level HCl and no HF in the fire products so the main fire retardant used would be Bromine based. The gases released

contained high levels of $NH_3$ and $NO_x$ and this indicates that possibly Ammonium bromide was the fire retardant [137].

The PEP fire had the longest period of burning (1033 s of total time) with an ignition at 62 s and a flame out at 1095s. The HBr was low for this material and so the included fire retardant would be low. Meanwhile, the SB-P fire gave the shortest burning period of 716 s with an ignition at 62 s and a flame out at 778 s. This SB-P sample was the thinnest wall compared to other Polyethylene samples and this was the reason why this Polyethylene sample had the shortest burning period. Also SB-P had low HBr indicating that it was not significantly fire retarded.

**Table 6.1** Test details for Polyethylene fires.

| Test | Polyethylene Type | Thickness (mm) | Initial Mass (g) | Ignition (s) | Flame out (s) |
|---|---|---|---|---|---|
| 1 | PE-Y | 9 | 78.0 | 87 | 846 |
| 2 | PE-Blue | 9 | 77.9 | 114 | 866 |
| 3 | PE-Black | 8 | 77.9 | 81 | 1058 |
| 4 | SB-P | 2 | 15.7 | 62 | 778 |
| 5 | PEP | 15 | 49.4 | 62 | 1095 |

The time to ignition showed that PE-Yellow had the greater fire retardant performance with the longest time to ignition at the minimum ignition radiant flux.

The minimum radiant heat flux for piloted ignition and time to ignition at the minimum radiant heat flux is as follows.

a) PE-Yellow – Industrial bunding containers for flammable liquid spillages (15.5 kW/m$^2$, 1067 s)
b) PE-Blue – Industrial bunding containers for flammable liquid spillages (13.5 kW/m$^2$, 707 s)
c) PE-Black – Industrial bunding containers for flammable liquid spillages (18.5 kW/m$^2$, 738 s)
d) SB-P Purple storage boxes
e) PEP White Polyethylene pipes (domestic)

(a) Steel Bund (b) Stainless Steel Bund (c) Composite Bund

**Figure 6.1** Types of bunds used in industry.

### 6.2.1 Profile for Mass Reduction and Oxygen Changes

Figure 6.2 (a) and (b) shows the normalised mass loss and oxygen consumption as a function of time for Polyethylene fires at 35 kW/m$^2$ with free ventilation. The normalised mass loss for PE-Y, PE-Black and PEP were high at close to 100% and another two Polyethylene fires (PE-Blue and SB-P fires) gave a maximum 80% of total mass loss. For the SB-P fire, the sample mass reduced quickly within up to 150 s of burning period and after that time the SB-P sample burning became slower. Fig. 6.2 shows that SB-P had 30% mass loss in the first 100s, but there was no Oxygen consumption. This indicates that the PE was simply vaporised or pyrolysed but not burnt. This is supported by the toxic gas results reported later. In the first 100 s there was no primary HRR, total HC peaked at 50% and Acetylene at 7%. These high emissions are a calibration error as the FTIR was not calibrated for such high levels of Hydrocarbons. However, it does support the above conclusion that the PE was vaporised and pyrolysed into gaseous hydrocarbons. The toxic gas results also show in the first 100 s at peak HCN of 900 ppm and a peak $NO_x$ of 800 ppm (with no flame present), which are close to the calibration. This strongly indicates that this PE sample had significant N compounds in it, possibly likely from the dye used to give the purple colour, but more likely from the fire retardant if Ammonium bromide was used. It shows that polymers in fires are not only a problem from their flaming emissions but the action of radiation from a fire elsewhere is to produce toxic gas emissions even though there is no flame from the polymer.

GRP-Blue fire had consumed less Oxygen than the other Polyethylene fires with the maximum oxygen consumption of 5% by volume for the period of burning from 200 s until 400 s. The highest Oxygen consumption of 15% by

volume was shown by PE-Black fire at 300 s to 1000 s of test time. This is shown later to have the second highest HBr toxic gas concentration and with PE-blue, which had the highest HBr, the mass loss rate was the lowest. However, once ignited PE-blue had the highest HRR with the lowest oxygen level.

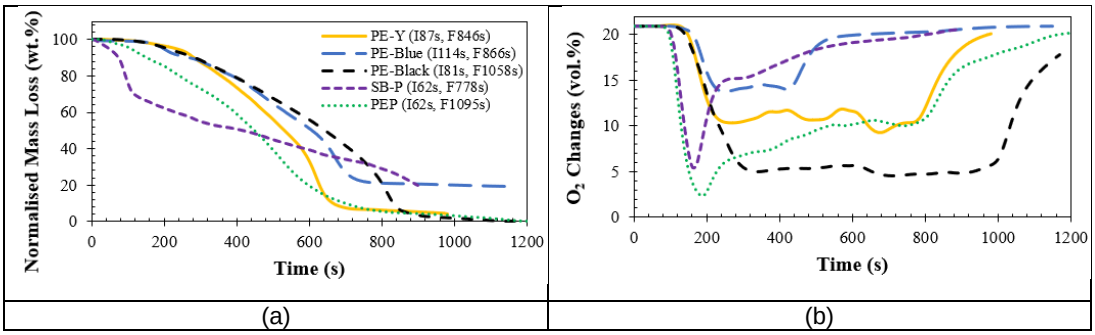


**Figure 6.2** Normalised mass loss and oxygen changes against time for Polyethylene fires at 35 kW/m$^2$ with free ventilation.

### 6.2.2 MLR and ER

Figure 6.3 shows the mass loss rate (MLR) and equivalence ratio (ER) for Polyethylene fires as a function of time. This show that the SB-P PE sample behaved differently to the others. As noted above initially in the first 100 s Hydrocarbons were vaporised but not burnt and this gave a very rich peak (over rich as the FTIR was off-scale in these tests). Once the gases auto-ignited the mass loss rate was low relative to the pyrolysis period and the combustion occurred in the lean region. The mass loss rate during the flaming combustion period was relatively low compared to the other samples. All the other four samples behaved in a similar way with a near linear increase in the mass loss rate until most of the mass was consumed, as shown in Figure 6.2. Near the end of the fire the PE samples which started off thermally thick were thermally thin and there was a sudden increase in the mass loss rate, just before the PE was burnt out and this gave a peak in the equivalence ratio. The PEP did not show this final peak in mass loss rate, possible because the pipe structure collapsed at the end of the test. The very large variations in the oxygen in Figure 6.2 combined with the rich equivalence ratios in Figure 6.3 show that the combustion efficiency must be low for some PE and higher for others. Rich mixtures in a fire should have low Oxygen and this has not occurred in these fires and this is because all the fuel pyrolysed has not burnt.

Figure 6.2 Oxygen levels show that PE-Black burnt well with low Oxygen but PE-Blue burnt poorly, as did SB-P. PE-Blue had high HBr emissions (see later) and indicates that it was fire retarded. This gives poor flames in the fire and very high toxic gas emissions as the fire does not generate the higher temperatures necessary to consume the fuel. In Table 6.1 it is shown that PE-Blue had a longer ignition delay, but this was not a major change from the non-fire retarded PE samples. Thus the addition of this brominated fire retardant made the fire toxicity worse as it prevented complete combustion of the PE. The equivalence ratio in the PE-Blue fire was close to stoichiometric and this led to high fire temperatures and relatively low toxic gas emissions.

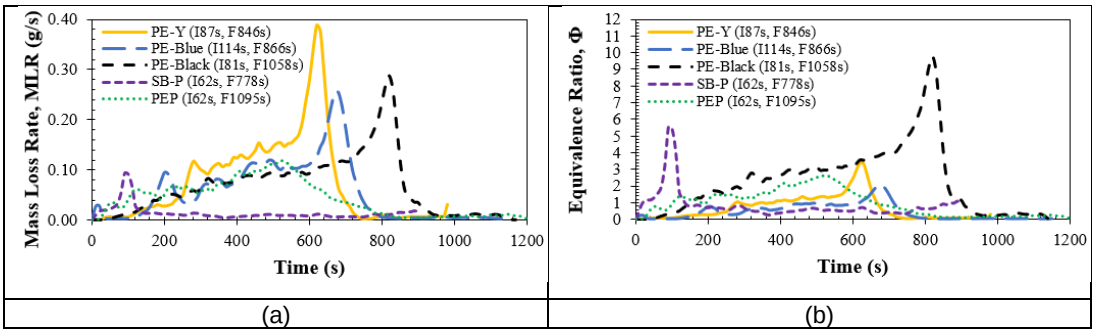


(a) (b)

**Figure 6.3** MLR and ER against time for Polyethylene fires at 35 kW/m$^2$ with free ventilation.

### 6.2.3 Heat Release Rate (HRR) for Polyethylene Fires

The HRR is shown in Figure 6.4 as a function of time on a mass loss basis and on an oxygen consumption basis for all five PE samples. The trends in the MLR based HRR were the same as for the MLR discussed above. However, the HRR based on oxygen consumption was completely different and with much lower peak HRR. The MLR HRR assumes that all the mass lost is consumed and fully releases the heat. This is not the case in these fires and in most practical fires.

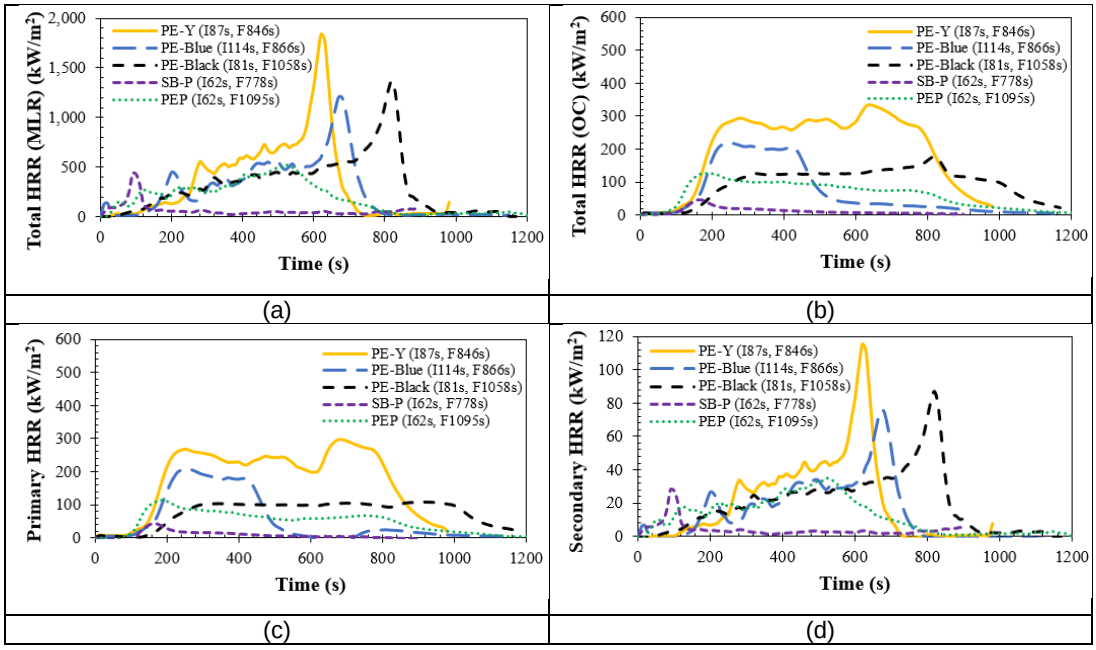


**Figure 6.4** HRRs against time for Polyethylene fires at 35 kW/m$^2$ with free ventilation.

## 6.3 Determination of Ignition Time and Temperature Profile for Polyethylene and GRP Fires with Pilot Ignition and Free Ventilation Condition

Other than Polyethylene materials (PE-Y, PE-Blue and PE-Black), Glass Reinforced Plastic (GRP-Blue) is also used as a bunding material in industry for storing flammable liquids. In the present work, determination of critical heat fluxes, ignition time and surface temperature of these polymer fires in the Cone Calorimeter with **pilot ignition** and free ventilation condition were also carried out. Surface temperatures were recorded using an Infrared camera. Note that in this work pilot ignition was used and NOT auto-ignition as in most of the rest of the thesis. Pilot ignition is determined by the time to reach a flammable gas concentration so that a spark above the sample ignited the mixture. Usually the pilot ignition time is shorter than the auto-ignition time. It will be shown in the toxic gas emissions section that high levels of Hydrocarbons are emitted during the ignition delay, which mix with air to give a flammable mixture that is spark ignited.

### 6.3.1 Ignition Time and Test Data for Polyethylene and GRP Fires

Various fire tests were conducted and repeated in determination of the critical heat flux for Polyethylene and GRP samples under free ventilation condition and piloted ignition. The details of test for all three Polyethylene samples and a GRP sample were summarised in the following Table 6.2 to Table 6.5.

PE-Y sample was burnt at various heat fluxes starting from the highest heat flux of 35 kW/m$^2$. Recorded ignition time was increased with the decrease in the heat flux value where lower heating temperature would require more time to ignite the fuel. As summarised in Table 6.2, the PE-Y fires at different heat fluxes had burned within a different burning period which PE-Y fire at a lower heat flux would burn longer than the PE-Y fire at a higher heat flux. Minimum heat flux to piloted ignition for this PE-Y fire was about 15.5 kW/m$^2$. The critical heat flux that determined for this PE-Y sample was 9 kW/m$^2$. At this heat flux, the maximum surface temperature of the sample recorded by the Infrared camera was about 283$^o$C at time of 1020 s. The PE-Y sample would start to ignite when reaching over this temperature level.

**Table 6.2** Test details for PE-Y fires.

| PE-Y Fires, Critical Heat Flux = 9 (kW/m$^2$) | | | | | | | | | | | |
|---|---|---|---|---|---|---|---|---|---|---|---|
| Test Details | | | | | | | | | | | |
| Heat Flux (kW/m$^2$) | 35 | 25 | 20 | 18 | 17 | 16 | 15 (1) | 15 (2) | 15 (3) | 15 (4) | 15 (5) |
| Set Cone Temperature (°C) | 708 | 630 | 590 | 565 | 548 | 540 | 530 | 530 | 530 | 530 | 530 |
| Ignition Time (s) | 109 | 284 | 512 | 892 | 893 | 1067 | No | No | No | No | No |
| Flame out Time (s) | 930 | 1317 | 1506 | 1866 | 1940 | 2218 | No | No | No | No | No |
| Sample Thickness (mm) | 9 | 8 | 9.5 | 9.6 | 9.3 | 8.5 | 8.2 | 8.2 | 8.9 | 9 | 9 |
| Sample Size (mm) | 98 x 98 | 99.2 x 99.2 | 99 x 99 | 99 x 99 | 98 x 99 | 99 x99 | 99 x 98.6 | 99 x 99 | 99 x 99 | 99 x99 | 98.5 x 98.5 |
| Weight Start of Test (g) | 80.9 | 72.6 | 86.5 | 86.9 | 84.9 | 76.6 | 75.8 | 73.3 | 79.6 | 81.8 | 80.2 |
| Weight End of Test (g) | 9.2 | 23.4 | 13.9 | 23.8 | 21.2 | 33.4 | 75.2 | 73.3 | 79.6 | 81.7 | 80.1 |
| *Before Ignition:-* Maximum Surface Temperature (°C) | 409 | 392 | 393 | 437 | 388 | 283 | No | No | No | No | No |
| (Before Ignition) Time (s) | 107 | 280 | 500 | 835 | 860 | 1020 | No | No | No | No | No |

Table 6.3 shows the test details for PE-Blue fires. The determined critical heat flux for this PE-Blue sample was 7.8 kW/m$^2$ with the minimum heat flux to piloted ignition of about 16.5 kW/m$^2$. The maximum sample surface temperature for this PE-Blue fire was 393$^o$C at time of 820 s. There were no ignition observed for heat fluxes lower than the minimum heat flux. PE-Blue sample took about 874 s to be ignited at the minimum heat flux level and would burn up to 2000 s before flame out.

**Table 6.3** Test details for PE-Blue fires.

| PE-Blue Fires, Critical Heat Flux = 7.8 (kW/m$^2$) | | | | | | | |
|---|---|---|---|---|---|---|---|
| Test Details | | | | | | | |
| Heat Flux (kW/m$^2$) | 35 | 25 | 20 | 18 | 17 | 16 | 15 (1) |
| Set Cone Temperature (°C) | 708 | 630 | 590 | 565 | 548 | 540 | 530 |
| Ignition Time (s) | 143 | 335 | 615 | 1007 | 874 | No | No |
| Flame out Time (s) | 925 | 1369 | 2184 | 2184 | 1866 | No | No |
| Sample Thickness (mm) | 8.8 | 8.2 | 8.8 | 8.8 | 8.5 | 9 | 9 |
| Sample Size (mm) | 100 x 99.2 | 100 x 99.2 | 99 x 100 | 99 x 99 | 98.5 x 99.5 | 99 x 99 | 99.5 X 99.5 |
| Weight Start of Test (g) | 78.8 | 76.4 | 79.3 | 81.1 | 76.7 | 80.3 | 80.6 |
| Weight End of Test (g) | - | 10 | 26.3 | 12.8 | 11.4 | 80.3 | 80.5 |
| *Before Ignition:-* Maximum Surface Temperature (°C) | 489 | - | 456 | 448 | 393 | No | No |
| (Before Ignition) Time (s) | 130 | - | 590 | 960 | 820 | No | No |

Compared to PE-Y and PE-Blue samples, PE-Black sample took shortest time to ignite for most fires at various heat fluxes. It took the longest burning duration before reaching flame out compared to other two Polyethylene fires. This PE-Black sample had the minimum heat flux to piloted ignition of about 18.5 kW/m$^2$ with an ignition at 738 s and a flame out at 2025 s. The determined critical heat flux was 12.2 kW/m$^2$. The maximum surface temperature of the sample recorded at this minimum heat flux was about 562$^o$C at time of 720 s, 18 s before the start of ignition. Test details for PE-Black fire were included in Table 6.4.

**Table 6.4** Test details for PE-Black fires.

| PE-Black Fires, Critical Heat Flux = 12.2 (kW/m$^2$) | | | | | | | | | | |
|---|---|---|---|---|---|---|---|---|---|---|
| Test Details | | | | | | | | | | |
| Heat Flux (kW/m$^2$) | 35 | 25 | 22 | 21 | 20 | 19 | 18 | 17 | 16 | 15 (1) |
| Set Cone Temperature (°C) | 708 | 630 | 606 | 597 | 590 | 575 | 365 | 548 | 540 | 530 |
| Ignition Time (s) | 92 | 193 | 507 | 661 | 944 | 738 | No | No | No | No |
| Flame out Time (s) | 982 | 1502 | 1427 | 1807 | 2158 | 2025 | No | No | No | No |
| Sample Thickness (mm) | 8.5 | 8.8 | 8.1 | 8 | 8.7 | 8.7 | 8.2 | 8.7 | 8.5 | 8.7 |
| Sample Size (mm) | 99 x 99 | 99 x99 | 98.5 x 98.5 | 98 x 99 | 99 x 99 | 99 x 99 | 99 x99 | 99 x 99 | 99 x99 | 99 x99 |
| Weight Start of Test (g) | 75.5 | 70.8 | 70.5 | 70 | 76.7 | 76.1 | 70.7 | 76.3 | 73.5 | 74.6 |
| Weight End of Test (g) | 8.6 | 1.9 | 4.8 | 1 | 6.6 | 6 | - | - | 73.2 | 74.2 |
| *Before Ignition:-* Maximum Surface Temperature (°C) | 467 | 444 | 464 | 466 | 482 | 562 | No | No | No | No |
| (Before Ignition) Time (s) | 90 | 190 | 490 | 625 | 900 | 720 | No | No | No | No |

The minimum heat flux to piloted ignition for this GRP-Blue fire was about 13.5 kW/m$^2$ with the determined critical heat flux of 3.7 kW/m$^2$. Test details for this GRP-Blue fire was shown in Table 6.5. Between these four bunding materials, GRP-Blue sample gave the lowest minimum heat flux value with the ignition time of 707 s and the flame out time of 1389 s. At this minimum heat flux level, the maximum sample surface temperature of about 366$^o$C was recorded by Infrared camera for this polymer fire. The critical heat flux for this bunding material fire was also the lowest if compared with the critical heat flux for other three Polyethylene fires.

**Table 6.5** Test details for GRP-Blue fires.

| GRP-Blue Fires, Critical Heat Flux = 3.7 (kW/m$^2$) | | | | | | | | |
|---|---|---|---|---|---|---|---|---|
| Test Details | | | | | | | | |
| Heat Flux (kW/m$^2$) | 35 | 25 | 20 | 18 | 16 | 14 | 13 | 12 |
| Set Cone Temperature (°C) | 708 | 630 | 590 | 565 | 540 | 515 | 500 | 486 |
| Ignition Time (s) | 79 | 138 | 200 | 308 | 454 | 707 | No | No |
| Flame out Time (s) | 701 | 786 | 881 | 1174 | 1284 | 1389 | No | No |
| Sample Thickness (mm) | 4 | 4 | 4 | 4.5 | 4 | 4 | 4.2 | 4 |
| Sample Size (mm) | 100 x 100 | 100 x 100 | 100 x 100 | 100 x 100 | 100 x 100 | 100 x100 | 100 x 100.2 | 100 x100 |
| Weight Start of Test (g) | 53.4 | 52.4 | 52.1 | 60.2 | 55.6 | 54 | 59.6 | 52.5 |
| Weight End of Test (g) | 14.2 | 14.4 | 17.6 | 19.6 | 18.2 | 18.15 | 57.2 | 51.5 |
| *Before Ignition:-* Maximum Surface Temperature (°C) | 408 | 387 | 396 | 371 | 373 | 366 | No | No |
| (Before Ignition) Time (s) | 70 | 125 | 190 | 290 | 420 | 680 | No | No |

## 6.3.2 Surface Temperature for Polyethylene and GRP Burning Samples

Surface temperatures for four bunding material fires as a function of time at various heat fluxes and free ventilation condition are shown in Figure 6.5 for a range of radiant heating intensities. This shows that all material will produce flammable gases that can be spark ignited, at all radiant intensities, but the time to an ignitable concentration decreases as the radiant intensity increases and was very short at 35 kW/m$^2$, the condition for all the toxicity tests. At 14 kW/m$^2$ it took 10 minutes to achieve sufficient flammable gases to reach a spark ignition concentration. During this period significant toxic gases were released that are presented later for 35 kW/m$^2$, as they had a different composition to the main flaming combustion and the later smouldering or char combustion.

The ignition temperature was difficult to determine accurately as the sample approached the final temperature slowly, it also relies on human observation of the flame occurring with the spark continuously on. The observed ignition temperature for these bunding materials was above 350$^{o}$C with PE-Y fire gave an average ignition temperature of 390$^{o}$C (this has the highest HBr emissions and also had the highest HCl and was thus fire retarded, yet the ignition temperature was the lowest, which was not expected), PE-Blue fire was 405$^{o}$C (this has high HBr emissions and was thus fire retarded, but this was not as great as PE-Y), PE-Black fire was 430$^{o}$C and GRP-Blue fire was 370$^{o}$C (this was also fire retarded). There was thus no link between the ignition temperature and the level of halogenated fire retardants. The literature value of the ignition temperature for PE is 340$^{o}$C and for autoignition 350$^{o}$C both in the absence of fire retardants [138].

Infrared images for Polyethylene and GRP fires during the flaming condition are shown in the following Figure 6.6. This was difficult to do as it is impossible to get a view from vertically above the test specimen, as the conical heater is there. The image produced was critical to the angle of the camera and the image shown is the bottom one with the test material at an oblique angle to the camera. The images show a non-uniform temperature with usually one hot spot away from the edges.

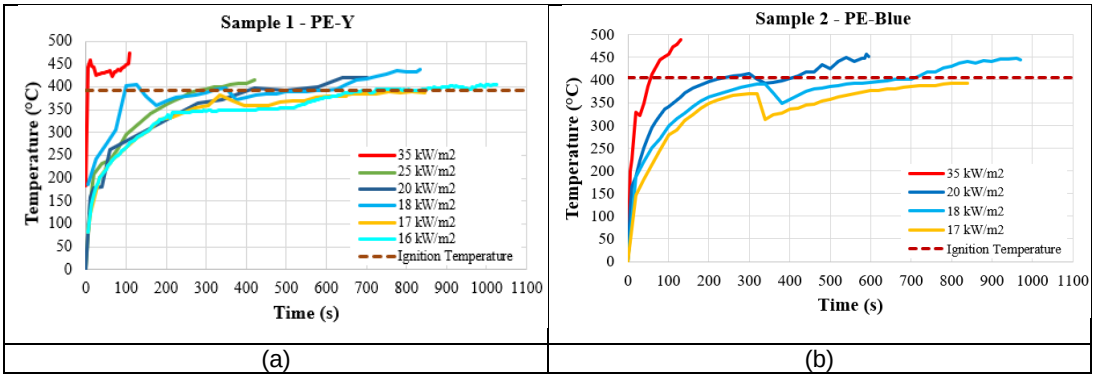


(a) (b)

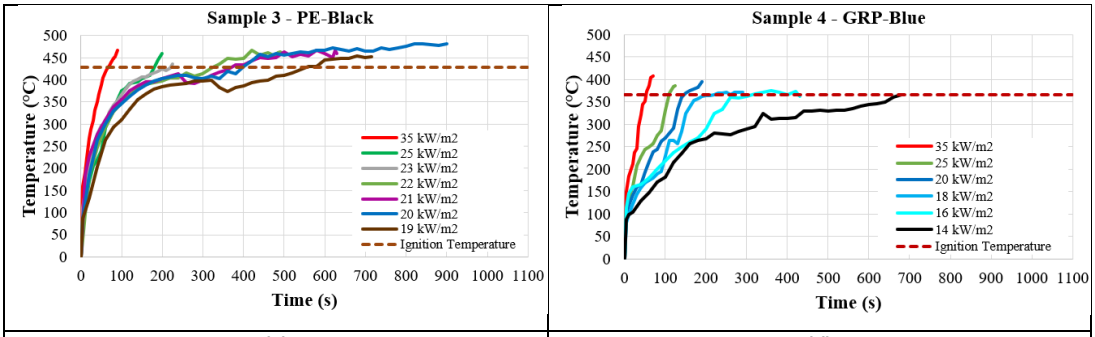


(c) (d)

**Figure 6.5** Surface temperature profiles for Polyethylene and GRP fires at various heat fluxes and free ventilation.

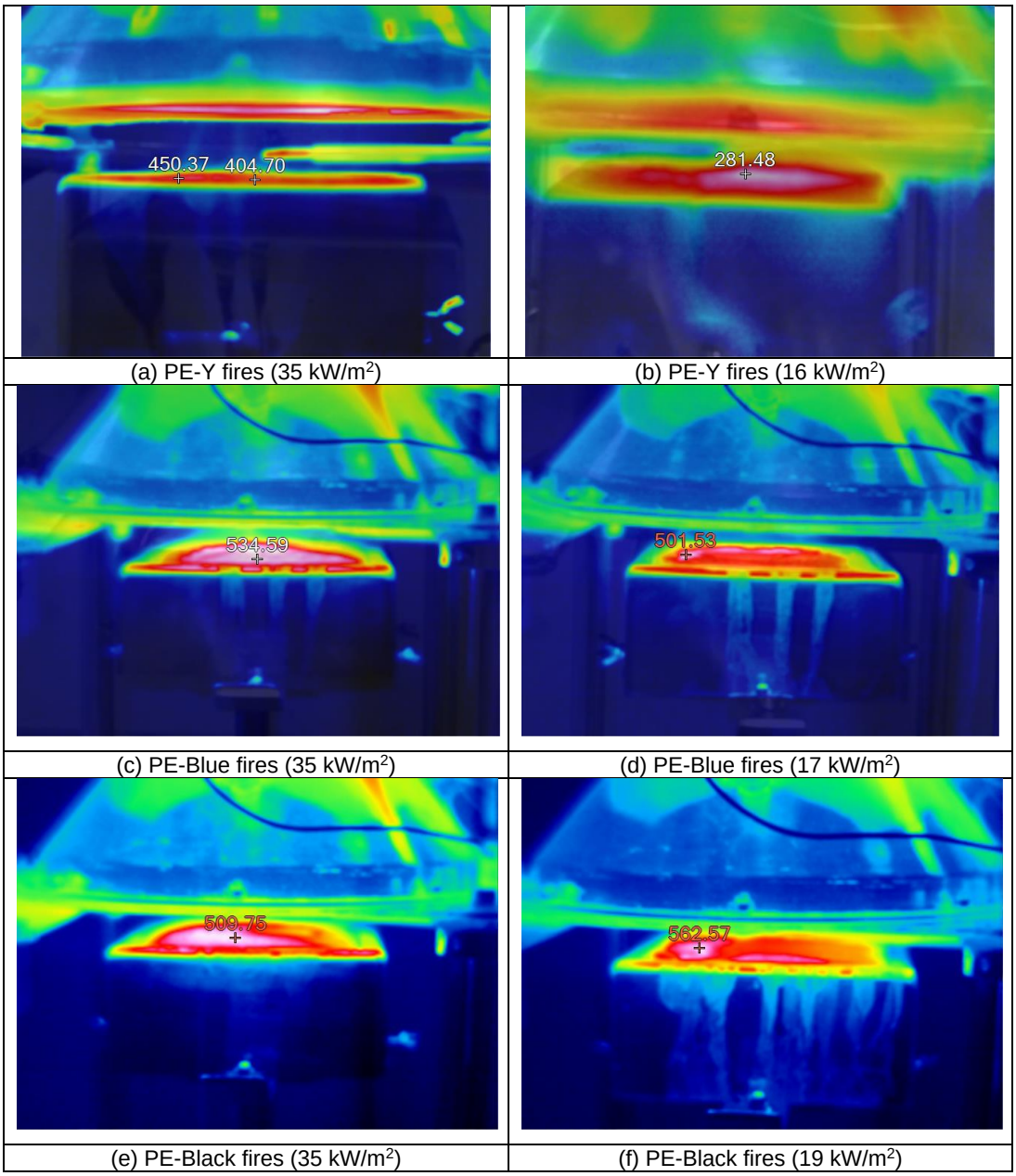


(a) PE-Y fires (35 kW/m$^2$) (b) PE-Y fires (16 kW/m$^2$)

(c) PE-Blue fires (35 kW/m$^2$) (d) PE-Blue fires (17 kW/m$^2$)

(e) PE-Black fires (35 kW/m$^2$) (f) PE-Black fires (19 kW/m$^2$)

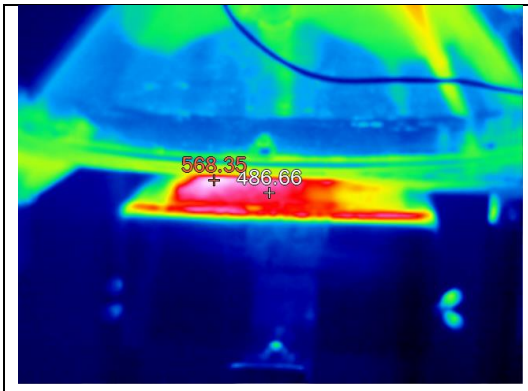


(g) GRP-Blue fires (35 kW/m$^2$)

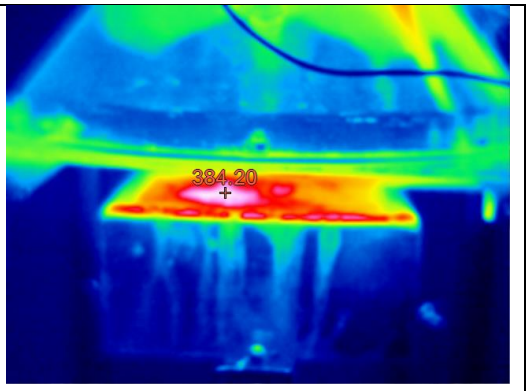


(h) GRP-Blue fires (14 kW/m$^2$)

**Figure 6.6** Infrared images for Polyethylene and GRP fires during the flaming condition, with the peak temperature indicated.

## 6.4 Toxicity of Polyethylene Fires

### 6.4.1 Gas Concentration as a Function of Time

The toxic gases released in Polyethylene fires were determined at a constant irradiation level of 35 kW/m$^2$ with free ventilation. There is a problem with the results in that the toxic gas emissions were so high that they exceeded the calibration range of the FTIR instrument by a long way, apart from CO and $CO_2$ which were calibrated through to 20%. Most of the other gases were calibrated to 500 ppm or 1000 ppm as detailed in Chapter 3. Thus, concentrations much higher than this, which are shown below, are based on calibration extrapolations. The FTIR curve fits the calibration and used this equation to determine higher concentrations. The accuracy of this deteriorates the higher the measured concentration. However, the key result is that very high concentrations of many species are released, even though the fire is freely ventilated.

The results for the 15 most important species from a toxicity viewpoint are given as a function of time in Figure 6.7. The concentrations in these graphs are within calibration or reasonable extrapolation of the calibration for some gases and way out of calibration for others, as shown in Table 6.6.

**Table 6.6** FTIR species that are in or well outside the calibration range.

| **In calibration with concentrations ,1000 ppm or close to this** | **Well outside the calibration range, >>1000 ppm** |
|---|---|
| CO (calibrated to 20%) | Benzene |
| HCN | Acetylene |
| HCl | THC |
| Formaldehyde | HBr |
| Acrolein | Toluene |
| $NO_2$ | |
| $NO_x$ | |
| $SO_2$ | |
| $NH_3$ | |
| Acetaldehyde | |

The HBr levels are very high and well above calibration. However, this does show that the samples with high HBr must have had high doses of brominated fire retardants. All the major Hydrocarbons were out of calibration range including the toxic gases Benzene and Toluene. Thus the THC, which is the sum of all the measured HC on a C1 equivalence basis, was well outside calibration and unreliable. For the unreliable gases the emission index reported later are also not reliable, as shown by the yields being greater than 1 for PE-Black, which is impossible. However, most of the yields are realistic, especially for the toxic gases that are within their calibration range such as Acrolein and HCl.

The interpretation of the toxic gas concentration results should be made with reference to the equivalence ratio determined by Carbon balance in Figure 6.3. This shows that for PE-Y the fire was richer than stoichiometric after 300 s and until 700 s; for PE-Black it was 200 s to 900 s and for PE-Blue it was lean combustion for all of the fire time apart from a short time 650-750 s. The PE Pipe (PEP) was rich after 100 s until 500 s. The SB-P storage box PE was very rich initially, due to rapid pyrolysis of volatile, but became lean after 150 s and remained lean for the rest of the fire. These equivalence ratio differences explain most of the differences in the five types of PE samples.

PE-Black gave the highest concentration for most of major toxic gases as it had the richest mixtures. This was followed by PEP, PE-Y, PE-Blue and SB-P and this follows the order expected from the equivalence ratio differences. CO concentration for PE-Black was the highest up to 50000 ppm at 300 s to 800 s of test time, due to the very rich combustion conditions. HBr emissions

were high for all these Polyethylene fires with PE-Y and PE-Black giving the highest HBr concentration of about 16000 ppm. Benzene concentration was really high for PE-Black compared to other Polyethylene fires. Other toxic gases such as $NO_2$ (<150 ppm), $SO_2$ (<100 ppm), HF (<20 ppm) showed very low concentration values. From Figure 6.7 (c) shows that HCl emissions for these Polyethylene fires were also significant but low compared with the HBr emissions. However, it does indicate that the fire retardant had Chlorine as well as Bromine in it.

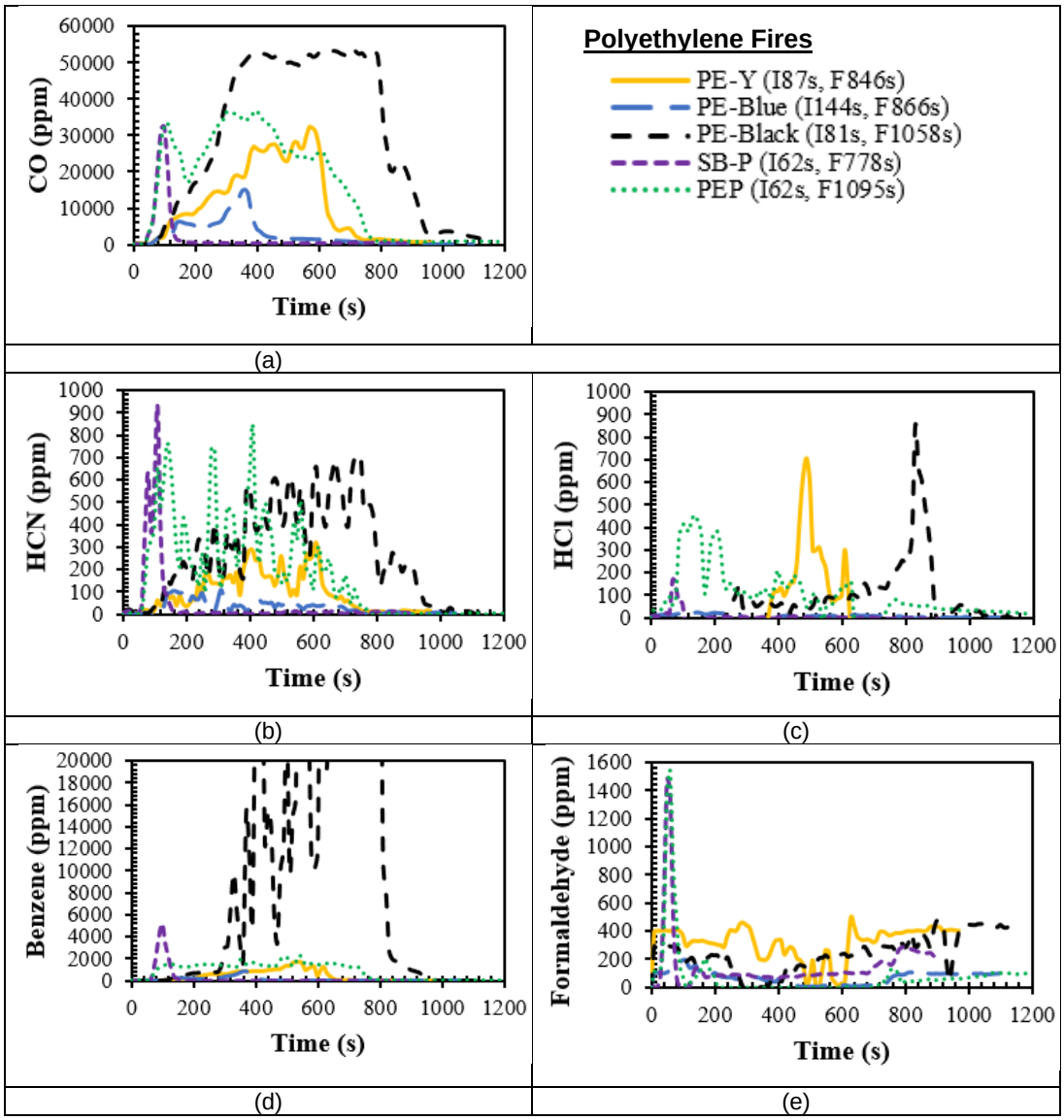

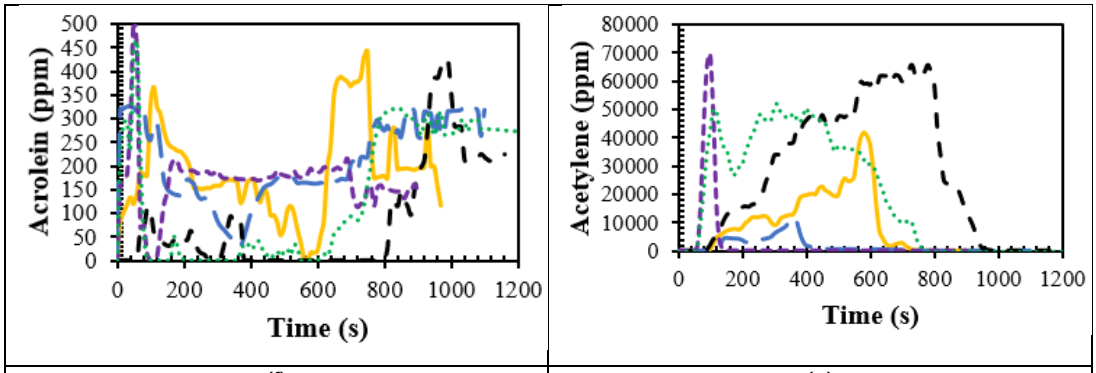
Acrolein (ppm)
Time (s)

(f)


Acetylene (ppm)
Time (s)

(g)

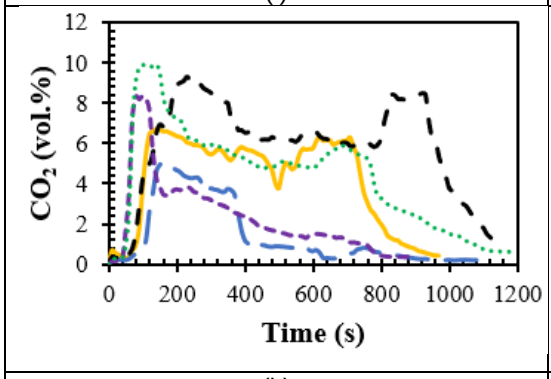
CO2 (vol.%)
Time (s)

(h)

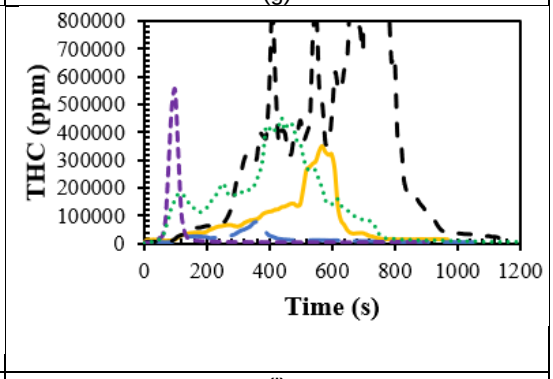
THC (ppm)
Time (s)

(i)

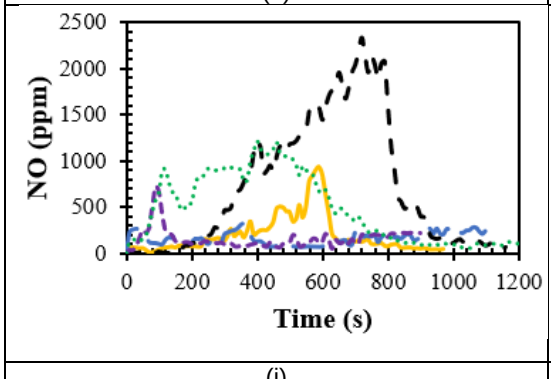
NO (ppm)
Time (s)

(j)

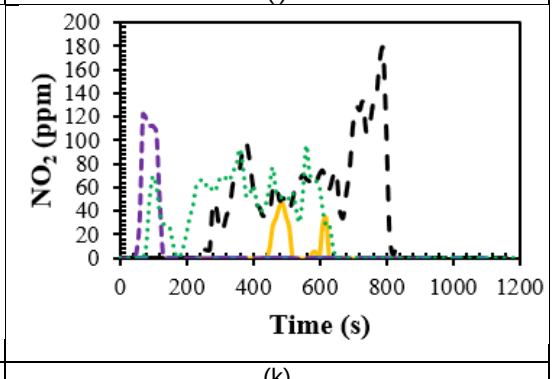
NO2 (ppm)
Time (s)

(k)

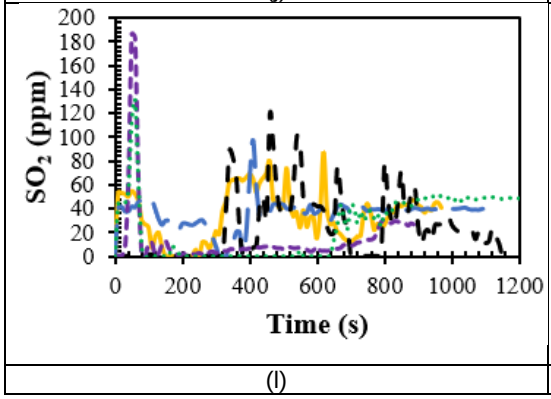
SO2 (ppm)
Time (s)

(l)

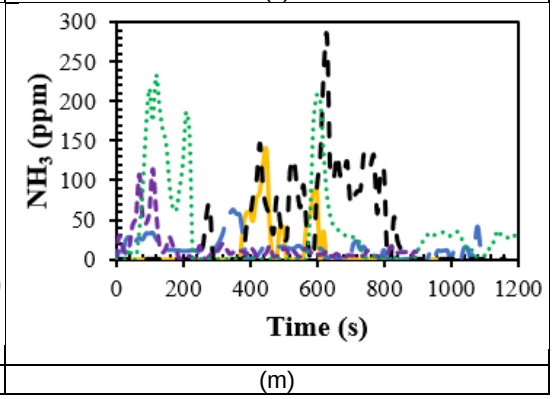
NH3 (ppm)
Time (s)

(m)

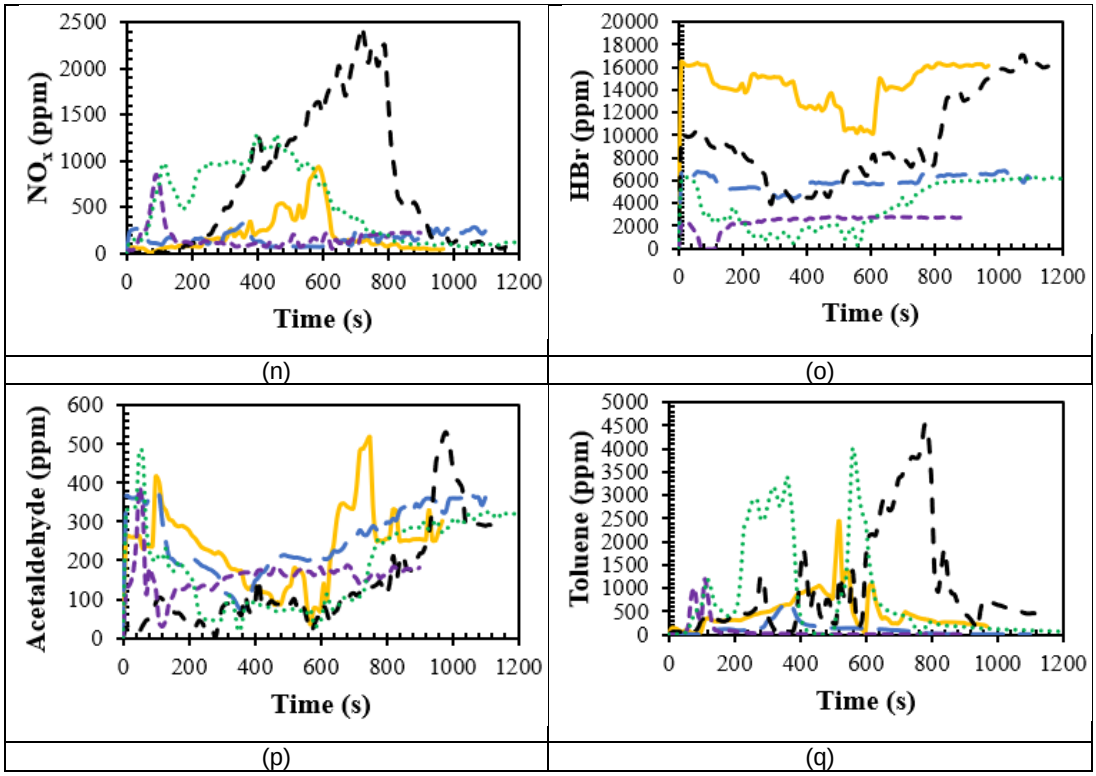


**Figure 6.7** Gas concentrations for Polyethylene fires at 35 kW/m$^2$ with free ventilation.

### 6.4.2 Gas Yields for Polyethylene Fires at 35 kW/m$^2$ with Free Ventilation

Figure 6.8 shows the gas yield as a function of time for the five Polyethylene fires at 35 kW/m$^2$ radiant heating with free ventilation. Among the Polyethylene fires, PE-Blue fire gave the highest CO yield of about 0.44 g/g at 100 s. PE-Y fire showed a CO gas yield profile with three main peaks with the gas yield value for the first peak was 0.20 g/g, the second highest yield peak of 0.35 g/g and the third yield peak was 0.25 g/g. The highest gas yield was given by PE-Black at about 0.35 g/g meanwhile, for PEP fire was 0.28 g/g and for SB-P was 0.2 g/g. The low CO yield for SB-P was due to the lean combustion discussed above. From Figure 6.8 (d), Benzene yield was the highest for PE-Black fire which above 0.25 g/g. For HCl and HBr yields, PE-Y showed the highest values compared to other four Polyethylene fires. In overall, PE-Blue contributed to the highest yields of NO and $NH_3$ which also showing the highest $NO_x$ in comparison with other Polyethylene fires. For THC yield, PE-Black fire had the highest yield value of above 6.5 g/g at 800 s of test time.

PEP fire showed the lowest yield for all gases that considered compared to other Polyethylene fires.

The HBr yields >1 are impossible and this is due to the concentrations being well above the calibration range for the FTIR and thus unreliable. However, this does not detract from the conclusion that these brominated fire retardants are resulting in massive releases of toxic HBr under fire conditions. The yield values for HBr could be x10 above the actual levels, but this would still be extremely high releases.

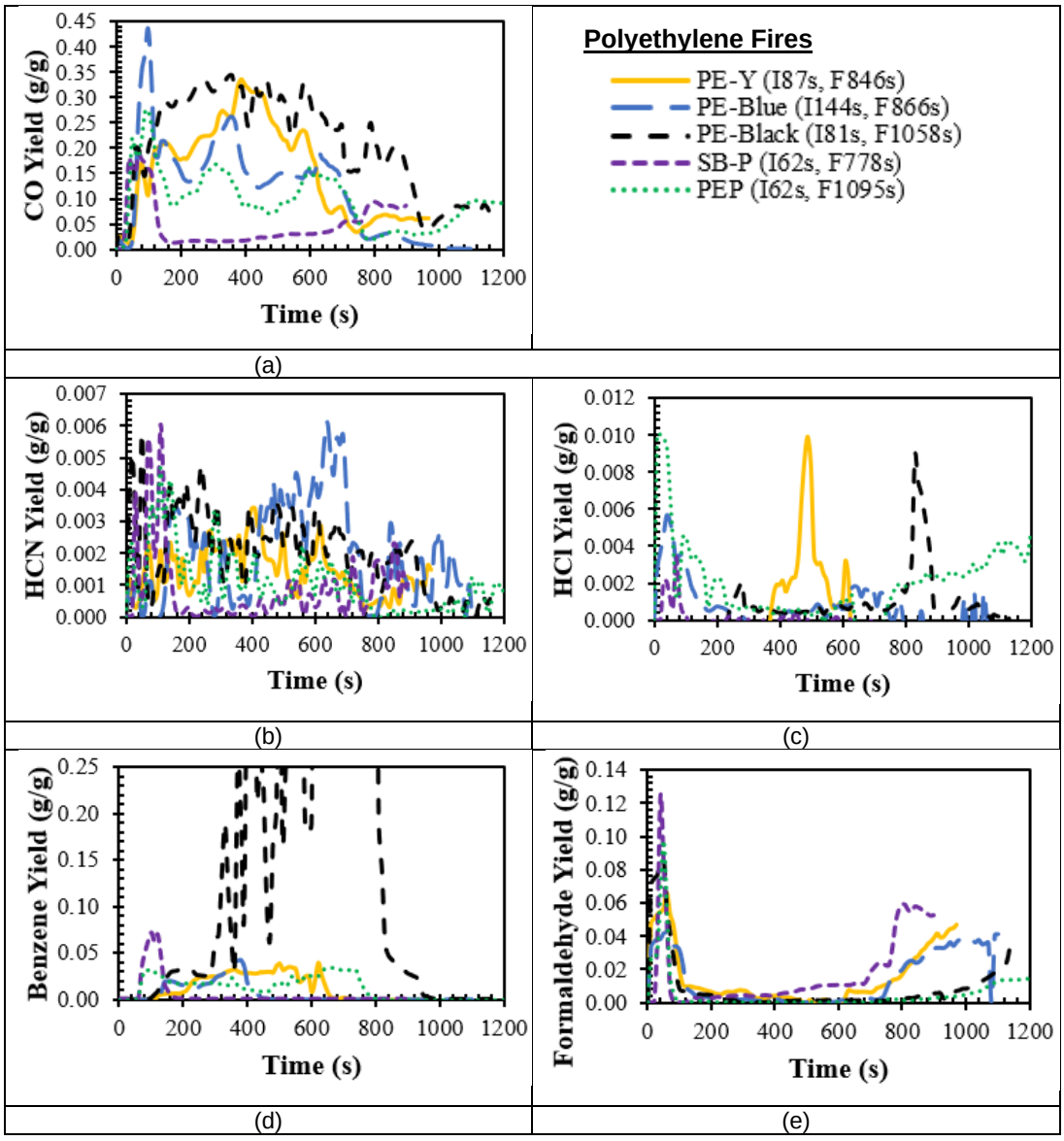

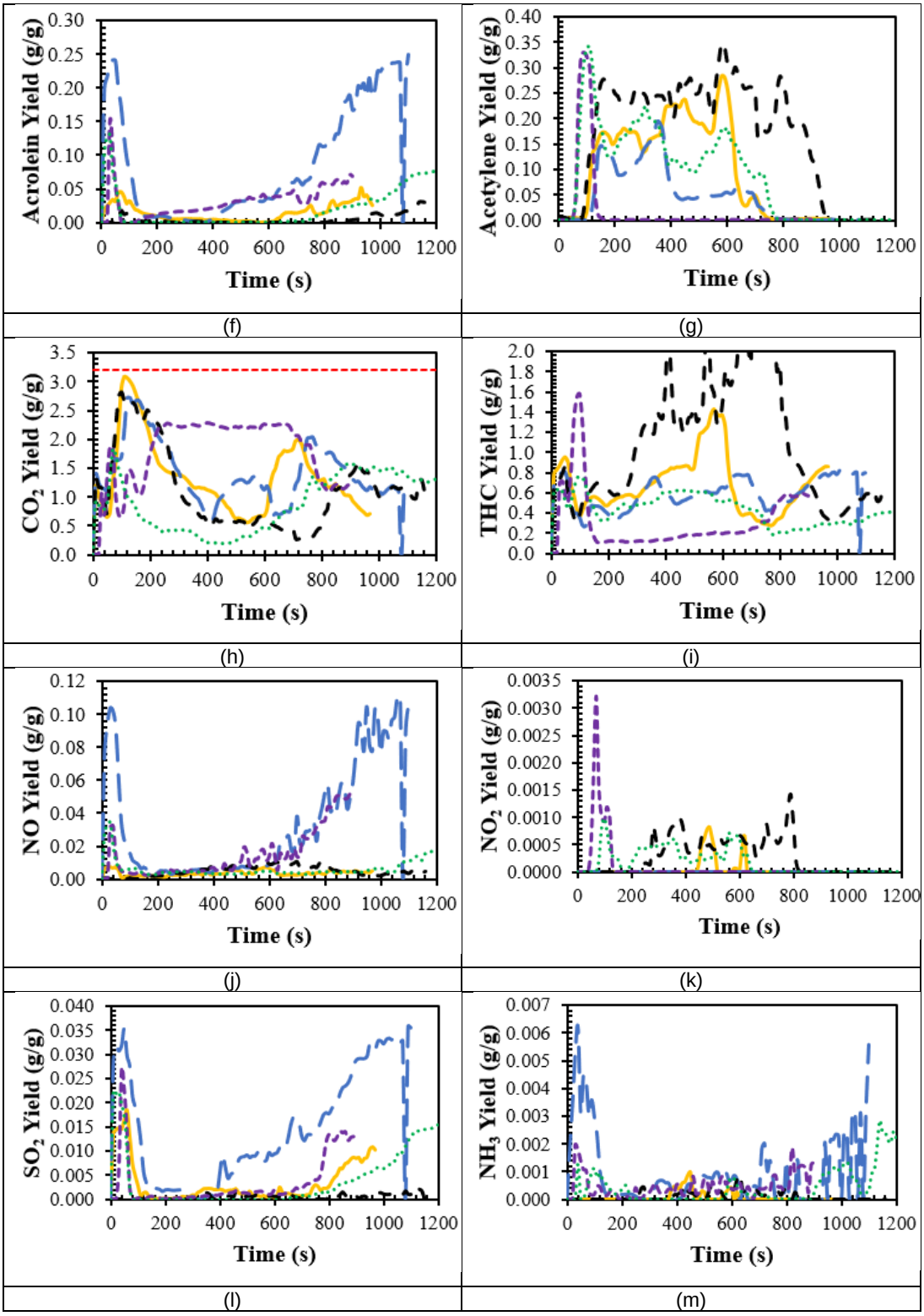
Acrolein Yield (g/g)
Time (s)
(f)
Acetylene Yield (g/g)
Time (s)
(g)
CO2 Yield (g/g)
Time (s)
(h)
THC Yield (g/g)
Time (s)
(i)
NO Yield (g/g)
Time (s)
(j)
NO2 Yield (g/g)
Time (s)
(k)
SO2 Yield (g/g)
Time (s)
(l)
NH3 Yield (g/g)
Time (s)
(m)

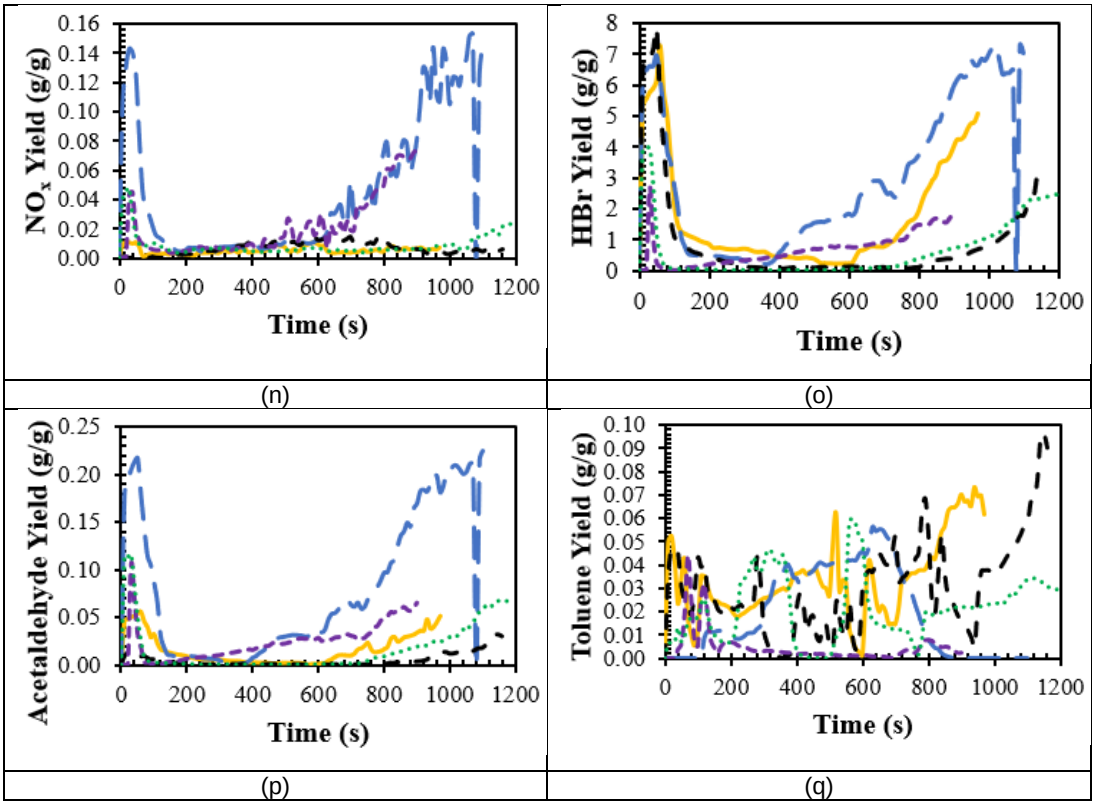


**Figure 6.8** Gas yields for Polyethylene fires at 35 kW/m$^2$ with free ventilation.

An unusual feature of the yield results is that for $NO_x$ in Figure 6.8 (n). This shows very high yields for PE-Blue and SB-P in the pre-flaming combustion phase and in the post flaming combustion phase. This is not a feature of the other PE samples and is not explained by the equivalence ratio variation which are quite different for the two PE samples, as shown in Figure 6.7. Also there is no corresponding HCN peak, which would be expected if the source was an organic fuel bound Nitrogen compound in the polymer such as an Acrylic or Amide. It could be that a N containing textile fibre has been used as a reinforcing component to add strength to the polymer. However, this is of academic interest as $NO_2$ is not sufficiently high to be a major toxic hazard. However, it could be that Ammonium bromide has been used in the fire retardant and this is the source of the $NO_x$. If this was the case it would only be the PE-Blue and SB-P that had this fire retardant.

The high emissions of CO and THC indicate a poor combustion efficiency. However, although the emissions index of CO is reliable that of THC is not, due to FTIR calibrations not being valid for the high concentrations of Hydrocarbons that occurred in the fires. The poor combustion efficiency is also

shown by the large difference in HRR based on mass consumption and Oxygen consumption, that was discussed above. This difference is not influenced by the FTIR calibration so the very poor combustion efficiencies are genuine results. A low combustion efficiency also results in a low $CO_2$ yield, as shown in Figure 6.8 (h). The high $CO_2$ yields are high combustion efficiency and low yields are low combustion efficiency. For a pure $CH_2$ polymer that completely burns the yield can be calculated as 3.2 kg/kg, which is marked on Figure 6.8 (h).

The combustion efficiency, η, for the five Polyethylene fires at 35 kW/m$^2$ radiant heating under free ventilation is shown in Figure 6.9. PE-Y, PE-Blue and SB-P fires had reached the highest combustion efficiency of more than 90% at certain burning time, which was due to leaner combustion. SB-P fire showed a constant combustion efficiency close to 85-90% from 200 s until 800 s, which was due to the lean mixture throughout this time shown in Figure 6.3. PE-Blue fire gave a constant combustion efficiency at test time from 400 s to 800 s. Several peaks of combustion efficiency were shown by PE-Y fire at 300 s, 650 s and 1000 s with 40%, 80% and 100% of efficiency rate. For PE-Black fire, the highest combustion efficiency was in a range of 60% to 70% within the burning duration from 50 s to 200 s with equivalence ratio values changed from lean (0.2) to rich (2.0). The combustion efficiency rate of PE-Black fire had reduced to the minimum before having the second efficiency peak of 70% at 850 s with fire equivalence ratio of 6.0. Three peaks of efficiency rate (50%, 80% and 85%) were given by PEP fire at burning time of 100 s, 750 s and 1100 s with the highest efficiency rate was achieved when the fire closest to flame out stage.

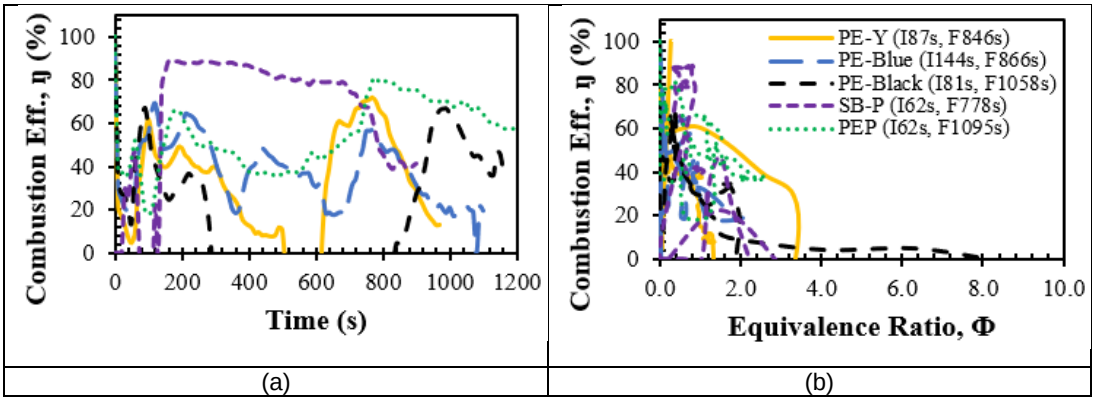


(a) (b)

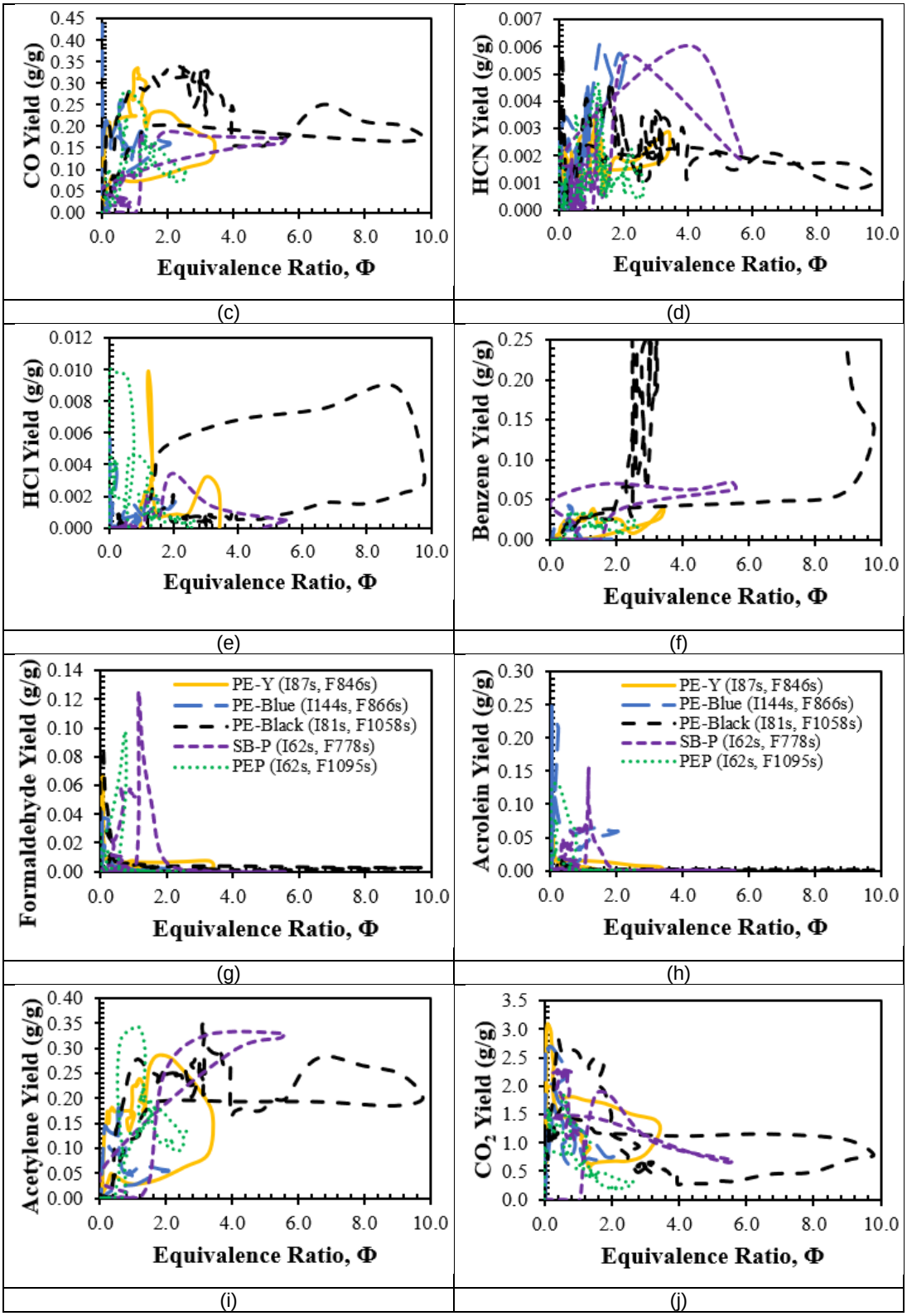
CO Yield (g/g)
Equivalence Ratio, Φ
(c)
HCN Yield (g/g)
Equivalence Ratio, Φ
(d)
HCl Yield (g/g)
Equivalence Ratio, Φ
(e)
Benzene Yield (g/g)
Equivalence Ratio, Φ
(f)
Formaldehyde Yield (g/g)
PE-Y (I87s, F846s)
PE-Blue (I144s, F866s)
PE-Black (I81s, F1058s)
SB-P (I62s, F778s)
PEP (I62s, F1095s)
Equivalence Ratio, Φ
(g)
Acrolein Yield (g/g)
PE-Y (I87s, F846s)
PE-Blue (I144s, F866s)
PE-Black (I81s, F1058s)
SB-P (I62s, F778s)
PEP (I62s, F1095s)
Equivalence Ratio, Φ
(h)
Acetylene Yield (g/g)
Equivalence Ratio, Φ
(i)
CO2 Yield (g/g)
Equivalence Ratio, Φ
(j)

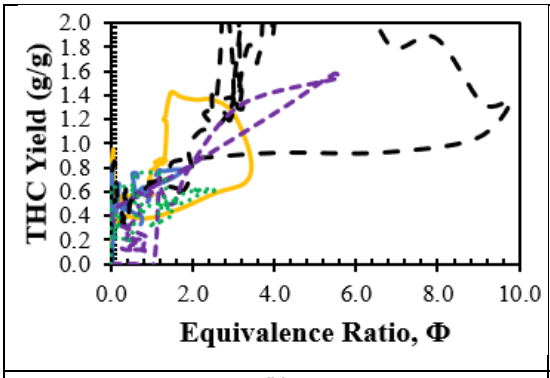
THC Yield (g/g)
Equivalence Ratio, Φ

(k)

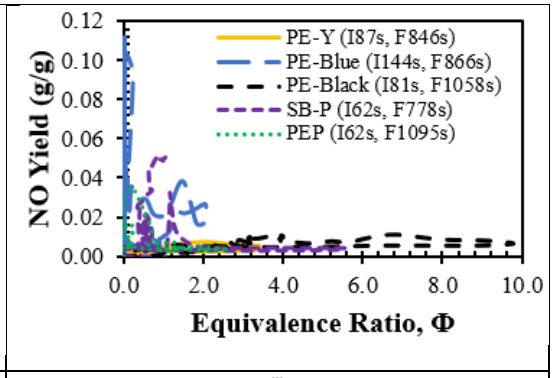
NO Yield (g/g)
PE-Y (I87s, F846s)
PE-Blue (I144s, F866s)
PE-Black (I81s, F1058s)
SB-P (I62s, F778s)
PEP (I62s, F1095s)
Equivalence Ratio, Φ

(l)

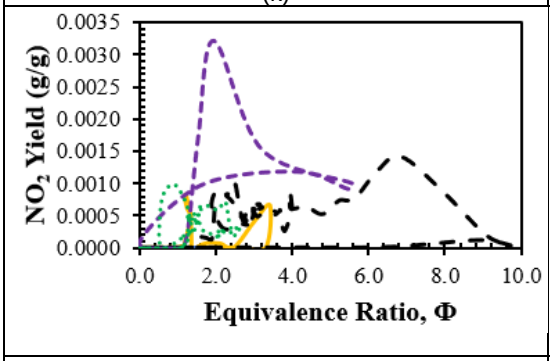
NO2 Yield (g/g)
Equivalence Ratio, Φ

(m)

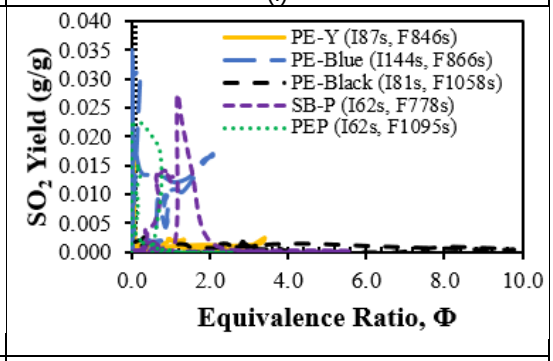
SO2 Yield (g/g)
PE-Y (I87s, F846s)
PE-Blue (I144s, F866s)
PE-Black (I81s, F1058s)
SB-P (I62s, F778s)
PEP (I62s, F1095s)
Equivalence Ratio, Φ

(n)

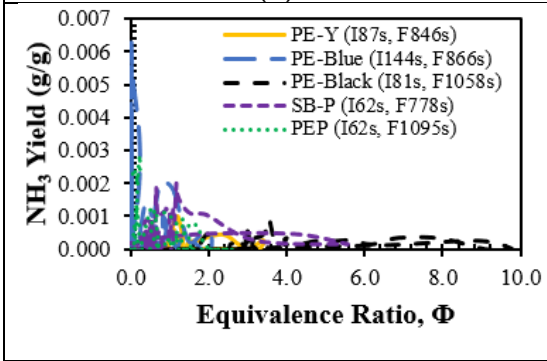
NH3 Yield (g/g)
PE-Y (I87s, F846s)
PE-Blue (I144s, F866s)
PE-Black (I81s, F1058s)
SB-P (I62s, F778s)
PEP (I62s, F1095s)
Equivalence Ratio, Φ

(o)

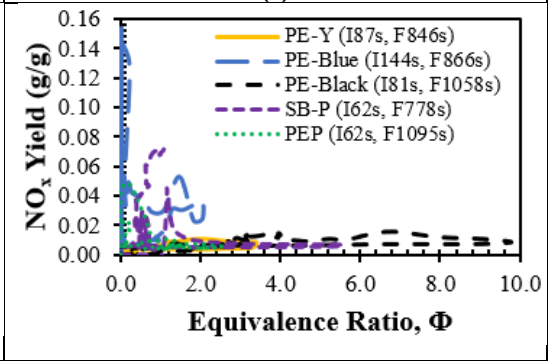
NOx Yield (g/g)
PE-Y (I87s, F846s)
PE-Blue (I144s, F866s)
PE-Black (I81s, F1058s)
SB-P (I62s, F778s)
PEP (I62s, F1095s)
Equivalence Ratio, Φ

(p)

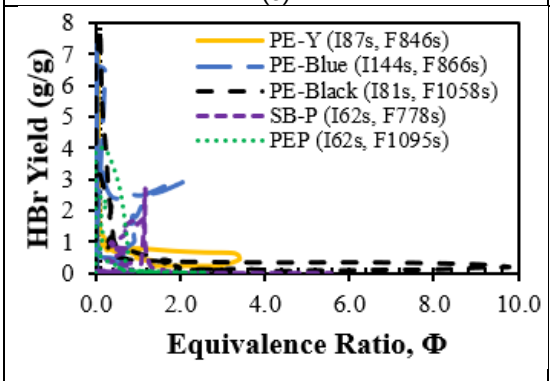
HBr Yield (g/g)
PE-Y (I87s, F846s)
PE-Blue (I144s, F866s)
PE-Black (I81s, F1058s)
SB-P (I62s, F778s)
PEP (I62s, F1095s)
Equivalence Ratio, Φ

(q)

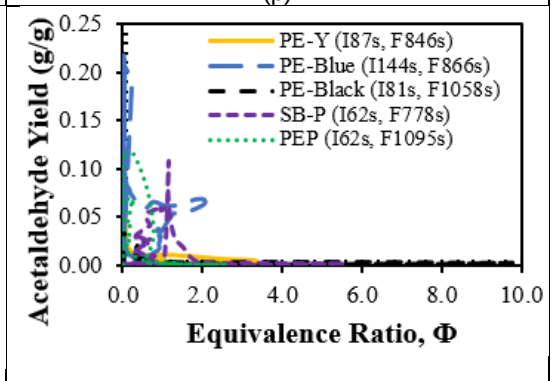
Acetaldehyde Yield (g/g)
PE-Y (I87s, F846s)
PE-Blue (I144s, F866s)
PE-Black (I81s, F1058s)
SB-P (I62s, F778s)
PEP (I62s, F1095s)
Equivalence Ratio, Φ

(r)

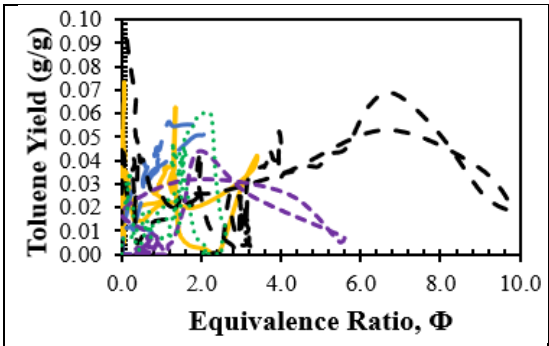


(s)

**Figure 6.9** Combustion efficiency, ŋ and gas yields as a function of equivalence ratio for Polyethylene fires at 35 kW/m$^2$ with free ventilation.

PE-Blue, SB-P and PEP fires had the highest combustion efficiency in lean fire condition, meanwhile other two Polyethylene (PE-Y and PE-Black) fires had the highest combustion efficiency in rich fire condition. The combustion efficiency was mainly controlled by the fire equivalence ratio as shown in Figure 6.9 (b) where all the high efficiencies were for lean or near stoichiometric mixtures and all the poor combustion efficiencies were for rich mixtures. The same trends are shown for $CO_2$ as a function of the equivalence ratio in Figure 6.9 (d) which shows a low yield for rich mixtures and a high yield for lean mixtures. The equivalence ratio was also important in most of the yield plots, as shown in Figure 6.9.

The peak yields for the five PE samples are compared in Table 6.7. Yields >1 are impossible apart from for $CO_2$ and CO and these have been marked in red. The come from FTIR calibration problems when the concentrations are much higher than the calibrated range. The average gas yield values for these PE materials are also presented as in Table 6.8. Cumulative mass graphs for CO species are shown in Appendix E.

**Table 6.7** Maximum gas yields for Polyethylene fires at irradiation level of 35 kW/m$^2$ with free ventilation.

| Polymer Type | PE-Y | PE-Blue | PE-Black | SB-P | PEP |
|---|---|---|---|---|---|
| **Test Condition** | **35 FV** | | | | |
| **Species** | **Maximum Yields (g/g)** | | | | |
| CO | 0.3344 | 0.4360 | 0.3448 | 0.1887 | 0.2769 |
| HCN | 0.0034 | 0.0061 | 0.0057 | 0.0060 | 0.0047 |
| HCl | 0.0099 | 0.0057 | 0.0088 | 0.0034 | 0.0101 |
| HF | 0.0009 | 0.0009 | 0.0015 | 0.0007 | 0.0003 |
| Benzene | 0.0397 | 0.0424 | 2709.7823 | 0.0712 | 0.0339 |
| Formaldehyde | 0.0661 | 0.0418 | 0.0866 | 0.1242 | 0.0974 |
| Acrolein | 0.0516 | 0.2504 | 0.0312 | 0.1497 | 0.1298 |
| Acetylene | 0.2847 | 0.1935 | 0.3477 | 0.3311 | 0.3417 |
| $CO_2$ | 3.0850 | 2.7250 | 2.8182 | 2.2937 | 1.8356 |
| THC | 1.4293 | 0.8273 | 3339.3689 | 1.5814 | 0.7599 |
| NO | 0.0075 | 0.1116 | 0.0107 | 0.0535 | 0.0346 |
| $NO_2$ | 0.0008 | 0.0000 | 0.0014 | 0.0032 | 0.0010 |
| $SO_2$ | 0.0184 | 0.0359 | 0.0025 | 0.0269 | 0.0226 |
| $NH_3$ | 0.0010 | 0.0062 | 0.0009 | 0.0020 | 0.0029 |
| $NO_x$ | 0.0103 | 0.1536 | 0.0160 | 0.0736 | 0.0477 |
| HBr | 7.2792 | 7.2945 | 7.7917 | 2.7070 | 3.9830 |
| Acetaldehyde | 0.0556 | 0.2242 | 0.0317 | 0.1050 | 0.1168 |
| Toluene | 0.0735 | 0.0560 | 0.0965 | 0.0441 | 0.0600 |

**Table 6.8** Mean gas yields for Polyethylene fires at irradiation level of 35 kW/m$^2$ with free ventilation.

| Polymer Type | PE-Y | PE-Blue | PE-Black | SB-P | PEP |
|---|---|---|---|---|---|
| **Test Condition** | **35 FV** | | | | |
| **Initial Mass (g)** | 78.21 | 78.22 | 77.20 | 15.67 | 50.30 |
| **Total Mass Loss (g)** | 74.83 | 63.15 | 77.20 | 12.53 | 50.29 |
| **Total Time (s)** | 970 | 1100 | 1140 | 900 | 1200 |
| **Mean ER, Φ** | 0.85 | 0.22 | 2.18 | 0.29 | 1.62 |
| **Species** | **Mean Yields (g/g)** | | | | |
| CO | 0.2084 | 0.1513 | 0.2423 | 0.0820 | 0.1153 |
| HCN | 0.0019 | 0.0032 | 0.0021 | 0.0016 | 0.0013 |
| HCl | 0.0010 | 0.0006 | 0.0013 | -0.0001 | 0.0011 |
| HF | 0.0001 | 0.0001 | 0.0000 | 0.0001 | 0.0000 |
| Benzene | 0.0238 | 0.0065 | 78.4292 | 0.0188 | 0.0178 |
| Formaldehyde | 0.0047 | 0.0027 | 0.0020 | 0.0164 | 0.0020 |
| Acrolein | 0.0050 | 0.0390 | 0.0009 | 0.0254 | 0.0041 |
| Acetylene | 0.1708 | 0.0661 | 0.2316 | 0.0908 | 0.1368 |
| $CO_2$ | 1.1261 | 1.1958 | 0.7966 | 1.4958 | 0.5304 |
| THC | 0.8555 | 0.6206 | 97.5980 | 0.5999 | 0.5201 |
| NO | 0.0040 | 0.0144 | 0.0066 | 0.0134 | 0.0043 |
| $NO_2$ | 0.0001 | 0.0000 | 0.0005 | 0.0004 | 0.0003 |
| $SO_2$ | 0.0013 | 0.0092 | 0.0004 | 0.0035 | 0.0009 |
| $NH_3$ | 0.0001 | 0.0006 | 0.0002 | 0.0005 | 0.0002 |
| $NO_x$ | 0.0056 | 0.0198 | 0.0094 | 0.0188 | 0.0061 |
| HBr | 0.5815 | 1.7590 | 0.2029 | 0.5316 | 0.1417 |
| Acetaldehyde | 0.0046 | 0.0391 | 0.0014 | 0.0199 | 0.0041 |
| Toluene | 0.0280 | 0.0368 | 0.0289 | 0.0081 | 0.0204 |

### 6.4.3 Total Toxicity for Polyethylene Fires at 35 kW/m$^2$ with Free Ventilation

Total normalised toxicity, n, for LC50, $COSHH_{15min}$ and AEGL-2 for each species was determined and then the total normalised toxicity was added to give a total normalised toxicity, N. N as a function of time in the fires is shown in Figure 6.10. All PE samples had a normalised toxicity >1 at all times in the fires and for all three toxicity assessment methods. The values of normalised toxicity would be increased by the FTIR calibration issues shown in Table 6.7. This is most important for HBr, but is also significant for Benzene and Toluene. In future work the total toxicity should be evaluated omitting these three off scale species or only putting in the maximum calibrated value into the normalised total toxicity.

Between all five Polyethylene fires, PE-Black fire gave the highest total toxicity for all three total LC50, $COSHH_{15min}$ and AEGL-2. For total LC50 basis, PE-Black fire had the highest toxicity peak of 16 and this was relevant to the very high CO emissions measured during the test as presented earlier in Figure 6.7 (a). The PE-Black fire also contributed to the highest total $COSHH_{15min}$ of 150000 and this value contributed by a very high Benzene concentration released from this Polyethylene fire.

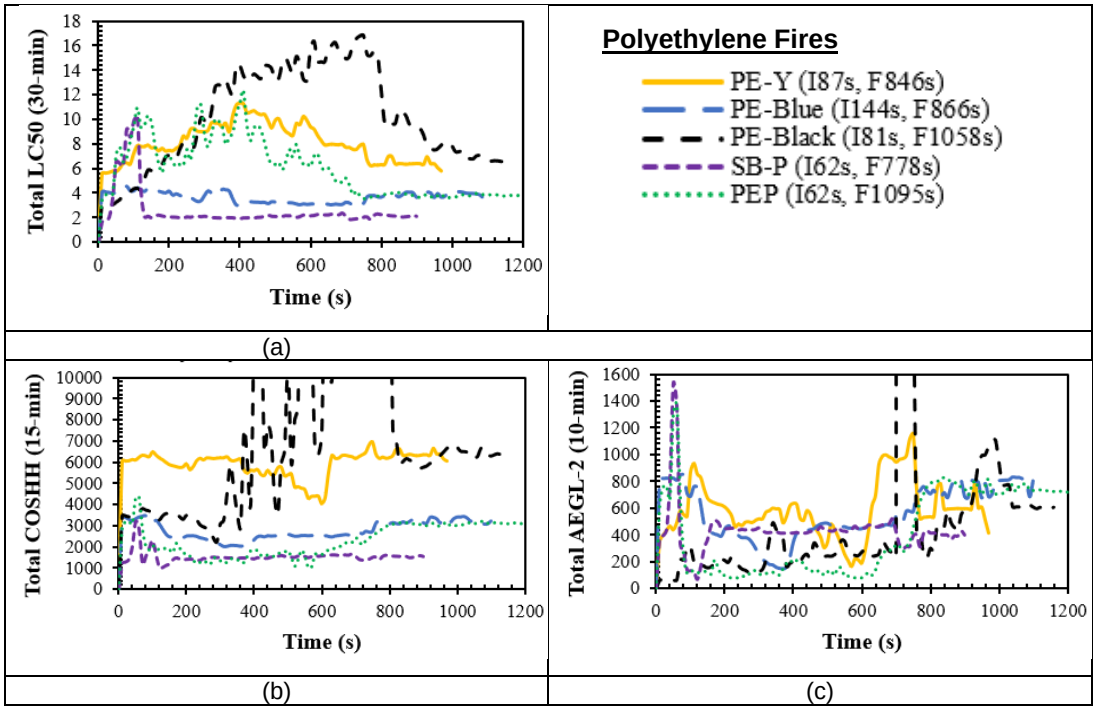


**Figure 6.10** Total toxicity for Polyethylene fires at 35 kW/m$^2$ with free ventilation.

### 6.4.4 Major Gases Contribution for Polyethylene Fires at 35 kW/m$^2$ with Free Ventilation

For all five tested Polyethylene materials, HBr was a major species that contributed to overall fire toxicity of Polyethylene fires and this HBr contribution had not been indicated by other tested polymer fires including the electrical cable fires. The % contribution to the total $LC_{50}$ toxicity is shown in Figure 6.11 as a function of time for all five Polyethylene fires. The toxic gas species that showed a high contribution were CO, Acrolein, HCN and Formaldehyde. For other tested polymeric materials like Polyurethane, Polyisocyanurate, Polystyrene and Polyvinyl chloride, the contribution of

Formaldehyde from these polymer fires was high but for Polyethylene fires it showed a low toxicity contribution. CO had a high contribution to the fire toxicity throughout the total test time for all four Polyethylene fires except for SB-P fire which only showed the CO contribution as a major species from start test time up to 200 s, this was because the combustion was lean after this time. Between Polyethylene bunding materials (PE-Y, PE-Blue and PE-Black), contribution percentage of CO and HCN were the highest for PE-Black fire, meanwhile the PE-Blue fire showed the lowest percentage for those two species. Polyethylene pipe fire also had a very high percentage for CO and HCN contributions which about 70% of CO and 20% of HCN within 800 s of burning period.

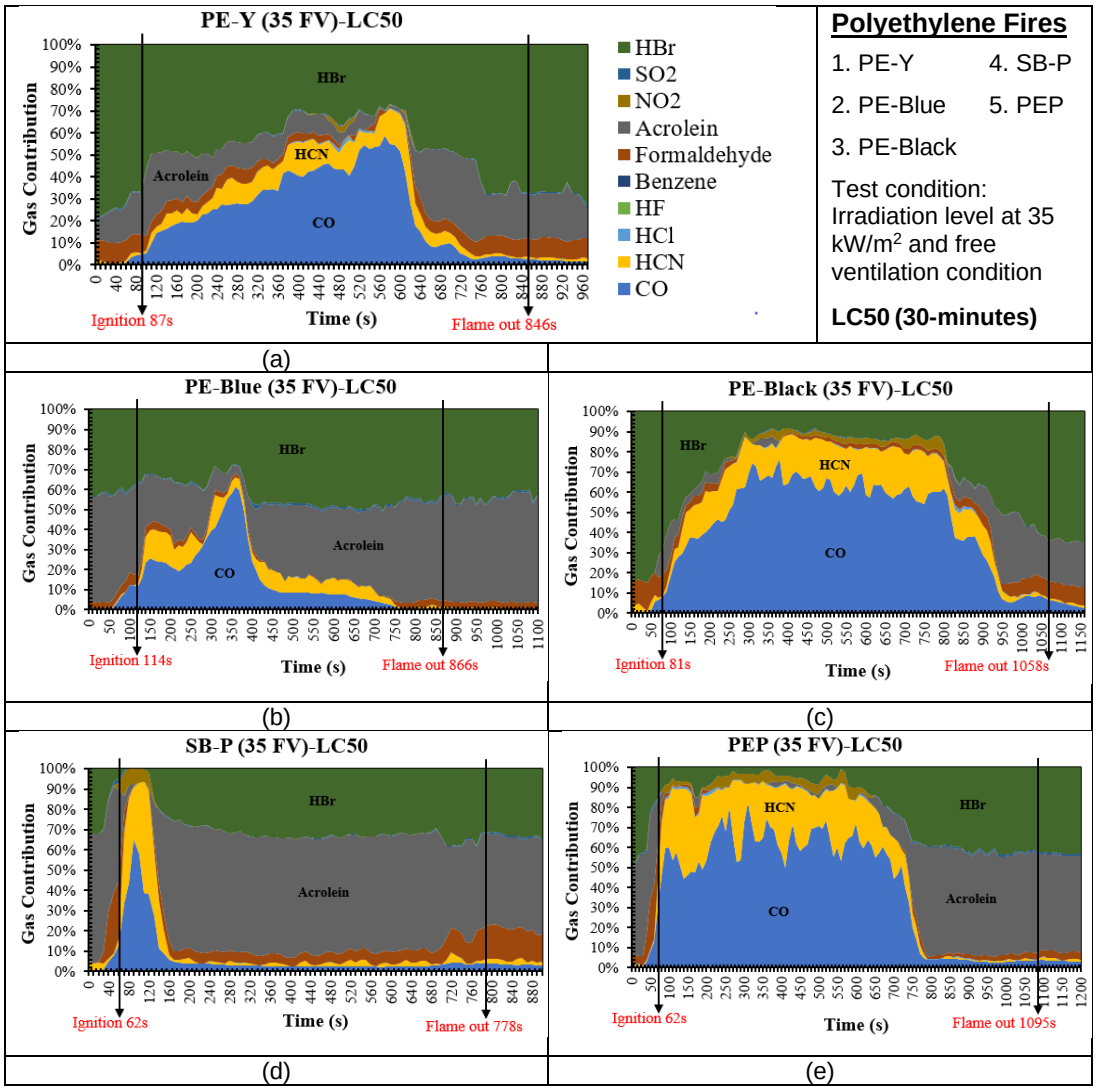


**Figure 6.11** Contribution of major gases (based $LC50_{30min}$) for Polyethylene fires at 35 kW/m$^2$ with free ventilation.

Among these Polyethylene samples, PE-Black gave the highest contribution percentage of Benzene for $COSHH_{15min}$ basis. High emissions of HBr and Acrolein were also proofing that these species also dominated the total toxicity of Polyethylene fires. From Figure 6.12 (a), it showed that PE-Y fire gave about 80% contribution percentage of HBr throughout the whole test time of 800 s and the highest if compared with other Polyethylene fires. According to this FEC $COSHH_{15min}$ shown in Figure 6.10, CO contribution was also significant especially for PEP fire other than the mentioned first three major species (Benzene, HBr and Acrolein) for all Polyethylene samples that tested. Other toxic species such as Formaldehyde, HCN and HCl that in consideration had also contributed to the fire toxicity of Polyethylene fires but the contribution was not really significant.

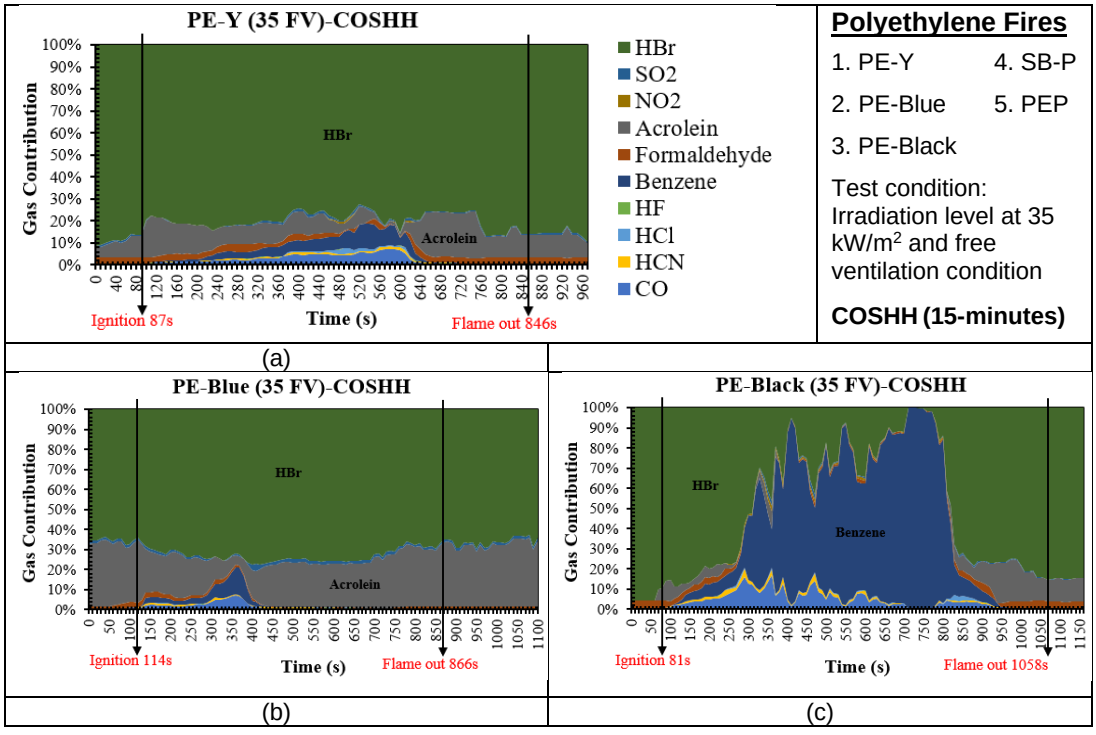

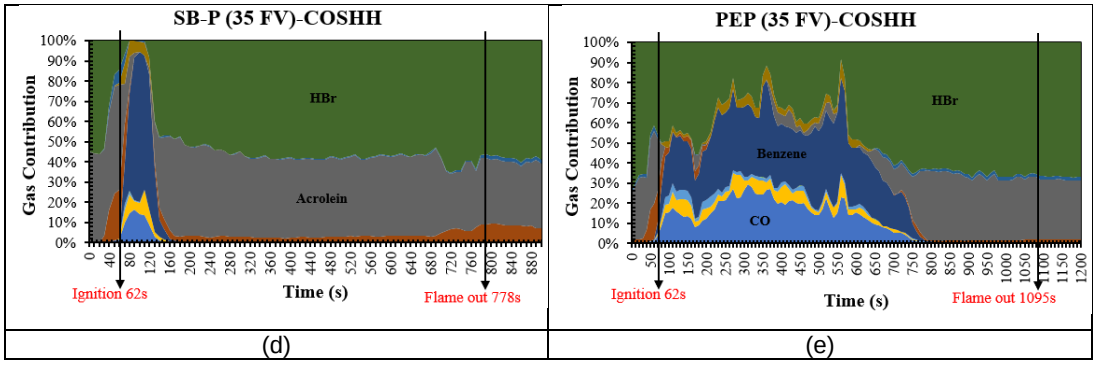


(d) (e)

**Figure 6.12** Contribution of major gases (based $COSHH_{15min}$) for Polyethylene fires at 35 kW/m$^2$ with free ventilation.

Figure 6.12 shows that $COSHH_{15min}$ impairment of escape toxic gas normalised concentrations. These are completely different to the $LC_{50}$ or death toxicity considerations. This means the gases that will impair escape are different from those that will kill you. Figure 6.12 shows that CO is never an issue in impairment of escape. In all the five PE fires HBr was the dominant toxic gas and Acrolein was the next most important, apart from PEP where Benzene was the second most important. This shows that the use of Bromine compounds in the fire retardancy of these polymers creates a major problem in the toxic gases containing HBr and impairing escape. Also these fire retardants are not very active at suppressing the fire development as the ignition temperature is only just above that for pure Ethylene with no fire retardant. Thus it may be concluded that the brominated fire retardants are ineffective and dangerous in making escape more difficult.

Figure 6.13 showed the % contribution to the AEGL-2 impairment of escape total toxicity. The most significant and dominant species for most of Polyethylene fires according to AEGL-2 was Acrolein. COSHH places a higher toxic limit on HBr than AEGL-2. Acrolein was the major toxic species that would cause an impairment of escape for Polyethylene fires under these fire conditions. This species gave the highest percentage contribution for SB-P fire which was more than 90% from the overall percentage (see Figure 6.13 (d)). In comparison between all five Polyethylene fires, PE-Blue fire contribution showed the least significant contribution of CO species to the fire toxicity than the other Polyethylene fires. $SO_2$ contribution was also significant for these Polyethylene fires. The first six major species for various Polyethylene fires are summarised and included in Table 6.9 for each stage of fire.

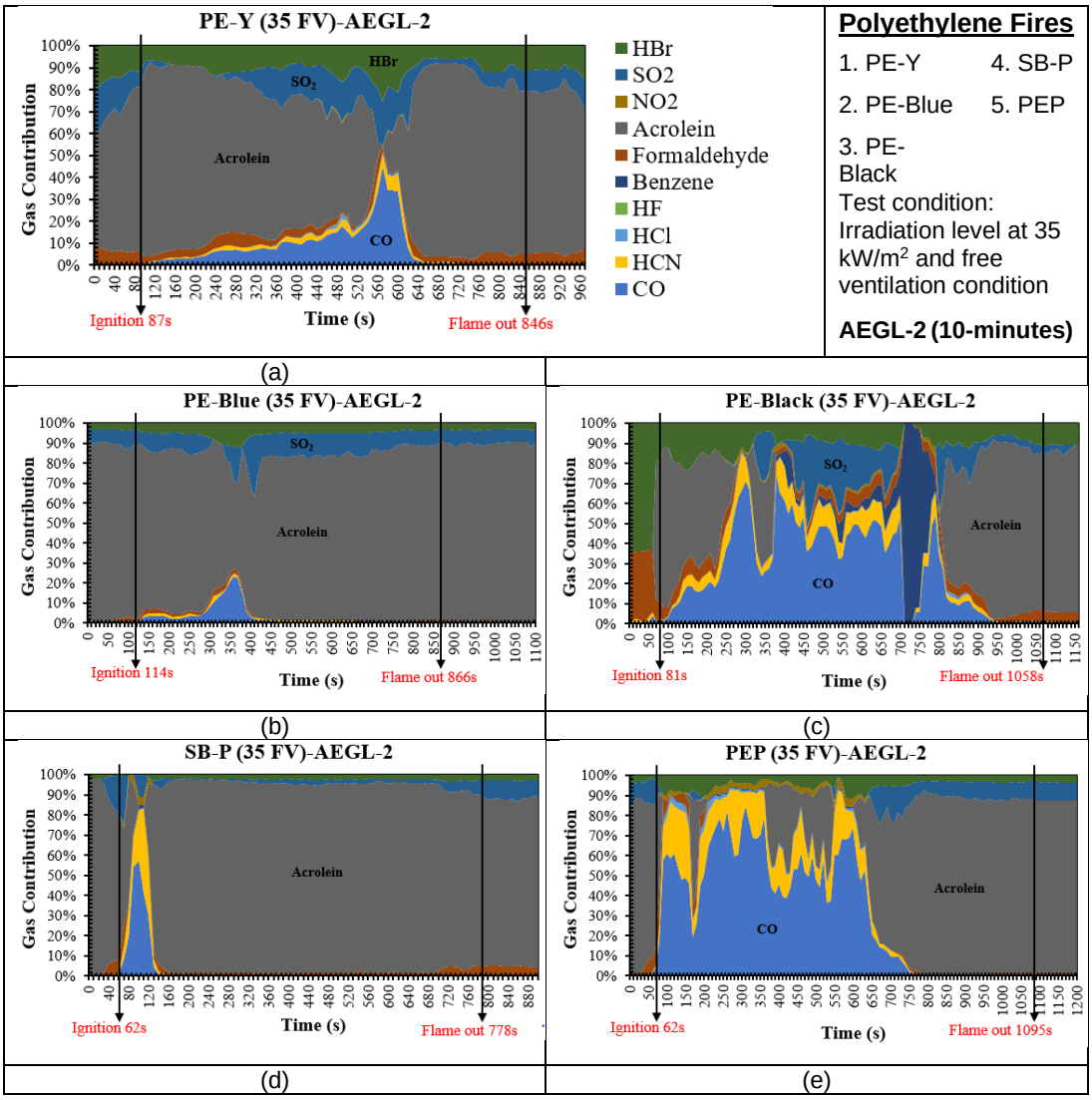


**Figure 6.13** Contribution of major gases (based AEGL-$2_{10min}$) for Polyethylene fires at 35 kW/m$^2$ with free ventilation.

**Table 6.9** First six major species for various Polyethylene fires.

| POLYETHYLENE FIRES | | | | | | | | | | | |
|---|---|---|---|---|---|---|---|---|---|---|---|
| **Test** | **Test Details** | **Mean ER, Φ (Chan)** | **Time (s)** | **Fire Stage** | **TT** | **Major Species** | | | | | |
| | | | | | | **1** | **2** | **3** | **4** | **5** | **6** |
| 1 | PE-Y | 0.3 | <87 | Ignition | LC50 | HBr | Acrolein | Formaldehyde | HCN | CO | $SO_2$ |
| | 35 FV | 2.5 (peak) | 87 - 640 | Flaming 1 | | CO | HBr | Acrolein | HCN | Formaldehyde | $NO_2$ |
| | I = 87 s | 0.7 | 640 - 846 | Flaming 2 | | HBr | Acrolein | Formaldehyde | CO | HCN | - |
| | F = 846 s | 0.2 | >846 | Post-flaming | | HBr | Formaldehyde | Acrolein | HCN | CO | - |
| | | 0.3 | <87 | Ignition | COSHH | HBr | Acrolein | Formaldehyde | $SO_2$ | - | - |
| | | 2.5 (peak) | 87 - 640 | Flaming 1 | | HBr | Acrolein | Benzene | CO | Formaldehyde | HCN |
| | | 0.7 | 640 - 846 | Flaming 2 | | HBr | Acrolein | Formaldehyde | $SO_2$ | - | - |
| | | 0.2 | >846 | Post-flaming | | HBr | Acrolein | Formaldehyde | $SO_2$ | - | - |
| | | 0.3 | <87 | Ignition | AEGL-2 | Acrolein | HBr | $SO_2$ | Formaldehyde | HCN | - |
| | | 2.5 (peak) | 87 - 640 | Flaming 1 | | Acrolein | CO | $SO_2$ | HBr | Formaldehyde | HCN |
| | | 0.7 | 640 - 846 | Flaming 2 | | Acrolein | HBr | $SO_2$ | Formaldehyde | - | - |
| | | 0.2 | >846 | Post-flaming | | Acrolein | HBr | $SO_2$ | Formaldehyde | - | - |
| 2 | PE-Blue | 0.3 | <114 | Ignition | LC50 | Acrolein | HBr | Formaldehyde | CO | HCN | $SO_2$ |
| | 35 FV | 0.9 (peak) | 114 - 750 | Flaming 1 | | HBr | Acrolein | CO | HCN | Formaldehyde | $SO_2$ |
| | I = 114 s | 0.2 | 750 - 866 | Flaming 2 | | Acrolein | HBr | Formaldehyde | HCN | $SO_2$ | - |
| | F = 866 s | 0.1 | >866 | Post-flaming | | Acrolein | HBr | Formaldehyde | HCN | $SO_2$ | - |
| | | 0.3 | <114 | Ignition | COSHH | HBr | Acrolein | Formaldehyde | $SO_2$ | - | - |
| | | 0.9 (peak) | 114 - 750 | Flaming 1 | | HBr | Acrolein | Benzene | CO | Formaldehyde | $SO_2$ |
| | | 0.2 | 750 - 866 | Flaming 2 | | HBr | Acrolein | Formaldehyde | $SO_2$ | - | - |
| | | 0.1 | >866 | Post-flaming | | HBr | Acrolein | Formaldehyde | $SO_2$ | - | - |

| | | | | | | | | | | | |
|---|---|---|---|---|---|---|---|---|---|---|---|
| | | 0.3 | <114 | Ignition | **AEGL-2** | Acrolein | $SO_2$ | HBr | Formaldehyde | CO | HCN |
| | | 0.9 (peak) | 114 - 750 | Flaming 1 | | Acrolein | $SO_2$ | CO | HBr | Formaldehyde | HCN |
| | | 0.2 | 750 - 866 | Flaming 2 | | Acrolein | $SO_2$ | HBr | Formaldehyde | - | - |
| | | 0.1 | >866 | Post-flaming | | Acrolein | $SO_2$ | HBr | Formaldehyde | - | - |
| 3 | PE-Black | 0.2 | <81 | Ignition | **LC50** | HBr | Formaldehyde | HCN | Acrolein | CO | - |
| | 35 FV | 4.0 (max. 7.5) | 81 - 950 | SS Flaming | | CO | HBr | HCN | Acrolein | Formaldehyde | $NO_2$ |
| | I = 81 s | 0.8 | 950 - 1058 | Flaming | | HBr | Acrolein | Formaldehyde | CO | HCN | - |
| | F = 1058 s | 0.3 | >1058 | Post-flaming | | HBr | Acrolein | Formaldehyde | CO | HCN | - |
| | | 0.2 | <81 | Ignition | **COSHH** | HBr | Formaldehyde | Acrolein | - | - | - |
| | | 4.0 (max. 7.5) | 81 - 950 | SS Flaming | | Benzene | HBr | CO | Acrolein | Formaldehyde | HCN |
| | | 0.8 | 950 - 1058 | Flaming | | HBr | Acrolein | Formaldehyde | - | - | - |
| | | 0.3 | >1058 | Post-flaming | | HBr | Acrolein | Formaldehyde | - | - | - |
| | | 0.2 | <81 | Ignition | **AEGL-2** | HBr | Formaldehyde | Acrolein | HCN | CO | - |
| | | 4.0 (max. 7.5) | 81 - 950 | SS Flaming | | CO | Acrolein | HBr | $SO_2$ | Benzene | HCN |
| | | 0.8 | 950 - 1058 | Flaming | | Acrolein | HBr | $SO_2$ | Formaldehyde | - | - |
| | | 0.3 | >1058 | Post-flaming | | Acrolein | HBr | Formaldehyde | $SO_2$ | - | - |
| 4 | SB-P | 0.2 | <62 | Ignition | **LC50** | Acrolein | HBr | Formaldehyde | HCN | CO | $SO_2$ |
| | 35 FV | 2.8 (peak) | 62 -160 | Flaming | | CO | HCN | Acrolein | HBr | $NO_2$ | Formaldehyde |
| | I = 62 s | 0.4 | 160 - 778 | SS Flaming | | Acrolein | HBr | Formaldehyde | HCN | CO | $SO_2$ |
| | F = 778 s | 0.1 | >778 | Post-flaming | | Acrolein | HBr | Formaldehyde | HCN | CO | $SO_2$ |
| | | 0.2 | <62 | Ignition | **COSHH** | Acrolein | HBr | Formaldehyde | $SO_2$ | $NO_2$ | CO |
| | | 2.8 (peak) | 62 -160 | Flaming | | Benzene | Acrolein | HBr | CO | HCN | Formaldehyde |
| | | 0.4 | 160 - 778 | SS Flaming | | HBr | Acrolein | Formaldehyde | $SO_2$ | - | - |
| | | 0.1 | >778 | Post-flaming | | HBr | Acrolein | Formaldehyde | $SO_2$ | - | - |
| | | 0.2 | <62 | Ignition | **AEGL-2** | Acrolein | $SO_2$ | Formaldehyde | HBr | HCN | - |
| | | 2.8 (peak) | 62 -160 | Flaming | | Acrolein | CO | HCN | $SO_2$ | Formaldehyde | HBr |
| | | 0.4 | 160 - 778 | SS Flaming | | Acrolein | Formaldehyde | HBr | $SO_2$ | - | - |
| | | 0.1 | >778 | Post-flaming | | Acrolein | $SO_2$ | Formaldehyde | HBr | - | - |

| | | | | | | | | | | | | |
|---|---|---|---|---|---|---|---|---|---|---|---|---|
| 5 | PEP | 0.4 | <62 | Ignition | **LC50** | Acrolein | HBr | Formaldehyde | CO | HCN | $SO_2$ |
| | 35 FV | 3.0 (max. 6.0) | 62 - 780 | Flaming 1 | | CO | HCN | HBr | Acrolein | $NO_2$ | Formaldehyde |
| | I = 62 s | 0.3 | 780 - 1095 | Flaming 2 | | Acrolein | HBr | CO | Formaldehyde | HCN | $SO_2$ |
| | F = 1095 s | 0.1 | >1095 | Post-flaming | | Acrolein | HBr | Formaldehyde | CO | HCN | $SO_2$ |
| | | 0.4 | <62 | Ignition | **COSHH** | HBr | Acrolein | Formaldehyde | $SO_2$ | Benzene | CO |
| | | 3.0 (max. 6.0) | 62 - 780 | Flaming 1 | | HBr | Benzene | CO | Acrolein | HCN | $NO_2$ |
| | | 0.3 | 780 - 1095 | Flaming 2 | | HBr | Acrolein | Formaldehyde | $SO_2$ | - | - |
| | | 0.1 | >1095 | Post-flaming | | HBr | Acrolein | Formaldehyde | $SO_2$ | - | - |
| | | 0.4 | <62 | Ignition | **AEGL-2** | Acrolein | $SO_2$ | Formaldehyde | HBr | CO | HCN |
| | | 3.0 (max. 6.0) | 62 - 780 | Flaming 1 | | CO | Acrolein | HCN | HBr | $NO_2$ | Formaldehyde |
| | | 0.3 | 780 - 1095 | Flaming 2 | | Acrolein | $SO_2$ | HBr | Formaldehyde | - | - |
| | | 0.1 | >1095 | Post-flaming | | Acrolein | $SO_2$ | HBr | Formaldehyde | - | - |

## 6.5 Findings and Conclusion from Polyethylene Fire Tests

Various conducted Polyethylene fires in the Cone Calorimeter at irradiation level of 35 kW/m$^2$ and free ventilation had come out with several significant findings as listed follow:

- The highest MLR was ~0.4 g/s for PE-Y fire followed by PE-Black (~0.3 g/s), PE-Blue (~0.28 g/s), PEP (~0.12 g/s) and SB-P (~0.1 g/s). The SB-P fire was the quickest reaching the maximum peak MLR at <100 s compared to other Polyethylene fires which reached the maximum peak MLR after 500 s of burning period.
- These PE foam fires experienced a fuel rich burning condition with giving fire equivalence ratios above 1.0 (up to 8.0 for PE-Black fire). The peak total HRR (MLR) for most of these PE fires were more than 500 kW/m$^2$ with PE-Y fire gave up to 2000 kW/m$^2$ of the maximum heat release rate value.3.7 kW/m$^2$. Most of these bund material samples mainly Polyethylene materials would reach the point of ignition when its surface temperature >350$^o$C.
- For the tests with piloted ignition for determination of critical heat flux of Polyethylene fires, among the three PE bund materials (PE-Y, PE-Blue and PE-Black), the lowest determined critical heat flux of 7.8 kW/m$^2$ was given by the PE-Blue fire. Other type of bund material, the GRP-Blue, the result showed that the critical heat flux for this material was 3.7 kW/m$^2$.
- Under these test conditions, all Polyethylene fires showed high HBr concentrations with PE-Y and PE-Black samples had the highest value of HBr emissions, as shown in Figure 6.7 (o), which were a major contribution to the FEC (Fractional Effective Concentration) LC50 total toxicity as presented in Figure 6.10. This PE-Yellow had the second highest total toxicity, as shown in Figure 6.10. The results show that the halogenated fire retardants, particularly HBr, have a significant contribution to the total toxicity, but that other combustion generated toxic gases are also important.
- Total toxic emissions from all five PE samples had FECs of LC50 greater than 1.0 with the highest peak ~17, but the worst toxicity was for the three flammable liquid bunds with high HBr toxic emissions.
- In terms of the impairment of escape the COSHH$_{15min}$ and AEGL-2 toxic limits had different conclusions and this was due to COSHH$_{15min}$ placing

a lower concentration for HBr. This resulted in HBr being the most important toxic gas under the $COSHH_{15min}$ assessment compared with Acrolein under the AEGL-2 assessment, which was the second most toxic gas under $COSHH_{15min}$.

- CO yields of these Polyethylene fires were below 0.45 g/g with PE-Blue gave the highest yield value. These Polyethylene fires had given $CO_2$ yields <3.0 g/g. Some of yield values presented were insensible and this could be due to the out of measurement range by the FTIR for certain species like Benzene and HBr.
- The two most dominant toxic species were Acrolein and HBr for these Polyethylene fires. Other toxic species like Benzene, Formaldehyde, $SO_2$, CO, HCN and $NO_2$ were also the major contributors to the fire toxicities for this polymer fires.

# Chapter 7
# Polystyrene Fires with Free Ventilation in the Cone Calorimeter Test

## 7.1 General Combustion Properties of Various Polystyrene Fires

Table 7.1 shows the test details for Polystyrene fires at test conditions of 35 kW/m$^2$ of irradiation level and free ventilation. All eight types of Polystyrenes were tested and the results were compared. Polystyrene sheets like PS2, PS-CB and PS-CB 2 were used as wall insulation, meanwhile PS-TV was used as packaging material for television. Polystyrene sheets with a cardboard layer (PS-CB and PS-CB 2), both were actually same type. The difference only was the arrangement of each sample in the sample holder before the fire test which PS-CB fire with Polystyrene layer was facing up and PS-CB 2 fire with cardboard layer was facing up. Other tested Polystyrenes such as PS-COVE sheet was normally used as coving materials for roof or ceiling and skirting board (SB-W H) was usually used as a cover for roof or wall liners. Clear glass Polystyrene sheets (Clear PS2 and Clear PS4) were widely used as building windows. These two clear glass Polystyrene sheets have different thicknesses which 2 mm (Clear PS2) and 4 mm (Clear PS4).

**Table 7.1** Test details for Polystyrene fires.

| Test | Polystyrene Type | Thickness (mm) | Initial Mass (g) | Density (g/cm$^3$) | Ignition (s) | Flame out (s) |
|---|---|---|---|---|---|---|
| 1 | PS2 | 2 | 0.3 | 0.0150 | No | No |
| 2 | PS-TV | 23 | 4.5 | 0.0196 | 50 | 235 |
| 3 | PS-CB | 3 | 2.5 | 0.0833 | 13 | 29 |
| 4 | PS-CB 2 | 3 | 2.4 | 0.0800 | No | No |
| 5 | PS COVE | 10 | 8.6 | 0.0860 | 51 | 303 |
| 6 | SB-W H | 7.5 | 32.7 | 0.4360 | 34 | 849 |
| 7 | Clear PS2 | 2 | 18.2 | 0.9100 | 37 | 593 |
| 8 | Clear PS4 | 4 | 38.8 | 0.9700 | 107 | 667 |

All eight Polystyrenes were divided to two groups while plotting the graphs based on the time duration of each Polystyrene took while burning until reaching the flame out condition. PS2, PS-TV, PS-CB and PS-CB 2 were in the first group of Polystyrenes and the second group of Polystyrenes were PS-COVE, SB-W H, Clear PS2 and Clear PS4. In terms of weight and

hardness, the first group Polystyrenes were much lighter and less hard than the second group of Polystyrene.

For the first group, the longest duration of test time was taken by PS-TV fire with flame out time was about 235 s. PS2 and PS-CB 2 burnings were happened so fast where there was no flaming condition was observed. For the second group of Polystyrenes, SB-W H took the shortest time to have an ignition (34 s) and the longest time (849 s) to reach flame out condition compared to PS COVE, Clear PS2 and Clear PS4. Between these four Polystyrenes in the second group, PS COVE was physically softest and could be a reason for it having the quickest burning compared to another three Polystyrenes.

### 7.1.1 Profile for Mass Reduction and Oxygen Changes

The normalised mass loss values for most of the tested Polystyrenes as shown in Figure 7.1 indicate zero except for Polystyrenes with the cardboard layer (PS-CB and PS-CB 2). It showed that about 20% of unburned residue was still left. From the Oxygen consumption graph (Figure 7.2), it showed clearly that the Polystyrene with the longer burning process had consumed more Oxygen compared to the Polystyrene with the shorter burning process.

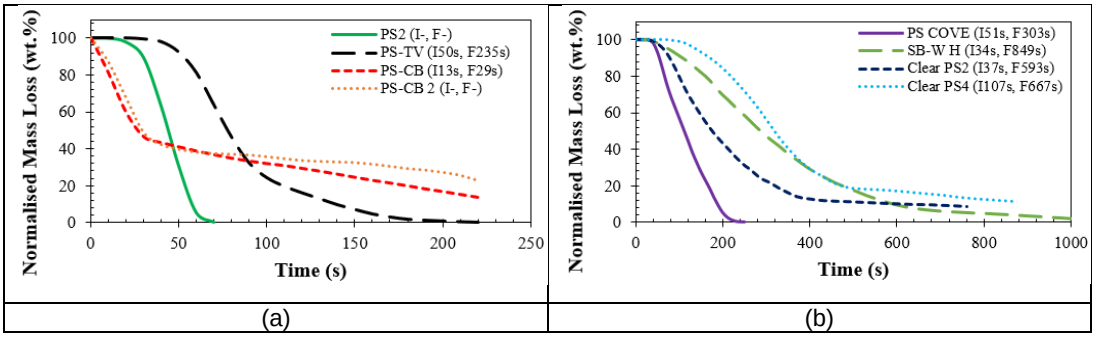


**Figure 7.1** Normalised mass loss profiles for Polystyrene fires.

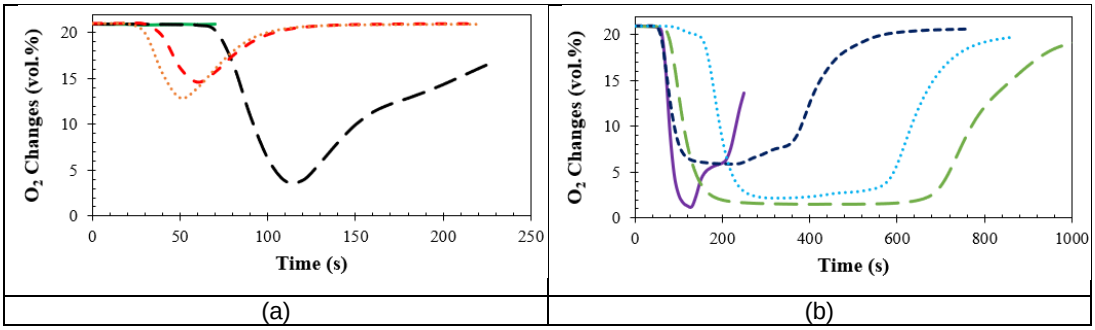


**Figure 7.2** Oxygen changes during polystyrene fire tests.

### 7.1.2 Correlations between MLR and ER

A key difference in the fire performance was in the speed and duration of the fires. Polystyrene foams (PS2, PS-CB and PS-CB 2) have a low density so the fuel mass was low and the fire spread was rapid, but short lived. Figure 7.3 showed the mass loss rate values as a function of time and Figure 7.4 showed the equivalence ratios as a function of time for various Polystyrene fires. The highest mass loss rate (MLR) of 0.12 g/s was given by the SB-W H fire at test time about 300 s. PS-TV, PS COVE, Clear PS2 and Clear PS4 gave the same peak of average MLR (0.08 g/s). Meanwhile PS2, PS-CB and PS-CB 2 showed the lowest MLR values which less than 0.01 g/s. From the equivalence ratio (ER) values, PS2, PS-CB and PS-CB 2 indicated the fuel lean burning condition with low ER values (<0.5). For other Polystyrenes like PS-TV, PS COVE, SB-W H, Clear PS2 and Clear PS4, the rich fuel burning condition were shown with equivalence ratios about 1.0 and above.

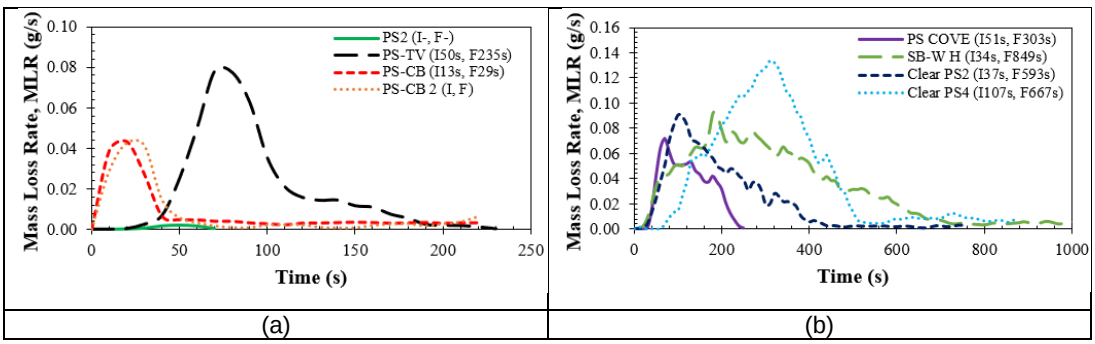


**Figure 7.3** Mass loss rate (MLR) as a function of time.

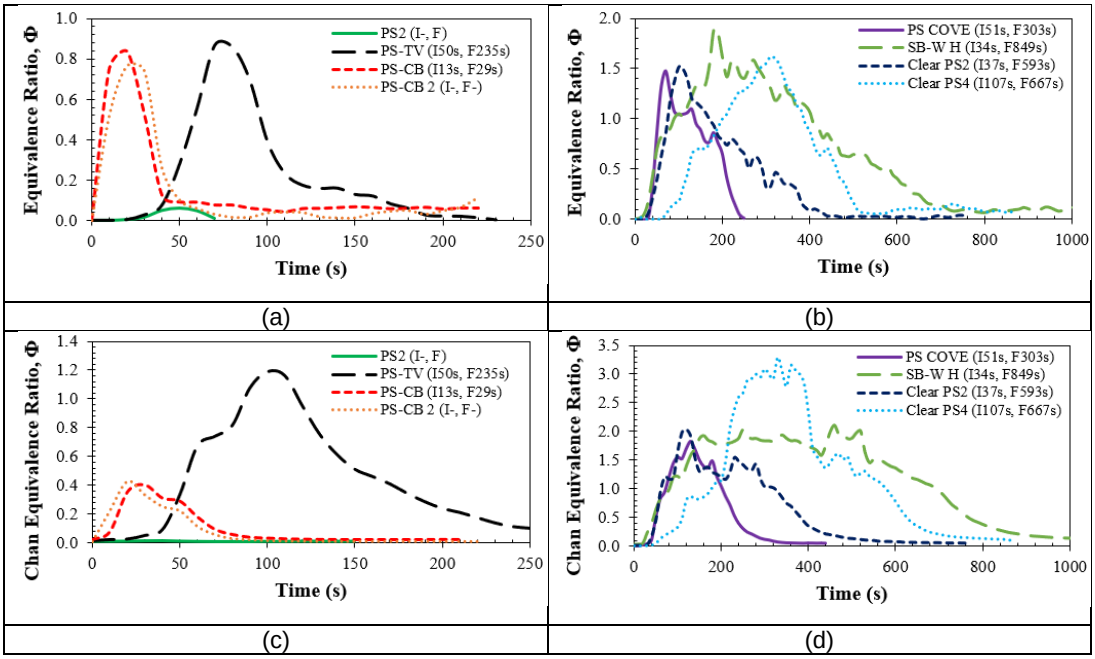


**Figure 7.4** Equivalence ratio (ER) as a function of time.

### 7.1.3 Heat Release Rate (HRR) Profiles for Polystyrene Fires

Heat release rate (HRR) is proportionate with the MLR. A higher MLR indicates a higher burning rate of the burned material. This will also contribute to a higher HRR. SB-W H gave the highest peak HRR of 500 kW/m$^2$, followed by PS-TV, PS COVE, Clear PS2 and Clear PS4 with the second highest of peak HRR about 300 kW/m$^2$. The wall insulation foams (PS2, PS-CB and PS-CB 2) showed a very low HRR compared to other Polystyrenes. HRR based MLR contributed a higher value than the HRR based Oxygen consumption (OC) as shown in Figure 7.5 (a) and Figure 7.5 (b). From Figure 7.5 (c), it can be seen that the highest primary HRR that determined was about 300 kW/m$^2$ and it can be estimated that the value of air flowrate for these Polystyrene fires with free ventilation condition was above that (>0.986 g/s or 48 L/min).

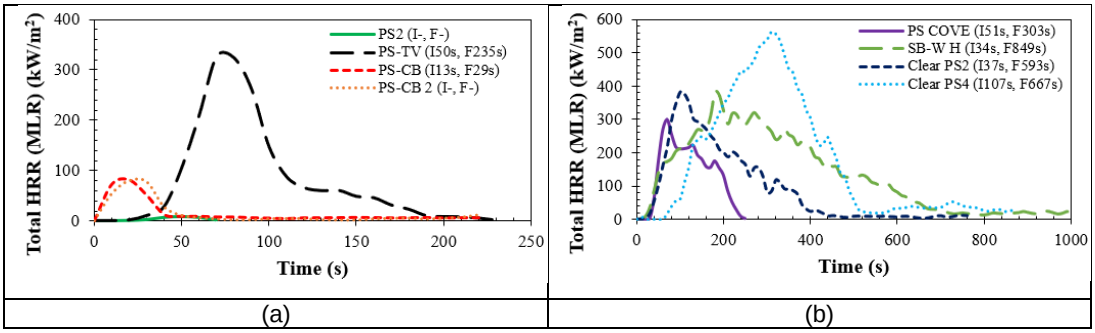

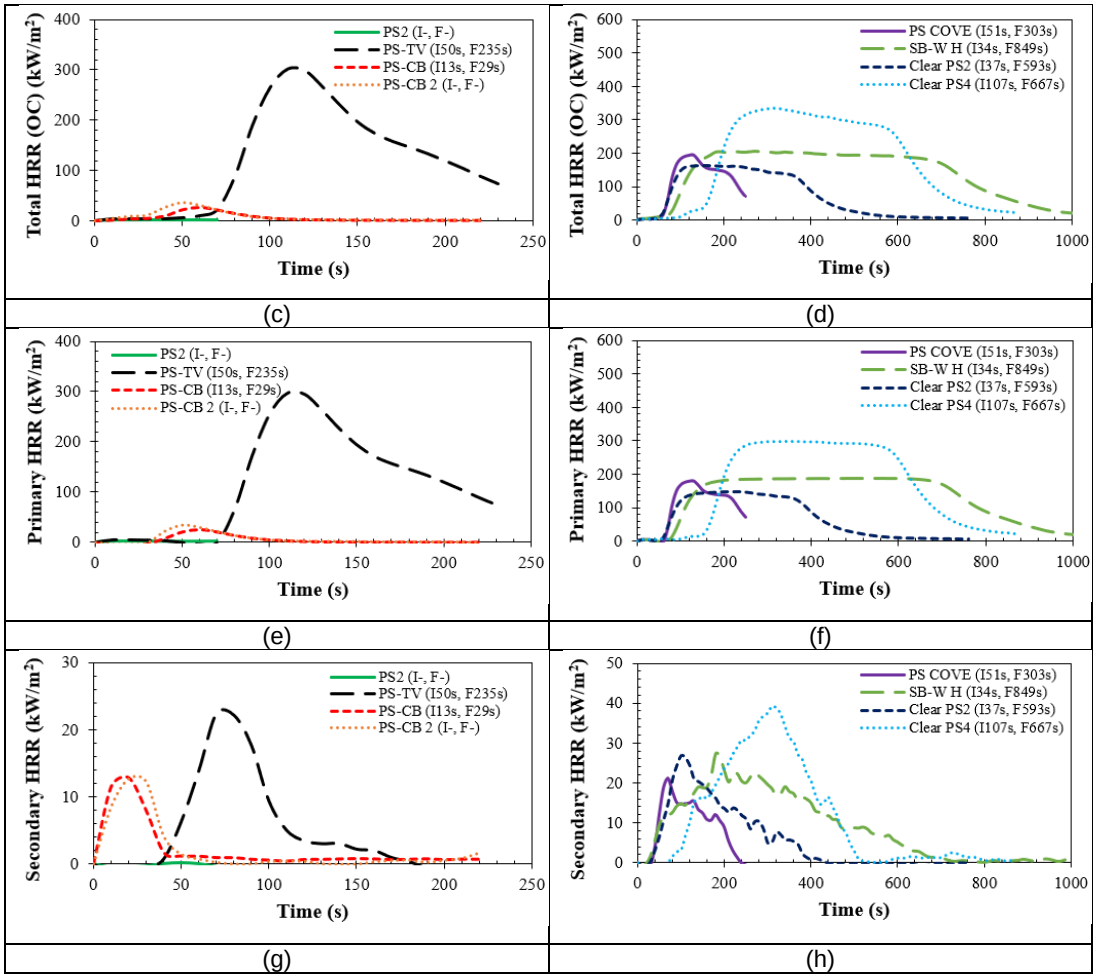


**Figure 7.5** Heat release rates for various Polystyrene fires at 35 kW/m$^2$ of irradiation level and free ventilation condition.

## 7.2 Toxicity of Polystyrene Fires

### 7.2.1 Gas Concentration as a Function of Time

Eight materials made from Polystyrene were tested and the toxic products determined. Figure 7.6 (a) shows the very high CO emissions for all samples, except for the foam ceiling boards (PS2, PS-CB and PS-CB 2) burnt very fast and the solid skirting board (SB-WH) burnt slowly and this had the worst CO emissions. Hydrocarbon emissions were very high as shown in Figure 7.6 (i) and the worst case was the same as for CO. One of the major components on the THC was Acetylene, as shown in Figure 7.6 (g). This is a major intermediate gas in the formation of soot.

Another aromatic hydrocarbon that is directly toxic to humans is Benzene and these emissions were high for all samples, especially in the early stages of

the fire. Again Benzene is an intermediate in the formation of soot, which is why soot emissions from Polystyrene fires is so high. Formaldehyde, Acrolein and Acetaldehyde were all high for most of the Polystyrene samples. Figure 7.6 (b) and Figure 7.6 (c) show very high levels of HCN and HCl, which indicates a Chlorine halogen fire retardant and a Nitrogen based material was used, apart from in the foams.

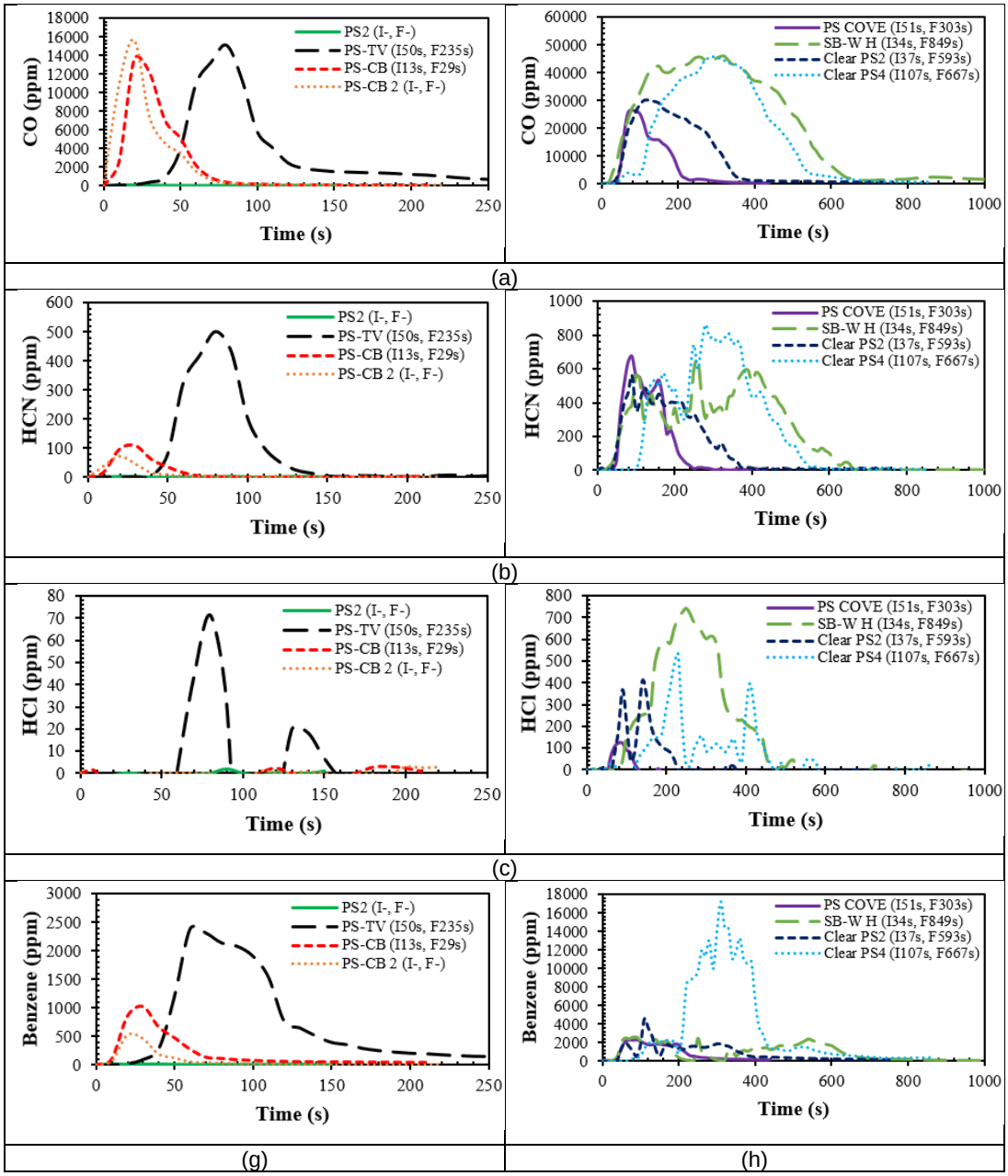

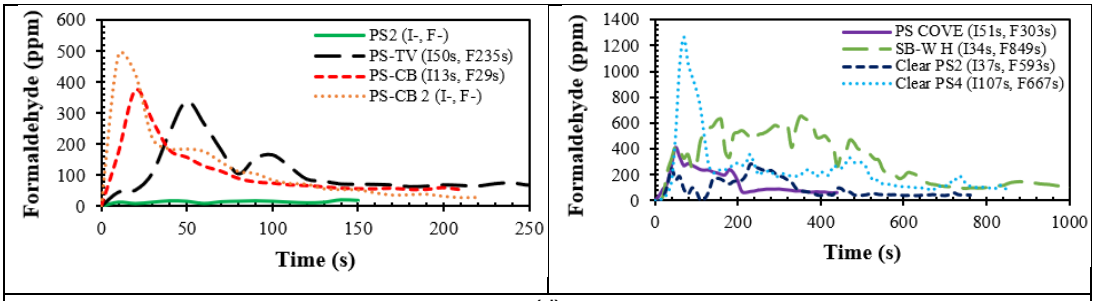
Formaldehyde (ppm)
Time (s)
PS2 (I-, F-)
PS-TV (I50s, F235s)
PS-CB (I13s, F29s)
PS-CB 2 (I-, F-)
PS COVE (I51s, F303s)
SB-W H (I34s, F849s)
Clear PS2 (I37s, F593s)
Clear PS4 (I107s, F667s)

(d)

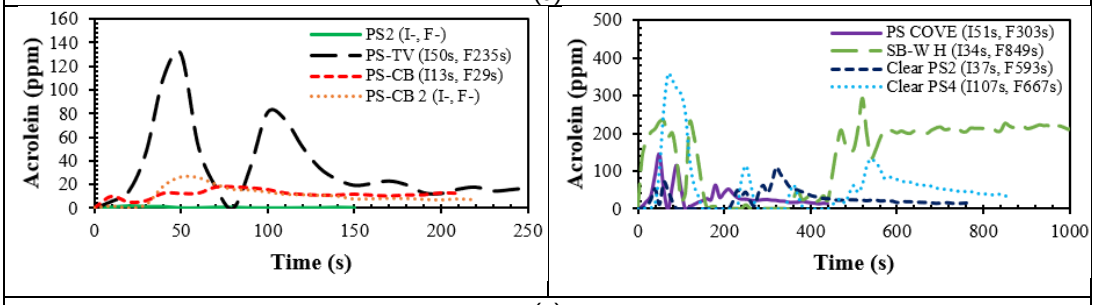
Acrolein (ppm)
Time (s)
PS2 (I-, F-)
PS-TV (I50s, F235s)
PS-CB (I13s, F29s)
PS-CB 2 (I-, F-)
PS COVE (I51s, F303s)
SB-W H (I34s, F849s)
Clear PS2 (I37s, F593s)
Clear PS4 (I107s, F667s)

(e)

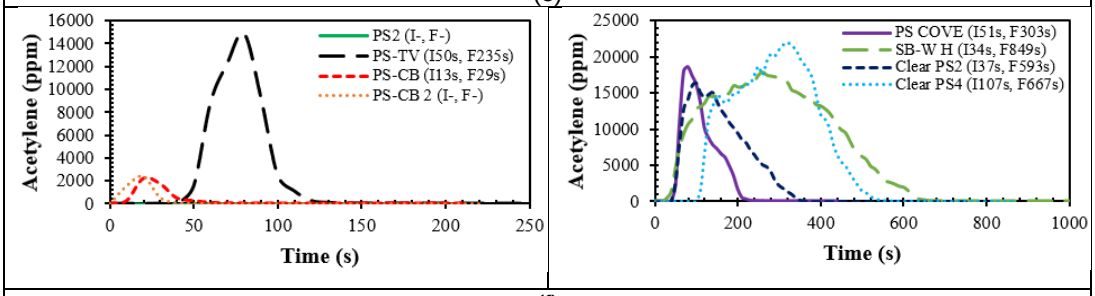
Acetylene (ppm)
Time (s)
PS2 (I-, F-)
PS-TV (I50s, F235s)
PS-CB (I13s, F29s)
PS-CB 2 (I-, F-)
PS COVE (I51s, F303s)
SB-W H (I34s, F849s)
Clear PS2 (I37s, F593s)
Clear PS4 (I107s, F667s)

(f)

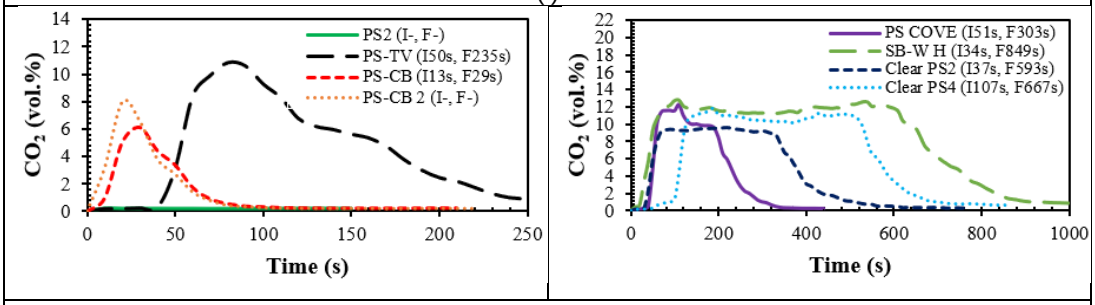
CO2 (vol.%)
Time (s)
PS2 (I-, F-)
PS-TV (I50s, F235s)
PS-CB (I13s, F29s)
PS-CB 2 (I-, F-)
PS COVE (I51s, F303s)
SB-W H (I34s, F849s)
Clear PS2 (I37s, F593s)
Clear PS4 (I107s, F667s)

(g)

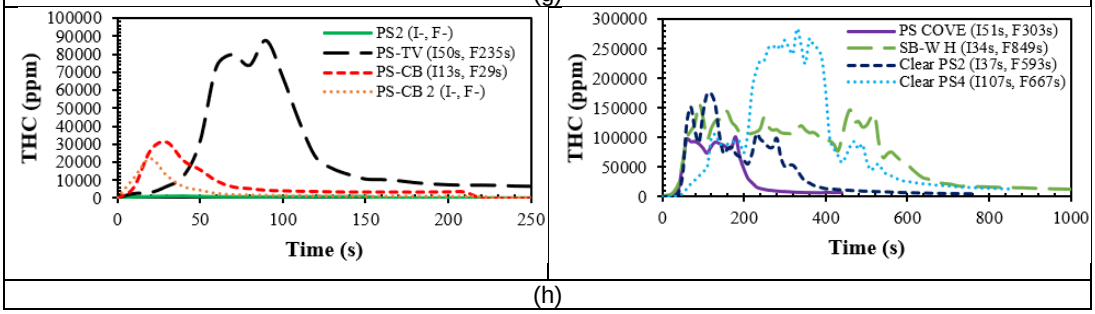
THC (ppm)
Time (s)
PS2 (I-, F-)
PS-TV (I50s, F235s)
PS-CB (I13s, F29s)
PS-CB 2 (I-, F-)
PS COVE (I51s, F303s)
SB-W H (I34s, F849s)
Clear PS2 (I37s, F593s)
Clear PS4 (I107s, F667s)

(h)

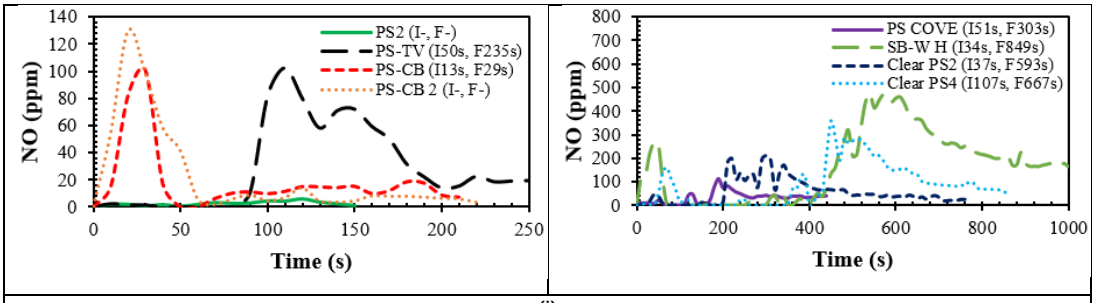
NO (ppm)
PS2 (I-, F-)
PS-TV (I50s, F235s)
PS-CB (I13s, F29s)
PS-CB 2 (I-, F-)
Time (s)
PS COVE (I51s, F303s)
SB-W H (I34s, F849s)
Clear PS2 (I37s, F593s)
Clear PS4 (I107s, F667s)

(i)

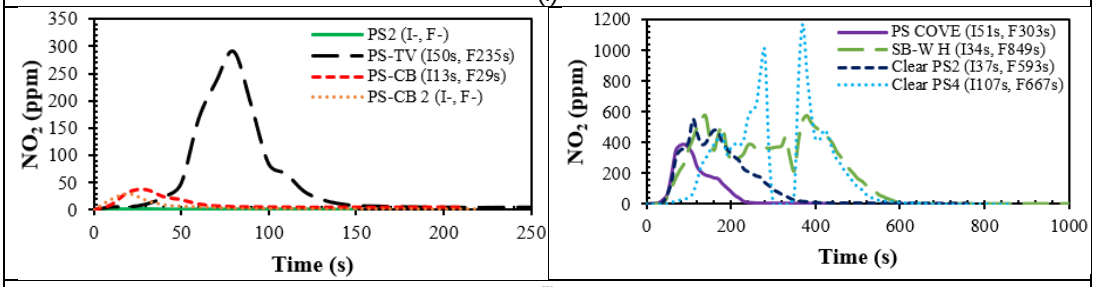
NO2 (ppm)
PS2 (I-, F-)
PS-TV (I50s, F235s)
PS-CB (I13s, F29s)
PS-CB 2 (I-, F-)
Time (s)
PS COVE (I51s, F303s)
SB-W H (I34s, F849s)
Clear PS2 (I37s, F593s)
Clear PS4 (I107s, F667s)

(j)

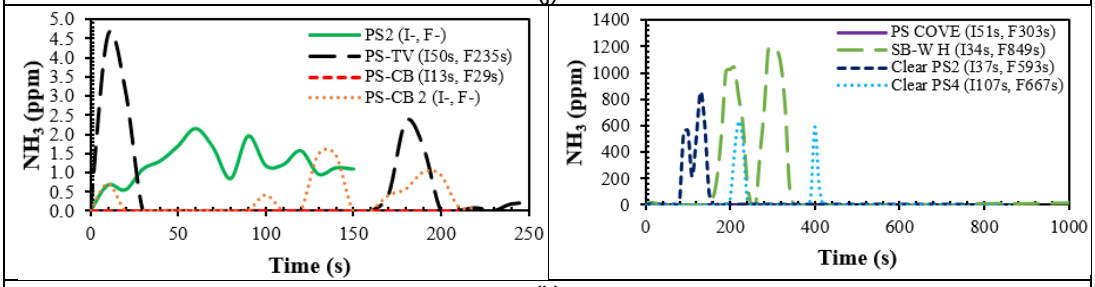
NH3 (ppm)
PS2 (I-, F-)
PS-TV (I50s, F235s)
PS-CB (I13s, F29s)
PS-CB 2 (I-, F-)
Time (s)
PS COVE (I51s, F303s)
SB-W H (I34s, F849s)
Clear PS2 (I37s, F593s)
Clear PS4 (I107s, F667s)

(k)

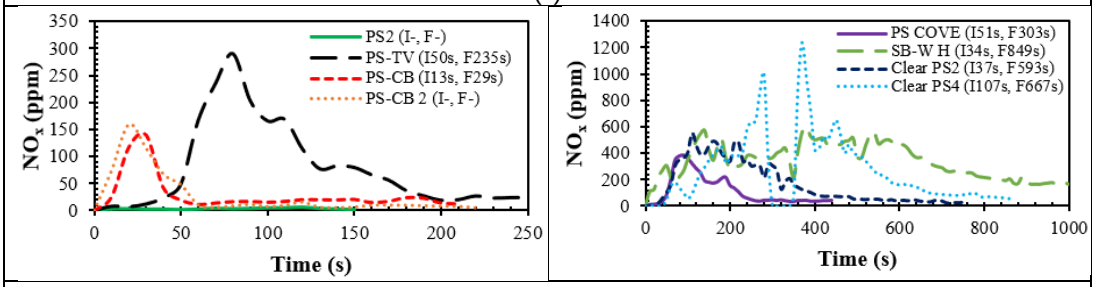
NOx (ppm)
PS2 (I-, F-)
PS-TV (I50s, F235s)
PS-CB (I13s, F29s)
PS-CB 2 (I-, F-)
Time (s)
PS COVE (I51s, F303s)
SB-W H (I34s, F849s)
Clear PS2 (I37s, F593s)
Clear PS4 (I107s, F667s)

(l)

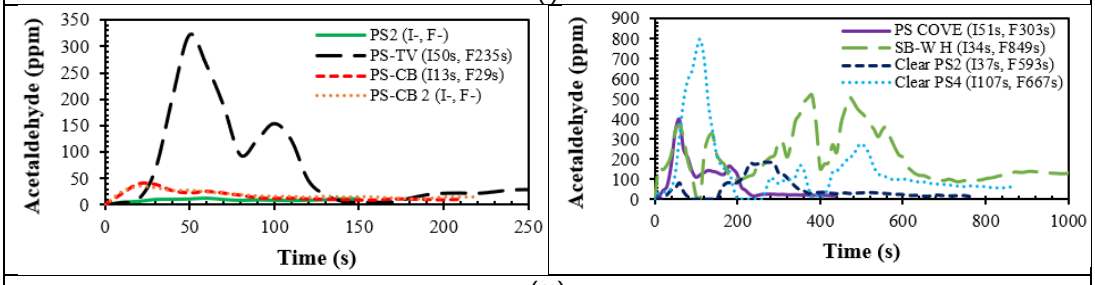
Acetaldehyde (ppm)
PS2 (I-, F-)
PS-TV (I50s, F235s)
PS-CB (I13s, F29s)
PS-CB 2 (I-, F-)
Time (s)
PS COVE (I51s, F303s)
SB-W H (I34s, F849s)
Clear PS2 (I37s, F593s)
Clear PS4 (I107s, F667s)

(m)

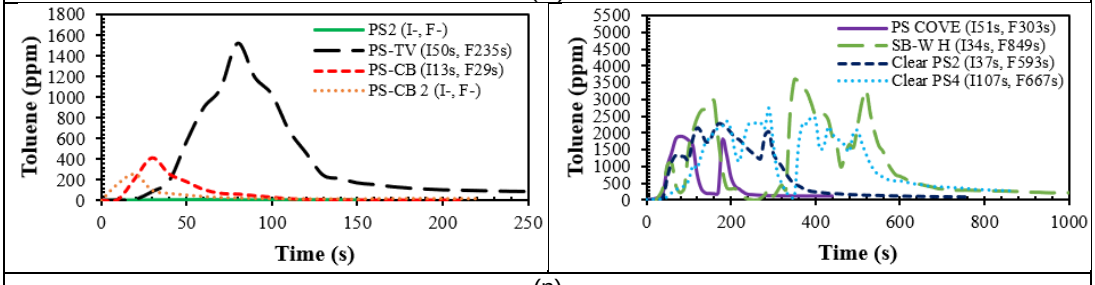
Toluene (ppm)
PS2 (I-, F-)
PS-TV (I50s, F235s)
PS-CB (I13s, F29s)
PS-CB 2 (I-, F-)
Time (s)
PS COVE (I51s, F303s)
SB-W H (I34s, F849s)
Clear PS2 (I37s, F593s)
Clear PS4 (I107s, F667s)

(n)

**Figure 7.6** Toxic gas concentrations as a function of time for various Polystyrene fires at 35 kW/m$^2$ with free ventilation.

### 7.2.2 Gas Yields for Polystyrene Fires at 35 kW/m$^2$ with Free Ventilation

Yield of each gas or species produced from a fire was depended to the chemical compound of the burned material that reacted with the supplied Oxygen in certain fire conditions. Certain weight of sample burned would produce certain weight of species that was determined as the combustion products. Yield for each species produced under fire conditions of 35 kW/m$^2$ and free ventilation for various Polystyrene fires against test time is shown in the following Figure 7.7. From the yield graph, it indicated clearly the yield value in weight percentage for each toxic species. CO Yield in Figure 7.7 showed that Clear PS4 had the highest CO yield of 0.5 g/g at 200 s of test time than other Polystyrene fires and also had a lower CO yield peak of <0.3 g/g after 400 s. The CO yield peak of 0.25 g/g was given by PS-TV fire at 80 s and the similar highest peak was observed for PS-CB 2 fire at ~20 s. PS COVE and Clear PS2 fires gave the CO yields <0.4 g/g and other Polystyrene fires such as PS2 and PS-CB fires had given less than 0.2 g/g of CO yield.

In overall, the higher density Polystyrene fires such as PS COVE, SB-W H, Clear PS2 and Clear PS4 fires, it gave a much higher yield for most considered toxic species if compared to the lower density Polystyrene fires (PS2, PS-TV, PS-CB and PS-CB 2 fires). Among these Polystyrene fires, Clear PS4 had shown the highest yield value for Benzene (0.25 g/g), Formaldehyde (0.12 g/g), $NO_2$ (0.01 g/g) and $SO_2$ (0.012 g/g) while SB-W H contributed to the highest yield of 0.008 g/g for HCl, 0.08 g/g for Acrolein and 0.08 g/g for Acetaldehyde. The maximum and average yields of toxic species for these Polystyrene fires are summarised and included in Table 7.2 and 7.3.

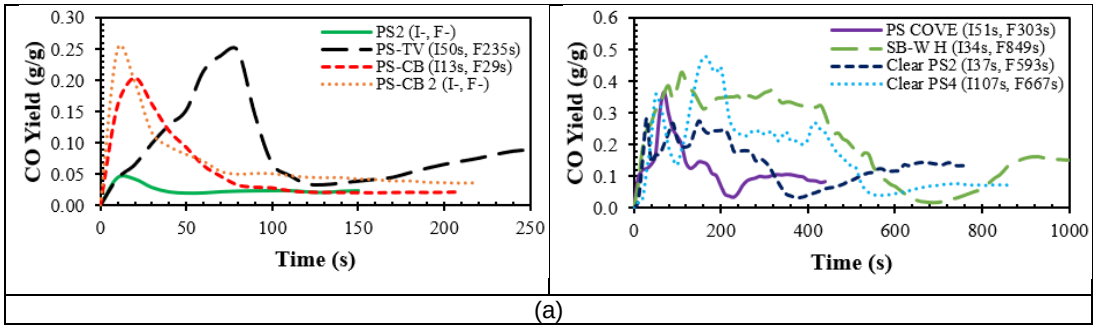


(a)

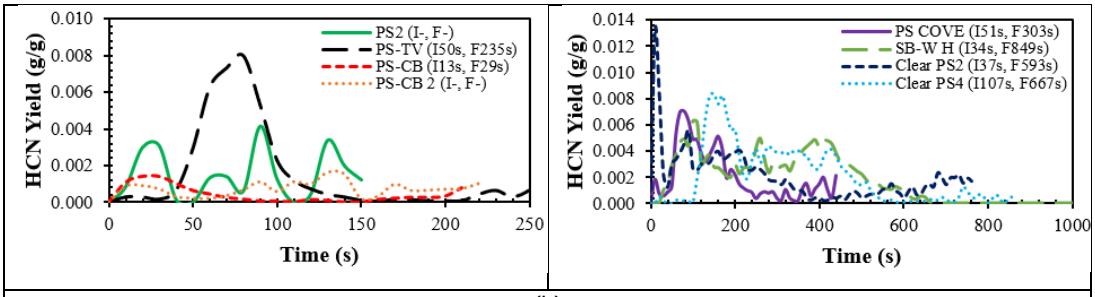
HCN Yield (g/g)
Time (s)
PS2 (I-, F-)
PS-TV (I50s, F235s)
PS-CB (I13s, F29s)
PS-CB 2 (I-, F-)
PS COVE (I51s, F303s)
SB-W H (I34s, F849s)
Clear PS2 (I37s, F593s)
Clear PS4 (I107s, F667s)

(b)

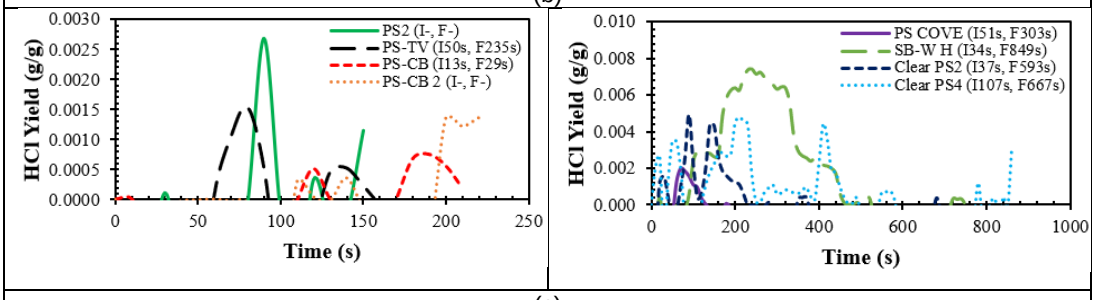
HCl Yield (g/g)
Time (s)
PS2 (I-, F-)
PS-TV (I50s, F235s)
PS-CB (I13s, F29s)
PS-CB 2 (I-, F-)
PS COVE (I51s, F303s)
SB-W H (I34s, F849s)
Clear PS2 (I37s, F593s)
Clear PS4 (I107s, F667s)

(c)

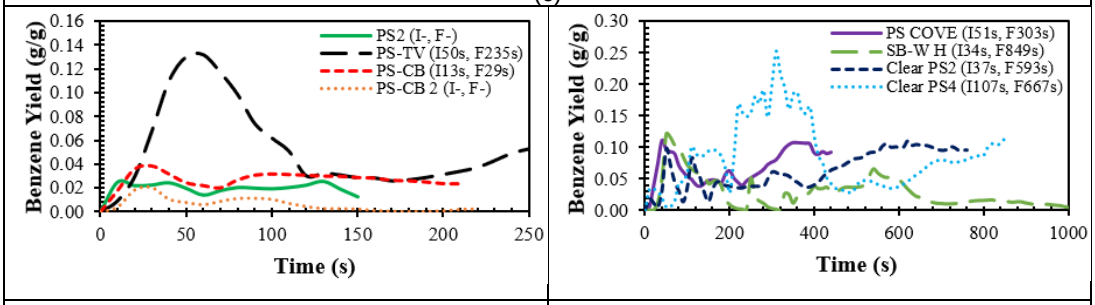
Benzene Yield (g/g)
Time (s)
PS2 (I-, F-)
PS-TV (I50s, F235s)
PS-CB (I13s, F29s)
PS-CB 2 (I-, F-)
PS COVE (I51s, F303s)
SB-W H (I34s, F849s)
Clear PS2 (I37s, F593s)
Clear PS4 (I107s, F667s)

(g) (h)

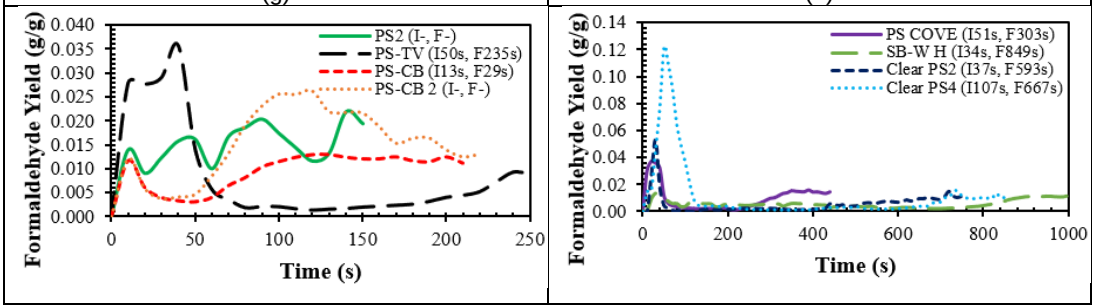
Formaldehyde Yield (g/g)
Time (s)
PS2 (I-, F-)
PS-TV (I50s, F235s)
PS-CB (I13s, F29s)
PS-CB 2 (I-, F-)
PS COVE (I51s, F303s)
SB-W H (I34s, F849s)
Clear PS2 (I37s, F593s)
Clear PS4 (I107s, F667s)

(d)

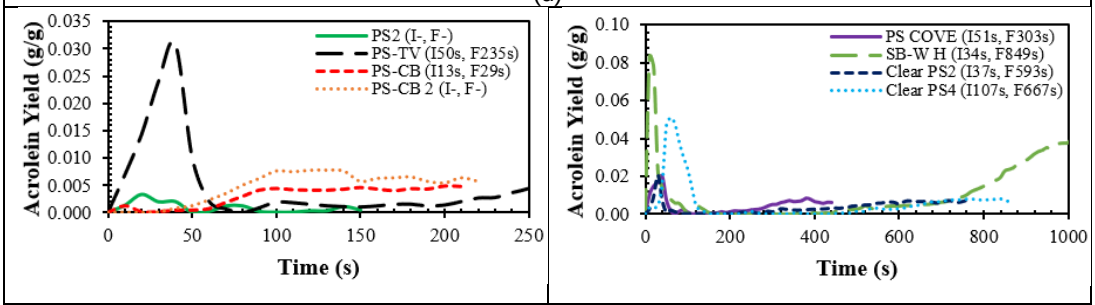
Acrolein Yield (g/g)
Time (s)
PS2 (I-, F-)
PS-TV (I50s, F235s)
PS-CB (I13s, F29s)
PS-CB 2 (I-, F-)
PS COVE (I51s, F303s)
SB-W H (I34s, F849s)
Clear PS2 (I37s, F593s)
Clear PS4 (I107s, F667s)

(e)

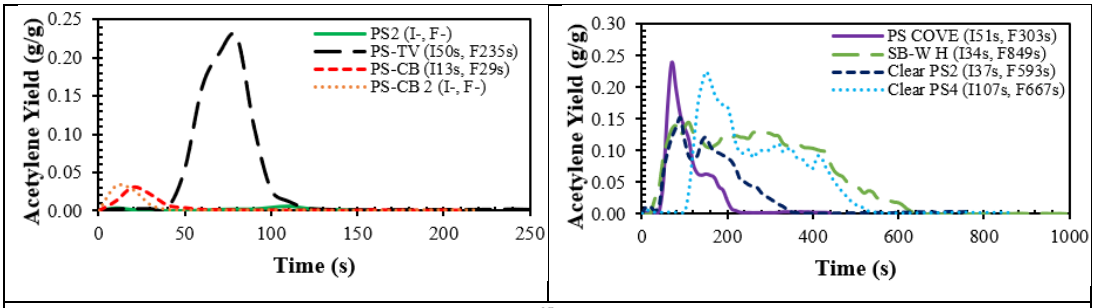
Acetylene Yield (g/g)
Time (s)
PS2 (I-, F-)
PS-TV (I50s, F235s)
PS-CB (I13s, F29s)
PS-CB 2 (I-, F-)
PS COVE (I51s, F303s)
SB-W H (I34s, F849s)
Clear PS2 (I37s, F593s)
Clear PS4 (I107s, F667s)

(f)

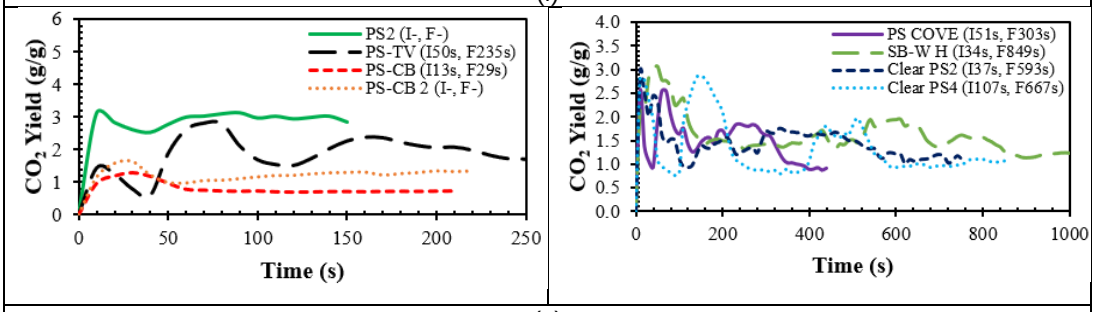
CO2 Yield (g/g)
Time (s)
PS2 (I-, F-)
PS-TV (I50s, F235s)
PS-CB (I13s, F29s)
PS-CB 2 (I-, F-)
PS COVE (I51s, F303s)
SB-W H (I34s, F849s)
Clear PS2 (I37s, F593s)
Clear PS4 (I107s, F667s)

(g)

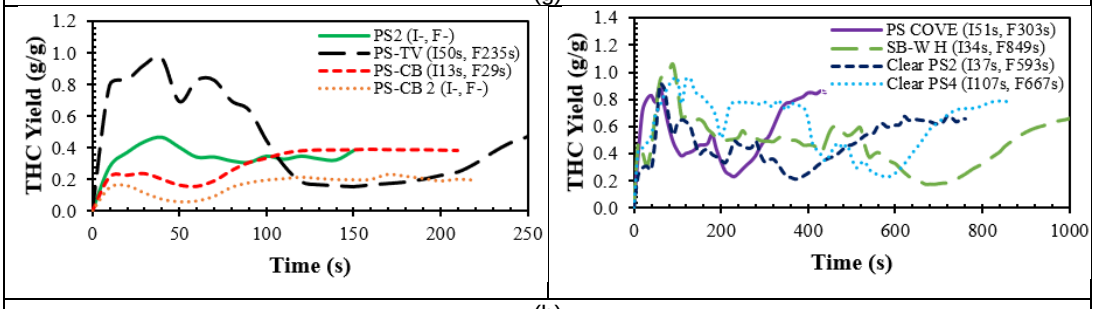
THC Yield (g/g)
Time (s)
PS2 (I-, F-)
PS-TV (I50s, F235s)
PS-CB (I13s, F29s)
PS-CB 2 (I-, F-)
PS COVE (I51s, F303s)
SB-W H (I34s, F849s)
Clear PS2 (I37s, F593s)
Clear PS4 (I107s, F667s)

(h)

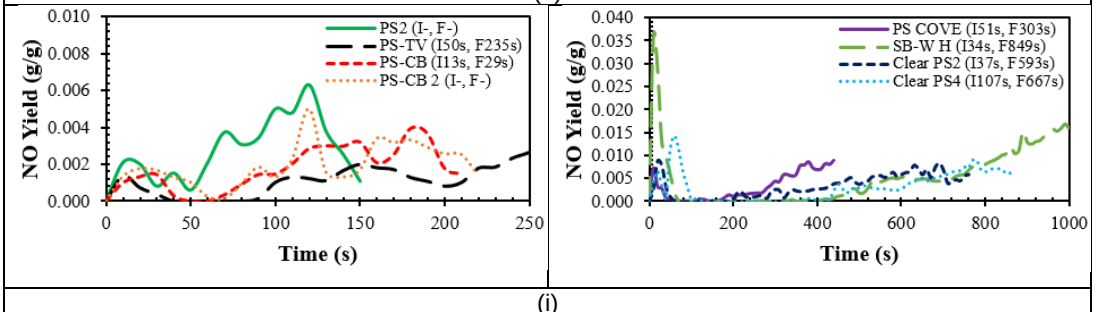
NO Yield (g/g)
Time (s)
PS2 (I-, F-)
PS-TV (I50s, F235s)
PS-CB (I13s, F29s)
PS-CB 2 (I-, F-)
PS COVE (I51s, F303s)
SB-W H (I34s, F849s)
Clear PS2 (I37s, F593s)
Clear PS4 (I107s, F667s)

(i)

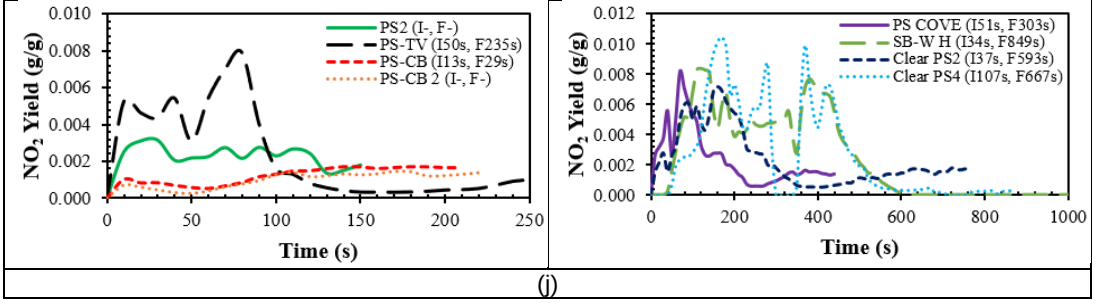
NO2 Yield (g/g)
Time (s)
PS2 (I-, F-)
PS-TV (I50s, F235s)
PS-CB (I13s, F29s)
PS-CB 2 (I-, F-)
PS COVE (I51s, F303s)
SB-W H (I34s, F849s)
Clear PS2 (I37s, F593s)
Clear PS4 (I107s, F667s)

(j)

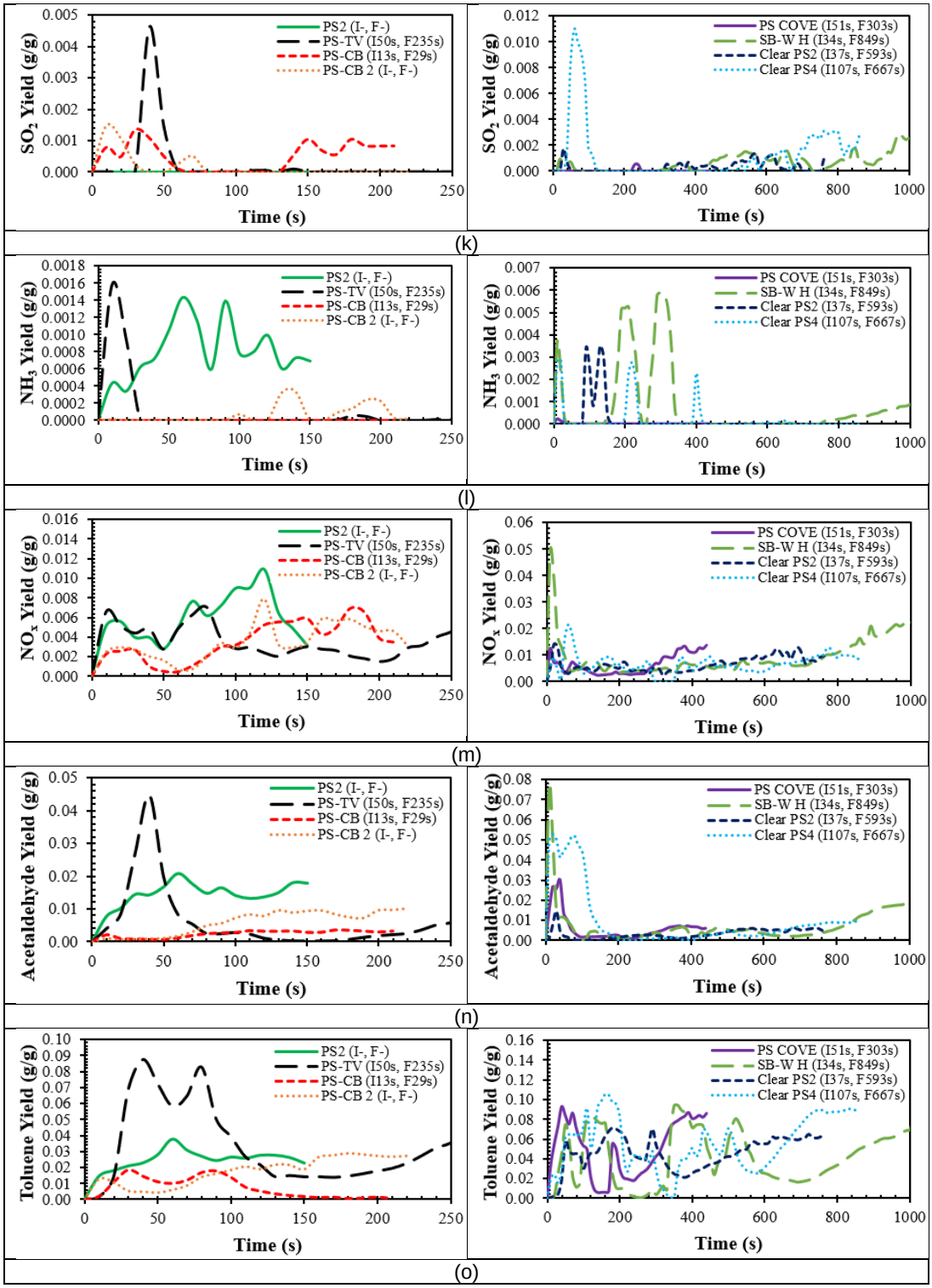


**Figure 7.7** Gas yields for Polystyrene fires at 35 kW/m$^2$ with free ventilation.

From the combustion efficiency (ŋ) graphs in Figure 7.8, for the Group 1 Polstyrene, PS-CB and PS-CB 2 fires had shown the highest percentage of 80% within 100 s of test time compared to PS2 and PS-TV fires. The Group 2

Polystyrene fires indicated efficiency rate <80%. Clear PS2 fire gave its highest peak of combustion efficiency at 600 s. Before 400 s, the combustion efficiency peak of Clear PS2 was about 40%. Meanwhile, PS2 fire had a peak of combustion efficiency of 60% at 70 s, PS-TV fire was shown a combustion efficiency peak of 30% at 50 s and Clear PS4 fire had its highest combustion efficiency peak of 80% at 600 s of test time. Based on personal understanding, these Polystyrenes were possibly produced by the manufacturer as less combustible polymers unlike the pure Polystyrene that had reduced the combustion rate and efficiency of the materials except the PS-CB and PS-CB 2 samples. Table 7.2 and Table 7.3 show the maximum yields and the mean yields of toxic species for various Polystyrene fires. CO cumulative mass for these polymer fire is illustrated in the graphs in Appendix E.

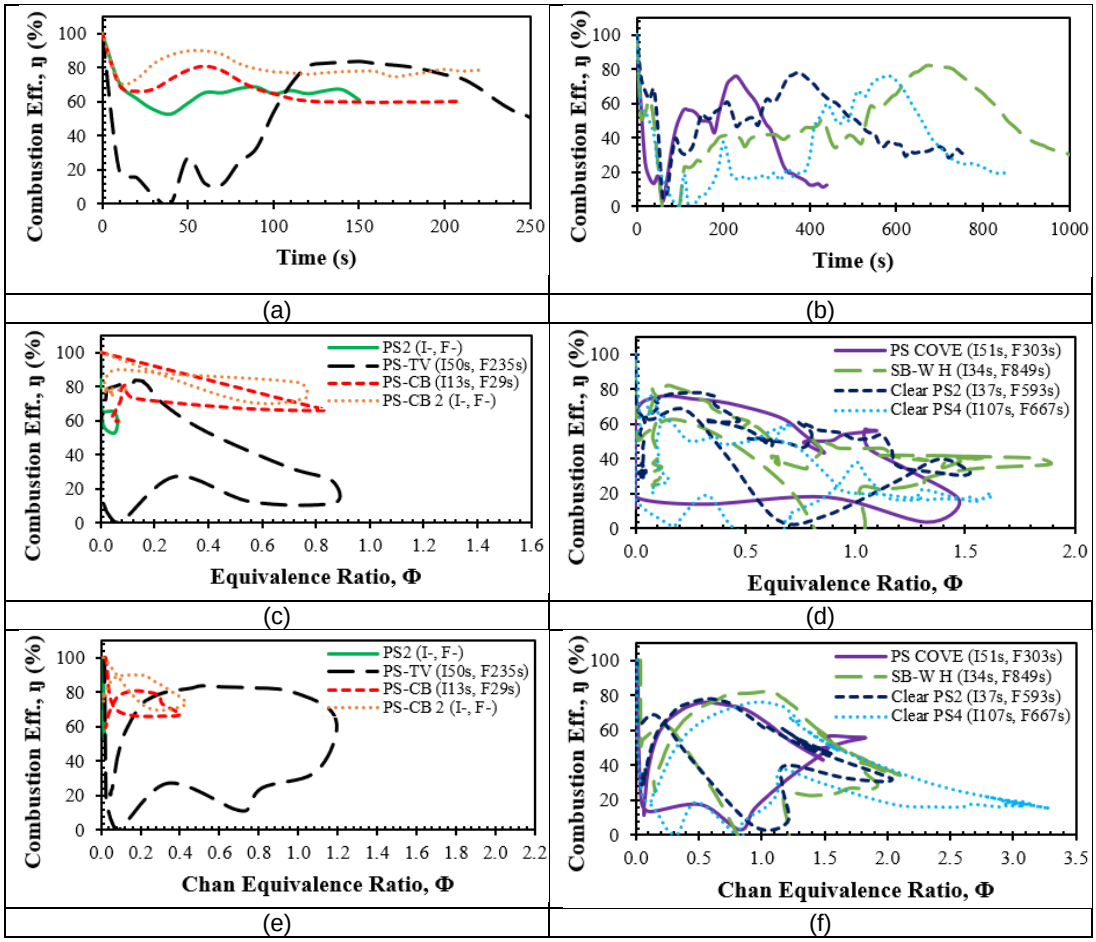


**Figure 7.8** Combustion efficiency, η for Polystyrene fires at 35 kW/m$^2$ with free ventilation.

**Table 7.2** Maximum gas yields for Polystyrene fires.

| Polymer Type | PS2 | PS-TV | PS-CB | PS-CB 2 | PS COVE | SB-W H | Clear PS2 | Clear PS4 |
|---|---|---|---|---|---|---|---|---|
| **Test Condition** | **35 FV** | | | | | | | |
| **Species** | **Maximum Yields (g/g)** | | | | | | | |
| CO | 0.0440 | 0.2481 | 0.2049 | 0.2485 | 0.3670 | 0.4299 | 0.2837 | 0.4752 |
| HCN | 0.0041 | 0.0080 | 0.0014 | 0.0016 | 0.0070 | 0.0063 | 0.0132 | 0.0084 |
| HCl | 0.0027 | 0.0015 | 0.0007 | 0.0014 | 0.0020 | 0.0074 | 0.0049 | 0.0048 |
| HF | 0.0024 | 0.0005 | 0.0003 | 0.0006 | 0.0005 | 0.0014 | 0.0007 | 0.0013 |
| Benzene | 0.0257 | 0.1314 | 0.0380 | 0.0204 | 0.1107 | 0.1214 | 0.1107 | 0.2529 |
| Formaldehyde | 0.0219 | 0.0358 | 0.0129 | 0.0262 | 0.0368 | 0.0129 | 0.0526 | 0.1213 |
| Acrolein | 0.0034 | 0.0308 | 0.0049 | 0.0078 | 0.0202 | 0.0833 | 0.0204 | 0.0507 |
| Acetylene | 0.0051 | 0.2281 | 0.0311 | 0.0330 | 0.2390 | 0.1449 | 0.1518 | 0.2244 |
| $CO_2$ | 3.1217 | 2.8094 | 1.2884 | 1.6484 | 2.5582 | 3.0661 | 2.9675 | 2.8696 |
| THC | 0.4691 | 0.9643 | 0.3908 | 0.2323 | 0.8947 | 1.0603 | 0.9082 | 0.9564 |
| NO | 0.0063 | 0.0053 | 0.0039 | 0.0050 | 0.0090 | 0.0359 | 0.0088 | 0.0143 |
| $NO_2$ | 0.0032 | 0.0079 | 0.0017 | 0.0014 | 0.0082 | 0.0084 | 0.0072 | 0.0105 |
| $SO_2$ | 0.0000 | 0.0046 | 0.0014 | 0.0015 | 0.0005 | 0.0029 | 0.0017 | 0.0110 |
| $NH_3$ | 0.0014 | 0.0016 | 0.0000 | 0.0003 | 0.0002 | 0.0059 | 0.0035 | 0.0029 |
| $NO_x$ | 0.0109 | 0.0088 | 0.0070 | 0.0079 | 0.0136 | 0.0494 | 0.0141 | 0.0215 |
| HBr | 0.0000 | 0.0000 | 0.0000 | 0.0000 | 0.0000 | 0.0000 | 0.0000 | 0.0000 |
| Acetaldehyde | 0.0208 | 0.0446 | 0.0036 | 0.0101 | 0.0299 | 0.0766 | 0.0147 | 0.0527 |
| Toluene | 0.0375 | 0.0876 | 0.0182 | 0.0287 | 0.0924 | 0.1260 | 0.0712 | 0.1060 |

**Table 7.3** Mean gas yields for Polystyrene fires.

| Polymer Type | PS2 | PS-TV | PS-CB | PS-CB 2 | PS COVE | SB-W H | Clear PS2 | Clear PS4 |
|---|---|---|---|---|---|---|---|---|
| **Test Condition** | **35 FV** | | | | | | | |
| **Initial Mass (g)** | 0.06 | 4.46 | 2.05 | 2.20 | 8.34 | 32.44 | 18.11 | 39.05 |
| **Total Mass Loss (g)** | 0.06 | 4.46 | 1.74 | 1.70 | 8.34 | 32.03 | 16.55 | 34.58 |
| **Total Time (s)** | 70 | 230 | 210 | 220 | 250 | 1050 | 760 | 860 |
| **Mean ER, Φ** | 0.01 | 0.49 | 0.10 | 0.09 | 0.97 | 1.11 | 0.61 | 1.14 |
| **Species** | **Mean Yields (g/g)** | | | | | | | |
| CO | 0.0217 | 0.1563 | 0.1285 | 0.1404 | 0.1898 | 0.2987 | 0.1947 | 0.2489 |
| HCN | 0.0008 | 0.0046 | 0.0009 | 0.0008 | 0.0043 | 0.0029 | 0.0030 | 0.0037 |
| HCl | -0.0018 | 0.0001 | -0.0002 | -0.0002 | 0.0003 | 0.0031 | 0.0012 | 0.0012 |
| HF | 0.0005 | 0.0002 | 0.0000 | 0.0001 | 0.0002 | 0.0001 | 0.0001 | 0.0000 |
| Benzene | 0.0197 | 0.0850 | 0.0287 | 0.0122 | 0.0610 | 0.0328 | 0.0453 | 0.1332 |
| Formaldehyde | 0.0141 | 0.0040 | 0.0082 | 0.0085 | 0.0038 | 0.0045 | 0.0020 | 0.0032 |
| Acrolein | 0.0009 | 0.0021 | 0.0015 | 0.0015 | 0.0015 | 0.0028 | 0.0008 | 0.0012 |
| Acetylene | 0.0003 | 0.1156 | 0.0148 | 0.0149 | 0.1011 | 0.0962 | 0.0783 | 0.0978 |
| $CO_2$ | 2.7589 | 2.2852 | 1.0055 | 1.4038 | 1.7592 | 1.6212 | 1.3748 | 1.2954 |
| THC | 0.4056 | 0.5908 | 0.2558 | 0.1427 | 0.5302 | 0.5453 | 0.4944 | 0.7018 |
| NO | 0.0014 | 0.0005 | 0.0014 | 0.0017 | 0.0003 | 0.0015 | 0.0009 | 0.0008 |
| $NO_2$ | 0.0023 | 0.0043 | 0.0010 | 0.0007 | 0.0041 | 0.0044 | 0.0043 | 0.0045 |
| $SO_2$ | 0.0000 | 0.0002 | 0.0007 | 0.0006 | 0.0000 | 0.0003 | 0.0001 | 0.0002 |
| $NH_3$ | 0.0010 | 0.0000 | 0.0000 | 0.0000 | 0.0000 | 0.0014 | 0.0008 | 0.0003 |
| $NO_x$ | 0.0041 | 0.0045 | 0.0029 | 0.0029 | 0.0041 | 0.0060 | 0.0050 | 0.0051 |
| HBr | 0.0000 | 0.0000 | 0.0000 | 0.0000 | 0.0000 | 0.0000 | 0.0000 | 0.0000 |
| Acetaldehyde | 0.0169 | 0.0050 | 0.0017 | 0.0024 | 0.0042 | 0.0040 | 0.0012 | 0.0027 |
| Toluene | 0.0283 | 0.0526 | 0.0087 | 0.0115 | 0.0447 | 0.0406 | 0.0478 | 0.0464 |

### 7.2.3 Total Toxicity for Polystyrene Fires at 35 kW/m$^2$ with Free Ventilation

The Fractional Effective Concentration (FEC) method of toxicity analysis was used with each of the 60 toxic gases measured divided by the toxic limit to give an N factor and the N for each species was summated to give the total toxic hazard, as shown in Figure 7.9, Figure 7.10 and Figure 7.11 for $LC50_{30min}$, $COSHH_{15min}$ and $AEGL\text{-}2_{10min}$ impairment of escape toxic assessments. All three methods of toxic gas assessment showed very high toxicity for most forms of the tested Polystyrenes with PS2 fire showed the lowest toxicity level compared to other tested Polymers. According to LC50 based total toxicity in Figure 7.9, PS2, PS-CB and PS-CB 2 fires gave the total toxicity value less than 1. But, for other two toxic assessments ($COSHH_{15min}$ and AEGL-2) the effect of impairment to escape was significant.

Total toxicity was extremely high on an LC50 and impairment of escape $COSHH_{15min}$ and AEGL-2 basis. Solid skirting board (SB-W H) and glass like Clear PS2 and Clear PS4 took longer to burn and had the highest toxicity. PS COVE fire had the similar value of total toxicity peak with the Clear PS2 fire giving total toxicities about 10 for LC50, about 2000 for $COSHH_{15min}$ and about 200 for AEGL-2 basis of toxic assessment methods.

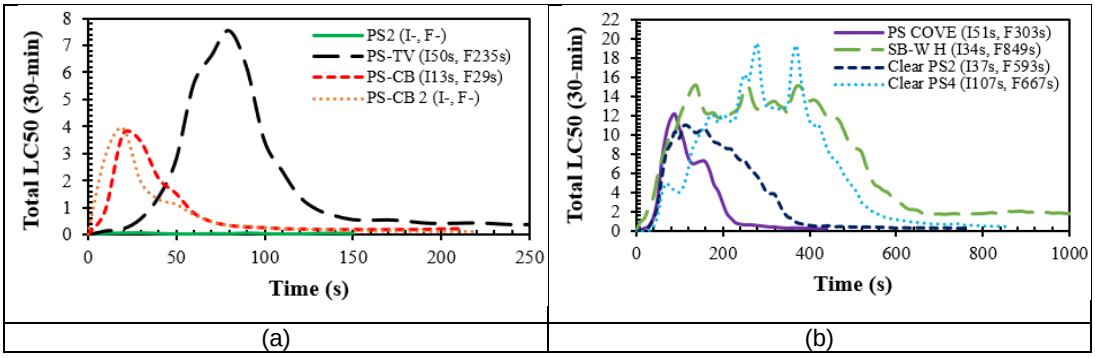


(a) (b)

**Figure 7.9** Total toxicity LC50 for Polystyrene fires at 35 kW/m$^2$ with free ventilation.

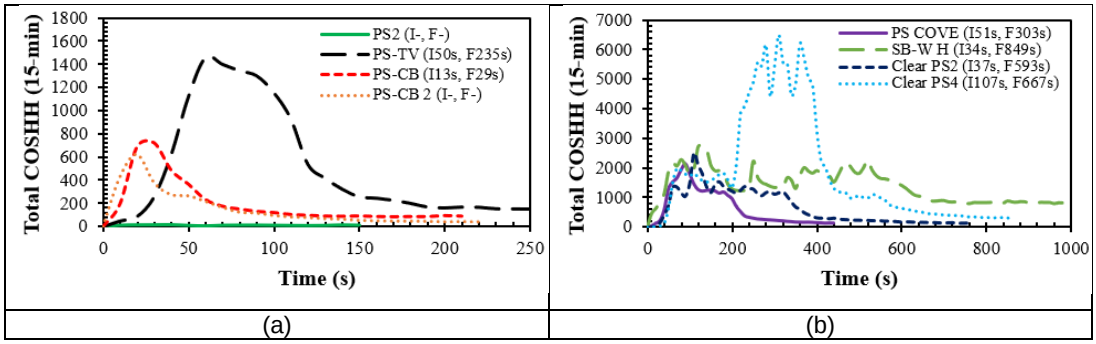


**Figure 7.10** Total toxicity $COSHH_{15min}$ for Polystyrene fires at 35 kW/m$^2$ with free ventilation.

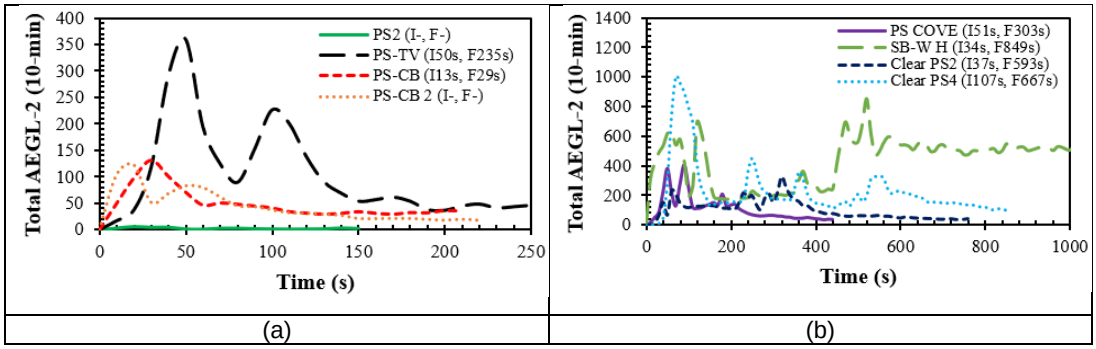


**Figure 7.11** Total toxicity AEGL-2 for Polystyrene fires at 35 kW/m$^2$ with free ventilation.

### 7.2.4 Major Gases Contribution for Polystyrene Fires at 35 kW/m$^2$ with Free Ventilation

As shown in Figure 7.12, for LC50 toxic assessment method, the major species that contributed to the high toxicity were CO, HCN, Formaldehyde, Acrolein and $NO_2$. CO contribution was about 10% for the low density polymer fire like PS2 and the contribution had seen to be around 40% in average for the other Polystyrene fires. Other Asphyxiant such as HCN, its contribution was also clearly indicated and realised. Polystyrene was a synthetic aromatic hydrocarbon polymer with a chemical formula of $(C_8H_8)_n$. The existence of major species like HCN and $NO_2$ in these Polystyrene fires were already mentioned in the previous chapters and it could be due to the Nitrogen addition into these polymer compound during the manufacturing process.

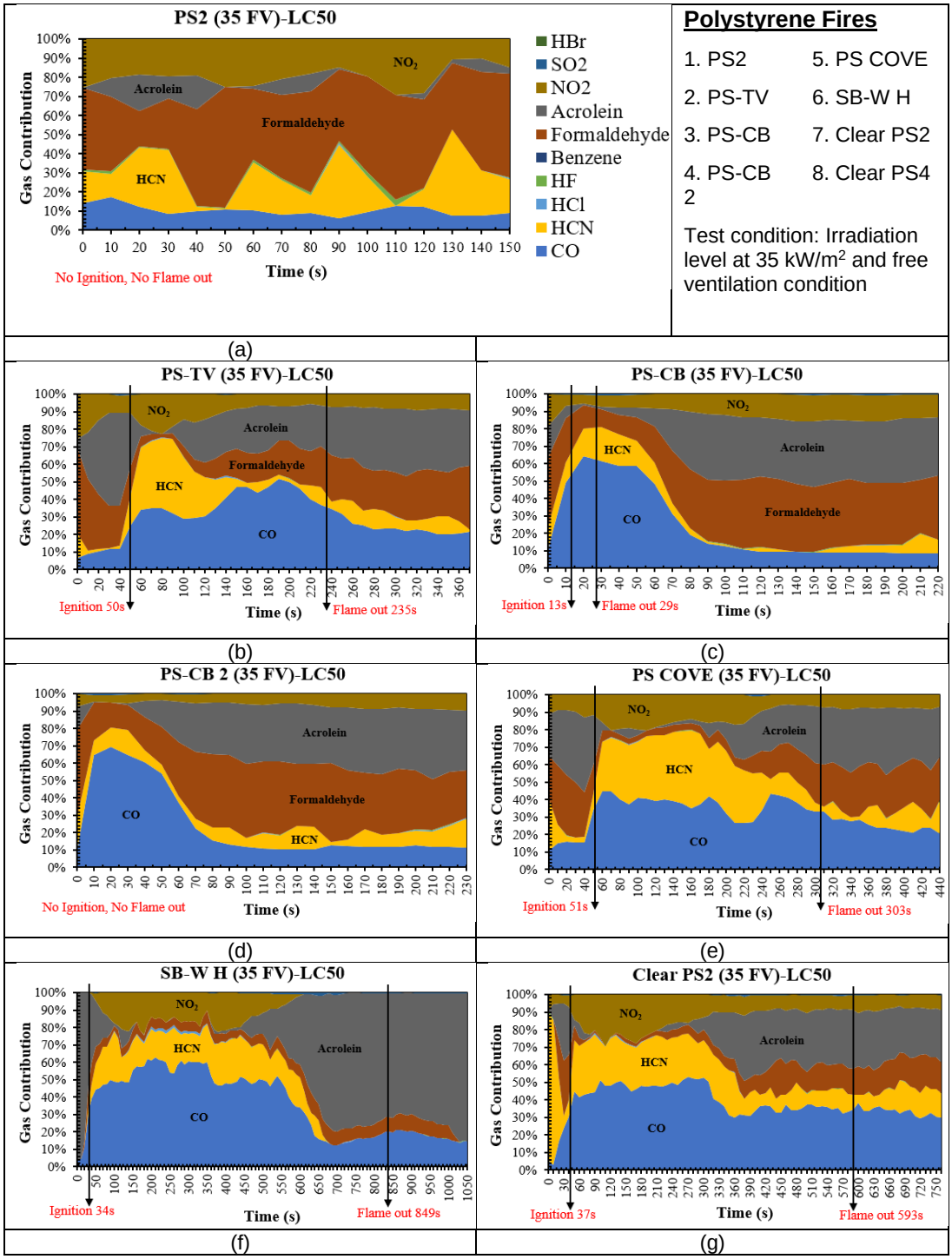
PS2 (35 FV)-LC50
Gas Contribution
Time (s)
No Ignition, No Flame out
HBr
SO2
NO2
Acrolein
Formaldehyde
Benzene
HF
HCl
HCN
CO
Polystyrene Fires
1. PS2
2. PS-TV
3. PS-CB
4. PS-CB 2
5. PS COVE
6. SB-W H
7. Clear PS2
8. Clear PS4 2
Test condition: Irradiation level at 35 kW/m2 and free ventilation condition
(a)
PS-TV (35 FV)-LC50
Ignition 50s
Flame out 235s
(b)
PS-CB (35 FV)-LC50
Ignition 13s
Flame out 29s
(c)
PS-CB 2 (35 FV)-LC50
No Ignition, No Flame out
(d)
PS COVE (35 FV)-LC50
Ignition 51s
Flame out 303s
(e)
SB-W H (35 FV)-LC50
Ignition 34s
Flame out 849s
(f)
Clear PS2 (35 FV)-LC50
Ignition 37s
Flame out 593s
(g)

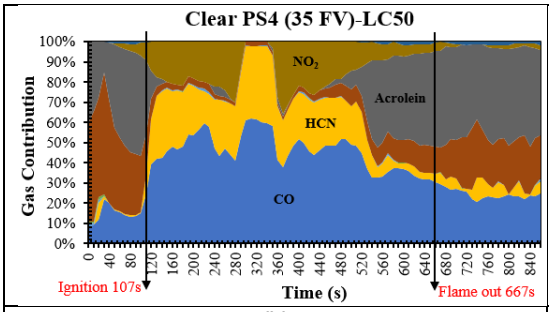


LC50 (30-minutes)

(h)

**Figure 7.12** Contribution of major gases (based $LC50_{30min}$) for Polystyrene fires at 35 kW/m$^2$ with free ventilation.

For $COSHH_{15min}$ based of assessment in Figure 7.13, as expected, Benzene's percentage contribution was really high for most of the conducted Polystyrene fires. Styrene is the derivative of Benzene which used to form Polystyrene, that is why it would release Benzene when burned. CO, Formaldehyde and Acrolein were the common major species as usual for most of hydrocarbon fires. Under this $COSHH_{15min}$ basis, PS2, Clear PS2 and Clear PS4 fires indicated that HF had also contributed to the total toxicity even at a low contribution level. Unlike other Polystyrene fires, SB-W H and Clear PS4 fires had shown that HCl was also the major species that contributing to the overall total toxicity on $COSHH_{15min}$ basis.

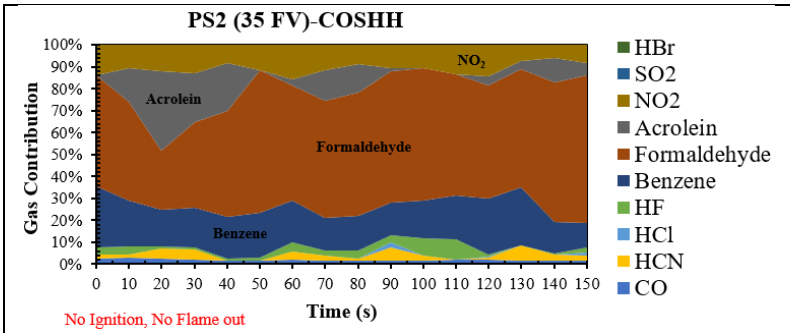


**Polystyrene Fires**

1. PS2
2. PS-TV
3. PS-CB
4. PS-CB 2
5. PS COVE
6. SB-W H
7. Clear PS2
8. Clear PS4

Test condition: Irradiation level at 35 kW/m$^2$ and free ventilation condition

(a)

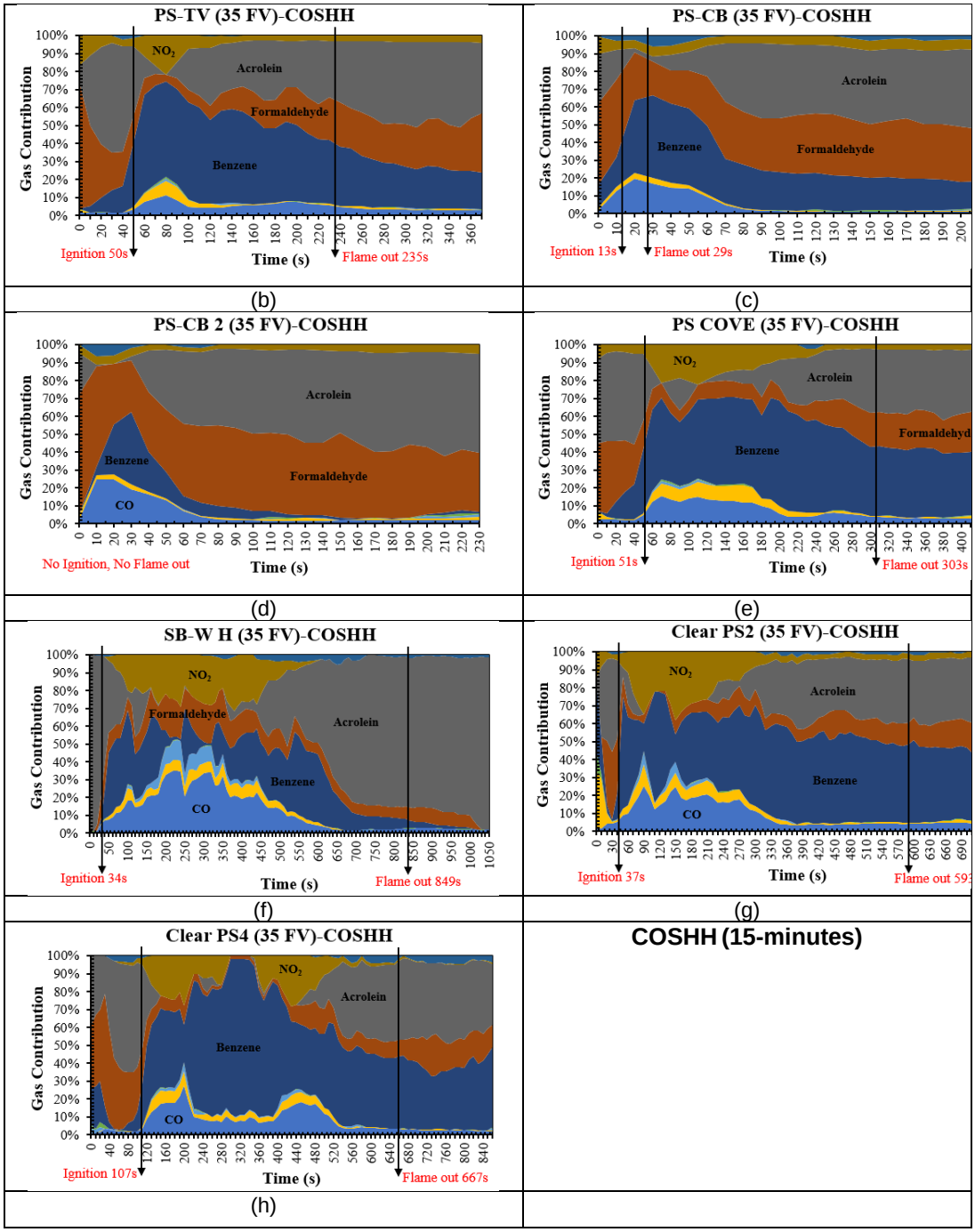


**Figure 7.13** Contribution of major gases (based $COSHH_{15min}$) for Polystyrene fires at 35 kW/m$^2$ with free ventilation.

Figure 7.14 showed the major gas contribution based on AEGL-2 toxic assessment method for Polystyrene fires at 35 kW/m$_2$ of irradiation level and free ventilation conditions. Under this AEGL-2 assessment, the main species were maintained the same as the COSHH15min assessment but only the percentage contribution of each species was different. For AEGL-2 basis,

Acrolein seemed to be the first major toxic species in Polystyrene fires than the other common species like CO, HCN and Formaldehyde. Benzene contribution had not been realised so much in Figure 7.14 due to a very high limit concentration value of Benzene (2000 ppm) for AEGL-2 basis compared to COSHH15min basis which only 3 ppm. $SO_2$ also one of the major species that indicated in Figure 7.14 for most of Polystyrene fires except for PS2 and PS COVE fires. Variation in every Polystyrene compound had given a variation in the profiles for major gas contribution graphs. It proved that synthetic Polystyrenes produced nowadays were chemically complex and much different from the pure Polystyrenes due to added additives into the original compound and this could contribute to more severe total fire toxicity. Six major species for various Polystyrene fires are summarised in Table 7.4 following the order for each fire stage from the point before ignition, during the steady state flaming and flaming conditions and also during post-flaming.

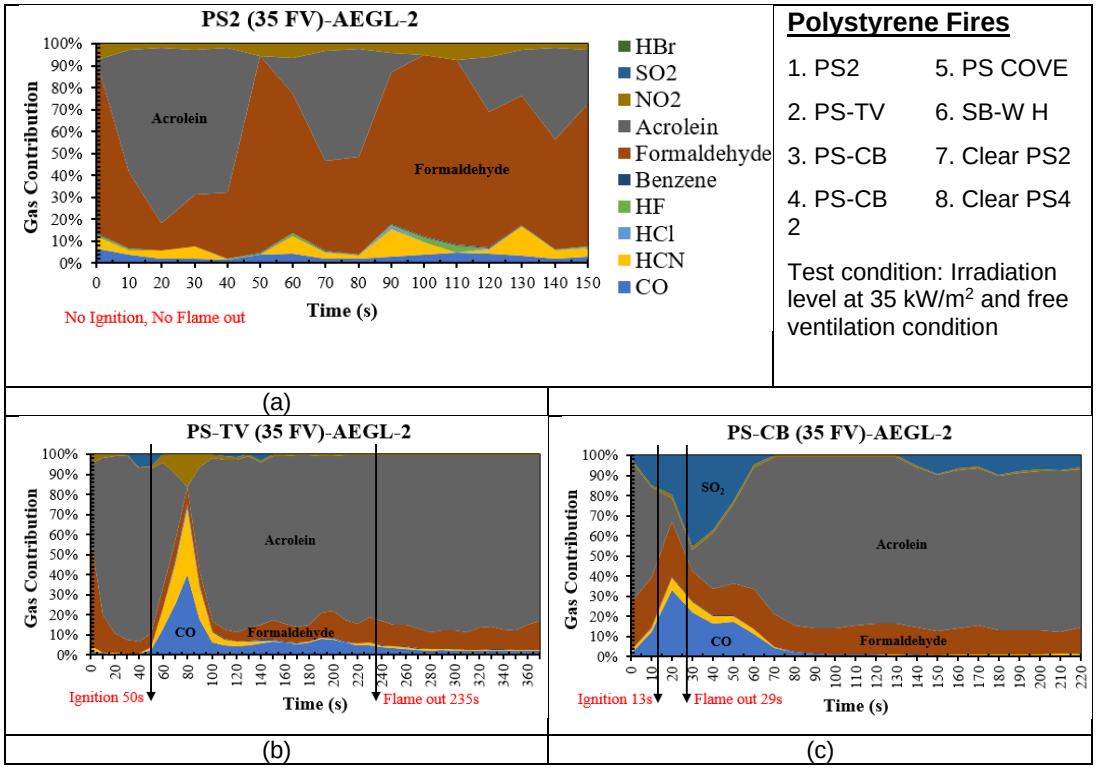

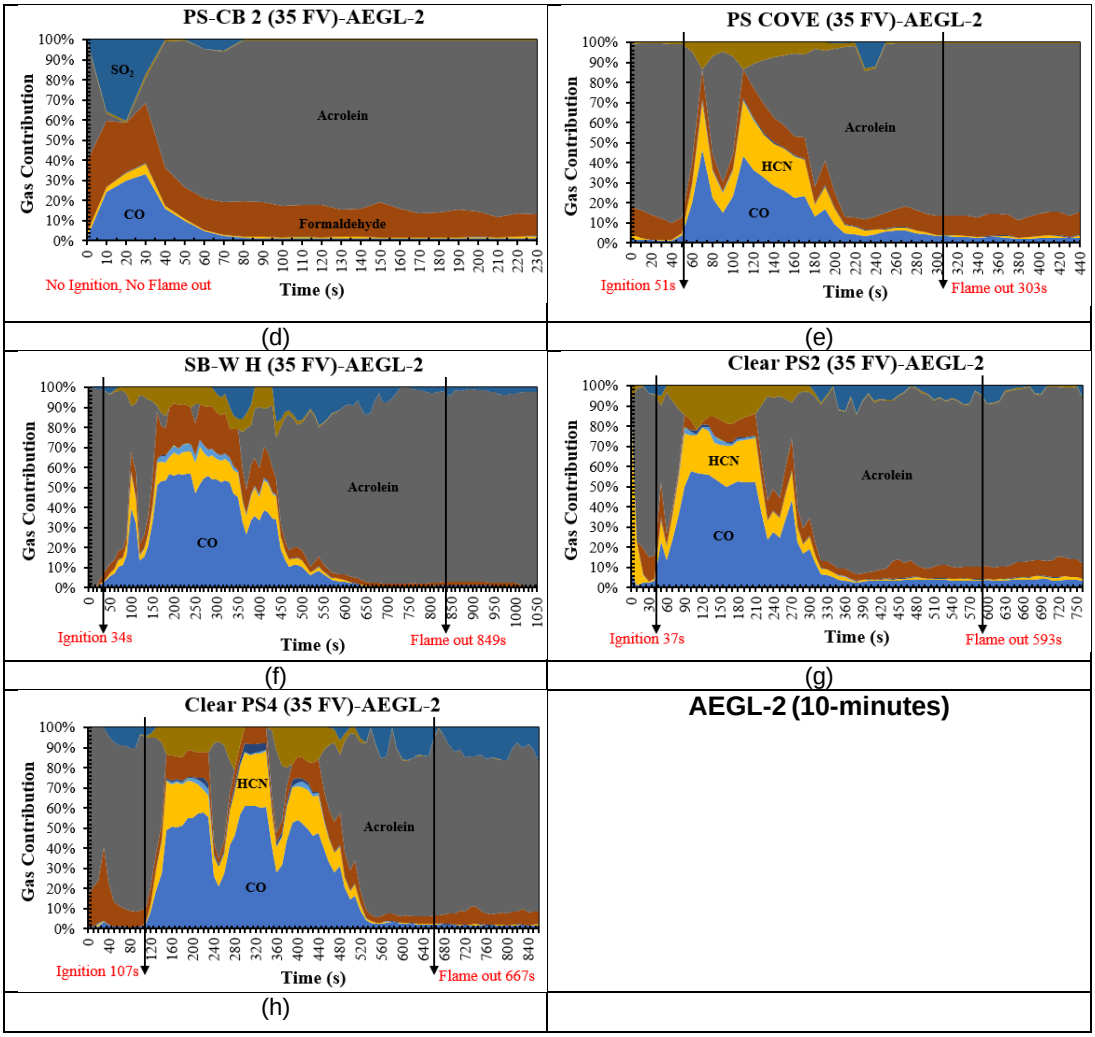


**Figure 7.14** Contribution of major gases (based AEGL-$2_{10min}$) for Polystyrene fires at 35 kW/m$^2$ with free ventilation.

**Table 7.4** First six major species for various Polystyrene fires.

| POLYSTYRENE FIRES | | | | | | | | | | | |
|---|---|---|---|---|---|---|---|---|---|---|---|
| **Test** | **Test Details** | **Mean ER, Φ (Chan)** | **Time (s)** | **Fire Stage** | **TT** | **Major Species** | | | | | |
| | | | | | | **1** | **2** | **3** | **4** | **5** | **6** |
| 1 | PS2 | 0.012 | <20 | - | **LC50** | Formaldehyde | $NO_2$ | HCN | CO | Acrolein | HF |
| | 35 FV | 0.014 (peak) | 20 - 120 | SS | | Formaldehyde | $NO_2$ | HCN | CO | Acrolein | HF |
| | I = No | 0.012 | >120 | - | | Formaldehyde | HCN | $NO_2$ | CO | Acrolein | HF |
| | F = No | 0.012 | <20 | - | **COSHH** | Formaldehyde | Benzene | Acrolein | $NO_2$ | HF | HCN |
| | | 0.014 (peak) | 20 - 120 | SS | | Formaldehyde | Benzene | $NO_2$ | Acrolein | HF | HCN |
| | | 0.012 | >120 | - | | Formaldehyde | Benzene | $NO_2$ | Acrolein | HCN | HF |
| | | 0.012 | <20 | - | **AEGL-2** | Acrolein | Formaldehyde | HCN | $NO_2$ | CO | HF |
| | | 0.014 (peak) | 20 - 120 | SS | | Formaldehyde | Acrolein | HCN | $NO_2$ | CO | HF |
| | | 0.012 | >120 | - | | Formaldehyde | Acrolein | HCN | $NO_2$ | CO | HF |
| 2 | PS-TV | 0.3 | <50 | Ignition | **LC50** | Acrolein | Formaldehyde | $NO_2$ | CO | HCN | - |
| | 35 FV | 1.2 (peak) | 50 - 110 | Flaming 1 | | HCN | CO | $NO_2$ | Acrolein | Formaldehyde | HCl |
| | I = 50 s | 0.6 | 110 - 235 | SS Flaming 2 | | CO | Acrolein | Formaldehyde | $NO_2$ | HCN | HCl |
| | F = 235 s | 0.1 | >235 | Post-flaming | | Acrolein | Formaldehyde | CO | HCN | $NO_2$ | - |
| | | 0.3 | <50 | Ignition | **COSHH** | Acrolein | Formaldehyde | Benzene | $NO_2$ | CO | HCN |
| | | 1.2 (peak) | 50 - 110 | Flaming 1 | | Benzene | Acrolein | $NO_2$ | Formaldehyde | CO | HCN |
| | | 0.6 | 110 - 235 | SS Flaming 2 | | Benzene | Acrolein | Formaldehyde | CO | $NO_2$ | HCN |
| | | 0.1 | >235 | Post-flaming | | Acrolein | Benzene | Formaldehyde | $NO_2$ | CO | HCN |
| | | 0.3 | <50 | Ignition | **AEGL-2** | Acrolein | Formaldehyde | $SO_2$ | $NO_2$ | CO | HCN |
| | | 1.2 (peak) | 50 - 110 | Flaming 1 | | Acrolein | CO | HCN | Formaldehyde | $NO_2$ | $SO_2$ |
| | | 0.6 | 110 - 235 | SS Flaming 2 | | Acrolein | Formaldehyde | CO | HCN | $NO_2$ | $SO_2$ |
| | | 0.1 | >235 | Post-flaming | | Acrolein | Formaldehyde | CO | HCN | $NO_2$ | - |

| | | | | | | | | | | | |
|---|---|---|---|---|---|---|---|---|---|---|---|
| 3 | PS-CB | 0.10 | <13 | Ignition | **LC50** | CO | Formaldehyde | HCN | Acrolein | $NO_2$ | $SO_2$ |
| | 35 FV | 0.40 (peak) | 13 - 29 | Flaming | | CO | HCN | Formaldehyde | $NO_2$ | Acrolein | $SO_2$ |
| | I = 13 s | 0.18 | 29 - 90 | Post-flaming | | CO | Formaldehyde | Acrolein | HCN | $NO_2$ | $SO_2$ |
| | F = 29 s | 0.04 | >90 | SS Post-flaming | | Formaldehyde | Acrolein | $NO_2$ | CO | HCN | $SO_2$ |
| | | 0.10 | <13 | Ignition | **COSHH** | Formaldehyde | Benzene | Acrolein | CO | $NO_2$ | $SO_2$ |
| | | 0.40 (peak) | 13 - 29 | Flaming | | Benzene | Formaldehyde | CO | $NO_2$ | Acrolein | $SO_2$ |
| | | 0.18 | 29 - 90 | Post-flaming | | Benzene | Formaldehyde | Acrolein | CO | $NO_2$ | $SO_2$ |
| | | 0.04 | >90 | SS Post-flaming | | Acrolein | Formaldehyde | Benzene | $NO_2$ | $SO_2$ | CO |
| | | 0.10 | <13 | Ignition | **AEGL-2** | Acrolein | Formaldehyde | $SO_2$ | CO | HCN | $NO_2$ |
| | | 0.40 (peak) | 13 - 29 | Flaming | | CO | Formaldehyde | $SO_2$ | Acrolein | HCN | $NO_2$ |
| | | 0.18 | 29 - 90 | Post-flaming | | Acrolein | Formaldehyde | $SO_2$ | CO | HCN | $NO_2$ |
| | | 0.04 | >90 | SS Post-flaming | | Acrolein | Formaldehyde | $SO_2$ | $NO_2$ | - | - |
| 4 | PS-CB 2 | 0.20 | <10 | - | **LC50** | CO | Formaldehyde | HCN | $NO_2$ | Acrolein | $SO_2$ |
| | 35 FV | 0.45 (peak) | 10 - 100 | - | | CO | Formaldehyde | Acrolein | HCN | $NO_2$ | $SO_2$ |
| | I = No | 0.02 | >100 | SS | | Formaldehyde | Acrolein | CO | HCN | $NO_2$ | - |
| | F = No | 0.20 | <10 | - | **COSHH** | Formaldehyde | CO | Acrolein | $NO_2$ | $SO_2$ | HCN |
| | | 0.45 (peak) | 10 - 100 | - | | Formaldehyde | Acrolein | Benzene | CO | $NO_2$ | $SO_2$ |
| | | 0.02 | >100 | SS | | Acrolein | Formaldehyde | $NO_2$ | CO | Benzene | HCN |
| | | 0.20 | <10 | - | **AEGL-2** | Formaldehyde | Acrolein | $SO_2$ | CO | HCN | - |
| | | 0.45 (peak) | 10 - 100 | - | | Acrolein | Formaldehyde | CO | $SO_2$ | HCN | - |
| | | 0.02 | >100 | SS | | Acrolein | Formaldehyde | HCN | CO | - | - |
| 5 | PS COVE | 0.8 | <51 | Ignition | **LC50** | Acrolein | Formaldehyde | CO | $NO_2$ | HCN | - |
| | 35 FV | 1.8 (peak) | 51 - 250 | Flaming 1 | | CO | HCN | $NO_2$ | Acrolein | Formaldehyde | - |
| | I = 51 s | 0.3 | 250 - 303 | Flaming 2 | | CO | Acrolein | Formaldehyde | HCN | $NO_2$ | - |
| | F = 303 s | 0.1 | >303 | Post-flaming | | Acrolein | Formaldehyde | CO | HCN | $NO_2$ | - |

| | | | | | | | | | | | | |
|---|---|---|---|---|---|---|---|---|---|---|---|---|
| | | 0.8 | <51 | Ignition | **COSHH** | Acrolein | Formaldehyde | Benzene | $NO_2$ | CO | HCN |
| | | 1.8 (peak) | 51 - 250 | Flaming 1 | | Benzene | $NO_2$ | Acrolein | CO | Formaldehyde | HCN |
| | | 0.3 | 250 - 303 | Flaming 2 | | Benzene | Acrolein | Formaldehyde | CO | $NO_2$ | HCN |
| | | 0.1 | >303 | Post-flaming | | Benzene | Acrolein | Formaldehyde | $NO_2$ | CO | HCN |
| | | 0.8 | <51 | Ignition | **AEGL-2** | Acrolein | Formaldehyde | CO | $NO_2$ | HCN | - |
| | | 1.8 (peak) | 51 - 250 | Flaming 1 | | Acrolein | CO | HCN | Formaldehyde | $NO_2$ | $SO_2$ |
| | | 0.3 | 250 - 303 | Flaming 2 | | Acrolein | Formaldehyde | CO | HCN | $NO_2$ | - |
| | | 0.1 | >303 | Post-flaming | | Acrolein | Formaldehyde | CO | HCN | $NO_2$ | - |
| 6 | SB-W H | 0.3 | <34 | Ignition | **LC50** | Formaldehyde | CO | HCN | Formaldehyde | - | - |
| | 35 FV | 1.6 (max. 2.0) | 34 - 700 | Flaming 1 | | CO | HCN | Acrolein | $NO_2$ | Formaldehyde | HCl |
| | I = 34 s | 0.7 | 700 - 849 | Flaming 2 | | Acrolein | CO | Formaldehyde | $SO_2$ | - | - |
| | F = 849 s | 0.2 | >849 | Post-flaming | | Acrolein | CO | Formaldehyde | - | - | - |
| | | 0.3 | <34 | Ignition | **COSHH** | Acrolein | Formaldehyde | CO | Benzene | - | - |
| | | 1.6 (max. 2.0) | 34 - 700 | Flaming 1 | | Acrolein | CO | Benzene | Formaldehyde | $NO_2$ | HCl |
| | | 0.7 | 700 - 849 | Flaming 2 | | Acrolein | Benzene | Formaldehyde | $SO_2$ | CO | - |
| | | 0.2 | >849 | Post-flaming | | Acrolein | Formaldehyde | Benzene | CO | $SO_2$ | - |
| | | 0.3 | <34 | Ignition | **AEGL-2** | Acrolein | Formaldehyde | $SO_2$ | CO | - | - |
| | | 1.6 (max. 2.0) | 34 - 700 | Flaming 1 | | Acrolein | CO | Formaldehyde | HCN | $SO_2$ | $NO_2$ |
| | | 0.7 | 700 - 849 | Flaming 2 | | Acrolein | $SO_2$ | Formaldehyde | CO | - | - |
| | | 0.2 | >849 | Post-flaming | | Acrolein | $SO_2$ | Formaldehyde | CO | - | - |
| 7 | Clear PS2 | 0.1 | <37 | Ignition | **LC50** | HCN | Formaldehyde | Acrolein | CO | $NO_2$ | - |
| | 35 FV | 1.4 (max 2.0) | 37 - 380 | Flaming 1 | | CO | HCN | $NO_2$ | Acrolein | Formaldehyde | HCl |
| | I = 37 s | 0.4 | 380 - 593 | Flaming 2 | | CO | Acrolein | Formaldehyde | HCN | $NO_2$ | - |
| | F = 593 s | 0.1 | >593 | Post-flaming | | CO | Acrolein | Formaldehyde | HCN | $NO_2$ | - |

| | | | | | | | | | | | |
|---|---|---|---|---|---|---|---|---|---|---|---|
| | | 0.1 | <37 | Ignition | **COSHH** | Acrolein | Formaldehyde | HCN | Benzene | $NO_2$ | CO |
| | | 1.4 (max 2.0) | 37 - 380 | Flaming 1 | | Benzene | $NO_2$ | CO | Acrolein | Formaldehyde | HCN |
| | | 0.4 | 380 - 593 | Flaming 2 | | Benzene | Acrolein | Formaldehyde | CO | $NO_2$ | $SO_2$ |
| | | 0.1 | >593 | Post-flaming | | Benzene | Acrolein | Formaldehyde | CO | $NO_2$ | HCN |
| | | 0.1 | <37 | Ignition | **AEGL-2** | Acrolein | HCN | Formaldehyde | CO | $NO_2$ | $SO_2$ |
| | | 1.4 (max 2.0) | 37 - 380 | Flaming 1 | | Acrolein | CO | HCN | $NO_2$ | Formaldehyde | $SO_2$ |
| | | 0.4 | 380 - 593 | Flaming 2 | | Acrolein | $SO_2$ | Formaldehyde | CO | HCN | - |
| | | 0.1 | >593 | Post-flaming | | Acrolein | Formaldehyde | CO | $SO_2$ | HCN | - |
| 8 | Clear PS4 | 0.4 | <107 | Ignition | **LC50** | Formaldehyde | Acrolein | CO | HCN | $NO_2$ | $SO_2$ |
| | 35 FV | 2.3 (max. 3.3) | 107 - 550 | Flaming 1 | | CO | HCN | $NO_2$ | Acrolein | Formaldehyde | HCl |
| | I = 107 s | 0.8 | 550 - 667 | Flaming 2 | | Acrolein | CO | Formaldehyde | HCN | $NO_2$ | $SO_2$ |
| | F = 667 s | 0.2 | >667 | Post-flaming | | Acrolein | CO | Formaldehyde | HCN | $NO_2$ | $SO_2$ |
| | | 0.4 | <107 | Ignition | **COSHH** | Acrolein | Formaldehyde | Benzene | $SO_2$ | CO | HCl |
| | | 2.3 (max. 3.3) | 107 - 550 | Flaming 1 | | Benzene | $NO_2$ | CO | Acrolein | Formaldehyde | HCN |
| | | 0.8 | 550 - 667 | Flaming 2 | | Benzene | Acrolein | Formaldehyde | CO | $SO_2$ | $NO_2$ |
| | | 0.2 | >667 | Post-flaming | | Acrolein | Benzene | Formaldehyde | $SO_2$ | CO | $NO_2$ |
| | | 0.4 | <107 | Ignition | **AEGL-2** | Acrolein | Formaldehyde | $SO_2$ | CO | - | - |
| | | 2.3 (max. 3.3) | 107 - 550 | Flaming 1 | | CO | Acrolein | HCN | $NO_2$ | Formaldehyde | $SO_2$ |
| | | 0.8 | 550 - 667 | Flaming 2 | | Acrolein | $SO_2$ | Formaldehyde | CO | HCN | - |
| | | 0.2 | >667 | Post-flaming | | Acrolein | $SO_2$ | Formaldehyde | CO | HCN | - |

## 7.3 Findings and Conclusion from Polystyrene Fire Tests

Pure Polystyrene is a synthetic aromatic hydrocarbon compound which containing Carbon and Hydrogen elements. This polymer has a high burning rate such as other natural hydrocarbon types. With addition of some additives to the pure Polystyrene, it was believed that it had changed its physical properties and the process had contributed to many variations of Polystyrene based products nowadays. These version of Polystyrenes would produce many toxic gases when burned in fire that may risk humans' life. Toxic species that produced from Polystyrene fires may lead to the death even at a very low concentration like HCN. Benzene which is carcinogenic may cause cancer to the people who exposed to it. It is important to realise and be aware of the health effects of this kind of fire hazard on the new generations through a strict prevention from the point while processing and producing these kind of polymers in order to ensure safer life for all. Several main findings from these Polystyrene fire tests were summarised as follow:

- PS2, PS-CB and PS-CB 2 burnings had consumed lower Oxygen <10% by volume while other Polystyrene fires had shown an Oxygen consumption >15% by volume. The peak MLR values for most of these Polystyrene fires were above 0.06 g/s with Clear PS4 gave the highest MLR value up to 0.14 g/s. The low density Polystyrene materials like PS2, PS-TV, PS-CB and PS-CB 2 had a lean burning condition with ER<0.8 and other four Polystyrene materials (PS COVE, SB-W H, Clear PS2 and Clear PS4) with a higher density had shown a rich fire condition with ER up to 2.0.
- The total HRR (MLR) released gave the highest peak of ~600 kW/m$^2$ for Clear PS4 fire while PS-TV, PS COVE, SB-W H and Clear PS2 showed maximum total HRR values in between 300 to 400 kW/m$^2$. Other Polystyrene fires (PS2, PS-CB and PS-CB 2) gave HRR values <100 kW/m$^2$. These polymer fires gave the primary HRR <300 kW/m$^2$ with the secondary HRR <40 kW/m$^2$. Compared to the HRR values from Polyethylene fires, these Polystyrene fires had released three times lower of heat release rates.
- For Polystyrene fires that had been conducted at 35 kW/m$^2$ of heat irradiation under free ventilation, the longest time delay was about less than two minutes (107 s) for these polymers being ignited. Total HRR values were significant for Polystyrene fires especially for high density

Polystyrenes. Some Polystyrene fires like PS2 and PS-CB 2 fires had still released toxic gases even there was non-flaming fire condition experienced and this was not an exception on contributing to the overall fire toxicity of these polymer fires.

- Total LC50 values for the higher density of Polystyrene fires were up to 22. Meanwhile, the low density Polystyrene fires such as PS-TV fire had given the total LC50 up to 8. Other three Polystyrene fires showed the total LC50 values <4. These Polystyrene fires resulted to a maximum total $COSHH_{15min}$ of ~7000 which in a factor of 7 compared with the maximum total toxicity based on AEGL-2 that determined for these polymer fires.
- Similar to the result obtained from the conducted Polyethylene fires, these Polystyrene fires had also given $CO_2$ yields <3.0 g/g. The maximum CO yield (~0.5 g/g) for the higher density Polystyrene fires were higher than the low density Polystyrene fires which the value was almost double.
- Major species for most of tested Polystyrenes were asphyxiants such as CO and HCN and incapacitating irritants such as Benzene, Formaldehyde, Acrolein and $NO_2$. $SO_2$ presence and its contribution as a major species were also identified especially before the ignition started and during the post-flaming period.

# Chapter 8
# Other Polymer Fires with Free Ventilation in the Cone Calorimeter Test

## 8.1 General Combustion Properties of Other Polymer Fires

In this chapter, other polymer fires such as blue Glass Reinforced Plastic sheet (GRP-Blue), clear Acrylic sheet (Clear A-B), Polyvinyl chloride square tube (PVC ST-W) and Ferrybridge's Rubber Butyl sheet fires were also included and compared. These polymers were tested in the Cone Calorimeter at irradiation level of 35 kW/m$^2$ with free ventilation condition. Test details for other polymer fires were summarised in Table 8.1. These tested polymers were used in different applications. GRP-Blue was commonly used in industry as a bunding material for flammable liquid storage. Clear Acrylic glass was usually used as doors or windows for houses and buildings. Meanwhile, PVC square tube was used as a cable trunk to lay, cover and protect the small wires or cables from damages and dangers in buildings. The black Rubber Butyl sheet was used as an insulation for Ferrybridge power station tower.

GRP-Blue was the fastest being ignited at 59 s from the start test compared to Clear A-B (65 s), PVC ST-W (no ignition) and RBS FB (66 s). PVC ST-W which was a Chloride containing material showed non flaming condition throughout the conducted test. During test, Ferrybridge's Rubber Butyl fire was observed giving much black smoke than other three polymer fires. This might be due to Carbon rich burning condition it had experienced while burning. Instead of having the shortest time to ignition than other polymer fires, the GRP-Blue fire also had the longest flaming time before extinguished at 754 s. Clear A-B and RBS FB took about the same time before ignited but the flame out time for both fires showed a time gap about two minutes from each other with Clear A-B fire extinguished first at 316 s. It seemed that heavier and thicker polymeric materials took longer burning time than the lighter and thinner materials. PVC ST-W was not having a flaming fire might be because this material was fire retardant type.

**Table 8.1** Test details for other polymer fires.

| Test | Polymer Type | Thickness (mm) | Initial Mass (g) | Ignition (s) | Flame out (s) |
|---|---|---|---|---|---|
| 1 | GRP-Blue | 4 | 52.7 | 59 | 754 |
| 2 | Clear A-B | 2 | 20.5 | 65 | 316 |
| 3 | PVC ST-W | 25 | 74.1 | No | No |
| 4 | RBS FB | 3 | 43.0 | 66 | 450 |

### 8.1.1 Profile for Mass Reduction and Oxygen Changes

From the normalised mass loss profile in Figure 8.1 (a), it showed that Clear A-B had the highest percentage of mass loss which was about 100% within 400 s burning period. GRP-Blue fire showed 70% of mass loss, meanwhile PVC ST-W and RBS FB fires, each gave 60% and 50% of mass loss. For the first 200 s, PVC square tube burnt at the slowest rate compared to other polymer fires and it increased later to reach the maximum mass loss percentage of 60% at about 500 s. As shown in Figure 8.1 (b), in comparison with low burning of materials like GRP-Blue and PVC ST-W, Rubber Butyl and Clear A-B fires had shown a high $O_2$ reduction profile. It indicated that high $O_2$ consumption was experienced by Rubber Butyl and Clear A-B fires and this contributed to a high burning rate profile.

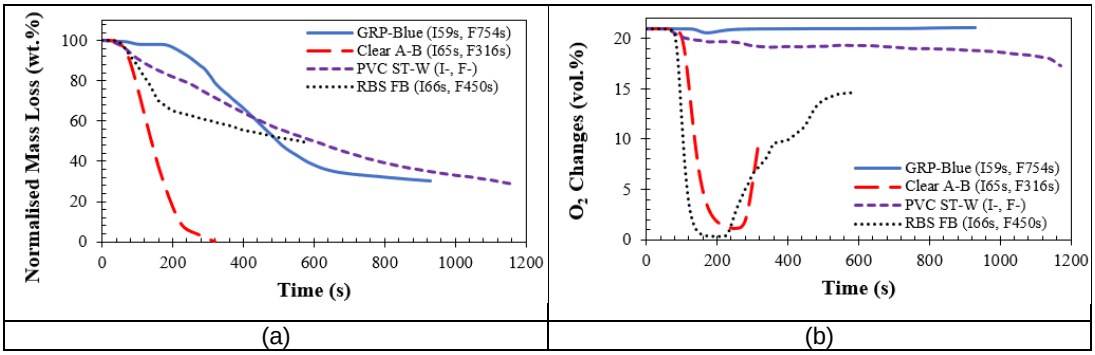


(a) (b)

**Figure 8.1** Mass loss and oxygen consumption profiles for other tested polymer fires at 35 kW/m$^2$ with free ventilation.

### 8.1.2 Correlations between MLR and ER

Figure 8.2 (a) showed the mass loss rates (MLR) and Figure 8.3 (b) showed the equivalence ratios, Φ (ER) as a function of time for polymer fires at 35 kW/m$^2$ with free ventilation. From Figure 8.2, it could be seen that MLR peak was at 0.14 g/s for Clear A-B fire at test time about 170 s and equivalence

ratio of 3.0. Clear A-B fire had fuel rich burning which contributed to the high MLR value. The maximum MLR for RBS FB fire was almost same with the maximum MLR for Clear A-B fire, about 0.13 g/s. At this peak MLR, RBS FB fire showed the equivalence ratio about 1.0, at test time of 100 s. There were two MLR peaks showed by the PVC ST-W fire which the first peak (0.1 g/s) at 100 s and the second peak (0.08 g/s) at 300 s. The first MLR peak for PVC ST-W fire gave the lean equivalence ratio (Φ equal to 0.6) and the second peak gave the equivalence ratio was about 0.5. The highest MLR value for GRP-Blue was 0.1 g/s at time of 500 s under very lean equivalence ratio condition.

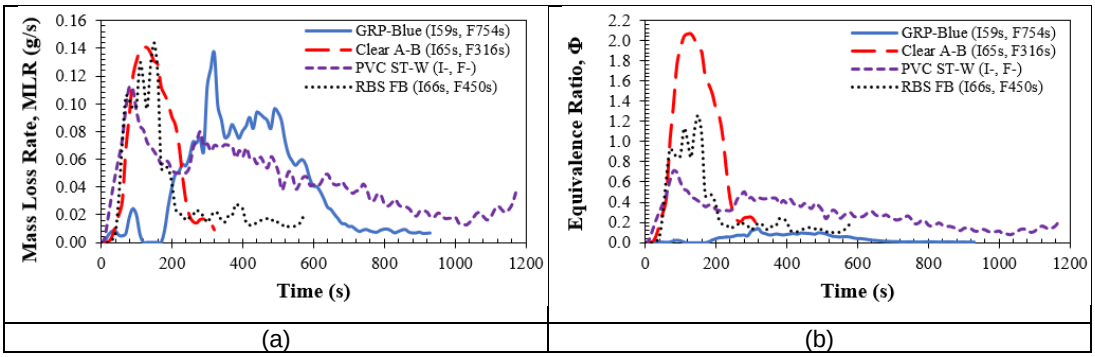


(a) (b)

**Figure 8.2** MLR and ER for other tested polymer fires at 35 kW/m$^2$ with free ventilation.

### 8.1.3 Heat Release Rate (HRR) Profiles

Heat release rate (HRR) profile as a function of time for polymer fires were shown in Figure 8.3 ((a) to (d)). The highest HRR of 400 kW/m$^2$ was given by Rubber Butyl (RBS FB) fire at time below 200 s and the second highest HRR was shown by Clear A-B fire, about 380 kW/m$^2$. For PVC ST-W and GRP-Blue fires, both gave the maximum HRR peak at 200 kW/m$^2$ with the highest HRR peak for PVC ST-W was at 100 s and the highest HRR peak for GRP-Blue was at 500 s.

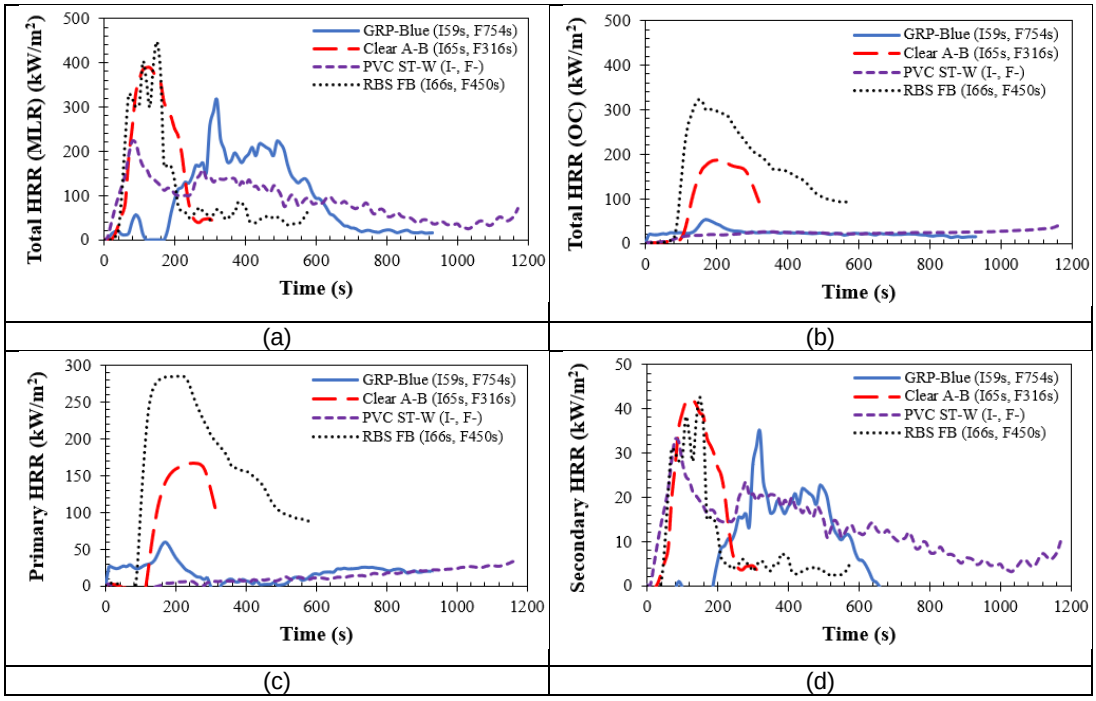


**Figure 8.3** HRR profiles for other tested polymer fires at 35 kW/m$^2$ with free ventilation.

## 8.2 Toxicity of Other Polymer Fires

Hydrocarbons including polymers would release gases or smoke when burnt in fire. Most of gases produced from an incomplete combustion were toxic and dangerous to human's health. People who inhaled toxic gases which were over their concentration limit may die. Some toxic gases such as HCN would lead to an immediate death even had exposed to it at low concentration level. High concentration of toxic gases produced from a fire would contribute to a high fire toxicity. Comparison of toxicity data for four different types of polymer fires were done and discussed in this section.

### 8.2.1 Gas Concentration as a Function of Time

Figure 8.4 showed comparison for gas concentrations between four different polymers which were GRP-Blue, Clear A-B, PVC ST-W and RBS FB. For most of presented gas concentration graphs in Figure 8.4, Clear A-B and RBS FB contributed to higher concentration values for most of gases compared to GRP-Blue and PVC ST-W. This might be due to resistance burning characteristic of the GRP-Blue (blue Glass Reinforced Plastic material) and

fire-retarded type of the PVC ST-W (Polyvinyl chloride white square tube) which contributed to low burning rates, hence contributing to low gas concentrations. From the analysis, non-flaming PVC ST-W fire gave a very significant value in HCl concentration (~40000 ppm) compared to another three polymers which the concentration values were small and negligible. It showed that HCl formation was still produced at high concentration at this operating temperature even this PVC ST-W fire had very low burning rate. Other analysed graphs for low toxic gas concentrations such as HF (<50 ppm), $NO_2$ (<250 ppm), HBr and Acetaldehyde were not presented.

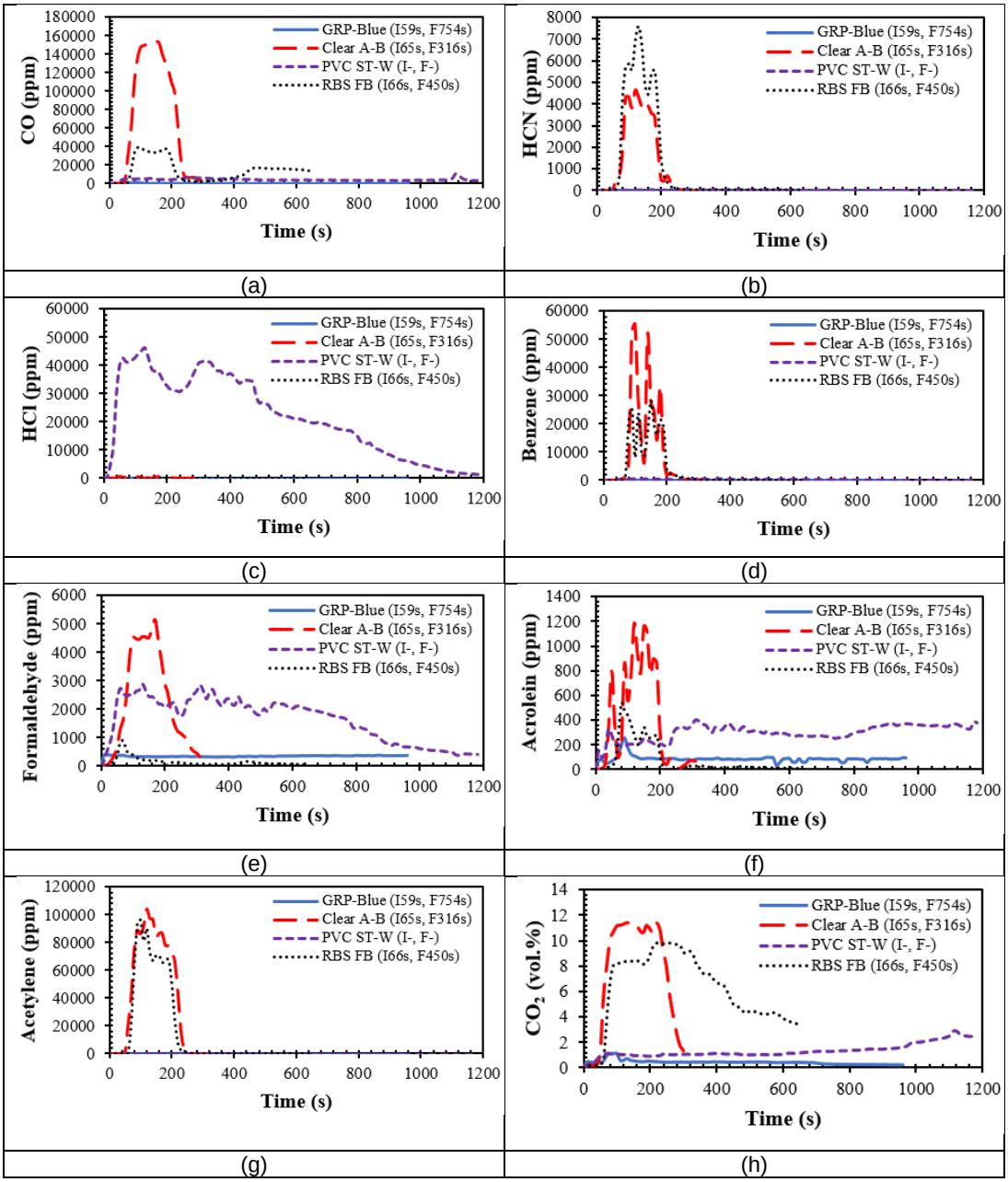

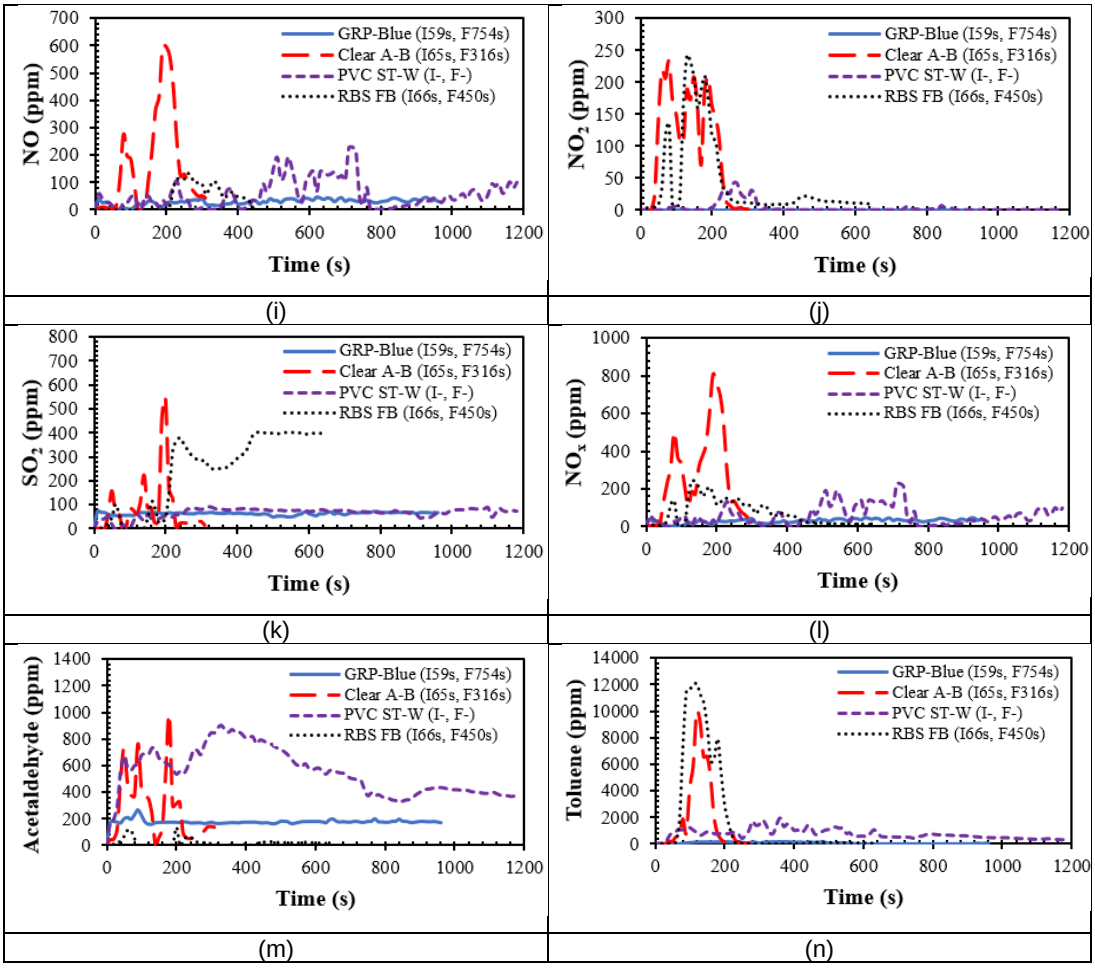


**Figure 8.4** Gas concentrations for other tested polymer fires at 35 kW/m$^2$ with free ventilation.

## 8.2.2 Gas Yields

Figure 8.5 showed the yield values for various species from four different polymer fires as a function of time. There were two peaks of CO yield observed for Clear A-B fire which the first peak of 0.4 g/g at 50 s and the second peak of 0.3 g/g at 200 s. The other three polymer fires gave the CO yields <0.1 g/g before 300 s with the RBS FB fire had its highest CO yield peak of 0.4 g/g after that period. In comparison between these four polymer fires, Clear A-B fire had the highest yield value for toxic species like HCN, Benzene, Acrolein, $NO_2$, Acetaldehyde and Toluene. HCl yield values were high throughout the burning period for PVC ST-W with the highest peak of 0.8 at time <100 s while HCl yields shown in Figure 8.4 (c) for other polymer fires were low and insignificant. This high HCl yield was always the expected result for PVC based material like PVC square tube. Other than HCl yield, the yield values of

other species were lower for this PVC ST-W fire compared to other three polymer fires. Yields of CO, HCN, Benzene, Formaldehyde, Acetylene, $CO_2$, $NO_2$, $SO_2$ and Toluene were all high and identifiable for RBS FB fire. For Clear A-B fire, Benzene yield was up to 0.35 g/g and the highest compared to other polymer fires. The maximum and mean yields for these polymer fires are shown in Table 8.2 and Table 8.3.

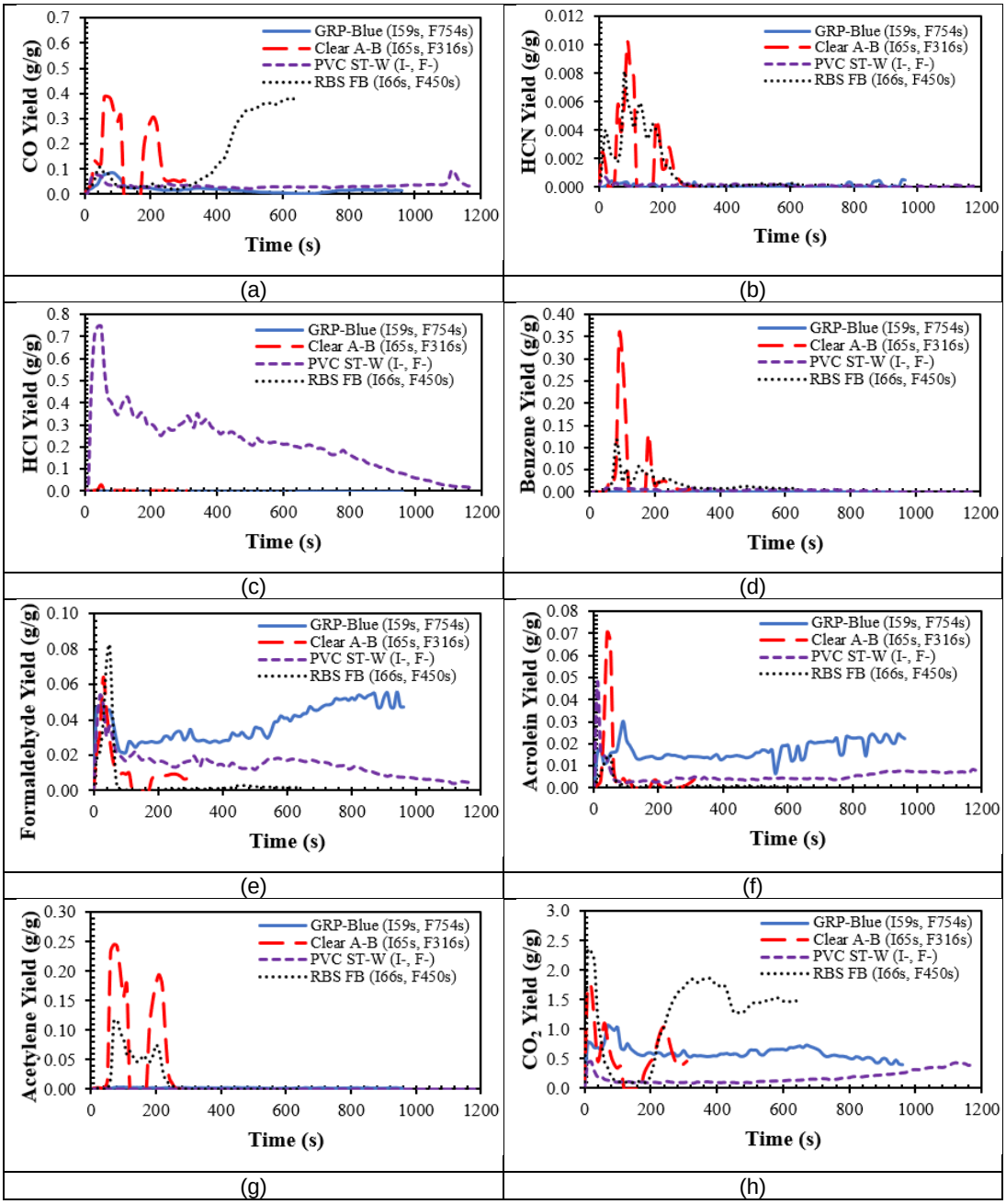

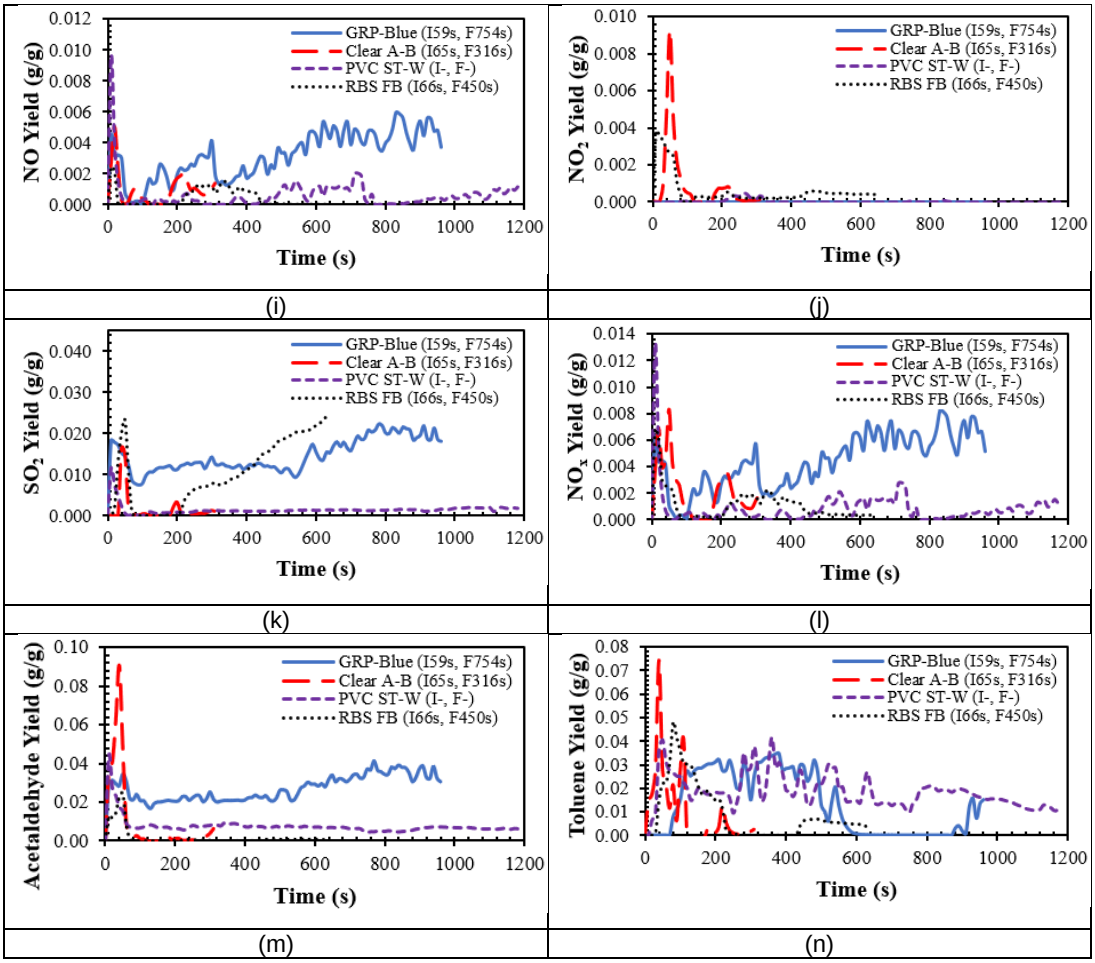


**Figure 8.5** Gas yields for other tested polymer fires at 35 kW/m$^2$ with free ventilation.

As shown in Figure 8.6, GRP-Blue and PVC ST-W fires gave a maximum combustion efficiency of about 60% with showing a leaner fire equivalence ratio, less than 0.7 while other two polymer fires (Clear A-B and RBS FB fires) had a maximum combustion efficiency peak of 90% with a richer fire equivalence ratio. The combustion efficiency percentage dropped to the zero for Clear A-B and RBS FB fires at 80 s before increased to the maximum efficiency rate after 200 s with equivalence ratio up to 1.5. A fuel lean burning condition were shown by GRP-Blue and PVC ST-W fires. In fact, the higher combustion efficiency rate indicates that the more complete of combustion process. For these polymer fires, the efficiency rate were low (below 60%) and the fires seemed experiencing an incomplete combustion with producing high amount of toxic species. Fire retardant material like PVC ST-W fire maintained giving a range from 60% to 70% of combustion efficiency throughout burning period with showing a slow increasing pattern in efficiency rate. A constant

and lower efficiency rate of ~50% was shown by GRP-Blue fire throughout the burning. It is likely that this GRP-Blue sample is a fire resistant material. The maximum and average gas yields for these polymer fires are summarised in Table 8.2 and Table 8.3 and in the Appendix E, graphs of CO cumulative mass produced from these polymer fires are also included for reference.

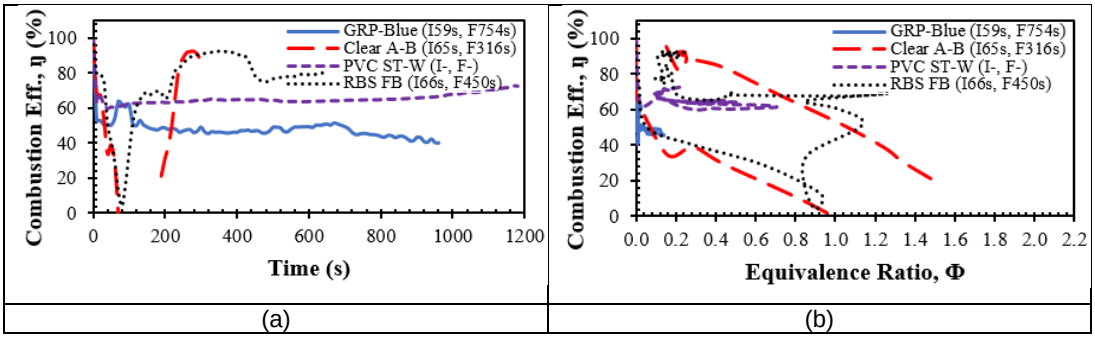


**Figure 8.6** Combustion efficiency, η for other tested polymer fires at 35 kW/m$^2$ with free ventilation.

**Table 8.2** Maximum gas yields for other polymer fires.

| Polymer Type | GRP-Blue | Clear A-B | PVC ST-W | RBS FB |
|---|---|---|---|---|
| Test Condition | 35 FV | | | |
| Species | Maximum Yields (g/g) | | | |
| CO | 0.0841 | 0.3866 | 0.0946 | 0.3841 |
| HCN | 0.0005 | 0.0102 | 0.0007 | 0.0080 |
| HCl | 0.0002 | 0.0298 | 0.7486 | 0.0059 |
| HF | 0.0008 | 0.0021 | 0.0002 | 0.0010 |
| Benzene | 0.0000 | 0.3536 | 0.0102 | 0.1172 |
| Formaldehyde | 0.0559 | 0.0639 | 0.0536 | 0.0816 |
| Acrolein | 0.0300 | 0.0705 | 0.0481 | 0.0150 |
| Acetylene | 0.0035 | 0.2445 | 0.0016 | 0.1175 |
| $CO_2$ | 1.0666 | 1.7367 | 0.4579 | 2.3591 |
| THC | 0.5924 | 1.4192 | 0.3703 | 0.9388 |
| NO | 0.0060 | 0.0050 | 0.0096 | 0.0024 |
| $NO_2$ | 0.0000 | 0.0093 | 0.0005 | 0.0038 |
| $SO_2$ | 0.0224 | 0.0166 | 0.0114 | 0.0246 |
| $NH_3$ | 0.0002 | 0.0016 | 0.0006 | 0.0009 |
| $NO_x$ | 0.0082 | 0.0083 | 0.0132 | 0.0068 |
| HBr | 0.0000 | 0.0000 | 0.0000 | 0.0000 |
| Acetaldehyde | 0.0414 | 0.0903 | 0.0439 | 0.0243 |
| Toluene | 0.0345 | 0.0743 | 0.0414 | 0.0481 |

**Table 8.3** Mean gas yields for other polymer fires.

| Polymer Type | GRP-Blue | Clear A-B | PVC ST-W | RBS FB |
|---|---|---|---|---|
| **Test Condition** | **35 FV** | | | |
| **Initial Mass (g)** | 52.70 | 20.59 | 72.61 | 41.47 |
| **Total Mass Loss (g)** | 43.31 | 20.47 | 52.59 | 34.48 |
| **Total Time (s)** | 960 | 310 | 1180 | 640 |
| **Mean ER, Φ** | 0.06 | 1.78 | 0.45 | 0.83 |
| **Species** | **Mean Yields (g/g)** | | | |
| CO | 0.0167 | 0.1566 | 0.0330 | 0.1917 |
| HCN | 0.0001 | 0.0027 | 0.0001 | 0.0020 |
| HCl | -0.0021 | 0.0009 | 0.2661 | 0.0005 |
| HF | 0.0004 | 0.0000 | 0.0000 | 0.0000 |
| Benzene | 0.0000 | 0.0666 | 0.0044 | 0.0233 |
| Formaldehyde | 0.0353 | 0.0061 | 0.0158 | 0.0029 |
| Acrolein | 0.0162 | 0.0024 | 0.0046 | 0.0008 |
| Acetylene | 0.0020 | 0.0915 | 0.0003 | 0.0284 |
| $CO_2$ | 0.5696 | 0.3125 | 0.1512 | 0.9356 |
| THC | 0.5281 | -22.0732 | 0.3376 | 0.2627 |
| NO | 0.0030 | 0.0006 | 0.0004 | 0.0001 |
| $NO_2$ | 0.0000 | 0.0006 | 0.0000 | 0.0004 |
| $SO_2$ | 0.0137 | 0.0007 | 0.0011 | 0.0118 |
| $NH_3$ | 0.0000 | -3.8798 | 0.0000 | 0.0001 |
| $NO_x$ | 0.0041 | 0.0013 | 0.0007 | 0.0005 |
| HBr | 0.0000 | 0.0000 | 0.0000 | 0.0000 |
| Acetaldehyde | 0.0252 | 0.0022 | 0.0074 | 0.0008 |
| Toluene | 0.0197 | 0.0081 | 0.0204 | 0.0139 |

### 8.2.3 Total Toxicity

Total toxicity profiles for the conducted other polymer fires under test conditions of 35 kW/m$^2$ of irradiation heat and free ventilation according to LS50, COSHH$_{15min}$ and AEGL-2 toxic assessments were shown in Figure 8.7. From the LC50 profile basis in Figure 8.7 (a), clear Acrylic sheet (Clear A-B) fire gave the highest total toxicity value of 65, followed by Rubber Butyl sheet (RBS FB) fire (50) and Polyvinyl chloride white square tube (PVC ST-W) fire (20). GRP-Blue (blue Glass Reinforced Plastic) fire showed the lowest Total LC50 which was less than 5 for a test duration of 800 s. As shown in Figure 8.8 (a), (b) and (c), Clear A-B fire showed the highest total toxicity for all three LC50, COSHH$_{15min}$ and AEGL-2 toxic assessment methods compared to other three polymer fires. PVC square tube fire gave more than 10000 times of toxic limit concentration for COSHH$_{15min}$ based method and about 1000 times for AEGL-2 based method. And the total toxicities for PVC square tube fire were about half from the total toxicities indicated by the Clear A-B fire for all three

assessment methods that were considered. The PVC tube fire released a very high HCl concentration and this irritant or toxic species was the usual major species for PVC type fire that also contributing to the high total toxicity values. Between these polymer fires, the GRP-Blue had the lowest burning rate and this could be the reason why the total toxicity values from the GRP-Blue fire were the lowest. In overall, all these polymer fires contributed to very high toxicities and total toxicities that may impair people from escape and may lead to the death.

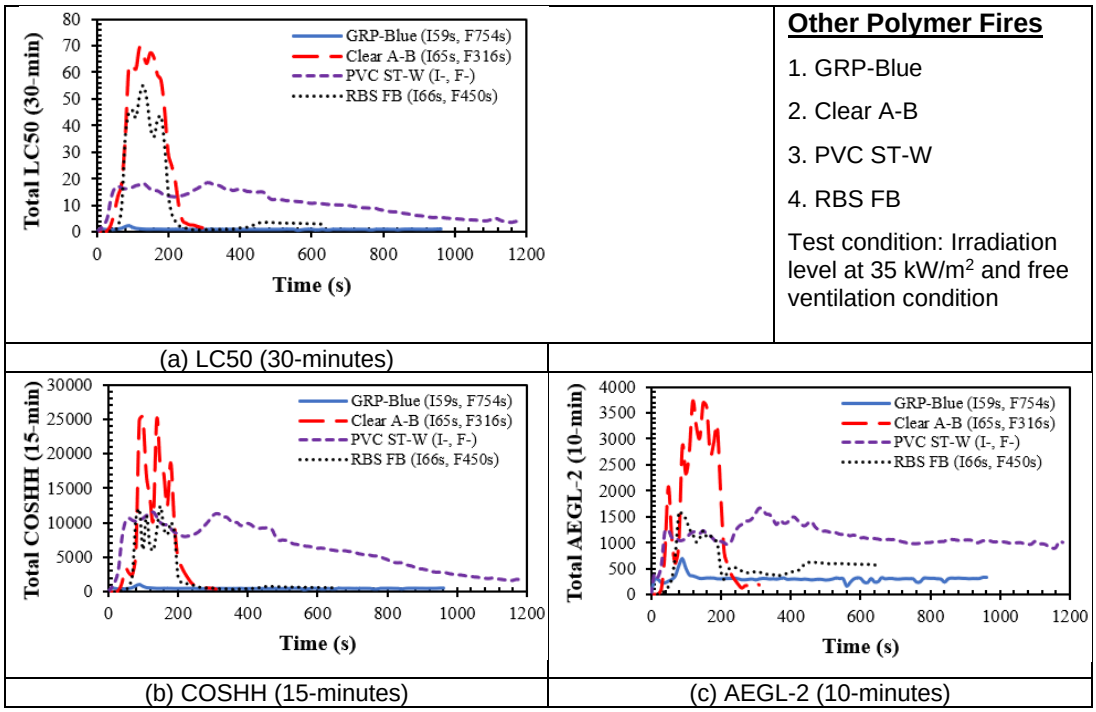


**Figure 8.7** Total toxicities for other tested polymer fires at 35 kW/m$^2$ with free ventilation.

### 8.2.4 Major Gases Contribution

Figure 8.8 showed the contribution of major species for four polymer fires under test conditions of 35 kW/m$^2$ of irradiate heat flux and free ventilation according to LC50 basis of toxic assessment. Formaldehyde and Acrolein were two major species with high percentage contribution to fire toxicity for GRP-Blue fire. These two species also the major species for other three polymer fires. For fire retarded square tube (PVC ST-W) fire, HCl was the first major species that contributing to the highest percentage. HCN contribution were also high and significant for clear Acrylic (Clear A-B) and rubber Butyl

(RBS FB) fires. Among these polymer fires, CO had shown (see Figure 8.8 (b) and (d)) the highest contribution peak at about 70% for Clear A-B and RBS FB fires with less 10% of contribution by other two polymer fires (GRP-Blue and PVC ST-W fires). $NO_2$ contribution as one of main toxic species were also identified for Clear A-B and RBS FB fires.

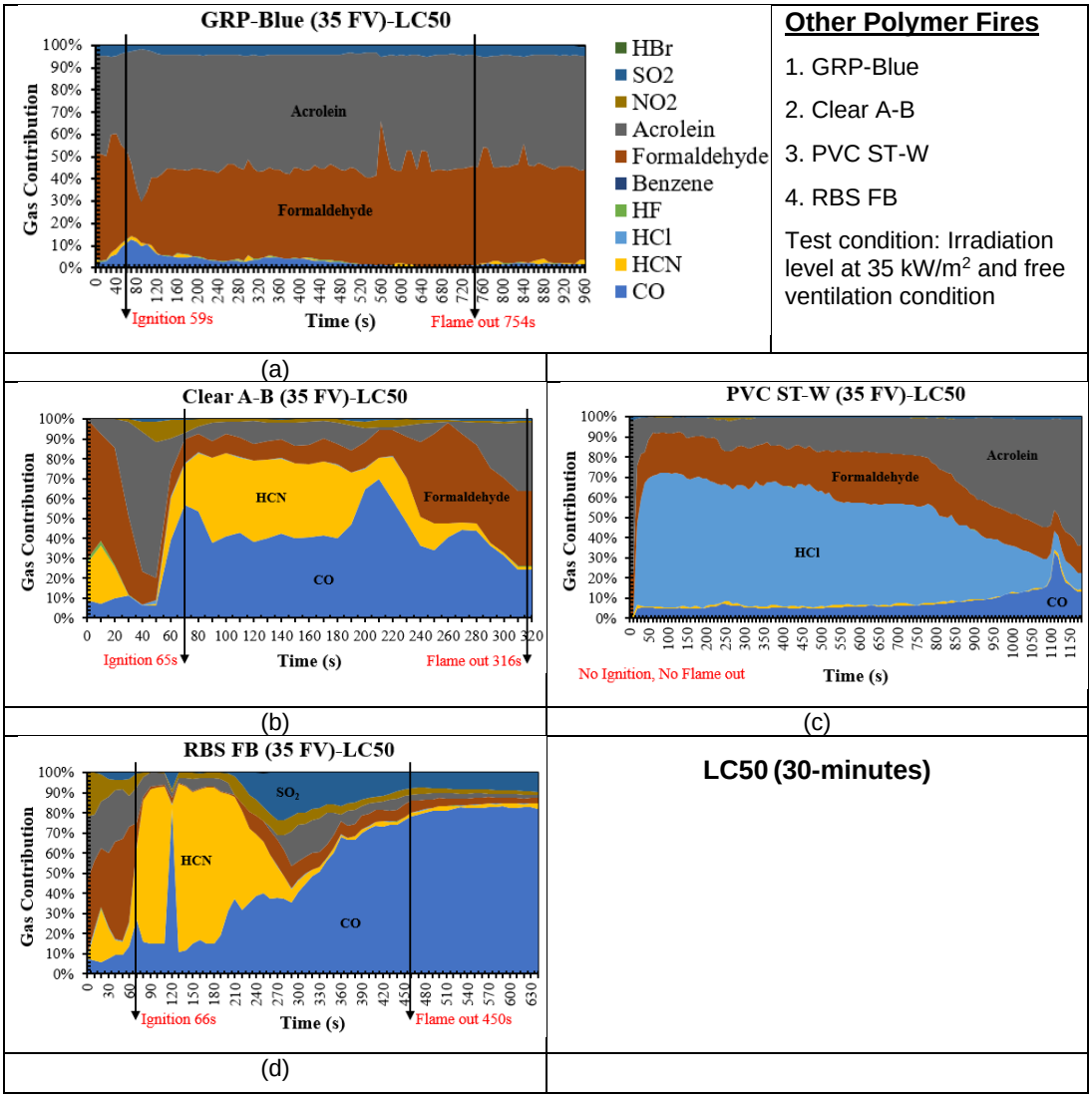


**Figure 8.8** Contribution of major gases (based $LC50_{30min}$) for other tested polymer fires at 35 kW/m$^2$ with free ventilation.

According to $COSHH_{15min}$ toxic assessment method as shown in the following Figure 8.9, Formaldehyde and Acrolein were still two common species for these polymer fires. The toxicity contribution by $SO_2$ were also realised for this method for most of these polymer fires especially for RBS FB fire, $SO_2$ was

high after 200 s of test time until end of its burning. Benzene was the major species with high contribution percentage for Clear A-B and RBS FB fire within burning period less than 200 s. Unlike Clear A-B and RBS FB fires, GRP-Blue and PVC ST-W fires showed that only few species dominated the fire toxicity with Formaldehyde, Acrolein and $SO_2$ were the dominant species for GRP-Blue fire meanwhile HCl, Formaldehyde and Acrolein were the dominant species for PVC ST-W fire.

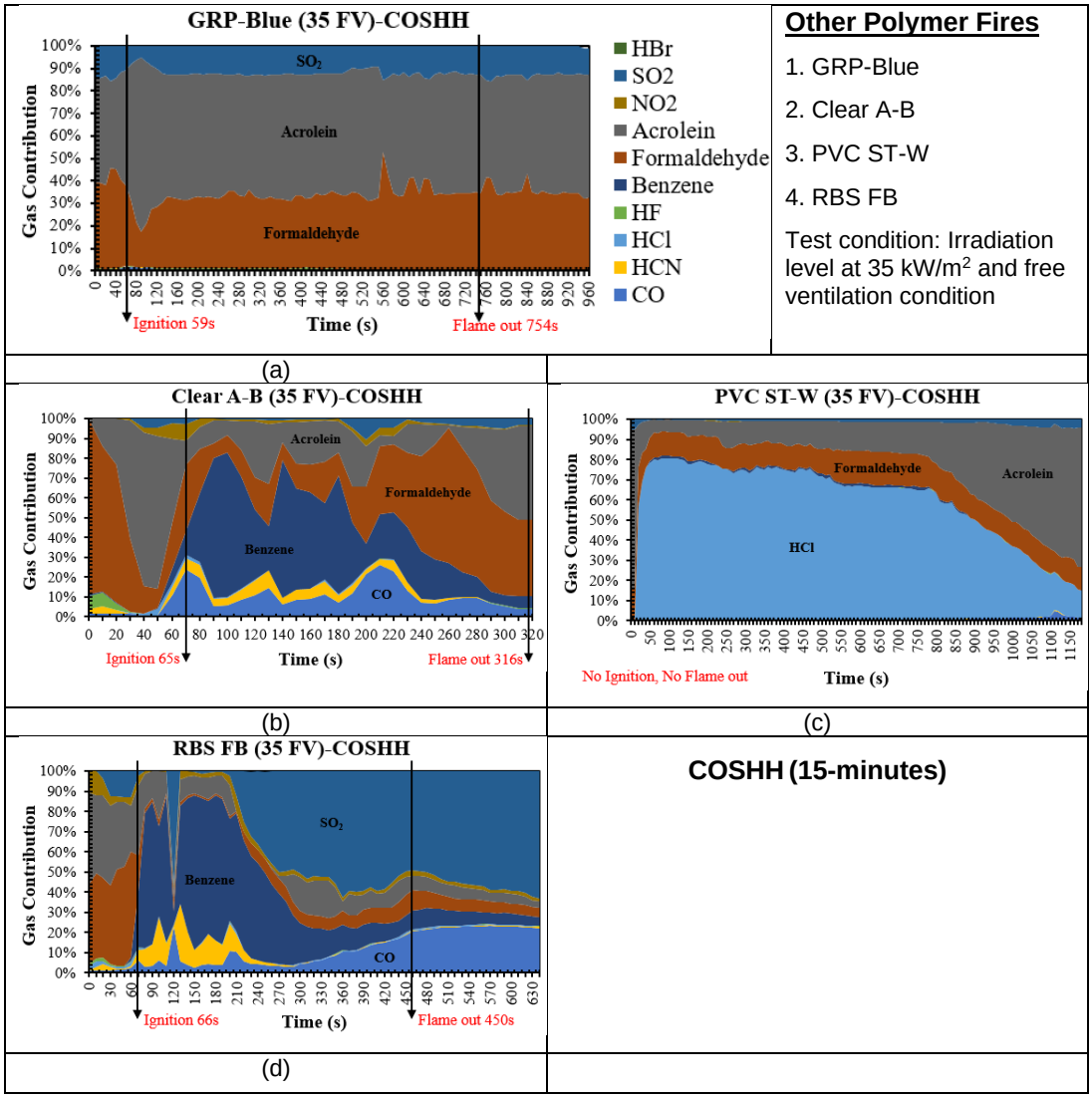


**Figure 8.9** Contribution of major gases (based $COSHH_{15min}$) for other tested polymer fires at 35 kW/m$^2$ with free ventilation.

From figures of major gas contribution based AEGL-2 assessment in Figure 8.10, Acrolein was observed to be the first major species for most of these

polymer fires. GR-P Blue fire had the highest contribution percentage of Acrolein, about 70% within 700 s of its burning period with a constant contributing profile. $SO_2$ contribution to fire toxicity was more significant for all four polymer fires for this assessment method than the other two LC50 and $COSHH_{15min}$ methods. For PVC ST-W non-flaming fire, HCl contribution was still high according to AEGL-2 basis even the determined dominant major species was Acrolein. All these toxic species were irritants and could cause irritancy when in contact with human's body which causing an impairment from escape during a fire. In overall, form all 10 toxic species that were taken into this consideration of major species contribution, HF and HBr contributions to fire toxicity were minor and insignificant for these four polymer fires. Table 8.4 shows a summary of the first six major species for other polymer fires

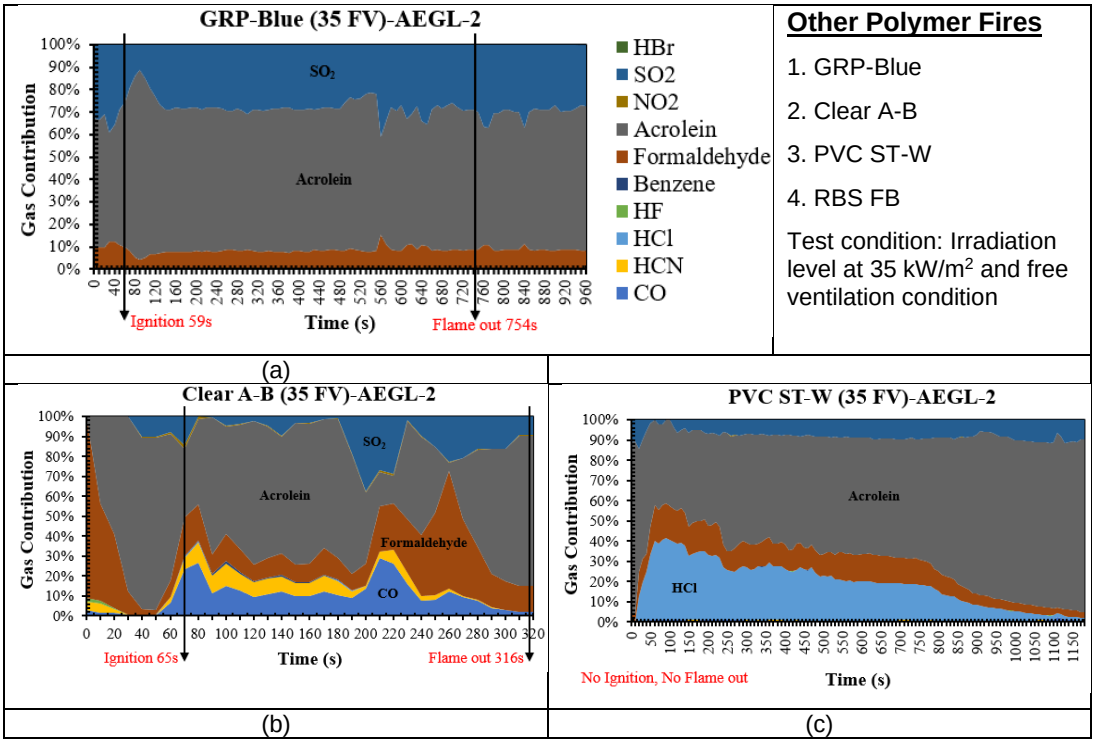

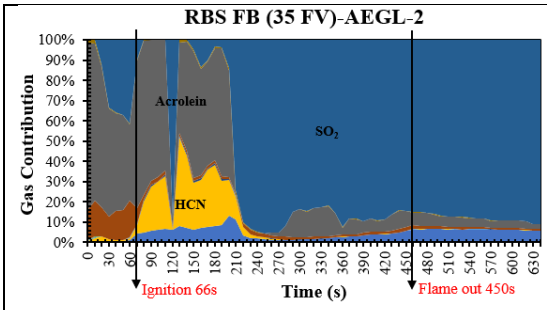


**AEGL-2 (10-minutes)**

(d)

**Figure 8.10** Contribution of major gases (based AEGL-$2_{10min}$) for other tested polymer fires at 35 kW/$m^2$ with free ventilation.

**Table 8.4** First six major species for other polymer fires.

| OTHER POLYMER FIRES | | | | | | | | | | | | |
|---|---|---|---|---|---|---|---|---|---|---|---|---|
| **Test** | **Test Details** | **Mean ER, Φ (Chan)** | **Time (s)** | **Fire Stage** | **TT** | **Major Species** | | | | | | |
| | | | | | | **1** | **2** | **3** | **4** | **5** | **6** |
| 1 | GRP-Blue | 0.05 | <59 | Ignition | **LC50** | Formaldehyde | Acrolein | CO | $SO_2$ | HCN | - |
| | 35 FV | 0.10 (peak) | 59 - 90 | Flaming | | Acrolein | Formaldehyde | CO | $SO_2$ | HCN | - |
| | I = 59 s | 0.07 | 90 - 754 | SS Flaming | | Acrolein | Formaldehyde | $SO_2$ | CO | HCN | - |
| | F = 754 s | 0.06 | >754 | Post-flaming | | Acrolein | Formaldehyde | $SO_2$ | CO | HCN | - |
| | | 0.05 | <59 | Ignition | **COSHH** | Acrolein | Formaldehyde | $SO_2$ | CO | - | - |
| | | 0.10 (peak) | 59 - 90 | Flaming | | Acrolein | Formaldehyde | $SO_2$ | CO | - | - |
| | | 0.07 | 90 - 754 | SS Flaming | | Acrolein | Formaldehyde | $SO_2$ | - | - | - |
| | | 0.06 | >754 | Post-flaming | | Acrolein | Formaldehyde | $SO_2$ | - | - | - |
| | | 0.05 | <59 | Ignition | **AEGL-2** | Acrolein | Formaldehyde | $SO_2$ | - | - | - |
| | | 0.10 (peak) | 59 - 90 | Flaming | | Acrolein | Formaldehyde | $SO_2$ | - | - | - |
| | | 0.07 | 90 - 754 | SS Flaming | | Acrolein | Formaldehyde | $SO_2$ | - | - | - |
| | | 0.06 | >754 | Post-flaming | | Acrolein | Formaldehyde | $SO_2$ | - | - | - |
| 2 | Clear A-B | 0.2 | <65 | Ignition | **LC50** | Formaldehyde | Acrolein | CO | HCN | $NO_2$ | $SO_2$ |
| | 35 FV | 8.4 (peak) | 65 - 190 | SS Flaming | | CO | HCN | Formaldehyde | Acrolein | $NO_2$ | - |
| | I = 65 s | - | 190 - 316 | Flaming | | CO | Formaldehyde | Acrolein | HCN | $NO_2$ | $SO_2$ |
| | F = 316 s | - | >316 | Post-flaming | | Formaldehyde | Acrolein | CO | HCN | $NO_2$ | $SO_2$ |
| | | 0.2 | <65 | Ignition | **COSHH** | Formaldehyde | Acrolein | $NO_2$ | $SO_2$ | HF | HCN |
| | | 8.4 (peak) | 65 - 190 | SS Flaming | | Benzene | Acrolein | Formaldehyde | CO | HCN | $NO_2$ |
| | | - | 190 - 316 | Flaming | | Formaldehyde | Acrolein | Benzene | CO | $SO_2$ | HCN |
| | | - | >316 | Post-flaming | | Acrolein | Formaldehyde | Benzene | CO | $SO_2$ | - |

| | | | | | | | | | | | |
|---|---|---|---|---|---|---|---|---|---|---|---|
| | | 0.2 | <65 | Ignition | **AEGL-2** | Acrolein | Formaldehyde | $SO_2$ | CO | HCN | HF |
| | | 8.4 (peak) | 65 - 190 | SS Flaming | | Acrolein | CO | Formaldehyde | HCN | $SO_2$ | Benzene |
| | | - | 190 - 316 | Flaming | | Acrolein | Formaldehyde | $SO_2$ | CO | HCN | - |
| | | - | >316 | Post-flaming | | Acrolein | Formaldehyde | $SO_2$ | CO | HCN | - |
| 3 | PVC ST-W | 0.02 | <20 | - | **LC50** | HCl | Acrolein | Formaldehyde | HCN | $SO_2$ | CO |
| | 35 FV | 0.55 (max. 0.70) | 20 - 800 | SS | | HCl | Formaldehyde | Acrolein | CO | HCN | $NO_2$ |
| | I = No | 0.40 | 800 - 1130 | - | | Acrolein | HCl | Formaldehyde | CO | HCN | $SO_2$ |
| | F = No | 0.30 | >1130 | - | | Acrolein | CO | HCl | Formaldehyde | HCN | $SO_2$ |
| | | 0.02 | <20 | - | **COSHH** | HCl | Acrolein | Formaldehyde | $SO_2$ | - | - |
| | | 0.55 (max. 0.70) | 20 - 800 | SS | | HCl | Formaldehyde | Acrolein | Benzene | $SO_2$ | - |
| | | 0.40 | 800 - 1130 | - | | HCl | Acrolein | Formaldehyde | $SO_2$ | CO | - |
| | | 0.30 | >1130 | - | | Acrolein | HCl | Formaldehyde | $SO_2$ | CO | - |
| | | 0.02 | <20 | - | **AEGL-2** | Acrolein | $SO_2$ | Formaldehyde | HCl | - | - |
| | | 0.55 (max. 0.70) | 20 - 800 | SS | | Acrolein | HCl | Formaldehyde | $SO_2$ | - | - |
| | | 0.40 | 800 - 1130 | - | | Acrolein | $SO_2$ | HCl | Formaldehyde | - | - |
| | | 0.30 | >1130 | - | | Acrolein | $SO_2$ | Formaldehyde | HCl | - | - |
| 4 | RBS FB | 0.04 | <66 | Ignition | **LC50** | Formaldehyde | Acrolein | HCN | $NO_2$ | CO | $SO_2$ |
| | 35 FV | 8.00 (peak) | 66 - 200 | Flaming 1 | | HCN | CO | Acrolein | $NO_2$ | Formaldehyde | $SO_2$ |
| | I = 66 s | - | 200 - 450 | Flaming 2 | | CO | $SO_2$ | HCN | Acrolein | Formaldehyde | $NO_2$ |
| | F = 450 s | - | >450 | Post-flaming | | CO | $SO_2$ | Formaldehyde | Acrolein | HCN | $NO_2$ |
| | | 0.04 | <66 | Ignition | **COSHH** | Formaldehyde | Acrolein | $SO_2$ | $NO_2$ | HCN | CO |
| | | 8.00 (peak) | 66 - 200 | Flaming 1 | | Benzene | HCN | Acrolein | CO | $SO_2$ | $NO_2$ |
| | | - | 200 - 450 | Flaming 2 | | $SO_2$ | Benzene | CO | Acrolein | Formaldehyde | $NO_2$ |
| | | - | >450 | Post-flaming | | $SO_2$ | CO | Benzene | Formaldehyde | Acrolein | $NO_2$ |

| | | | | | | | | | | | |
|---|---|---|---|---|---|---|---|---|---|---|---|
| | | 0.04 | <66 | Ignition | **AEGL-2** | Acrolein | $SO_2$ | Formaldehyde | HCN | CO | - |
| | | 8.00 (peak) | 66 - 200 | Flaming 1 | | Acrolein | HCN | $SO_2$ | CO | Formaldehyde | - |
| | | - | 200 - 450 | Flaming 2 | | $SO_2$ | Acrolein | CO | Formaldehyde | HCN | - |
| | | - | >450 | Post-flaming | | $SO_2$ | CO | Acrolein | Formaldehyde | HCN | - |

## 8.3 Particle Size Distributions from Other Polymer Fires

### 8.3.1 Particle Number and Mass Distributions for Rubber Butyl Sheet Fire

Figure 8.11 shows particle number and mass distributions as a function of particle size for Rubber Butyl Sheet (RBS FB) fire at heat flux of 35 kW/m$^2$ and free ventilation. After 10 s the test started, number concentration for <50 nm particles was higher compared to larger particles. The number concentration was lower for <50 nm particles than larger particles at 50 s of burning. After the ignition started at 66 s, the generation of <100 nm particles had increased which giving a high number concentration up to 1E+10 p/cm$^3$ throughout the burning period. The mass concentration profile for this rubber fire had shown an increase with the increase of particle size. In the early test at time = 10 s, the mass concentration of particles was at the same level with no particles larger than 500 nm were presence. >500 nm particles had shown an increase in mass distribution after that period when approaching the ignition state.

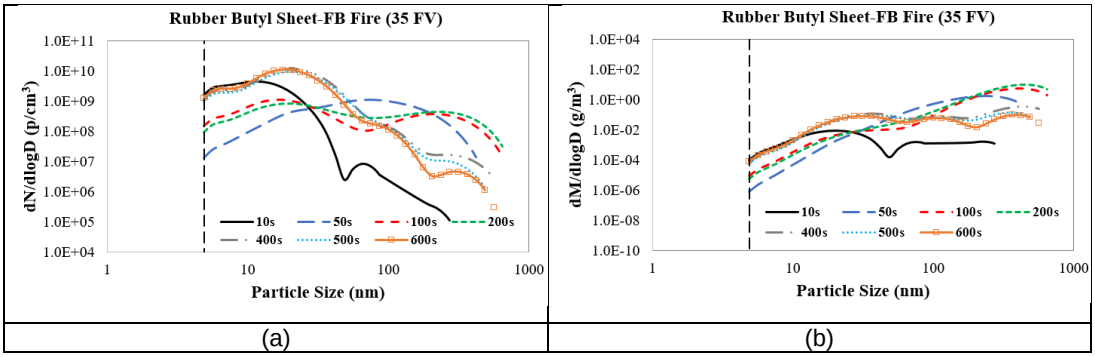


**Figure 8.11** Particle number and mass distributions for Rubber Butyl Sheet (RBS FB) fire at heat flux of 35 kW/m$^2$ and free ventilation.

Particle number and mass distributions in 3D Waterfall plot for Rubber Butyl Sheet (RBS FB) fire at heat flux of 35 kW/m$^2$ and free ventilation are shown in the following Figure 8.12. Number concentration for particles with the size less than 100 nm was higher compared to particles >100 nm while the mass concentration for these smaller particles was lower than the larger particles. The number of 5 nm to 100 nm particles reached the highest concentration up to 1E+10 p/cm$^3$. Larger particles with the size >100 nm had shown a decrease

in number concentration profile at the end of burning period where it might be due to an increase in agglomeration rate of the generated particles from this rubber fire. As shown in Figure 8.12 (b), particles above 100 nm gave a higher mass distribution compared to particles less than 100 nm. Under free ventilation condition, the supplied air could increase the agglomeration rate of the small particles to form bigger size of particles by cooling down the surrounding temperature. With the decrease in temperature, smaller particles which are mainly aerosols would attach to each other and had changed from the gas phase to form liquid droplets with a larger size.

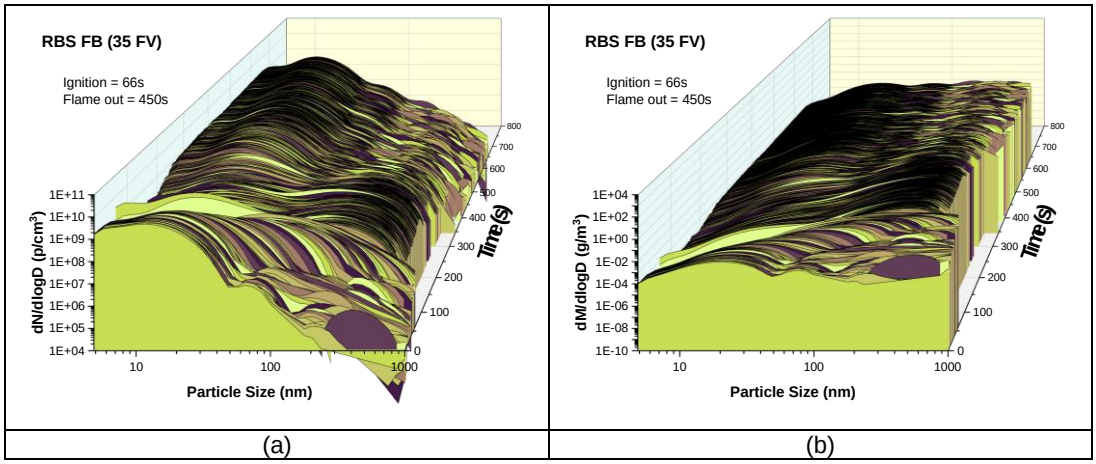


(a) (b)

**Figure 8.12** Particle number and mass distributions in 3D Waterfall plot for Rubber Butyl Sheet (RBS FB) fire at heat flux of 35 kW/m$^2$ and free ventilation.

Figure 8.13 shows size distributions for 10 nm, 50 nm and 100 nm particles for Rubber Butyl Sheet (RBS FB) fire at heat flux of 35 kW/m$^2$ and free ventilation. Before the ignition, RBS FB fire show a higher number of 10 nm particles with a lower number of 50 nm and 100 nm particles. Within this period, aerosols were produced from the pyrolysis process when the sample exposed to the cone heater. After start of ignition at 66 s, number distribution for 50 nm and 100 nm had increased to the same level as 10 nm particles up to 200 s of burning period. From 200 s until the end of test, the generation of 10 nm, 50 nm and 100 nm were constant with 100 nm gave the lower number distribution of about 1E+08 p/cm$^3$ and 10 nm and 50 nm particles gave 10 times higher number concentration of above 1E+09 p/cm$^3$. Mass concentration for 50 nm and 100 nm particles was higher than 10 nm particles as illustrated in Figure 8.13 (b).

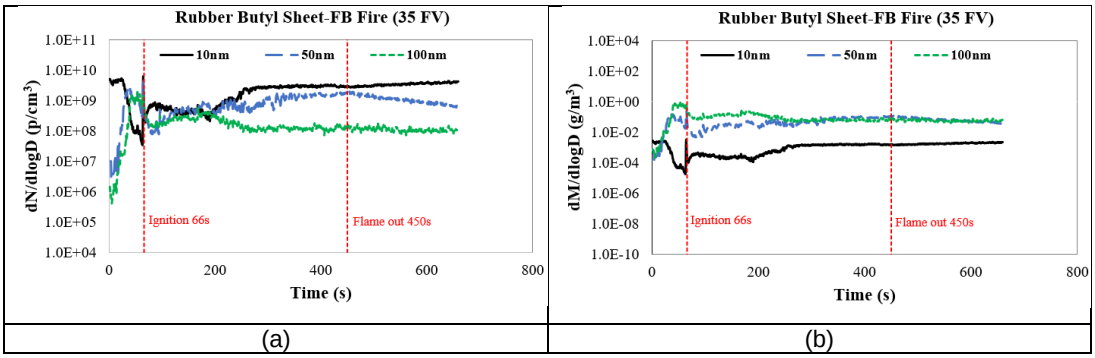


**Figure 8.13** Size distributions for 10 nm, 50 nm and 100 nm particles for Rubber Butyl Sheet (RBS FB) fire at heat flux of 35 kW/m$^2$ and free ventilation.

Particulate cumulative mass for Rubber Butyl Sheet (RBS FB) fire in the Cone Calorimeter at heat flux of 35 kW/m$^2$ and free ventilation is shown in Figure 8.14. Rubber Butyl Sheet (RBS FB) fire had an ignition at 66 s and flame out at 450 s. Particulate cumulative mass had increased with the increasing of burning time for all size of particles from 5 nm to 1000 nm. The peak of cumulative mass for this rubber fire was about 100 g/m$^3$ at the time of ignition with the highest number of 200 nm particles. Meanwhile, at the flame out time, the highest cumulative mass was represented by 400 nm particles with the cumulative mass value of ~3000 g/m$^3$. After the flame out, the cumulative mass for larger particles with the size >400 nm decreased and this had shown that the number of large particles were decreased during that period. During this period, the agglomeration of small particles occurred to form larger particles. Particles below 100 nm produced from RBS FB fire gave a cumulative mass <100 g/m$^3$ which the value much more lower compared to other larger size of particles.

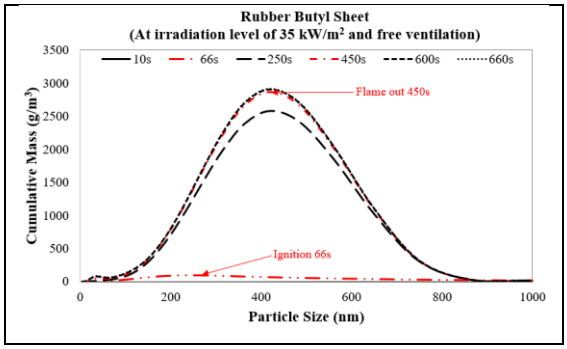


**Figure 8.14** Particulate cumulative mass for Rubber Butyl Sheet (RBS FB) fire at heat flux of 35 kW/m$^2$ and free ventilation.

## 8.3.2 Particulate Yields for Rubber Butyl Sheet Fire

Number and mass yields for 10 nm, 50 nm and 100 nm particles for RBS FB fire at 35 kW/m$^2$ and free ventilation are shown in Figure 8.15. From the result as shown in Figure 8.15, the average number yields of 10 nm particles (~1.0E+10 p/kg) were higher than the average number yields for 50 nm and 100 nm particles (~1.0E+04 p/kg). Before the ignition point at 66 s, the number yields of particulate gave a higher maximum yield value compared to the number yields produced after the ignition. From the graph trends, for particle size above 50 nm, it could be expected to give lower number yields than the particle size smaller than 50 nm. The calculated equivalence ratios by Chan method for this Rubber fire had shown a rich fire condition with ER > 8.0 at certain burning period. Black soot was produced as observed manually during the fire test of this Rubber sample. If compared with other polymer fires such as PIR solid foam fires and Polyethylene fires in the present work, this RBS FB fire had a higher particulate yield values. From Figure 8.15 (c), the tabulated mass yield values for these particle sizes were in the same range, from 1.0E-05 g/g up to 1.0E+00 g/g.

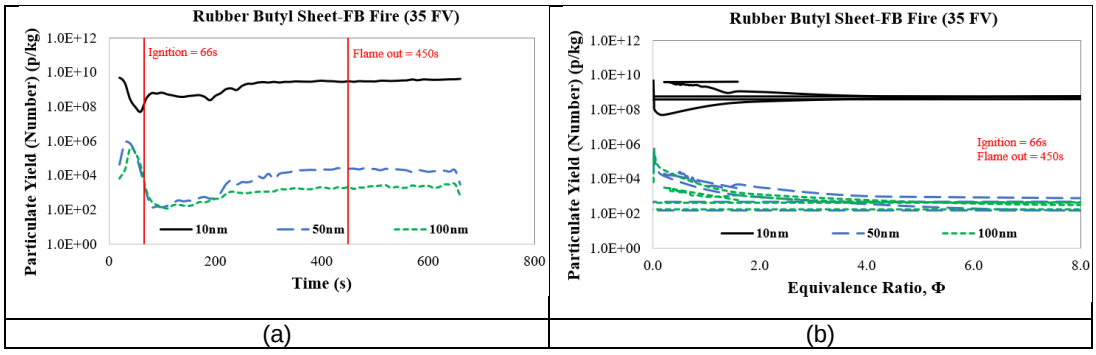

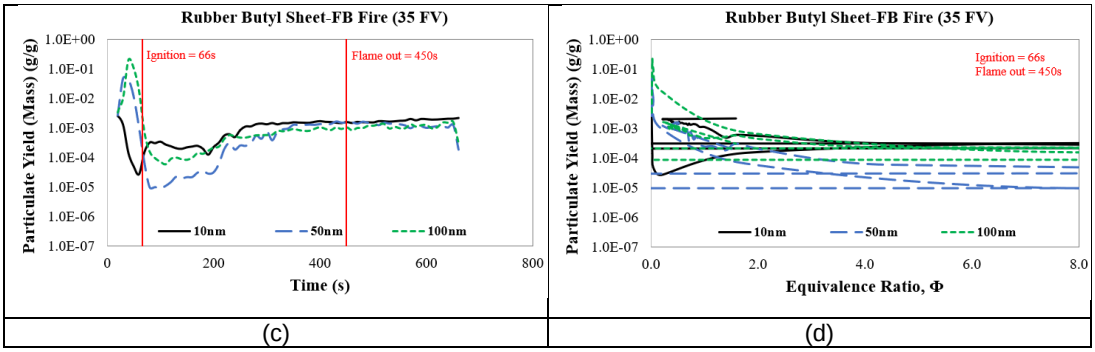


(c) (d)

**Figure 8.15** Particulate yields (number and mass) for RBS FB fire at 35 kW/m$^2$ and free ventilation.

## 8.4 Findings and Conclusion from Other Polymer Fire Tests

Chapter 8 includes the results for four different types of polymer fires which were tested for toxicity data separately. The main findings from these polymer fires as the following list:

- Clear A-B fire gave the highest normalised mass loss % of ~100% with MLR value , while other three polymers showed a normalised mass loss <70%. The Oxygen consumption was higher for Clear A-B and RBS FB fires (~20%) while GRP-Blue and PVC ST-W gave a lower Oxygen consumption of <5%. The GRP-Blue used as a flammable liquid storage in the industry application is likely a fire resistance material and the PVC ST-W pipe is a fire retardant material containing Chlorine.
- Most of these polymer fires gave the maximum MLR (0.12-0.14 g/s) before 200 s of test time except the GRP-Blue fire which had reached the highest MLR peak of 0.14 g/s later at 300 s. A lean burning condition was shown by GRP-Blue and PVC ST-W fires with ER<0.7 and a rich burning experienced by Clear A-B and RBS FB samples with ER >1.0. The peak HRR (MLR) value for these polymer fires was in a range from 200 to 450 kW/m$^2$ with the primary HRR <300 kW/m$^2$ and secondary HRR <45 kW/m$^2$.
- Clear A-B and RBS FB fires produced a higher concentration of toxic gases than other two polymers with GRP-Blue gave the lowest toxic gas concentrations. The highest HCl concentration of 40000 ppm was given by PVC ST-W fire while insignificant HCl concentration was shown by other three polymers. HCN emissions were significant for

Clear A-B and RBS FB fires with a maximum concentration of 8000 ppm showed by Clear A-B fire, about double than the RBS FB fire.

- Within 300 s of test time, Clear A-B fire gave the highest CO yield peak of 0.4 g/g which ~4 times higher than other polymer fires (<0.1 g/g). The result had a good agreement with the CO emissions produced from these polymer fires which the CO concentration shown by Clear A-B fire was ~160000 ppm while the CO concentration for RBS FB and other two polymer fires was <40000 ppm. The highest HCl yield peak of ~0.8 g/g was given by the chlorinated polymer fire, the PVC ST-W.
- Among all tested electrical cables and polymers in the present work, total LC50 for these four polymer fires were high and most significant especially for Clear A-B and RBS FB fires which giving the total LC50 peaks >55. PVC pipe (PVC ST-W) fire gave the total LC50 ~20 and the total LC50 values <5 were shown by GRP-Blue fire. For $COSHH_{15min}$ and AEGL-2 basis, the total toxicities were the highest for Clear A-B fire with 25000 of total $COSHH_{15min}$ peak and 3800 of AEGL-2 peak.
- Formaldehyde, Acrolein and CO were the three major species for these polymer fires according to the LC50 toxic assessment method. Compared to Formaldehyde and Acrolein contributions on the fire total toxicity, CO contribution was lower for GRP-Blue and PVC ST-W fires than the Clear A-B and RBS FB fires. Based on $COSHH_{15min}$ toxic assessment method, HCN and Benzene were also a major species for Clear A-B and RBS FB fires. For PVC ST-W fire, HCl was a dominant species and contributed to the highest total toxicity % for LC50 and $COSHH_{15min}$ methods.
- The number concentration of 10 nm particles (>1.0E+09 p/$cm^3$) was higher than 50 nm and 100 particles while the mass concentration of 10 nm particles (<1.0E-02 g/$m^3$) was lower than 50 nm and 100 particles. Particles <100 nm gave the cumulative of ~100 g/$m^3$, ~30 times lower compared to 400 nm particles.
- Number yield for 10 nm (1.0E+10 p/kg) was much higher than 50 nm and 100 particles (1.0E+05 p/kg) but all these three size of particles gave a same average mass yield of 1.0E-03 g/g.

# Chapter 9
# Development and Testing in the Purser Furnace

## 9.1 Improved Design of the New Purser Furnace System

### 9.1.1 The Purser Furnace Method for Fire Toxicity Measurements and Its Design Problems

The steady state Purser Furnace System (ISO/TS 19700) [104] is a controlled equivalence ratio method for the determination of toxic emissions from materials under fire conditions. For the work described here reference was made to the 2013 version of the ISOTS19700 tube furnace standard [104]. Significant modifications were made for the current (2016) standard but were not considered in this work The Purser furnace [104] is a good method for fire toxicity measurements as a function of the fire equivalence ratio and temperature. In the present work, an improved version of the Purser furnace was designed and constructed, with several modifications to improve on the original design of the Purser furnace.

The Purser furnace uses a furnace to simulate fire temperatures and is normally operated at about 600$^{o}$C, but the temperature can be varied. A Quartz tube passes into the furnace and the fire material is place as a long sample in a Quartz half tube that acts as a container for the fire sample that can be traversed into the furnace. An air flow passes into the furnace and the ratio of the air flow to the material inflow rate enables a metered fire equivalence ratio to be set up prior to the test. The basis of the method is to provide a dynamic steady state specimen combustion, maintaining a constant rate of combustion and constant defined combustion conditions by introducing the test specimen through the furnace at a constant mass rate under a constant mass flow of air. The combustion products are expelled from the furnace tube into a mixing chamber where they are cooled and diluted by a introduction of a secondary air supply to provide a total flow through the mixing chamber of 50 L/min.

If a raw hot gas sample had been taken from the end of the tube and transported to a gas analyser using heated lines and pumps, then the problems of the Purser method could have been avoided. Most fire toxicity laboratories do not have the heated gas sample equipment necessary to analyse the fire gases hot and the practice in fire research has been to cool the gas samples by dilution, which keeps the water vapour in the combustion

products in the gas phase. If the water condenses so will several other toxic species with low boiling points. The standard Cone Calorimeter for example, used in this research, dilutes the products of combustion by a large factor. This is why the present use of the Cone calorimeter used heated raw gas sampling from a chimney at the exit from the conical heater.

The Purser Furnace uses a bypass air flow that mixes with the raw products of combustion in a discharge mixing volume and an exit pipe from this chamber is then sent to a flue extract. The method was developed of using a total air flow of 50 LPM with up to 10 LPM sent down the furnace test tube and the rest bypassing the test tube and then mixing in the discharge volume. The minimum dilution ratio is 4/1 when 10 LPM is used in the Quartz tube and the maximum dilution ratio is 25/1 when 2 LPM is used in the Quartz tube. The principle is still to prevent water condensation and the condensation of any other fire product gas. The purpose of the dilution and mixing of the primary combustion products from the furnace tube with secondary air in the mixing chamber is to provide a cooled and diluted atmosphere suitable for animal toxicity exposures and similar to that likely to be inhaled by fire victims away from an immediate combustion zone. The dilution stage is also used to reduce combustion atmosphere concentrations to levels suitable for measurements of gas and smoke particulate compositions. In existing apparatus the secondary air plume is blown directly into the emerging primary air plume to ensure rapid mixing and reduce the plume temperature to eliminate secondary oxidation. The distance from the furnace to the chamber is a short as possible to minimise any condensation of products in the unheated end of the furnace tube.

Many fire toxic gases dissolve in water so a thermally cooled sampling system cannot be used as the water condenses and this condensate then dissolves some of the gases that are required to be measured.

Potential issues with the original TS19700 “Purser Furnace” are:

a) The method requires constant defined conditions in terms of flaming or non-flaming behaviour. It is therefore necessary to observe down the tube during a run to ensure that the combustion remains in the desired state. Where intermittent flaming occurs, the run should be repeated with a higher furnace temperature (to ensure constant flaming) or a lower temperature (to ensure constant non-flaming) decomposition.

b) The combustion conditions (equivalence ratio) are highly dependent on the accuracy of the rate of fuel introduction and the primary air flow over the specimen. It is particularly important that these are calibrated and confirmed.

c) During the early stages of a run as the leading edge of the specimen enters the furnace the combustion conditions may vary immediately after the specimen ignites. Data of gas and smoke yield analysis are therefore taken only during the steady state period of at least 10 minutes once conditions have settled to constant conditions as shown by constant gas and smoke concentrations. The steady state period enables batch sampling for particular products and multiple gas measurements.

d) During a run after a flame is established in the hot zone of the furnace, for some materials the flame may spread rapidly back along the unburned specimen, disrupting the steady state combustion. In order to prevent this the standard requires a minimum of rate of sample introduction of 40 mm/min, providing a total 20-minute test run.

e) A potential issue with measurement of gas and smoke concentrations in the chamber occurs if the products are not well mixed. For the original method this was achieved by introducing the secondary air flow directly into the plume emerging from the furnace tube. This also ensured rapid cooling of the plume to <40$^{o}$C. Even mixing with the chamber was confirmed by sampling from multiple locations within the chamber.

f) Potential issues with the determination of the fuel/air equivalence ratio can occur if there is any secondary oxidation of partially burned fuel products in the plume emerging from the furnace tube as it mixes with dilution air under fuel rich combustion conditions, or if there is any backflow of air from the mixing chamber into the heated end of the furnace tube. Since the calculation of fuel/air equivalence ratio is based on the assumption that only the primary air supply is available for combustion, any secondary oxidation or combustion resulting from air in or form the mixing chamber will result in additional oxidation of products and an actual equivalence ratio somewhat lower than the calculated value.

g) During early development of the method secondary flames were formed in the mixing chamber at the end of the furnace tube for some runs involving highly fuel rich mixtures at high furnace temperatures

and low primary air flows at 1 L/min. Modifications with higher flow rates have eliminated these occurrences although a blow-out panel is fitted for safety purposes. Minor non-flaming secondary oxidation is prevented by rapid cooling as the plume enters the chamber.

h) For early versions of the apparatus using a much wider tube problems were encountered in obtaining stable combustion for fuel rich mixtures. This was found to be due to layer formation and possibly back pressure differences resulting in air flowing into the furnace tube from the mixing chamber. Once identified, this problem was solved by using the standard narrower tube and the use of a flow restrictor at the end of the furnace tube. Analysis of early data using the standard tube also showed some evidence for limited additional oxidation from air entry near the end of the furnace tube for fuel rich conditions (especially for polyethylene) when the primary air flow rate was <2 L/min. Following this the use of a flow restrictor for lower flow fuel rich runs was recommended. The effects with and without the flow restrictor were examined for the round robin experiments prior to the latest version of the standard. The results showed no difference in equivalence ratio or CO yields between runs with and without a flow restrictor, and no evidence of air flow entering from the mixing chamber. To ensure that this secondary combustion could not occur in future tests a flow restrictor was required in.

A feature of the Purser Furnace is that as the fire load is gradually introduce there is present in the sample a range of fire conditions. The first burnt fuel will have the highest residence time and will burn the fire load to a char as the fuel is advanced and the new fuel being introduced at the leading edge of the fire will be undergoing pyrolysis and in the middle will be flaming combustion. Thus all stages of a fire are present at once. This should be an advantage of the method as all phases of the fire process are present in real fires, but some have seen this as a disadvantage. The Cone Calorimeter also has all phases of a fire present. The top surface is char and below this as the heat is conducted material is undergoing pyrolysis and then flowing upwards through the char layer.

### 9.1.2 The Redesigned Furnace for Toxic Gas and Particulate Measurements

For the Leeds Purser Furnace some design changes were made to solve the design problems in the original equipment identified in the previous section.

a) Potential secondary combustion explosion problem
   I was considered that the risk of an explosion in the discharge volume is protected by an inadequately sized vent. Prof. G.E. Andrews, as an expert in gas explosion vent design, re-designed the vent size using NFPA 68 2007. The EU vent design method produced a vent size large than could be fitted into one side of the discharge volume.
b) Potential back flow problem
   The back flow of dilution is into the reaction tube was prevented by adding an orifice plate at the end of the Quartz tube. This created a static pressure in the reaction tube greater than the discharge volume pressure. Also, the pipe connecting the dilution volume to the discharge was made much larger so that the back pressure of the outflow was minimised. This combination of measures ensured that no back flow could occur.
c) Diluted Sampling Point – potential mixing problem
   The diluted sample for analysis was taken from the middle of the mixing chamber in the original design and it was considered that the two-flow stream may not have mixed and reacted completely at this sample point. The uncertainty was how to make sure that the point was well mixed. To overcome this problem the sample was taken using a multi-hole sample probe in the large diameter discharge pipe after a $90^{o}$ bend, which would help the mixing. This improved mean gas sample point was used for the particulate mass and particle size and the test rig was fitted with three separate sample points so that particle mass, particle size and gas analysis could be done from the mixed discharge gases simultaneously.
d) Secondary Oxidation avoidance of potential secondary combustion
   The problem of secondary oxidation by diluted air is a problem with all bench-scale methods that do not use raw gas sampling, which is most fire research test rigs. In order to prevent dilution air entering the furnace tube from the mixing chamber restrictor (reduced diameter discharge orifice plate) was fixed to the end of the furnace tube.
e) Raw Gas Sampling

The physical composition of a hot fire effluent plume changes significantly from just beyond the flame zone as it entrains air, cools and flows downstream. As the effluent cools water and some organic vapours condense into droplets. Carbonaceous smoke particulates agglomerate to form greater concentrations of larger particles. Acid gases dissolve in water droplets and are partly adsorbed onto smoke particles, as are organic vapours. As the effluents are further diluted distant from the source some liquid droplets may then evaporate as the vapour pressure decreases.

The tube furnace apparatus has been designed to provide a cooled, diluted atmosphere such as is likely to be inhaled by a fire victim some distance from a fire combustion zone and at temperatures below those capable of causing pain or respiratory burns, in order to measure the toxicity of the inhaled effluents. The diluted atmosphere was also necessary for sampling and analysis by gas and smoke analytical equipment.

For the study reported here the particulates were measured from cooled diluted atmosphere from the mixing chamber, but for the gases and organic vapours it was considered of interest to sample and measure the hot, raw effluents, which was possible using the Leeds FTIR analyser. This ensured that the water and organics did not condense and remained in the vapour phase.

The diluted flow changes the dew point of the mixture so that the water in the products of combustion does not condense and the condensation of other species is also prevented. However, this is at the expense of continuing oxidation of unburnt toxic species so that toxic yields are underestimated. The only solution to this problem is to use raw gas sampling from the Quartz tube well upstream of the discharge point. The raw gas sampler would pull air from the discharge volume, but this is prevented by the use of the discharge orifice with an adequate back pressure to prevent the gas sample suction pump entraining gases from the dump volume. In this work the raw gas sample was an uncooled stainless steel tube mounted on the centreline of the Quartz tube and passing across the discharge volume to a heated sample line connected to the heated pump and filter for the FTIR and finally through another heated sample line to the heated FTIR and from there to a water condenser and then to the Oxygen analyser.

## 9.2 Engineered Design

The diagram of the old version of Purser Furnace and the engineering drawings of the new Purser furnace design are shown in Figure 9.1 (a) and (b). The detailed of assembly drawings are also attached in Appendix F.

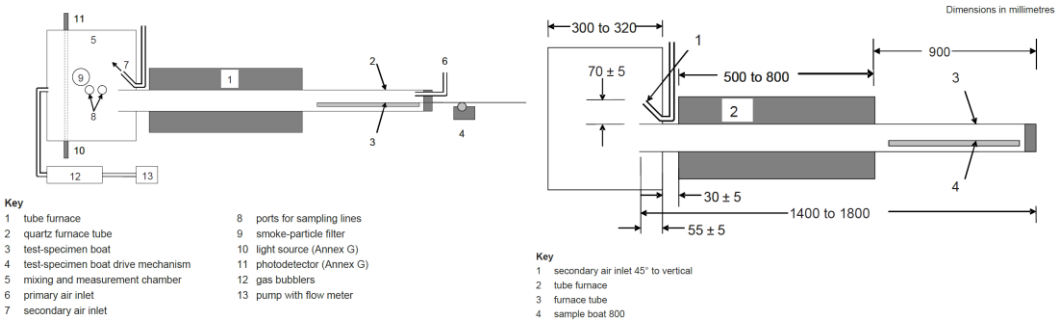


**Figure 9.1 (a)** Diagram of the old version Purser Furnace System [104].

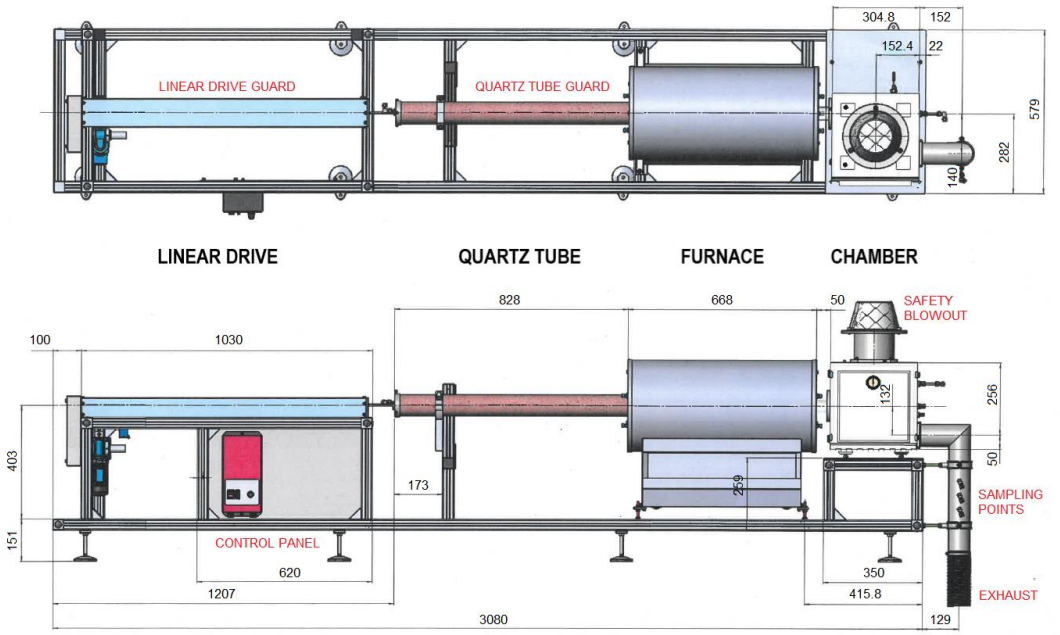


**Figure 9.1 (b)** Overall diagram of the new Purser Furnace System.

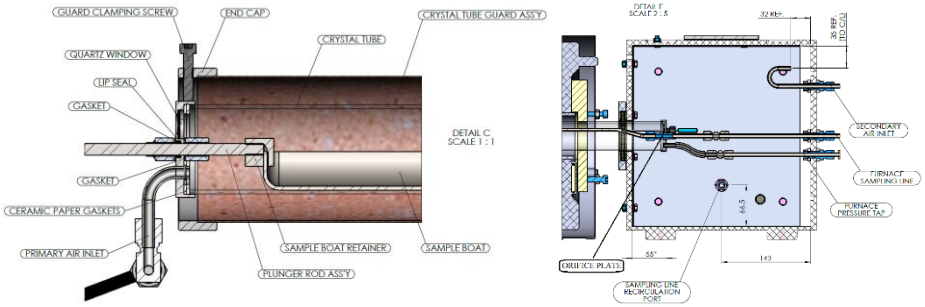


**Figure 9.1 (c)** Quartz tube ends were sealed using the end caps.

As shown in Figure 9.1 (c), the end of the Quartz tube was sealed against the tube and for the passage of the boat traverse using the end caps. The Quartz window was sealed within the end cap using high temperature silicon. The lip seal was sealed and positively retained within the end cap by means of 2 compressed gaskets. With the Quartz tube guard assembly in position, 3-off guard clamping screws could be tightened about the end cap to retain the crystal tube in place. The location of the dilution air and the way it impinges on the dilution chamber wall to increase mixing with the discharge gases is shown in Figure 9.1 (c).

### 9.2.1 Insertion of Orifice Plate to Overcome Back Flow Problem

An orifice plate was placed at the end of the furnace tube in the chamber. This orifice cause a greater than 90 % flow blockage and was 3 mm diameter. Two manometers were also used to measure the pressure difference in the furnace and the mixing chamber. It was ensured that the pressure inside the furnace was always more than the mixing chamber during the time of the test.

### 9.2.2 Mixing Improvement in the Measurement Chamber

Secondary air was supplied into the measurement chamber to dilute the gas effluents before being discharged safely through the exhaust pipe. A pipe with a bend end was used for supplying the secondary air to provide more time for mixing to come up with reasonable and more realistic results. With the secondary air tube end was placed facing back to the chamber wall and the supplied air would disperse back to all directions inside the chamber, it would help and improve a mixing of the air and gas effluent mixture to become more homogenous before further samplings in the exhaust line.

### 9.2.3 Explosion Vent Installation

When the test was continued without the existence of a flame, flammable vapour fuel was produced, and that could lead to an explosion. The safety blowout vent was used to prevent such event. The design of the vent area was corresponding to the US standards as for the EU standards; the vent size was greater than the size of the wall. Also the discharge volume was smaller than the EU standard was applicable for. The explosion vent was installed at the top of the dilution and consisted of commercial Aluminium foil. The foil was prevented from accidental damage using a steel net bolted at the top end of the vent, as shown in Figure 9.1.

### 9.2.4 Direct Heated Gas and Diluted Samplings

The conventional Purser Furnace design takes the toxic gas sample from the middle point inside the measurement chamber. In the current design of the new Purser Furnace, there were four sampling points that were available: one was designed for a raw undiluted gas sample and three sampling points were available on the exhaust line for the diluted gas sampling by different external analysers. In the present work, the FTIR analyser was attached to the heated gas sampling line for toxic gas measurement, meanwhile the DMS500 Particle Sizer and the particle mass Smoke Meter were attached to the diluted sampling points for measurements of particle size and soot mass.

## 9.3 Construction Works of the Modified Furnace System

The new developed furnace system, the Purser furnace has four separate main sections which are the driving mechanism system, the glass furnace tube, the tube furnace and the mixing and measuring chamber. Each section was designed separately before being assembled during the installation. A proper equipment frame and base was at first designed and installed as a stable place and a support system for placement and assembly of all those new furnace sections.

### 9.3.1 Driving Mechanism System

During the fire toxicity test, the fuel is placed uniformly in the sample boat inside the crystal tube. It is fed through the crystal tube into the furnace by the driving components which function to push the sample boat through the crystal tube into the tube furnace at a desired speed rate. For a complete drive mechanism, it includes a driven shaft, a driving motor and a controller system. The drive mechanism system which is constructed in the present study as shown in Figure 9.2.

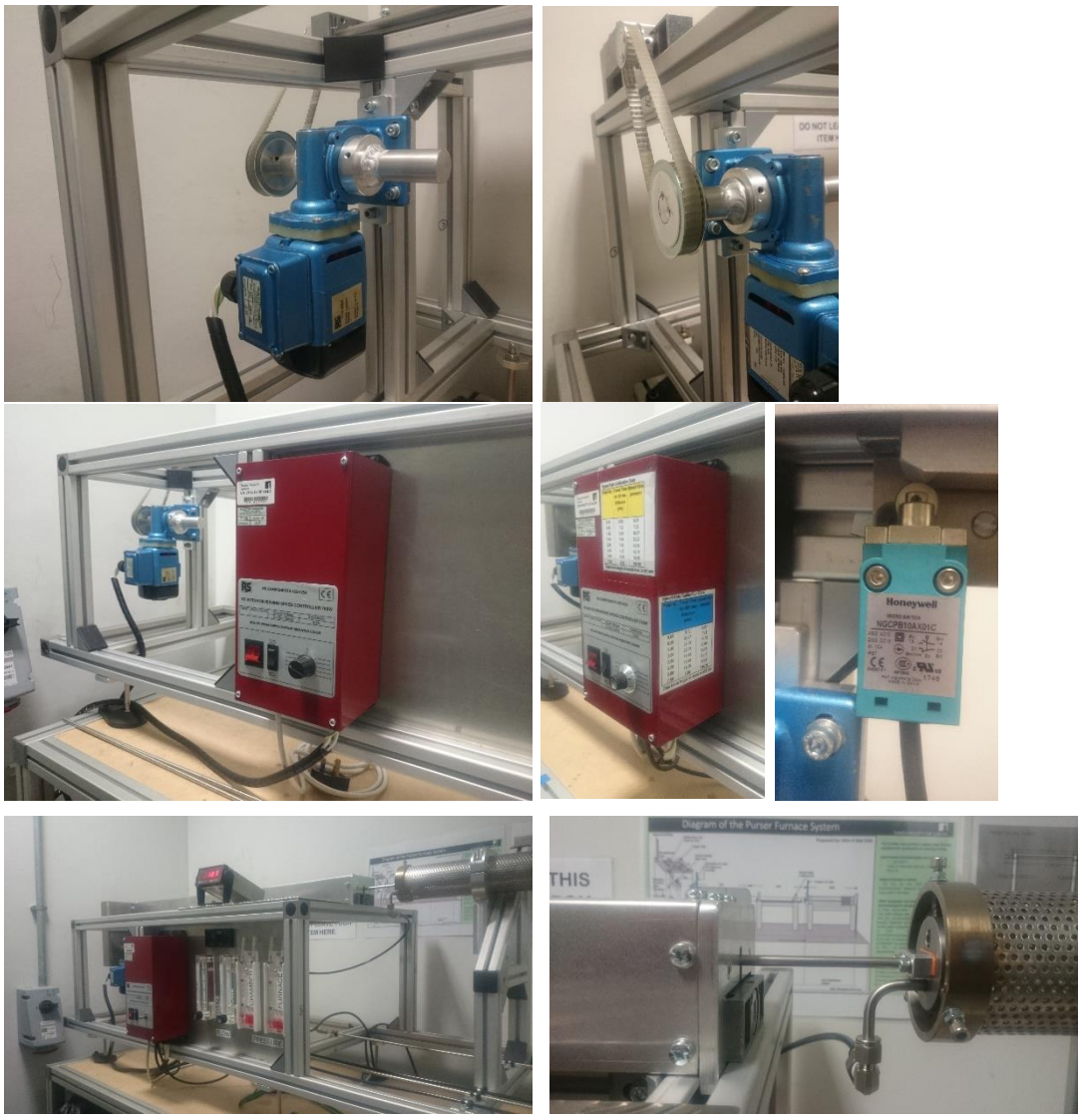

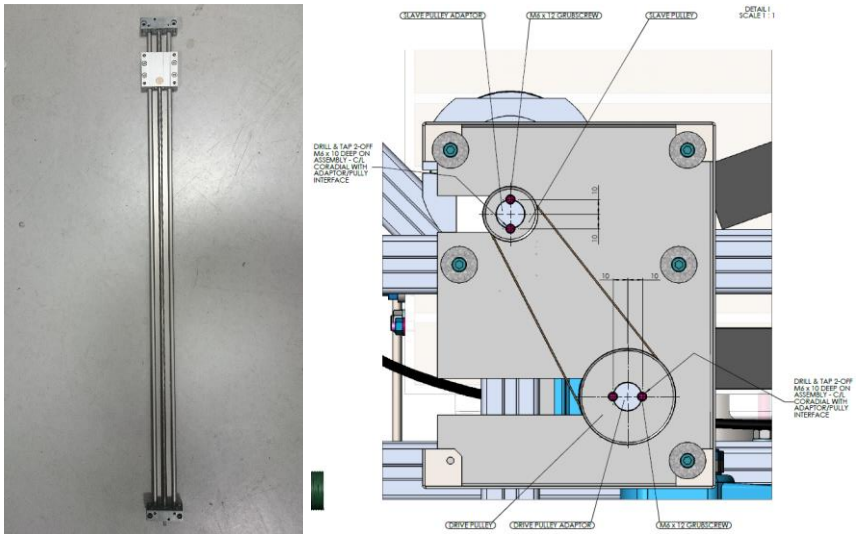

**Figure 9.2** Driving motor, driving belt and driving controller.

### 9.3.1.1 Gear Ratio Calculations

Combination of suitable gears is selected based on the determination of the gear ratios. Gear or velocity ratio ratios are calculated as the following calculations.

Output speed from the driving motor = 55 rpm (This is the desired input speed at the driver gear).

1st pulley/gear – 40 teeth

2nd pulley/gear – 22 teeth

$$Gear\ Ratio = \frac{Driven\ Gear}{Drive\ Gear} = \frac{40}{22} = 1.88 \qquad (35)$$

Output speed at the driven gear = 55 x 1.88 = 103.4 rpm

*2 mm linear drive screw pitch (Pitch is the distance between teeth).

Shaft speed = 103.4 x 2 = 206.8 mm/min

In the standard the fuel feed rate is 60mm/min for fast burning materials. If the maximum shaft speed is 70 mm/min, the best combination of pulleys or gears will be as follows:

Output Speed = 70/2 = 35 rpm

Gear Ratio = 35/55 = 0.64

So, a larger (drive gear) to a smaller gear (driven gear) combination is needed. Available gear combination with the appropriate number of teeth were selected based on the closest required specification and item availability.

1st pulley/gear – 22 teeth (driven gear)

2nd pulley/gear – 34 teeth (drive gear)

Gear Ratio = 22/34 = 0.65

### 9.3.1.2 Verification of Driving Speed

In order to verify the driving speed of the drive mechanism, RPM (revolutions per minute) reading device is used in measuring the actual produced speed by the driving system. Calibration of fuel feed rate was also determined by measuring time manually with a stopwatch at several moving distances of the sample boat with the maximum travel length of 685 mm. The determined speed rate values as function of travel time and dial number is shown in Figure 9.3 and some points were summarised and included in Table 9.1. Each dial or point number represented certain fuel feed rates by the sample boat and this proportionate to certain equivalence ratio values (refer Table 3.9) which could be set before the start of test in the Purser Furnace System.

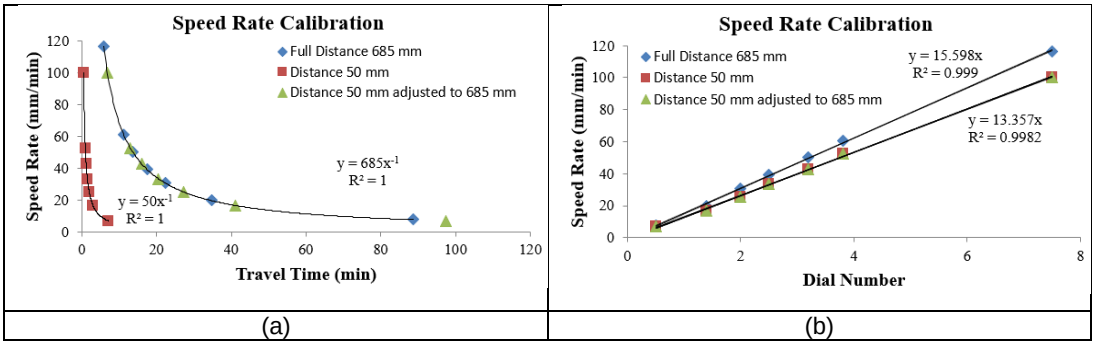


(a) (b)

**Figure 9.3** Speed rate values as a function of travel time (a) and dial number (b).

**Table 9.1** Calibrated values for fuel feed rate at corresponding dial or point number.

**Speed Rate Calibration Data**

| Point No. | Travel Time for 685 mm Distance (min) | Speed Rate (mm/min) |
|---|---|---|
| 0.00 | 0.00 | 0.00 |
| 0.50 | 88.57 | 7.73 |
| 1.40 | 34.73 | 19.72 |
| 2.00 | 22.33 | 30.68 |
| 2.50 | 17.45 | 39.26 |
| 3.20 | 13.65 | 50.18 |
| 3.80 | 11.25 | 60.89 |
| 7.50 | 5.88 | 116.50 |

*Total travel length of driver is 685 mm*

### 9.3.2 Quartz Tube

Transparent glass was a good choice and recommended to be used in the present work for easy observation of fire performance during conducted fire tests. However in order to protect the Quartz tube from broken in case of mishandling and for safety reason such as to prevent from a direct contact with possible hot surface of the glass tube during equipment operation, a perforated metal tube cover was installed. Furnace Quartz tube with metal tube cover as shown in Figure 9.4. Another way had been applied in the present work in order to observe the flames during the conducted furnace tests by placing a glass mirror at centre of the linear drive guard end or Quartz tube start end which could reflect the flame image in the furnace.

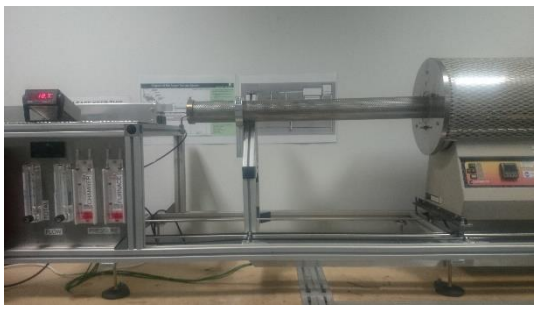

**Figure 9.4** Furnace Quartz tube.

### 9.3.3 Tube Furnace

The tube furnace (Carbolite) as shown in the following Figure 9.5 was used to fix the test at a specific temperature during the test so different fire stages could be obtained. For example, the temperature was about 650$^{o}$C and 850$^{o}$C for well-ventilated and post-flashover respectively. It should be noted that the temperature of the furnace that was maintained manually was the temperature of furnace walls, not hot gases temperature. For PE-Y fire toxicity tests in the present work, the furnace temperature was set at 600$^{o}$C with varying equivalence ratios. Temperature profiles (see Figure 9.8) in the Purser Furnace during tests were measured by the Thermocouples and could be observed properly throughout the experiment.

**Figure 9.5** Main section of the tube furnace.

### 9.3.4 Mixing and Measurement Chamber

Figure 9.6 showed the configuration of measurement chamber for Purser Furnace System. A 12 inch square clear Acrylic box or chamber was used to collect the toxic product gases. The sampling was taken from the middle of the box from the original design of the tube furnace. For the modified design, the sampling were taken in the middle at the end furnace tube for raw gas sampling and the sampling point could be adjusted and varied as desired.

Other sampling points were also available and accessible by measuring devices on the exhaust pipe for diluted gas sampling.

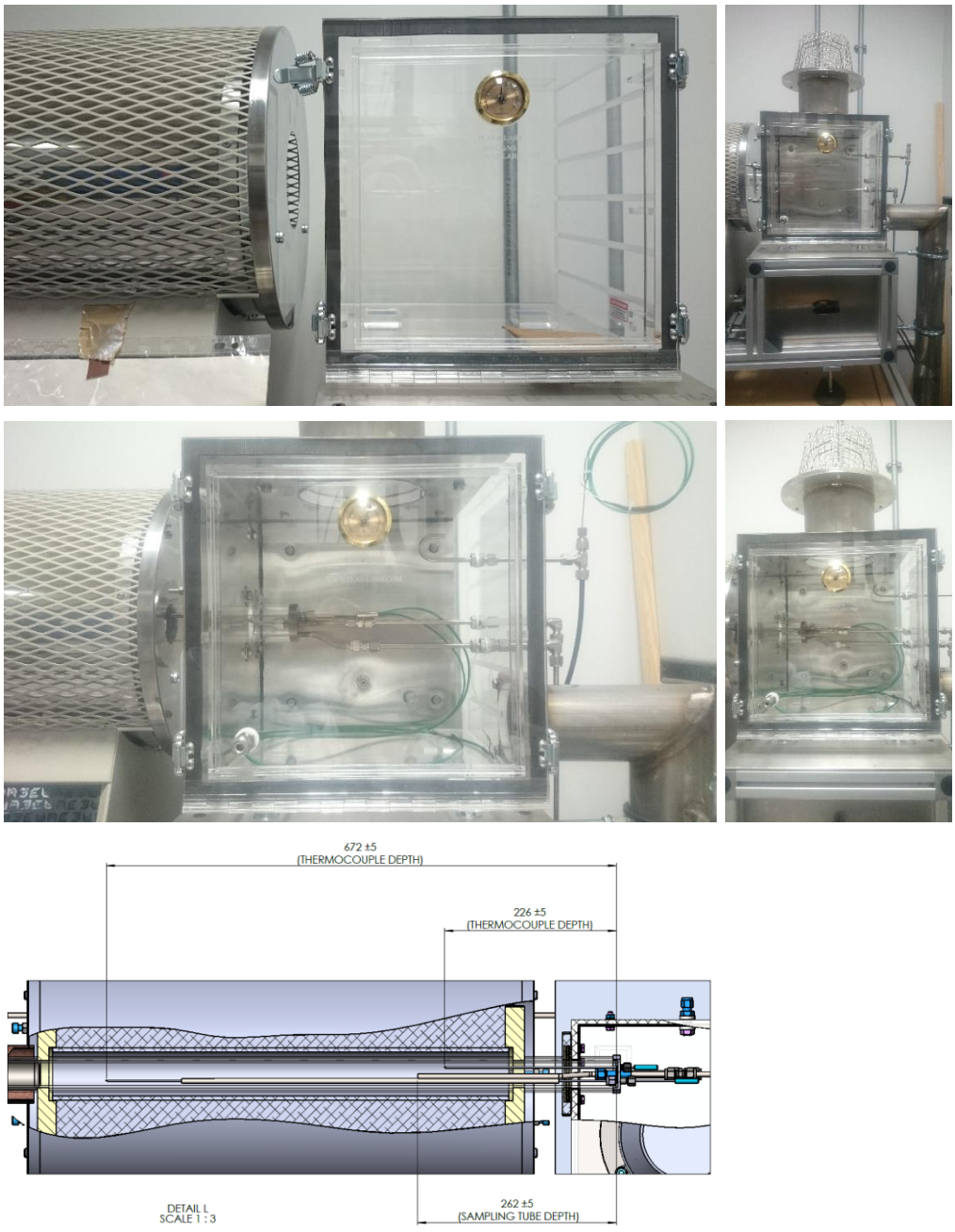


**Figure 9.6** Transparent chamber of the new furnace rig.

## 9.4 Commissioning and operation of New Purser Furnace System

For commissioning and operation of the new .Purser Furnace, using the same Polyethylene (PE-Y) material that was used in the Cone Calorimeter. Photos taken before, during and after test are shown in Figure 9.7. The flame was observed using a glass mirror placed centrally at the end of the linear drive guard that viewed the flame through a Quartz window of 10 mm diameter. A mirror was used externally so that the flame could be viewed during the experimental. Details of the Test Procedure for the Purser Furnace is included in Appendix C.

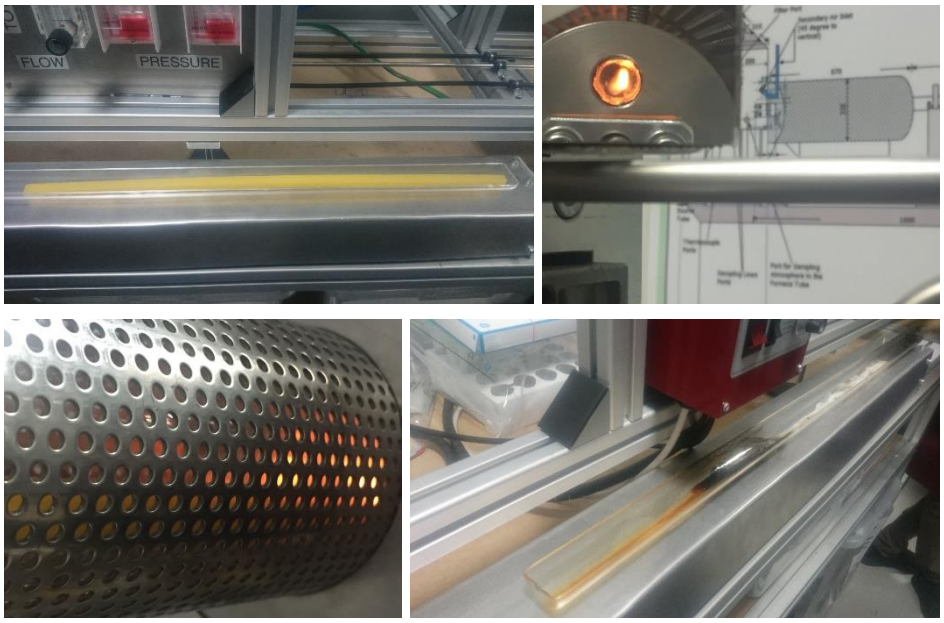


**Figure 9.7** Before, during and after test observations.

## 9.5 Experimental Data

PE-Y samples with 9 mm thickness and 600 mm length were tested at two different metered mean equivalence ratios, ER = 2.0 and ER = 0.8. An ER of 0.8 represents the early stages of a fire and ER of 2.0 represents the later post flash over stages of a fire. The results were also compared with the PE-Y fire in the Cone Calorimeter. Table 9.2 shows the calculated traverse motor speed to achieve the desired equivalence ratio. The initial air flowrate was set to 10 L/min (~0.2 g/s) for both tests with different fuel feed rates into the

furnace to achieve the desired equivalence ratio, The comparison of the results for both fires in the Purser Furnace were presented in this chapter and were also compared with the result for PE-Y fire in the Cone Calorimeter from Chapter 6.

**Table 9.2** Calculated details and parameters prior to Purser Furnace tests.

| Information | Test No. | |
|---|---|---|
| | **T1 31.07.2018** | **T2 01.08.2018** |
| Fuel Type | PE-Y | PE-Y |
| Mass (g) | 49.3 | 47.3 |
| Fuel Length (mm) | 600 | 600 |
| Mass Per Unit Length (g/mm) | 0.0822 | 0.0788 |
| Speed Rate (mm/min) | 19.72 | 7.73 |
| Speed Rate (mm/s) | 0.3287 | 0.1288 |
| Fuel Mass Flow Rate (g/s) | 0.0270 | 0.0102 |
| Air Flow Rate (L/min) | 10 | 10 |
| Daily Air Density ($g/m^3$) | 1204.1 | 1204.1 |
| Air Flow Rate (g/s) | 0.2007 | 0.2007 |
| AFR Actual | 7.4312 | 19.7594 |
| AFR Stoic. | 14.92 | 14.92 |
| Equivalence Ratio, $\phi$ | 2.0 | 0.8 |

The furnace tube was also instrumented with inlet and exit Type K mineral insulated thermocouples and the temperature as a function of time are shown in Figure 9.8. The temperature values at an average of 500$^o$C at the furnace start point and 450$^o$C at the furnace end point before the ignition and after the flame out, about 100$^o$C to 150$^o$C difference with the set furnace temperature (600$^o$C). The maximum average flame temperature was slightly higher for rich PE-Y fire (ER = 2.0) but for lean PE-Y fire (ER = 0.8), the flame temperature had reached the maximum point at about 700$^o$C. The ER 0.8 test had a significant temperature rise due to the heat release immediately after a flame was observed. For a short time this heat release gave a temperature higher than the set furnace temperature. There was no equivalent event for the rich mixture.

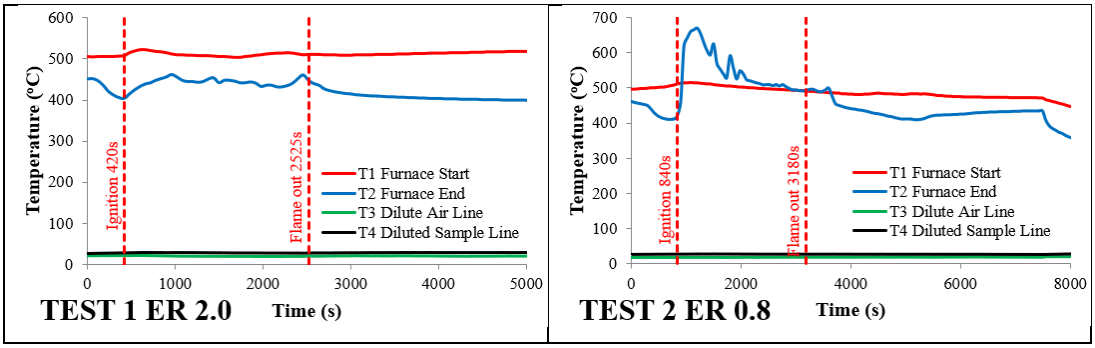


**Figure 9.8** Temperature profiles in the Purser Furnace tests: Test 1 is ER 2.0 and Test 2 is ER 0.8.

Table 9.3 includes the details for PE-Y fires in the Purser Furnace and Cone Calorimeter. Rich PE-Y fire in the Purser Furnace had reached an ignition at 420 s and flame out at 2525 s while lean PE-Y fire had an ignition delay of 840 s, double that of the rich PE-Y fire with a longer burning period before flame out at 3180 s. Compared with PE-Y fire in the Cone Calorimeter with irradiation level of 35 kW/m$^2$ and free ventilation, it gave an ignition at 87 s and a flame out at 846 s.

**Table 9.3** Test details for the Purser Furnace tests.

| Test | Polyethylene Type | Test Condition | Thickness (mm) | Initial Mass (g) | Ignition (s) | Flame out (s) |
|---|---|---|---|---|---|---|
| **PURSER FURNACE** | | | | | | |
| 1 | PE-Y | ER 2.0 | 9 | 49.3 | 420 | 2525 |
| 2 | PE-Y | ER 0.8 | 9 | 47.3 | 840 | 3190 |
| **CONE CALORMETER** | | | | | | |
| 3 | PE-Y | 35 FV | 9 | 78.0 | 87 | 846 |

### 9.5.1 General Combustion Properties

The initial mass of PE-Y samples were included in Table 9.3 with CC 35 FV sample = 78.0 g, PFS T1 ER 2.0 = 49.3 g and PFS T2 ER 0.8 = 47.3 g. From Figure 9.9 (b), for the tests in the Purser Furnace, PFS T1 ER 2.0 fire had given a lower mass loss (wt.%) than PFS T2 ER 0.8 fire. In under ventilated fire condition, less amount of fuel was burned compared to well ventilated fire condition. The higher total mass fuel burned, the higher mass loss would be. This is showed by the PE-Y fire in the cone which giving a higher mass loss than PE-Y fires in the furnace. The maximum $O_2$ consumption (11%) by the PE-Y fire in the Cone Calorimeter with free ventilation condition was about

half than the $O_2$ consumption by the PE-Y fires in the Purser Furnace with restricted ventilation condition. The Purser furnace Oxygen measurements did not seem to relate to the set equivalence ratio with the lean mixture having very low Oxygen. This would indicate that its actual combustion ER was richer than the set value.

The MLR for the Purser Furnace (where mass is not directly measured) was calculated from the Carbon balance A/F (Chan Equation) and the measured air flow rate. The HRR could be calculated for the Purser Furnace from this calculated mass loss rate or by the Oxygen consumption method. The MLR was at the highest of ~0.4 g/s (at 700 s) for PE-Y fire in the cone while the MLR values for PE-Y fires in the furnace were not more than 0.1 g/s (less than quarter compared to the PE-Y fire in the cone).

The PE-Y fire in the cone had reached the maximum HRR of ~1800 kW/m$^2$ while PE-Y fire in the furnace had given the highest HRR less than 400 kW/m$^2$. In comparison between PE-Y fires in the furnace, HRR was higher for PE-Y fire with ER = 2.0 (rich fire condition) than PE-Y fire with ER = 0.8 (lean fire condition). These PE-Y fire samples had experienced rich burning condition with equivalence ratios above 1.0 as shown in Figure 9.9 (e). The following Figure 9.9 shows general combustion properties for PE-Y fires in the Cone Calorimeter and Purser Furnace at different fire conditions.

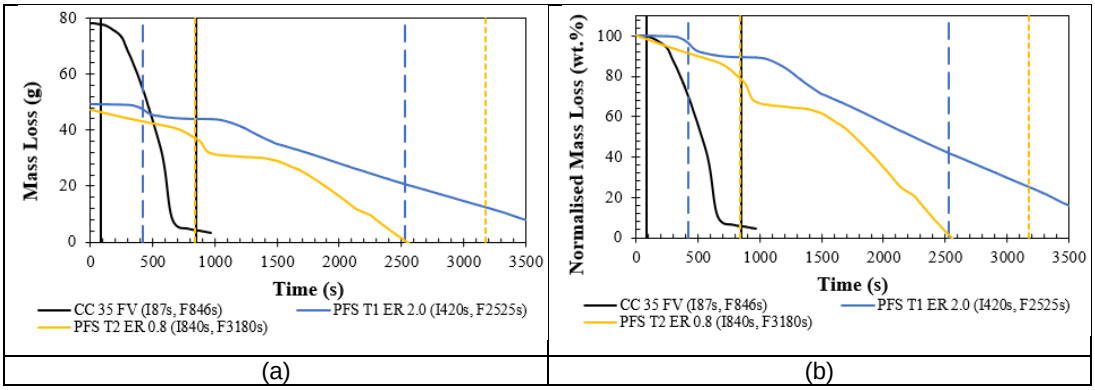


(a) (b)

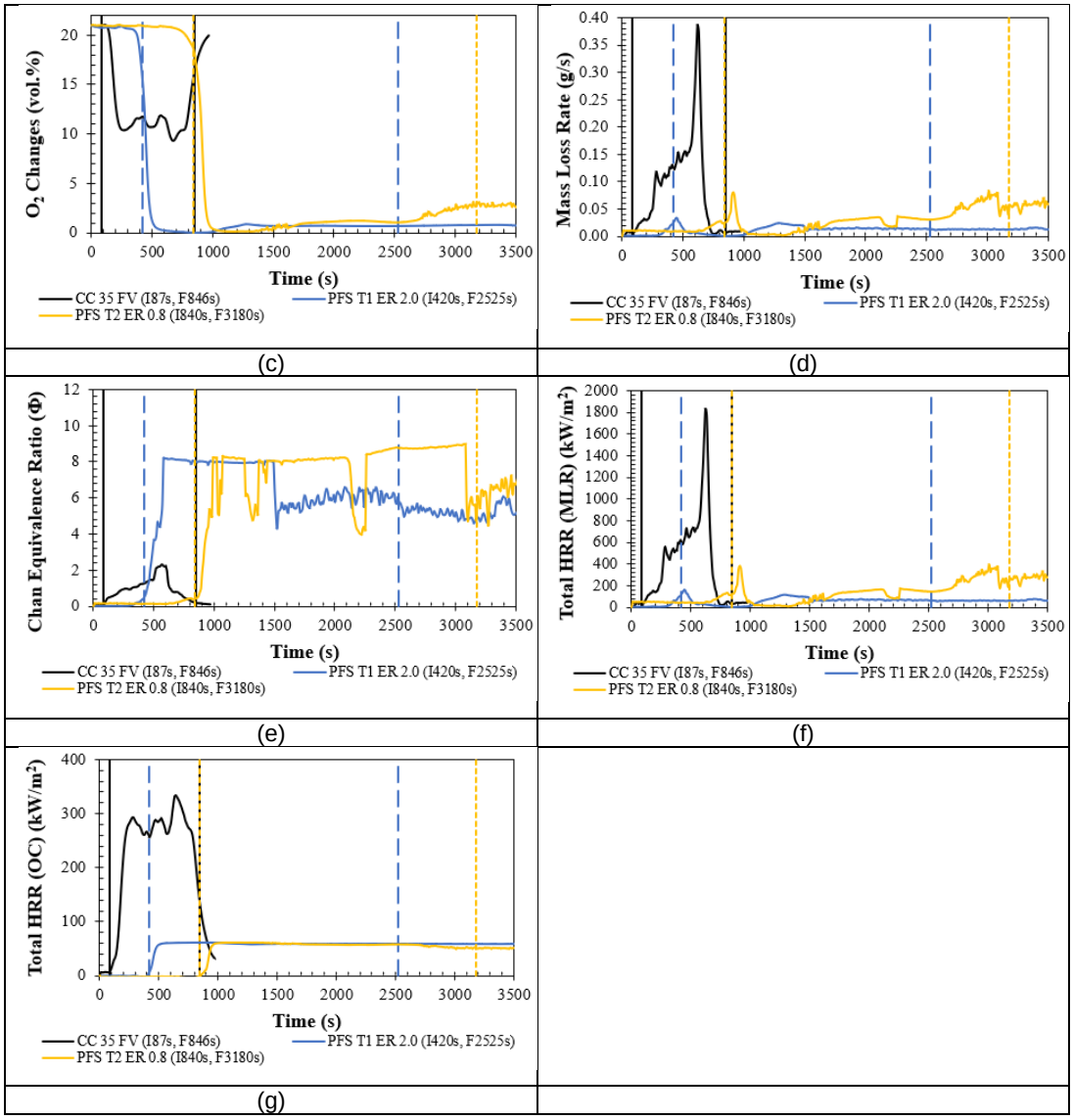


**Figure 9.9** General combustion properties for PE-Y fires in the Cone Calorimeter and Purser Furnace at different fire conditions.

## 9.5.2 Toxicity of Polyethylene Fires in the Cone Calorimeter and Purser Furnace Tests

### 9.5.2.1 Gas Concentration (Raw Gas Samples)

Gas concentrations measured by the FTIR were compared between Cone Calorimeter and Purser Furnace methods, considering a fire period from the start of ignition until the flame out state. This consideration was taken due to a limitation of measurement scale by the FTIR which giving very high concentrations for several species especially after the flame extinguished. Figure 9.10 shows the concentration of gases for PE-Y fires in the Cone

Calorimeter and Purser Furnace at different fire conditions. CO concentration was the highest of ~3200 ppm at burning time of 500 s for PE-Y fire in the Cone Calorimeter. At the same burning time, the PE-Y in the Purser Furnace with ER = 2.0 gave the highest CO peak of ~3000 ppm, slightly lower compared to the PE-Y fire in the Cone Calorimeter test. Meanwhile, the PE-Y fire with ER = 0.8 (fuel lean concentration) had given a CO peak of about 3000 ppm at 1000 s. The CO concentration for these fires from both methods were in the same average.

The concentration of HCN produced from PE fires was less than 800 ppm for the total burning period of 3500 s. Irritants like HCl and HF were giving concentration less than 800 ppm and 70 ppm. From Figure 9.10 (p), HBr concentration measured was very high (peak of 16000 ppm) for PE-Y in the Cone Calorimeter while for the Purser Furnace tests, the HBr peak was 16 times lower than that. It is likely that this was due to different Bromine fire retardant concentrations in the two species of PE-Y, although we were assured by the industrial suppliers of the materials that they were the same sample.

This HBr problem is possibly because the limit of the calibration range which caused the out of measurement scale when measuring this species concentration. This is only a problem for the sample of PE-Y tested on the cone, as the HBr levels are much lower for the PE-Y tested on the Purser furnace, but the HF levels are much higher. This indicates that these two PE-Y samples are not the same, in spite of the colour being the same.

The maximum $CO_2$ concentration was higher for PE-Y fires in the furnace test (10% vol.%) than the cone test (7 vol.%). This was because of the higher combustion efficiency when the fire temperature was maintained by the electrical heated furnace. In overall, gas concentration of PE-Y fires in the furnace test were higher than in the PE-Y fire cone test especially for Hydrocarbons.

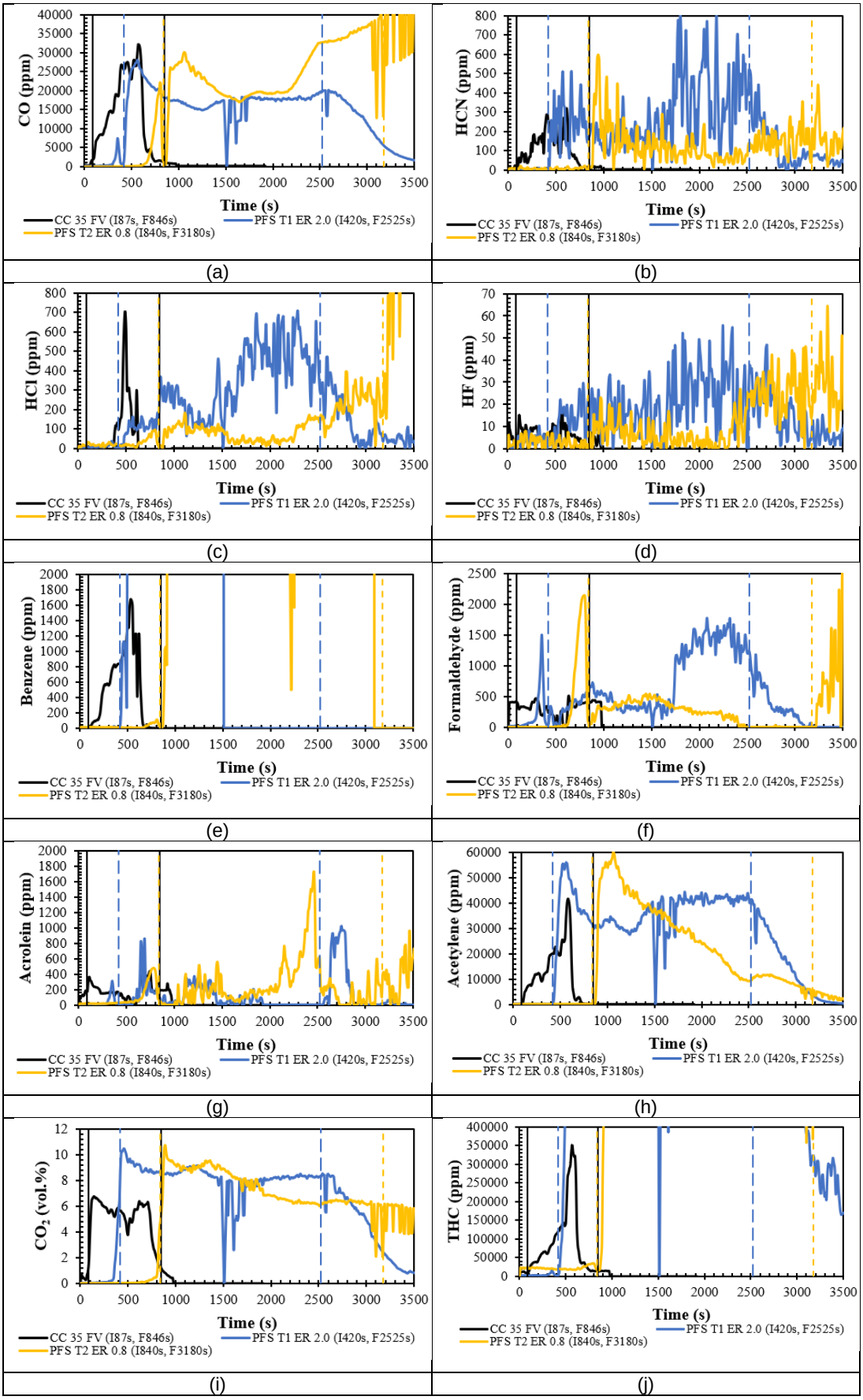
CO (ppm)
Time (s)
CC 35 FV (I87s, F846s)
PFS T1 ER 2.0 (I420s, F2525s)
PFS T2 ER 0.8 (I840s, F3180s)
(a)
HCN (ppm)
Time (s)
CC 35 FV (I87s, F846s)
PFS T1 ER 2.0 (I420s, F2525s)
PFS T2 ER 0.8 (I840s, F3180s)
(b)
HCl (ppm)
Time (s)
CC 35 FV (I87s, F846s)
PFS T1 ER 2.0 (I420s, F2525s)
PFS T2 ER 0.8 (I840s, F3180s)
(c)
HF (ppm)
Time (s)
CC 35 FV (I87s, F846s)
PFS T1 ER 2.0 (I420s, F2525s)
PFS T2 ER 0.8 (I840s, F3180s)
(d)
Benzene (ppm)
Time (s)
CC 35 FV (I87s, F846s)
PFS T1 ER 2.0 (I420s, F2525s)
PFS T2 ER 0.8 (I840s, F3180s)
(e)
Formaldehyde (ppm)
Time (s)
CC 35 FV (I87s, F846s)
PFS T1 ER 2.0 (I420s, F2525s)
PFS T2 ER 0.8 (I840s, F3180s)
(f)
Acrolein (ppm)
Time (s)
CC 35 FV (I87s, F846s)
PFS T1 ER 2.0 (I420s, F2525s)
PFS T2 ER 0.8 (I840s, F3180s)
(g)
Acetylene (ppm)
Time (s)
CC 35 FV (I87s, F846s)
PFS T1 ER 2.0 (I420s, F2525s)
PFS T2 ER 0.8 (I840s, F3180s)
(h)
CO2 (vol.%)
Time (s)
CC 35 FV (I87s, F846s)
PFS T1 ER 2.0 (I420s, F2525s)
PFS T2 ER 0.8 (I840s, F3180s)
(i)
THC (ppm)
Time (s)
CC 35 FV (I87s, F846s)
PFS T1 ER 2.0 (I420s, F2525s)
PFS T2 ER 0.8 (I840s, F3180s)
(j)

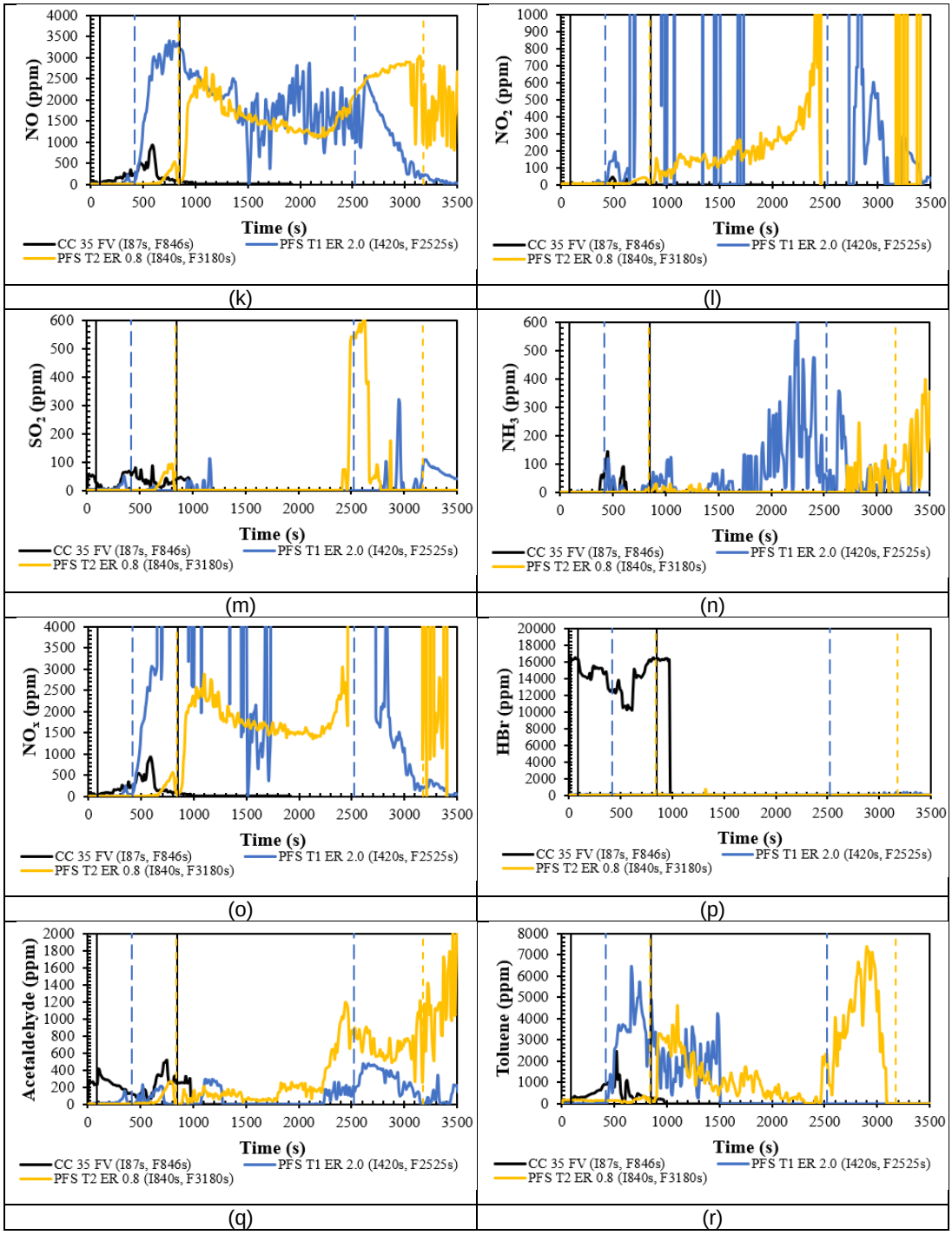


**Figure 9.10** Concentration of gases for PE-Y fires in the Cone Calorimeter and Purser Furnace at different fire conditions.

### 9.5.2.2 Gas Yields

CO yield for Polyethylene fire in the steady state tube furnace (SSTF) reported by Purser [139] was about 0.025 g/g for ER = 0.8 and 0.2 g/g for ER = 1.7. Compared with present work, maximum CO yield for ER = 0.8 was ~0.76 g/g

and for ER = 2.0 was 0.23 g/g. The average CO yield obtained for PE-Y fire in the Purser Furnace was <1.0 g/g for fire equivalence ratio of 0.8 (fuel lean burning) and ~0.2 g/g for fire equivalence ratio of 2.0. CO yield produced from PE-Y fire for under ventilated fire by the present study was in a good agreement with the result reported by Purser [139] for Polyethylene fire in the SSTF.

Figure 9.11 shows yield of gases for PE-Y fires in the Cone Calorimeter and Purser Furnace at different fire conditions. Comparing these PE-Y fires in both methods, HCN yield gave a maximum value of 0.01 g/g. Irritants like HCl and HF each had given a maximum yield of <0.018 g/g and <0.08 g/g as shown in Figure 9.11 (c) and (d). The maximum and mean yields for the three Polyethylene fires in the Cone Calorimeter and Purser Furnace are given in Table 9.4.

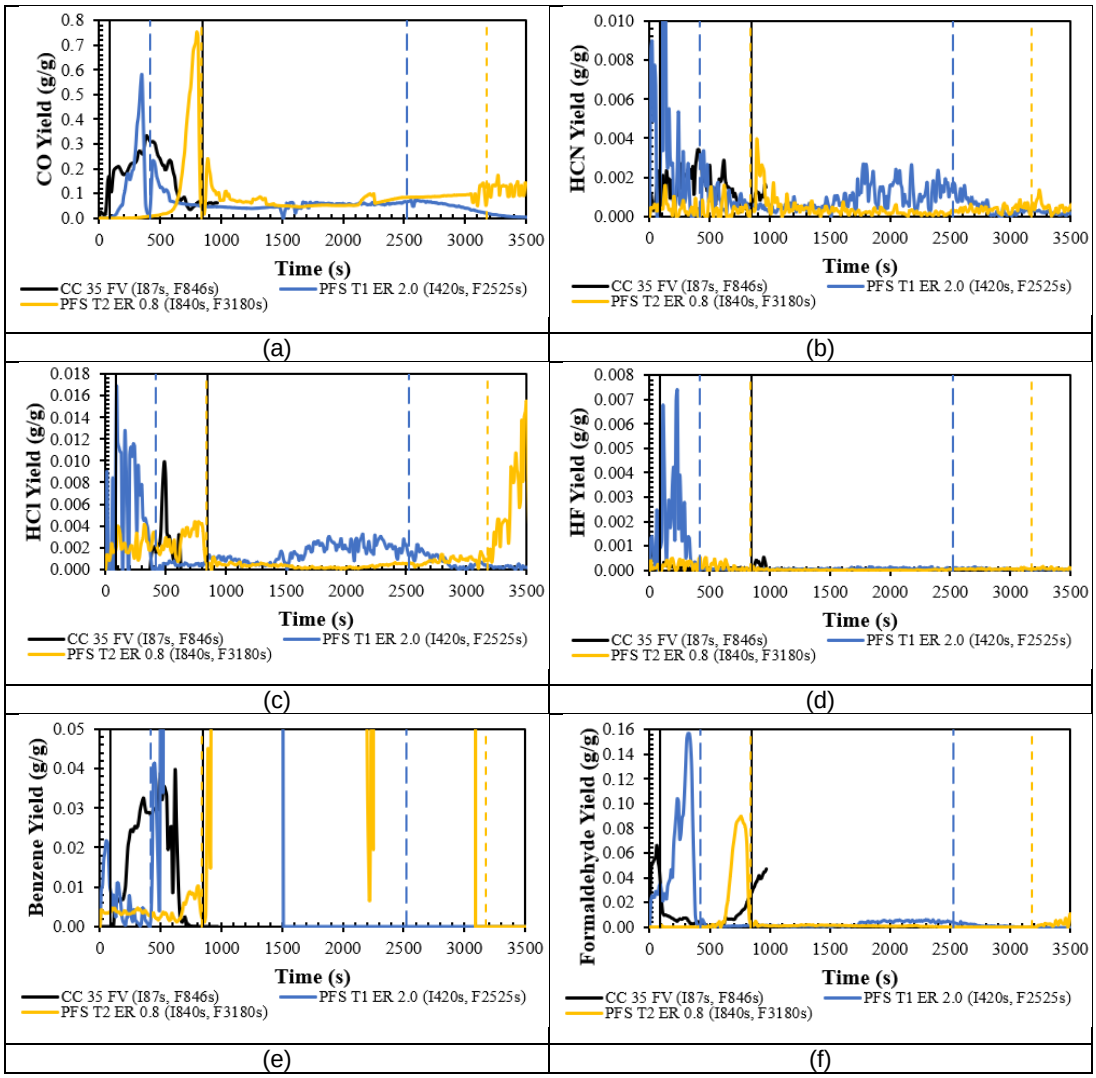

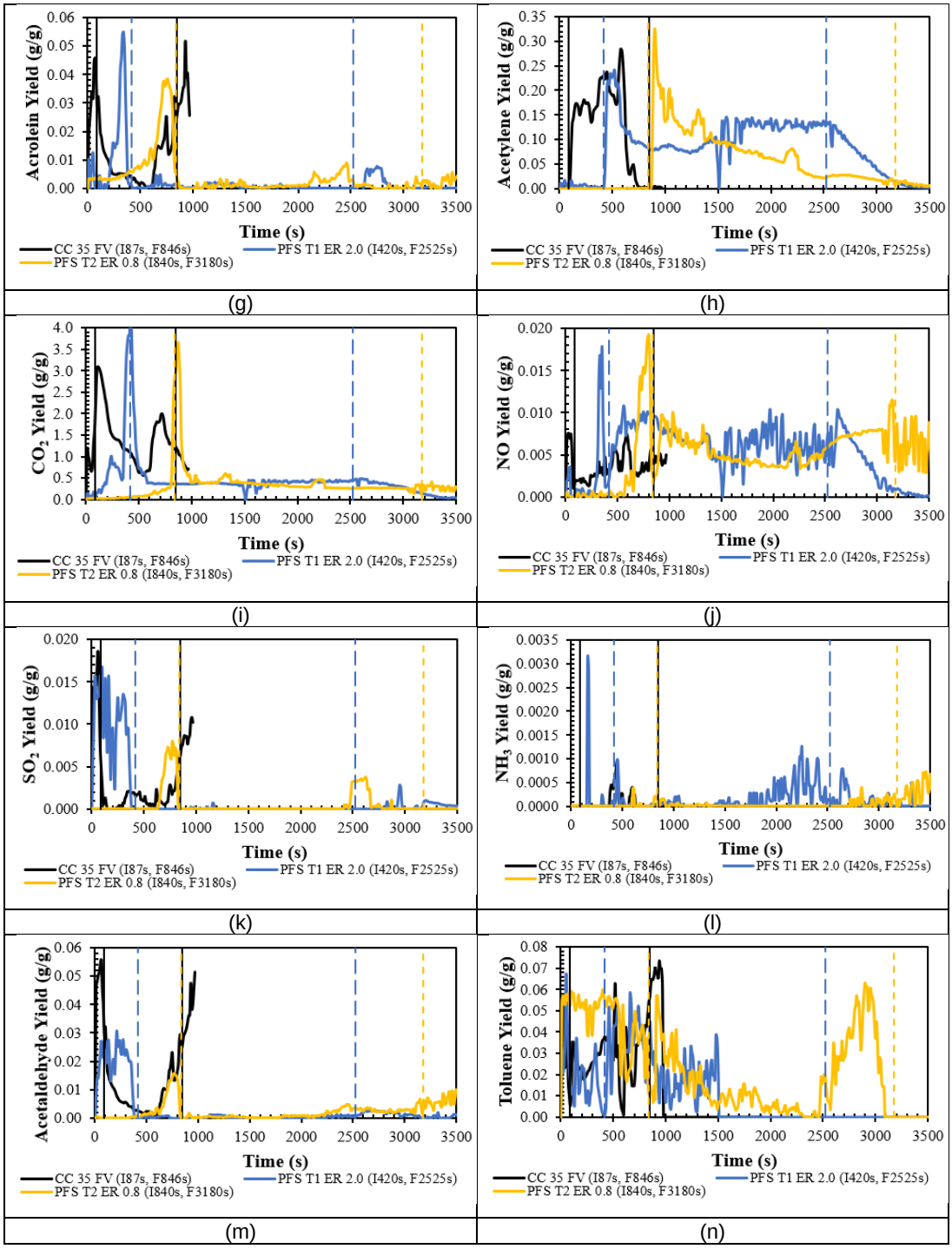


**Figure 9.11** Yield of gases for PE-Y fires in the Cone Calorimeter and Purser Furnace at different fire conditions.

Combustion efficiency, ŋ for PE-Y fires in the Cone Calorimeter and Purser Furnace at different fire conditions is shown in Figure 9.11. Combustion efficiency of these Polyethylene fires were less than 95%. PE-Y fire in the cone test had two peaks of efficiency rate of 60% and 70% at early burning

(~100 s) and near flame out state (~800 s). The highest peak was given at the point when ignition started for PE-Y fires in the furnace tests. CO and $CO_2$ showed a high yield value at the peaks of combustion efficiency rate.

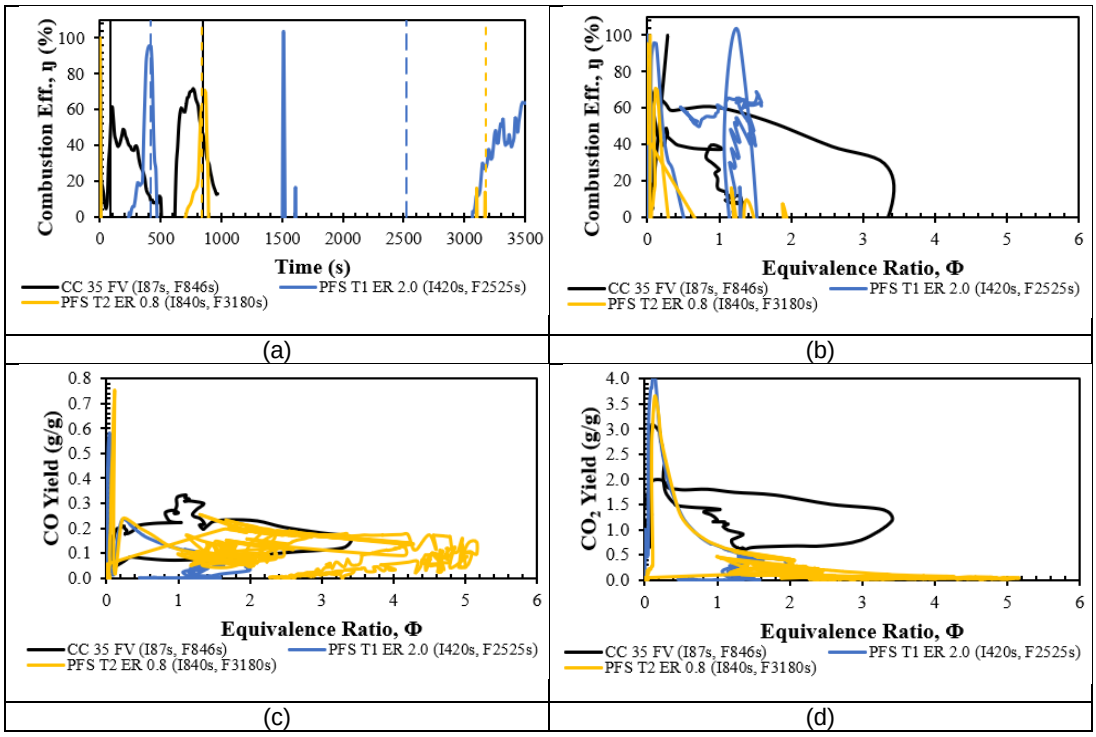


**Figure 9.12** Combustion efficiency, ŋ for PE-Y fires in the Cone Calorimeter and Purser Furnace at different fire conditions.

**Table 9.4** Maximum gas yields for Polyethylene fires in the Cone Calorimeter and Purser Furnace tests.

| Test Method | PURSER FURNACE | | CONE CALORIMETER | | | | |
|---|---|---|---|---|---|---|---|
| **Polymer Type** | **TEST 1 PE-Y** | **TEST 2 PE-Y** | **PE-Y** | **PE-Blue** | **PE-Black** | **SB-P** | **PEP** |
| **Test Condition** | **Φ = 2.0** | **Φ = 0.8** | **35 FV** | | | | |
| **Time Range (s)** | **400-3000** | **800-4000** | **0-970** | **0-1100** | **0-1160** | **0-900** | **0-1200** |
| **Species** | **Maximum Yields (g/g)** | | **Maximum Yields (g/g)** | | | | |
| CO | 0.2337 | 0.7551 | 0.3344 | 0.4360 | 0.3448 | 0.1887 | 0.2769 |
| HCN | 0.0034 | 0.0039 | 0.0034 | 0.0061 | 0.0057 | 0.0060 | 0.0047 |
| HCl | 0.0032 | 894.1868 | 0.0099 | 0.0057 | 0.0088 | 0.0034 | 0.0101 |
| HF | 0.0001 | 0.0002 | 0.0009 | 0.0009 | 0.0015 | 0.0007 | 0.0003 |
| Benzene | 7518.4802 | 7539.6301 | 0.0397 | 0.0424 | 2709.7823 | 0.0712 | 0.0339 |
| Formaldehyde | 0.0064 | 0.0779 | 0.0661 | 0.0418 | 0.0866 | 0.1242 | 0.0974 |
| Acrolein | 0.0076 | 0.0308 | 0.0516 | 0.2504 | 0.0312 | 0.1497 | 0.1298 |
| Acetylene | 0.2407 | 0.3245 | 0.2847 | 0.1935 | 0.3477 | 0.3311 | 0.3417 |
| $CO_2$ | 4.1885 | 3.6563 | 3.0850 | 2.7250 | 2.8182 | 2.2937 | 1.8356 |
| THC | 9265.5298 | 13652.9954 | 1.4293 | 0.8273 | 3339.3689 | 1.5814 | 0.7599 |
| NO | 0.0108 | 0.0192 | 0.0075 | 0.1116 | 0.0107 | 0.0535 | 0.0346 |
| $NO_2$ | 94.2856 | 1276.5985 | 0.0008 | 0.0000 | 0.0014 | 0.0032 | 0.0010 |
| $SO_2$ | 0.0028 | 0.0072 | 0.0184 | 0.0359 | 0.0025 | 0.0269 | 0.0226 |
| $NH_3$ | 0.0013 | 929.7483 | 0.0010 | 0.0062 | 0.0009 | 0.0020 | 0.0029 |
| $NO_x$ | 84.6468 | 1146.0278 | 0.0103 | 0.1536 | 0.0160 | 0.0736 | 0.0477 |
| HBr | 0.0078 | 0.0082 | 7.2792 | 7.2945 | 7.7917 | 2.7070 | 3.9830 |
| Acetaldehyde | 0.0028 | 0.0145 | 0.0556 | 0.2242 | 0.0317 | 0.1050 | 0.1168 |
| Toluene | 0.0580 | 0.0632 | 0.0735 | 0.0560 | 0.0965 | 0.0441 | 0.0600 |

*Yield values in the RED mark are not sensible

**Table 9.5** Mean gas yields for Polyethylene fires in the Cone Calorimeter and Purser Furnace tests.

| Test Method | PURSER FURNACE | | CONE CALORIMETER | | | | |
|---|---|---|---|---|---|---|---|
| Polymer Type | TEST 1 PE-Y | TEST 2 PE-Y | PE-Y | PE-Blue | PE-Black | SB-P | PEP |
| Test Condition | Φ = 2.0 | Φ = 0.8 | 35 FV | | | | |
| Initial Mass (g) | 49.30 | 47.30 | 78.21 | 78.22 | 77.20 | 15.67 | 50.30 |
| Total Mass Loss (g) | 34.75 | 30.99 | 74.83 | 63.15 | 77.20 | 12.53 | 50.29 |
| Total Time (s) | 3000 | 4000 | 970 | 1100 | 1140 | 900 | 1200 |
| Mean ER, Φ | 5.47 | 6.13 | 0.85 | 0.22 | 2.18 | 0.29 | 1.62 |
| Species | Mean Yields (g/g) | | | | | | |
| CO | 0.0692 | 0.1091 | 0.2084 | 0.1513 | 0.2423 | 0.0820 | 0.1153 |
| HCN | 0.0009 | 0.0004 | 0.0019 | 0.0032 | 0.0021 | 0.0016 | 0.0013 |
| HCl | 0.0013 | 12.7715 | 0.0010 | 0.0006 | 0.0013 | -0.0001 | 0.0011 |
| HF | 0.0001 | 0.0001 | 0.0001 | 0.0001 | 0.0000 | 0.0001 | 0.0000 |
| Benzene | 857.1181 | 1111.9700 | 0.0238 | 0.0065 | 78.4292 | 0.0188 | 0.0178 |
| Formaldehyde | 0.0049 | 0.0041 | 0.0047 | 0.0027 | 0.0020 | 0.0164 | 0.0020 |
| Acrolein | 0.0016 | 0.0030 | 0.0050 | 0.0390 | 0.0009 | 0.0254 | 0.0041 |
| Acetylene | 0.1046 | 0.0301 | 0.1708 | 0.0661 | 0.2316 | 0.0908 | 0.1368 |
| $CO_2$ | 0.6067 | 0.3061 | 1.1261 | 1.1958 | 0.7966 | 1.4958 | 0.5304 |
| THC | 1058.4125 | 2609.2142 | 0.8555 | 0.6206 | 97.5980 | 0.5999 | 0.5201 |
| NO | 0.0060 | 0.0047 | 0.0040 | 0.0144 | 0.0066 | 0.0134 | 0.0043 |
| $NO_2$ | 17.8081 | 38.7079 | 0.0001 | 0.0000 | 0.0005 | 0.0004 | 0.0003 |
| $SO_2$ | 0.0003 | 0.0003 | 0.0013 | 0.0092 | 0.0004 | 0.0035 | 0.0009 |
| $NH_3$ | 0.0002 | 45.7170 | 0.0001 | 0.0006 | 0.0002 | 0.0005 | 0.0002 |
| $NO_x$ | 15.9950 | 34.7553 | 0.0056 | 0.0198 | 0.0094 | 0.0188 | 0.0061 |
| HBr | 0.0006 | 0.0000 | 0.5815 | 1.7590 | 0.2029 | 0.5316 | 0.1417 |
| Acetaldehyde | 0.0010 | 0.0042 | 0.0046 | 0.0391 | 0.0014 | 0.0199 | 0.0041 |
| Toluene | 0.0084 | 0.0142 | 0.0280 | 0.0368 | 0.0289 | 0.0081 | 0.0204 |

### 9.5.2.3 Total Toxicity

Total toxicities of LC50, $COSHH_{15min}$ and AEGL-2 basis for PE-Y fires in the Cone Calorimeter and Purser Furnace at different fire conditions are shown in Figure 9.13. Hydrocarbon like Benzene was the major species that contributed to the total toxicity values in Figure 9.13 especially for PE fire with ER = 0.8 in the Purser Furnace. For PE-Y fire in the Cone Calorimeter, HBr was the major species that contributed to the Total COSHH as shown in Figure 9.13 (b) where the graph pattern was similar to the HBr emission in Figure 9.10. Average Total LC50 for this polymer fires was about 12 while the average total toxicity for AEGL-2 was less than 2000. In this present work, the plotted graphs for total toxicity had taken in consideration of 10 number of species for purpose of comparison between both methods. However, clearer comparison could be made if considering less number of species with uncounted the species which were out from the FTIR measurement scale.

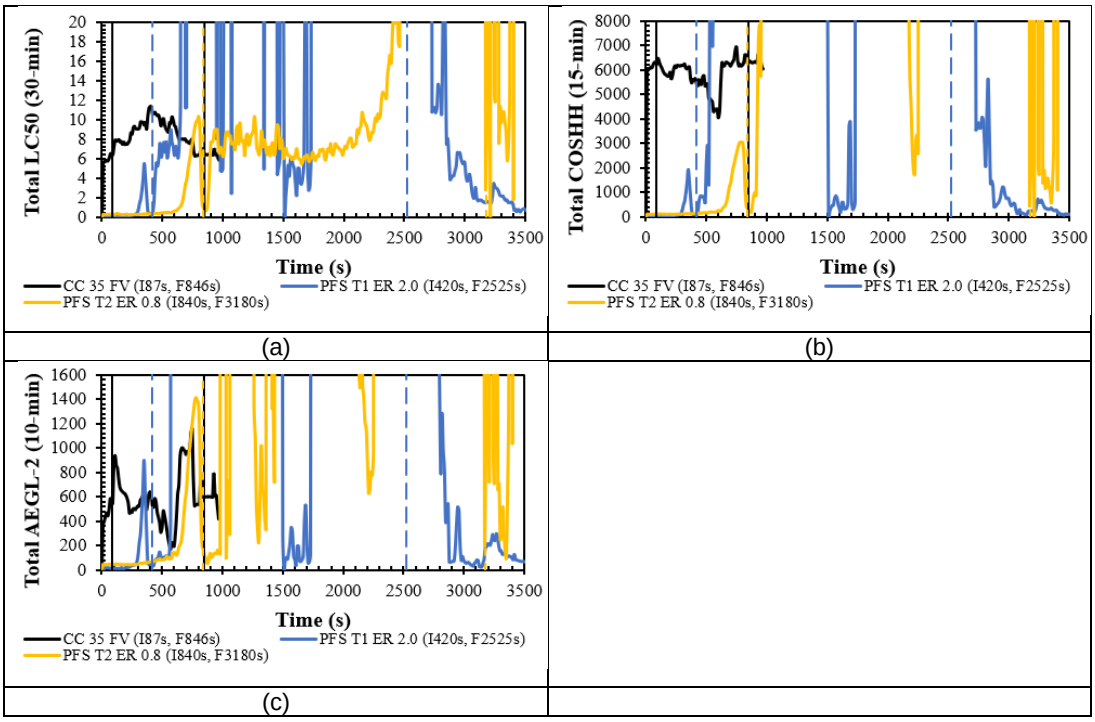


**Figure 9.13** Total toxicity for PE-Y fires in the Cone Calorimeter and Purser Furnace at different fire conditions.

### 9.5.2.4 Major Gases Contribution

Figure 9.14 shows the graphs for contribution of major toxic gases for the Purser Furnace tests at two different equivalence ratios. For PE-Y fires in both cone and furnace tests, according to LC50 toxic assessment method, the dominated toxic species were CO, HCN, Formaldehyde and Acrolein. From the gas contribution graphs of LC50 basis in Figure 6.11 (a) and Figure 9.14, other main species that dominated was HBr for the Cone Calorimeter test and $NO_2$ for the Purser Furnace tests. HBr emissions were high for all five conducted Polyethylene fires in the Cone Calorimeter at heat flux of 35 kW/m$^2$ and under free ventilation. Meanwhile, NO2 emissions were high for Polyethylene fires in the Purser Furnace for both set equivalence ratios of 0.8 and 2.0 (lean and rich fires) with the restricted ventilation. For $COSHH_{15min}$ and AEGL-2 based methods, Benzene and $SO_2$ were also the major species that contributed to the total toxicity. The first six major species for PE-Y fires in the Cone Calorimeter and Purser Furnace are summarised in Table 9.6.

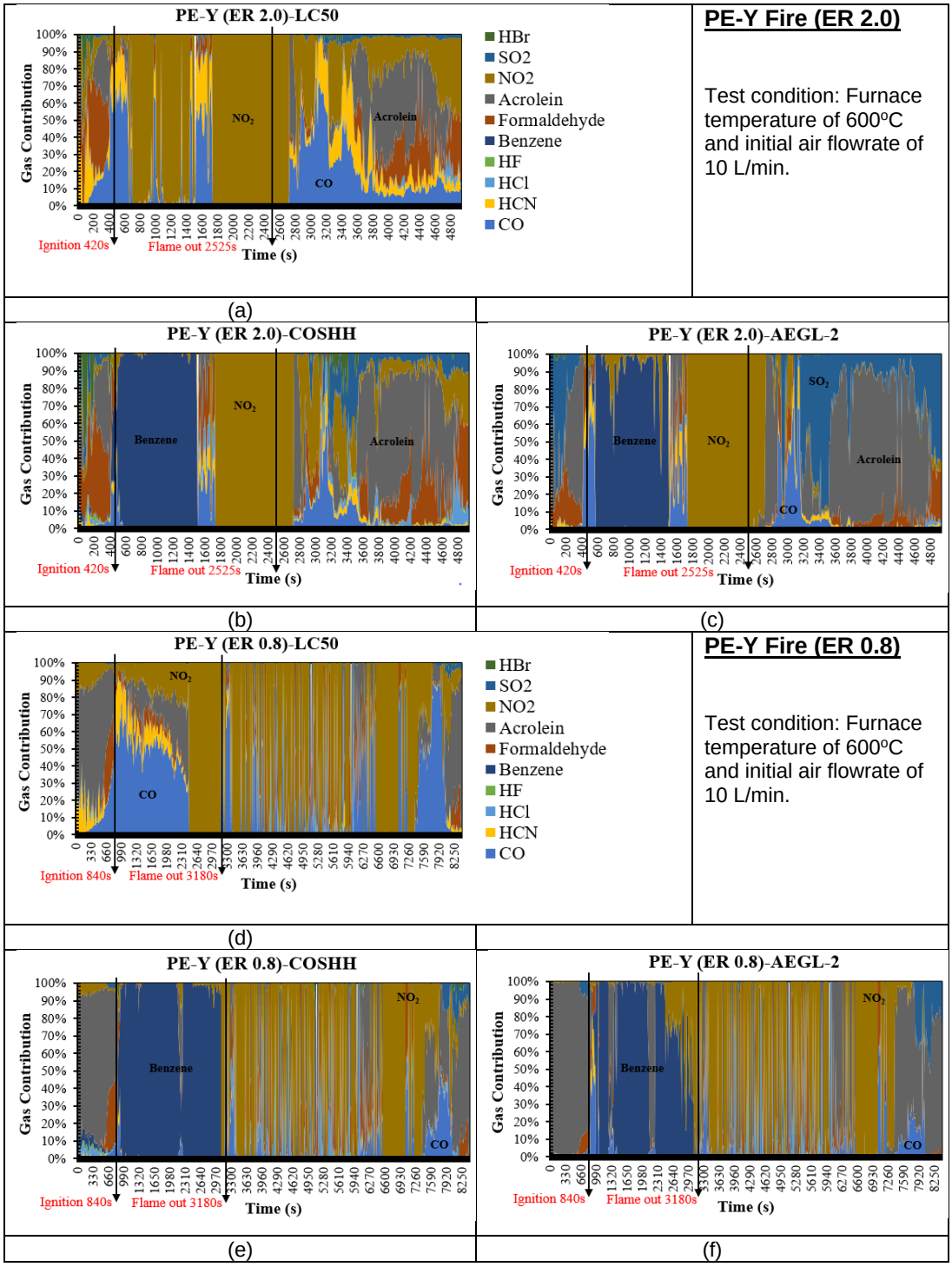


**Figure 9.14** Contribution of major toxic gases for the Purser Furnace tests at two different equivalence ratios.

**Table 9.6** First six major species for PE-Y fires in the Cone Calorimeter and Purser Furnace.

| POLYETHYLENE (PE-Y) FIRES | | | | | | | | | | | | |
|---|---|---|---|---|---|---|---|---|---|---|---|---|
| **Test** | **Test Details** | **Mean ER, Φ (Chan)** | **Time (s)** | **Fire Stage** | **TT** | **Major Species** | | | | | | |
| | | | | | | **1** | **2** | **3** | **4** | **5** | **6** |
| **CONE CALORIMETER** | | | | | | | | | | | | |
| 1 | PE-Y | 0.3 | <87 | Ignition | **LC50** | HBr | Acrolein | Formaldehyde | HCN | CO | $SO_2$ |
| | 35 FV | 2.5 (peak) | 87 - 640 | Flaming 1 | | CO | HBr | Acrolein | HCN | Formaldehyde | $NO_2$ |
| | I = 87 s | 0.7 | 640 - 846 | Flaming 2 | | HBr | Acrolein | Formaldehyde | CO | HCN | - |
| | F = 846 s | 0.2 | >846 | Post-flaming | | HBr | Formaldehyde | Acrolein | HCN | CO | - |
| | | 0.3 | <87 | Ignition | **COSHH** | HBr | Acrolein | Formaldehyde | $SO_2$ | - | - |
| | | 2.5 (peak) | 87 - 640 | Flaming 1 | | HBr | Acrolein | Benzene | CO | Formaldehyde | HCN |
| | | 0.7 | 640 - 846 | Flaming 2 | | HBr | Acrolein | Formaldehyde | $SO_2$ | - | - |
| | | 0.2 | >846 | Post-flaming | | HBr | Acrolein | Formaldehyde | $SO_2$ | - | - |
| | | 0.3 | <87 | Ignition | **AEGL-2** | Acrolein | HBr | $SO_2$ | Formaldehyde | HCN | - |
| | | 2.5 (peak) | 87 - 640 | Flaming 1 | | Acrolein | CO | $SO_2$ | HBr | Formaldehyde | HCN |
| | | 0.7 | 640 - 846 | Flaming 2 | | Acrolein | HBr | $SO_2$ | Formaldehyde | - | - |
| | | 0.2 | >846 | Post-flaming | | Acrolein | HBr | $SO_2$ | Formaldehyde | - | - |
| **PURSER FURNACE** | | | | | | | | | | | | |
| 2 | PE-Y | 0.4 | <420 | Ignition | **LC50** | Formaldehyde | HCN | CO | Acrolein | $NO_2$ | HBr |
| | Φ = 2.0 | 8.0 | 420 - 1500 | SS Flaming 1 | | $NO_2$ | CO | HCN | Acrolein | Formaldehyde | - |
| | I = 420 s | 6.0 | 1500 - 2525 | Flaming 2 | | $NO_2$ | CO | HCN | Formaldehyde | Acrolein | - |
| | F = 2525 s | 5.0 | >2525 | Post-flaming | | CO | Acrolein | $NO_2$ | HCN | Formaldehyde | $SO_2$ |
| | | 0.4 | <420 | Ignition | **COSHH** | Formaldehyde | Acrolein | HBr | $SO_2$ | $NO_2$ | CO |
| | | 8.0 | 420 - 1500 | SS Flaming 1 | | Benzene | CO | $NO_2$ | HCN | - | - |
| | | 6.0 | 1500 - 2525 | Flaming 2 | | $NO_2$ | CO | Formaldehyde | Acrolein | HCN | HCl |
| | | 5.0 | >2525 | Post-flaming | | Acrolein | $NO_2$ | $SO_2$ | CO | Formaldehyde | HCl |

| | | | | | | | | | | | | |
|---|---|---|---|---|---|---|---|---|---|---|---|---|
| | | 0.4 | <420 | Ignition | **AEGL-2** | Acrolein | $SO_2$ | Formaldehyde | CO | HCN | HBr |
| | | 8.0 | 420 - 1500 | SS Flaming 1 | | Benzene | CO | $NO_2$ | HCN | Formaldehyde | - |
| | | 6.0 | 1500 - 2525 | Flaming 2 | | $NO_2$ | CO | Acrolein | HCN | Formaldehyde | - |
| | | 5.0 | >2525 | Post-flaming | | Acrolein | $SO_2$ | CO | $NO_2$ | Formaldehyde | HCN |
| 3 | PE-Y | 0.6 | <840 | Ignition | **LC50** | Acrolein | $NO_2$ | CO | HCN | Formaldehyde | $SO_2$ |
| | Φ = 0.8 | 8.0 | 840 - 2400 | SS Flaming 1 | | CO | Acrolein | $NO_2$ | HCN | Formaldehyde | - |
| | I = 840 s | 8.4 (max. 9.0) | 2400 - 3180 | SS Flaming 2 | | $NO_2$ | - | - | - | - | - |
| | F = 3180 s | 8.0 | >3180 | Post-flaming | | $NO_2$ | CO | Acrolein | Formaldehyde | HCN | $SO_2$ |
| | | 0.6 | <840 | Ignition | **COSHH** | Acrolein | Formaldehyde | $NO_2$ | Benzene | HCl | $SO_2$ |
| | | 8.0 | 840 - 2400 | SS Flaming 1 | | Benzene | Acrolein | $NO_2$ | CO | - | - |
| | | 8.4 (max. 9.0) | 2400 - 3180 | SS Flaming 2 | | Benzene | $NO_2$ | - | - | - | - |
| | | 8.0 | >3180 | Post-flaming | | $NO_2$ | CO | Acrolein | Formaldehyde | $SO_2$ | HBr |
| | | 0.6 | <840 | Ignition | **AEGL-2** | Acrolein | Formaldehyde | $SO_2$ | $NO_2$ | CO | - |
| | | 8.0 | 840 - 2400 | SS Flaming 1 | | Benzene | Acrolein | CO | HCN | Formaldehyde | $NO_2$ |
| | | 8.4 (max. 9.0) | 2400 - 3180 | SS Flaming 2 | | Benzene | $NO_2$ | - | - | - | - |
| | | 8.0 | >3180 | Post-flaming | | $NO_2$ | Acrolein | CO | $SO_2$ | Formaldehyde | - |

### 9.5.3 Particle Mass from Polyethylene Fires in the Purser Furnace Test

Filter paper based Smoke Meter was used to collect and measure the total particulate mass (PM) from the PE-Y fires in the Purser Furnace. TGA analysis on the filters was used to determine the soot, volatile, and ash fraction. It will be shown that the PM mass was predominantly ash. This was not expected as the PE-Y sample in Table 3.11 only has 0.72% of ash. Again it is likely that the PE-Y sample analysed by TGA in Table 3.11 was not the same sample as that used on the Cone Calorimeter or the Purser Furnace.

The high ash in the PM would indicate that a fire retardant was used that decomposed to ash was in the PE-Y used in the Purser tests. Sodium bicarbonate, Calcium carbonate or Aluminium hydroxide would be three possibilities. The ash was a problem in the tests as it came out the orifice at the end of the Quartz tube like a molten lava and accumulated on the floor of the dilution chamber underneath the Quartz tube exit. There was so much ash that it started to block the flow exit from the Quartz tube.

Figure 9.15 shows the pictures of filter paper samples collected from the Purser Furnace tests. A black colour indicates Carbon is present, grey filters are dominated by ash and brown filters normally indicate Hydrocarbon volatiles. Most of the filters are grey indicating a high ash content, that the TGA analysis confirms. There were 12 filter paper samples for Test 1 (ER = 2.0) and 11 filter paper samples for Test 2 (ER = 0.8).

The PM mass was determined by weight different of the filter paper samples measured by the mass balance before and after the test. These filter paper samples were also analysed with TGA to determine the moisture, volatile, Carbon and ash content (refer Table 9.8) and some were analysed by SEM for morphology analysis. Measured PM mass collected from filter paper equipment in the Purser Furnace tests were summarised in Table 9.7.

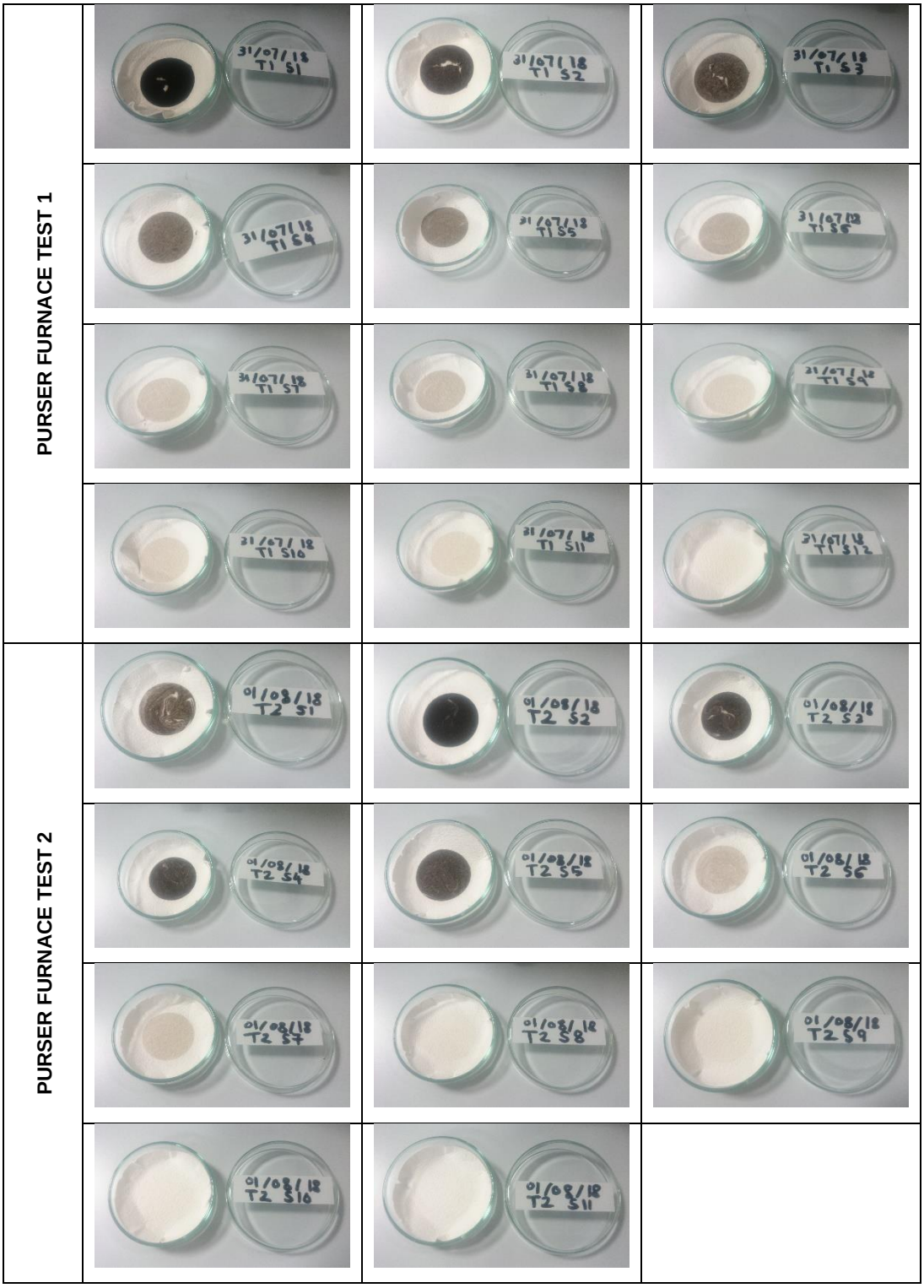


**Figure 9.15** Filter paper samples collected from the Purser Furnace tests.

**Table 9.7** PM mass collected from filter paper in the Purser Furnace tests.

| PM MASS FROM FILTER PAPER | | | | | | |
|---|---|---|---|---|---|---|
| **PURSER FURNACE - TEST 1 (ER 2.0)** | | | | | | |
| **No.** | **Weight (mg)** | **Duration (min)** | **Weight After (mg)** | **Test Time (s)** | **PM Mass (g)** | **Remarks** |
| 1 | 179.22 | 5 | 193.20 | 300 | 0.013980 | 31/07/18 T1 S1 |
| 2 | 179.36 | 2 | 184.70 | 660 | 0.005340 | 31/07/18 T1 S2 |
| 3 | 177.14 | 1 | 184.06 | 840 | 0.006920 | 31/07/18 T1 S3 |
| 4 | 175.67 | 1 | 175.67 | 960 | 0.000000 | **Used to prevent burst |
| 5 | 176.15 | 1 | 179.89 | 960 | 0.003740 | 31/07/18 T1 S4 |
| 6 | 177.31 | 1 | 180.34 | 1080 | 0.003030 | 31/07/18 T1 S5 |
| 7 | 179.50 | 1 | 181.71 | 1200 | 0.002210 | 31/07/18 T1 S6 |
| 8 | 177.25 | 1 | 179.40 | 1320 | 0.002150 | 31/07/18 T1 S7 |
| 9 | 178.05 | 1 | 180.38 | 1440 | 0.002330 | 31/07/18 T1 S8 |
| 10 | 176.86 | 2 | 180.53 | 1560 | 0.003670 | 31/07/18 T1 S9 |
| 11 | 177.62 | 5 | 185.14 | 1740 | 0.007520 | 31/07/18 T1 S10 |
| 12 | 177.78 | 5 | 185.42 | 2100 | 0.007640 | 31/07/18 T1 S11 |
| 13 | 176.31 | 5 | 178.56 | 2460 | 0.002250 | 31/07/18 T1 S12 |
| **PURSER FURNACE - TEST 2 (ER 0.8)** | | | | | | |
| **No.** | **Weight (mg)** | **Duration (min)** | **Weight After (mg)** | **Test Time (s)** | **PM Mass (g)** | **Remarks** |
| 14 | 178.53 | 2 | 178.83 | 240 | 0.000300 | 01.08.2018 T2 S1 |
| 15 | 179.29 | 2 | 181.76 | 420 | 0.002470 | 01.08.2018 T2 S2 |
| 16 | 179.48 | 2 | 181.99 | 660 | 0.002510 | 01.08.2018 T2 S3 |
| 17 | 181.62 | 2 | 183.90 | 780 | 0.002280 | 01.08.2018 T2 S4 |
| 18 | 177.52 | 2 | 179.60 | 960 | 0.002080 | 01.08.2018 T2 S5 |
| 19 | 177.69 | 2 | 178.61 | 1140 | 0.000920 | 01.08.2018 T2 S6 |
| 20 | 178.08 | 5 | 180.51 | 1380 | 0.002430 | 01.08.2018 T2 S7 |
| 21 | 178.54 | 7 | 181.79 | 1680 | 0.003250 | 01.08.2018 T2 S8 |
| 22 | 177.80 | 10 | 182.31 | 2160 | 0.004510 | 01.08.2018 T2 S9 |
| 23 | 177.19 | 15 | 179.51 | 2820 | 0.002320 | 01.08.2018 T2 S10 |
| 24 | 177.69 | 13 | 178.53 | 3780 | 0.000840 | 01.08.2018 T2 S11 |

Figure 9.16 shows mass of PM as a function of time for PE-Y fires in the Purser Furnace. PM mass was high in the early stage of flaming condition for the Polyethylene fires before it decreased towards the end of the test. Then, after 1000 s of burning, the measured PM mass increased and had a second peak at 2000 s for both fires at different set equivalence ratios.

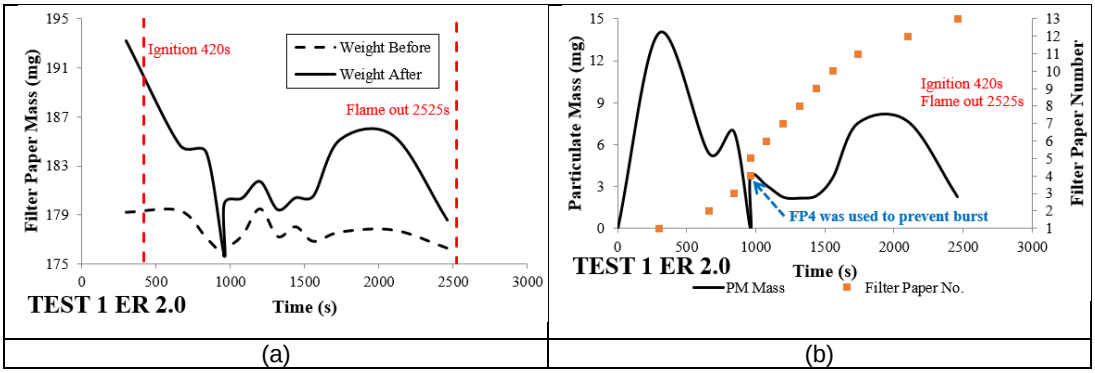


(a) (b)

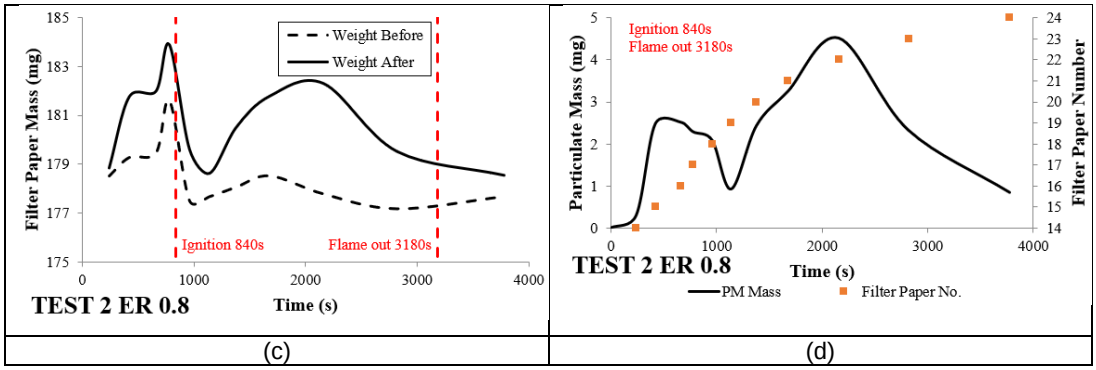


(c) (d)

**Figure 9.16** PM mass as a function of time for the Purser Furnace tests.

Average soot yields reported [140-142] for Polyethylene fires (during pre-flashover period) in the Cone Calorimeter were 0.06 kg/kg for solid Polyethylene, 0.06 kg/kg for other common forms of Polyethylene and in a range from 0.056 to 0.102 kg/kg for Polyethylene foam. The maximum soot yield for PE-Y fire in the Purser Furnace obtained from the present work was much more lower (less than 0.0003 g/g) compared to the published soot yields obtained from the cone tests. Soot yields as a function of time for PE-Y fires in the Purser Furnace are shown in the following Figure 9.17.

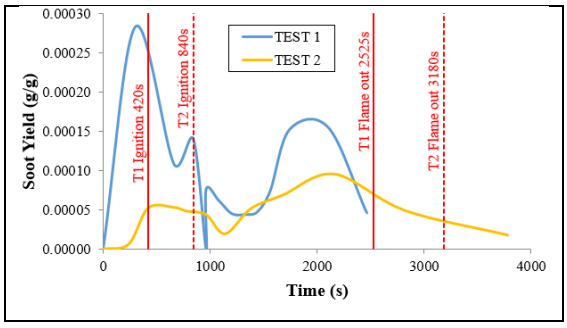


**Figure 9.17** Soot yields as a function of time for the Purser Furnace tests.

Post proximate analysis data by the TGA for the filter paper samples collected from PE-Y fires in the furnace were included in Table 9.8 while Figure 9.18 shows the contents (in wt.%) of moisture, volatiles, fixed Carbon and ash in the collected filter paper samples. Ash content for PE-Y fire with ER = 0.8 was more than 95% (up to >99%), this value was higher than PE-Y fire with ER = 2.0 (from 83% to 97%). The result showed that the unburnt fuel amount left in the end of combustion was more for the PE-Y fire at the lean fire condition compared to the PE-Y fire at the rich fire condition.

**Table 9.8** Filter paper analysis by TGA for the Purser Furnace tests.

| PFS TEST 1 (ER 2.0) | | | | | |
|---|---|---|---|---|---|
| Material | Sample | Moisture | Volatile | Fixed Carbon | Ash |
| | | Wet Ash (wt.%) | | | |
| PE-Y | FP 1 | 0.58 | 9.26 | 7.12 | 83.05 |
| PE-Y | FP 2 | 0.20 | 5.40 | 0.35 | 94.05 |
| PE-Y | FP 3 | 0.26 | 6.81 | 0.16 | 92.77 |
| PE-Y | FP 4 | 0.22 | 4.38 | 0.06 | 95.34 |
| PE-Y | FP 5 | 0.01 | 3.63 | 0.24 | 96.12 |
| PE-Y | FP 6 | 0.15 | 3.20 | 0.24 | 96.41 |
| PE-Y | FP 7 | 0.03 | 3.37 | 0.21 | 96.39 |
| PE-Y | FP 8 | 0.14 | 3.51 | 0.22 | 96.13 |
| PE-Y | FP 9 | 0.17 | 5.08 | 0.19 | 94.56 |
| PE-Y | FP 10 | 0.26 | 8.63 | 0.24 | 90.88 |
| PE-Y | FP 11 | 0.18 | 8.46 | 0.16 | 91.21 |
| PE-Y | FP 12 | 0.13 | 2.55 | 0.17 | 97.15 |

| PFS TEST 2 (ER 0.8) | | | | | |
|---|---|---|---|---|---|
| Material | Sample | Moisture | Volatile | Fixed Carbon | Ash |
| | | Wet Ash (wt.%) | | | |
| PE-Y | FP 1 | 0.02 | 0.92 | 0.03 | 99.03 |
| PE-Y | FP 2 | 0.12 | 2.82 | 0.51 | 96.56 |
| PE-Y | FP 3 | 0.17 | 3.08 | 0.23 | 96.53 |
| PE-Y | FP 4 | 0.20 | 2.95 | 0.22 | 96.63 |
| PE-Y | FP 5 | 0.20 | 2.70 | 0.21 | 96.90 |
| PE-Y | FP 6 | 0.06 | 1.51 | 0.00 | 98.44 |
| PE-Y | FP 7 | 0.02 | 2.54 | 0.12 | 97.32 |
| PE-Y | FP 8 | 0.12 | 3.59 | 0.24 | 96.06 |
| PE-Y | FP 9 | 0.03 | 4.51 | 0.13 | 95.34 |
| PE-Y | FP 10 | 0.08 | 2.92 | 0.24 | 96.76 |
| PE-Y | FP 11 | 0.06 | 1.97 | 0.23 | 97.74 |
| - | Blank P | 0.00 | 0.72 | 0.17 | 99.12 |

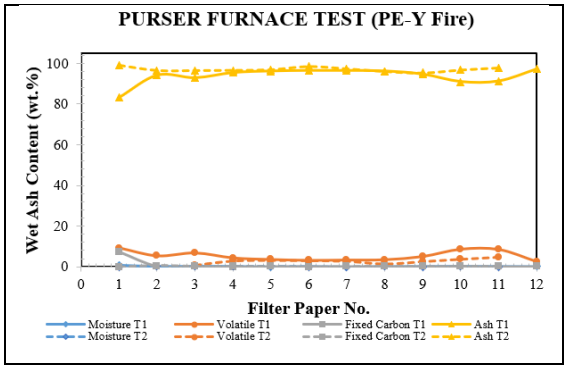


**Figure 9.18** Wet ash contents from filter paper analysis by the TGA for the Purser Furnace tests.

## 9.5.4 Particle Size Distributions of Polyethylene Fires in the Purser Furnace Test

### 9.5.4.1 Particle Number and Mass Distributions

Particle number and mass distributions for PE-Y fires in the Purser Furnace at two different equivalence ratios are shown in the following Figure 9.19. Particle number distribution as a function of time for rich PE-Y fire was higher than lean PE-Y fire. For the lean PE-Y fire, the number distribution was lower after 1500 s and this might be due to a higher agglomeration rate for this well ventilated fire where a higher number of smaller particles had agglomerated to form a lower number of larger particles. From Figure 9.19 (d), the particle mass distribution after 1500 s for the lean PE-Y fire was lower for smaller size of particles (<100 nm) compared with larger size of particles. Meanwhile, the

particle mass distribution of all size of particles (5 nm to 1000 nm) was high within 3000 s of burning period for the rich PE-Y fire.

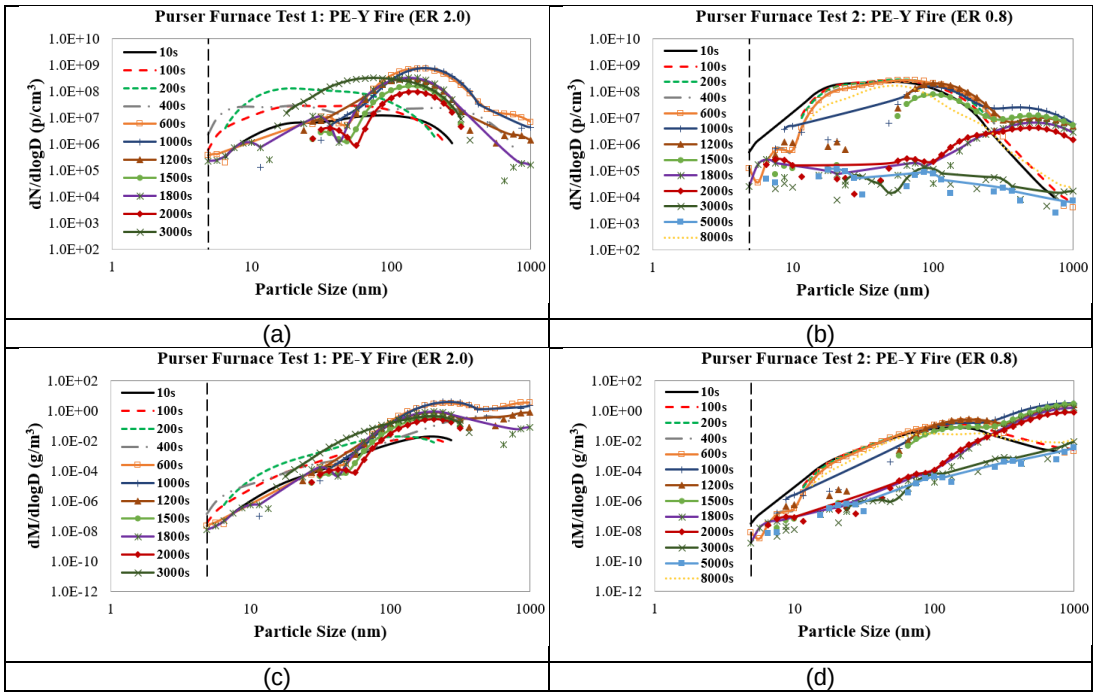


**Figure 9.19** Particle number and mass distributions for PE-Y fires in the Purser Furnace at two different equivalence ratios.

Figure 9.18 shows particle number and mass distributions in 3D Waterfall plot for the Purser Furnace tests at two different equivalence ratios. PE-Y fire with fuel rich burning condition was giving a higher particle number and mass distributions. This is due to more fuel amount burned in the rich fire equivalence ratio condition compared to the lean fire condition. The particle number distribution were high throughout the burning period of up to 4000 s for rich PE-Y fire at ER = 2.0, while for the same burning period, the lean PE-Y fire at ER = 0.8 had shown a lower particle number distribution with a decreasing particle number profile after 1000 s. In Figure 9.18 (a), there are three main peaks indicated which showing a very high number of particles with size less than 100 nm. It showed that high number of volatiles present in the rich PE-Y fire and this was tally with the result of higher volatile contents obtained from the TGA analysis (refer Table 9.6) compared to the lean PE-Y fire.

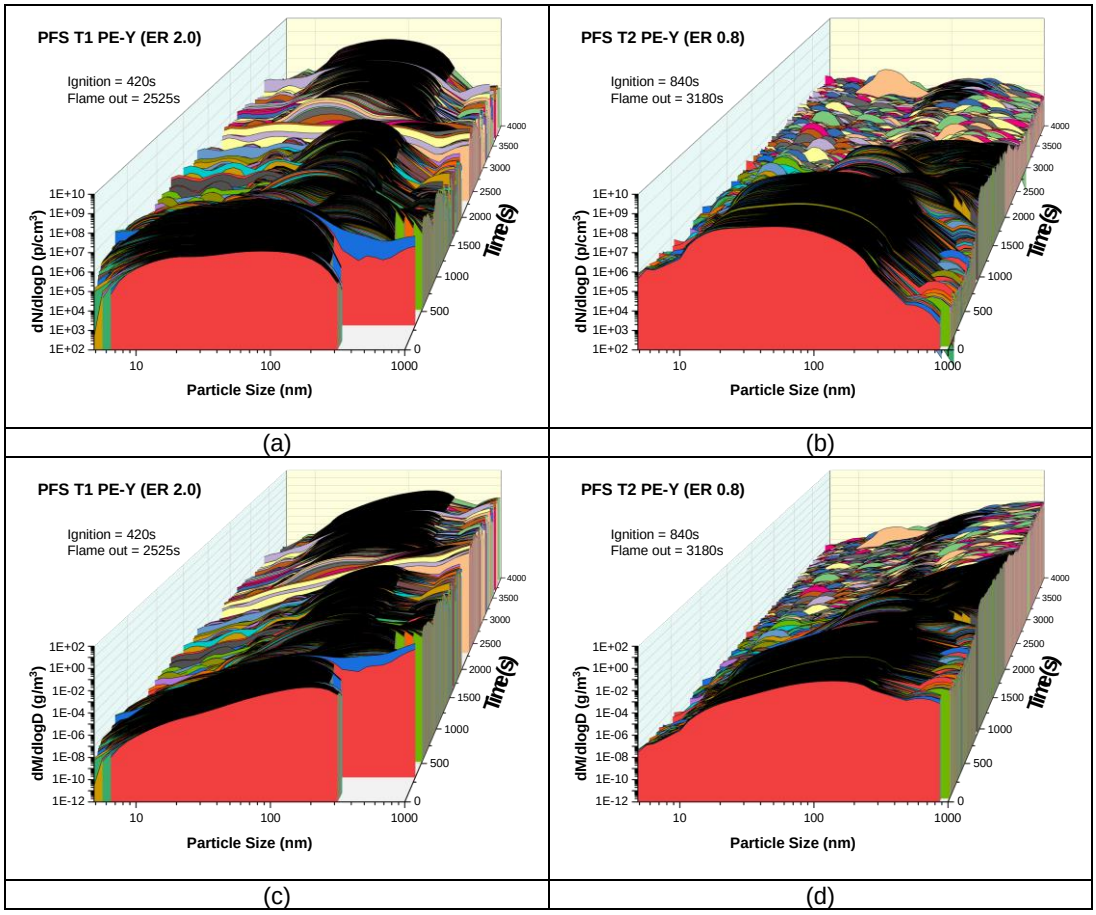


**Figure 9.20** Particle number and mass distributions in 3D Waterfall plot for PE-Y fires in the Purser Furnace at two different equivalence ratios.

Compared to 100 nm particles, smaller particles (10 nm) had a lower particle number and mass distributions for these PE-Y fires. This is not expected and it is quite rare to have the particle number of large particles bigger than small particles. This indicates that the particle number is dominated by ash which does not form chemically in the way soot does, but condenses as large particles. It is likely that the 10 nm particles are Carbon and as the mass of Carbon in the PM is low this gives the low number. Nevertheless, the health hazards of fine particles are not related to their composition, so fine particles that are ash are still a health hazard.

10 nm and 100 nm particles were having the same particle distribution throughout the burning period for the rich PE-Y fire while the particle distribution of these particle sizes had decreased after 1500 s for the lean PE-Y fire. Figure 9.21 shows 10 nm and 100 nm particle distributions for PE-Y fires in the Purser Furnace at two different equivalence ratios. The highest peak of particle number distribution was about 1.0E+09 p/cm$^3$ and the highest

peak of particle mass distribution was about 1.0E+00 g/m$^3$ for both rich and lean PE-Y fires.

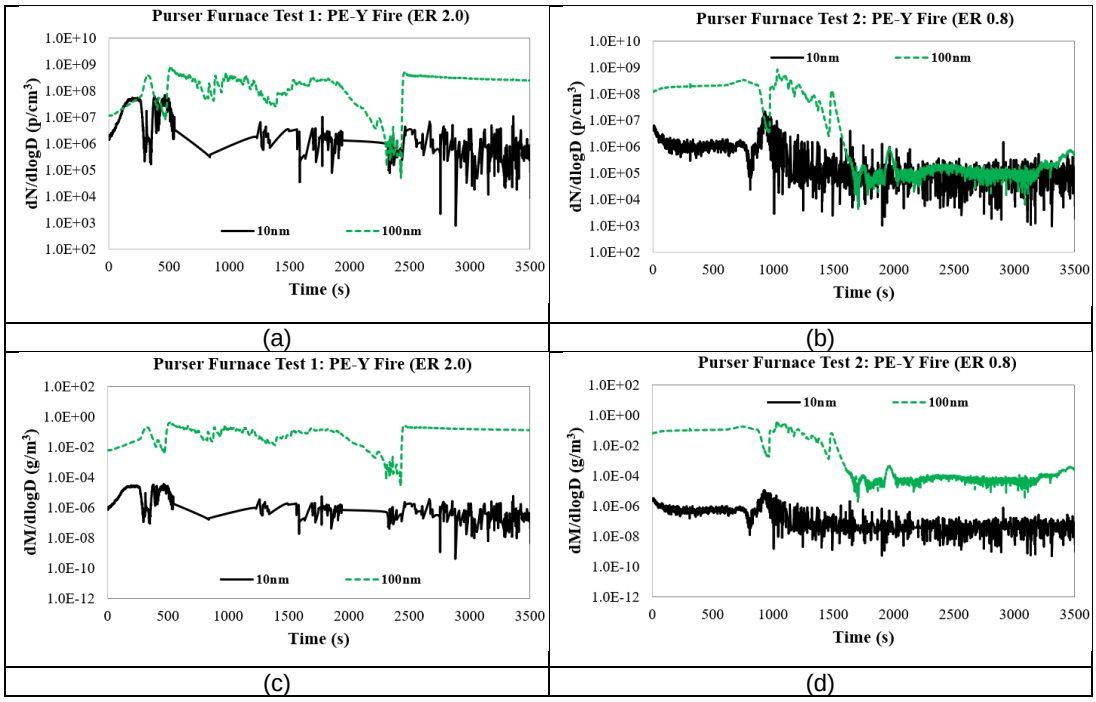


**Figure 9.21** 10 nm and 100 nm particle distributions for PE-Y fires in the Purser Furnace at two different equivalence ratios.

Particulate cumulative mass as a function of particle size for PE-Y fires in the Purser Furnace at two different equivalence ratios is shown in Figure 9.22. The particulate cumulative mass had increased with the increase of burning time with at the time of ignition, the cumulative mass of the particulate was much more lower for these PE-Y fires compared to at the time of flame out. At the flame out time of 2525 s for rich PE-Y fire (ER = 2.0), the cumulated particulate mass was about 4000 g/m$^3$, slightly lower compared to the lean PE-Y fire (ER = 0.8, ~4200 g/m$^3$). The lean PE-Y fire gave lower particulate cumulative mass for all sizes of particle after the fire extinguished while the rich PE-Y fires had shown a higher particulate cumulative mass after the fire extinguished. For fuel rich burning, the more fuel burned would produce more particles. 200 nm particles were giving the highest cumulative mass for rich PE-Y fire and particles with the size >400 nm were giving a higher cumulative mass for the lean PE-Y fire. However, particle sizes less than 100 nm were focused more in presenting the results due to the health effect either short or

long term effect of these ultra-fine particles to the human more critical than the larger particles.

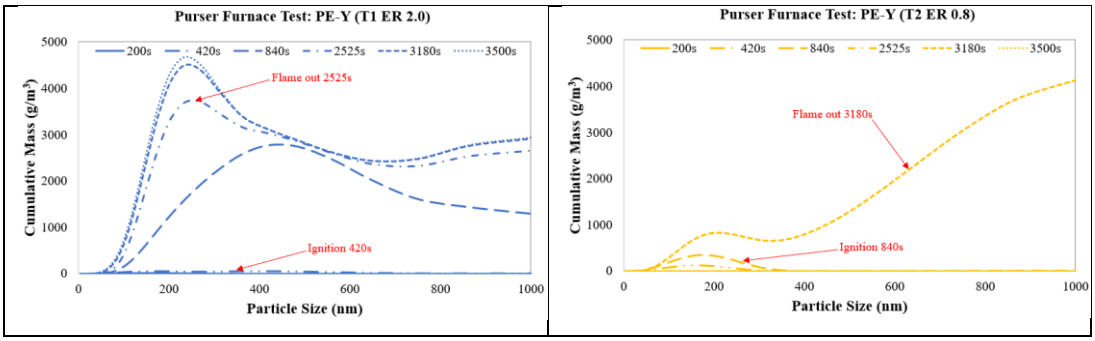


**Figure 9.22** Particulate cumulative mass as a function of particle size for PE-Y fires in the Purser Furnace at two different equivalence ratios.

### 9.5.4.2 Particulate Yields

Yields of particulate for 10 nm and 100 nm particles as a function of time and fire equivalence ratio for PE-Y fires in the Purser Furnace are shown in the following Figure 9.23. The average number yields of 100 nm particles (1.0E+02 p/kg) for PE-Y fire at ER = 2.0 were higher compared to the PE-Y fire at ER = 0.8 (1.0E-02 p/kg). For 10 nm particles, the number yields were about 1.0E+08 p/kg for PE-Y fire at ER = 2.0 while for PE-Y fire at ER = 0.8, the number yields had a maximum peak of 1.0E+07 p/kg (at 1000 s). A leaner fire equivalence ratio (<4.0) by PE-Y fire (at ER = 2.0) had contributed to a higher number yields of 10 nm particles compared to PE-Y fire at ER = 0.8. For 100 nm particles, the number yields for both PE-Y fires were high with both Polyethylene fires showing a rich burning condition. The result showed that different fire equivalence ratios or burning conditions would produce a different number of certain size of particles. In terms of mass based particulate yields, 100 nm particles showed higher yield values than 10 nm particles. In a richer fire condition, mass yields for large particles are expected to be higher if compared with a leaner fire condition as the results obtained in the present work (refer Figure 9.23) due to a higher amount unburned fuel left at the end of the burning process and a higher soot formation.

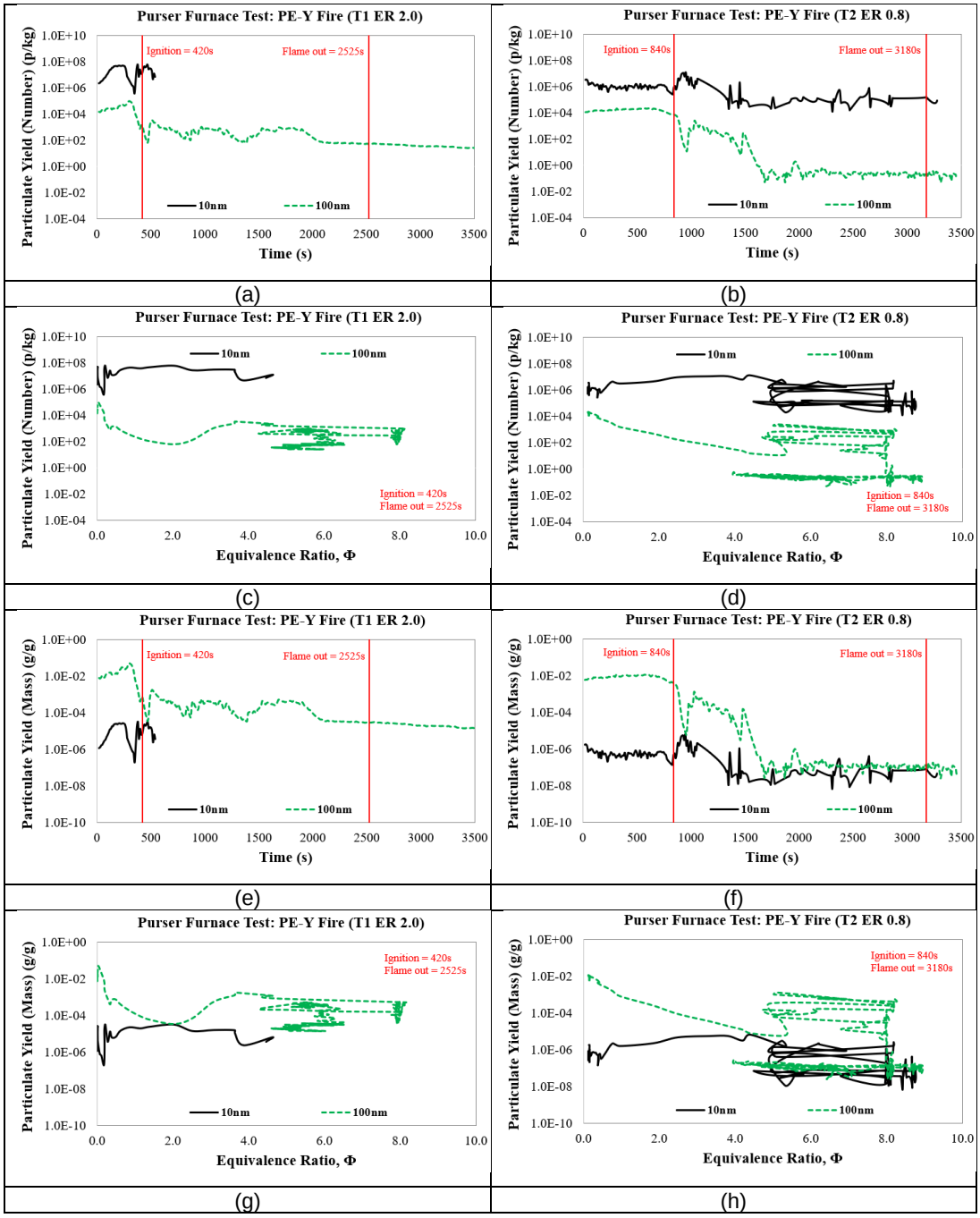


**Figure 9.23** Particulate yields (number and mass) for PE-Y fires in the Purser Furnace at two different equivalence ratios.

## 9.6 Findings and Conclusion from PE-Y Fire Tests in the Cone Calorimeter and Purser Furnace

This chapter resulted to the following findings and conclusion for the experimental works done on Polyethylene (PE-Y) fires in both Cone Calorimeter and Purser Furnace:

- The Purser Furnace data are preliminary, and the combustion conditions cannot be defined due to problems with the runs. The data presented here represent the results of the tests as run but cannot be related to the intended ER conditions. It is not therefore possible to make any realistic comparison between results from the tube furnace and the Cone Calorimeter under defined combustion conditions.
- PE-Y fire in the Cone Calorimeter had a shorter burning period (<1000 s) compared to the fires in the Purser Furnace (~3300 s). The fire equivalence ratio was richer for PE-Y fires in the Purser Furnace, ~4 times richer than PE-Y fire in the Cone Calorimeter (ER~2.0). Richer PE-Y fires in the Purser Furnace had consumed high Oxygen (~21% by volume) while the leaner PE-Y fire in the Cone Calorimeter had consumed a maximum Oxygen consumption up to 10%.
- The MLR was higher for PE-Y fire in the Cone Calorimeter with giving the highest MLR peak of 0.4 g/s at 600 s of burning period while PE-Y fires in the Purser Furnace showed MLR values <0.1 g/s. A shorter burning period taken by PE-Y fire in the Cone Calorimeter contributed to a higher MLR value, hence also contributing to a higher HRR (MLR) value. PE-Y fire in the Cone Calorimeter gave a maximum HRR peak of 1800 kW/m$^2$ while these Polyethylene fires in the furnace gave lower HRR values <400 kW/m$^2$.
- PE-Y fires in both test methods had the same CO concentration peak of 30000 ppm at <1500 s. For the same test period, these PE-Y fires gave the same level of HCl, $SO_2$ and Acetaldehyde emissions while for other toxic species, the PE-Y fires in the furnace showed the higher concentration than the PE-Y fire in the cone. This contributed to the higher total LC50, $COSHH_{15min}$ and AEGL-2 values for the PE-Y fires in the Purser Furnace than the fires in the Cone Calorimeter.
- CO yields were higher for PFS T1 ER 2.0 and PFS T2 ER 0.8 fires compared to CC 35 FV fire with PFS T1 ER 2.0 fire gave the maximum CO yield of 0.8 g/g at 1000 s, PFS T2 ER 0.8 and CC 35 FV fires had the maximum CO yield peak of 0.6 g/g and 0.3 g/g at ~300 s. PE-Y fire

in the cone gave a higher Acetaldehyde yield compared to the PE-Y fires in the furnace. These Polyethylene fires had shown the same average of Acetylene (0.25 g/g) and Toluene yields (0.06 g/g). In overall, PE-Y fires with air flowrate of 10 L/min in the Purser Furnace gave the higher yield values for most of toxic species compared to the PE-Y fire in the Cone Calorimeter with free ventilation condition.

- Formaldehyde, Acrolein, CO and Benzene were the four common major species observed for most of conducted polymer fires including Polyethylene materials. HBr was also the major species which dominating the total toxicity for PE-Y fire in the Calorimeter. $NO_2$ contribution was significant and this species also a major species from the PE-Y fires in the Purser Furnace.
- Soot mass collected from the filter papers was higher in a factor of 3 for PFS T1 ER 2.0 than the PFS T2 ER 0.8. Two soot yield peaks were given by these two PE-Y fires with PFS T2 ER 0.8 fire gave lower soot yields than the PFS T1 ER 2.0 fire. The maximum soot yield of 0.0003 g/g was shown by PFS T1 ER 2.0 fire at <500 s while the PFS T2 ER fire 0.8 gave the maximum soot yield of 0.0001 g/g at >2000 s.
- Number and mass distributions for 10 nm particles were lower than the 100 nm particles for both PE-Y fires in the furnace for the first 1500 s. Within the same burning period, the mass concentration of 10 nm (1.0E-06 g/$m^3$) and 100 nm (1.0E-02 g/$m^3$) particles had shown the same average level for both PE-Y fires. At the flame out state, the cumulative mass for 200 nm particles was 4 times (~4000 g/$m^3$) higher for PFS T1 ER 2.0 fire compared to PFS T2 ER 0.8 fire. The cumulative mass of 600 nm particles was same, ~2000 g/$m^3$ for both PE-Y fires while for larger particles (>600 nm), PFS T2 ER 0.8 fire gave a higher cumulative mass than the PFS T1 ER 2.0 fire.
- Number yields for 10 nm particles were higher than 100 nm particles for both PE-Y fires in the Purser Furnace while for the mass yields, the values were higher for 100 nm particles compared to 10 nm particles. 10 nm particulate yields were produced before 700 s of test time when the fire equivalence ratio <4.0 for the PFS T1 ER 2.0 fire with the average number and mass yields of 1.0E+08 p/kg and 1.0E-04 g/g.
- In overall, CC 35 FV fire in the cone had contributed to a lower fire toxicity than the PFS T1 ER 2.0 and PFS T2 ER 0.8 fires in the furnace. The PFS T1 ER 2.0 fire was more toxic compared to the PFS T2 ER 0.8 fire for the tests conducted in the Purser Furnace.

# Chapter 10
# Conclusion and Recommendation

## 10.1 General Discussion of Significant of Findings

The restricted Cone Calorimeter is designed to provide some control over the fuel/air mixture during specimen combustion so that the yields of toxic combustion products can be measured over a range of equivalence ratios typical of those occurring during compartment fires. By varying the ventilation conditions, it is possible theoretically to vary the fuel/air ratio during combustion and examine the effect on yields of toxic fire gases and particulates. In practice complications were found in that:

- The pyrolysis rate of the fuel depends on the applied heat flux and the rate of combustion
- The combustion behaviour flaming or non-flaming depends on the applied heat flux
- The combustion behaviour is also affected by the air flow over the specimen
- The mass loss rate and composition of the fuel mass loss varies throughout the test run and depends upon the composition of the specimen (especially whether it is a char former or not).

### 10.1.1 Main Findings

- The general pattern with a Cone Calorimeter run is that there is an early stage after exposure to the radiant heat when the specimen heats up and begins to pyrolyze, but before flaming ignition occurs. The products during this period are generally rich in CO and small particles including condensed aerosols of organic vapours. After a short period (typically <100 seconds) the fuel rich gas phase products ignite and there is typically a short period of intense, relatively fuel rich combustion (ER ~1.2) resulting in higher concentrations of gases and particulates as measured form the chimney above the Cone heater. Following this the fuel/air ratio and product concentrations tend to decrease somewhat as the specimen continues to burn. For non-char forming thermoplastic materials such as PE, there is generally then a period of steady burning as the specimen pool is consumed, with some changes toward the end of the run. With char forming materials the situation is more complex,

since the composition of the specimen changes throughout the run. At the beginning of the run more volatile organic pyrolysis products are given off, while as the run progresses the proportion of Carbon char increases, so that towards the end of the run the main fuel remaining is the Carbon char.

- At low radiant heat the pyrolysis rate is low and ignition may fail to occur. The dominant mode of decomposition is then oxidative pyrolysis and the ER is low and does not affect decomposition.
- At middle and higher radiation levels the fuel pyrolysis rate is sufficient to result in maintain flaming combustion for most of the run. Under these conditions it was possible to observe some variation in ER during the run, but this was generally over a relatively narrow range between approximately 0.8 – 1.2 is. This was because limited air low tended to reduce the mass loss rate, so it was difficult to obtain ERs in the 1.5-3.0 range typical of under ventilated and post flashover compartment fires.
- At higher ventilation rates in the controlled cone the high air flow was found to inhibit flaming, resulting in somewhat inhibited well ventilated combustion.
- Surprisingly, the fuel air ratio in the primary combustion zone under the Cone heater was found to be somewhat higher under free ventilation conditions than under controlled ventilation conditions, because the space between the open specimen and the cone limited air flow under free ventilation, but the forced ventilation in the controlled ventilation Cone actually provided a higher fuel/air ratio. This demonstrates that in the standard Cone Calorimeter, the combustion as measured in the duct, which is always well-ventilated, results mainly from secondary combustion of primary products above the Cone heater, while the primary combustion under the Cone is relatively fuel rich.
- The overall finding with the controlled ventilation Cone Calorimeter is that the combustion conditions vary considerably throughout a run so that the product yields are very variable, but in general the combustion condition operate in a range between ER ~0.8 and 1.2, which is typical of some compartment fires, but does not include the more under ventilated range occurring in many situations.
- A wide range of materials were tested for this study to examine the range and yields of toxic gases and particulates evolved.

## 10.2 Conclusion

### 10.2.1 Restricted Ventilation Fire Tests in the Cone Calorimeter

The restricted ventilation fire tests with varying heat flux in the Cone Calorimeter resulted in the following general findings.

***PVC Prysmian A Electrical Cable Fires:***

- CO emissions increased with the increase of heat flux value. CO concentration showed a maximum value of ~70000 ppm at heat flux of 50 kW/m$^2$ compared to the cable fires at heat flux of 25 kW/m$^2$ (<16000 ppm) and heat flux of 35 kW/m$^2$ (<25000 ppm). These cable fires gave the highest peak of HCl concentration ~20000 ppm.
- The total toxicity based LC50 basis increased with the increase of heat flux value giving the maximum total LC50 values of <12 (25 kW/m$^2$), <14 (35 kW/m$^2$) and <20 (50 kW/m$^2$). The total $COSHH_{15min}$ for these cable fire gave the same average of ~6000. While for AEGL-2 basis, the total toxicities were >2 times higher (~1500) for cable fire at heat flux of 25 kW/m$^2$ compared to the higher heat fluxes (<600).
- CO yields produced were higher for the higher heat flux of 50 kW/m$^2$, <0.2 g/g with ER<0.3 while the lower heat fluxes showed a rich burning with ER>1.4 and CO yields <0.12 g/g. HCl yields were <0.3 g/g for these cable fires. The higher heat flux had the lowest minimum combustion efficiency of ~70% compared to the lower heat fluxes (>80%) due to the increase of CO emissions.
- HCl, CO, Formaldehyde and Acrolein were the first four major toxic gases that contributing to the fire toxicity for these cable fires.
- 10 nm particles had a higher number concentration than 100 nm particles for most of these cable fires. Particulate yields for 10 nm and 100 nm particles were in a range from 1.0E-05 g/g to 1.0E-02 g/g with the yields for 10 nm particles were lower than 100 particles at the initial burning while the values increased to be higher in the middle of burning (~400 s) compared to 100 nm particles for most of these cable fires.

The Cone Calorimeter as used this work with a restricted atmosphere enclosure can be used to test material under realistic fire ventilation conditions. Even with free ventilation the raw gases are rich locally and a range of equivalence ratios are generated in the tests.

### 10.2.2 Free-ventilated Fire Tests in the Cone Calorimeter

The free-ventilated fire tests for various electrical cables and polymeric materials with heat flux of 35 kW/m$^2$ and free ventilation in the Cone Calorimeter resulted in the following general findings.

***Various Electrical Cable Fires:***

- Prysmian A and EC-GB cables were the PVC type of electrical cable which produced HCl when burned. However the HCl concentration were much lower for EC-GB cable fires (<500 ppm) compared to Prysmian A cable fire (~20000 ppm). HCl yields for EC-GB cable fires were <0.02 g/g. Unexpectedly for FLEX1-BG cable sample which was not specified as PVC cable, the HCl emissions (~50000 ppm) from this cable fire were >2 times higher than the PVC cable fires with the maximum HCl yield ~0.4 g/g. The HCl emissions for FLEX2-W cable fire were also high (~5000 ppm) but far lower compared to the PVC Prysmian A and FLEX1-BG cable fires.
- Under these test conditions, PVC cable fires (Prysmian A and EC-GB) gave lower CO yields compared to other electrical cable fires with the maximum CO yield (~0.08 g/g) for Prysmian A cable fire was double than the CO yield for the two EC-GB cable fires. Wind Turbine cable fires had the CO yields <0.1 g/g while other cable fires showed the CO yield peak up to 0.16 g/g. PVC Prysmian A and most of LSZH and FLEX cable fires had shown a rich burning condition with the ER up to 2.0 except for the PVC EC-GB, Solar Energy and Wind Turbine cable fires which gave ER less than 0.8.The combustion efficiency rate, ŋ for these cables were in a range from 60% up to 100% with the two EC-GB cable fires had the maximum combustion efficiency peak of 80%.
- Based on the LC50 method, the first three major species for most of these cable fires were Acrolein, Formaldehyde and CO for the flaming fire condition. For $COSHH_{15min}$, Benzene was in the list of first three major species that contributed to the total toxicity of these cable fires except for EC-GB and FLEX1-BG cable fires which this species was still a major species but was not in the first three.
- Particle number distributions from PVC Prysmian A cable fire have an average of 1.0E+09 p/cm$^3$ for 10 and 100 nm particles with the average mass of 10 nm particles (1.0E+00 g/m$^3$) was higher than the 100 nm particles (1.0E-03 g/m$^3$). While the LSZH cable fires (including the Wind

Turbine cable fires) gave the particle number and mass concentration in between 1.0E+08 to 1.0E+10 p/$m^3$ and 1.0E-04 to 1.0E+00 g/$m^3$.

- With a rich fire condition (ER~2.5), the PVC Prysmian A cable fire gave a mass yield of 1.0E-03 p/kg for 100 nm particles which higher than the mass yield for 10 nm particles (<1.0E-03 p/kg). Compared to the PVC Prysmian cable fire, the average mass yield of 100 nm particles for the three LSZH cable (AMI-B, Prysmian B and 6701B-W) fires was higher (~1.0E-01 g/m3). Most of these cable fires had the same average number yield of 1.0E+10 p/kg for 10 nm particles and 1.0E+04 p/kg for 100 nm particles.

***PU and PIR Solid Foam Fires:***

- CO emissions for PU-FM and PU-FB fires (the maximum concentration peak of 70000 ppm) were >2 times higher compared to other two foam (PU-FSC and PIR-F GT) fires. The PIR-F GT fire gave the HCN concentration <400 ppm, 5 times lower than the PU-FSC foam fire while the PU-FM and PU-FB fires gave a higher HCN emission of 4000 ppm. This significant HCN concentration was expected for these Nitrogen containing materials. The highest peak of HCl emission (~2500 ppm) was shown by the PU-FSC foam fire and was higher compared to <500 ppm.of HCl peak by the PIR-F GT foam fire. There were none significant HCl emissions observed by PU-FM and PU-FB foam fires. Other species like Formaldehyde, the concentration was higher for PIR foam fire (<1400 ppm) than the three PU foam fires (<400 ppm) while Acrolein concentration was <400 ppm for these PU and PIR foam fires.
- The three PU foam fires gave CO yields from 0.3 up to 0.5 g/g while the CO yields for PIR foam fire <0.4 g/g. The HCN yields (<0.01 g/g) for PIR foam fire were >3 times lower than the PU foam fires. Both PU and PIR foam fires showed the $CO_2$ yields in between 0.5 to 3.0 g/g during the burning with the PIR foam fire gave the highest CO yield peak. The THC yield for PIR foam fire (0.2 g/g) was lower in a factor of 3 if compared with the PU foam fires.
- The total FEC LC50 values (<40) were the highest for PU-FM and PU-FB foam fires if compared to PU-FSC foam fire (<20) and PIR foam fire (<5). The total LC50 values were high for these polymer fires with the value up to 40 but it was lower if compared to the clear Acrylic or rubber fires (from 50 up to 70). According to the total $COSHH_{15min}$ assessment,

PIR foam burning was less toxic (total $COSHH_{15min}$ <500) than the PU foam burning (total $COSHH_{15min}$ >2000), the same with the AEGL-2 method which the PIR foam fire gave a lower total toxicity compared to the three PU foam fires.

- HCN was the first major toxic species that contributing to the highest percentage of the total LC50, ~55% followed by CO (~35%) and other species such as Formaldehyde, Acrolein, $NO_2$ (<10%) within of the flaming state of these foam fires.

***Polyethylene Fires:***

- HBr emissions produce were much more higher for these Polyethylene fires compared to other polymer fires which this species was the major species contributed to the overall LC50 total toxicity of these polymer fires. Concentration of other toxic gases was also significant especially the Benzene and THC with over the range of measurement values.
- Total toxic emissions from all five PE samples had FECs of LC50 greater than 1.0 with the highest peak ~17, but the worst toxicity was for the three flammable liquid bunds with high HBr toxic emissions.
- In terms of the impairment of escape the $COSHH_{15min}$ and AEGL-2 toxic limits had different conclusions and this was due to $COSHH_{15min}$ placing a lower concentration for HBr. This resulted in HBr being the most important toxic gas under the $COSHH_{15min}$ assessment compared with Acrolein under the AEGL-2 assessment, which was the second most toxic gas under $COSHH_{15min}$.
- CO yields of these Polyethylene fires were below 0.45 g/g with PE-Blue gave the highest yield value. These Polyethylene fires had given $CO_2$ yields <3.0 g/g. Some of yield values presented were insensible and this could be due to the out of measurement range by the FTIR especially for the toxic Hydrocarbons.
- The two most dominant toxic species were Acrolein and HBr for these Polyethylene fires. Other toxic species like Benzene, Formaldehyde, $SO_2$, CO, HCN and $NO_2$ were also the major contributors to the fire toxicities for this polymer fires.

***Polystyrene Fires:***

- Some Polystyrene fires like PS2 and PS-CB 2 fires had still released toxic gases even there was non-flaming fire condition experienced and

this was not an exception on contributing to the overall fire toxicity of these polymer fires.

- Total LC50 values for the higher density of Polystyrene fires were up to 22 while for the low density Polystyrene fires such as PS-TV, the fire had contributed to the total LC50 up to 8. Other three Polystyrene fires showed the total LC50 values <4. These Polystyrene fires resulted to a maximum total $COSHH_{15min}$ of ~7000 which in a factor of 7 compared with the maximum total toxicity based on AEGL-2 that determined for these polymer fires.
- Similar to the result obtained from the conducted Polyethylene fires, these Polystyrene fires had also given $CO_2$ yields <3.0 g/g. The maximum CO yield (~0.5 g/g) for the higher density Polystyrene fires were higher than the low density Polystyrene fires which the value was almost double.
- Asphyxiants such as CO and HCN and incapacitating irritants such as Benzene, Formaldehyde, Acrolein and $NO_2$. $SO_2$ were the major species for these polymer fires and its contribution was significant especially before the point of ignition when the pyrolysis of material occurred and during the post-flaming period.

***Other Polymer Fires:***

- Clear A-B and RBS FB fires produced a higher concentration of toxic gases than other two polymers with GRP-Blue gave the lowest toxic gas concentrations. The highest HCl concentration of 40000 ppm was given by the PVC ST-W fire while insignificant HCl concentration was shown by the other three polymers. HCN emissions were significant for Clear A-B and RBS FB fires with a maximum concentration of 8000 ppm showed by Clear A-B fire, about double than the RBS FB fire.
- Within 300 s of test time, Clear A-B fire gave the highest CO yield peak of 0.4 g/g which ~4 times higher than other polymer fires (<0.1 g/g). The result had a good agreement with the CO emissions produced from these polymer fires which the CO concentration shown by Clear A-B fire was ~160000 ppm while the CO concentration for RBS FB and other two polymer fires was <40000 ppm. The highest HCl yield peak of ~0.8 g/g was given by the chlorinated polymer fire, the PVC ST-W.
- Among all the tested electrical cables and polymers in the present work, total LC50 for these four polymer fires were high and most significant especially for Clear A-B and RBS FB fires which giving the

total LC50 peaks >55. The PVC pipe (PVC ST-W) fire gave the total LC50 ~20 and the total LC50 values <5 were shown by GRP-Blue fire. For $COSHH_{15min}$ and AEGL-2 basis, the total toxicities were the highest for Clear A-B fire with 25000 of total $COSHH_{15min}$ peak and 3800 of AEGL-2 peak.

- Formaldehyde, Acrolein and CO were the three major toxic species for these polymer fires according to the LC50 toxic assessment method. Compared to Formaldehyde and Acrolein contributions on the fire total toxicity, CO contribution was lower for GRP-Blue and PVC ST-W fires than the Clear A-B and RBS FB fires. Based on $COSHH_{15min}$ toxic assessment method, HCN and Benzene were also a major species for Clear A-B and RBS FB fires. For PVC ST-W fire, HCl was a dominant species and contributed to the highest total toxicity % for LC50 and $COSHH_{15min}$ methods.
- For the rubber fire, the number concentration of 10 nm particles (>1.0E+09 p/cm$^3$) was higher than 50 nm and 100 particles while the mass concentration of 10 nm particles (<1.0E-02 g/m$^3$) was lower than 50 nm and 100 particles. Particles <100 nm gave the cumulative of ~100 g/m$^3$, ~30 times lower compared to 400 nm particles.
- Number yield for 10 nm (1.0E+10 p/kg) was much higher than 50 nm and 100 particles (1.0E+05 p/kg) but all these three size of particles that produced from the RBS FB fire gave a same average mass yield of 1.0E-03 g/g.

### 10.2.3 Fire Tests in the Purser Furnace System

The results for Polyethylene fires in the Purser Furnace with two different mean metered equivalence ratios were compared and the results were also compared with the results from the Cone Calorimeter test. The main findings are listed as follow:

***Polyethylene (PE-Y) Fires:***

- PE-Y fires in both test methods had the same CO concentration peak of 30000 ppm at <1500 s. For the same test period, these PE-Y fires gave the same level of HCl, $SO_2$ and Acetaldehyde emissions while for other toxic species, the PE-Y fires in the furnace showed the higher concentration than the PE-Y fire in the cone. This contributed to the

higher total LC50, $COSHH_{15min}$ and AEGL-2 values for the PE-Y fires in the Purser Furnace than the fires in the Cone Calorimeter.

- CO yields were higher for PFS T1 ER 2.0 and PFS T2 ER 0.8 fires compared to CC 35 FV fire with PFS T1 ER 2.0 fire gave the maximum CO yield of 0.8 g/g at 1000 s, PFS T2 ER 0.8 and CC 35 FV fires had the maximum CO yield peak of 0.6 g/g and 0.3 g/g at ~300 s. PE-Y fire in the cone gave a higher Acetaldehyde yield compared to the PE-Y fires in the furnace. These Polyethylene fires had shown the same average of Acetylene (0.25 g/g) and Toluene yields (0.06 g/g). In overall, PE-Y fires with air flowrate of 10 L/min in the Purser Furnace gave the higher yield values for most of toxic species compared to the PE-Y fire in the Cone Calorimeter with free ventilation condition.
- Formaldehyde, Acrolein, CO and Benzene were the four common major species observed for most of conducted polymer fires including Polyethylene materials. HBr was also the major species which dominating the total toxicity for PE-Y fire in the Calorimeter. $NO_2$ contribution was significant and this species also a major species from the PE-Y fires in the Purser Furnace.
- Soot mass collected from the filter papers was higher in a factor of 3 for PFS T1 ER 2.0 than the PFS T2 ER 0.8. Two soot yield peaks were given by these two PE-Y fires with PFS T2 ER 0.8 fire gave lower soot yields than the PFS T1 ER 2.0 fire. The maximum soot yield of 0.0003 g/g was shown by PFS T1 ER 2.0 fire at <500 s while the PFS T2 ER fire 0.8 gave the maximum soot yield of 0.0001 g/g at >2000 s.
- Number and mass distributions for 10 nm particles were lower than the 100 nm particles for both PE-Y fires in the furnace for the first 1500 s. Within the same burning period, the mass concentration of 10 nm (1.0E-06 $g/m^3$) and 100 nm (1.0E-02 $g/m^3$) particles had shown the same average level for both PE-Y fires. At the flame out state, the cumulative mass for 200 nm particles was 4 times (~4000 $g/m^3$) higher for PFS T1 ER 2.0 fire compared to PFS T2 ER 0.8 fire. The cumulative mass of 600 nm particles was same, ~2000 $g/m^3$ for both PE-Y fires while for larger particles (>600 nm), PFS T2 ER 0.8 fire gave a higher cumulative mass than the PFS T1 ER 2.0 fire.
- Number yields for 10 nm particles were higher than 100 nm particles for both PE-Y fires in the Purser Furnace while for the mass yields, the values were higher for 100 nm particles compared to 10 nm particles. 10 nm particulate yields were produced before 700 s of test time when

the fire equivalence ratio <4.0 for the PFS T1 ER 2.0 fire with the average number and mass yields of 1.0E+08 p/kg and 1.0E-04 g/g.

### 10.2.4 Comparison of Results for Fire Tests in the Cone Calorimeter and Purser Furnace System

***Polyethylene (PE-Y) Fires:***

- HBr emissions from the PE-Y fire in the Cone Calorimeter were higher and more significant than the PE-Y fire in the Purser Furnace. From the analysis by the TGA and the test results, it is a high possibility that the chemical composition of these two PE-Y samples is different even both samples were physically looked the same with the same colour identification.
- In overall, CC 35 FV fire in the cone had contributed to a lower fire toxicity than the PFS T1 ER 2.0 and PFS T2 ER 0.8 fires in the furnace. The PFS T1 ER 2.0 fire was more toxic compared to the PFS T2 ER 0.8 fire for the tests conducted in the Purser Furnace.

## 10.3 Recommendation

For the Cone Calorimeter tests, the measurement of sample temperature at the point of ignition can be done by placing Thermocouples in the samples. In the present work, instead of using the Thermocouples, the Infrared camera had been used to determine the sample temperature only for bunding material fires (Polyethylene and GRP fires) with piloted ignition. Further investigations on the sample temperature during the burning in the Cone Calorimeter could be done in future for other types of polymeric material.

For the new Purser Furnace, some useful recommendations to the future operators as follow:

a) Method for observation of flame should be improved. Instead of using a mirror to observe the flame, it is recommended to use a camera or recorder as a proper way to observe, capture and record the flame behaviour.
b) It is not an easy work to clean the sample boat, internal furnace tube and the chamber wall. In example, Polyethylene residues which were left in the end of test would stick to the chamber wall and other area

inside the furnace system especially when the temperature was cooled down naturally after the test. It would require the use of strong chemical solution to dissolve the residue and remove it off from the system. To reduce the effort on cleaning the system with chemical solution, the unburned residues could be burned completely by rising up the furnace temperature to a high temperature (800$^{o}$C).

c) Suitable range of driving controller's dial should be used for an easy adjustment during the fire tests and for an accurate setting of the fuel feed rates to represent certain equivalence ratios.
d) Measurement of toxic gases by the FTIR analyser should be done for both raw and diluted sampling points for comparison purposes and as a reference when analysing the results.

Regarding the calibrated measurement range of the FTIR, it is recommended to have a wider measurement range to be able to measure very high concentrations of toxic species released from certain polymer fires to avoid any insensible results.

## 10.4 Future Works

For the next research project, an initial plan is to focus more on the aging process of the particulates in order to understand how the particles behave on a longer term and to predict the particle behaviour and toxicity in fires. The aging is probably will be different depending to the amount of particles and the type of substances found in the particles. This is mainly related to the post analysis of the tested polymers in the present work through an application of the Scanning Electron Microscopy (SEM). Further analysis on the soot samples collected on filter papers could also be done using Gas Chromatography Mass Spectrometry (GC/MS) in order to determine the presence of Polycyclic Aromatic Hydrocarbons (PAHs) in the soot. However, it would be good too to continue with other fire toxicity tests from the work done in the present work as mentioned in the following sections.

### 10.4.1 Fire Tests with and without Thermodenuder attached to the Particle Sizer in the Cone Calorimeter and Purser Furnace System

In Chapter 3 Research Methodology, it was elaborated a bit about the Dekati Thermodenuder. Although the author did not have a chance to use it while

doing the fire tests, it included in the future works to be done. It is important to compare the results of particle size measurement with and without using the Thermodenuder together with the Particle Sizer. This analyser functions to remove volatiles from the fire effluents before particle size measurement takes place by the Particle Sizer equipment. It will allow in differentiating between particle only profile and volatile and particle mixture profile which is obtained from the plotted graph as in the present study.

### 10.4.2 More Fire Tests in the New Developed Purser Furnace System Burning Various Fuels

For the new developed Purser Furnace, these were preliminary experiments. The results show problems with the operation of the apparatus and that these issues need to be investigated for any further work.

In the present work, only several fire tests were done in the new developed Purser Furnace System involving one test material only. Many tests could be done using this fire rig in future with burning various polymers that had been tested in the present work using the Cone Calorimeter for comparison in the results from both fire test methods. Variation in initial parameters like initial air flowrate and fuel speed rate set in the Purser furnace would vary the test conditions. Hence it also varies the experimental result on fire toxicities. Unlike the Cone Calorimeter, the Purser furnace was expected to give a constant burning of materials. This makes Purser furnace a better method in control to assess fire toxicities.

Further investigation on the furnace operation temperature is also significant and highly recommended for the future works in order to study the furnace temperature profile and its effects on the material burning. As the recorded temperatures inside the furnace in the present work showed a large different from the furnace set temperature (600$^{o}$C).

### 10.4.3 More Restricted Ventilation Fire Tests in the Cone Calorimeter Burning Various Polymers

Most of restricted ventilation fire tests in the present work involved the burning of various electrical cables (about 12 types). The heat fluxes and air flowrates were varied for some electrical cable fires. But for polymer groups such as Polyethylene, PIR and PU foams, Polystyrene and other polymers, fire tests

were conducted under free ventilation condition only, with some of the tests with varying irradiation levels and either with auto or piloted ignition. The same polymers could be tested under restricted ventilation conditions in the Cone Calorimeter in the future for result comparison with the free ventilation tests.

# List of References


1. *Fire & rescue incident statistics, England, year ending September 2019.* 2019.
2. *CTIF Centre of Fire Statistics-World Fire Statistics:*. 2018.
3. Alarifi, A., H.N. Phylaktou, and G.E. Andrews, *What Kills People in a Fire? Heat or Smoke?* 2016.
4. *National Statistics-Fire Statistics: Great Britain April 2013 to March 2014*. 2014.
5. Hertzberg, T., et al., *Particles and isocyanates from fires*. 2003: SP Swedish National Testing and Research Institute, Fire Technology.
6. Goo, J., *Study on the real-time size distribution of smoke particles for each fire stage by using a steady-state tube furnace method.* Fire Safety Journal, 2015. **78**: p. 96-101.
7. Lingard, J.J., et al., *Observations of urban airborne particle number concentrations during rush-hour conditions: analysis of the number based size distributions and modal parameters.* Journal of Environmental Monitoring, 2006. **8**(12): p. 1203-1218.
8. BBC. *Grenfell Tower: What happened*. 2019 [cited 2020 01.09.2020].
9. Purser, D.A., *Effects of exposure of Grenfell occupants to toxic fire products— Causes of incapacitation and death. Phase 1 Report: General description of hazards excluding comprehensive references to individual occupants*. 2018.
10. Moore, J. and V. Hrymak, *Fire Safety in 17 Irish Nursing Homes.* 2012.
11. BBC. *BBC News 2011: Rosepark care home deaths 'preventable' inquiry finds*. 2011.
12. Purser, D.A., *Effects of pre-fire age and health status on vulnerability to incapacitation and death from exposure to carbon monoxide and smoke irritants in Rosepark fire incident victims.* Fire and Materials, 2017.
13. Miller, K., *Piper Alpha and the Cullen Report.* Indus. LJ, 1991. **20**: p. 176.
14. Cullen, L.W.D., *The public inquiry into the Piper Alpha disaster.* Drilling Contractor;(United States), 1993. **49**(4).
15. Fennel, D., *Investigation into the King's Cross Underground Fire*, in *Fennel Report*. 1988.
16. *How air pollution can cause cancer*. 2016.
17. *CBS News - FDNY: 9/11 illness kills 3 retired firefighters in one day*. 2014.
18. *The Building Regulations 2010 - Fire Safety (Approved Document B)*, H. Government, Editor. 2019: England.
19. *BS 7974:2001 - Application of fire safety engineering principles to the design of buildings. Code of practice. (2001).* 2012.
20. *BS 9999:2017 - Fire safety in the design, management and use of buildings. Code of practice. (2017).* 2017.
21. Kaczorek, K., A.A. Stec, and T.R. Hull, *Carbon monoxide generation in fires: effect of temperature on halogenated and aromatic fuels.* Fire Safety Science, 2011. **10**: p. 253-263.

22. Fraser, T.M., *Toxic Chemicals in the Workplace: A Manager's Guide to Recognition Evaluation Control*. 1996: Gulf Publishing Company.
23. Tan, K.-H. and T.-L. Wang, *Asphyxiants: simple and chemical.* Ann Disaster Med Vol, 2005. **4**: p. 1.
24. Michael A.T. Marro, M.A.P., J. Houston Miller, *Strategy for the simplification of nitric oxide chemistry in a laminar methane/air diffusion flamelet.* Combustion and Flame, 1997. **111**(3): p. Pages 208-221.
25. Stec, A. and T.R. Hull, *Fire toxicity and its assessment.* Fire retardancy of polymeric materials, Second edn. CRC Press, Boca Raton, FL, 2010: p. 453-477.
26. Stec, A.A., *Fire Toxicity and its Measurement*. 2007, The University of Bolton.
27. Mehlman, M., *Health Effects and Toxicity of Phosgene: Scientific Review.* Defence Science Journal, 2014. **37**(2): p. 269-279.
28. Faroon, O., et al., *Acrolein health effects.* Toxicology and industrial health, 2008. **24**(7): p. 447-490.
29. Organization, W.H., *Exposure to benzene: a major public health concern.* Geneva: WHO Document Production Services, 2010.
30. Pierini, C., *A Health-Destroying Toxin We Can't Avoid And Must Detoxify.*
31. Bruce, R.M., J. Santodonato, and M.W. Neal, *Summary review of the health effects associated with phenol.* Toxicology and Industrial Health, 1987. **3**(4): p. 535-568.
32. Sakurai, H., et al., *Health effects of acrylonitrile in acrylic fibre factories.* British journal of industrial medicine, 1978. **35**(3): p. 219-225.
33. Stec, A.A., et al., *The effect of temperature and ventilation condition on the toxic product yields from burning polymers.* Fire and Materials, 2008. **32**(1): p. 49-60.
34. Purser, D. *The application of exposure concentration and dose to evaluation of the effects of irritants as components of fire hazard*. in *Interflam, conference proceedings*. 2007.
35. Purser, D., *Behavioural impairment in smoke environments.* Toxicology, 1996. **115**(1–3): p. 25-40.
36. Stec, A.A., et al., *Comparison of toxic product yields from bench-scale to ISO room.* Fire Safety Journal, 2009. **44**(1): p. 62-70.
37. Stec, A.A. and T.R. Hull, *Assessment of the fire toxicity of building insulation materials.* Energy and Buildings, 2011. **43**(2–3): p. 498-506.
38. *Fire Statistics United Kingdom 2007, Department for Communities and Local Government, London, August 2009, and preceding volumes.* 2009.
39. *BS ISO 13344:2015 - Estimation of the lethal toxic potency of fire effluents. (2016).* 2016.
40. *HSE. (2018). EH40/2005 Workplace exposure limits.3rd ed. UK: TSO, part of Williams Lea Tag*. 2018.
41. *EPA, Environmental Protection Agency. (2018). Compiled Acute Exposure Guideline Values (AEGLs)*. 2018.

42. Purser, D.A., *Toxic product yields and hazard assessment for fully enclosed design fires.* Polymer International, 2000. **49**(10): p. 1232-1255.
43. Purser, D.A., *Review of human response to thermal radiation, HSE contract research report No. 97/1996: S. M. Hockey and P. J. Rew. HSE Books, PO Box 1999, Sudbury, Suffolk CO10 6FS, UK 1996, 49 pp., £15·00 net, ISBN 0 7176 1083 7, paperback.* Fire Safety Journal, 1997. **28**(3): p. 290-291.
44. Forbes. *This Is How A Volcano's Pyroclastic Flow Will Kill You*. 2017 [cited 2020 01.09.2020].
45. Hartin, E., *Fire development and fire behavior indicators.* FireHouse. Accessed August, 2008. **10**.
46. Purser, D., *Influence of fire retardants on toxic and environmental hazards from fires.* Fire retardancy of polymers: new strategies and mechanisms. Royal Society of Chemistry, 2009: p. 381-404.
47. Hull, T.R., et al., *Factors affecting the combustion toxicity of polymeric materials.* Polymer Degradation and Stability, 2007. **92**(12): p. 2239-2246.
48. Hull, T.R. and K.T. Paul, *Bench-scale assessment of combustion toxicity—A critical analysis of current protocols.* Fire Safety Journal, 2007. **42**(5): p. 340-365.
49. Stec, A.A., T.R. Hull, and K. Lebek, *Characterisation of the steady state tube furnace (ISO TS 19700) for fire toxicity assessment.* Polymer Degradation and Stability, 2008. **93**(11): p. 2058-2065.
50. Stec, A.A., et al., *A comparison of toxic product yields obtained from five laboratories using the steady state tube furnace (ISO TS 19700).* Fire Safety Science, 2008. **9**: p. 653-664.
51. Stec, A.A. and J. Rhodes, *Bench scale generation of smoke particulates and hydrocarbons from burning polymers.* Fire Safety Science, 2011. **10**: p. 629-639.
52. Stec, A.A. and J. Rhodes, *Smoke and hydrocarbon yields from fire retarded polymer nanocomposites.* Polymer Degradation and Stability, 2011. **96**(3): p. 295-300.
53. Hull, T.R., et al., *Combustion toxicity of fire retarded EVA.* Polymer Degradation and Stability, 2002. **77**(2): p. 235-242.
54. Hull, R.T., A.A. Stec, and J. Robinson. *Development of Standards for Assessment of Fire Effluent Toxicity and their Application to Cable Installations*. 2008.
55. Hull, T.R., et al., *Comparison of toxic product yields of burning cables in bench and large-scale experiments.* Fire Safety Journal, 2008. **43**(2): p. 140-150.
56. Carman, J.M., et al., *Experimental parameters affecting the performance of the Purser furnace: a laboratory-scale experiment for a range of controlled real fire conditions.* Polymer International, 2000. **49**(10): p. 1256-1258.
57. Chan, S., *An Exhaust Emissions Based Air–Fuel Ratio Calculation for Internal Combustion Engines.* Proceedings of the Institution of Mechanical Engineers, Part D: Journal of Automobile Engineering, 1996. **210**(3): p. 273-280.

58. Chan, S. and J. Zhu, *Sensitivity analysis of an exhaust-emissions-based air: fuel ratio model for gasoline engines.* Journal of the Institute of Energy, 1996. **69**(480): p. 144-154.
59. Chan, S. and J. Zhu, *Exhaust Emission Based Air-Fuel Ratio Model (I): Literature Reviews and Modelling*. 1996, SAE Technical Paper.
60. Chan, S. and J. Zhu, *Exhaust Emission Based Air-Fuel Ratio Model (II): Divergence Analysis and Emission Estimations*. 1996, SAE Technical Paper.
61. Chan, S. and J. Zhu, *Divergence analysis of an emissions-based air—fuel ratio model and exhaust oxygen estimation.* Proceedings of the Institution of Mechanical Engineers, Part D: Journal of Automobile Engineering, 1997. **211**(2): p. 137-144.
62. Purser, D.A., *Recent developments in understanding the toxicity of PTFE thermal decomposition products.* Fire and Materials, 1992. **16**(2): p. 67-75.
63. Purser, D. and J. Purser, *HCN yields and fate of fuel nitrogen for materials under different combustion conditions in the ISO 19700 tube furnace and large-scale fires.* Fire Safety Science, 2008. **9**: p. 1117-1128.
64. Blomqvist, P., et al., *Detailed determination of smoke gas contents using a small-scale controlled equivalence ratio tube furnace method.* Fire and Materials, 2007. **31**(8): p. 495-521.
65. Hirschler, M.M. and D.A. Purser, *Irritancy of the smoke (non-flaming mode) from materials used for coating wire and cable products, both in the presence and absence of halogens in their chemical composition.* Fire and Materials, 1993. **17**(1): p. 7-20.
66. Hull, T.R., K. Lebek, and J.E. Robinson, *Acidity, Toxicity And European Cable Classification.* 2006.
67. Hull, T.R., J.M. Carman, and D.A. Purser, *Prediction of CO evolution from small-scale polymer fires.* Polymer International, 2000. **49**(10): p. 1259-1265.
68. Purser, D.A., *Modelling Toxic and Physical Hazard in Fire.* Fire Safety Science, 1989. **2**: p. 391-400.
69. Purser, D.A., P. Grimshaw, and K.R. Berrill, *Intoxication by cyanide in fires: a study in monkeys using polyacrylonitrile.* Archives of Environmental Health: An International Journal, 1984. **39**(6): p. 394-400.
70. Purser, D.A., *A bioassay model for testing the incapacitating effects of exposure to combustion product atmospheres using cynomolgus monkeys.* Journal of fire Sciences, 1984. **2**(1): p. 20-36.
71. Purser, D. and P. Grimshaw, *The incapacitative effects of exposure to the thermal decomposition products of polyurethane foams.* Fire and Materials, 1984. **8**(1): p. 10-16.
72. Purser, D. and W. Woolley, *Biological effects of combustion atmospheres.* J. Fire Sci, 1982. **1**: p. 118-144.
73. Purser, D.A. and K.R. Berrill, *Effects of carbon monoxide on behavior in monkeys in relation to human fire hazard.* Archives of Environmental Health: An International Journal, 1983. **38**(5): p. 308-315.

74. Purser, D.A. and M.S. Rose, *The toxicity and renal handling of paraquatin cynomolgus monkeys.* Toxicology, 1979. **15**(1): p. 31-41.
75. Purser, D., *Validation of additive models for lethal toxicity of fire effluent mixtures.* Polymer Degradation and Stability, 2012. **97**(12): p. 2552-2561.
76. Stec, A.A., et al., *Analysis of toxic effluents released from PVC carpet under different fire conditions.* Chemosphere, 2013. **90**(1): p. 65-71.
77. Mahalingam, A., et al., *Numerical investigation of tube furnace toxicity measurement method (ISO 19700).* Fire and Materials, 2012. **36**(1): p. 17-30.
78. Babrauskas, V., *Effective measurement techniques for heat, smoke, and toxic fire gases.* Fire Safety Journal, 1991. **17**(1): p. 13-26.
79. Babrauskas, V., et al., *Toxic potency measurement for fire hazard analysis.* Fire technology, 1991. **28**(2): p. 163-167.
80. Marquis, D.M., et al., *Usage of controlled-atmosphere cone calorimeter to provide input data for toxicity modelling.* Proceeding in the 12th. International Fire and Material., San Francisco, 2011.
81. Parker, W.J., *Calculations of the heat release rate by oxygen consumption for various applications.* Journal of fire Sciences, 1984. **2**(5): p. 380-395.
82. Stec, A.A. and T.R. Hull. *Assessment of fire toxicity from polymer nanocomposites*. in *Conference information: 11th Meeting on fire retardant polymers, Bolton, UK, Fire retardancy of polymers: new strategies and mechanisms*. 2009.
83. Babrauskas, V., *Development of the cone calorimeter—a bench-scale heat release rate apparatus based on oxygen consumption.* Fire and Materials, 1984. **8**(2): p. 81-95.
84. Babrauskas, V. and G. Mulholland, *Smoke and soot data determinations in the cone calorimeter*, in *Mathematical Modeling of Fires*. 1988, ASTM International.
85. Babrauskas, V. and W.J. Parker, *Ignitability measurements with the cone calorimeter.* Fire and Materials, 1987. **11**(1): p. 31-43.
86. 5660-1, B.I., *Cone Calorimeter Standard: Reaction-to-fire tests — Heat release, smoke production and mass loss rate*. 2015.
87. Babrauskas, V., *Toxic hazard from fires: a simple assessment method.* Fire Safety Journal, 1993. **20**(1): p. 1-14.
88. Pei, B., G.-y. Song, and C. Lu, *The Application of Cone Calorimeter on the Study of Burning Performance of Liquorices.* Procedia Engineering, 2014. **71**: p. 291-295.
89. Hull, T.R. and A.A. Stec, *Polymers and fire.* Fire retardancy of polymers–new strategies and mechanisms, ed. TR Hull and BK Kandola, The Royal Society of Chemistry, Cambridge, 2009: p. 8.
90. Stec, A.A., et al., *Quantification of fire gases by FTIR: Experimental characterisation of calibration systems.* Fire Safety Journal, 2011. **46**(5): p. 225-233.
91. Babrauskas, V., et al., *Toxic potency measurement for fire hazard analysis.* Fire technology, 1992. **28**(2): p. 163-167.
92. Babrauskas, V., et al., *A cone calorimeter for controlled-atmosphere studies.* Fire and Materials, 1992. **16**(1): p. 37-43.

93. Babrauskas, V., et al., *The phi meter: A simple, fuel-independent instrument for monitoring combustion equivalence ratio.* Review of scientific instruments, 1994. **65**(7): p. 2367-2375.
94. Babrauskas, V., *Fire safety improvements in the combustion toxicity area: is there a role for LC50 tests?* Fire and Materials, 2000. **24**(2): p. 113-119.
95. Babrauskas, V. and R.D. Peacock, *Heat release rate: the single most important variable in fire hazard.* Fire Safety Journal, 1992. **18**(3): p. 255-272.
96. Guillaume, E., D.M. Marquis, and C. Chivas, *Experience plan for controlled-atmosphere cone calorimeter by Doehlert method.* Fire and Materials, 2013. **37**(2): p. 171-176.
97. Guillaume, E., et al., *Effect of gas cell pressure in FTIR analysis of fire effluents.* Fire and Materials, 2015. **39**(7): p. 675-684.
98. Guillaume, E., D. Marquis, and L. Saragoza, *Calibration of flow rate in cone calorimeter tests.* Fire and Materials, 2014. **38**(2): p. 194-203.
99. Guillaume, E., C. Chivas, and A. Sainrat, *Regulatory issues and flame retardant usage in upholstered furniture in Europe.* Fire & Building Safety in the Single European Market. School of Engineering and Electronics, University of Edinburgh, 2008: p. 3.
100. Irshad, A., Andrews, G.E., Phylaktou, H.N. and Gibbs, B.M. *Development of the Controlled Atmosphere Cone Calorimeter to Simulate Compartment Fires*. in *Proc. Ninth Int. Sem.on Fire and Explosion Hazards (ISFEH9)*. 2019. Saint Petersburg, Russia: Published by Saint-Petersburg Polytechnic University Press.
101. 19700, I.T., *Controlled equivalence ratio method for the determination of hazardous components of fire effluents*. 2007.
102. Purser, J., et al., *Repeatability and reproducibility of the ISO/TS 19700 steady state tube furnace.* Fire Safety Journal, 2013. **55**: p. 22-34.
103. *DIN 53436-1 - Generation of Thermal Decomposition Products from Materials for Their Analytic - Toxicological Testing*. 2015.
104. 19700, I., *Controlled equivalence ratio method for the determination of hazardous components of fire effluents - The steady state tube furnace*. 2013.
105. Alarifi, A.A., *Compartment Fire Toxicity: Measurements and Aspects of Modelling*, in *School of Chemical and Process Engineering*. 2016, University of Leeds: Leeds, UK.
106. Irshad, A., *Gasification Burning of Biomass*, in *School of Chemical and Process Engineering*. 2017, University of Leeds: Leeds, UK.
107. Mustafa, B.G., *Toxic Species and Particulate Emissions from Wood and Pool Fires*, in *School of Chemical and Process Engineering*. 2019, University of Leeds: Leeds, UK.
108. Aljumaiah, O.A.O., *Combustion products from ventilation controlled fires: toxicity assessment and modelling*. 2012, The University of Leeds.
109. Andrews, G., et al., *FTIR investigations of toxic gases in air starved enclosed fires.* Fire Safety Science, 2005. **8**: p. 1035-1046.

110. Hakkarainen, T., et al., *Smoke gas analysis by Fourier transform infrared spectroscopy.* VTT Building Technology, Final report of the SAFIR project, 1999.
111. Speitel, L.C., *Fourier transform infrared analysis of combustion gases.* Journal of fire sciences, 2002. **20**(5): p. 349-371.
112. Abdulaziz A. Alarifi, H.N.P.a.G.E.A. *Toxic Gas Analysis from Compartment Fires using Heated Raw Gas Sampling with Heated FTIR 50+ Species Gas Analysis*. in *Proc. of the First International Fire Safety Symposium*. 2015. Coimbra, Portugal.
113. Abdulaziz A. Alarifi, H.N.P.a.G.E.A. *Heated Raw Gas Sampling with Heated FTIR Analysis of Toxic Effluents from Small and Large Scale Fire Tests*. in *Proceedings of the IAFSS, 10th Asia-Oceania Symposium on Fire Science and Technology, 10th AOSFST*. 2015. Tsukuba, Japan.
114. Alarifi, A., Andrews, G. E., Witty, L., & Phylaktou, H. N. *Ignition and toxicity of selected aircraft interior materials using the cone calorimeter and FTIR analysis*. in *In Conference Proceedings, Interflam2013*. 2013. Royal Holloway College - University of London. UK: Interscience Communications Ltd.
115. Aljumaiah, O., Andrews, G.E., Alqahtani, A.M., Husain, B.F., Singh, P. and Phylaktou, H.N. *Air Starved Acrylic Curtain Fire Toxic Gases using an FTIR*. in *Sixth International Seminar on Fire and Explosion Hazards*. 2010. University of Leeds, UK.
116. Andrews, G.E., Boulter, S., Burell, G., Cox, M., Daham, B, Li, H. and Phylaktou, H.N., *Toxic Gas Measurements Using FTIR for Combustion of COH Materials in Air Starved Enclosed Fires*, in *The European Combustion Institute Meeting, Chania, Crete, April, 2007.* 2007.
117. Andrews, G.E., et al., *Aircraft Blanket Ignition and Toxic Emission in Simulated Aircraft Cabin Fires Using the Cone Calorimeter.* Fire and Materials 2015, 2015: p. 734-748.
118. Mat Kiah, M.H., Mustafa, B.G., Andrews, G.E., Phylaktou, H.N. and Li, H. *PVC Sheathed Electrical Cable Fire Smoke Toxicity*. in *Proc. Ninth Int. Sem.on Fire and Explosion Hazards (ISFEH9)*. 2019. Saint Petersburg, Russia: Published by Saint-Petersburg Polytechnic University Press.
119. Mustafa, B.G., Mat Kiah, M.H., Andrews, G.E., Phylaktou, H.N. and Li, H. *Smoke Particle Size Distributions in Pine Wood Fires*. in *Proc. Ninth Int. Sem.on Fire and Explosion Hazards (ISFEH9)*. 2019. Saint Petersburg, Russia: Published by Saint-Petersburg Polytechnic University Press.
120. 19702, I., *Toxicity testing of fire effluents - Guidance for analysis of gases and vapours in fire effluents using FTIR gas analysis*. 2006.
121. 19701, B.I., *Methods for sampling and analysis of fire effluents*. 2013: International Organization for Standardization: Geneva.
122. Fardell, P. and E. Guillaume, *Sampling and measurement of toxic fire effluent.* Flammability testing of materials used in construction, transport and mining (ISBN 978-1-85573-935-2) This authoritative text reviews flammability tests for buildings and their contents,

including wood products, cladding, sandwich panels, floor and ceiling materials, upholstered furniture and mattresses, cables and electrical appliances. It also covers, 2010: p. 385.
123. Ltd., C., *User Manual - DMS500 Fast Particulate Spectrometer with Heated Sample Line High Ratio Diluter*. 2011: United Kingdom.
124. Reavell, K., Hands, T., and Collings, N., *A Fast Response Particulate Spectrometer for Combustion Aerosols 2002-01-2714.* 2002.
125. Kittelson, D., Tim Hands, Chris Nickolaus, Nick Collings, Ville Niemelä, and Martyn Twigg, *Mass Correlation of Engine Emissions with Spectral Instruments, JSAE paper number 20045462.* 2004.
126. Held, A., et al., *Aerosol size distributions measured in urban, rural and high-alpine air with an electrical low pressure impactor (ELPI).* Atmospheric Environment, 2008. **42**(36): p. 8502-8512.
127. Coudray, N., et al., *Density measurement of fine aerosol fractions from wood combustion sources using ELPI distributions and image processing techniques.* Fuel, 2009. **88**(5): p. 947-954.
128. Liang, B., et al., *Comparison of PM emissions from a gasoline direct injected (GDI) vehicle and a port fuel injected (PFI) vehicle measured by electrical low pressure impactor (ELPI) with two fuels: Gasoline and M15 methanol gasoline.* Journal of Aerosol Science, 2013. **57**: p. 22-31.
129. Elmer, P., *Thermogravimetric analysis (TGA) a beginner 0 s guide.* United States of America: Perkin Elmer, 2010.
130. D.T. Gottuk, R.J.R., *Effect of combustion conditions on species production*, in *SFPE handbook of fire protection engineering*. 1995, Quincy, Mass. : National Fire Protection Association ; Boston, Mass. : Society of Fire Protection Engineers. p. p. 2-64 – 2-84.
131. Schaschke, C., *Antoine equation.* In A Dictionary of Chemical Engineering, 2014.
132. Huggett, C., *Estimation of rate of heat release by means of oxygen consumption measurements.* Fire and Materials, 1980. **4**(2): p. 61-65.
133. M., J., *Calorimetry. In: Hurley M.J. et al. (eds) SFPE Handbook of Fire Protection Engineering*. 2016, Springer, New York, NY.
134. Abdul-Khalek, I., D. Kittelson, and F. Brear, *The Influence of Dilution Conditions on Diesel Exhaust Particle Size Distribution Measurements*. 1999, SAE International.
135. Alarifi, A.A., et al., *Ignition and Toxicity Evaluation of Selected Aircraft Interior Materials Using the Cone Calorimeter and FTIR Analysis.* InterFlam2013, 2013: p. 37-48.
136. Purser, D., A. Stec, and T. Hull, *Effects of the material and fire conditions on toxic product yields.* Fire toxicity. Cambridge, UK.: Woodhead Publishing Limited, 2010: p. 515-38.
137. Lewin, M. and E.D. Weil, *2 - Mechanisms and modes of action in flame retardancy of polymers*, in *Fire Retardant Materials*, A.R. Horrocks and D. Price, Editors. 2001, Woodhead Publishing. p. 31-68.
138. Price, D., G. Anthony, and P. Carty, *1 - Introduction: polymer combustion, condensed phase pyrolysis and smoke formation*, in *Fire*

*Retardant Materials*, A.R. Horrocks and D. Price, Editors. 2001, Woodhead Publishing. p. 1-30.
139. Purser, D.A., *Toxic Combustion Product Yields as a Function of Equivalence Ratio and Flame Retardants in Under-Ventilated Fires: Bench-Large-Scale Comparisons.* Polymers, 2016. **8**: p. 1-23.
140. Wade, A.P.R.a.C.A., *Branz Study Report 185: Soot Yield Values for Modelling Purposes - Residential Occupancies*. 2008, Branz.
141. Guillaume, E., *Effects of Fire on People: Bibliography Summary - July 2006*. 2006, Laboratorie National de Metrologie et d'Essais (LNE): Paris, France.
142. Tewarson, A., *Generation of Heat and Chemical Compounds in Fires*, in *SFPE Handbook of Fire Protection Engineering*. 1988, National Fire Protection Association: Quincy, MA, USA.

# List of Abbreviations

ER: Equivalence Ratio

HRR: Heat Release Rate

MLR: Mass Loss Rate

PIR: Polyisocyanurate

PU: Polyurethane

ASET: Available Safe Egress Time

PE: Polyethylene

FTIR: Fourier Transform Infrared Spectroscopy

DMS: Differential Mobility Spectrometer

COSHH: Control of Substances Hazardous to Health Regulations

AEGL: Acute Exposure Guideline Levels of Hazardous Substances

FED: Fractional Exposure Dose

ISO: International Organisation for Standardization

LC50: Lethal Concentration resulting to death of 50% of the population

LDPE: Low-Density Polyethylene

PEP: Polyethylene Pipe

PMMA: Poly (methyl methacrylate)

PP: Polypropylene

PPE: Personal Protective Equipment

PS: Polystyrene

PVC: Polyvinyl chloride

SB-P: Storage Box Purple

UK: United Kingdom

A/F: Air to fuel ratio

BSI: British Standards Institution

RSET: Required Safe Escape Time

TGA: Thermal Gravimetrical Analysis

SEM: Scanning Electron Microscopy

TEM: Transform Electron Microscopy

OC: Oxygen Consumption

BC: Bomb Calorimeter

CHNS-O: Carbon Hydrogen Nitrogen Sulphur Oxygen Analyser

TT: Total Toxicity, Total Toxicities

FEC: Fractional Effective Concentration

I: Ignition

F: Flame out

Daf: Dry Ash Basis

GCV: Gross Calorific Value

# Appendix A
# Papers and Presentations

## A.1 List of Papers and Publications

### A.1.1 PVC Electrical Cable Fires

1) Mat Kiah M.H., Mustafa B.G., Andrews G.E., Phylaktou H.N., Li H (2019). PVC Sheathed Electrical Cable Fire Smoke Toxicity, Proceedings of the Ninth International Seminar on Fire and Explosion Hazards, St. Petersburg, Russia (April, 2019).
2) Draft – Particle size emissions from PVC electrical cable fires, FIRE SAFETY 2017.

### A.1.2 Solid Foam Fires

1) Draft – Toxic Gases from PU and PIR Foam Fires, ISFEH9 2019.

### A.1.3 Other Submitted Abstracts

1) FRPM19 2019 – Turku, Finland, June 26-28, 2019, HCl, HBr and HF emissions from halogenated fire retarded PU and PIR Foam Fires (Accepted for Poster).
2) FRPM19 2019 – Turku, Finland, June 26-28, 2019, HBr Toxic Gas Emissions from Fire Retarded Polyethylene (Accepted for Poster).
3) Interflam 2019 – Royal Holloway College, United Kingdom, July 1-3, 2019, Particle Size Number Distribution from PIR Foam Fires.
4) Interflam 2019 – Royal Holloway College, United Kingdom, July 1-3, 2019, Toxic Emissions from Different forms of Polystyrene.
5) Interflam 2019 – Royal Holloway College, United Kingdom, July 1-3, 2019, PU and PIR foam fire toxicity.

### A.1.4 Other Joint Publications

1) Bintu G. Mustafa, Rosmawati Zahari, Yangfu Zeng, Miss H. Mat Kiah, Gordon E. Andrews and Herodotos N. Phylaktou (2020). Pine Wood Crib Fires: Toxic Gas Emissions Using a 5m$^3$ Compartment Fire, Wood and Fire Safety 2020, 9$^{th}$ International Scientific Conference, Strbske Pleso, Slovakia (May, 2020).
2) Bintu Grema Mustafa, Miss H. Mat Kiah, Gordon E. Andrews, Herodotos N. Phylaktou, Hu Li (2020). Toxic Gas Emissions from Plywood Fires, Wood and Fire Safety 2020, 9$^{th}$ International Scientific Conference, Strbske Pleso, Slovakia (May, 2020).

3) Bintu G. Mustafa, Miss H. Mat Kiah, Juma Al-Nahdi, Gordon E. Andrews, Herodotos N. Phylaktou, Hu Li (2019). Toxic Emissions from Processed Wood in Cone Calorimeter Tests. Submitted to Fire and Materials (under review).
4) B.G. Mustafa, M.H. Mat Kiah, A. Irshad, G.E. Andrews, H.N. Phylaktou, H. Li and B.M. Gibbs (2019). Rich Biomass Combustion: Gaseous and Particle Number Emissions, Fuel (July, 2019).
5) Mustafa B.G., Mat Kiah M.H., Andrews G.E., Phylaktou H.N., Li H (2019). Smoke particle size distribution in pine wood fires, Proceedings of the Ninth International Seminar on Fire and Explosion Hazards, St. Petersburg, Russia (April, 2019).

## A.2 List of Conferences and Presentations

1) ISFEH9 2019 – St. Petersburg, Russia, April 21-26, 2019, PVC Sheathed Electrical Cable Fire Smoke Toxicity, (Oral).
2) ISFEH9 2019 – St. Petersburg, Russia, April 21-26, 2019, Toxic Gases from PU and PIR Foam Fires (Poster).
3) Fired-UP 2018 – University of Edinburgh, United Kingdom, May 17-18, 2018, Toxicity of electrical cable fires under restricted and free ventilations in the Cone Calorimeter (Oral).
4) Cambridge Particle Meeting 2017 – University of Cambridge, United Kingdom, June 23, 2017.
    a) Particle size distribution as a function of time during pine wood combustion on a cone calorimeter (Oral, presented by Dr Hu Li).
    b) Particle size emissions from PVC electrical cable fires (Poster).
5) MySECON2017 2017 – University of Manchester, United Kingdom, May 12, 2017. Toxic species and particle size distribution from PVC cable fires (Poster).

# Appendix B
# The Modified Cone Calorimeter

## B.1 Standard Test Procedure and Check List

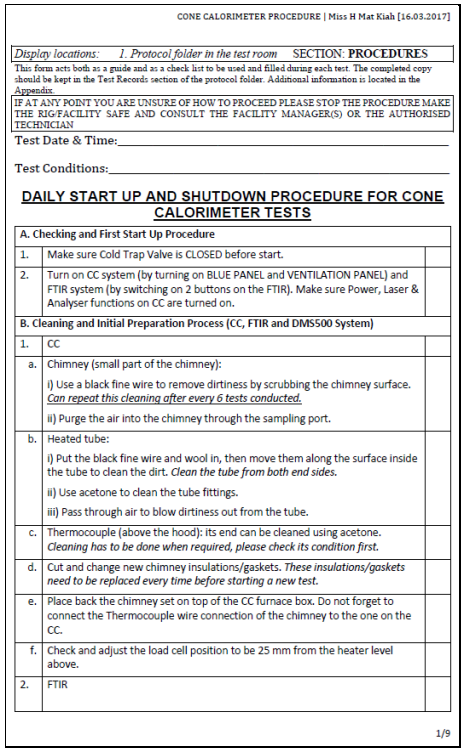

CONE CALORIMETER PROCEDURE | Miss H Mat Kiah [16.03.2017]

*Display locations: 1. Protocol folder in the test room* SECTION: **PROCEDURES**

This form acts both as a guide and as a check list to be used and filled during each test. The completed copy should be kept in the Test Records section of the protocol folder. Additional information is located in the Appendix.

IF AT ANY POINT YOU ARE UNSURE OF HOW TO PROCEED PLEASE STOP THE PROCEDURE MAKE THE RIG/FACILITY SAFE AND CONSULT THE FACILITY MANAGER(S) OR THE AUTHORISED TECHNICIAN

Test Date & Time:_____

Test Conditions:_____

**DAILY START UP AND SHUTDOWN PROCEDURE FOR CONE CALORIMETER TESTS**

| | | |
|---|---|---|
| **A. Checking and First Start Up Procedure** | | |
| 1. | Make sure Cold Trap Valve is CLOSED before start. | |
| 2. | Turn on CC system (by turning on BLUE PANEL and VENTILATION PANEL) and FTIR system (by switching on 2 buttons on the FTIR). Make sure Power, Laser & Analyser functions on CC are turned on. | |
| **B. Cleaning and Initial Preparation Process (CC, FTIR and DMS500 System)** | | |
| 1. | CC | |
| a. | Chimney (small part of the chimney):<br>i) Use a black fine wire to remove dirtiness by scrubbing the chimney surface. *Can repeat this cleaning after every 6 tests conducted.*<br>ii) Purge the air into the chimney through the sampling port. | |
| b. | Heated tube:<br>i) Put the black fine wire and wool in, then move them along the surface inside the tube to clean the dirt. *Clean the tube from both end sides.*<br>ii) Use acetone to clean the tube fittings.<br>iii) Pass through air to blow dirtiness out from the tube. | |
| c. | Thermocouple (above the hood): its end can be cleaned using acetone. *Cleaning has to be done when required, please check its condition first.* | |
| d. | Cut and change new chimney insulations/gaskets. *These insulations/gaskets need to be replaced every time before starting a new test.* | |
| e. | Place back the chimney set on top of the CC furnace box. Do not forget to connect the Thermocouple wire connection of the chimney to the one on the CC. | |
| f. | Check and adjust the load cell position to be 25 mm from the heater level above. | |
| 2. | FTIR | |

1/9

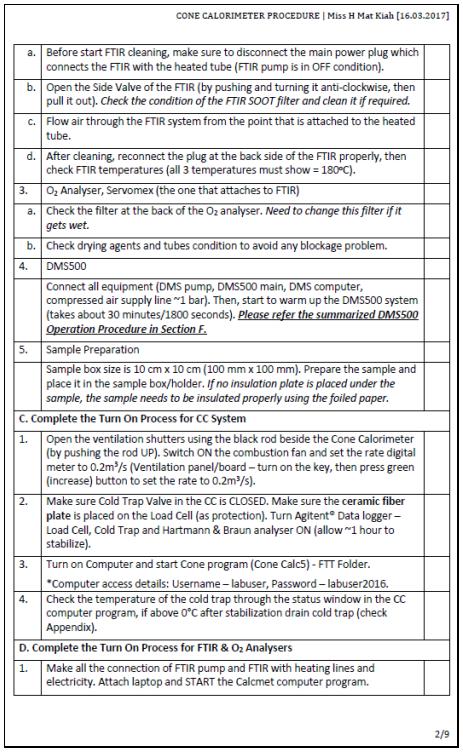

CONE CALORIMETER PROCEDURE | Miss H Mat Kiah [16.03.2017]

| | | |
|---|---|---|
| a. | Before start FTIR cleaning, make sure to disconnect the main power plug which connects the FTIR with the heated tube (FTIR pump is in OFF condition). | |
| b. | Open the Side Valve of the FTIR (by pushing and turning it anti-clockwise, then pull it out). *Check the condition of the FTIR SOOT filter and clean it if required.* | |
| c. | Flow air through the FTIR system from the point that is attached to the heated tube. | |
| d. | After cleaning, reconnect the plug at the back side of the FTIR properly, then check FTIR temperatures (all 3 temperatures must show = 180ºC). | |
| 3. | $O_2$ Analyser, Servomex (the one that attaches to FTIR) | |
| a. | Check the filter at the back of the $O_2$ analyser. *Need to change this filter if it gets wet.* | |
| b. | Check drying agents and tubes condition to avoid any blockage problem. | |
| 4. | DMS500 | |
| | Connect all equipment (DMS pump, DMS500 main, DMS computer, compressed air supply line ~1 bar). Then, start to warm up the DMS500 system (takes about 30 minutes/1800 seconds). ***Please refer the summarized DMS500 Operation Procedure in Section F.*** | |
| 5. | Sample Preparation | |
| | Sample box size is 10 cm x 10 cm (100 mm x 100 mm). Prepare the sample and place it in the sample box/holder. *If no insulation plate is placed under the sample, the sample needs to be insulated properly using the foiled paper.* | |
| **C. Complete the Turn On Process for CC System** | | |
| 1. | Open the ventilation shutters using the black rod beside the Cone Calorimeter (by pushing the rod UP). Switch ON the combustion fan and set the rate digital meter to 0.2$m^3$/s (Ventilation panel/board – turn on the key, then press green (increase) button to set the rate to 0.2$m^3$/s). | |
| 2. | Make sure Cold Trap Valve in the CC is CLOSED. Make sure the **ceramic fiber plate** is placed on the Load Cell (as protection). Turn Agitent® Data logger – Load Cell, Cold Trap and Hartmann & Braun analyser ON (allow ~1 hour to stabilize). | |
| 3. | Turn on Computer and start Cone program (Cone Calc5) - FTT Folder.<br>*Computer access details: Username – labuser, Password – labuser2016. | |
| 4. | Check the temperature of the cold trap through the status window in the CC computer program, if above 0°C after stabilization drain cold trap (check Appendix). | |
| **D. Complete the Turn On Process for FTIR & $O_2$ Analysers** | | |
| 1. | Make all the connection of FTIR pump and FTIR with heating lines and electricity. Attach laptop and START the Calcmet computer program. | |

2/9

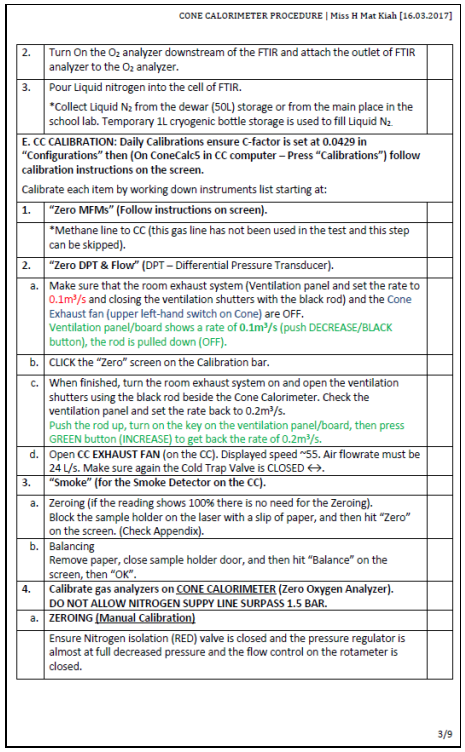

CONE CALORIMETER PROCEDURE | Miss H Mat Kiah [16.03.2017]

| | | |
|---|---|---|
| 2. | Turn On the $O_2$ analyzer downstream of the FTIR and attach the outlet of FTIR analyzer to the $O_2$ analyzer. | |
| 3. | Pour Liquid nitrogen into the cell of FTIR.<br>*Collect Liquid $N_2$ from the dewar (50L) storage or from the main place in the school lab. Temporary 1L cryogenic bottle storage is used to fill Liquid $N_2$. | |
| **E. CC CALIBRATION: Daily Calibrations ensure C-factor is set at 0.0429 in "Configurations" then (On ConeCalc5 in CC computer – Press "Calibrations") follow calibration instructions on the screen.** | | |
| | Calibrate each item by working down instruments list starting at: | |
| 1. | **"Zero MFMs" (Follow instructions on screen).** | |
| | *Methane line to CC (this gas line has not been used in the test and this step can be skipped). | |
| 2. | **"Zero DPT & Flow"** (DPT – Differential Pressure Transducer). | |
| a. | Make sure that the room exhaust system (Ventilation panel and set the rate to 0.1$m^3$/s and closing the ventilation shutters with the black rod) and the Cone Exhaust fan (upper left-hand switch on Cone) are OFF.<br>Ventilation panel/board shows a rate of **0.1$m^3$/s** (push DECREASE/BLACK button), the rod is pulled down (OFF). | |
| b. | CLICK the "Zero" screen on the Calibration bar. | |
| c. | When finished, turn the room exhaust system on and open the ventilation shutters using the black rod beside the Cone Calorimeter. Check the ventilation panel and set the rate back to 0.2$m^3$/s.<br>Push the rod up, turn on the key on the ventilation panel/board, then press GREEN button (INCREASE) to get back the rate of 0.2$m^3$/s. | |
| d. | Open **CC EXHAUST FAN** (on the CC). Displayed speed ~55. Air flowrate must be 24 L/s. Make sure again the Cold Trap Valve is CLOSED ↔. | |
| 3. | **"Smoke" (for the Smoke Detector on the CC).** | |
| a. | Zeroing (if the reading shows 100% there is no need for the Zeroing).<br>Block the sample holder on the laser with a slip of paper, and then hit "Zero" on the screen. (Check Appendix). | |
| b. | Balancing<br>Remove paper, close sample holder door, and then hit "Balance" on the screen, then "OK". | |
| 4. | **Calibrate gas analyzers on CONE CALORIMETER (Zero Oxygen Analyzer).<br>DO NOT ALLOW NITROGEN SUPPY LINE SURPASS 1.5 BAR.** | |
| a. | **ZEROING [Manual Calibration]** | |
| | Ensure Nitrogen isolation (RED) valve is closed and the pressure regulator is almost at full decreased pressure and the flow control on the rotameter is closed. | |

3/9

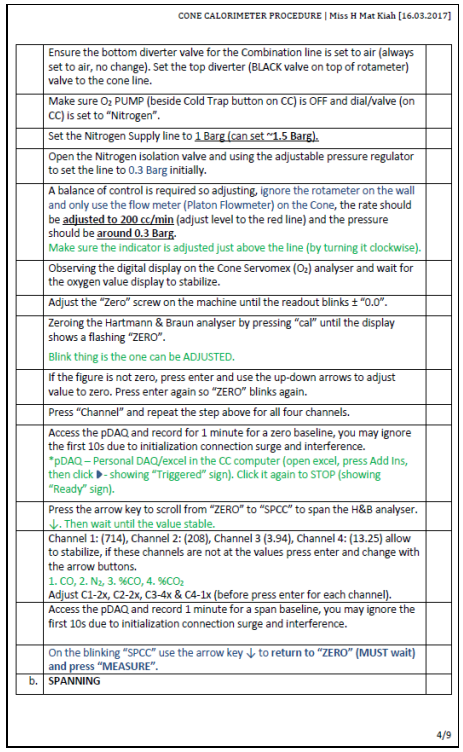

CONE CALORIMETER PROCEDURE | Miss H Mat Kiah [16.03.2017]

| | |
|---|---|
| | Ensure the bottom diverter valve for the Combination line is set to air (always set to air, no change). Set the top diverter (BLACK valve on top of rotameter) valve to the cone line. |
| | Make sure $O_2$ PUMP (beside Cold Trap button on CC) is OFF and dial/valve (on CC) is set to "Nitrogen". |
| | Set the Nitrogen Supply line to 1 Barg (can set ~1.5 Barg). |
| | Open the Nitrogen isolation valve and using the adjustable pressure regulator to set the line to 0.3 Barg initially. |
| | A balance of control is required so adjusting, ignore the rotameter on the wall and only use the flow meter (Platon Flowmeter) on the Cone, the rate should be **adjusted to 200 cc/min** (adjust level to the red line) and the pressure should be **around 0.3 Barg**.<br>Make sure the indicator is adjusted just above the line (by turning it clockwise). |
| | Observing the digital display on the Cone Servomex ($O_2$) analyser and wait for the oxygen value display to stabilize. |
| | Adjust the "Zero" screw on the machine until the readout blinks ± "0.0". |
| | Zeroing the Hartmann & Braun analyser by pressing "cal" until the display shows a flashing "ZERO".<br>Blink thing is the one can be ADJUSTED. |
| | If the figure is not zero, press enter and use the up-down arrows to adjust value to zero. Press enter again so "ZERO" blinks again. |
| | Press "Channel" and repeat the step above for all four channels. |
| | Access the pDAQ and record for 1 minute for a zero baseline, you may ignore the first 10s due to initialization connection surge and interference.<br>*pDAQ – Personal DAQ/excel in the CC computer (open excel, press Add Ins, then click ▶- showing "Triggered" sign). Click it again to STOP (showing "Ready" sign). |
| | Press the arrow key to scroll from "ZERO" to "SPCC" to span the H&B analyser. ↓. Then wait until the value stable. |
| | Channel 1: (714), Channel 2: (208), Channel 3 (3.94), Channel 4: (13.25) allow to stabilize, if these channels are not at the values press enter and change with the arrow buttons.<br>1. CO, 2. $N_2$, 3. %CO, 4. %$CO_2$<br>Adjust C1-2x, C2-2x, C3-4x & C4-1x (before press enter for each channel). |
| | Access the pDAQ and record 1 minute for a span baseline, you may ignore the first 10s due to initialization connection surge and interference. |
| | On the blinking "SPCC" use the arrow key ↓ to **return to "ZERO" (MUST wait) and press "MEASURE".** |
| b. | **SPANNING** |

4/9

| | | |
|---|---|---|
| | Turn off $N_2$ supply (RED) valve, switch the diverter on the cone to "Air" and turn ON the CC PUMP. | |
| | After turn dial/valve to "Air" and immediately **adjust flow rate to 200 cc/min (Platon Flowmeter on CC)**. | |
| | Wait for the oxygen value display to stabilize (on the CC Servomex). Can check the Cold Trap Temperature (~3ºC). | |
| | Adjust "Span" screw on Cone until readout blinks between 20.9and 21.0 | |
| 5. | **"Mass" (for the CC Load Cell).** | |
| a. | Ensure that the heat shutter is CLOSED. Then remove any sample from Load Cell followed by "Tare" (push "Tare" button on CC). | |
| b. | Press "Zero" (on CC computer) when the values are about stable after "Tare". | |
| c. | Span mass balance (if necessary) using 100g weight (span/load) by placing it on the Load Cell. | |
| d. | Press "Span" on the CC computer, then press "Ok" and "Main". | |
| e. | Remove the span/load and replace it with a temporary sample (ceramic fiber plate). | |
| f. | Place a sample holder with the foiled paper (insulation) on the Load Cell, then "Tare". | |
| g. | Tare TEST SAMPLE + foiled paper + sample holder, record the initial sample mass (g). | |
| h. | Press "Start" on the CC computer, then "Ok", File (keep in details: Description, Material ID, Mass, Thickness, Heat Flux, then press "Ok", Calibration-press "No", and "Ok") and save it. | |
| i. | Open EXCEL, Add Ins, wait to press ▶ (must press/start at the same time with ConeCalc5 & FTIR Calcmet2-Temet Instruments software). | |
| j. | POUR Liquid $N_2$ into the FTIR system. | |
| 6. | **Zeroing of the FTIR and $O_2$ analyzer downstream of the FTIR analyzer.** | |
| a. | Attach data logger connections and switch on the Laptop (OPEN Calcmet2 – Temet Instruments). | |
| b. | Switch the **top diverter** (BLACK valve on top of the rotameter for $N_2$ supply) to the FTIR line directed towards the zero gas inlet. | |
| c. | Set the dial of the FTIR pump to ZERO GAS. | |
| d. | Set the Nitrogen supply line to 1 Barg (can set ~1.5 Barg). | |
| e. | Open the RED valve. Ensure the pressure in the Nitrogen line is at 0.3 Barg. Use the control valve to set the flow of $N_2$ from the flow meter between 2-4 L/m. Then, $O_2$ analyser will go to ZERO. | |
| f. | Just re-check again CC Servomex ($O_2$), must show **20.9**. | |





| | | |
|---|---|---|
| g. | Wait for the values of % oxygen stable on $O_2$ analyzer downstream of FTIR. When it becomes stable set the "Zero" with a screw driver until it blinks ± "0.0". (If $O_2$ analyzer is not present just wait for 5 minutes before recording on the pDAQ on CC computer for 1 minute). | |
| h. | First press 3M on the Calcmet(2) program, then CANCEL it. Go to OPTION, click AUTOSAVING and RENAME it, then press OK. | |
| i. | To zero the FTIR, go on the Laptop Calcmet program, on the **"Measure"** tab, click "Zero" in order to get zero calibration. Calcmet program will return a background reading. | |
| j. | Run the program for a 3 min sample, check that zero line is straight and at zero. If not check for leakages in the system and/or check the detection cell temperature is at **-196.0°C** on **View, Hardware Status** (TOP UP the liquid nitrogen if it's not the correct temperature). | |
| k. | Press 5s on the Calcmet program (check the graph must show a straight line, ± 0.5s). | |
| l. | Close $N_2$ supply line, close RED Valve. | |
| m. | Set the dial of FTIR pump towards SAMPLE/SPAN gas. | |
| n. | To span the $O_2$ analyzer downstream of FTIR, START the FTIR PUMP. | |
| o. | Wait for 5 minutes to get the values of % oxygen stable on $O_2$ analyzer. When it becomes stable set the dial to between 20.9and 21.0 then record on the pDAQ for 1 minute. | |
| p. | Adjust air flowrate as DESIRED (e.g. 9.4 L/min), open cooling water, SPAN $O_2$ analyser to 20.9 (by adjusting the SPAN button manually). | |
| q. | Refill Liquid $N_2$ if required. | |
| r. | Check and make sure again that FTIR PUMP, AIR FLOWRATE & COOLING WATER are OPENED. | |
| s. | Check again the DMS500 (must already "AUTOZERO ALL"). | |
| t. | Set CC Temperature as DESIRED by pressing ▲ (Eurotherm). Now it is READY to RUN the TEST. | |
| 7. | **Heat Flux Calibration** | |
| a. | Make sure COOLING WATER is opened and CC temperature is at the test irradiation level (i.e. 40 kW, 695°C). | |
| b. | Bottom Valve to be OPENED and Side Valve to be CLOSED. | |
| c. | Place the heat flux device properly on the specified holder inside the cone box. Be careful with the end part of the device (very sensitive and easy to damage). Square body part of the device should be placed with **its end must be same level with the vertical line of the device holder.** | |
| d. | Start the calibration process by following instructions stated in the CC computer (Cone Calc5 – Heat Flux Calibration). | |





| | | |
|---|---|---|
| e. | The reading which is shown by the software Cone Calc5 must similar to the temperature of the tested irradiation level. | |
| f. | Remove the heat flux device and place it properly with its end can be CLOSED using the CAP (as protection). | |
| **F. DMS500 Operation Procedure.** | | |
| 1. | Switch on the computer where DMS 500 software is installed. | |
| 2. | Open the software via CD-R, Cambustion, My V4.11, Start DMS. | |
| 3. | Select File Dialog: Biomondal_m7_m2cqw21.dmd. | |
| 4. | Turn on the compressed air (2bar) and the DMS unit (Green bottom on the equipment). | |
| 5. | Turn the DMS equipment to ON from STAND BY, and wait 30 mins for warming up the DMS equipment. | |
| 6. | AUTOZERO ALL after the warming up, and decide where the experiment data should be logged to. | |
| 7. | Start and stop logging data. After pressing "Start Logging", RENAME the file and SAVE it. **Change "ZERO" mode to "SAMPLE" mode.** FIRE EVENTS can be stated in the MEMO. | |
| 8. | After the experiment, turn the equipment from ON to STAND BY, and click EXIT from the FILE MENU. | |
| 9. | Close the software and shut down the DMS equipment. | |
| 10. | Turn off the compressed air. | |
| **G. Run Test(s).** | | |
| | **Start Test** | |
| | Start Baseline on Conecalc program & pDAQ (excel, by pressing ▶) on the CC computer and start FTIR program (by pressing Ω) at the same time. | |
| | Put the sample into the CC box on the Load Cell, then close the box door and open the heater shutter (Immediately start the test by pressing START TEST on the ConeCalc program in the CC computer). When seeing a flame, press I for ignition.<br>* Shout Start Test or Ignition to the lab partner for her to press START TEST / I). | |
| | **Stop Test** | |
| | Stop Test on Conecalc program & pDAQ (excel, by pressing ▶) on the CC computer and start FTIR program (by pressing **CANCEL**) at the same time. | |
| | Close heater shutter, set/decrease CC Temperature (Eurotherm) to 0oC by pressing ▼ continuously, close FTIR pump. | |
| | Take out the burned sample from the CC box, put in in the ventilation equipment, take pictures and cover it with the foiled paper. | |





| | | |
|---|---|---|
| | Proceed with flushing the system with $N_2$. Change FTIR Valve from SAMPLE/SPAN to ZERO. Then, open $N_2$ supply line and turn on the RED Valve. | |
| | SAVE all data in the CC computer (ConeCalc & pDAQ excel). | |
| | Put DMS500 program as "STANDBY" (DMS pump will be OFF), turn off the DMS500, then can close air valve and compressed air supply line, switch off the power supply to the DMS pump. | |
| | COPY the results/data. | |
| **H. Normal Shut Down Procedure.** | | |
| 1. | The prescribed shutdown does not turn everything off, in order to keep the electronics stable and avoid an excessive warm-up period on the following day. The following CC devices shall remain ON: **i) ANALYSER, ii) POWER SUPPLY & iii) LASER.** | |
| 2. | Turn off CC heater (by lowering the temperature down to 0°C in the heater controller). | |
| 3. | Turn off FTIR pump. | |
| 4. | Set the FTIR pump valve to zero gas and flush the FTIR and $O_2$ analyser with $N_2$. | |
| 5. | Turn off all gas supplies. Observe the pressure gauges to check they are off. | |
| 6. | Turn off Load cell and Cold Trap (Cold Trap VALVE needs to be turn ON before leaving the room). | |
| 7. | Save all your files and copy data.<br>* 7 data **(excel)** files from CC computer (5 files in the Documents & 2 files in CC52-Data) , 1 data folder from FTIR computer (in the Calcmet Sample) and 1 data **(excel)** file from DMS computer (in the Fire Group folder). | |
| 8. | Values to stabilize, then turn off CC pump. | |
| 9. | Turn off DMS500 equipment, turn off its compressed air VALVE (green valve) and switch off the DMS pump. | |
| 10. | Shut down Cone software and turn off Computers. | |
| 11. | Sweep/vacuum floor free from any ash/debris. | |
| 12. | Switch off the combustion fan (Ventilation Panel) and close the ventilation shutters (by pulling down the black rod). | |
| **I. EMERGENCY SHUTDOWN Procedure.** | | |
| 1. | **Turn off the heater (by switching off the "Analysers" on the Cone).** | |
| 2. | **Make your way to the nearest Fire Exit.** | |
| 3. | **In the event of smoke accumulation and alarm failure, use manual "Purge" switch to operate emergency ventilation (Ventilation shutters should be open, otherwise evacuate and contact local technician).** | |

| **J. Periodic Maintenance.**<br>**(Note: Check Daily, Weekly and Monthly maintenance log).** | | |
|---|---|---|
| 1. | Check maintenance logs and appendix for a comprehensive list of periodic maintenance. | |
| 2. | Gloves must be worn during cleaning. Lab coat is recommended. | |
| 3. | Turn on compressed airline and check for leaks or blockages in oxygen line (either by ear or visually with a soap solution). | |
| 4. | Repair any leaks, turn off airline and return oxygen line to standard configuration. | |

## B.2 Pictures of Cone Calorimeter Tests

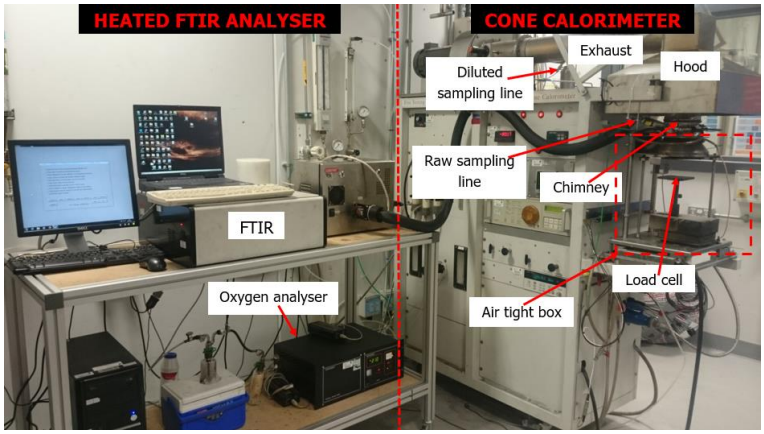


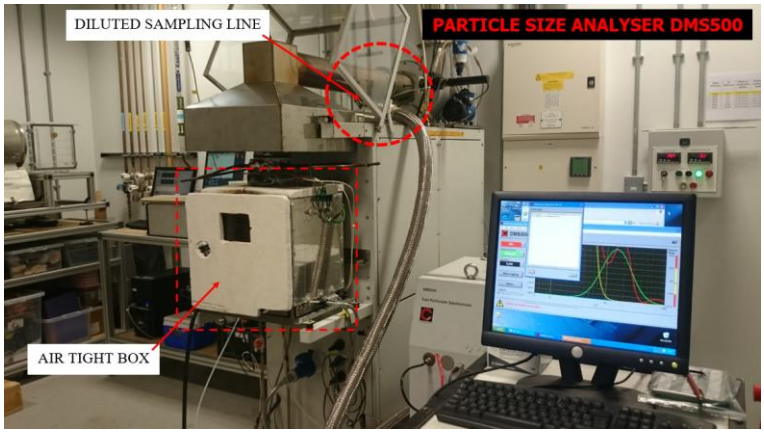


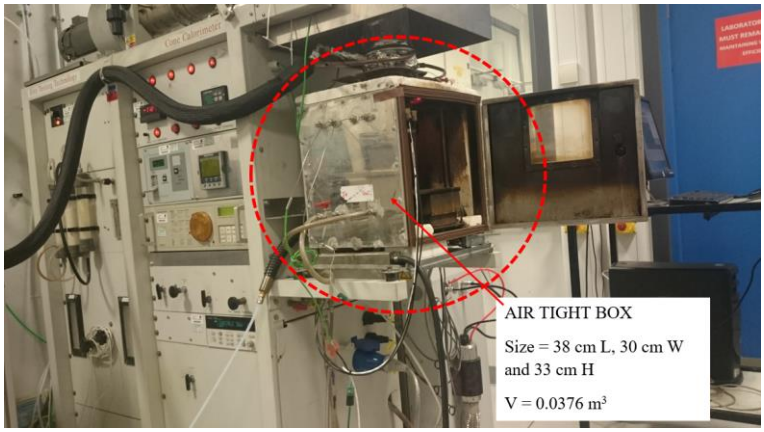

# Appendix C
# The Modified Purser Furnace

## C.1 Standard Test Procedure and Check List

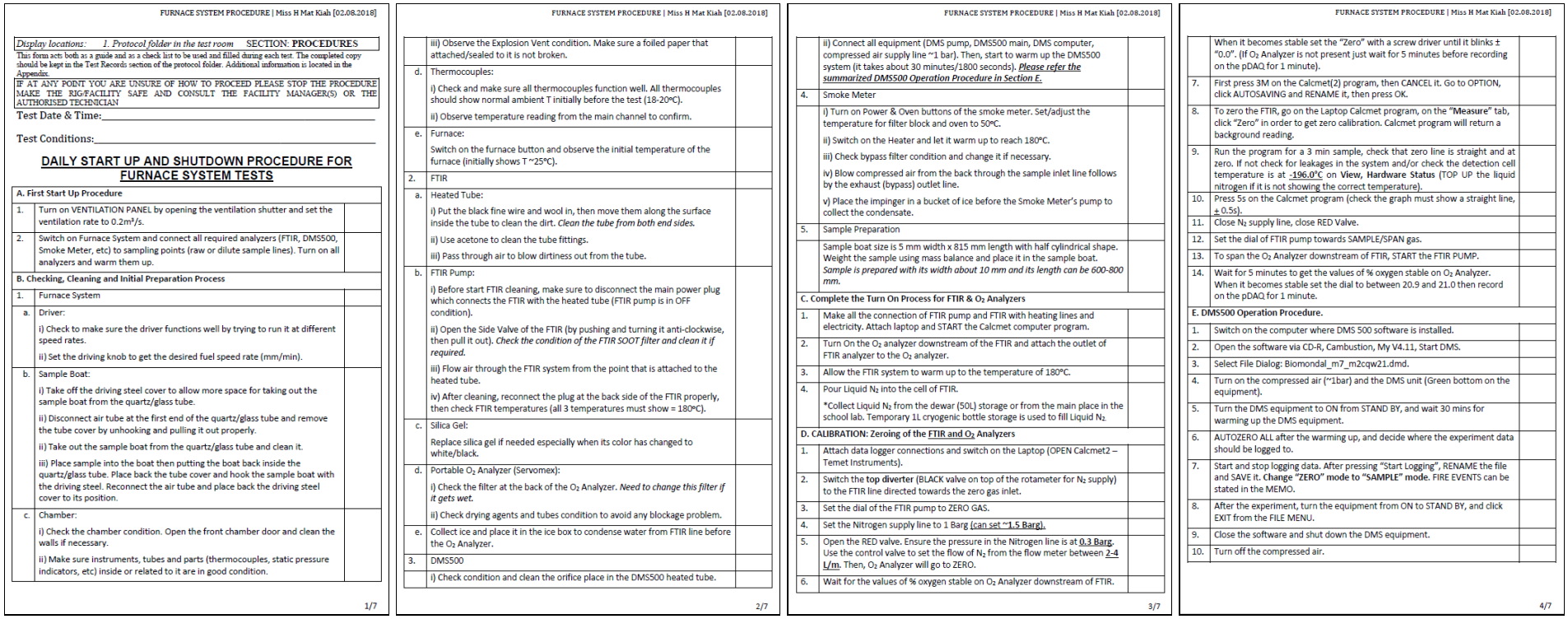

FURNACE SYSTEM PROCEDURE | Miss H Mat Kiah [02.08.2018]

*Display locations: 1. Protocol folder in the test room* SECTION: **PROCEDURES**

This form acts both as a guide and as a check list to be used and filled during each test. The completed copy should be kept in the Test Records section of the protocol folder. Additional information is located in the Appendix.

IF AT ANY POINT YOU ARE UNSURE OF HOW TO PROCEED PLEASE STOP THE PROCEDURE MAKE THE RIG/FACILITY SAFE AND CONSULT THE FACILITY MANAGER(S) OR THE AUTHORISED TECHNICIAN

Test Date & Time:_____

Test Conditions:_____

**DAILY START UP AND SHUTDOWN PROCEDURE FOR FURNACE SYSTEM TESTS**

| | | |
|---|---|---|
| **A. First Start Up Procedure** | | |
| 1. | Turn on VENTILATION PANEL by opening the ventilation shutter and set the ventilation rate to 0.2m³/s. | |
| 2. | Switch on Furnace System and connect all required analyzers (FTIR, DMS500, Smoke Meter, etc) to sampling points (raw or dilute sample lines). Turn on all analyzers and warm them up. | |
| **B. Checking, Cleaning and Initial Preparation Process** | | |
| 1. | Furnace System | |
| a. | Driver:<br>i) Check to make sure the driver functions well by trying to run it at different speed rates.<br>ii) Set the driving knob to get the desired fuel speed rate (mm/min). | |
| b. | Sample Boat:<br>i) Take off the driving steel cover to allow more space for taking out the sample boat from the quartz/glass tube.<br>ii) Disconnect air tube at the first end of the quartz/glass tube and remove the tube cover by unhooking and pulling it out properly.<br>ii) Take out the sample boat from the quartz/glass tube and clean it.<br>iii) Place sample into the boat then putting the boat back inside the quartz/glass tube. Place back the tube cover and hook the sample boat with the driving steel. Reconnect the air tube and place back the driving steel cover to its position. | |
| c. | Chamber:<br>i) Check the chamber condition. Open the front chamber door and clean the walls if necessary.<br>ii) Make sure instruments, tubes and parts (thermocouples, static pressure indicators, etc) inside or related to it are in good condition. | |

1/7

FURNACE SYSTEM PROCEDURE | Miss H Mat Kiah [02.08.2018]

| | | |
|---|---|---|
| | iii) Observe the Explosion Vent condition. Make sure a foiled paper that attached/sealed to it is not broken. | |
| d. | Thermocouples:<br>i) Check and make sure all thermocouples function well. All thermocouples should show normal ambient T initially before the test (18-20ºC).<br>ii) Observe temperature reading from the main channel to confirm. | |
| e. | Furnace:<br>Switch on the furnace button and observe the initial temperature of the furnace (initially shows T ~25ºC). | |
| 2. | FTIR | |
| a. | Heated Tube:<br>i) Put the black fine wire and wool in, then move them along the surface inside the tube to clean the dirt. *Clean the tube from both end sides.*<br>ii) Use acetone to clean the tube fittings.<br>iii) Pass through air to blow dirtiness out from the tube. | |
| b. | FTIR Pump:<br>i) Before start FTIR cleaning, make sure to disconnect the main power plug which connects the FTIR with the heated tube (FTIR pump is in OFF condition).<br>ii) Open the Side Valve of the FTIR (by pushing and turning it anti-clockwise, then pull it out). *Check the condition of the FTIR SOOT filter and clean it if required.*<br>iii) Flow air through the FTIR system from the point that is attached to the heated tube.<br>iv) After cleaning, reconnect the plug at the back side of the FTIR properly, then check FTIR temperatures (all 3 temperatures must show = 180ºC). | |
| c. | Silica Gel:<br>Replace silica gel if needed especially when its color has changed to white/black. | |
| d. | Portable $O_2$ Analyzer (Servomex):<br>i) Check the filter at the back of the $O_2$ Analyzer. *Need to change this filter if it gets wet.*<br>ii) Check drying agents and tubes condition to avoid any blockage problem. | |
| e. | Collect ice and place it in the ice box to condense water from FTIR line before the $O_2$ Analyzer. | |
| 3. | DMS500 | |
| | i) Check condition and clean the orifice place in the DMS500 heated tube. | |

2/7

FURNACE SYSTEM PROCEDURE | Miss H Mat Kiah [02.08.2018]

| | | |
|---|---|---|
| | ii) Connect all equipment (DMS pump, DMS500 main, DMS computer, compressed air supply line ~1 bar). Then, start to warm up the DMS500 system (it takes about 30 minutes/1800 seconds). ***Please refer the summarized DMS500 Operation Procedure in Section E.*** | |
| 4. | Smoke Meter | |
| | i) Turn on Power & Oven buttons of the smoke meter. Set/adjust the temperature for filter block and oven to 50ºC.<br>ii) Switch on the Heater and let it warm up to reach 180ºC.<br>iii) Check bypass filter condition and change it if necessary.<br>iv) Blow compressed air from the back through the sample inlet line follows by the exhaust (bypass) outlet line.<br>v) Place the impinger in a bucket of ice before the Smoke Meter's pump to collect the condensate. | |
| 5. | Sample Preparation | |
| | Sample boat size is 5 mm width x 815 mm length with half cylindrical shape. Weight the sample using mass balance and place it in the sample boat. *Sample is prepared with its width about 10 mm and its length can be 600-800 mm.* | |
| **C. Complete the Turn On Process for FTIR & $O_2$ Analyzers** | | |
| 1. | Make all the connection of FTIR pump and FTIR with heating lines and electricity. Attach laptop and START the Calcmet computer program. | |
| 2. | Turn On the $O_2$ analyzer downstream of the FTIR and attach the outlet of FTIR analyzer to the $O_2$ analyzer. | |
| 3. | Allow the FTIR system to warm up to the temperature of 180ºC. | |
| 4. | Pour Liquid $N_2$ into the cell of FTIR.<br>*Collect Liquid $N_2$ from the dewar (50L) storage or from the main place in the school lab. Temporary 1L cryogenic bottle storage is used to fill Liquid $N_2$ | |
| **D. CALIBRATION: Zeroing of the FTIR and $O_2$ Analyzers** | | |
| 1. | Attach data logger connections and switch on the Laptop (OPEN Calcmet2 – Temet Instruments). | |
| 2. | Switch the **top diverter** (BLACK valve on top of the rotameter for $N_2$ supply) to the FTIR line directed towards the zero gas inlet. | |
| 3. | Set the dial of the FTIR pump to ZERO GAS. | |
| 4. | Set the Nitrogen supply line to 1 Barg (can set ~1.5 Barg). | |
| 5. | Open the RED valve. Ensure the pressure in the Nitrogen line is at 0.3 Barg. Use the control valve to set the flow of $N_2$ from the flow meter between 2-4 L/m. Then, $O_2$ Analyzer will go to ZERO. | |
| 6. | Wait for the values of % oxygen stable on $O_2$ Analyzer downstream of FTIR. | |

3/7

FURNACE SYSTEM PROCEDURE | Miss H Mat Kiah [02.08.2018]

| | | |
|---|---|---|
| | When it becomes stable set the "Zero" with a screw driver until it blinks ± "0.0". (If $O_2$ Analyzer is not present just wait for 5 minutes before recording on the pDAQ for 1 minute). | |
| 7. | First press 3M on the Calcmet(2) program, then CANCEL it. Go to OPTION, click AUTOSAVING and RENAME it, then press OK. | |
| 8. | To zero the FTIR, go on the Laptop Calcmet program, on the **"Measure"** tab, click "Zero" in order to get zero calibration. Calcmet program will return a background reading. | |
| 9. | Run the program for a 3 min sample, check that zero line is straight and at zero. If not check for leakages in the system and/or check the detection cell temperature is at -196.0ºC on **View, Hardware Status** (TOP UP the liquid nitrogen if it is not showing the correct temperature). | |
| 10. | Press 5s on the Calcmet program (check the graph must show a straight line, ± 0.5s). | |
| 11. | Close $N_2$ supply line, close RED Valve. | |
| 12. | Set the dial of FTIR pump towards SAMPLE/SPAN gas. | |
| 13. | To span the $O_2$ Analyzer downstream of FTIR, START the FTIR PUMP. | |
| 14. | Wait for 5 minutes to get the values of % oxygen stable on $O_2$ Analyzer. When it becomes stable set the dial to between 20.9 and 21.0 then record on the pDAQ for 1 minute. | |
| **E. DMS500 Operation Procedure.** | | |
| 1. | Switch on the computer where DMS 500 software is installed. | |
| 2. | Open the software via CD-R, Cambustion, My V4.11, Start DMS. | |
| 3. | Select File Dialog: Biomondal_m7_m2cqw21.dmd. | |
| 4. | Turn on the compressed air (~1bar) and the DMS unit (Green bottom on the equipment). | |
| 5. | Turn the DMS equipment to ON from STAND BY, and wait 30 mins for warming up the DMS equipment. | |
| 6. | AUTOZERO ALL after the warming up, and decide where the experiment data should be logged to. | |
| 7. | Start and stop logging data. After pressing "Start Logging", RENAME the file and SAVE it. **Change "ZERO" mode to "SAMPLE" mode.** FIRE EVENTS can be stated in the MEMO. | |
| 8. | After the experiment, turn the equipment from ON to STAND BY, and click EXIT from the FILE MENU. | |
| 9. | Close the software and shut down the DMS equipment. | |
| 10. | Turn off the compressed air. | |

4/7

| | | |
|---|---|---|
| **F. Smoke Meter Operation Procedure.** | | |
| 1. | Make sure the Power and Oven buttons are on. Switch on the Heater and allow it to heat up to 180ºC. Set the Filter Block and Oven temperatures to 50ºC (47 to 50ºC). Wait for the system to reach the set temperatures. | |
| 2. | Put the system on Bypass button always when no sampling made. Adjust the Bypass valve to the flow rate of 10 L/min. Smoke Meter's pump is in off condition. | |
| 3. | Place a filter paper in the sample holder/block and close it. Turn on the Smoke Meter's pump and put the system on Sample button to start sampling process. Immediately adjust the Sample valve flow rate to 10 L/min. | |
| 4. | *Record the time every time when starting filter paper sampling after changing the filter paper. Filter paper is changed every 2 to 5 minutes depending to amount of soot that collected. Change time reduces if soot amount increases. | |
| 5. | Put the system on Bypass button, switch off the pump, open the filter paper holder/block and change a new filter paper. Transfer the used filter paper and place it temporarily in the desiccator before weighing its weight to determine the soot mass. Repeat the same steps during the test until completed. | |
| **G. Before Test(s).** | | |
| 1. | Make sure that the room exhaust system is ON and set to 0.2m³/s. | |
| 2. | Set and increase Furnace temperature (Eurotherm) to the desired test temperature (i.e. 600ºC). | |
| 3. | Put and arrange a test sample into the sample boat properly. | |
| 4. | Turn on the main compressed air supply valve. Set the diverter on the furnace to "Air". Set the Total Flowmeter to 50 L/min and set the Primary Air Flowmeter to the desired value (e.g. 10 L/min) depending to the required equivalence ratio. ***Please refer the prepared Excel Table for test conditions with various equivalence ratios.*** | |
| 5. | Refill Liquid $N_2$ into the FTIR cell if required. | |
| 6. | Check and make sure again that FTIR PUMP is ON and $O_2$ value is ~20.9. | |
| 7. | Check again the DMS500 (must already "AUTOZERO ALL"). Start logging first before the furnace test is started. | |
| 8. | Make sure the first filter paper is placed in the filter holder/block and all temperatures on the Smoke Meter are correct and in the required range. | |
| 9. | Recheck again to make sure total and primary air flow rates are at the set values. | |
| 10. | Set the speed rate of the driver and get READY to START the TEST. | |





| | | |
|---|---|---|
| **H. Run Test(s).** | | |
| 1. | **Start Test** | |
| a. | Start Baseline/Sampling on FTIR program, pDAQ and DMS500 computer at the same time. | |
| b. | Test is started by switching on the driver to feed the sample at certain speed rate into the tube furnace. Test start time is recorded. | |
| c. | Ignition/flame is observed through a mirror and test details are recorded. | |
| d. | $O_2$ levels that shown by the $O_2$ Analyzer are observed throughout the test and recorded. | |
| 2. | **Stop Test** | |
| a. | Stop Test/Sampling on FTIR program, pDAQ and DMS500 computer at the same time. | |
| b. | Decrease the furnace temperature (Eurotherm) to the minimum value. | |
| c. | Allow the primary and secondary air flows to keep flowing through the Furnace System for certain duration of time (at least 5 minutes) to cool down the whole Furnace System. System needs to be cooled down below 300ºC to avoid any further reaction and self-ignition. | |
| d. | Turn off FTIR pump. Change FTIR Valve from SAMPLE/SPAN to ZERO. Proceed with flushing the FTIR & $O_2$ Analyzers with $N_2$. | |
| e. | Pull or reverse back the sample boat to the first end of quartz/glass tube by controlling the driver. Doing this will avoid any further reaction on the fuel when keep staying in hot furnace. | |
| f. | SAVE all recorded data (FTIR program, pDAQ excel and DMS500 computer). | |
| g. | Put DMS500 program as "STANDBY" (DMS pump will be OFF), turn off the DMS500, then can close air valve and compressed air supply line. | |
| h. | COPY the recorded results/data. | |
| **I. Normal Shut Down Procedure.** | | |
| 1. | Shut down software and turn off computers. | |
| 2. | Switch off all power supplies to the equipment and analyzers. | |
| 3. | Turn off all gas supplies. Observe the pressure gauges to check they are off. | |
| 4. | Sweep/vacuum floor free from any ash/debris. | |
| 5. | Switch off the exhaust fan (Ventilation Panel) and close the ventilation shutters (by pulling down the black rod). | |
| **J. EMERGENCY SHUTDOWN Procedure.** | | |
| 1. | **Turn off the heater (by switching off the "Tube Furnace" on the Furnace System).** | |





| | | |
|---|---|---|
| 2. | **Make your way to the nearest Fire Exit.** | |
| 3. | **In the event of smoke accumulation and alarm failure, use manual "Purge" switch to operate emergency ventilation (Ventilation shutters should be open, otherwise evacuate and contact local technician).** | |
| **K. Periodic Maintenance.** **(Note: Check Daily, Weekly and Monthly maintenance log).** | | |
| 1. | Check maintenance logs and appendix for a comprehensive list of periodic maintenance. | |
| 2. | Gloves must be worn during cleaning. Lab coat is recommended. | |
| 3. | Turn on compressed airline and check for leaks or blockages in oxygen line (either by ear or visually with a soap solution). | |
| 4. | Repair any leaks, turn off airline and return oxygen line to standard configuration. | |

## C.2 Pictures of Purser Furnace Tests

# Appendix D
# List of Fire Toxicity Tests

| No. | Material Type | Material Group | Sample Preparation | Pre and Post Analysis | | | | | | | | Ignition Type | Air Flow Rate (L/min) | Heat Flux (kW/m$^2$) | Data Collection | | | | |
|---|---|---|---|---|---|---|---|---|---|---|---|---|---|---|---|---|---|---|---|
| | | | | CHNS | CHNS2 | TGA1 (Raw Sample) | TGA2 (Burned Sample) | Bomb C | GC | TGA3 (Filter Paper) | SEM / TEM | | | | Cone | FTIR | DMS500 / SMPS | Smoke Meter | Infra-RED Camera |
| **CONE CALORIMTER TESTS** | | | | | | | | | | | | | | | | | | | |
| 1 | PVC P A | EC | Y | Y | Y | Y | Y | Y | N | N | Y | Auto | 9.4 | 25 | Y | Y | Y | N | N |
| 2 | PVC P A | EC | Y | Y | Y | Y | Y | Y | N | N | Y | Auto | 9.4 | 30 | Y | Y | Y | N | N |
| 3 | PVC P A | EC | Y | Y | Y | Y | Y | Y | N | N | Y | Auto | 9.4 | 50 | Y | Y | Y | N | N |
| 4 | PVC P A | EC | Y | Y | N | Y | Y | Y | N | N | Y | Auto | 18 | 25 | Y | Y | Y | N | N |
| 5 | PVC P A | EC | Y | Y | Y | Y | Y | Y | N | N | Y | Auto | 18 | 30 | Y | Y | Y | N | N |
| 6 | PVC P A | EC | Y | Y | Y | Y | Y | Y | N | N | Y | Auto | 18 | 50 | Y | Y | Y | N | N |
| 7 | PVC P A | EC | Y | Y | N | Y | Y | Y | N | N | Y | Auto | 28 | 25 | Y | Y | Y | N | N |
| 8 | PVC P A | EC | Y | Y | Y | Y | Y | Y | N | N | Y | Auto | 28 | 30 | Y | Y | Y | N | N |
| 9 | PVC P A | EC | Y | Y | Y | Y | Y | Y | N | N | Y | Auto | 28 | 50 | Y | Y | Y | N | N |
| 10 | PVC P A | EC | Y | Y | N | Y | N | Y | N | N | Y | Auto | Free | 35 | Y | Y | Y | N | N |
| 11 | P B | EC | Y | Y | N | Y | N | Y | N | N | Y | Auto | 9.4 | 50 | Y | Y | N | N | N |
| 12 | P B | EC | Y | Y | N | Y | N | Y | N | N | Y | Auto | Free | 35 | Y | Y | Y | N | N |
| 13 | AMI-G | EC | Y | Y | N | Y | N | Y | N | N | N | Auto | 9.4 | 50 | Y | Y | N | N | N |
| 14 | AMI-G | EC | Y | Y | N | Y | N | Y | N | N | N | Auto | Free | 35 | Y | Y | Y | N | N |
| 15 | 6701B-W | EC | Y | Y | N | Y | N | Y | N | N | N | Auto | 9.4 | 50 | Y | Y | N | N | N |
| 16 | 6701B-W | EC | Y | Y | N | Y | N | Y | N | N | N | Auto | Free | 35 | Y | Y | Y | N | N |
| 17 | AMI-B | EC | Y | Y | N | Y | N | Y | N | N | N | Auto | Free | 35 | Y | Y | Y | N | N |
| 18 | RBS | Rubber | Y | Y | N | Y | N | Y | N | N | N | Auto | Free - NC | 29 | Y | N | N | N | N |
| 19 | RBS | Rubber | Y | Y | N | Y | N | Y | N | N | N | Auto | Free - NC | 30 | Y | N | N | N | N |
| 20 | RBS | Rubber | Y | Y | N | Y | N | Y | N | N | N | Auto | Free - NC | 35 | Y | N | N | N | N |
| 21 | RBS | Rubber | Y | Y | N | Y | N | Y | N | N | N | Auto | Free | 35 | Y | Y | Y | N | N |
| 22 | RBS | Rubber | Y | Y | N | Y | N | Y | N | N | N | Auto | Free - NC | 40 | Y | N | N | N | N |
| 23 | RBS | Rubber | Y | Y | N | Y | N | Y | N | N | N | Auto | Free - NC | 45 | Y | N | N | N | N |
| 24 | RBS | Rubber | Y | Y | N | Y | N | Y | N | N | N | Auto | Free - NC | 50 | Y | N | N | N | N |
| 25 | RBS | Rubber | Y | Y | N | Y | N | Y | N | N | N | Auto | Free - NC | 55 | Y | N | N | N | N |
| 26 | PIRF-GT | PIR | Y | Y | N | Y | N | Y | N | N | Y | Auto | Free | 25 | Y | Y | Y | N | N |

| No. | Material Type | Material Group | Sample Preparation | Pre and Post Analysis | | | | | | | | Ignition Type | Air Flow Rate (L/min) | Heat Flux (kW/m$^2$) | Data Collection | | | | |
|---|---|---|---|---|---|---|---|---|---|---|---|---|---|---|---|---|---|---|---|
| | | | | CHNS | CHNS2 | TGA1 (Raw Sample) | TGA2 (Burned Sample) | Bomb C | GC | TGA3 (Filter Paper) | SEM / TEM | | | | Cone | FTIR | DMS500 / SMPS | Smoke Meter | Infra-RED Camera |
| **CONE CALORIMTER TESTS** | | | | | | | | | | | | | | | | | | | |
| 27 | PIRF-GT | PIR | Y | Y | N | Y | N | Y | N | N | Y | Auto | Free | 28 | Y | Y | Y | N | N |
| 28 | PIRF-GT | PIR | Y | Y | N | Y | N | Y | N | N | Y | Auto | Free | 30 | Y | Y | Y | N | N |
| 29 | PIRF-GT | PIR | Y | Y | N | Y | N | Y | N | N | Y | Auto | Free | 35 | Y | Y | Y | N | N |
| 30 | PIRF-GT | PIR | Y | Y | N | Y | N | Y | N | N | Y | Auto | Free | 50 | Y | Y | Y | N | N |
| 31 | PS-CB | PS | Y | Y | N | Y | N | Y | N | N | N | Auto | Free | 35 | Y | Y | N | N | N |
| 32 | PU-FM | PU | Y | Y | N | Y | N | Y | N | N | Y | Auto | Free | 35 | Y | Y | N | N | N |
| 33 | TEC2-W | EC | Y | Y | N | Y | N | Y | N | N | N | Auto | Free | 35 | Y | Y | N | N | N |
| 34 | FL2-W | EC | Y | Y | N | Y | N | Y | N | N | N | Auto | Free | 35 | Y | Y | N | N | N |
| 35 | PS-TV W | PS | Y | Y | N | Y | N | Y | N | N | N | Auto | Free | 35 | Y | Y | N | N | N |
| 36 | RBG | Rubber | Y | Y | N | Y | N | Y | N | N | N | Auto | Free - NC | 30 | Y | N | N | N | N |
| 37 | RBG | Rubber | Y | Y | N | Y | N | Y | N | N | N | Auto | Free - NC | 35 | Y | N | N | N | N |
| 38 | RBG | Rubber | Y | Y | N | Y | N | Y | N | N | N | Auto | Free - NC | 40 | Y | N | N | N | N |
| 39 | RBG | Rubber | Y | Y | N | Y | N | Y | N | N | N | Auto | Free - NC | 45 | Y | N | N | N | N |
| 40 | RBG-B | Rubber | Y | Y | N | Y | N | Y | N | N | N | Auto | Free - NC | 35 | Y | N | N | N | N |
| 41 | RBG-B | Rubber | Y | Y | N | Y | N | Y | N | N | N | Auto | Free - NC | 40 | Y | N | N | N | N |
| 42 | RBG-B | Rubber | Y | Y | N | Y | N | Y | N | N | N | Auto | Free - NC | 45 | Y | N | N | N | N |
| 43 | RBG-B | Rubber | Y | Y | N | Y | N | Y | N | N | N | Auto | Free - NC | 50 | Y | N | N | N | N |
| 44 | RBG-B | Rubber | Y | Y | N | Y | N | Y | N | N | N | Auto | Free - NC | 55 | Y | N | N | N | N |
| 45 | HV1 | EC | Y | Y | N | Y | N | Y | N | N | N | Auto | Free | 35 | Y | Y | N | N | N |
| 46 | HV2 | EC | Y | Y | N | Y | N | Y | N | N | N | Auto | Free | 35 | Y | Y | N | N | N |
| 47 | DC1 | EC | Y | Y | N | Y | N | Y | N | N | N | N | N | N | N | N | N | N | N |
| 48 | DC2 | EC | Y | Y | N | Y | N | Y | N | N | N | N | N | N | N | N | N | N | N |
| 49 | CT (B) & (S) | Other | Y | Y | N | Y | N | Y | N | N | N | N | N | N | N | N | N | N | N |
| 50 | Foam B | PU | Y | Y | N | Y | N | Y | N | N | N | Auto | Free | 35 | Y | Y | N | N | N |
| 51 | FL1-BG | EC | Y | Y | N | Y | N | Y | N | N | N | Auto | Free | 35 | Y | Y | N | N | N |
| 52 | PEP | PE | Y | Y | N | Y | N | Y | N | N | N | Auto | Free | 35 | Y | Y | N | N | N |
| 53 | SB-P | PE | Y | Y | N | Y | N | Y | N | N | N | Auto | Free | 35 | Y | Y | N | N | N |
| 54 | PP Rope10 | Other | Y | Y | N | Y | N | Y | N | N | N | N | N | N | N | N | N | N | N |
| 55 | SB-W H | PS | Y | Y | N | Y | N | Y | N | N | N | Auto | Free | 35 | Y | Y | N | N | N |
| 56 | PVC ST | PVC | Y | Y | N | Y | N | Y | N | N | N | Auto | Free | 35 | Y | Y | N | N | N |
| 57 | Clear PS2 | PS | Y | Y | N | Y | N | Y | N | N | N | Auto | Free | 35 | Y | Y | N | N | N |

| No. | Material Type | Material Group | Sample Preparation | Pre and Post Analysis | | | | | | | | Ignition Type | Air Flow Rate (L/min) | Heat Flux (kW/m$^2$) | Data Collection | | | | |
|---|---|---|---|---|---|---|---|---|---|---|---|---|---|---|---|---|---|---|---|
| | | | | CHNS | CHNS2 | TGA1 (Raw Sample) | TGA2 (Burned Sample) | Bomb C | GC | TGA3 (Filter Paper) | SEM / TEM | | | | Cone | FTIR | DMS500 / SMPS | Smoke Meter | Infra-RED Camera |
| **CONE CALORIMTER TESTS** | | | | | | | | | | | | | | | | | | | |
| 58 | Clear PS4 | PS | Y | Y | N | Y | N | Y | N | N | N | N | N | N | N | N | N | N | N |
| 59 | PS2 | PS | Y | Y | N | Y | N | Y | N | N | N | Auto | Free | 35 | Y | Y | N | N | N |
| 60 | CA-B | Other | Y | Y | N | Y | N | Y | N | N | N | Auto | Free | 35 | Y | Y | N | N | N |
| 61 | PS Cove S | PS | Y | Y | N | Y | N | Y | N | N | N | Auto | Free | 35 | Y | Y | N | N | N |
| 62 | TEC1-G/EC-GB1 | EC | Y | Y | N | Y | N | Y | N | N | N | Auto | Free | 35 | Y | Y | N | N | N |
| 63 | TEC3-G/EC-GB2 | EC | Y | Y | N | Y | N | Y | N | N | N | Auto | Free | 35 | Y | Y | N | N | N |
| 64 | TEC4-G/EC-GB3 | EC | Y | Y | N | Y | N | Y | N | N | N | N | N | N | N | N | N | N | N |
| 65 | TEC5-G/SK1-GB | EC | Y | Y | N | Y | N | Y | N | N | N | N | N | N | N | N | N | N | N |
| 66 | TEC6-G/SK2-GS | EC | Y | Y | N | Y | N | Y | N | N | N | N | N | N | N | N | N | N | N |
| 67 | PMMA-Black | Other | Y | Y | N | Y | N | Y | N | N | N | Pilot | Free | 50 | Y | N | N | N | Y |
| 68 | PE-Y | PE | Y | Y | N | Y | N | Y | N | N | N | Pilot | Free | 15 | Y | N | N | N | Y |
| 69 | PE-Y | PE | Y | Y | N | Y | N | Y | N | N | N | Pilot | Free | 16 | Y | N | N | N | Y |
| 70 | PE-Y | PE | Y | Y | N | Y | N | Y | N | N | N | Pilot | Free | 20 | Y | N | N | N | Y |
| 71 | PE-Y | PE | Y | Y | N | Y | N | Y | N | N | N | Pilot | Free | 25 | Y | N | N | N | Y |
| 72 | PE-Y | PE | Y | Y | N | Y | N | Y | N | N | N | Pilot | Free | 35 | Y | N | N | N | Y |
| 73 | PE-Y | PE | Y | Y | N | Y | N | Y | N | N | N | Auto | Free | 35 | Y | Y | N | N | N |
| 74 | PE-Blue | PE | Y | Y | N | Y | N | Y | N | N | N | Pilot | Free | 15 | Y | N | N | N | Y |
| 75 | PE-Blue | PE | Y | Y | N | Y | N | Y | N | N | N | Pilot | Free | 16 | Y | N | N | N | Y |
| 76 | PE-Blue | PE | Y | Y | N | Y | N | Y | N | N | N | Pilot | Free | 17 | Y | N | N | N | Y |
| 77 | PE-Blue | PE | Y | Y | N | Y | N | Y | N | N | N | Pilot | Free | 20 | Y | N | N | N | Y |
| 78 | PE-Blue | PE | Y | Y | N | Y | N | Y | N | N | N | Pilot | Free | 25 | Y | N | N | N | Y |
| 79 | PE-Blue | PE | Y | Y | N | Y | N | Y | N | N | N | Pilot | Free | 35 | Y | N | N | N | Y |
| 80 | PE-Blue | PE | Y | Y | N | Y | N | Y | N | N | N | Auto | Free | 35 | Y | Y | N | N | N |
| 81 | PE-Black | PE | Y | Y | N | Y | N | Y | N | N | N | Pilot | Free | 15 | Y | N | N | N | Y |
| 82 | PE-Black | PE | Y | Y | N | Y | N | Y | N | N | N | Pilot | Free | 16 | Y | N | N | N | Y |
| 83 | PE-Black | PE | Y | Y | N | Y | N | Y | N | N | N | Pilot | Free | 17 | Y | N | N | N | Y |
| 84 | PE-Black | PE | Y | Y | N | Y | N | Y | N | N | N | Pilot | Free | 18 | Y | N | N | N | Y |
| 85 | PE-Black | PE | Y | Y | N | Y | N | Y | N | N | N | Pilot | Free | 19 | Y | N | N | N | Y |
| 86 | PE-Black | PE | Y | Y | N | Y | N | Y | N | N | N | Pilot | Free | 20 | Y | N | N | N | Y |
| 87 | PE-Black | PE | Y | Y | N | Y | N | Y | N | N | N | Pilot | Free | 25 | Y | N | N | N | Y |

| No. | Material Type | Material Group | Sample Preparation | Pre and Post Analysis | | | | | | | | Ignition Type | Air Flow Rate (L/min) | Heat Flux ($kW/m^2$) | Data Collection | | | | |
|---|---|---|---|---|---|---|---|---|---|---|---|---|---|---|---|---|---|---|---|
| | | | | CHNS | CHNS2 | TGA1 (Raw Sample) | TGA2 (Burned Sample) | Bomb C | GC | TGA3 (Filter Paper) | SEM / TEM | | | | Cone | FTIR | DMS500 / SMPS | Smoke Meter | Infra-RED Camera |
| **CONE CALORIMTER TESTS** | | | | | | | | | | | | | | | | | | | |
| 88 | PE-Black | PE | Y | Y | N | Y | N | Y | N | N | N | Pilot | Free | 35 | Y | N | N | N | Y |
| 89 | PE-Black | PE | Y | Y | N | Y | N | Y | N | N | N | Auto | Free | 35 | Y | Y | N | N | N |
| 90 | GRP-Blue | Other | Y | Y | N | Y | N | Y | N | N | N | Pilot | Free | 12 | Y | N | N | N | Y |
| 91 | GRP-Blue | Other | Y | Y | N | Y | N | Y | N | N | N | Pilot | Free | 13 | Y | N | N | N | Y |
| 92 | GRP-Blue | Other | Y | Y | N | Y | N | Y | N | N | N | Pilot | Free | 14 | Y | N | N | N | Y |
| 93 | GRP-Blue | Other | Y | Y | N | Y | N | Y | N | N | N | Pilot | Free | 16 | Y | N | N | N | Y |
| 94 | GRP-Blue | Other | Y | Y | N | Y | N | Y | N | N | N | Pilot | Free | 20 | Y | N | N | N | Y |
| 95 | GRP-Blue | Other | Y | Y | N | Y | N | Y | N | N | N | Pilot | Free | 25 | Y | N | N | N | Y |
| 96 | GRP-Blue | Other | Y | Y | N | Y | N | Y | N | N | N | Pilot | Free | 35 | Y | N | N | N | Y |
| 97 | GRP-Blue | Other | Y | Y | N | Y | N | Y | N | N | N | Auto | Free | 35 | Y | Y | N | N | N |
| 98 | PS-CB2 | Other | Y | Y | N | Y | N | Y | N | N | N | Auto | Free | 35 | Y | Y | N | N | N |
| 99 | FL3-W | EC | Y | Y | N | Y | N | Y | N | N | N | N | N | N | N | N | N | N | N |
| 100 | PM-Green | PU | Y | Y | N | Y | N | Y | N | N | N | N | N | N | N | N | N | N | N |
| 101 | Lamp1-C | Other | Y | Y | N | Y | N | Y | N | N | N | N | N | N | N | N | N | N | N |
| 102 | Lamp2-Y | Other | Y | Y | N | Y | N | Y | N | N | N | N | N | N | N | N | N | N | N |
| 103 | PS-CB2 | PS | Y | Y | N | Y | N | Y | N | N | N | Auto | Free | 35 | Y | Y | N | N | N |
| 104 | PU-FSC | PU | Y | Y | N | Y | N | Y | N | N | N | Auto | Free | 35 | Y | Y | N | N | N |
| **NEW DEVELOPED PURSER FURNACE TESTS (Varied Fuel Feed Rates)** | | | | | | | | | | | | | | | | | | | |
| 105 | PE-Y | PE | Y | Y | N | Y | N | Y | N | N | N | Auto | 10 | ~30 (600°C) | N | Y | Y | Y | N |
| 106 | PE-Y | PE | Y | Y | N | Y | N | Y | N | N | N | Auto | 10 | ~30 (600°C) | N | Y | Y | Y | N |

# Appendix E
# Cumulative Mass of CO for Various Polymer Fires

**CONE CALORIMETER TESTS**
**VARIOUS ELECTRICAL CABLE FIRES**

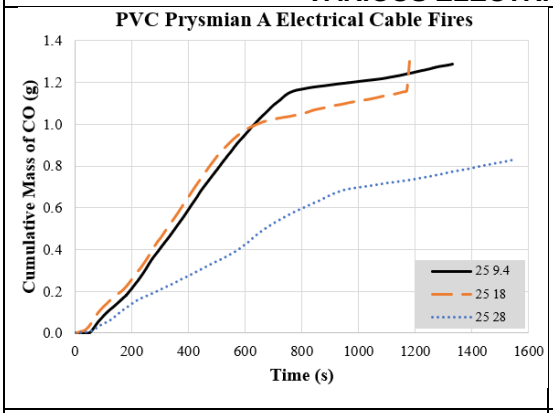


(a)

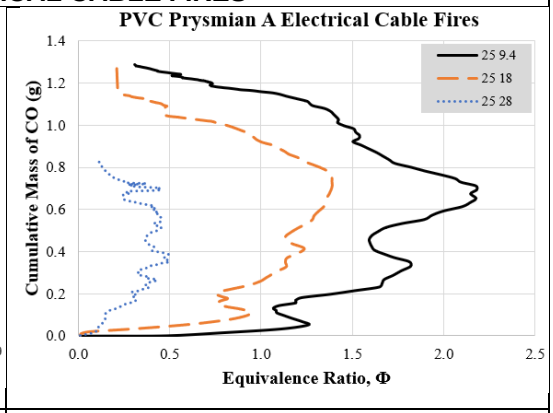


(b)

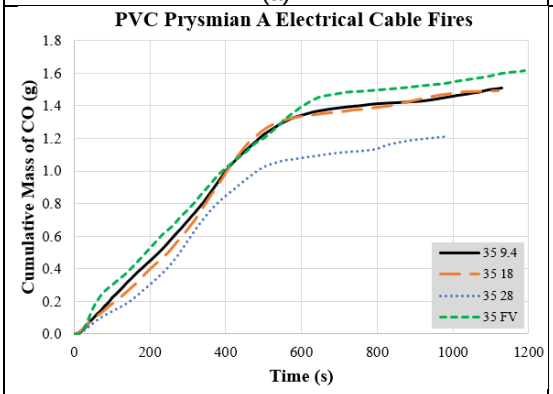


(c)

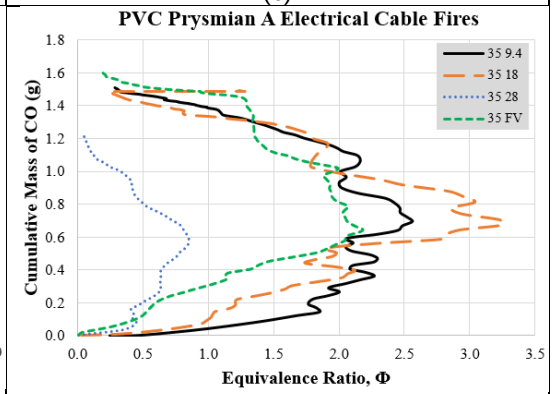


(d)

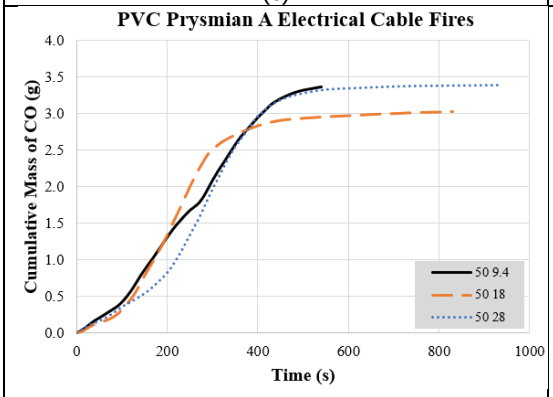


(e)

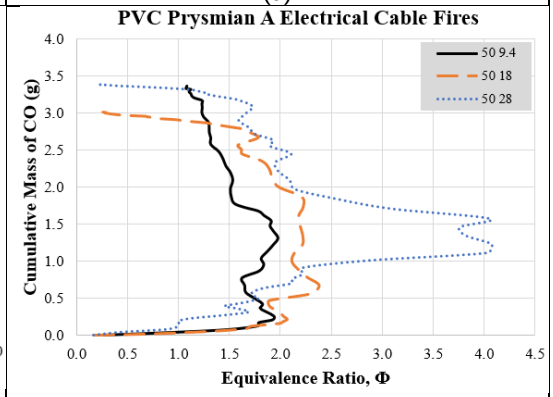


(f)

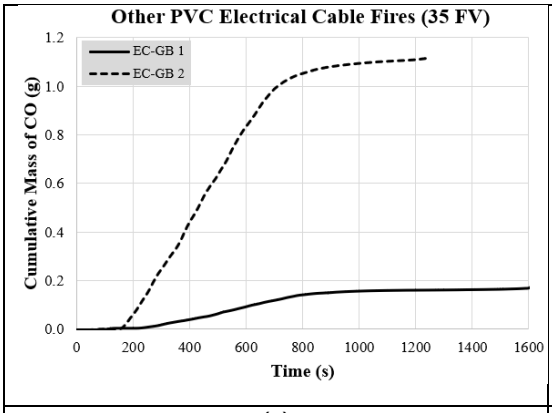
Other PVC Electrical Cable Fires (35 FV)
EC-GB 1
EC-GB 2
Cumulative Mass of CO (g)
Time (s)

(g)

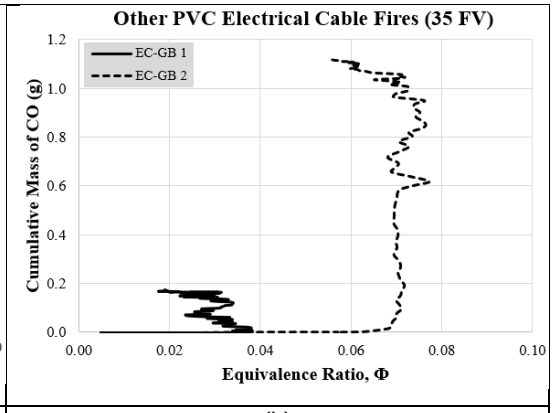
Other PVC Electrical Cable Fires (35 FV)
EC-GB 1
EC-GB 2
Cumulative Mass of CO (g)
Equivalence Ratio, Φ

(h)

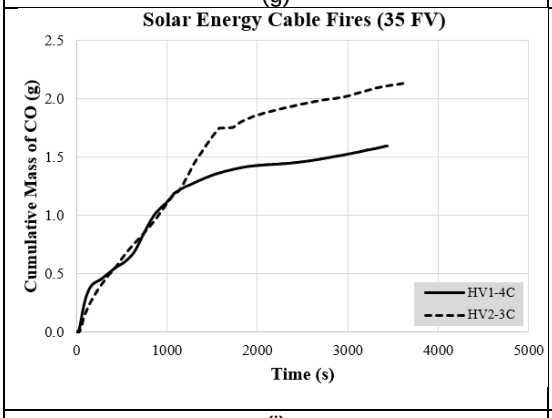
Solar Energy Cable Fires (35 FV)
HV1-4C
HV2-3C
Cumulative Mass of CO (g)
Time (s)

(i)

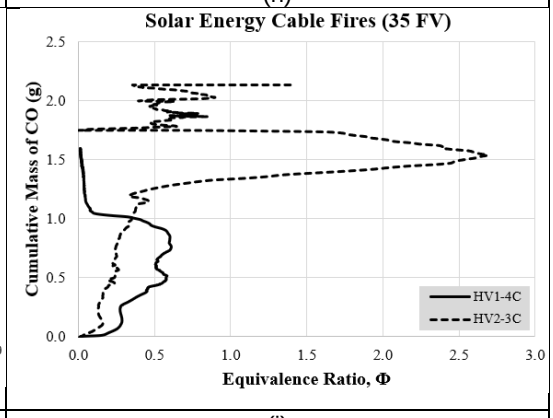
Solar Energy Cable Fires (35 FV)
HV1-4C
HV2-3C
Cumulative Mass of CO (g)
Equivalence Ratio, Φ

(j)

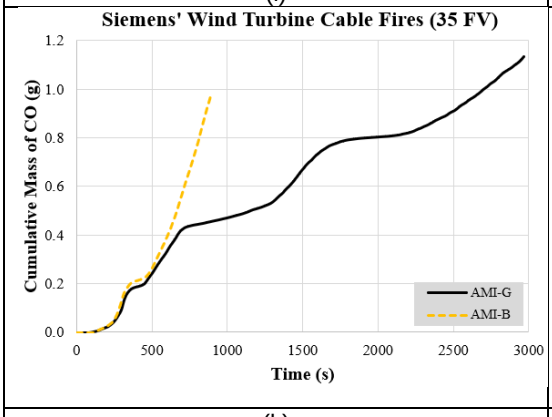
Siemens' Wind Turbine Cable Fires (35 FV)
AMI-G
AMI-B
Cumulative Mass of CO (g)
Time (s)

(k)

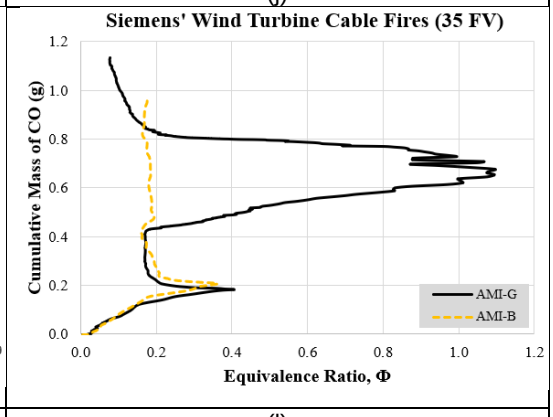
Siemens' Wind Turbine Cable Fires (35 FV)
AMI-G
AMI-B
Cumulative Mass of CO (g)
Equivalence Ratio, Φ

(l)

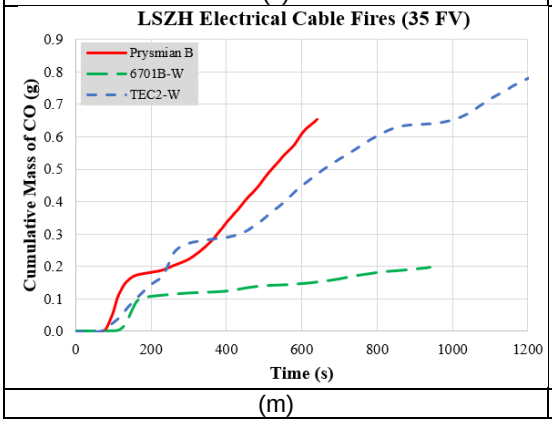
LSZH Electrical Cable Fires (35 FV)
Prysmian B
6701B-W
TEC2-W
Cumulative Mass of CO (g)
Time (s)

(m)

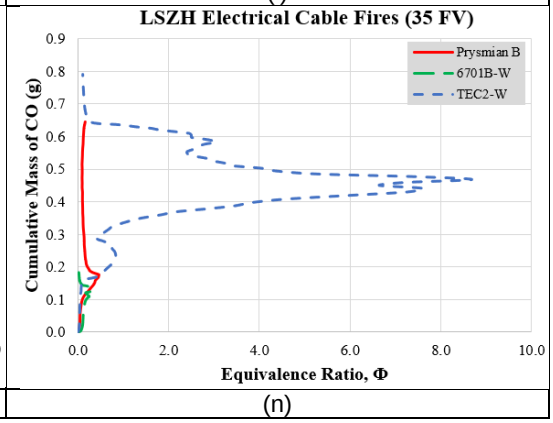
LSZH Electrical Cable Fires (35 FV)
Prysmian B
6701B-W
TEC2-W
Cumulative Mass of CO (g)
Equivalence Ratio, Φ

(n)

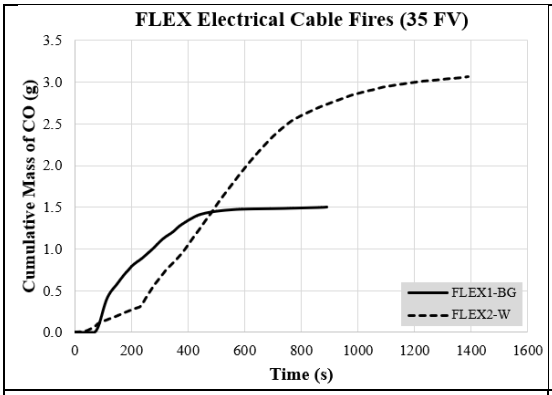


(o)

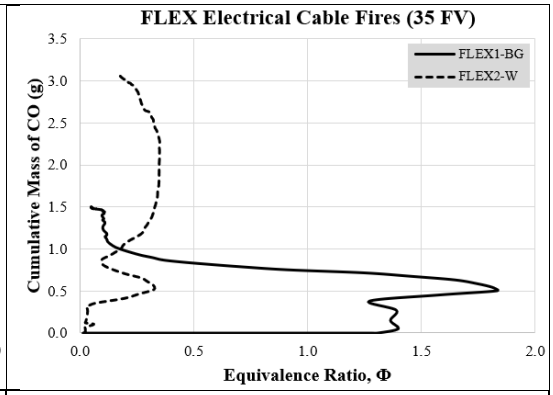


(p)

**VARIOUS POLYMER FIRES**

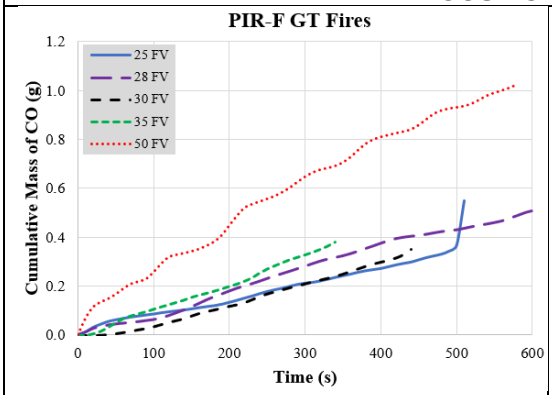


(a)

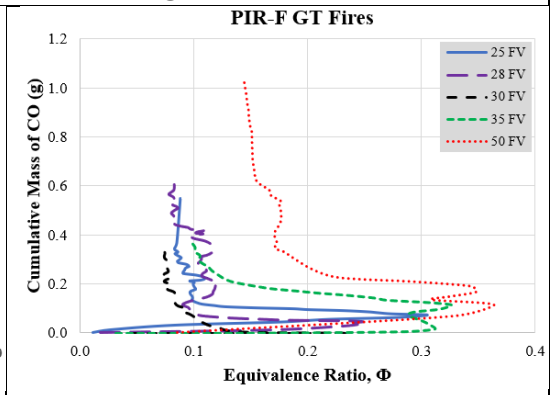


(b)

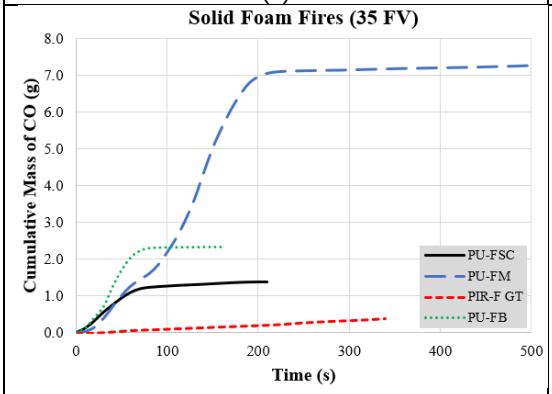


(c)

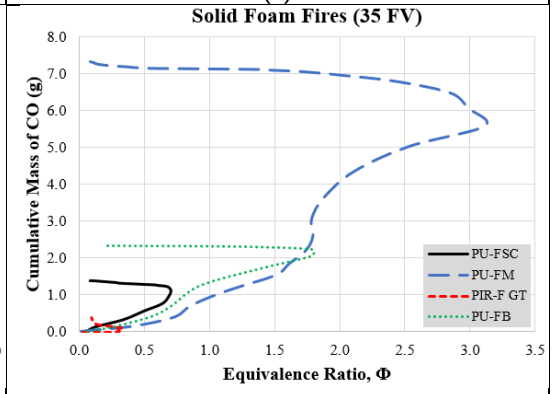


(d)

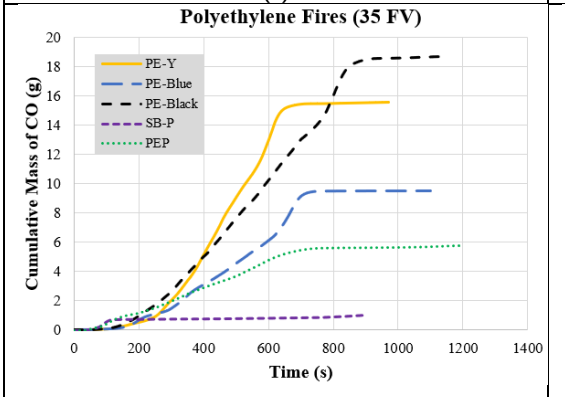


(e)

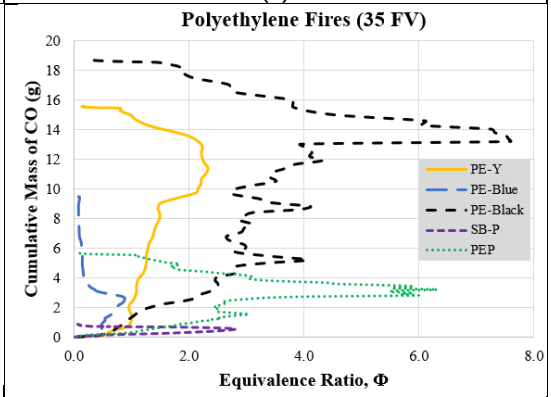


(f)

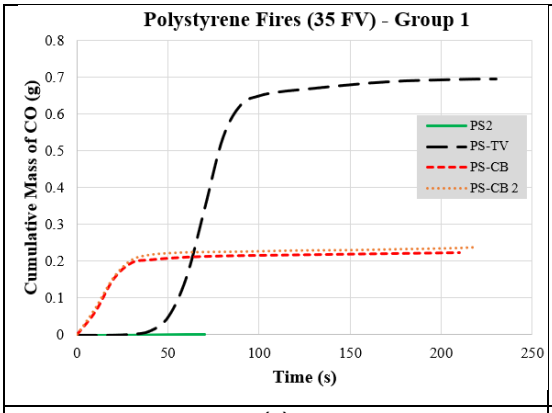
Polystyrene Fires (35 FV) - Group 1
Cumulative Mass of CO (g)
Time (s)
PS2
PS-TV
PS-CB
PS-CB 2

(g)

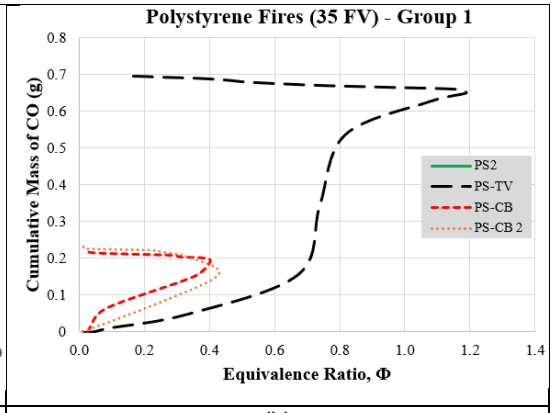
Polystyrene Fires (35 FV) - Group 1
Cumulative Mass of CO (g)
Equivalence Ratio, Φ
PS2
PS-TV
PS-CB
PS-CB 2

(h)

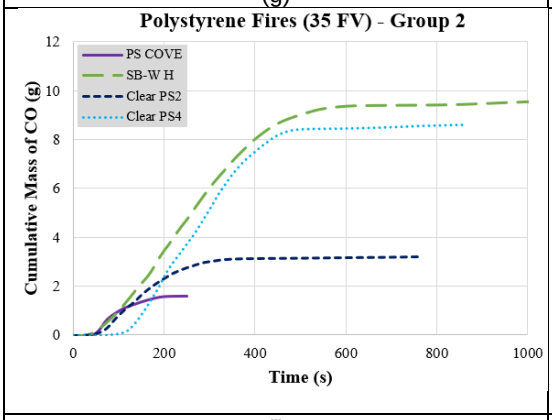
Polystyrene Fires (35 FV) - Group 2
Cumulative Mass of CO (g)
Time (s)
PS COVE
SB-W H
Clear PS2
Clear PS4

(i)

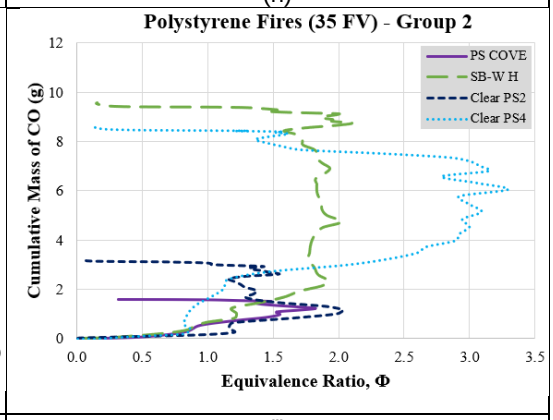
Polystyrene Fires (35 FV) - Group 2
Cumulative Mass of CO (g)
Equivalence Ratio, Φ
PS COVE
SB-W H
Clear PS2
Clear PS4

(j)

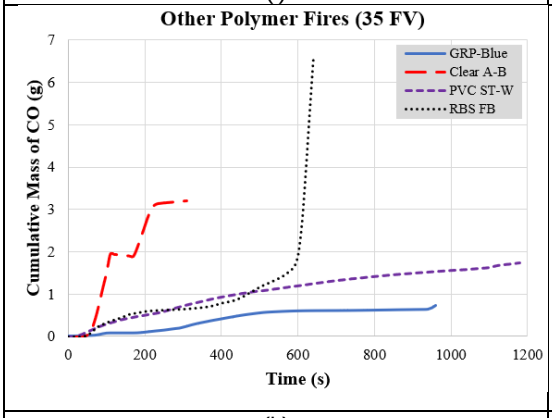
Other Polymer Fires (35 FV)
Cumulative Mass of CO (g)
Time (s)
GRP-Blue
Clear A-B
PVC ST-W
RBS FB

(k)

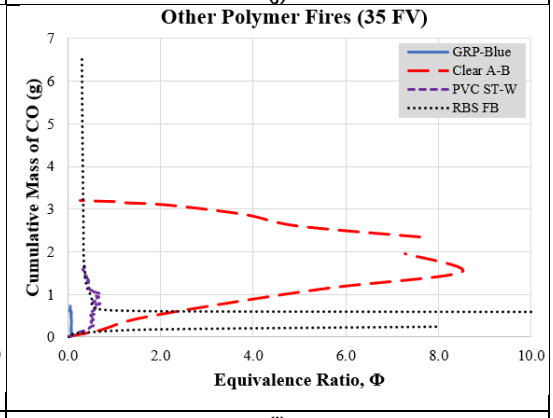
Other Polymer Fires (35 FV)
Cumulative Mass of CO (g)
Equivalence Ratio, Φ
GRP-Blue
Clear A-B
PVC ST-W
RBS FB

(l)

# Appendix F
# Assembly Drawings of the Modified Purser Furnace

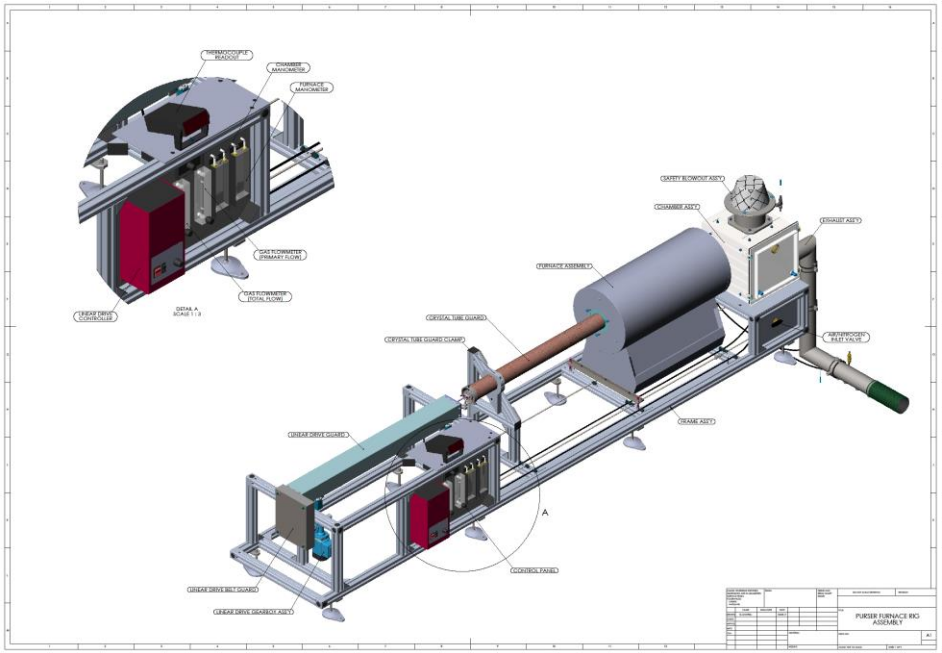


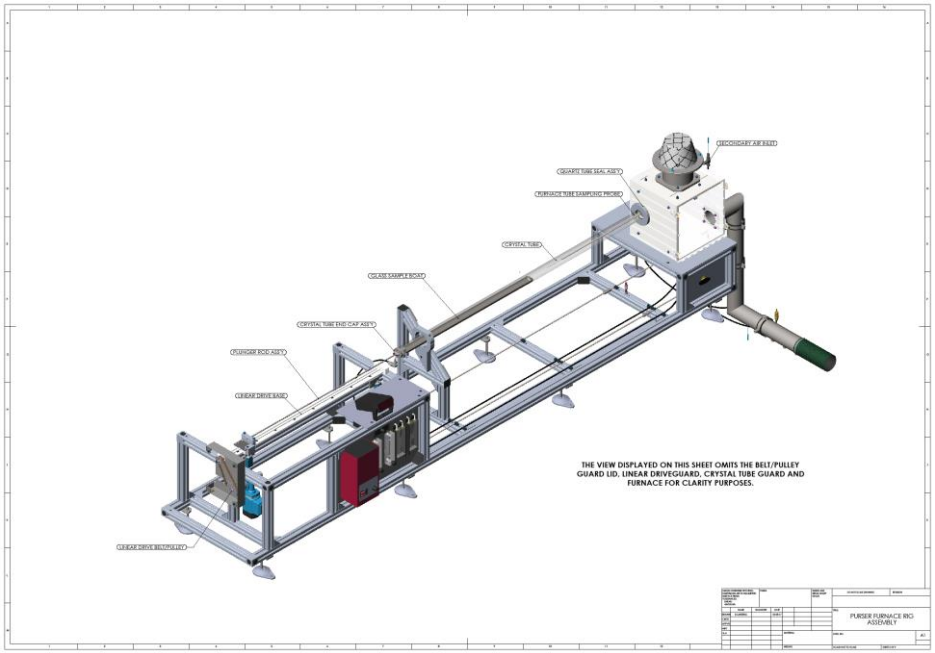

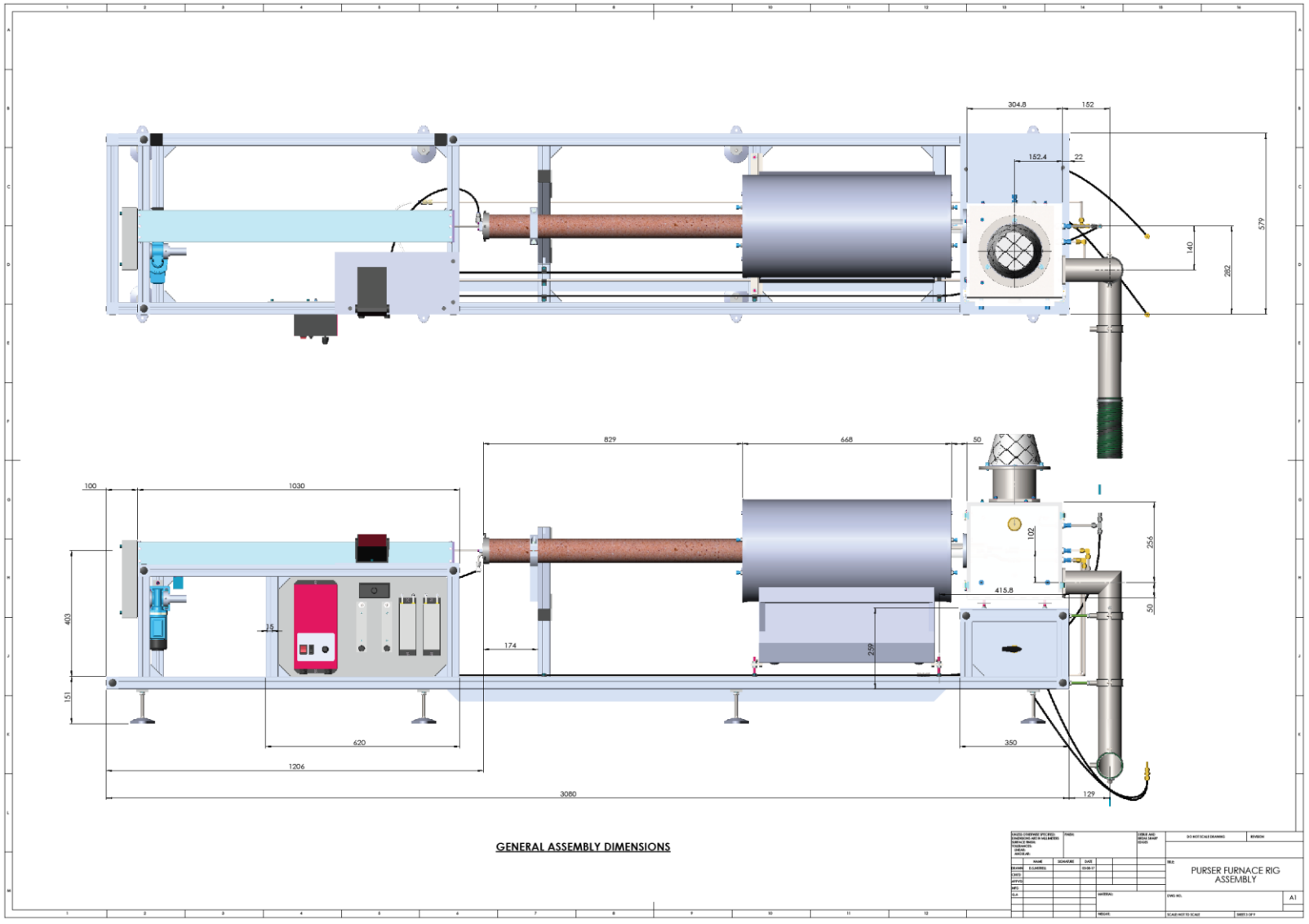


GENERAL ASSEMBLY DIMENSIONS

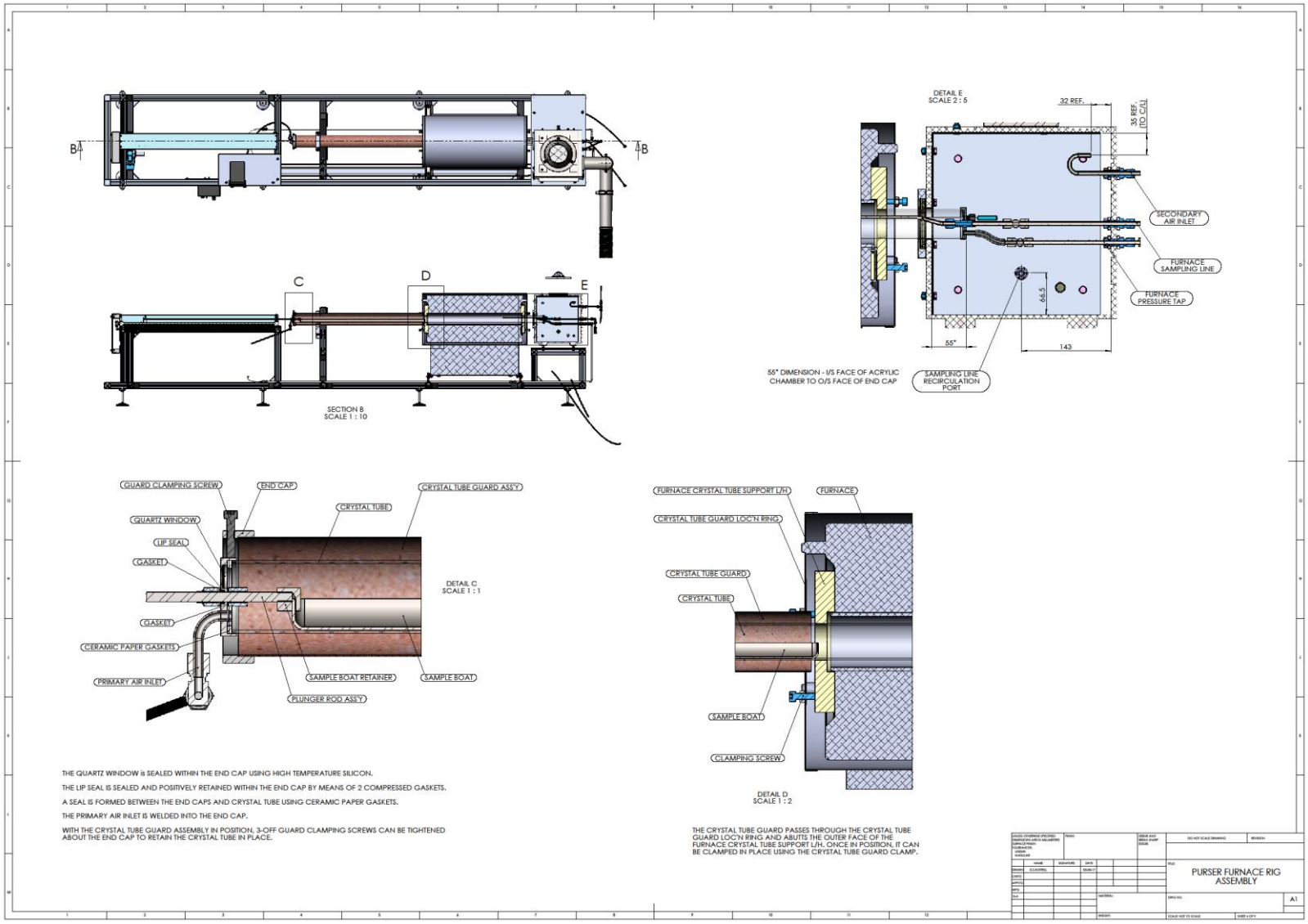
B
B
C
D
E
SECTION B
SCALE 1 : 10
DETAIL E
SCALE 2 : 5
32 REF.
35 REF.
(TO C/L)
SECONDARY AIR INLET
FURNACE SAMPLING LINE
FURNACE PRESSURE TAP
66.5
55*
143
55* DIMENSION - I/S FACE OF ACRYLIC CHAMBER TO O/S FACE OF END CAP
SAMPLING LINE RECIRCULATION PORT
GUARD CLAMPING SCREW
END CAP
CRYSTAL TUBE GUARD ASS'Y
CRYSTAL TUBE
QUARTZ WINDOW
LIP SEAL
GASKET
GASKET
CERAMIC PAPER GASKETS
PRIMARY AIR INLET
SAMPLE BOAT RETAINER
SAMPLE BOAT
PLUNGER ROD ASS'Y
DETAIL C
SCALE 1 : 1
FURNACE CRYSTAL TUBE SUPPORT L/H
FURNACE
CRYSTAL TUBE GUARD LOC'N RING
CRYSTAL TUBE GUARD
CRYSTAL TUBE
SAMPLE BOAT
CLAMPING SCREW
DETAIL D
SCALE 1 : 2
THE QUARTZ WINDOW is SEALED WITHIN THE END CAP USING HIGH TEMPERATURE SILICON.
THE LIP SEAL IS SEALED AND POSITIVELY RETAINED WITHIN THE END CAP BY MEANS OF 2 COMPRESSED GASKETS.
A SEAL IS FORMED BETWEEN THE END CAPS AND CRYSTAL TUBE USING CERAMIC PAPER GASKETS.
THE PRIMARY AIR INLET IS WELDED INTO THE END CAP.
WITH THE CRYSTAL TUBE GUARD ASSEMBLY IN POSITION, 3-OFF GUARD CLAMPING SCREWS CAN BE TIGHTENED ABOUT THE END CAP TO RETAIN THE CRYSTAL TUBE IN PLACE.
THE CRYSTAL TUBE GUARD PASSES THROUGH THE CRYSTAL TUBE GUARD LOC'N RING AND ABUTTS THE OUTER FACE OF THE FURNACE CRYSTAL TUBE SUPPORT L/H. ONCE IN POSITION, IT CAN BE CLAMPED IN PLACE USING THE CRYSTAL TUBE GUARD CLAMP.
DO NOT SCALE DRAWING
REVISION
PURSER FURNACE RIG ASSEMBLY
A1

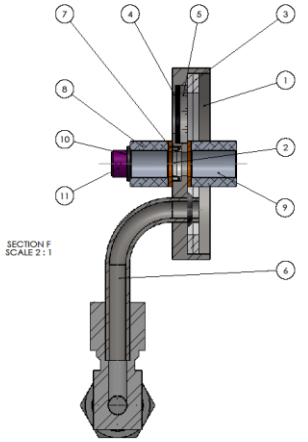


SECTION F
SCALE 2 : 1

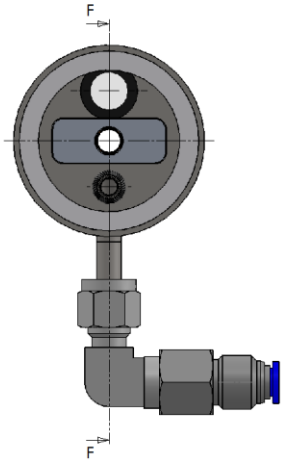


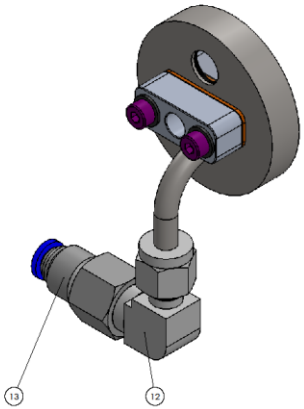


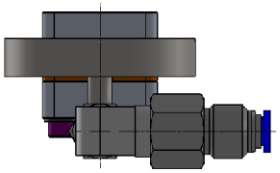

| ITEM NO. | PART NUMBER | QTY. |
|---|---|---|
| 1 | Alternative Quartz Tube End Cap | 1 |
| 2 | 1Turcon Variseal M25 6mmA | 1 |
| 3 | Alternative Quartz Tube End Cap Seal | 2 |
| 4 | Alternative Quartz Tube End Cap Window Sealant | 1 |
| 5 | Alternative Quartz Tube End Cap Window | 1 |
| 6 | Alternative Quartz Tube End Cap Air Inlet | 1 |
| 7 | Lip Seal Retainer Gasket | 2 |
| 8 | Lip Seal Retainer Outer | 1 |
| 9 | Lip Seal Retainer Inner | 1 |
| 10 | M4 Washer | 2 |
| 11 | M4 x 25 Capscrew | 2 |
| 12 | Male Elbow_SS-400-2-4RT | 1 |
| 13 | 1-4 Pneumatic Push-Fit Straight_I-PFS-04-04NPT | 1 |

**QUARTZ TUBE END CAP ASSEMBLY**

FOR FURTHER DETAILS OF HOW THIS SUB-ASSEMBLY FITS WITHIN THE OVERALL ASSEMBLY, PLEASE REFER TO SHEETS 2 & 4.

PURSER FURNACE RIG ASSEMBLY

A1

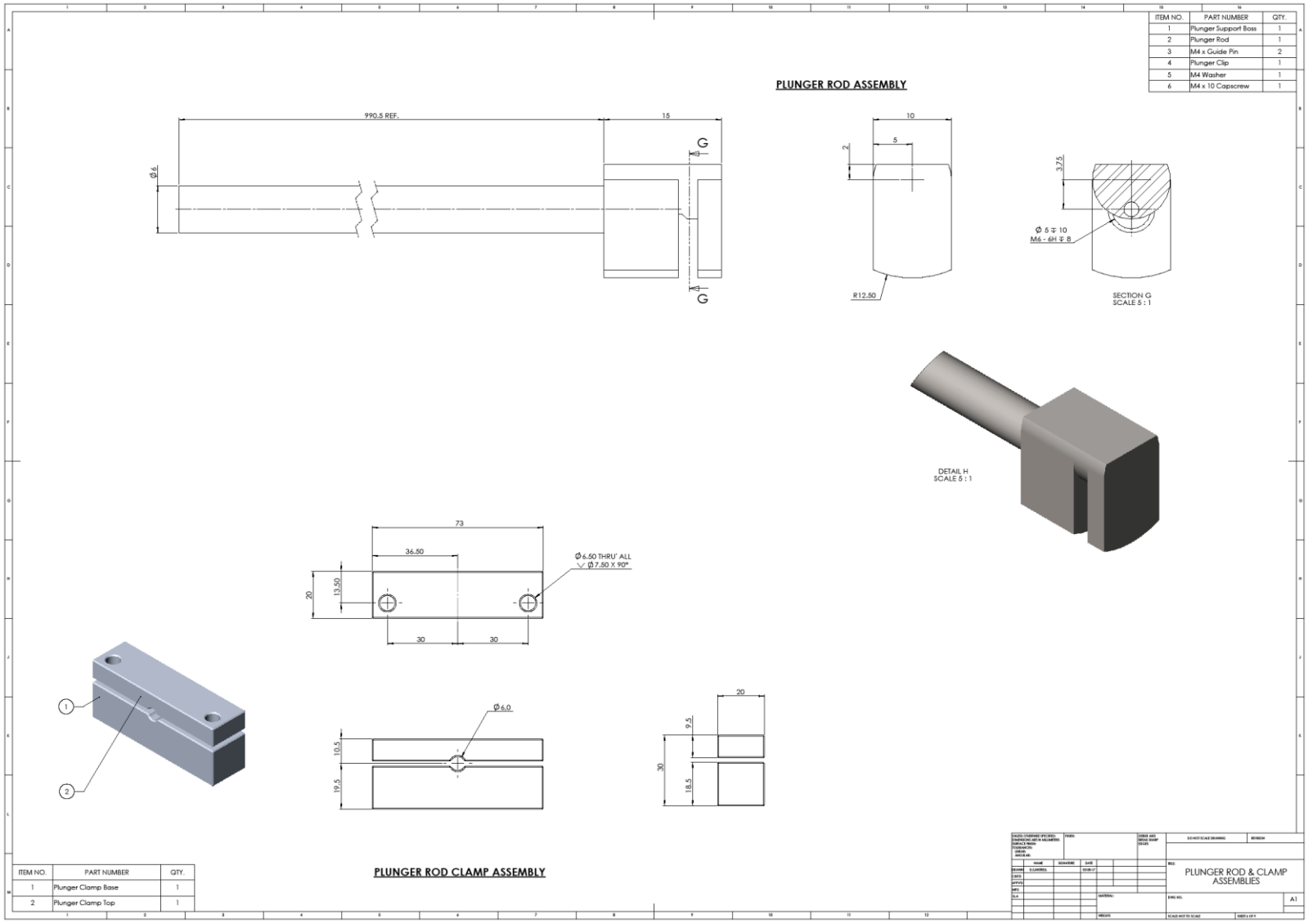
ITEM NO. | PART NUMBER | QTY.
1 | Plunger Support Boss | 1
2 | Plunger Rod | 1
3 | M4 x Guide Pin | 2
4 | Plunger Clip | 1
5 | M4 Washer | 1
6 | M4 x 10 Capscrew | 1
PLUNGER ROD ASSEMBLY
990.5 REF.
15
Ø6
G
10
5
2
R12.50
3.75
Ø 5 ↧ 10
M6 - 6H ↧ 8
SECTION G
SCALE 5 : 1
DETAIL H
SCALE 5 : 1
73
36.50
Ø6.50 THRU ALL
⌵ Ø7.50 X 90°
20
13.50
30
30
Ø6.0
10.5
19.5
20
9.5
30
18.5
1
2
ITEM NO. | PART NUMBER | QTY.
1 | Plunger Clamp Base | 1
2 | Plunger Clamp Top | 1
PLUNGER ROD CLAMP ASSEMBLY
PLUNGER ROD & CLAMP ASSEMBLIES
A1

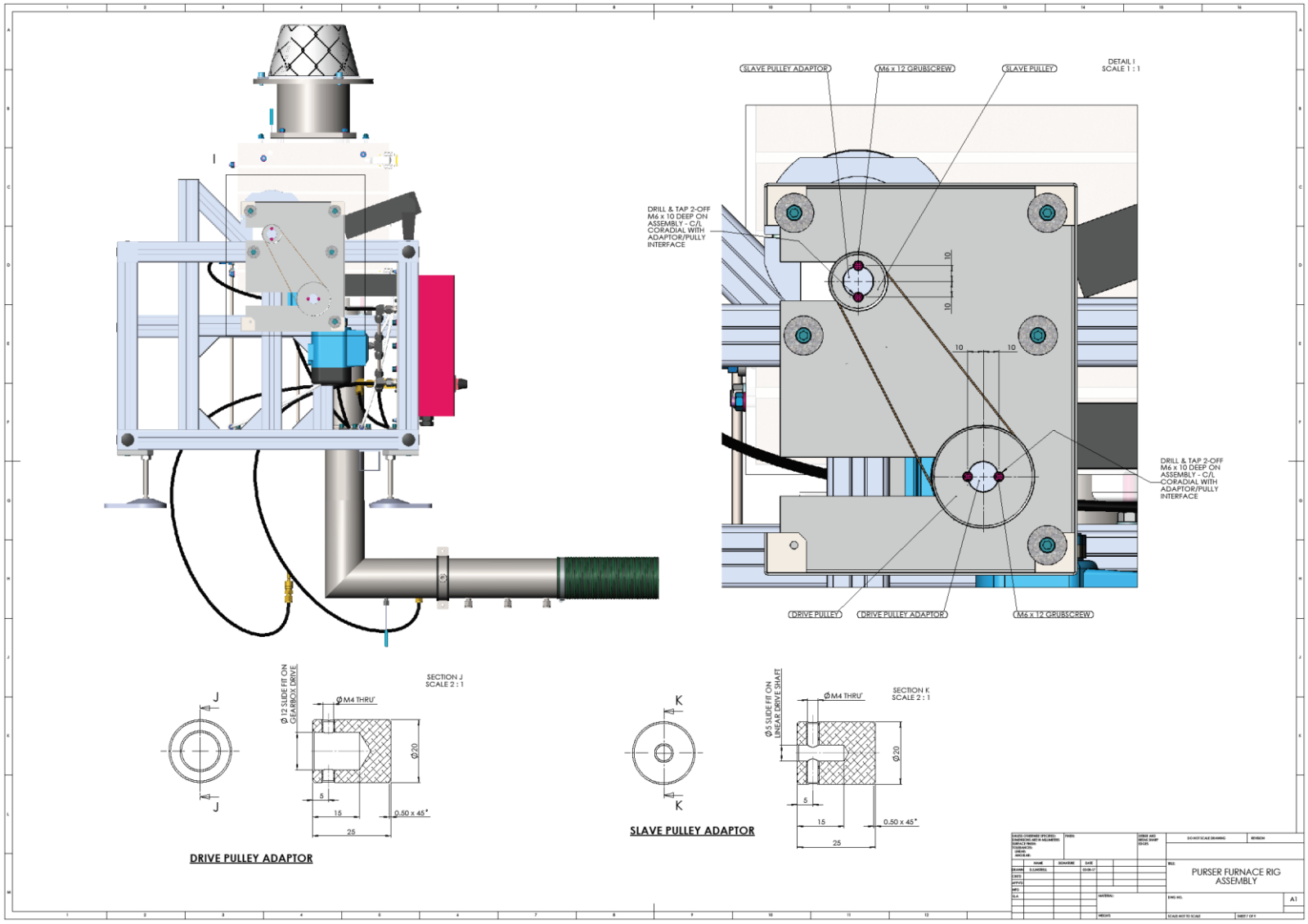
SLAVE PULLEY ADAPTOR
M6 x 12 GRUBSCREW
SLAVE PULLEY
DETAIL I
SCALE 1 : 1
DRILL & TAP 2-OFF M6 x 10 DEEP ON ASSEMBLY - C/L CORADIAL WITH ADAPTOR/PULLY INTERFACE
10
10
10
10
DRILL & TAP 2-OFF M6 x 10 DEEP ON ASSEMBLY - C/L CORADIAL WITH ADAPTOR/PULLY INTERFACE
DRIVE PULLEY
DRIVE PULLEY ADAPTOR
M6 x 12 GRUBSCREW
I
J
J
SECTION J
SCALE 2 : 1
Ø 12 SLIDE FIT ON GEARBOX DRIVE
ØM4 THRU'
Ø20
5
15
25
0.50 x 45°
DRIVE PULLEY ADAPTOR
K
K
SECTION K
SCALE 2 : 1
Ø5 SLIDE FIT ON LINEAR DRIVE SHAFT
ØM4 THRU'
Ø20
5
15
25
0.50 x 45°
SLAVE PULLEY ADAPTOR
PURSER FURNACE RIG ASSEMBLY
A1

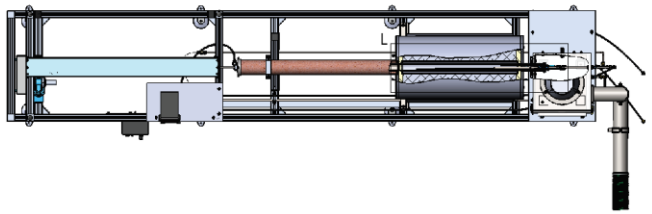


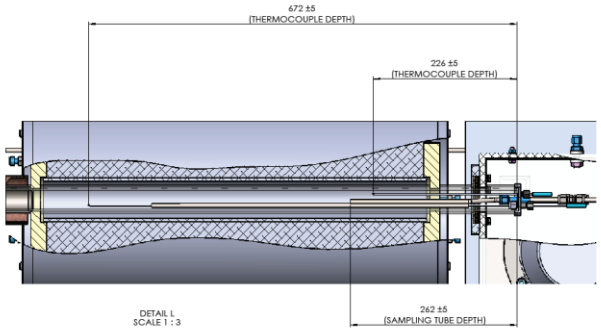


DETAIL L
SCALE 1 : 3

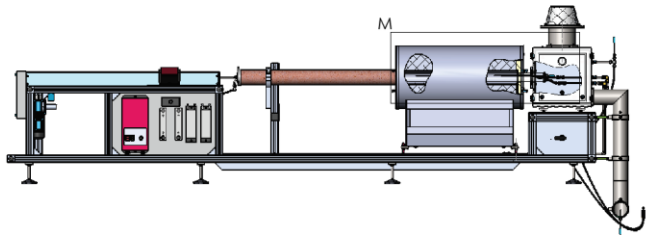


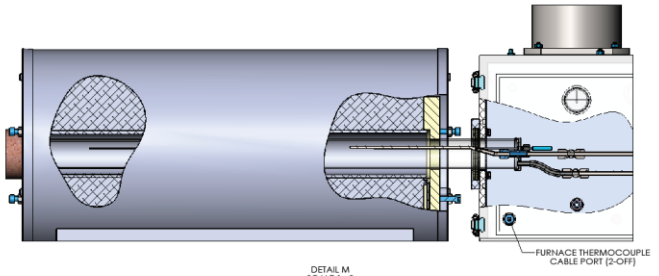


DETAIL M
SCALE 1 : 3

**FURNACE & SECONDARY AIR INLET**

**THERMOCOUPLE DIMENSIONS**

SAMPLING TUBE &
FURNACE THERMOCOUPLES

A1

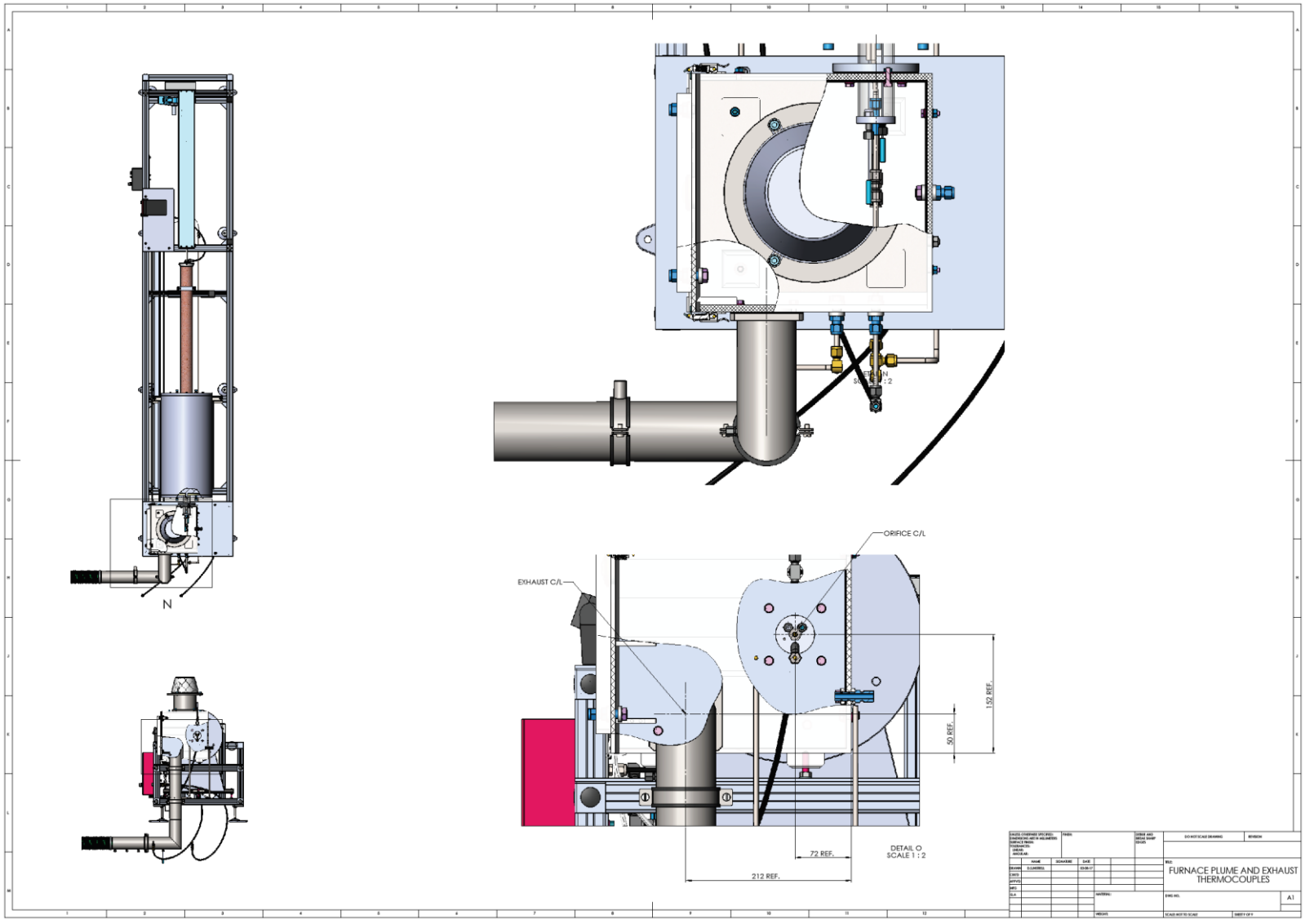
N
ORIFICE C/L
EXHAUST C/L
152 REF.
50 REF.
72 REF.
212 REF.
DETAIL O
SCALE 1 : 2
FURNACE PLUME AND EXHAUST THERMOCOUPLES
A1